Silyloxyarenes as C-O Electrophilic Coupling Partners Enabled by Nickel Catalysis

by

Eric M. Wiensch

A dissertation submitted in partial fulfillment
of the requirements for the degree of
Doctor of Philosophy
(Chemistry)
in the University of Michigan
2018

Doctoral Committee:

Professor John Montgomery, Chair
Professor Kenichi Kuroda
Professor Melanie Sanford
Professor John Wolfe

Eric M. Wiensch

ewiensch@umich.edu

ORCID iD: 0000-0003-1965-3258

Dedication

This dissertation is dedicated to my family for all the love and support they have provided. I would not be where I am without all of them. To my parents, Dave and Julie, for teaching me I can solve any problem with determination and logical thinking. To my brother, Josh, for sparking my curiosity for a more complete understanding. And to my wife, Ashley, for her intellectual prowess in teaching me how to look at things differently.

Acknowledgements

I would like to thank my advisor, John Montgomery for all his support and mentorship over my years in graduate school. Under his supervision, he has taught me much on how to think about problems and has helped me grow as a scientist. Thank you to Melanie Sanford and John Wolfe for the great experience teaching with both of them and, along with Kenichi Kuroda, for serving on my committee and all of the feedback through graduate school.

I would like to thank all current and former Montgomery group members that I have had the pleasure of working next to in lab. Thank you to everyone in lab for bouncing ideas off each other and working through problems together. I really appreciate all the support and mentorship from Evan Jackson and Hengbin Wang when I joined the group. A special thank you to David Todd and Wesley Pein for their collaborative contributions in the development and future exploration of projects discussed in my thesis. I would also like to acknowledge Kilian Muñiz and Calvin O'Brion at ICIQ for the wonderful experience I had in lab, as well as all of the students at ICIQ for their hospitality during my stay in Tarragona.

Finally, I would like to thank my family and friends for all their support.

Table of Contents

List of Tables

List of Figures

List of Equations

List of Schemes

List of Abbreviations

Me ..... methyl

Et ..... ethyl

n-Pr or Pr ..... *n*-propyl

i-Pr ..... *iso*-propyl

Ph ..... phenyl

n-Bu or Bu ..... *n*-butyl

i-Bu ..... *iso*-butyl

s-Bu ..... *sec*-butyl

Cy ..... cyclohexyl

t-Am ..... *tert*-amyl

t-Bu ..... *tert*-butyl

Py or Pyr ..... pyridine

Ad ..... adamantly

Cyp ..... cyclopenyl

TBS ..... *tert*-butyldimethylsilyl

TES ..... triethylsilyl

TBDPS ..... *tert*-butyldiphenylsilyl

TMS ..... trimethylsilyl

TIPS ..... triisopropylsilyl

Piv ..... pivaloyl

MOM..... methoxymethyl acetate

Tf..... trifluoromethanesulfonate

Ac..... acetyl

DMT..... 4,6-dimethoxy-1,3,5-triazine

TCT..... 2,4,6-trichloro-1,3,5-triazine

BOM ..... benzyloxymethyl acetal

Boc ..... *tert*-butyloxycarbonyl

eq..... equivalents

rt ..... room temperature

NHC ..... N-heterocyclic carbene

SIMes·HCl ..... 1,3-dimesityl-4,5-dihydro-1*H*-imidazol-3-ium chloride

IMes·HCl ..... 1,3-dimesityl-1*H*-imidazol-3-ium chloride

SIPr·HCl ..... 1,3-bis(2,6-diisopropylphenyl)-4,5-dihydro-1*H*-imidazol-3-ium chloride

IPr·HCl..... 1,3-bis(2,6-diisopropylphenyl)-1*H*-imidazol-3-ium chloride

IPr^{NMe2}·HCl..... 1,3-bis(2,6-diisopropylphenyl)-4,5-bis(dimethylamino)-1*H*-imidazol-3-ium chloride

IPr^{Me}·HCl ..... 1,3-bis(2,6-diisopropylphenyl)-4,5-dimethyl-1*H*-imidazol-3-ium chloride

IPr^{Cl}·HCl ..... 4,5-dichloro-1,3-bis(2,6-diisopropylphenyl)-1*H*-imidazol-3-ium chloride

$IMes^{Me}$·HCl..... 1,3-dimesityl-4,5-dimethyl-1*H*-imidazol-3-ium chloride

IPr^{Me}OMe·HCl..... 1,3-bis(2,6-diisopropyl-4-methoxyphenyl)-4,5-dimethyl-1*H*-imidazol-3-ium chloride

I(1-Ad)·HCl ..... 1,3-bis(1-adamantyl)imidazol-3-ium chloride

I(2-Ad)·HCl ..... 1,3-bis(2-adamantyl)imidazol-3-ium chloride

ICy·HCl..... 1,3-dicyclohexyl-1*H*-imidazol-3-ium chloride

$SIPr^{Ph}$·HCl..... 1,3-bis(2,6-diisopropylphenyl)-4,5-diphenyl-4,5-dihydro-1*H*-imidazol-3-ium chloride

IPr*OMe·HCl ..... 1,3-bis(2,6-dibenzhydryl-4-methoxyphenyl)-1*H*-imidazol-3-ium chloride

COD 1,5-cyclooctadiene

acac ..... acetylacetone

PMHS..... poly(methylhydrosiloxanne)

9-BBN ..... 9-borabicyclo[3.3.1]nonane

DMEDA..... N,N'dimethylethylenediamine

TMDSO..... 1,1,3,3-tetramethyldisiloxane

HMDS ..... hexamethyldisilazane

pin ..... pinacolato

nep..... neopentyl glycolato

dba..... dibenzylideneacetone

TBAF ..... tetrabutylammonium fluoride

DCM ..... dichloromethane

DMF ..... dimethylformamide

DME..... dimethoxyethane

DMSO ..... dimethylsulfoxide

THF ..... tetrahydrofuran

MeCN..... acetonitrile

NMP *N*-methyl-2-pyrrolidone

meo-mop ..... 2-(diphenylphosphino)-2'-methoxy-1, l'-binaphthyl

Xantphos ..... 4,5-bis(diphenylphosphino)-9,9-dimethylxanthene

DPPF ..... 1,1’-bis(diphenyl- phosphino)ferrocene

dcype ..... 1,2-bis(dicyclohexylphosphino)ethane

XPhos ..... 2-dicyclohexylphosphino-2’,4’,6’-triisopropylbiphenyl

XPhos-Pd-G2 ..... Chloro(2-dicyclohexylphosphino-2’,4’,6’-triisopropyl-1,1’-biphenyl)[2-(2’-amino-1,1’-biphenyl)]palladium(II)

dppp..... 1,3-bis(diphenylphosphino)propane

dtbbpy ..... 4,4'-di-tert-butyl-2,2'-bipyridine

Abstract

Silane protecting groups are traditionally only viewed as inert protecting groups to mask an alcohol functionality, allowing for orthogonal reactivity compared with other protecting groups and chemoselective protection or deprotection through silane attenuation. Therefore, due to the prevalence of silyl ethers in organic chemistry, they are attractive as C-O bond coupling partners that can be carried through syntheses for direct late-stage coupling without intermediate deprotection-activation strategies. However, silyloxyarenes have not been viewed as competent C-O coupling partners, and exploration of their C-O bond reactivity and general use as electrophilic coupling partners have not been previously developed as a general strategy.

In this thesis, silyloxyarene C-O bond reactivity has been explored through development of new silylation and reduction reactions, allowing for direct comparison to other electrophilic coupling partners. Additional cross-coupling reactions have been developed, including amination, borylation, and Suzuki couplings to display the utility of silyloxyarenes as C-O electrophiles. Orthogonal couplings with aryl methyl ethers have been developed where chemoselective coupling of either electrophile can be obtained by catalyst-controlled selectivity. Sequential coupling routes with silyloxyarene C-O bonds are described, demonstrating where current silyloxyarene C-O bond coupling reactions can be applied. Additionally, these routes display examples of carrying a silyloxyarene C-O bond through numerous steps for late-stage coupling. Finally, preliminary future work includes utilizing other classes of silyl-protected C-O bonds, developing an unrealized electrophile into a general handle for diversification.

Chapter 1

Late-Stage Functionalization of C-H and C-X Bonds

1.1 Introduction on Late-Stage Couplings

The development of pharmaceuticals and agrochemicals hinges on the ability to rapidly construct chemical libraries and screen molecules for activity. This allows medicinal chemists to explore structure-activity relationships and determine efficacy of complex molecules. Novel strategies to expediently access and diversify complex molecules are required to generate compound libraries. An approach that has been considered highly attractive, and broadly applicable in developing libraries of related compounds, is the use of methods for late-stage functionalization. Ideally, this approach allows for one general scaffold to be diversified with any functional group late in a synthetic route. (Scheme 1-1).

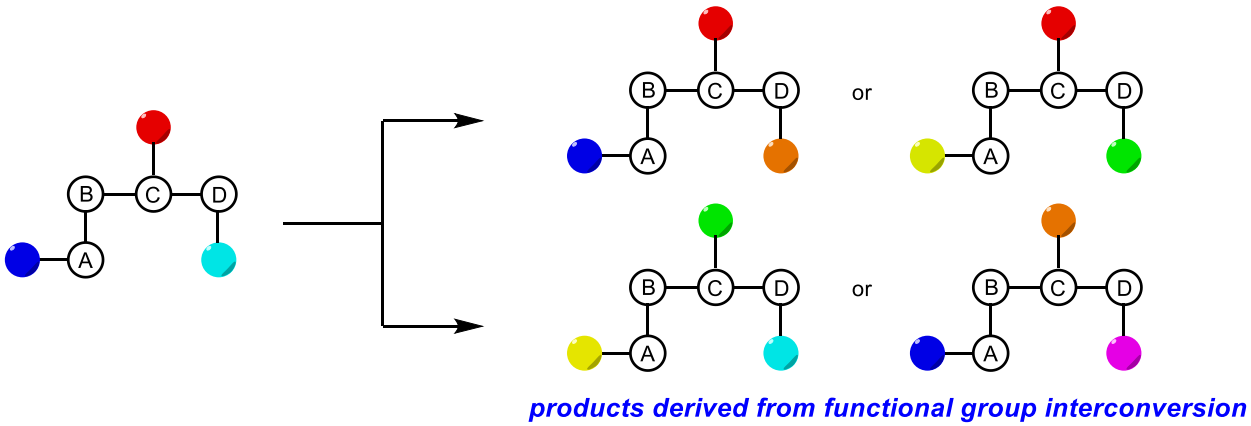

Scheme 1-1. Diversification through Late-Stage Functional Group Interconversion.

This strategy is advantageous over linear approaches that diverge early in a synthesis, as linear routes require separate syntheses for each compound in a library (Scheme 1-2). There has

been substantial interest in the chemical community to move away from linear syntheses due to the increased effort required for accessing related compounds. As such, numerous protocols have been developed for late-stage modification of complex molecules, including many examples utilizing transition metal catalysis. The ability to attenuate reactivity of a transition metal catalyst through their ligands allows for high functional group tolerance to be obtained.

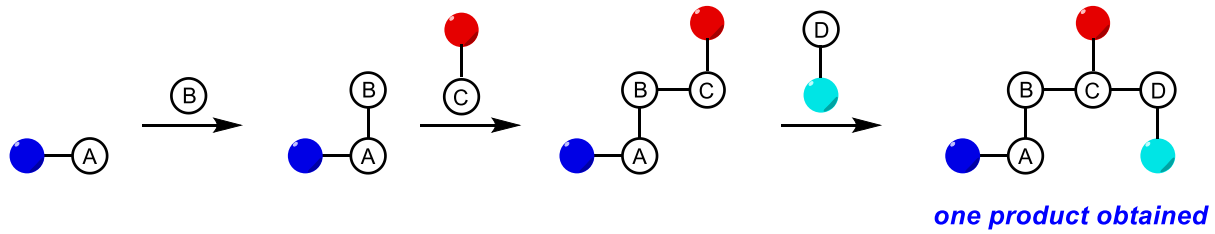

Scheme 1-2. Traditional Linear Synthesis Approach.

Countless methods exist for modification of alkyl scaffolds with or without transition metals. However, prior to the 1970's, no general method existed for derivatization of aryl C-sp^2 carbons that did not require harsh reaction conditions or specific electronic or steric environments. This gap in synthetic organic methods led to the cross-coupling revolution in organic synthesis, where modification of aryl scaffolds became possible. However, two general characteristics are required for late-stage coupling that limit additional activation steps: stability and reactivity. Traditional coupling methods have advanced to where reactivity of aryl halides is high; however, this limits their application in late-stage functionalization. As stability and reactivity are interconnected, an optimal group for late-stage coupling needs high stability while maintaining high reactivity towards a specific transition metal catalyst system. Therefore, there has been great interest in exploring new groups and transition metal catalysts for late-stage coupling, most prevalent being aryl C-H bonds and inert C-X bonds.

1.2 C-H Bond Derivatization

Due to the prevalence of C-H bonds in organic molecules, their selective modification has been a very attractive method. This has led to numerous reports of C-H bond functionalization for installation of nearly any group, making these powerful methods in organic chemistry. However, the prevalence of C-H bonds in organic molecules is also problematic, as selectivity between similar C-H bonds becomes challenging.

Two general solutions for high selectivity have been the use of directing groups and utilizing electronically or sterically differentiable C-H bonds.[1] However, this limits the generalizability of these methods as specific functional groups or substitution patterns are required for directed C-H functionalization. Without a directing group, electronic or steric biases are required for good selectivity. These restraints limit current methods to specific substitution patterns or require additional steps for installation and removal of directing groups. While there have been many creative solutions to solve these restrictions, improvement is still necessary for general application of C-H bond functionalization, particularly for late-stage applications. Therefore, utilizing a different functional group that can be carried through a synthesis and selectively derivatized at a late-stage would be preferred.

1.3 C-X Bond Derivatization

A method that removes problems of selectivity is the use of a pre-functionalized group that can be interconverted into nearly any desired group through transition metal catalysis. There have been many electrophilic or nucleophilic coupling partners employed in transition metal-catalyzed cross-couplings. Use of different electrophilic coupling partners allows for new reactivity that can be deployed alongside current methodology. Most prevalent are the halide derivatives, but more recently use of protected phenols and anilines have been explored as sources of renewable starting

materials. Furthermore, they have the ability to obtain complementary reactivity alongside other aryl electrophiles.

1.3.1 Aryl Halides as Electrophilic Cross-Coupling Partners

Use of transition metal-catalyzed cross-coupling reactions of alkyl and aryl halides has revolutionized synthesis of organic molecules due to their high selectivity and reactivity. Aryl halides have been the most influential as they have proved advantageous over previous methods. Currently, palladium has emerged as the most effective metal for cross-coupling aryl halides,[2,3,4] and is one of the most reliable homogeneous catalysts used in industry.[5,6] However, more abundant transition metals have also been utilized as alternatives to palladium, most commonly nickel.

Nickel catalysts have been shown to be competent replacements for palladium in cross-coupling and allow for new, complementary, or even improved reactivity. For example, a recent review of nickel catalyzed cross-couplings states,[7] "Comparative cross-coupling experiments of substituted aryl chloride with phenyl boronic acid demonstrated nearly uniformly higher yields for $Ni^{II}Cl_2$(dppf) than for $Pd^0(PPh_3)_4$, especially for electron-donating or nitrogenous substituents, thereby providing strong support for the assertion that Ni^0 catalysis is more robust for less reactive halide and pseudohalide leaving groups." Nickel has been shown to be more reactive to inert C-X bonds than palladium, which would be necessary for late-stage applications without intermediate activations.

Aryl fluorides are the most attractive aryl halide for late-stage application because they are more inert and this lower reactivity allows them to be carried through synthetic steps. Aryl C-F bonds have been shown to be competent electrophilic coupling partners under nickel catalysis.[8,9] Despite the several methods for aryl C-F coupling, limitations still remain in obtaining high reactivity due to the high C-F bond strength.[10]

In addition to direct transition metal-catalyzed C-F bond activation, nucleophilic aromatic substitution, S_NAr, is typically a milder method to utilize C-F bonds for derivatization, and is more amenable for late-stage applications.[11] This has solved reactivity problems but has introduced limitations on aryl functional groups which derive from the limited arene scope for S_NAr reactions. Together, both approaches work towards a dependable method of late-stage derivatization; however, availability of aryl fluorides is problematic. As many halides are often synthesized through C-H halogenations,[12] use of aryl halides does not actually remove selectivity issues observed in aryl C-H functionalization. Furthermore, aryl halides are not readily derived from renewable sources. Therefore, use of an abundant group that can be tuned for stability and reactivity would be advantageous.

1.3.2 Protected C-X bonds as Electrophilic Cross-Coupling Partners

Protected heteroatoms, such as anilines and phenols, are typically used as alternative electrophilic coupling partners to aryl halides. The advantages of utilizing aniline and phenol electrophiles include the ability to use starting materials derived from feedstock chemicals for green chemistry methods[13] and the access to new reactivity through tuning the protecting group. Unlike anilines,[14] phenols have been explored with a range of protecting groups, generating distinct classes of electrophilic C-O bond coupling partners. The array of protecting groups allows for tunable reactivity, which has led to numerous coupling reactions.[15,16,7,17,18,19,20,21,22]

1.3.2.1 Activated C-O bonds as Electrophilic Cross-Coupling Partners

Development of coupling methods for phenol C-O bond derivatives is challenging due to the strength of an aryl C-O bond, requiring high amounts of energy for activation. Therefore, initial development of C-O bonds as cross-coupling partners used strong activating groups and has since been extensively explored. An early example of using activated phenol C-O bonds as an

electrophilic coupling partner with palladium catalysts was in Heck and Sonogashira type reactions (Scheme 1-3).[23] Of all the fluorinated sulfonates that were explored, triflate (**1-1**) resulted in the best results. High yields were obtained using palladium catalysts with alkynes or alkenes to generate the arylated alkynes (**1-2**) or styrene (**1-3**) derivatives, respectively.

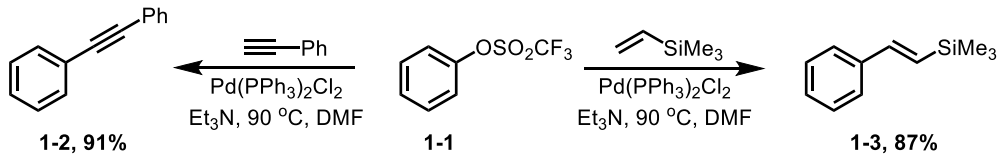

Scheme 1-3. Palladium-Catalyzed Coupling of Aryl Sulfonates.

However, the first coupling of an activated sp^2 C-O bond was not of an aryl system, but used vinyl triflates and organostannanes as reported by Stille.[24] Stoichiometric and catalytic reactions were explored to investigate the use of vinyl triflates as an extension to the use of allylic sulfonates for coupling reactions under palladium[25] or nickel[25] catalysis. The power of coupling enol C-O electrophiles was displayed by regioselectively generating the two isomeric vinyl triflates of 2-methylcyclohexanone (**1-5, 1-6**) using well known enolate chemistry. Subsequent C-O coupling of the vinyl triflates displayed the power of such C-O coupling methods by generating isomeric products which would be difficult to obtain through alternative methods (Scheme 1-4).

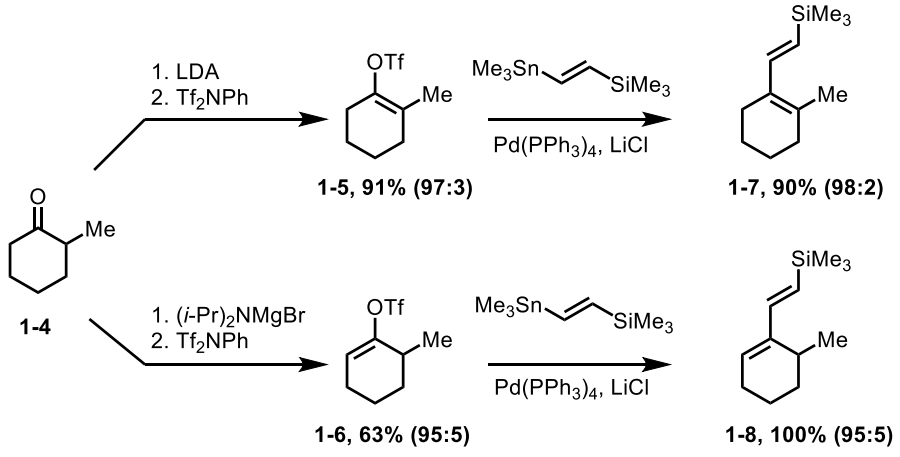

Scheme 1-4. Palladium-Catalyzed Coupling of Isomeric Vinyl Triflates with Organostannanes.

Following reports of these methods using vinyl and aryl triflates as electrophilic coupling partners, countless advances have been described with different coupling partners, catalysts, ligands, and protecting group variations. The first nickel-catalyzed method using activated phenol C-O bonds was reported by Yamashita in a homocoupling of aryl triflates with zinc as a reducing agent (Table 1-1).[26] Other sulfonate derivatives, such as methanesulfonate and *p*-toluenesulfonate, were explored but resulted in significantly lower yields.

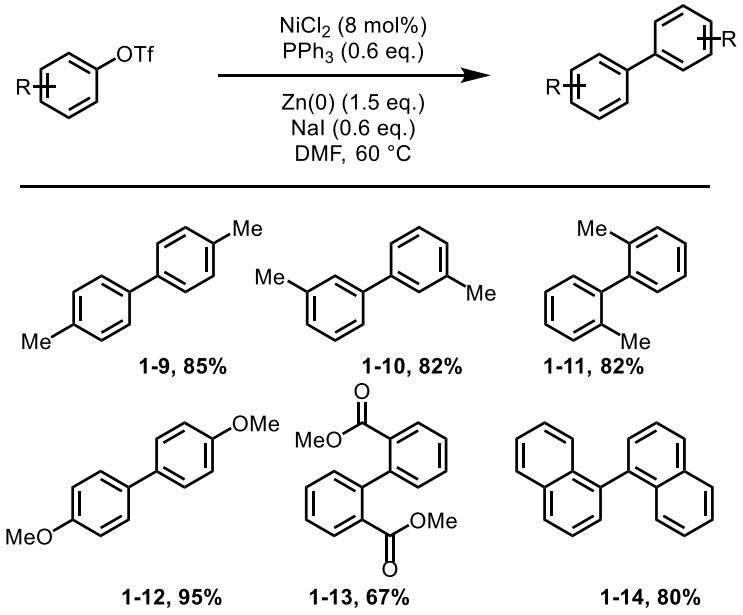

Table 1-1. Nickel-Catalyzed Homocoupling of Aryl Triflates.

Due to the high cost and low stability of triflates, other sulfonate protecting groups were explored. Early in their development as coupling partners, Percec investigated common sulfonates and observed reactivity for all of the sulfonates explored, with mesylate and tosylate giving slightly lower reactivity under nickel catalysis.[27] Since these initial reports using nickel catalysts for activated C-O bond couplings, the field has expanded immensely.[7] Some of the main activating groups that are commonly explored when developing new reactions or exploring new catalysts are the sulfonate, sulfamate, and phosphate derivatives.[28]

The use of activated C-O bonds has been very powerful; however, their direct application in late-stage diversification is not possible due to their high reactivity and instability across many common reaction conditions. In most cases, to conduct late-stage coupling of an activated C-O bond, the alcohol needs to be protected with a more stable protecting group as a placeholder, resulting in additional steps for deprotection-activation strategies, thereby lengthening syntheses.[29] An example of this approach is observed in the synthesis of 10,12-peroxycalamenene by the Woerpel group, where a silyl-protected alcohol (**1-15**) is carried through numerous synthetic steps, deprotected, activated to the aryl triflate (**1-18**), and then coupled in an intramolecular Heck reaction (Scheme 1-5).[30] Protecting group manipulations comprise a large number of steps in syntheses, both industrially and academically.[31,32]As such, the synthetic community has been pushing new methods that remove or limit protecting group manipulations.[33,34] Therefore, due to the instability of the pseudohalides, more robust C-O protecting groups would be needed for applications in late-stage diversification.

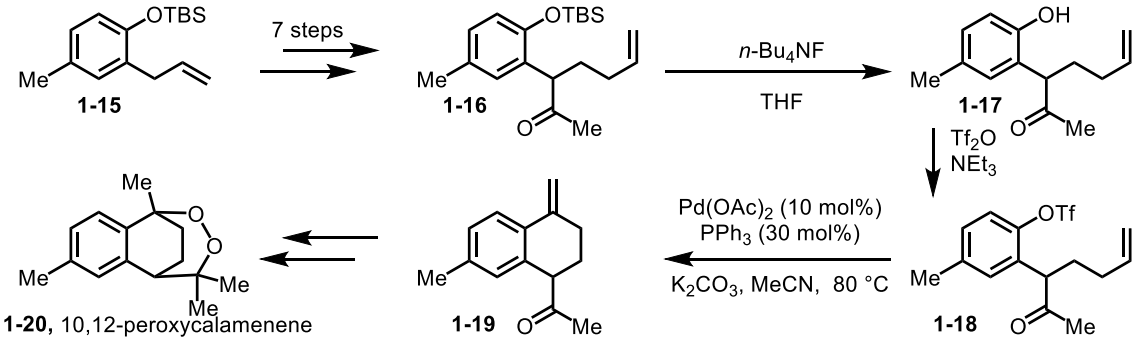

Scheme 1-5. Woerpel's Synthesis of 10,12-peroxycalamenene with Deprotection and Activation Strategy for C-O Coupling.

1.3.2.2 Inert C-O Bonds as Electrophilic Cross-Coupling Partners

Inert C-O bonds are derivatives that are attractive for applications in late-stage coupling because they are stable across a vast range of reaction conditions and can have high enough reactivity to be functionalized with the appropriate catalyst system. Aryl esters, carbamates, silyl

ethers, aryl ethers, and alkyl ethers are typically viewed as inert aryl C-O bonds. Palladium catalysts have not been widely shown to couple these aryl electrophiles and nickel has been the primary focus. There is a range of inert C-O bonds that balances reactivity of the C-O bond, or ease of oxidative addition to a nickel catalyst, and the stability of the protecting group (Figure 1-1). Ester, carbonate, carbamate, and some heterocyclic aryl derivatives have significantly higher reactivity over the simple ether derivatives, making them more analogous to the pseudohalide derivatives, and could be classified as semi-inert C-O bonds.

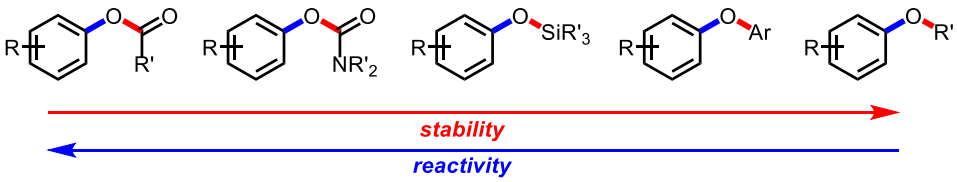

Figure 1-1. Stability and Reactivity of Inert C-O Bonds.

The range in reactivity can be rationalized by considering the conjugate acid pKa of the corresponding alcohol for the different protecting groups (Figure 1-2). However, this is only a general approximation as other factors need to be taken into consideration, most important of which is the ability of the protecting group to act as a directing group. Ester, carbonates, carbamate, and heterocyclic aryl protecting groups readily direct the nickel catalyst. Even simple aryl protecting groups for diaryl ethers can act as a weak directing group through η-coordination of the nickel catalyst to the π system of an aryl substituent. Another reason that conjugate acid pKa's of the protecting groups only provide an approximation is because the same catalyst system is not utilized for all inert C-O derivatives, leading to indirect comparisons.

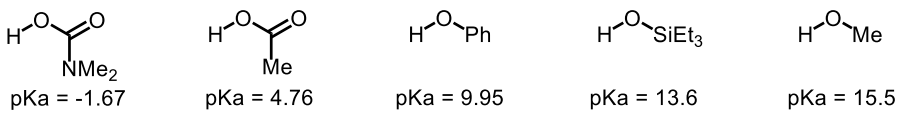

Figure 1-2. pKa Values of Common Inert C-O Protecting Groups

1.3.2.2.1 Carbamates, Carbonate and Esters as Electrophilic Cross-Coupling Partners

Nickel catalysts have primarily been the focus for C-O coupling of aryl carbamates, carbonates, and esters. This area of using carbamates or esters in cross-couplings has evolved independently, with initial reports of C-O coupling of carbamates reported in the early 1990's and esters being developed later in the 2000's. Of these two classes, the main protecting groups have included diethyl carbamates and pivalates due to their increased stability from electronic or steric effects, limiting deprotection.

Aryl carbamates were first used as C-O coupling partners with Grignard reagents without β-hydrogens under nickel catalysis by Snieckus.[35] Carbamates were displayed as attractive groups for directed ortho-metalation,[36] an advantage over previously developed aryl C-O electrophiles. After generation of the aryl carbamate (**1-21**), iterative ortho metalations, and subsequent quenching with an electrophile, resulted in a trisubstituted naphthyl substrate (**1-22**, Scheme 1-6). Finally, use of carbamates as traceless directing groups was displayed by removal of the aryl C-O bond through reduction with a nickel catalyst and a Grignard reagent with β-hydrogens.

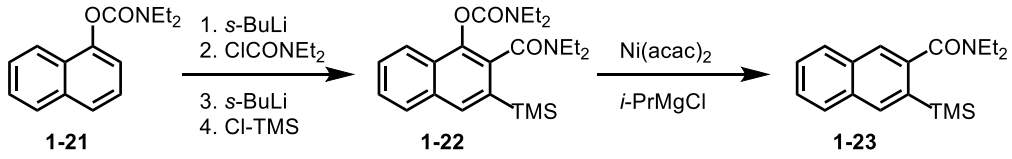

Scheme 1-6. C-O Coupling of Aryl Carbamates and Directed Ortho Metalation.

Since this initial report, many coupling reactions have been developed to explore new nucleophilic coupling partners in aryl carbamate C-O bond couplings (Scheme 1-7). In addition to Snieckus' display of carbamates as traceless directing groups with Grignard reagents containing β-hydrogens, silanes have also been shown as competent reductants for reductive deoxygenation of carbamate C-O bonds.[37]

However, there have also been numerous methods for installation of new functionality through C-O bond coupling (Scheme 1-7). Alkyl boranes have been utilized to install a variety of

alkyl substituents through in situ generation of coupling partners by hydroboration of olefins with 9-BBN.[38] Several methods have been developed to generate biaryl compounds by pairing the electrophilic C-O bond of aryl carbamates with common nucleophilic coupling partners, such as Grignard reagents,[35] boroxines,[39] boronic acids,[40,41] boronate esters,[42] silanes,[43] and aluminum reagents.[44,45] Other developed coupling reactions with aryl carbamate or carbonate C-O bonds include generation of aryl boron reagents,[46] anilines,[47,48] α-aryl ketones,[49,50] benzonitriles,[51] and biaryl compounds through C-H functionalization.[52]

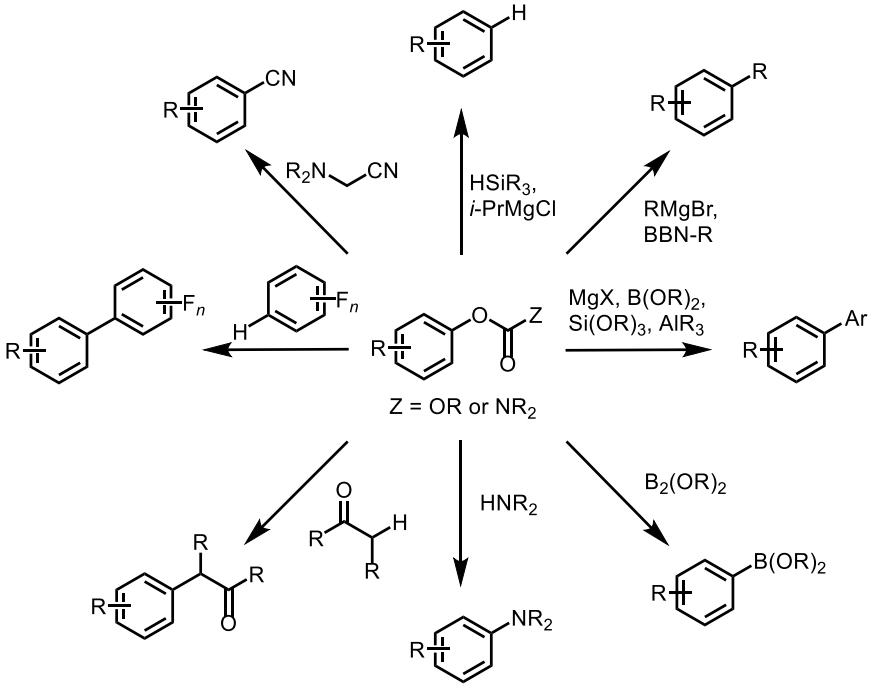

Scheme 1-7. Nickel-Catalyzed C-O Couplings with Aryl Carbamates.

It is important to note that different metals have been utilized besides nickel in C-O bond couplings of aryl carbamates, including cobalt for a directed C-H arylation.[53] Iron has been used for alkylations with Grignard reagents[54] and arylation with silanes.[43] Rhodium displayed arylation with boronate esters[55] or reductive deoxygenation with isopropanol.[56]

In addition to carbamates and carboxylates, esters have recently been explored in aryl C-O coupling. Garg and Shi independently reported the first nickel-catalyzed C-O coupling of aryl

esters with aryl boron reagents. Garg demonstrated C-O coupling of aryl pivalates with boronic acids,[57] while Shi reported coupling of aryl acetates with boroxines.[58] Since these initial reports, many different groups have developed C-O couplings with different nucleophilic coupling partners (Scheme 1-8). In addition to the aforementioned couplings of aryl esters with nickel catalysts, other nucleophiles include organozinc[59] and aluminum reagents[44,45] for aryl couplings. C-O bond coupling reactions with aryl esters also exist for generation of aryl phosphates,[60,61] styrene derivatives,[62] anilines,[63,64] and benzonitriles.[51] Removal of the C-O bond through reductive deoxygenation can also be accomplished with silanes[65] or sodium formate.[66] Several C-H/C-O couplings have been reported using heterocycles,[67] ortho-substituted phenols,[68] and α-carbonyls.[69,70] Aryl ester C-O coupling has also been shown with carbon dioxide,[71] isocyanates,[72] silylboron reagents,[73] and silyltin reagents.[74] Metals besides nickel have also been utilized in C-O couplings of aryl pivalates, including an iron catalyst in the coupling of aliphatic Grignard reagents,[75] and a rhodium catalyst for borylation.[76]

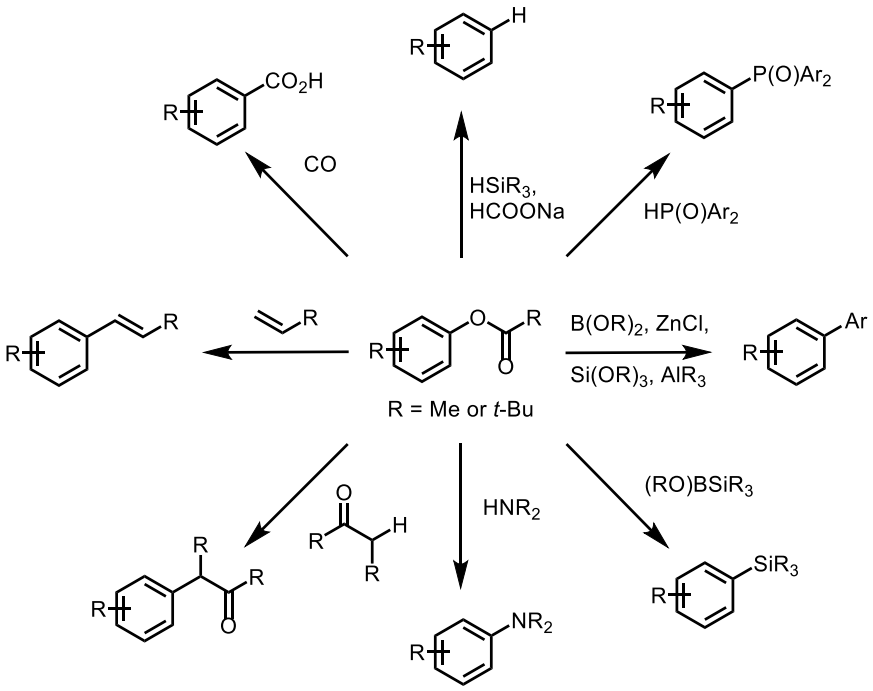

Scheme 1-8. Nickel-Catalyzed C-O Couplings of with Aryl Esters.

Despite the numerous methods developed for C-O coupling of carbamates, carbonates, and esters, there are stability issues with these C-O protecting groups, just like the pseudohalides. This is less of an issue with pivalates due to the increased sterics over acetates, but the presence of a carbonyl protecting group makes them generally unstable to basic conditions. There are also selectivity concerns with the ester derivatives due to the presence of an aryl C-O bond and an acyl C-O bond ((Scheme 1-9),[77,78] which can also be an issue for carbamates.[79,80] More inert protecting groups would be advantageous for the late-stage functionalization due to their increased stability.

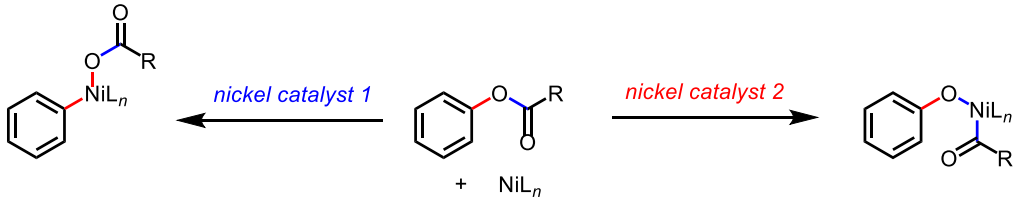

Scheme 1-9. Selectivity in Nickel-Catalyzed C-O Bond Activation of Esters.

1.3.2.2.2 Aryl and Alkyl Ethers as Electrophilic Cross-Coupling Partners

Very inert protecting groups for oxygen are the aryl or alkyl ethers, which were first explored as electrophilic coupling partners by Wenkert in Kumada couplings with a nickel catalyst (Scheme 1-10).[81] Only a small number of aryl methyl ethers were explored, with only extended aryl systems, such as naphthyl (**1-24**), resulting in high yields. Aryl methyl ether substrates with isolated aromatics resulted in poor yields.

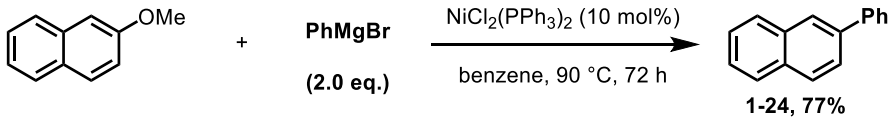

Scheme 1-10. Wenkert Nickel-Catalyzed C-O Coupling of Aryl Methyl Ethers with Grignard Reagents.

The lower reactivity of aryl methyl ether C-O bonds is an issue that hinders application for late-stage functionalization, as simple aryl systems show low activity. However, the Dankwardt group later improved the activity to allow coupling of isolated aromatics (**1-25**) by increasing catalyst reactivity with a more electron-rich phosphine ligand (Scheme 1-11).[82] This allowed for a

large substrate scope containing unprotected alcohols and amines. However, the use of such a strong nucleophilic coupling partner limits use of substrates with base-sensitive functionality. Therefore, milder nucleophilic coupling partners would be desired for applications in late-stage functionalization.

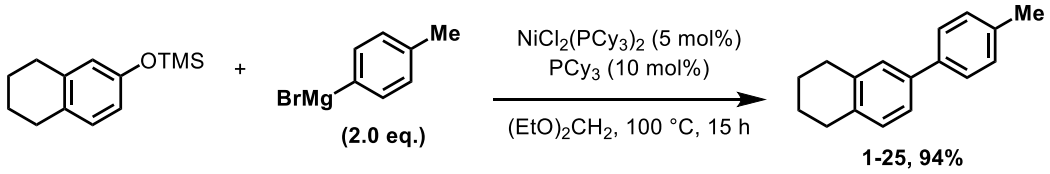

Scheme 1-11. Dankwardt C-O Coupling of Aryl Methyl Ethers with Grignard Reagents.

Since initial reports by Wenkert and Dankwardt, several new coupling methods with C-O bonds of aryl methyl ethers have been developed (Scheme 1-12). Reactions include other aryl couplings using Grignard reagents,[83,84,85,86] zinc reagents,[87] organolithiums,[88] aryl boronate esters,[89,90] and aryl bromides with metal reductants.[91] A number of alkyl groups without β-hydrogens have been coupled, employing Grignard,[92,93,94] organolithium,[95] and aluminum reagents.[96] More recently, a number these reactions have been expanded to compounds with β-hydrogens by use of different ligands, including aluminum,[97] Grignard,[98] and boron reagents.[99]

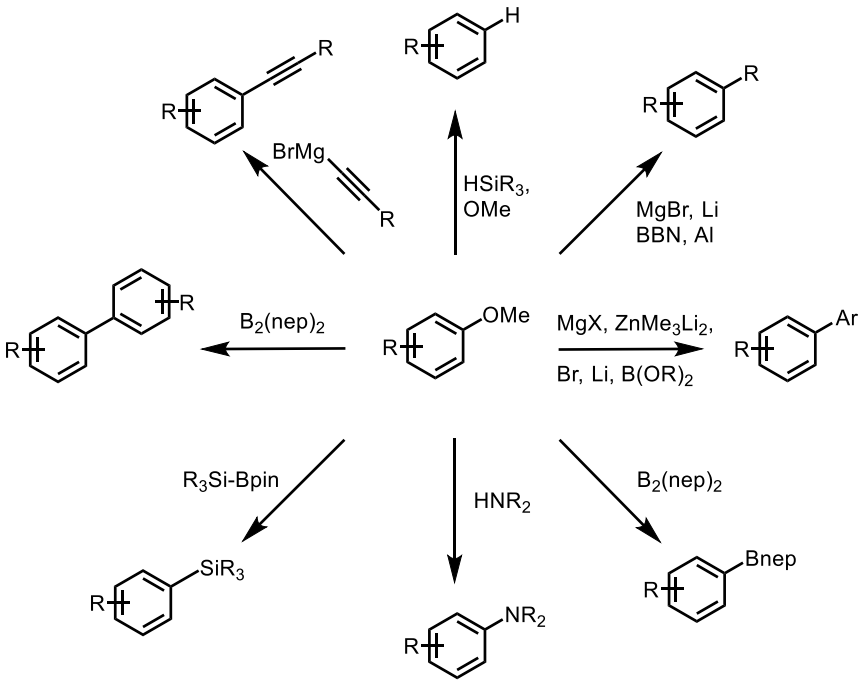

Scheme 1-12. Nickel-Catalyzed C-O Couplings with Aryl Methyl Ethers.

In addition to aryl and alkyl couplings, reductive deoxygenation reactions using silanes[100,65] or the methoxy group through β-hydride elimination[101] have been reported. Further couplings to increase diversity include alkynylation with Grignard reagents,[102] homocoupling with a diboron reductant,[103] silylation,[104] amination,[105,106] and borylation.[107] Despite the large number of coupling reactions developed with aryl methyl ethers under nickel catalysis, the low reactivity of aryl methyl ether C-O bonds still hinders these coupling reactions. This is apparent when moving away from strongly Lewis acidic or nucleophilic coupling partners, such as Grignard, organolithium, and zinc reagents. In these reactions with less nucleophilic coupling partners, lower reactivity is observed with biphenyl and completely isolated aromatic systems.

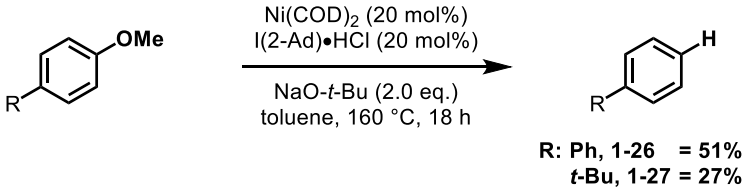

Scheme 1-13. Nickel-Catalyzed Amination of Aryl Methyl Ethers.

The lower reactivity with biphenyl and isolated phenyl systems is observed in reductive deoxygenation of aryl methyl ether C-O bonds (Scheme 1-13),[101] where moderate yields are obtained with biphenyl (**1-26**) and poor yields are observed with *tert*-butyl substrate **1-27**. In another reductive deoxygenation reaction with silane as the reductant, no product was observed with a biphenyl substrate[65] and a directing group was necessary to observe C-O bond activation.[100] Use of a directing group to overcome low reactivity of aryl methyl ether C-O bonds was further demonstrated in a borylation,[107] where an electron-deficient directing group was necessary to obtain moderate yields of isolated aromatic products. However, a directing group approach is not a long-term solution to the lower reactivity of aryl methyl ethers. There have been some developments in exploring new ligands to improve reactivity,[90] but has not led to significant improvements as low yields are still obtained (Scheme 1-14).

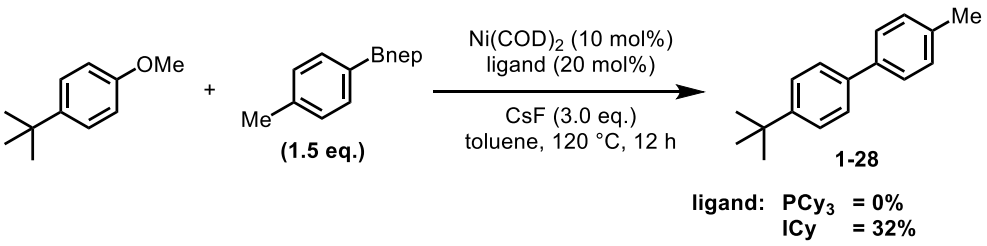

Scheme 1-14. Nickel-Catalyzed Suzuki Coupling of Aryl Methyl Ethers.

Diaryl ethers have also been explored as C-O electrophiles, although the focus has mainly been on applications for lignin degradation. One of the first major papers in this area was by the Hartwig group where they utilized a nickel catalyst to reduce the C-O bond of diaryl ethers with hydrogen gas (Scheme 1-15).[108] Since this report, there have been a number of follow-up papers focusing on heterogeneous catalysts,[109] selectivity,[110] and mechanistic analysis[111] of the C-O bond reduction of diaryl ethers. Although this methodology is exciting for lignin degradation, diaryl ethers are not particularly attractive as C-O electrophiles for cross coupling, as they are commonly synthesized through a coupling reaction themselves, not through a simple protection.

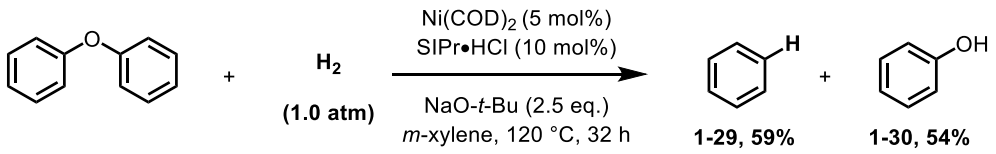

Scheme 1-15. Nickel-Catalyzed Hydrogenolysis of Diaryl Ethers.

Lower reactivity is also observed when moving away from a naphthyl substrate to a biphenyl or isolated aromatic in couplings of diaryl ethers. However, using the aryl protecting group as a directing group, such as 2-pyridyl, has been successful for improving conversion. Yet, yields can remain low and a more common approach has been the use of a 1,3,5-triazine group which has good directing capabilities and withdrawing influence to weaken the C-O bond. As such, significantly higher yields are observed using triazine as a protecting group over 2-pyridyl or simple phenyl groups (Scheme 1-16).[112]

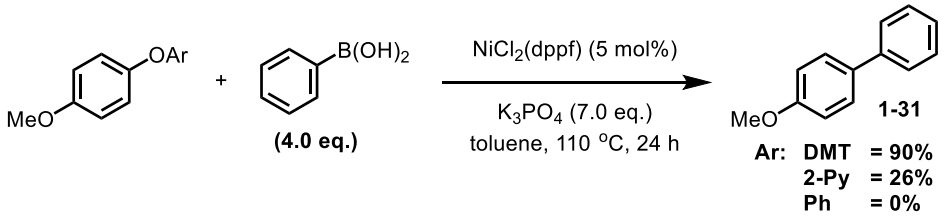

Scheme 1-16. Nickel-Catalyzed Comparison of Diaryl Ether Protecting Groups.

This higher reactivity of the triazine derivatives has led to the development of coupling reactions beyond the hydrogenolysis reaction mentioned above. A couple of examples exist with rhodium[113] or ruthenium,[114] but methods primarily focus on nickel. Aryl coupling reactions with a nickel catalyst include use of aryl boron[112,115] or Grignard reagents.[116] Other nickel-catalyzed reactions include borylation,[117] amination,[118,119] homocoupling,[120] and Heck couplings.[121] Additionally, methods for reductive deoxygenation have also been reported using alcohol reductants (Scheme 1-17).[120,122] Utilizing the 2-pyridyl or triazine group also allows for directed C-H functionalization at the ortho position, followed by coupling of the C-O bond.[123]

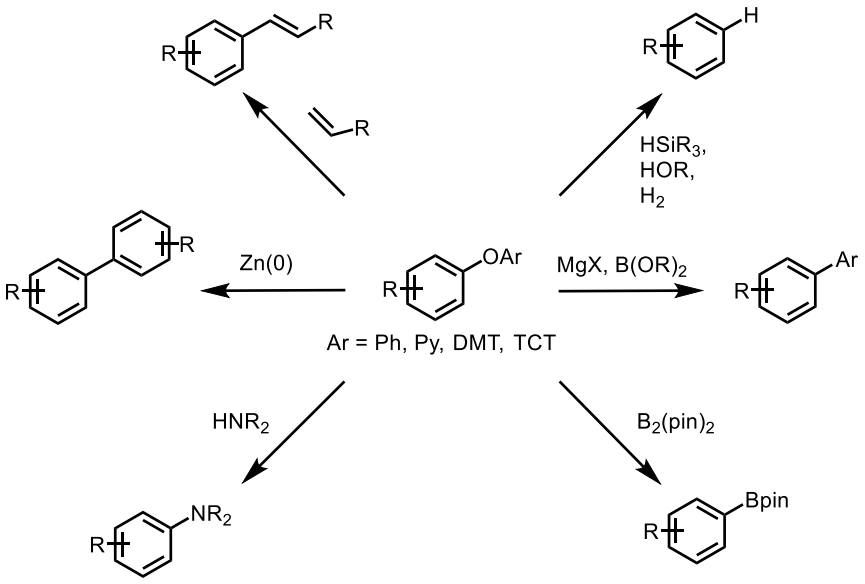

Scheme 1-17. Nickel-Catalyzed C-O Couplings of Diaryl Ethers.

Due to applications for lignin degradation, other methods have been utilized to reduce the strong C-O bond in aryl or alkyl ethers. Early work by Milstein described stoichiometric studies with rhodium, palladium, and nickel in activation of inert C-O bonds with pincer ligands.[124,125] Agapie also explored stoichiometric experiments with related ligands for reductive deoxygenation reactions.[126–128] Ruthenium was displayed in stoichiometric experiments by Murai[129] and Kakiuchi,[114] and developed catalytic couplings of olefins and aryl boronate esters with ortho-directing groups. Additional advances have been realized for catalytic coupling of alkyl ethers, including, ruthenium,[130,131] chromium,[132,133] iridium,[134] and a titanium Lewis acid.[135] However, nickel has been shown to be one of the few transition metals that can activate the inert C-O bond of aryl alkyl ethers without a directing group. There are a select few examples with other transition metals, such as iron[136] or cobalt,[137] but they typically require strong nucleophilic coupling partners and are proposed to undergo a range of different mechanisms,[138,139,140,141,142,143,144] as opposed to formal oxidative addition that is typically proposed for homogeneous nickel-catalyzed methods.

In exploration of the nickel-catalyzed mechanism, a nickel(0)-ate complex is commonly proposed to facilitate oxidative addition,[145,146] as a super-stoichiometric amount of base is typically employed. Other proposals for the base are to aid in coordination of the nickel catalyst to the aryl system,[147,148,149] to prevent off-cycle pathways,[111] and destabilization of the resting state.[150] Beyond the exploration of a Ni(0) complex for oxidative addition, Ni(I) intermediates have been proposed under certain reaction conditions when using silanes[151] or silyl boranes.[104,150]

Despite the many mechanistic papers, further developments to improve reactivity have not led to significant improvements or been reaction specific. One such example appears to be an advance in reactivity, allowing for silylation at room temperature.[104] However, this nickel-catalyzed silylation is very different than all of the other nickel-catalyzed C-O bond couplings as no ligand is utilized and the reaction proceeds at room temperature. Upon closer analysis, use of in situ generated, strong silyl anions result in the improved reactivity,[150] analogous to how strongly nucleophilic carbon coupling partners (e.g.: Grignard, organolithium, aryl zinc reagents) allow for coupling of aryl methyl ethers under nickel catalysis at room temperature. Due to the limitation of nickel-catalyzed C-O coupling of aryl and alkyl ethers, other methods that allow for higher reactivity while maintaining high stability would be advantageous for applications in late-stage functionalization.

1.3.2.2.3 Silyloxyarenes as Electrophilic Cross-Coupling Partners

Silyloxyarenes should have both high stability and higher C-O bond reactivity over aryl or alkyl ethers. Furthermore, silyloxyarenes are attractive as C-O electrophiles because silanes have become one of the most useful protecting groups in organic synthesis for oxygen functionalities. Silanes have many widely available structures, allowing for tunability and chemoselective protection or deprotection.[152,153,154,155] Common silane protecting groups utilized for organic

synthesis are trimethysilyl (TMS), triethylsilyl (TES), *tert*-butyldimethylsilyl (TBS), triisopropylsilane (TIPS), and *tert*-butyldiphenylsilyl (TBDPS) (Figure 1-3).

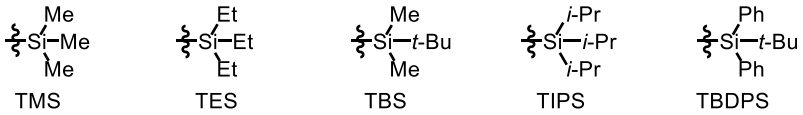

Figure 1-3. Common Silane Protecting Groups.

One reason silanes have become such a popular protecting group is their complementary deprotection with fluoride ions, making them orthogonal to other common protecting groups. Furthermore, sterics around the silicon allows for a range of stability, where more steric hinderance around silicon allows for less labile silane protecting groups. Additionally, electronics on the silane play an important role where withdrawing substitutes increases susceptibility for basic hydrolysis but decreases sensitivity for acidic hydrolysis. The ability to tune silane protecting groups has allowed for selective deprotections of more labile silanes in the presence of more stable silane protecting groups.[156,157] Remarkably, even small changes in sterics or electronics can result in selective deprotection, such as the example by Carreira where one primary TBS ether can be deprotected in the presence of another primary TBS ether (Scheme 1-18).[158]

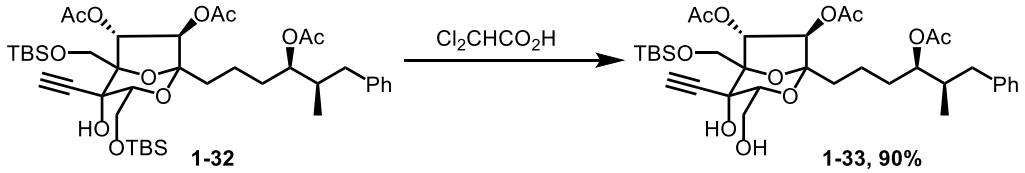

Scheme 1-18. Carreira Selective Deprotection Between two Primary Silyl Ethers.

Typically, selective protection of alcohols depends on the sterics and electronics of alcohols in a molecule. Generally, less sterically hindered and more electron-rich alcohols are protected before more hindered or less electron-rich alcohols. Analogues to selective deprotection, there are examples of only slight differences in either sterics or electronics for selective

protections, such as the example by Danishefsky where a secondary alcohol was protected in the presence of a secondary allylic alcohol (Scheme 1-19).[159]

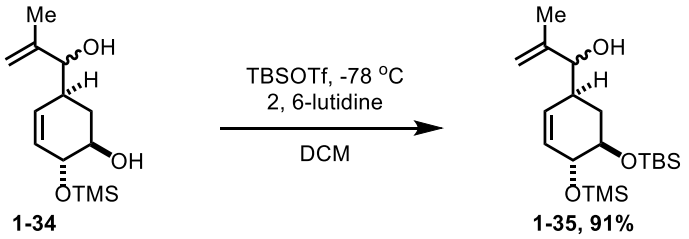

Scheme 1-19. Danishefsky Selective Protection of Secondary Alcohol over Secondary Allylic Alcohol.

These characteristics of silane protecting groups have enabled the synthesis of many complex molecules, such as the first synthesis of Taxol (**1-37**) by the Holton group (Figure 1-4).[160] This synthesis demonstrates the ability to sequentially deprotect various trialkylsilanes based on the sterics of the groups, where iterative deprotections of three secondary alcohols was described. Use of different deprotection conditions allowed for selective deprotection from most labile to most stable silane protecting group (TMS, TES, TBS). Being able to sequentially deprotect silyl-protected alcohols allowed for each of them to be derivatized chemoselectively. The unique characteristics and prevalence of silanes as protecting groups in organic chemistry presents silyl ethers as an attractive C-O coupling partner.

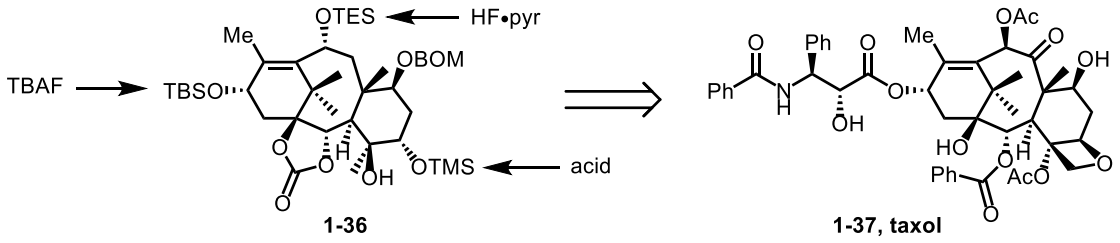

Figure 1-4. Use of Silane Protecting Groups in the Synthesis of Taxol.

Despite the advantage of silane protecting groups, silyloxyarene C-O bonds have not been viewed as competent coupling partners. Only a few examples exist and are limited to Kumada couplings. One of the first examples that explored silyloxyarene C-O bonds as aryl electrophilic coupling partners was by Dankwardt (Scheme 1-20), where he only explored two silyloxyarene

substrates in a protecting group screen.[82] However, these examples displayed the first use of silyl-protected phenol derivatives as electrophilic coupling partners.

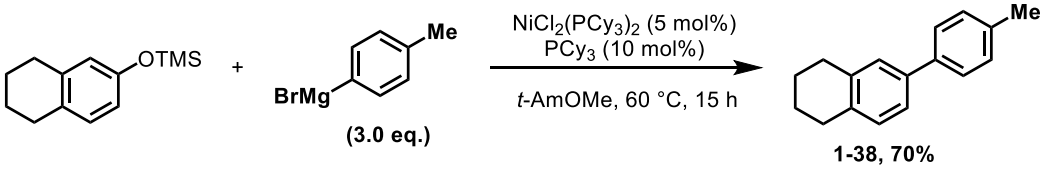

Scheme 1-20. Dankwardt Silyloxyarene Kumada Coupling.

Several other reports have also explored use of silyloxyarenes ac C-O coupling partners, but only explored their use in screening different protecting groups for methods developed for aryl alkyl ether C-O bond coupling.[92,83,88] Trimethylsilane was the silane protecting group typically used in these studies, which is the most labile trialkylsilane protecting group. Therefore, this ability to be readily deprotected under acid or basic conditions limits use in late-stage functionalization.

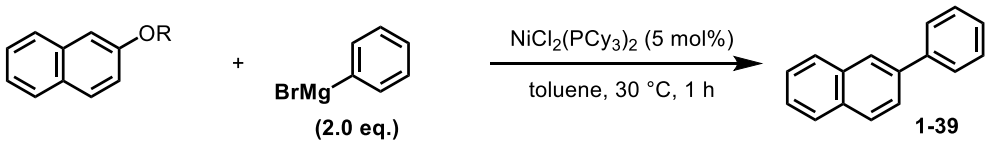

entry	R	yield
1	$SiMe_3$	**80%**
2	$SiEt_3$	**76%**
3	$Si(i\text{-}Pr)_3$	**89%**
4	$Si(t\text{-}Bu)Me_2$	**85%**
5	$SiPh_3$	**80%**
6	$SiPhMe_2$	**88%**

Table 1-2. Silane Protecting Groups in Kumada Coupling with Phenyl Magnesium Bromide.

A recent method by Shi was the first report that focused on developing silyloxyarenes as C-O electrophiles[161] and not simply showing one example in an optimization table. The scope was mostly limited to naphthyl substrates, where good yields were obtained. Few examples displayed use of isolated aromatic systems, which resulted in moderate yields. In the initial optimization, several different silane groups were also explored. Interestingly, all of the different silanes gave yields between 76 and 89 percent, even very labile silane protecting groups (Table 1-2). As

strongly basic nucleophiles are used, this is surprising that labile silane protecting groups are not deprotected and result in lower yields. Furthermore, bis(phenoxy)disilane **1-40** was also utilized as a substrate with four equivalents of Grignard reagent (Scheme 1-21). Typically, dialkoxy-silanes are not stable and rapidly deprotect under strongly acidic or basic conditions, suggesting that something else may be occurring in these reactions besides direct C-O bond coupling of the silyloxyarene.

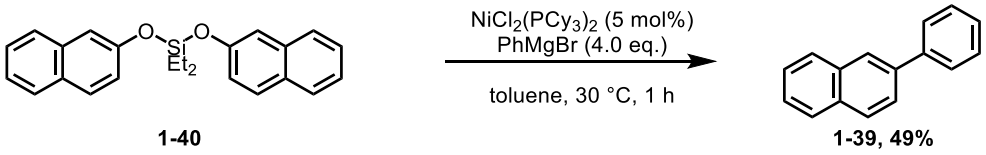

Scheme 1-21. C-O Bond Cleavage in Bis(2-naphthoxy)diethylsilane.

The Uchiyama group did state that using a trimethylsilyl protecting group in C-O bond coupling reactions with organolithium reagents, resulted in deprotected of starting material to 2-naphthol (Scheme 1-22).[88] However, increasing to a bulkier silane, *tert*-butyldimethylsilane, resulted in the desired product. Therefore, previous reports of using trimethylsilyl (TMS) protecting groups in C-O bond coupling reactions with Grignard reagents may have resulted in deprotection and C-O bond coupling was with the free phenol. Such coupling of free phenols with Grignard reagents has been reported before, where activation of the C-O bond is through coordination of a magnesium salt to generate a magnesium naphtholate complex.[162] However, in these examples, coupling was only described with naphthyl substrates and has not been shown with isolated phenols. Additionally, aggregation of phenyl magnesium bromide may lead to significantly different reactivity and could not deprotect trimethylsilyl as rapidly as phenyl lithium. Regardless of the identity of the C-O bond coupling partner, use of strongly nucleophilic coupling partners limit application to late-stage functionalization due to the inability to tolerate base-

sensitive functionality. Therefore, other reactions should be explored that use milder coupling partners with silyloxyarene C-O bonds.

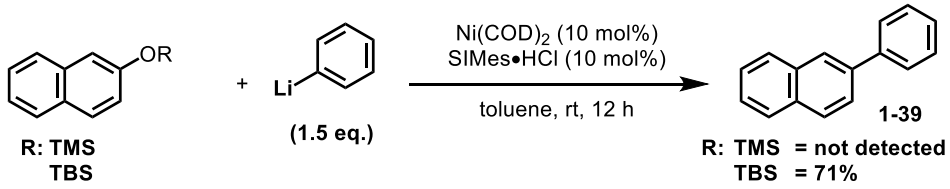

Scheme 1-22. Silyloxyarene Coupling with Organolithium.

The Nakao group explored the use of alkoxysilanes as in situ protecting groups and the reductant with a nickel catalyst for hydrogenolysis of phenols.[163] A mechanism was proposed (Scheme 1-23) that begins with nickel-catalyzed dehydrogenative silylation between the phenol (**1-41**) and silane. Upon generation of the silyloxyarene (**1-42**), oxidative addition of the C-O bond to the nickel(0) catalyst generates a nickel(II) silyloxy intermediate (**1-43**). This complex undergoes transmetallation with another equivalent of silane, producing a nickel hydride (**1-44**) and disiloxane byproduct. The nickel hydride then reductively eliminates to produce the desired product (**1-45**) and turnover the nickel catalyst.

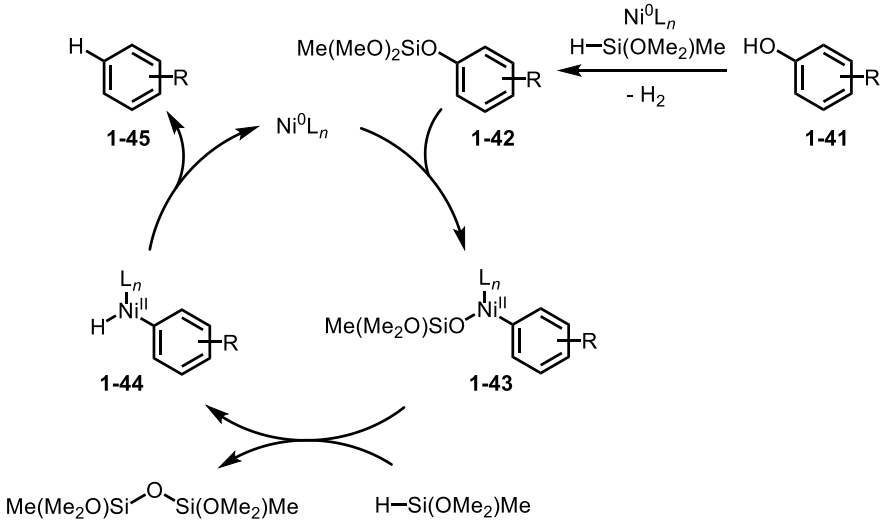

Scheme 1-23. Proposed Mechanism for Nickel-Catalyzed Hydrogenolysis of Phenols with Hydrosilanes.

Experiments were conducted to support the proposed mechanism. First, as hydrogen gas is generated through the proposed dehydrogenative silylation, hydrogen could be acting as the reductant for the hydrogenolysis step. However, the process was separated into two steps where an equimolar amount of silane and phenol (**1-46**) was utilized to generate the silyloxyarene (**1-47)**, which was verified by ^{1}H NMR. The reaction mixture was then transferred to a closed vessel, placed under two atmospheres of hydrogen gas, and set up under standard reaction conditions. It was found that only trace product (**1-48**) was observed with hydrogen. Additionally, they also conducted the same experiment but did not place the reaction under a hydrogen atmosphere and added another equivalent of silane, resulting in similar yields to the standard reaction setup. These experiments suggest that hydrogen produced from the dehydrogenative silylation is not playing a large role in this reaction, and the silane is acting as the protecting group and the reductant (Scheme 1-24).

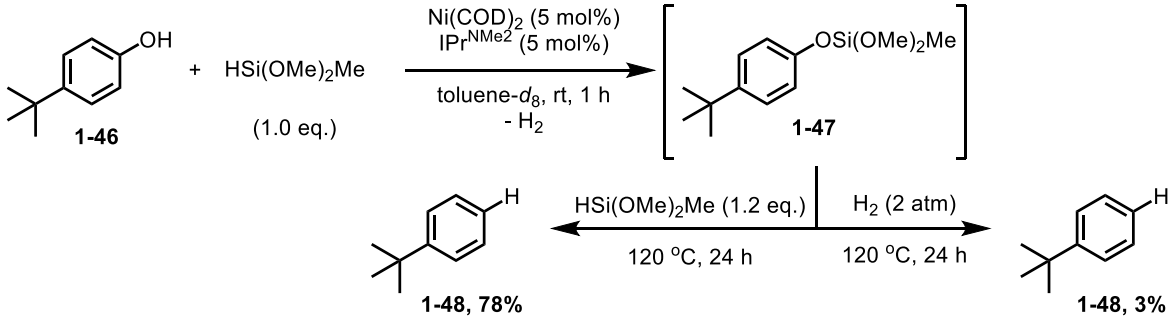

Scheme 1-24. Reductant Control in Hydrogenolysis of Phenols.

Another series of experiments were conducted to support the formation of a silyloxyarene substrate prior to C-O insertion (Table 1-3). Use of trimethylsilyl (TMS) protecting group was used to support the generation of a silyloxyarene, in situ, by starting with a discrete silyloxyarene substrate. The trimethylsilyl protected starting material was found to have analogous reactivity to the in-situ procedure under standard reaction conditions. Notably, there was a significant difference in yield between a biphenyl and *tert*-butyl substituted phenol, with the TMS-protected

tert-butyl phenol resulting in a 45% yield (entry 1, Table 1-3). Furthermore, the analogous phenols were also explored as their methyl ether counterparts, to compare reactivity of their C-O bonds. Lower yields were obtained with the aryl methyl ether derivatives with trace product for the isolated *tert*-butyl phenol derivative and modest yield for biphenyl. These experiments suggest that silyloxyarene C-O bonds have higher reactivity compared to aryl methyl ethers under these reaction conditions, presenting them as attractive coupling partners for late-stage functionalization.

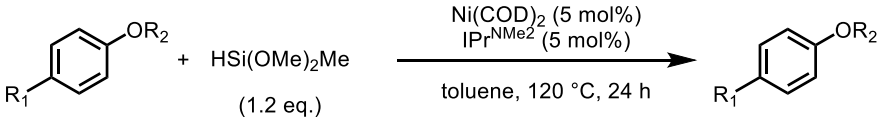

entry	R_1	R_2	yield
1	*t*-Bu	$SiMe_3$	**45%**
2	Ph	$SiMe_3$	**96%**
3	*t*-Bu	Me	**4%**
4	Ph	Me	**46%**

Table 1-3. Hydorgenolysis of Silyoxyarenes and Aryl Methyl Ethers.

1.4 Conclusions on Strategies for Late-Stage Functionalization of C-H and C-X Bonds

There has been substantial interest in the late-stage diversification of complex molecules and in the development of new methods for this efficient approach. An immense amount of effort has been directed towards developing selective C-H functionalization that allow for derivatization of complex scaffolds. However, the field is currently limited to the use of biased substrates or directing groups, limiting the generalizability of current methods.

However, the development of aryl halides as electrophilic coupling partners utilizes a pre-functionalized substrate to generate complex scaffolds without selectivity issues, as coupling occurs exclusively at the site of the halide. Methods using halides are extremely powerful and have revolutionized the synthesis of molecules since their discovery. Yet the desire to utilize an abundant starting material that could be accessed from natural sources has led to the development of alternative methods. One common approach has been the use of phenol derivatives with

activated protecting groups, allowing for the same type of coupling as aryl halides. These pseudohalides have similar reactivity to commonly employed aryl halides. However, halides and pseudohalides do not typically allow for their use in late-stage functionalization unless intermediate protecting group interconversions or activations are utilized.

Therefore, use of less activating protecting groups have been developed to attenuate the stability and reactivity of the C-O bond. Carbonyl-derived protecting groups, such as esters, carboxylates, and carbamates have high reactivity, due to the higher electron-withdrawing nature of the carbonyl and directing ability of the protecting group. However, they are also susceptible to deprotection under basic conditions or through competing transition metal-catalyzed C-O bond activation of the aryl or acyl C-O bond. These features make the carbonyl derivatives less advantageous for use as late-stage coupling surrogates over more other inert C-O bonds.

The aryl ether derivatives are the most inert C-O bond derivatives. Aryl methyl ethers have been the focus of significant research efforts, as they are an inert protecting group, allowing for them to be carried through nearly any organic reaction. However, their high stability results in a very low reactivity of the C-O bond, limiting possible types of coupling reactions and substrates. High reactivity is observed when strong nucleophiles or extended aryl systems are utilized; however, use of milder coupling partners and isolated aromatic systems result in poor yields. Diaryl ethers are also plagued by these limitations, along with limitations for their synthesis.

However, aryl silyl ethers, or silyloxyarenes, have been widely utilized in protecting group chemistry due to their tunable nature. This allows them to be highly stable and carried through numerous synthetic steps. The prevalence of silyl ethers in organic chemistry, and their tunable nature, makes them excellent candidates as electrophilic coupling partners for late-stage functionalization. Until now, silyloxyarenes have not been viewed as competent C-O coupling

partners and have not been explored beyond use in Kumada couplings. Therefore, their C-O bond reactivity has not been explored to determine if they will facilitate improved reactivity over aryl methyl ethers. Determination of silyloxyarene C-O bond reactivity, and subsequent development of useful coupling reactions, would be advantageous for diversification and synthesis of complex molecules.

Chapter 2

Nickel-Catalyzed Reduction and Silylation of Silyloxyarenes

2.1 Introduction on Reduction Reactions of C-O Bonds

Reduction of inert C-O bonds was first explored as a method of using C-O bonds as a traceless directing group. The protected C-O bond would allow for a directed functionalization on the aryl ring and could be removed through C-O bond coupling. Snieckus explored the use of carbamates with Grignard reagents containing β-hydrogens as the reducing agent (Scheme 1-6).[35] The reductive deoxygenation of aryl ether C-O bonds has also been explored for traceless directing group strategies. Martin explored the use of nickel catalysts with silanes as reducing agents for the reduction of aryl methyl ether C-O bonds (Scheme 2-1).[100] However, the lower reactivity of aryl methyl ether C-O bonds limited this method. Use of non-extended aryl systems required a directing group to be installed through ortho-functionalization that could direct the nickel catalyst to the aryl methyl ether C-O bond for activation.

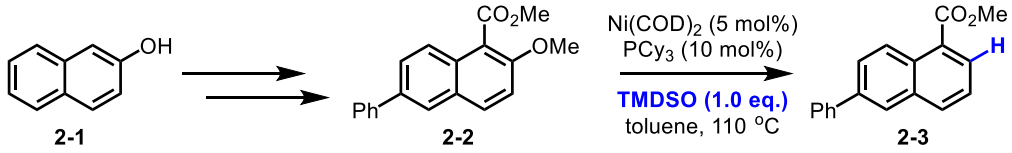

Scheme 2-1. Martin's Nickel-Catalyzed Reduction of Aryl Methyl Ether C-O bonds with Silanes.

Aryl ethers (**2-4**) have also been explored for C-O bond reduction under nickel catalysis. However, instead of applications in directed functionalization the main application has been for depolymerization of lignin. Hartwig described a nickel catalyst facilitated C-O bond reduction of diaryl ethers with silane or hydrogen gas as a reductant (Scheme 2-2).[108] These reductions did

require high catalyst loadings and stoichiometric trimethylaluminum for moderate yields in the reduction of more inert C-O bonds, such as aryl methyl ethers.

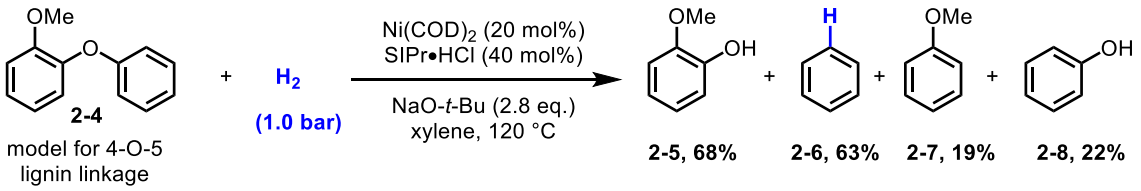

Scheme 2-2. Hartwig's Nickel-Catalyzed C-O Reduction of Diaryl Ethers.

Since these three initial papers in the field of inert C-O reduction, numerous papers have been reported using similar strategies and protecting groups to facilitate reduction of strong C(sp_2)-O bonds. For example, other carbonyl derived protecting groups (**2-9**), such as carbamate[37] and pivalate,[65] were used under nickel catalysis with silanes (Scheme 2-3). Recently, other reducing agents or metals have been used, including sodium formate[66] with pivalate C-O bonds, or alcohols containing β-hydrogens[56] with carbamates and rhodium catalysts.

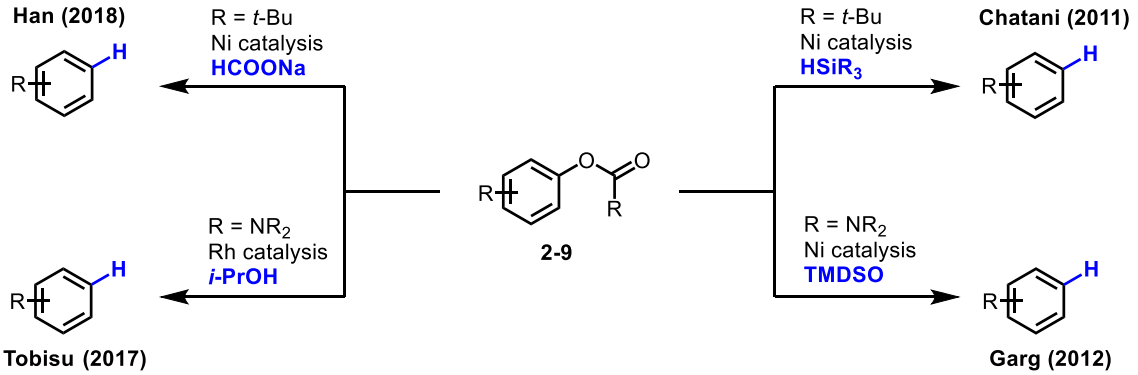

Scheme 2-3. Further Developments in Carbonyl Derivatives C-O Bond Reductions.

In addition to the carbonyl derivatives (**2-9**), several additional methods of aryl ether C-O reduction have been reported (**2-10**, Scheme 2-4). Shortly after Martin's report of aryl methyl ether C-O reduction with silanes, an analogous method was reported with trialkylsilanes.[65] Subsequent reports have focused on utilizing different transition metals or reductants. Iridium has been shown to be competent for aryl methyl ether C-O reductions using a directing group and alcohols

containing β-hydrogens.[134] Nickel can also utilize alcohols containing β-hydrogens as the reducing agent, even using the methoxy group derived from the aryl methyl ether protecting group.[101] Use of diaryl ethers has been further explored in heterogeneous nickel catalysts,[109,110] expanding on the initial report by Hartwig. More activated aryl substituents with directing capabilities have also been explored using homogeneous nickel catalysts and alcohols containing β-hydrogens as a reductant.[120,122]

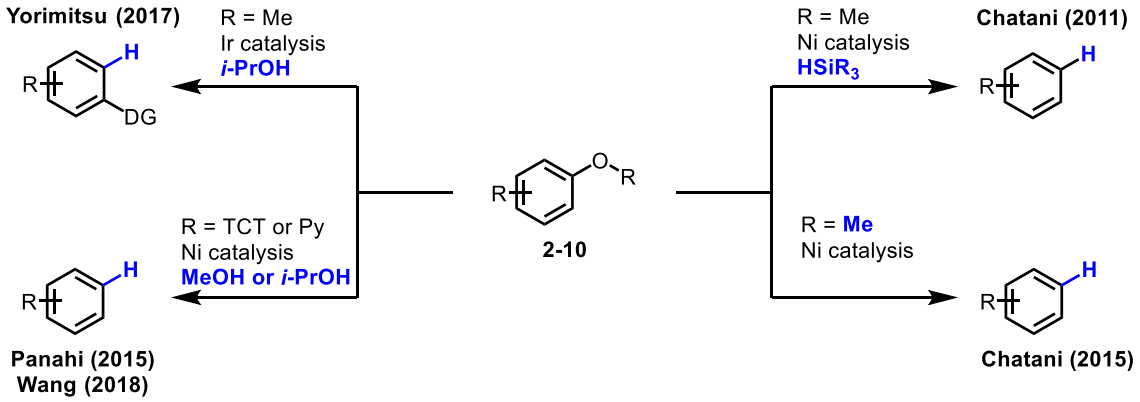

Scheme 2-4. Further Developments in Aryl and Alkyl Ether C-O Bond Reductions.

In addition to the most commonly employed inert aryl C-O bonds, there is one report of using in-situ generated silyloxyarenes as electrophiles for C-O reduction,[163] which was published towards the end of our studies. One key finding in the hydrogenolysis of phenols was the use of electron-rich, bulky NHC ligands (entry 1, Table 2-1). Phosphine ligands (entry 2, Table 2-1) did not result in the desired product (**2-12**). Additionally, other less electron-rich NHC ligands resulted in lower yields, with the least donating ligands resulting in the worst results (entries 3-6, Table 2-1). Use of a NHC salt of the starting ligand also did not result in the desired product, potentially due to the high pKa of electron-rich NHC ligand (entry 7, Table 2-1). Finally, only dimethoxymethylsilane resulted in appreciable yield, with other silanes explored resulted in poor results, including a trialkylsilane, trialkoxysilane, polymeric silane, and another mixed silane (entries 8-11, Table 2-1).

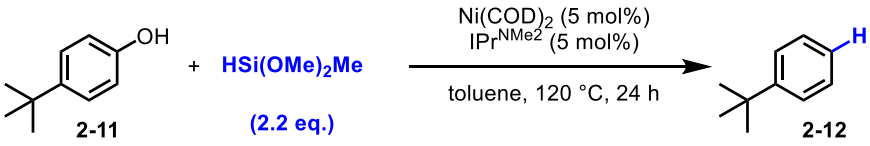

entry	variations	yield[a]
1	-	**88%**
2	PCy_3 (10 mol%)	**<1%**
3	IPr^{Cl}	**<1%**
4	IPr	**4%**
5	IPr^{Me}	**78%**
6	$IPr^{Me}OMe$	**85%**
7	IPr^{NMe2}•HOTf and 0.1 eq. Na(O-*t*-Bu)	**<1%**
8	$HSiEt_3$	**<1%**
9	$HSi(OTMS)_2Me$	**<1%**
10	$HSi(OEt)_3$	**6%**
11	PMHS	**39%**

(a) Yields were determined by GC analysis with undecane as internal standard.

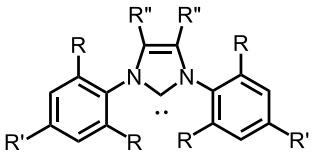

IPr^{NMe2}	R = *i*-Pr, R' = H, R" = NMe_2
IPr^{Cl}	R = *i*-Pr, R' = H, R" = Cl
IPr	R = *i*-Pr, R' = H, R" = H
IPr^{Me}	R = *i*-Pr, R' = H, R" = Me
$IPr^{Me}OMe$	R = *i*-Pr, R' = OMe, R" = Me

Table 2-1. Hydrogenolysis of 4-*tert*-butylphenol.

The phenol scope displayed a small number of substrates, with high yields shown for naphthyl, unhindered biphenyl, and some isolated aromatics (Table 2-2). However, basic functionalities beyond phenols or protected alcohols were not displayed, likely due to competing in-situ protection and consumption of the reductant. Some sterically encumbered and orthogonal functional groups were tolerated, such as ortho phenyl substituents (**2-16**) and silyl-protected benzylic alcohols (**2-17**). Interestingly, for the silyl-protected benzylic alcohol, a less electron-rich ligand, IPr^{Me}, was used. This could suggest that a more electron-rich ligand facilitates benzylic silyl ether C-O bond activation. Most importantly, the method was able to tolerate aryl methyl ethers, as good yields were obtained with ortho (**2-18**) or para (**2-19**) substituted anisole derivatives.

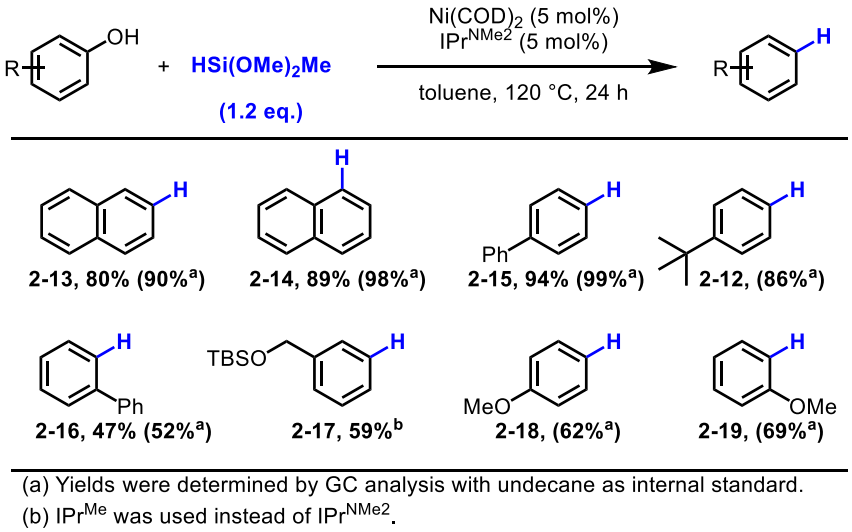

Table 2-2. Arene Scope for Hydrogenolysis of Phenols with Silanes.

The general trends in these inert aryl C-O reductions are that reductants such as silanes or alcohols with β-hydrogens are effective for reductive deoxygenation. Interestingly, in the case of C-O bonds, use of a silane reductant only results in arene product and generation of aryl silanes has not been observed. This is reversal in selectivity has been observed with more activated coupling partners under palladium catalysis.[164] There have been numerous reports for synthesis of aryl silanes using aryl halides and hydrosilanes.[165] However, selectivity between arene and aryl silane is often substrate dependent, based on electronics of the aryl halide[166] or the silane employed. Often electron deficient aryl halides and trialkyl silanes favor formation of the arene product.[164] There have been some reports utilizing trialkyl silanes to favor the aryl silane product,[167] but high ratios are still often limited to specific substrate classes based on electronics of the aryl electrophile (Scheme 2-5).[168]

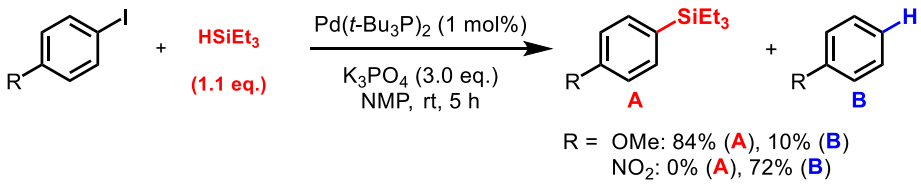

Scheme 2-5. Electronic Influence in Palladium-catalyzed Aryl Halide Silylation with Hydrosilanes.

Just as disilane reagents are commonly utilized for silylation of more activated aryl electrophiles,[169,170] use of silylboranes have been used for silylation of aryl C-O bonds with pivalate[73] or methyl[104] protecting groups. These methods show good functional group tolerance; however, use of silylboranes limits these methods as they are not readily available and need to be synthesized.[171] Therefore, we hoped to explore reactivity of discrete silyloxyarene C-O bonds in reduction reactions for a direct comparison to other inert C-O bonds. Furthermore, as silyloxyarenes have been rarely utilized in coupling reactions, new reactions or selectivities could be discovered that have not been previously reported for other C-O bonds.

2.2 Initial Discovery and Exploration into Reduction of Silyloxyarene C-O Bonds

Studies began by exploring nickel catalysts as they have been the primary transition metal utilized for inert C-O bond activation. NHC ligands were used due to previous group expertise on reversing selectivity based on ligand size.[172] A common triethylsilyl protecting group (**2-20**) was initially explored along with triethylsilane as the reductant. Initially, a mild Lewis acid, titanium isopropoxide, was employed to potentially weaken the C-O bond for coupling (Scheme 2-6). We hypothesized that coordination of the oxygen to titanium could lower the barrier of C-O bond activation and improve reactivity, as has been shown with related aryl and alkyl ether derivatives.[128]

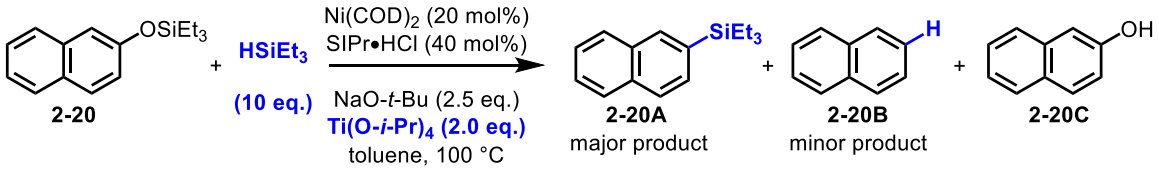

Scheme 2-6. Initial Exploration into Nickel-Catalyzed C-O Reductions of Silyloxyarenes.

Very excitingly, naphthalene (**2-20A**) was observed under these reaction conditions. However, naphthalene was the minor product and an unexpected aryl silane product **2-20B** was observed as the major product. This result was very interesting as all previous reports of utilizing

silanes as reductants with inert aryl C-O bonds exclusively yielded the reduced arene. Furthermore, access to aryl silanes from inert C-O bonds have only been shown from silylboranes and methods using commercially available silanes would be advantageous. Therefore, we explored the optimization of this reaction to obtain selectivity over the two reactions while exploring reactivity of the silyloxyarene C-O bond.

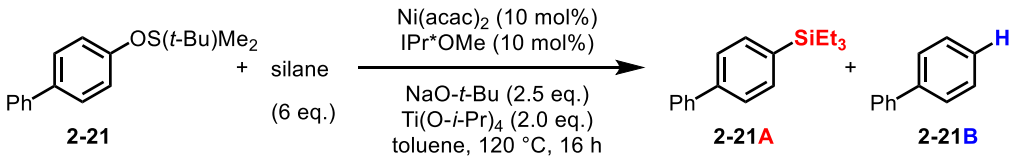

entry	variations	$HSiEt_3$ (A, A:B)[a]	$HSi(i\text{-}Pr)_3$ (B)[a]
1	-	**86%, 91:9**	**74%**
2	IPr for IPr*OMe	**38%, 70:30**	**64%**
3	IMes for IPr*OMe	**16%, 29:71**	**7%**
4	PCy_3 for IPr*OMe	**NR**	**NR**
5	KO-*t*-Bu for NaO-*t*-Bu	**NR**	**25%**
6	LiO-*t*-Bu for NaO-*t*-Bu	**2%**	**49%**
7	NaO-*i*-Pr for NaO-*t*-Bu	**NR, 7% B**	**NR**
8	1.5 eq. NaO-*t*-Bu	**7%**	**63%**
9	$Ni(COD)_2$ for $Ni(acac)_2$	**71%, 86:14**	**88%**
10	$OSiEt_3$ for $OS(t\text{-}Bu)Me_2$	**59%, 88:12**	**40%**

(a) Yields and ratios were determined by GCFID with decane as an internal standard.

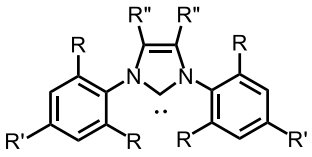

IMes R = Me, R' = Me, R" = H
IPr R = *i*-Pr, R' = H, R" = H
IPr*OMe R = $CHPh_2$, R' = OMe, R = H

Table 2-3. Initial Optimization of Nickel-Catalyzed C-O Reduction and Silylation of Silyloxyarenes.

Further optimization of the silylation and reduction reaction began with ([1,1'-biphenyl]-4-yloxy)(*tert*-butyl)dimethylsilane (**2-21**) as the model substrate (Table 2-3). This substrate was explored to optimize around a more challenging isolated aryl substrate where successful optimization would allow for coupling of these more challenging substrates and present higher reactivity over other inert C-O bond couplings. A larger silane protecting group was also used to decrease deprotection observed with the triethylsilyl group. Furthermore, a large silane, *tert*-

butyldimethylsilane, is more commonly used as a protecting group in organic synthesis. Development of C-O bond coupling methods of these derivatives would allow for direct coupling of a commonly used functionality.

Optimization of the reduction and silylation reactions uncovered divergent reactivity that appeared to derive from the silane. Larger trialkylsilane, such as triisopropylsilane, gave the reduction product (**2-21B**) and none of the corresponding silylation product. A large influence was also observed based on the ligand with small, aryl NHC ligands resulting in poor ratios. Small trialkylsilanes, such as triethylsilane, and large NHC ligands resulted in ratios of silylation (**2-21A**) over reduction (Table 2-3, Entries 1-3). Other common ligands, such as phosphines and alkyl NHC ligands did not result in the desired product (Table 2-3, Entry 4). An extremely bulky aryl NHC ligand, IPr*OMe, resulted in the best results for both reactions, with high yields and ratios of products.

Other bases were explored, with sodium *tert*-butoxide being uniquely effective for silylation, where other counterions resulting in poor yields (Table 2-3, Entries 5-6). Interestingly, base effects were less significant for the reduction reaction with triisopropylsilane. Sodium isoproxide did not work for silylation, and utilizing it as both the base and/or reductant did not work for the reduction reaction (Table 2-3, Entry 7). Fewer equivalents of base could be used, although lower yields were observed for both reactions (Table 2-3, Entry 8). Although higher yields were observed when using bis(1,5-cyclooctadiene)nickel(0) as a pre-catalyst in the reduction reaction with triisopropylsilane, lower yields were obtained for silylation (Table 2-3, Entry 9). However, due to the advantages of nickel(II) acetylacetonate, such as cost and air stability, it was used as the optimal nickel pre-catalyst. Finally, lower yields were observed in both

reactions when looking at triethylsilane as the protecting group due to deprotection (Table 2-3, Entry 10).

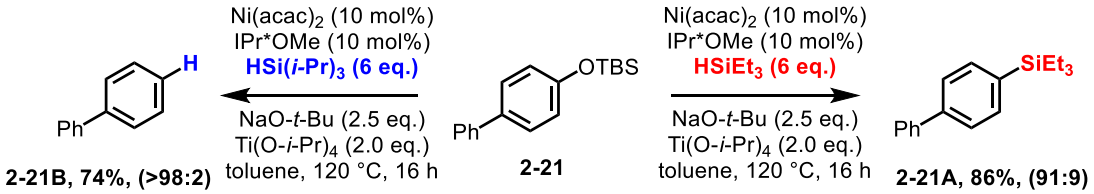

Scheme 2-7. Divergent Reduction Reactions with Silane Reductants.

Two novel reactions were developed where selectivity was observed based on silane choice, where small trialkylsilanes resulted in aryl silylation and large trialkylsilanes resulted in arenes (Scheme 2-7). Due to the large influence in silane identity, the silane scope was explored (Table 2-4). Small, trialkylsilanes resulted in the best yields and ratios, with small amounts of arene product observed for diethylmethylsilane (Table 2-4, entry 3) and ethyldimethylsilane (Table 2-4, entry 4). As mentioned previously, large trialkylsilanes do not result in any of the aryl silane product and arene is exclusively observed (Table 2-4, entry 2). Moving to larger alkyl substituents, tripropylsilane (Table 2-4, entry 5) gives larger amounts of arene product. The influence of steric hindrance of the silane can be observed by moving through the *tert*-butyldimethylsilane (Table 2-4, entry 6), di(*tert*-butyl)methylsilane (Table 2-4, entry 7), and tri(*tert*-butyl)silane (Table 2-4, entry 8) series. This series shows that the arene product is increasingly favored with larger substituents, and eventually reactivity decreases with no silylation product being observed. Other large silanes, such as triisobutylsilane (Table 2-4, entry 9) and di(*tert*-butyl)silane (Table 2-4, entry 10) result in low yields and exclusively generate the arene product. This method was limited to trialkylsilanes, as several alkoxysilanes did not result in the desired products. Although this was disappointing due to limited application of trialkylarylsilanes in Hiyama-Denmark couplings,[173,174] benzyldimethylsilane (Table 2-4, entry 11) could be used as a silane coupling partner.

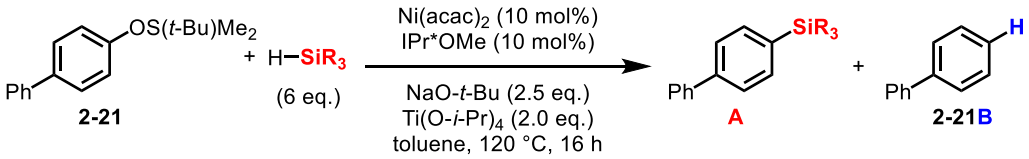

entry	H-SiR$_3$	yield A	yield 2-21B
1	HSiEt$_3$	81%	3%
2	Si(*i*-Pr)$_3$	0%	74%
3	SiEt$_2$Me	82%	6%
4	SiEtMe$_2$	71%	9%
5	Si(*n*-Pr)$_3$	70%	18%
6	Si(*t*-Bu)Me$_2$	29%	71%
7	Si(*t*-Bu)$_2$Me	0%	53%
8	Si(*t*-Bu)$_3$	0%	38%
9	Si(*i*-Bu)$_3$	0%	23%
10[a]	Si(*t*-Bu)$_2$H	0%	42%
11[a]	SiBnMe$_2$	45%	21%

(a) Yields and ratios were determined by GCFID with decane as an internal standard.

Table 2-4. Silane Scope for Divergent Silylation/Reduction Reactions.

Having explored trends in the silane utilized for silylation and reduction reactions, the silyloxyarene scope was next explored (Table 2-5). A range of naphthyl substrates were all coupled in good yield for both reactions, including naphthyl rings containing two silyloxy groups (**2-22**), other silane functionality (**2-23**), and a methoxy group (**2-24**). However, when using the disilyloxy naphthyl substrate (**2-22**), silylation only occurred at the 6-position and the 1-position remained untouched. This noted high sensitivity to sterics in the silylation reaction, which was not the case for the reduction reaction as both silyloxy groups were reduced. The ability to tolerate a methoxy group was exciting as it allowed for further functionalization.

Next, we began exploring other functional groups that could be tolerated, and further explored C-O bond reactivity by utilizing isolated aromatic systems. Biphenyl substrates containing unprotected alcohols (**2-25**), benzyl silyl ethers (**2-26**), and methyl ethers (**2-27**) were all tolerated for both reactions. Heterocycles could also be utilized, with carbazoles (**2-28**) and pyridines (**2-29**) resulting in good yields. Interestingly, benzylic silyl ethers resulted in good yield for silylation of the aryl C-O bond, with the benzylic C-O bond untouched. However, the reduction

reaction product could not be quantified as the proposed product was also the solvent for the reaction.

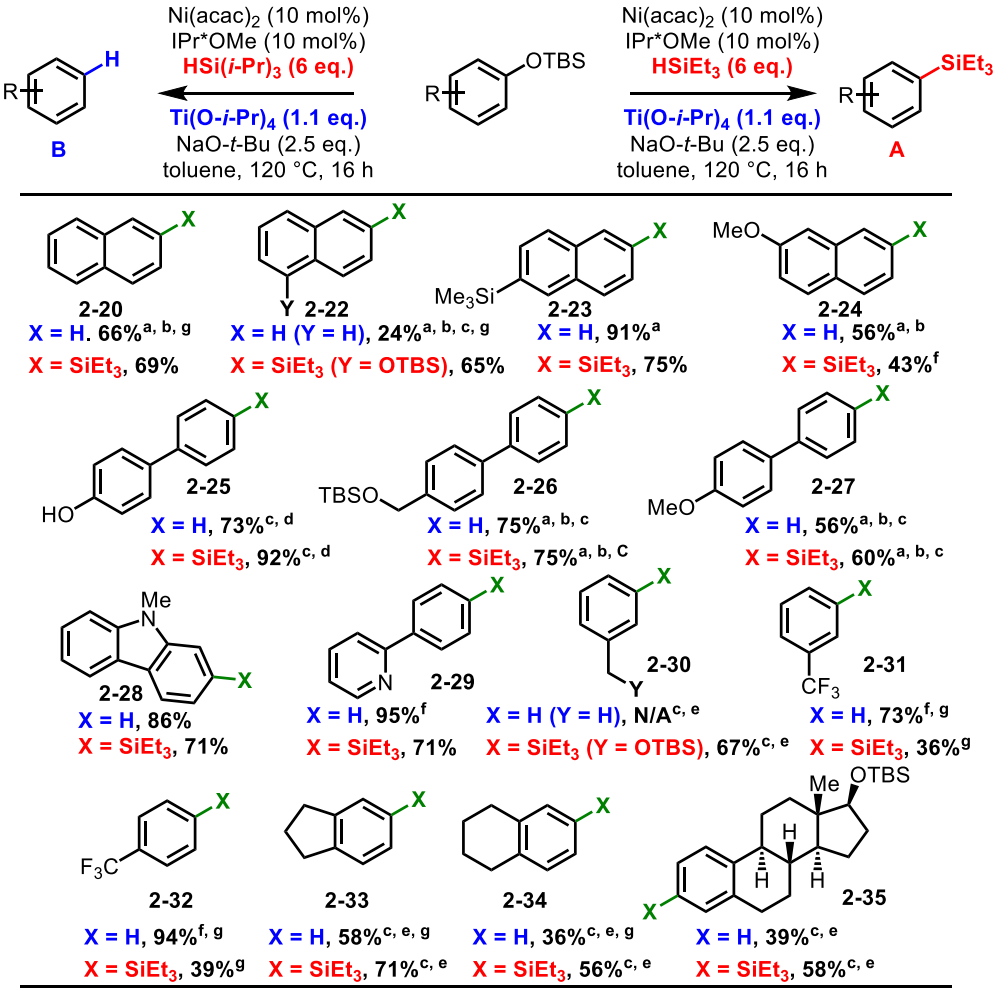

(a) Reaction run at 100 °C. (b) Reaction run for 8 hours. (c) Reaction run using 25 mol% $Ni(acac)_2$ and IPr*OMe. (d) Reaction run using 3 equivalents of $Ti(O^iPr)_4$. (e) Reaction run at 130 °C for 24 hours. (f) Reaction run for 5 hours. (g) Yield determined by GCFID with decane as standard. (h) Yield determined by GCFID with tridecane as standard.

Table 2-5. Silyloxyarene Scope for Divergent Silylation/Reduction Reactions.

Use of other isolated aromatic systems resulted in good yields, in contrast to current methods for aryl methyl ether activation. Electron-withdrawing substituents in the para or meta positions gave good yields for reduction, although yields for silylation were lower. However, with more electron-rich isolated aromatic systems, the opposite trend appears with high yields observed for silylation and lower yields for reduction. Thus, these two reactions appeared to have opposite influences from electronics on the aryl system, suggesting different mechanisms could be operable.

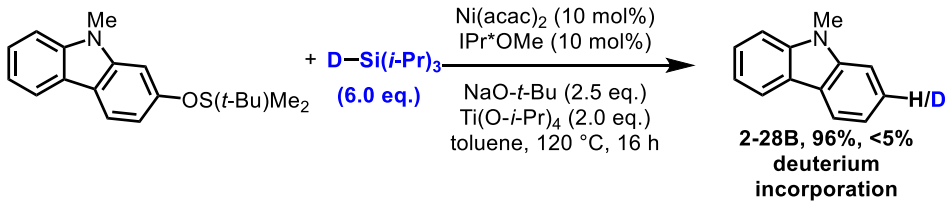

Scheme 2-8. Deuterium Labeling Experiment with Deuterated Triisopropylsilane.

We first started exploring the mechanism further by utilizing a deuterated triisopropylsilane to determine the reductant for the reaction. However, low deuterium incorporation was observed when using deuterated triisopropylsilane (Scheme 2-8). This led to a series of control experiments to further explore the role of each component in these reactions.

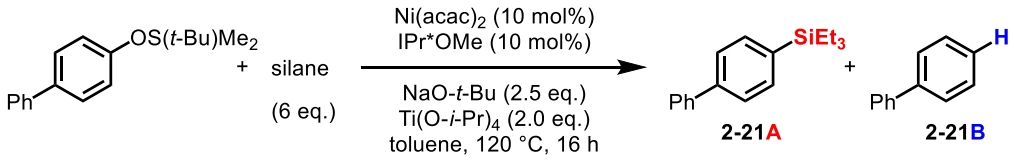

entry	variations	$HSiEt_3$ (A, A:B)[a]	$HSi(i\text{-}Pr)_3$ (B)[a]
1	-	**86%, 91:9**	**74%**
2	No $Ni(acac)_2$	**NR**	**NR**
3	No Ligand	**NR**	**NR**
4	No Base	**NR**	**NR**
5	No silane	**-**	**NR**
6	$Ni(COD)_2$, no silane	**-**	**14%**
7	No $Ti(O\text{-}i\text{-}Pr)_4$	**76%, 86:14**	**NR**

a) Yields and ratios were determined by GCFID with decane as an internal standard.

Table 2-6. Controls for Divergent Silylation/Reduction Reactions.

Both reactions showed no reactivity in the absence of nickel pre-catalyst, ligand, base, or silane (Table 2-6, Entries 2-5). However, when using a nickel(0) pre-catalyst, where reduction to the active nickel(0) is not necessary, exclusion of silane still resulted in reduction product. This led us to believe that silane was not necessary in the reduction reaction and that titanium isopropoxide was the reductant. Running the standard reaction conditions with triisopropylsilane and without titanium isopropoxide gave none of the arene product (Table 2-6, Entry 7). Titanium isopropoxide could have two roles as reductant and Lewis acid, which could be the reason for no

observed reactivity. However, this theory was refuted when only slightly lower yields were observed for silylation without titanium isopropoxide, showing titanium was not necessary for silylation.

2.3 C-O Bond Reduction of Silyloxyarenes under Nickel Catalysis with Titanium Reductants

When synthesizing a deuterated titanium isopropoxide and subjecting it to the reaction conditions without silane, high deuterium incorporation was observed (Scheme 2-9). However, when using both triisopropylsilane and deuterated titanium isopropoxide, deuterium incorporation was much lower (Scheme 2-10).

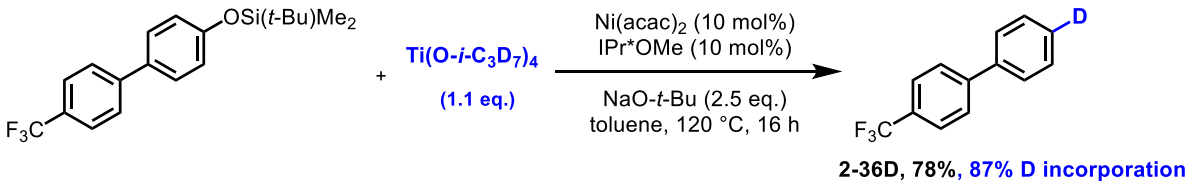

Scheme 2-9. Deuterium Labeling Experiment with Deuterated Titanium Isopropoxide Without Silane.

The lower deuterium incorporation when using silane and deuterated titanium isopropoxide suggests that there could be a synergistic influence when both are included in the reaction mixture, or that scrambling of a nickel hydride could be taking place prior to reductive elimination. To simplify the reaction and utilize exclusively titanium isopropoxide as reductant in C-O bond activation, further optimization was necessary as low yields were observed under previous conditions while excluding triisopropylsilane (Table 2-6, entries 5-6).

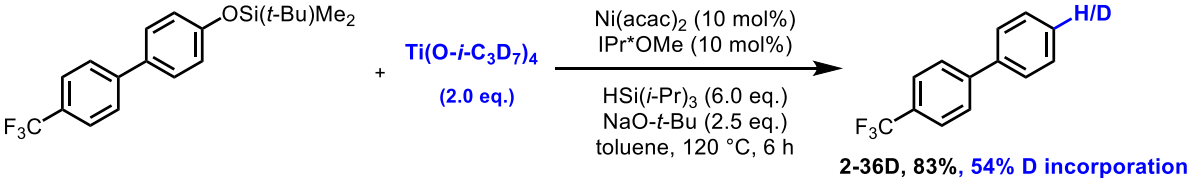

Scheme 2-10. Deuterium labeling of Reduction with Triisopropylsilane and Deuterated Titanium Isopropoxide.

2.3.1 Optimization for C-O Bond Reduction of Silyloxyarenes

Additional optimization found that comparable yields to the previous conditions could be obtained by using fewer equivalents of titanium isopropoxide, 2:1 ratio of nickel pre-catalyst to ligand, and shorter reaction times (Table 2-7, Entry 1). However, a different ligand, IPr^{Me}, resulted in superior results over the previous ligand (Table 2-7, Entry 2). The importance of the donating ability of the NHC ligand can be observed by looking at the IPr series from the most donating to least donating (IPr^{Me}, IPr, IPr^{Cl}). This comparison shows that more donating ligands result in higher yields (Table 2-7, entries 2-4). Other common phosphine ligands used for C-O bond activation, such as tricyclohexylphosphine, did not result in product formation (Table 2-7, entry 6). Other nickel pre-catalysts or reductants could be used, although lower yields were observed (Table 2-7, entries 7-9). Sodium isopropoxide was again explored as base and/or reductant but did not result in any product (Table 2-7, entries 10-11). Finally, because the reaction utilizes a nickel(II) pre-catalyst, the reaction does not require the use of a glovebox and can be set up on the benchtop (Table 2-7, entry 12).

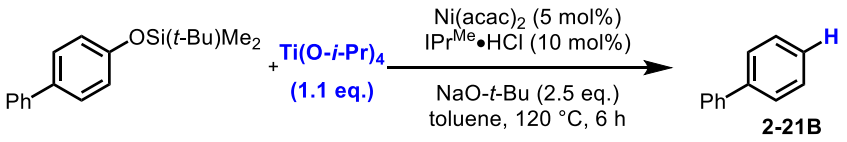

entry	variations	yields[a]
1	IPr*OMe•HCl for IPr^{Me}•HCl	**80%**
2	-	**94% (80%)**
3	IPr•HCl for IPr^{Me}•HCl	**72%**
4	IPr^{Cl}•HCl for IPr^{Me}•HCl	**49%**
5	IMes•HCl for IPr^{Me}•HCl	**16%**
6	PCy_3 for IPr^{Me}•HCl	**NP**
7	$Ni(COD)_2$ for $Ni(acac)_2$	**81%**
8	$Ti(OMe)_4$ for $Ti(O\text{-}i\text{-}Pr)_4$	**4%**
9	$Al(O\text{-}i\text{-}Pr)_3$ for $Ti(O\text{-}i\text{-}Pr)_4$	**55%**
10	NaO-*i*-Pr for NaO-*t*-Bu	**NP**
11	NaO-*i*-Pr for $Ti(O\text{-}i\text{-}Pr)_4$	**NP**
12	benchtop setup	**86%**

(a) Yields were determined by GCFID with tridecane as internal standard, isolated yields in parantheses.

Table 2-7. Optimization for Nickel-Catalyzed C-O Bond Reduction with Titanium Isopropoxide.

The aryl electrophile was further explored to compare and investigate silyloxyarene reactivity alongside other common aryl electrophiles (Table 2-8). Several different silane protecting groups were utilized, and for the reduction reaction with titanium isopropoxide, most large silane protecting groups work well (Table 2-8, entries 1-3). Smaller silane protecting groups, such as triethylsilane, give lower yields due to increased amounts of deprotection under the reaction conditions (Table 2-8, entry 4). Diaryl ethers gave slightly lower yields than the larger silane protecting groups, but other common aryl C-O electrophiles did not give good yields, with aryl methyl ethers, aryl pivalates, aryl triflate all resulting in poor yields (Table 2-8, entries 5-8). Finally, aryl bromides can be utilized but result in slightly lower yields than the silyloxyarene derivatives (Table 2-8, entry 9).

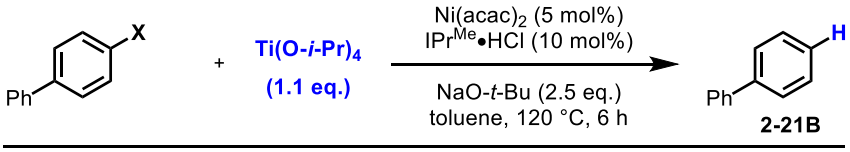

entry	X	yield[a]
1	OSi(*t*-Bu)Ph_2	**76%**
2	OSi(*i*-Pr)$_3$	**90%**
3	OSi(*t*-Bu)Me_2	**94%**
4	$OSiEt_3$	**49%**
5	OPh	**78%**
6	OMe	**16%**
7	OPiv	**trace**
8	OTf	**2%**
9	Br	**70%**

(a) Yields were determined by GCFID with tridecane as internal standard.

Table 2-8. Protecting Group Screen in Nickel-Catalyzed Reduction of C-O Bonds with Titanium Isopropoxide.

2.3.2 Substrate Scope for C-O Bond Reduction of Silyloxyarenes

Having found optimized conditions for the model substrate, the scope of the silyloxyarene was next explored (Table 2-9). Simple naphthyl substrates all gave good yields, including more sterically hindered *tert*-butyldimethyl(naphthalen-1-yloxy)silane (**2-37B**) and naphthyl substrates with silane functionality (**2-23B**). High reactivity was maintained moving from naphthyl to

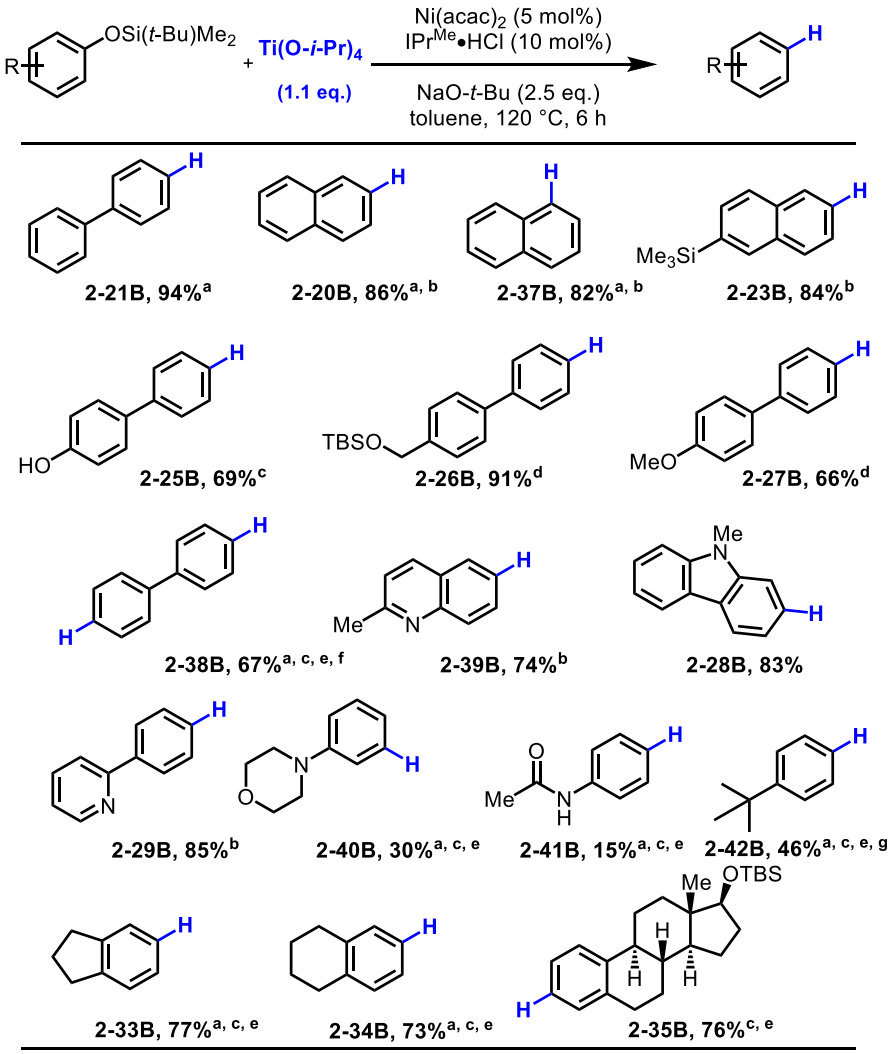

(a) Yield determined by GCFID with tridecane as internal standard. (b) Reaction run for 3 hours.
(c) Reaction run using 10 mol% $Ni(acac)_2$, 20 mol% IPr^{Me}•HCl, 4 eq. NaO-*t*-Bu for 16 hours.
(d) Reaction run for 16 hours. (e) Reaction run at 130 °C.
(f) Reaction run using 2.2 eq. $Ti(O\text{-}i\text{-}Pr)_4$. (g) Reaction run using $Ni(COD)_2$.

Table 2-9. Silyloxyarene Scope for Nickel-Catalyzed C-O Bond Reduction with Titanium Isopropoxide.

biphenyl, where several other functional groups were tolerated, including unprotected hydroxyls (**2-25B**), benzylic silyl ethers (**2-26B**), and aryl methyl ethers (**2-27B**). Double reduction was achieved in good yield with a disilyloxy substrate (**2-38B**). Several heterocycles were utilized and resulted in good yields, including quinoline (**2-39B**), carbazole (**2-28B**), and pyridines (**2-29B**). Very electron rich, isolated aromatics were coupled including 4-(3-((*tert*-butyldimethylsilyl)oxy)phenyl)morpholine (**2-40B**) and an acetaminophen derivative **2-41B**. Although yields were much lower for these substrates, the reactivity is high compared to aryl

methyl ethers, and a more thorough substrate-by-substrate optimization might be necessary for these lower yielding examples. However, slightly less electron rich isolated aromatic systems gave good yields, including an estradiol derivative (**2-35B**).

2.3.3 Mechanism for C-O Bond Reduction of Silyloxyarenes

Deuterium labeling studies were again conducted using the new reaction conditions and a deuterated titanium isopropoxide that was synthesized from titanium isopropoxide and deuterated isopropanol. High deuterium labeling was observed under the new reaction conditions using IPr^{Me} as ligand and $Ni(COD)_2$ as pre-catalysts (Scheme 2-11). This again confirmed that titanium isopropoxide was the reductant in our developed methodology.

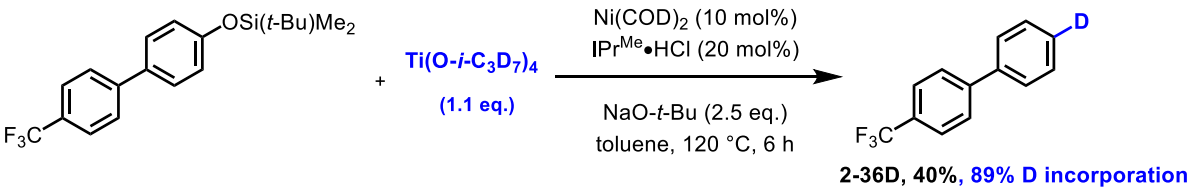

Scheme 2-11. Deuterium Labeling for C-O Bond Reduction of Silyloxyarenes under Nickel Catalysis with Titanium Isopropoxide.

Although no detailed mechanistic experiments have been conducted to fully elucidate the mechanism, a mechanistic proposal has been developed (Scheme 2-12). The proposed mechanism is based on deuterium labeling studies, empirical findings discovered through development of the methods, and computations from previously reported mechanisms of other inert C-O bonds. The catalytic cycle begins with generation of $Ni(IPr^{Me})_2$ from the nickel(II) pre-catalyst, IPr^{Me} ligand, and titanium isopropoxide. Displacement of one NHC ligand with *tert*-butoxide results in complex **A**, which then coordinates to the silyloxyarene substrate, through η^2 binding. The resulting complex (**B**) inserts into the silyloxyarene C-O bond and dissociates the silyloxy group to generate a neutral complex (**C**). The tri-substituted complex (**C**) undergoes a six-membered transition state to transfer a β-hydrogen from an isopropoxy group from titanium isopropoxide to nickel (**D**),

producing acetone and nickel hydride **E**. Finally, reductive elimination and association of sodium *tert*-butoxide completes the catalytic cycle and generates the desired product.

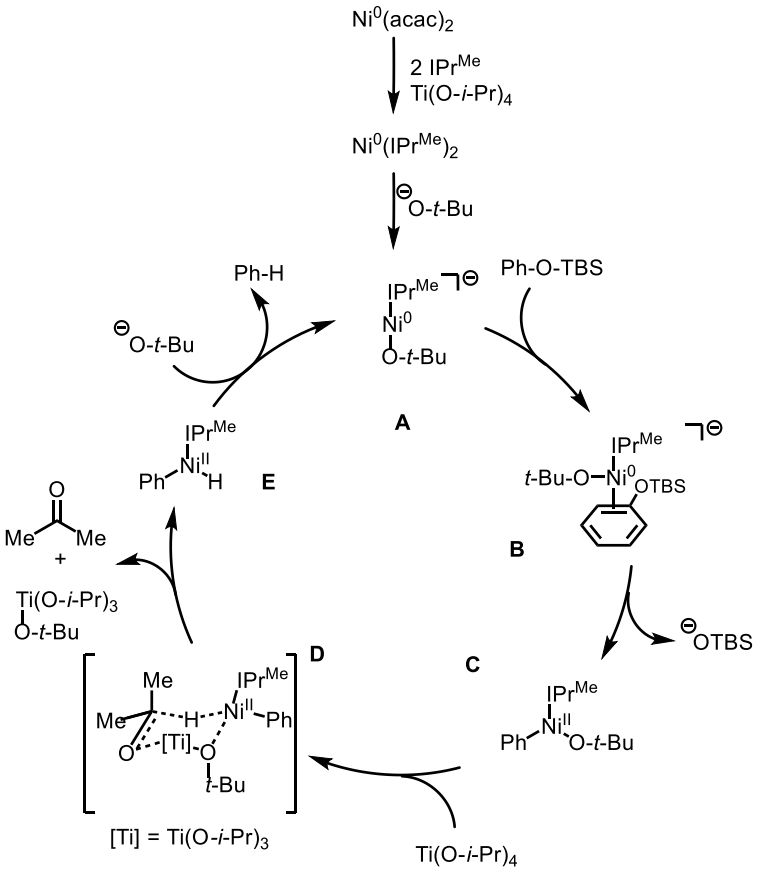

Scheme 2-12. Proposed Mechanism for Nickel-Catalyzed C-O Bond Reduction of Silyloxyarenes with Titanium Isopropoxide.

Many empirical results and reported computational studies on related C-O bond coupling reactions support the proposed mechanism for C-O bond reduction of silyloxyarenes. While interpreting the experimental data, it was noted that two equivalents of NHC ligand result in significantly higher yields than with one equivalent of NHC ligand. This is likely due to the stabilization of the nickel catalyst throughout the reaction, where another NHC ligand stabilizes highly reactive intermediates, preventing catalyst decompositions through comproportionation, and other unproductive pathways. Additionally, previous computational studies on related C-O bond activations using IPr ligands propose $Ni(IPr^{Me})_2$ and $Ni(IPr^{Me})(L_n)$ exist in equilibrium in

solution, with Ni(IPr^{Me})$_2$ typically being proposed to be more thermodynamically stable.[147] Furthermore, Ni(IPr^{Me})$_2$ was synthesized and shown to be competent under the reaction conditions (Table 2-10).

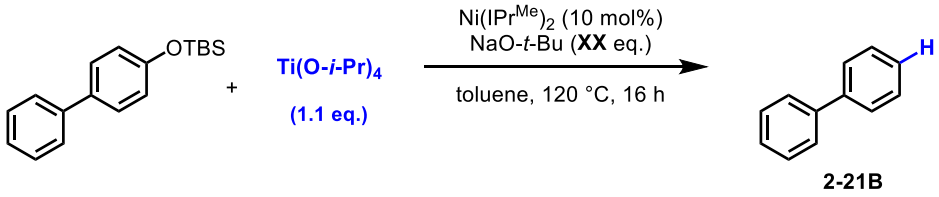

entry	NaO-*t*-Bu equivalents	yield[a]
1	0 eq. NaO-*t*-Bu	**60%**
2	0.25 eq. NaO-*t*-Bu	**65%**
3	2.5 eq. NaO-*t*-Bu	**64%**

(a) Yields were determined by GC-FID with tridecane as internal standard.

Table 2-10 Diligated Nickel-NHC Complex in Reductive Deoxygenation of Silyloxyarene C-O Bonds.

One of the possible ligands in equilibrium with the second IPr^{Me} ligand is proposed to be sodium *tert*-butoxide, which has been supported by literature precedent.[146] Another species in equilibrium is the silyloxyarene, where association through η-coordination is again supported by literature precedent in related reactions.[147] Often, η^2 is proposed to be the penultimate intermediate for C-O bond activation and is important for insertion into the C-O bond. Previous computations have shown that η^2 and η^6 coordination are very close in energy and help stabilize the complex.[148] The importance of coordination explains the small difference in reactivity between naphthyl, biphenyl, and isolated aromatics, as the more conjugated aryl systems would have more favorable coordination to the nickel(0) catalyst.[148] Furthermore, use of electron-withdrawing groups also supports this proposal as increased yields are observed with electron-deficient silyloxyarene substrates, where a more favorable η^2 coordination has also been shown computationally.[147] However, this increased reactivity could also involve a lower barrier to oxidative addition due to a weaker C-O bond with electron-deficient silyloxyarene substrates.

Oxidative addition to the silyloxyarene C-O bond is proposed to undergo a 3-centered, 2-electron transition state, which is typically proposed for oxidative addition to inert C-O bonds with nickel-NHC complexes.[111,146–148] Use of a titanium Lewis acid could also result in coordination to the silyloxyarene C-O bond, weakening the bond and facilitating oxidative addition. Improved reactivity for aryl methyl ether C-O bond has been widely shown with several Lewis acids, such as magnesium salts and trimethylaluminum.[128] However, due to the size of titanium isopropoxide and *tert*-butyldimethylsilane this interaction would likely be very small or non-existent.

Alternate pathways have also been explored in reported computational papers where coordination of *tert*-butoxide base to the nickel(0) pre-catalyst is not proposed.[146] This pathway is also possible in the reductive deoxygenation of silyloxyarene C-O bonds with titanium isopropoxide. However, due to the excess amounts of base and higher computed[146] transition state energy for oxidative addition without a nickelate, this is unlikely unless the presence of titanium isopropoxide and the silyloxy group results in significant changes of the energy barriers.

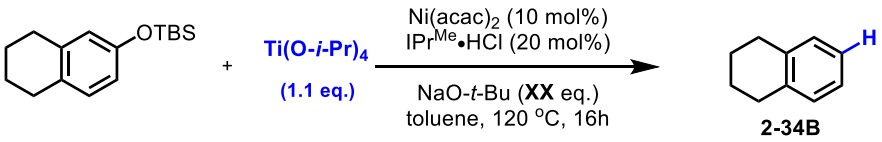

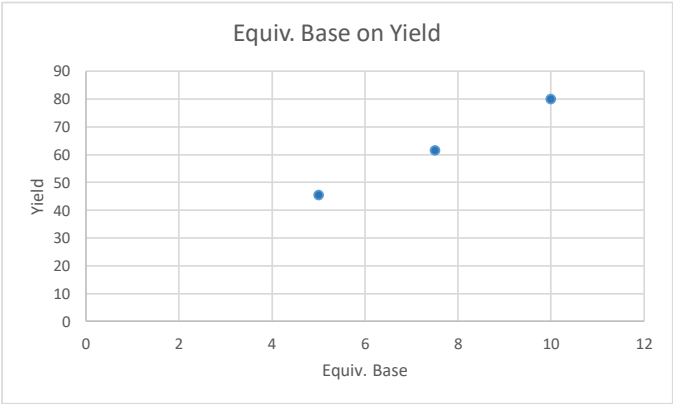

Table 2-11 Influence of Equivalents of Base on Yield for Reductive Deoxygenation of Silyloxyarenes.

There are two conflicting empirical results on how the importance of sodium *tert*-butoxide on the reductive deoxygenation reaction. First, in experiments using a discrete nickel(0)-NHC complex (Table 2-10**)**, base is not required for the reaction and does not have an influence on the yield. However, when using our standard reaction conditions for in-situ generation of the catalyst, higher amounts of base result in higher yields (Table 2-11). These finding are complicated using titanium isopropoxide due to the presence of isopropoxide in these reactions. Instead of *tert*-butoxide, isopropoxide or the silyloxy group could generate a nickelate. Furthermore, excess base is likely interacting with titanium isopropoxide in addition to the nickel catalyst. Other roles of base have also been proposed, including shifting the equilibrium from the $Ni(IPr^{Me})_2$ complex[148] or limiting off-cycle intermediates.[111]

2.4 C-O Bond Silylation of Silyloxyarenes under Nickel Catalysis with Silanes

Having found judicious choice of silane resulted in two very different reaction manifolds, and that titanium isopropoxide was not necessary for the silylation reaction, further optimization was necessary without titanium isopropoxide.

2.4.1 Optimization for C-O Bond Silylation of Silyloxyarenes

Unlike the reduction reaction, yields were found to be lower when using nickel(II) acetylacetonate as pre-catalyst without titanium isopropoxide. However, moving to bis(1,5-cyclooctadiene)nickel(0) resulted in a good yield (Table 2-12, entry 1). The decrease in reactivity is likely slower reduction of the nickel(II) pre-catalyst to the active nickel(0) catalyst in the absence of titanium isopropoxide. An increase in the ratio of silylation product to reduction product was observed, where only trace amounts of the arene product were observed, due to the absence of titanium isopropoxide. Having obtained an improved yield and ratio of products, a quick ligand screen again showed that the extremely bulky IPr*OMe ligand was uniquely effective in this

silylation reaction. Other large NHC ligands, such as IPr derivative, resulted in significantly lower yields and worse ratios of products (Table 2-12, entries 2-3). A smaller aryl NHC ligand also gave a lower yield and the opposite ratio of products, favoring the reduction product (Table 2-12, entry 4). Common phosphine ligands for C-O activation again did not result in any of the desired product (Table 2-12, entry 5). Finally, lowering equivalents of base and silane was found to be detrimental to the reaction, resulting in modest yields and lower ratios of products (Table 2-12, entries 7-9).

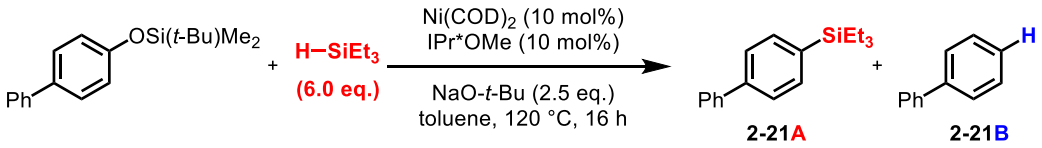

entry	variations	yields (A, B)[a]
1	-	**97% (91%), 1%**
2	IPr^{Me} for IPr*OMe	**18%, 5%**
3	IPr for IPr*OMe	**20%, 2%**
4	IMes for IPr*OMe	**10%, 14%**
5	PCy_3 for IPr*OMe	**NP**
7	1.5 eq. NaO-*t*-Bu	**47%, 1%**
8	3 eq. $HSiEt_3$	**74%, 3%**
9	1.5 eq. $HSiEt_3$	**68%, 16%**

(a) Yields were determined by GCFID with tridecane as internal standard, isolated yields in parantheses.

Table 2-12. Optimization of Nickel-Catalyzed C-O Bond Silylation of Silyloxyarenes.

The electrophile scope was also explored to determine whether this unique reactivity was limited to silyloxyarenes, or if other common aryl electrophiles could be utilized. A range of different silane protecting groups were explored. Large, sterically hindered silane protecting groups resulted in lower yields due to low conversion (Table 2-13, entries 1-2). Deprotection of the silyl group was not a problem, and smaller silane protecting groups, such as triethylsilane, gave similar results to *tert*-butyldimethylsilane (Table 2-13, entries 3-5). In general, other common aryl electrophiles resulted in poor yeilds and silyloxyarenes were uniquely effective for the reaction. Diaryl ethers gave the most similar results to the silyloxyarene derivatives with the aryl silane product being favored, although the yield and ratio of products was lower (Table 2-13, entry 6).

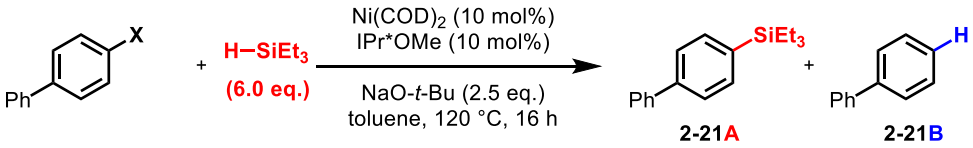

entry	X	yields (A, B)[a]
1	OSi(*t*-Bu)Ph_2	**34%, 1%**
2	OSi(*i*-Pr)$_3$	**32%, 2%**
3	OSi(*t*-Bu)Me_2	**97%, 1%**
4	OSiEt_3	**90%, 1%**
5	OTMS	**40%, 6%**
6	OPh	**42%, 8%**
7	OMe	**1%, 37%**
8	OPiv	**3%, 4%**
9	OTf	**25%, 25%**
10	Br	**5%, 44%**

(a) Yields were determined by GCFID with tridecane as internal standard.

Table 2-13. Electrophile Scope for Nickel-Catalyzed Silylation of Silyloxyarenes.

Interestingly, aryl methyl ethers resulted in low conversion and gave the opposite selectivity with only trace silylation product observed (Table 2-13, entry 7). This notes that simply changing the size of the electrophile completely switches the selectivity of the reaction. Further demonstration for the influence of the protecting group can be observed moving to a trimethylsilyl protecting group, where a larger ratio of biphenyl is observed. Although reversal in selectivity for aryl methyl ethers was unexpected, C-O bond reduction of aryl methyl ethers under nickel catalysis with silanes has been reported before.[100,65,151] This difference in reactivity for accessing the aryl silane instead of arene again showcases the new and unique reactivity discovered. More activated C-O electrophiles, such as pivalates or triflates, were unselective and resulted in poor yields due to deprotection (Table 2-13, entries 8-9). Aryl bromides gave similar results to aryl methyl ethers, with lower yields and the major product being arene with only small amounts of the aryl silane observed (Table 2-13, entry 10).

2.4.2 Substrate Scope for C-O Bond Silylation of Silyloxyarenes

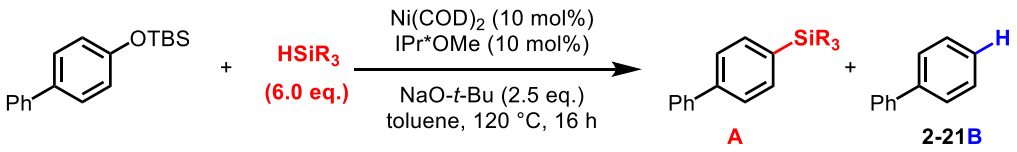

entry	H-SiR_3	yield A	yield 2-21B[a]
1	$SiEtMe_2$	73%	5%
2	$SiEt_2Me$	75%	3%
3	$SiEt_3$	91%	1%
4	Si(*i*-Pr)Me_2	79%	6%
5	Si(*n*-Pr)$_3$	85%	10%
6	Si(*t*-Bu)Me_2	32%	34%
7	Si(*i*-Pr)$_3$	0%	11%
8	$SiBnMe_2$	37%	11%

(a) Yields of biphenyl were determined by GCFID with tridecane as an internal standard.

Table 2-14. Silane Scope in Nickel-Catalyzed C-O Bond Silylation.

The silane scope was again explored due to the influence of titanium isopropoxide on the ratio of products. However, very similar results were obtained in comparison to reactions with titanium isopropoxide. Small, trialkylsilanes again gave the best yields and ratios of products, such as ethyldimethylsilane (Table 2-14, entry 1) and diethylmethylsilane (Table 2-14, entry 2), gave slightly lower yields. The lower yields could be due to the lower boiling points these silanes have compared to the reaction temperature. Larger silanes than triethylsilane gave lower yields and decreased ratios of silylation product to reduction product. Eventually increasing size up to *tert*-butyldimethylsilane (Table 2-14, entry 6) gave equivalent amounts of aryl silane and arene. Increasing size further to triisopropylsilane (Table 2-14, entry 7) resulted in low conversion and only small amounts of arene product. Low reactivity of triisopropylsilane explains why arene product was observed in the mixed system with titanium isopropoxide and triisopropylsilane. Benzyldimethylsilane (Table 2-14, entry 8) can also be used to generate aryl silanes that can be used for Hiyama-Denmark couplings. Although triethylsilylarenes have been shown to be competent in select couplings,[175] trimethylsilylarenes are more useful and should be accessible through our methodology with the correct equipment to handle trimethylsilane.

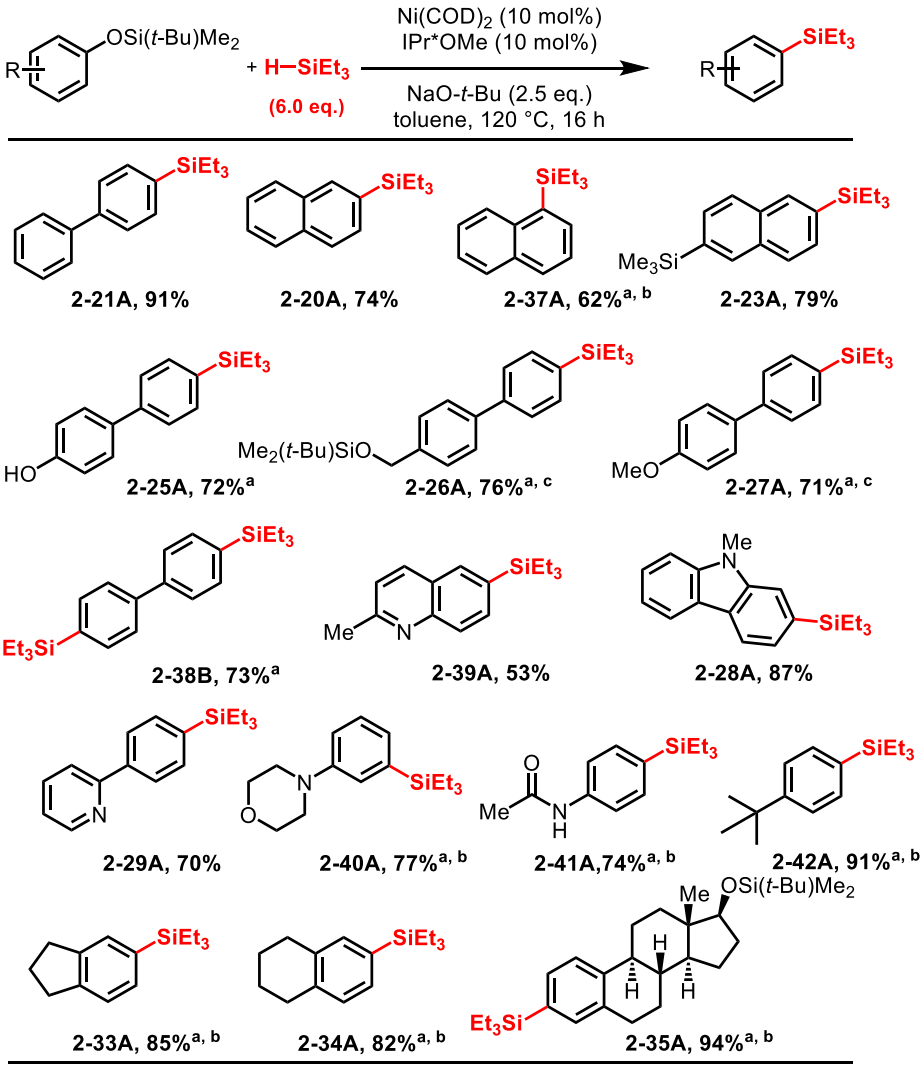

(a) Reactions run using 25 mol% $Ni(COD)_2$ and IPr^*OMe. (b) Reactions run at 130 °C for 24 hours.
(c) Reactions run at 100 °C for 8 hours.

Table 2-15. Silyloxyarene Substrate Scope in Nickel-Catalyzed C-O Silylation.

Having optimized the silylation reaction and explored other aryl electrophiles, the silyloxyarene substrate scope was explored next (Table 2-15). The scope was analogous to the reduction reaction with titanium isopropoxide. Substrates included a range of naphthyl substrates, including those more sterically hindered (**2-37A**) and those containing other aryl silane functionalities (**2-23A**). Unprotected phenols (**2-25A**), benzyl silyl ethers (**2-26A**), and aryl methyl ethers (**2-27A**) were again tolerated and resulted in good yields. Disilyloxy functionalities were also disilylated in good yield (**2-38A**). Several heterocyclic substrates resulted in good yields,

including quinoline (**2-39A**), carbazole (**2-28**), and pyridine (**2-29A**). There was not as dramatic of a decrease in yield moving from biphenyl substrates to very electron-rich isolated aromatic systems, as compared to the reduction reaction. A range of different isolated aromatics resulted in high yields. Acetaminophen (**2-41A**) and estradiol (**2-35A**) derivatives were coupled in very good yields, displaying tolerance of unprotected amides and aliphatic silyl ethers.

2.4.3 Mechanism for C-O Bond Silylation of Silyloxyarenes

The mechanism for C-O bond silylation of silyloxyarenes has also not been explored in detail and our proposed mechanism is based on empirical findings and related computational reports. The reactivity difference between aryl methyl ethers and silyloxyarenes with silane reductants is unique. Whereas, aryl methyl ether C-O bonds with silane reductants produces arene products, silyloxyarene C-O produce aryl silanes as the product. However, with aryl methyl ether C-O bonds, a unique mechanism is proposed with a nickel catalyst, phosphine ligands, and silanes.[151] The mechanism includes dearomatization and leads to a significant difference in reactivity between naphthyl substrates and isolated aromatics. If a similar pathway were operable under our reaction conditions, a dramatic difference between isolated and conjugated aryl systems would be observed. However, similar reactivity is observed for both classes of substrates. Furthermore, isolated aryl methyl ether substrates can also be utilized, suggesting that this mechanism is also not operable under our reaction conditions for either electrophile. One possibility for the change in mechanism derives from the ligand. Computations support formation of a nickel(I) complex in aryl methyl ether C-O bond couplings with phosphine ligands and silane.[151] However, reported computations on a aryl methyl ether silylation reaction suggest the same nickel(I) complexes are not operable with NHC ligands.[146]

The silylation reaction of aryl methyl ether C-O bonds with silylboranes has also been reported.[104] This reaction does not use added ligands and can be run at room temperature, where aryl methyl ether C-O bond activation is typically run at 100 °C. Computational papers on this aryl methyl ether silylation,[150,171] as well as empirical results from the original paper, suggest that a silyl anion is generated. Therefore, this would be analogous to use of strongly nucleophilic Grignard reagents and explains the mild reaction conditions. Additionally, the polarity of the silane is reversed between silanes and silylboranes, where the silane silicon is electrophilic and silylborane silicon atom is nucleophilic. Based on findings in our silylation methodology, it is unlikely that an analogous silyl anion is generated in situ using our method. First, high reaction temperatures are required and if a silyl anion was generated, lower reaction temperatures would be possible, as has been previously shown in silyloxyarene C-O bond Kumada couplings.[161]

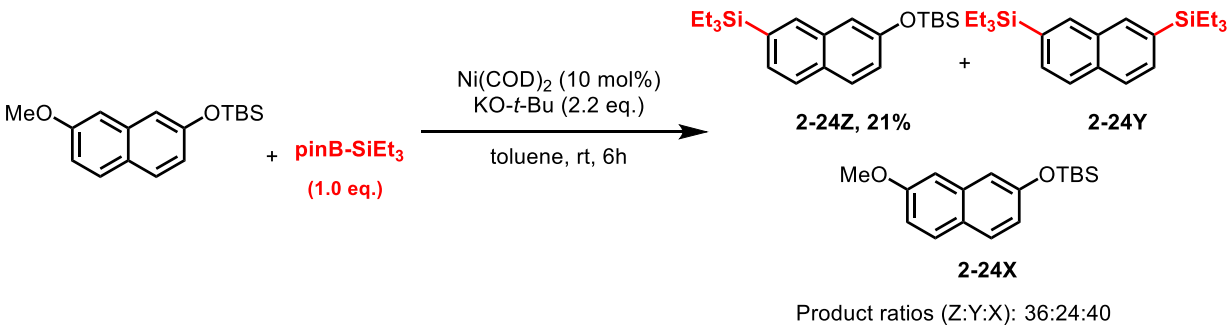

Scheme 2-13. Silylation of *tert*-butyl((7-methoxynaphthalen-2-yl)oxy)dimethylsilane with Silylborane.

Furthermore, use of an unbiased substrate with both methoxy and silyloxy C-O electrophiles, using reported conditions for aryl methyl ether silylation with silylboranes,[104] resulted in selectivity for the aryl methyl ether C-O bond. Although there are products derived from silyloxyarene C-O bond silylation, where both electrophiles were silylated, no product corresponding to initial silylation of the silyloxy group first is observed (Scheme 2-13). This is the opposite trend observed when using our reaction conditions, where the silyloxyarene C-O bond is preferred (Scheme 2-14). Furthermore, under our reaction conditions with the difunctionalized

compound, the only conversion of the aryl methyl ether C-O bond was reduction to the arene. (Scheme 2-14). Therefore, these experiments suggest that neither mechanism for aryl methyl ether C-O bond silylation with a silylborane or reduction with a silane is operable in our reaction.

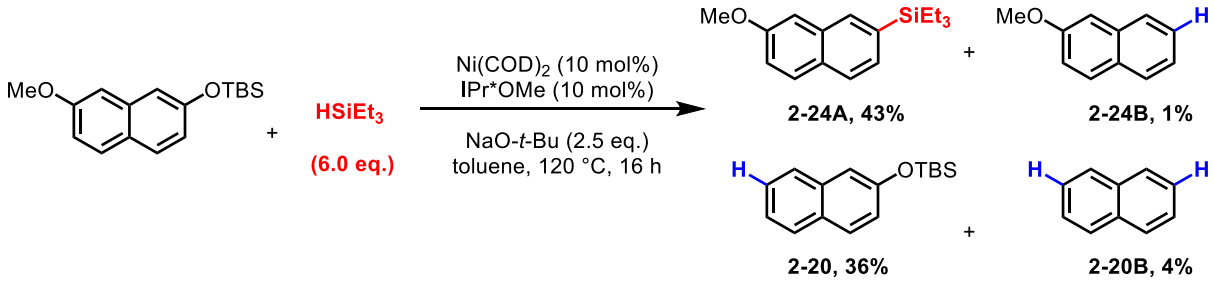

Scheme 2-14. Silyloxyarene C-O Bond Silylation of *tert*-butyl((7-methoxynaphthalen-2-yl)oxy)dimethylsilane.

Currently, our proposed mechanism begins with generation of a mono-ligated nickel(0)-NHC complex (**F)**, which coordinates the silyloxyarene through η^2 coordination (Scheme 2-15). A three-centered, two-electron oxidative addition generates complex **H**, which then undergoes sigma-bond metathesis with a silane through a four-membered transition state, generating *tert*-

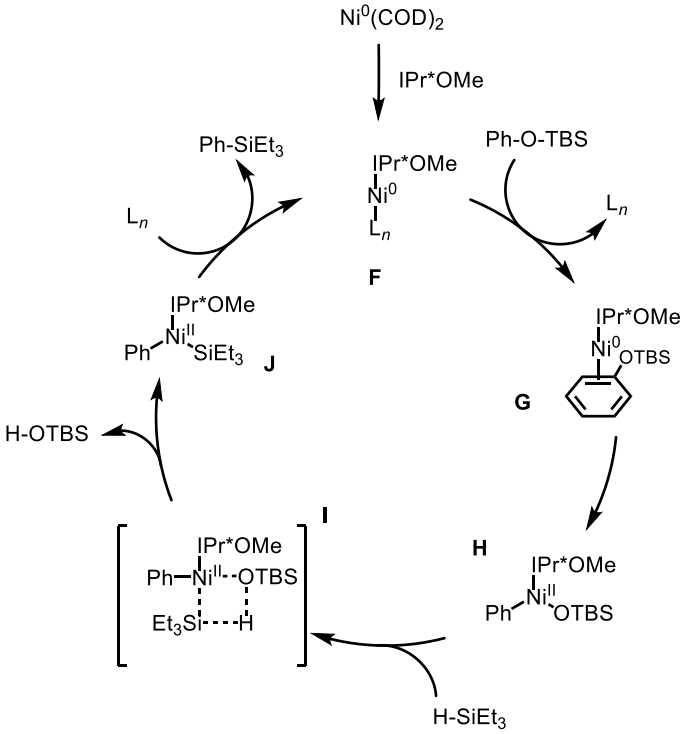

Scheme 2-15. Proposed Mechanism for Nickel-Catalyzed C-O Bond Silylation of Silyloxyarenes.

butyldimethylsilanol and nickel complex **J**. Finally, reductive elimination generates the aryl silane product and addition of another ligand completes the catalytic cycle, to generate the mono-ligated nickel(0)-NHC complex **F**.

The proposed mechanism is supported by empirical findings and computations on related C-O bond coupling reactions. Additionally, a more detailed discussion on some aspects of the silylation mechanism are covered in section 2.3.3. A diligated nickel(0)-NHC complex $Ni(NHC)_2$ is not proposed as only one equivalent of NHC ligand is used. Additionally, the increased size of IPr*OMe over IPr decreases the stability of $Ni(NHC)_2$ and would only be present in small concentrations under the reaction conditions.

Instead of another NHC ligand for complex **F**, the other ligand, L_n, could be several species in solution and is likely to be *tert*-butoxide, generating a nickelate. An alternative type of oxidative addition, such as an ion-pair (S_NAr-like) pathway, could also be operable instead of a traditional oxidative addition, as has been proposed through computations of related reactions.[146] However, these computations show that this pathway becomes less favorable with more substituted diaryl ethers and unsubstituted aryl alkyl ethers. Use of a silane protecting group could change the energetics of both pathways and could lead to competitive mechanisms for some substrates, although these possibilities are all speculative.

After C-O bond insertion, sigma-bond metathesis with an aryl or alkoxy group is possible to generate an aryl silane or alcohol. The selectivity observed in our reaction likely depends on this sigma bond metathesis transition state (**I**). We observe that a large ligand is important for high selectivity of the aryl silane product, where smaller ligands result in larger amounts of reduction product. This can be explained through generation of the more stable oxygen-silicon bond when using a smaller ligand. With a larger NHC ligand, increased steric interactions with the silane could

result in the opposite selectivity by potentially reversing orientation of the silane for sigma-bond metathesis. Additionally, this is further supported by observing lower conversions and larger ratios of reduction product with increased sterics at the ortho position on the aryl substituent.

This analysis can also be used to explain the increase in reduction product by increasing silane size from triethylsilane, and the absence of reactivity with triisopropylsilane. Increasing size of the silane plays a large role in the selectivity through steric interactions, where reversal in selectivity is observed until the silane becomes too large and is unable to approach for sigma bond metathesis. Other factors could also be responsible for the observed selectivity, such as influences from the protecting group, interactions of silane and base, or from the NHC ligand used in the reaction beyond what is mentioned above. These could be important differences compared to aryl methyl ether coupling with silanes as a different protecting group, no base, and phosphine ligands are used.

2.5 Conclusions and Future Directions for C-O Bond Reduction and Silylation of Silyloxyarenes

Exploration into the C-O bond reactivity of silyloxyarenes under nickel catalysis has led to the development of two new reactions. Initial investigation into the C-O bond reactivity of silyloxyarenes with silanes and Lewis acids led to the discovery of divergent silylation and reduction reactions. Further control experiments and optimization discovered the role of titanium isopropoxide as the reductant in generating arene products and a unique manifold for C-O coupling reactions with nickel catalysts and silane coupling reagents. Generation of aryl silanes from aryl C-O bonds with silanes, to the best of our knowledge, has not been previously reported with nickel catalysts. Portions of the work described in this chapter has been published: Wiensch, E. M.; Todd, D. P.; Montgomery, J. *ACS Catal.* **2017**, *7*, 5568–5571.

Future directions on this project would be to explore the mechanisms for these two reactions, especially silylation, as current mechanistic proposals do not fully explain all the observed selectivity in the reaction. There are also many synthetic future directions for both reduction and silylation methods, which are discussed in chapter 5.

Chapter 3

Nickel-Catalyzed C-O Bond Amination, Borylation, and Suzuki Coupling of Silyloxyarenes

3.1 General Introduction on Buchwald-Hartwig and Suzuki-Miyaura Couplings of C-O Bonds

Having explored the reactivity of silyloxyarenes under nickel catalysis, development of methods for late-stage diversification was explored. Reaction development focused on the two most utilized coupling reactions in organic synthesis, Buchwald-Hartwig aminations and Suzuki-Miyaura couplings for C-C bond formation. Development of these coupling reactions would then allow for use of silyloxyarenes C-O bonds as electrophilic coupling partners for diversification into a variety of commonly installed functionalities.

3.2 C-O Bond Amination of Silyloxyarenes under Nickel Catalysis

Initial exploration into Buchwald-Hartwig aminations focused on expanding previous work for amination of inert C-O bonds. There have been a few reports using aryl methyl ethers C-O bonds for aminations. However, there are not any reports of using silyloxyarene C-O bonds for aminations. Therefore, we sought to develop silyloxyarenes as a viable electrophile for Buchwald-Hartwig amination and hoped that exploring this new electrophilic coupling partner would allow for complementary reactivity to existing methods, thereby broadening the scope of C-N coupling partners for inert C-O bonds.

3.2.1 Background in Aminations of C-O Bonds

Since the groundbreaking work by Buchwald and Hartwig,[176] several advances have been made to improve catalyst loadings, coupling partners, and reproducibility. Recently, there has been increased interest in developing methods complementary to those using aryl halides, allowing for sequential and/or orthogonal couplings that can eliminate protecting group manipulations while utilizing renewable, feedstocks chemicals. Inert C-O bonds of phenol derivatives are one of the most explored green alternatives to aryl halides or pseudohalides because of their relative abundance, complementary reactivity, and tuneability derived from the protecting group installed. As such, they have been explored in amination reactions.

Initial reports by Chatani[63] and Garg[47] demonstrated semi-inert C-O bonds, such as carboxylates and carbamates, as electrophilic coupling partners with a range of secondary amines under nickel catalysis. The scope of amines displayed with aryl carbamate electrophiles was better as couplings with primary and secondary anilines were achieved. Although, use of acyclic secondary aliphatic amines resulted in moderate yields, this was an improvement over use of acyclic secondary aliphatic amines with aryl pivalates. However, primary aliphatic amines were not shown to be competent coupling partners in either report and were explicitly described by Garg as a limitation of the method. Since these two seminal reports, several advances have been made, including the utilization of an air-stable pre-catalyst.[48] More recently, a small number of examples have been shown for coupling specific primary aliphatic amines using unique ligand scaffolds.[177,178]

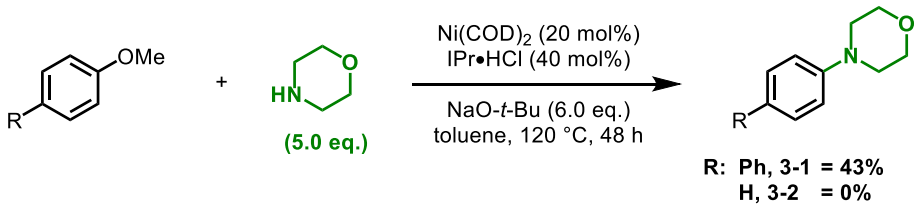

Scheme 3-1. Nickel-Catalyzed Amination of Isolated Aryl Methyl Ethers.

However, more inert C-O bonds are much more attractive than the carbonyl derivatives for late-stage coupling, due to their stability across a larger range of conditions. Reports of aminations using diaryl ether derivatives have utilized protecting groups that have directing capabilities, such as 2-pyridiyl.[119] These directing aryl protecting groups have led to advances in the substrate scope of these reactions due to higher reactivity of the C-O bond. However, these diaryl ethers are not attractive for cross-coupling due to use of a coupling reaction to install the aryl protecting group.

Aryl methyl ethers have been reported as competent electrophilic coupling partners with amines under nickel catalysis. Although high loadings of amine, base, and catalyst was used, an early example demonstrate aminations of aryl methyl ethers, where high yields were observed for aryl substrates with extended π systems.[105] However, the naphthyl problem was significant, as only 43% yield was obtained when moving to a biphenyl scaffold (**3-1**) and no product was observed when using anisole (**3-2**) (Scheme 3-1). The amine scope also had limitations as only cyclic, secondary aliphatic amines were displayed in good yields. Primary aliphatic amines were not shown and acyclic, secondary aliphatic amines resulted in modest yields.

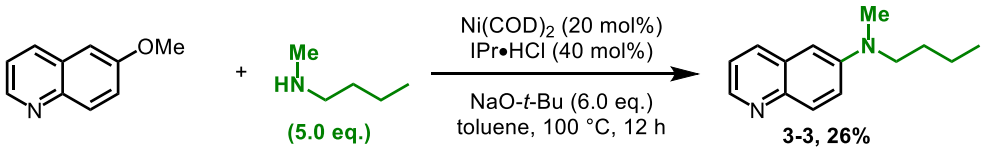

Scheme 3-2. Nickel-Catalyzed Amination of Heterocyclic Aryl Methyl Ethers.

The substrate scope was later expanded to use of heterocyclic aryl methyl ethers.[106] However, as the same catalyst system was utilized, the method was still limited to use of extended aryl systems for good yields. Furthermore, the amine scope was still limited to cyclic secondary aliphatic amines, where N-methylbutylamine gave 26% yield of the product with an activated naphthyl substrates (**3-3**, Scheme 3-2). Therefore, development of an amination with high

reactivity, broad amine scope, and use of an easily accessible or readily used inert C-O bond would be attractive.

3.2.2 Optimization for C-O Bond Amination of Silyloxyarenes

C-O bond amination of silyloxyarenes, mediated by nickel catalysis, was investigated using conditions analogous to those used in our reductive deoxygenation reaction. Having previously obtained high reactivity for silyloxyarene C-O bonds,[179] changing the catalyst system was not necessary. We were excited to find that simply introducing an amine coupling partner gave high yields of the aniline product (**3-4**) with the biphenyl model substrate (Table 3-1, entry 1).

Other variations on the catalyst system were also explored. As a secondary aliphatic amine with β-hydrogens was utilized, a nickel(II) pre-catalyst could be used in the reaction, where the nickel catalyst can be reduced to the active nickel(0) species with the amine. Although a slight decrease in yield is observed, use of the nickel(II) pre-catalyst allows for the reaction to be setup without the need of a glovebox (Table 3-1, entry 2). A 2:1 ratio of ligand to nickel proved to be optimal, where smaller ratios of ligand resulted in inferior results (Table 3-1, entries 3-4). A range of other ligands were also explored, focusing on electron-rich phosphine and NHC ligands.

Interestingly, another large, electron-rich NHC ligand, IPr*OMe, that was used in C-O bond silylation of silyloxyarenes resulted in no observed product with a 2:1 or 1:1 ratio of ligand to nickel pre-catalyst (Table 3-1, entries 5-6). This was surprising due to previous use of nickel and IPr*OMe for silyloxyarene C-O bond coupling and for aminations of aryl halides. A large dependence on the donating ability of the of the IPr derivative to the nickel center was observed, with low yields obtained using electron-withdrawing IPr^{Cl} (Table 3-1, entry 6), and increased yields from IPr (Table 3-1, entry 7) to the model ligand IPr^{Me} (Table 3-1, entry 1). Previous work in inert C-O bond activation also led to exploration of other common, large, and electron-rich NHC

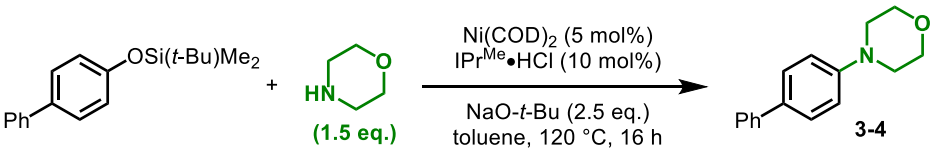

entry	variations	yield[a]
1	-	**93%**
2	$Ni(acac)_2$	**88%**
3	5 mol% IPr^{Me}•HCl	**62%**
4	7.5 mol% IPr^{Me}•HCl	**80%**
5	5 mol% $IPr^{*}OMe$•HCl for IPr^{Me}•HCl	**trace**
6	$IPr^{*}OMe$•HCl for IPr^{Me}•HCl	**trace**
7	IPr•HCl	**58%**
8	IPr^{Cl}•HCl	**13%**
9	$IMes^{Me}$•HCl	**NP**
10	IMes•HCl	**NP**
11	ICy•HCl	**NP**
12	IAd•HCl	**NP**
13	PCy_3	**trace**
14	dcype	**NP**
15	dppf	**NP**
16	dtbbpy	**NP**
17	1,10-phenanthroline	**NP**
18	LiO-*t*-Bu for NaO-*t*-Bu	**64%**
19	KO-*t*-Bu for NaO-*t*-Bu	**NP**
20	NaOMe for NaO-*t*-Bu	**NP**
21	NaOPh for NaO-*t*-Bu	**NP**
22	NaOTMS for NaO-*t*-Bu	**NP**
23	0.25M in toluene	**85%**
24	THF	**52%**
25	1,4-dioxanes	**80%**
26	6h	**78%**
27	100 °C	**70%**
28	1 eq. base	**70%**
29	1 eq. amine	**77%**

(a) Yields were determined by isolation. NP = no product observed.

Table 3-1. Optimization of Nickel-Catalyzed Amination of Silyloxyarene via C-O Bond Activation.

ligands, such as IMes, ICy and IAd. However, none of these ligands resulted in observable product (Table 3-1, entries 8-12). Several ligands beyond NHCs were also explored, including phosphines and bidentate N-donor ligands. Phosphine ligands used in aryl methyl ether C-O bond activation did not result in product with silyloxyarenes (Table 3-1, entries 13-14). Other phosphine ligands and bpy derivatives also did not result in any of the desired product (Table 3-1, entries 15-17).

Several variables beyond the catalyst were also explored. Intriguingly, of the many alkoxide bases deployed, only sodium (Table 3-1, entry 1) and lithium (Table 3-1, entry 18) *tert*-butoxide resulted in the desired product with several other bases not generating aniline (Table 3-1, entries 19-22). Concentration and solvent studies showed that the reaction could be run more dilute with a small decrease in yield (Table 3-1, entry 23), and other ethereal solvents could be employed with moderate to small decreases in yield (Table 3-1, entries 24-25). Finally, the reaction can be run for shorter reaction times, at lower temperatures, and with fewer equivalents of base or amine, although small decreases in yield are observed (Table 3-1, entries 26-29).

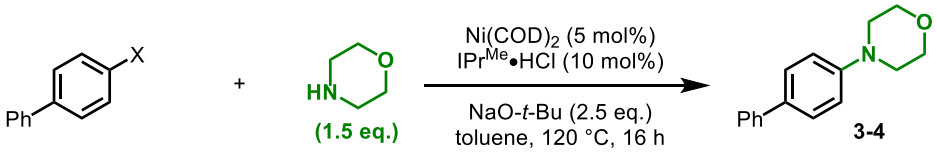

entry	X	yield[a]
1	OSi(*t*-Bu)Me_2	**93%**
2	OSi(*t*-Bu)Ph_2	**84%**
3	OSi(*i*-Pr)$_3$	**37%**
4	$OSiEt_3$	**67%**
5	OMe	**4%**
6	OPiv	**54%**
7	OTf	**78%**
8	OPh	**72%**
9	Br	**29%**
10	F	**39%**

(a) Yields were determined by isolation. NP = no product observed.

Table 3-2. Electrophile Scope in Nickel-Catalyzed C-O Bond Amination of Silyloxyarenes.

Other aryl electrophiles were also explored to compare reactivity of silyloxyarenes to commonly used coupling partners and to ensure that another silyloxyarene derivative did not give superior results. Exploring the use of other silyloxyarene derivatives showed a dependence on size and electronics of the silane protecting group, with TBS being optimal (Table 3-2, entry 1). Although, high yields were obtained with TBDPS (Table 3-2, entry 2), lower yields were observed with TIPS and TES (Table 3-2, entries 3-4). Other common aryl electrophiles resulted in inferior

results, with OMe (Table 3-2, entry 5) only showing trace product and other C-O electrophiles, including OPh, OPiv, or OTf (Table 3-2, entries 6-8), resulting in moderate yields. Finally, aryl halides (Br, F) resulted in low yields, due to conversion of the aryl halides to biphenyl by competing reduction through β-hydride elimination (Table 3-2, entries 9-10).

3.2.3 Substrate Scope for C-O Bond Amination of Silyloxyarenes

With optimized conditions in hand, the scope of amine coupling partners was explored. Several cyclic amines were coupled in good yields, including amines with basic functionality, such as a piperazine derivative (Table 3-3, **3-5**), and a more sterically hindered amine (**3-6**). However, increasing further to more a sterically hindered cyclic amine resulted in a lower yield (**3-7**). Exploring acyclic secondary aliphatic amines, a very sterically hindered amine, diisobutylamine (**3-8**), resulted in a lower yield but other acyclic secondary amines (**3-8, 3-9, 3-10**) coupled in high yields. Although secondary aniline derivatives (**3-11**) resulted in moderate yield, sterically hindered primary anilines (**3-12, 3-13**) resulted in good yields. Sterically hindered anilines were necessary as using an unhindered aniline (**3-14**) as a coupling partner only resulted in trace product. However, exploring the use of primary aliphatic amines showed promising results (**3-15, 3-16**), as these amines have been difficult to couple with inert C-O bonds using previously reported methods. Gratifyingly, use of unhindered, primary aliphatic amines provided the coupled products in high yield (**3-17, 3-18, 3-19**). A series of increasingly sterically encumbered nucleophilic primary amines were explored, with aliphatic amines from *n*-butyl (**3-17**) to cyclobutyl (**3-20**) all resulting in good yields. Increasing to more sterically hindered, *tert*-butylamine (**3-21**), did result in lower yield but even 1-adamantyl amine (**3-22**) was isolated in a high yield, showing the first example of a general coupling for primary aliphatic amines with inert C-O bonds.

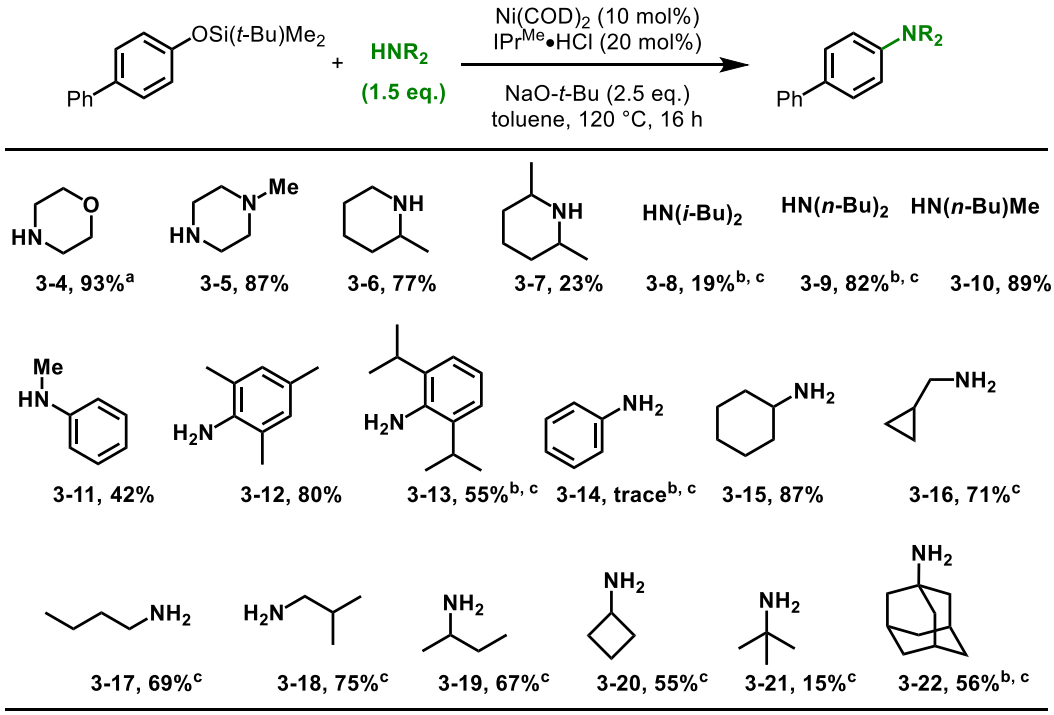

(a) Reaction used 5 mol% $Ni(COD)_2$ and 10 mol% IPr^{Me}•HCl. (b) Reaction used 15 mol% $Ni(COD)_2$ and 30 mol% IPr^{Me}•HCl. (c) Reaction used 2.5 eq. of amine.

Table 3-3. Amine Scope for Nickel-Catalyzed C-O Bond Amination of Silyloxyarenes.

However, despite the large amine scope for primary and secondary aliphatic amines, there were several amines that did not result in any observed product (Table 3-4). Due to the inability of aniline to act as coupling partner, generation of primary anilines appeared obtainable and a variety of coupling partners as primary amine equivalents were explored. However, ammonia, as a solution or as lithium amide, did not result in the free aniline. Furthermore, other primary amine equivalents did not result in product, including hexamethyldisilazane derivatives or diphenylmethanimine.

A range of small, low boiling amines were also unsuccessful coupling partners, including methylamine, dimethyl amine, cyclopropylamine, and allylamine. This is likely due to the high reaction temperatures utilized in our reactions and the low boiling points of these amines. Other extremely sterically hindered primary and secondary aliphatic amines did not give product, including 2,4,4-trimethylpentan-2-amine, dicyclohexylamine, dibenzylamine, diisopropylamine,

and 2,2,6,6-tetramethylpiperidine. Finally, non-nucleophilic amines did not result in any observable product, including amides, pyrroles, and primary unhindered anilines.

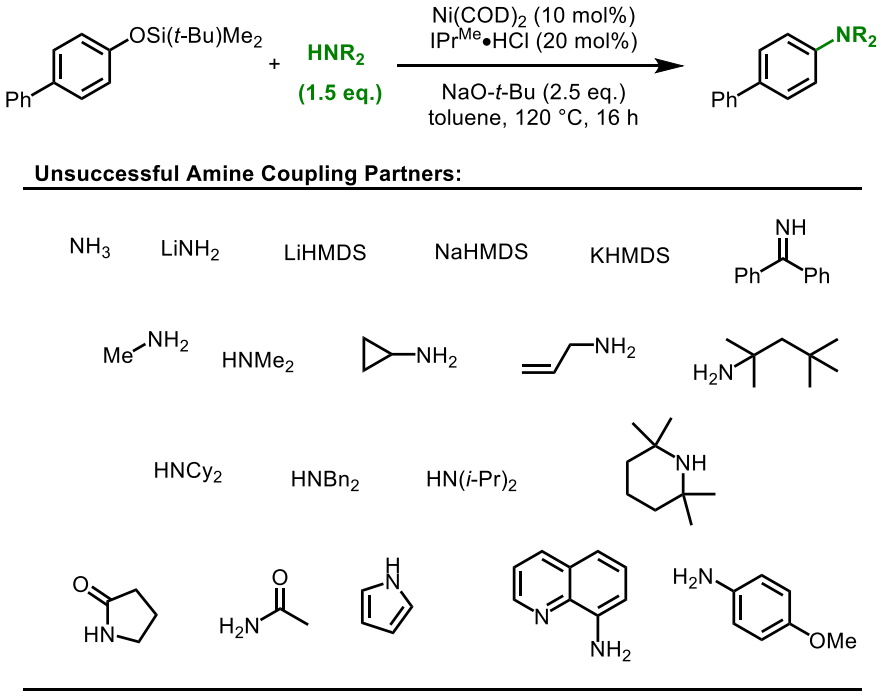

Table 3-4. Unsuccessful Amines in Nickel-Catalyzed Amination of Silyloxyarene C-O Bonds.

Having a good understanding of the limitations in the amine scope, the silyloxyarene component was next explored, utilizing a challenging amine or silyloxyarene as one of the coupling partners. Naphthyl substrates substituted at the 1 or 2 positions were coupled in good yield with primary aliphatic amines (Table 3, **3-23** and **3-24**). A variety of substitutions were tolerated on the silyloxyarene substrate, including silyl groups (**3-25**) and ortho substitution (**3-26**). However, large ortho substituents, such as phenyl, resulted low reactivity. For 2-phenylhydroquinone derivative **6**, the meta C-O bond was preferred in a 5.7:1 ratio of product **3-27** to 4-([1,1'-biphenyl]-3-yl)morpholine over the ortho position for this electron-rich silyloxyarene. A variety of heterocycles are tolerated, including quinoline, pyridine, and carbazole (**3-28**, **3-29**, and **3-30**). Additionally, C-O bonds substituted on the heterocycles are coupled in high yield, such as quinoline substrate **3-31**. Other protecting groups for alcohols or amines, such

as aryl methyl ethers or *tert*-butyloxycarbonyl are tolerated, allowing for further derivatization of complex substrates (**3-32** and **3-33**). Finally, C-O bonds substituted on isolated phenyl substrates are coupled, including very electron-rich silyloxyarenes (**3-34** and **3-35**), resulting in good yields. Acetaminophen derivative **3-35** also shows the tolerance of unprotected amides. High yields are observed with less electron-rich isolated aromatics (**3-36**), including estradiol derivative **3-37**.

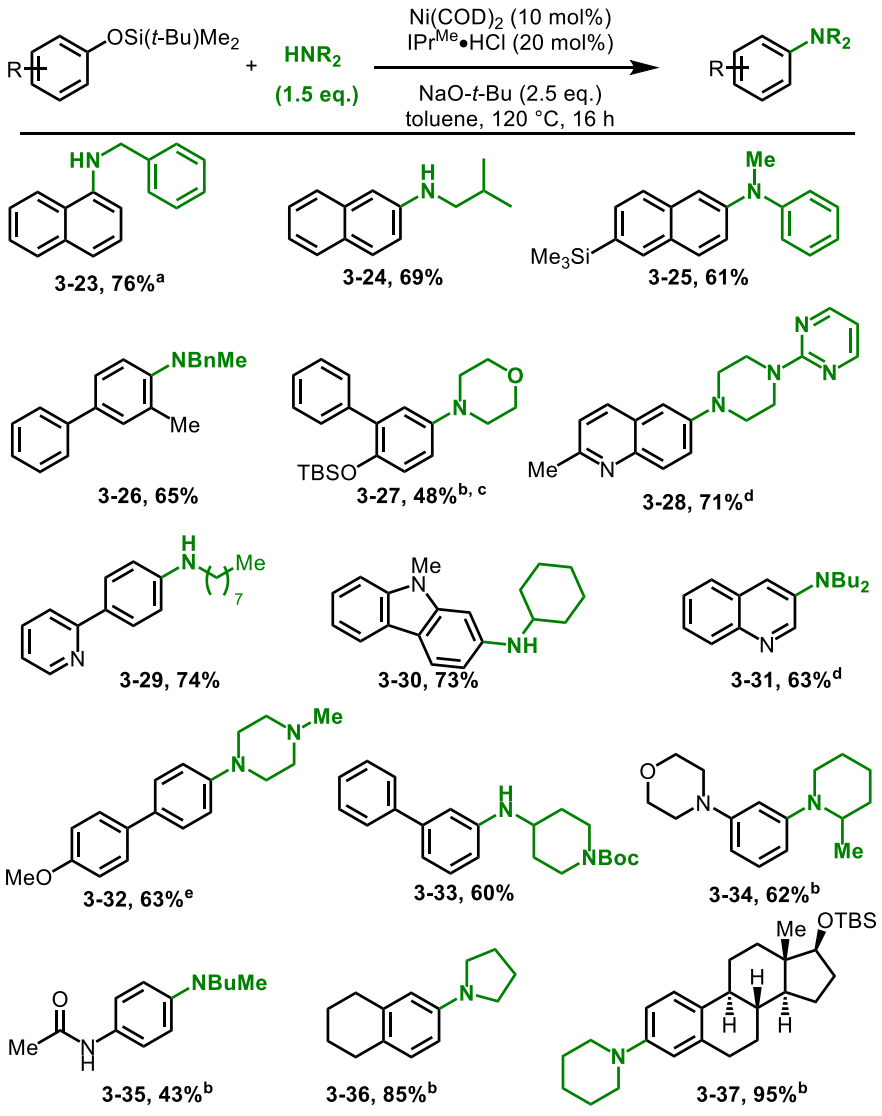

(a) Reaction used 4 eq. of base. (b) Reaction used 15 mol% $Ni(COD)_2$, 30 mol% IPr^{Me}•HCl, 4 eq. base, 2.5 eq. amine at 130 °C. (c) Reaction gave a 5.7:1 ratio of **6**:4-([1,1'-biphenyl]-3-yl)morpholine. (d) Reaction used 2.5 eq. of amine. (e) Reaction used 15 mol% $Ni(COD)_2$, 30 mol% IPr^{Me}•HCl and 4 eq. base.

Table 3-5. Silyloxyarene Scope for Nickel-Catalyzed C-O Amination of Silyloxyarenes.

3.2.4 Mechanism for C-O Bond Amination of Silyloxyarenes

The proposed mechanism for nickel-catalyzed C-O bond amination of silyloxyarenes is analogous to the proposed mechanism for our titanium mediated reduction reaction due to the use of the same catalysts system. Generation of $Ni(NHC)_2$ from the nickel pre-catalyst, followed by displacement of one NHC ligand with sodium *tert*-butoxide, generates the active nickelate complex **F** (Scheme 3-3). Coordination of silyloxyarene substrate generates complex **G**, which explains the small reactivity differences between extended and isolated aromatic systems due the stronger η^2 coordination with extended aryl systems. Oxidative addition of the aryl C-O bond to nickel generates neutral complex **G** after dissociation of an alkoxide. Exchange of an amine with the remaining alkoxide generates a nickel amido (**I**), which undergoes deprotonation to generate complex **J**. Reductive elimination and association of *tert*-butoxide completes the catalytic cycle.

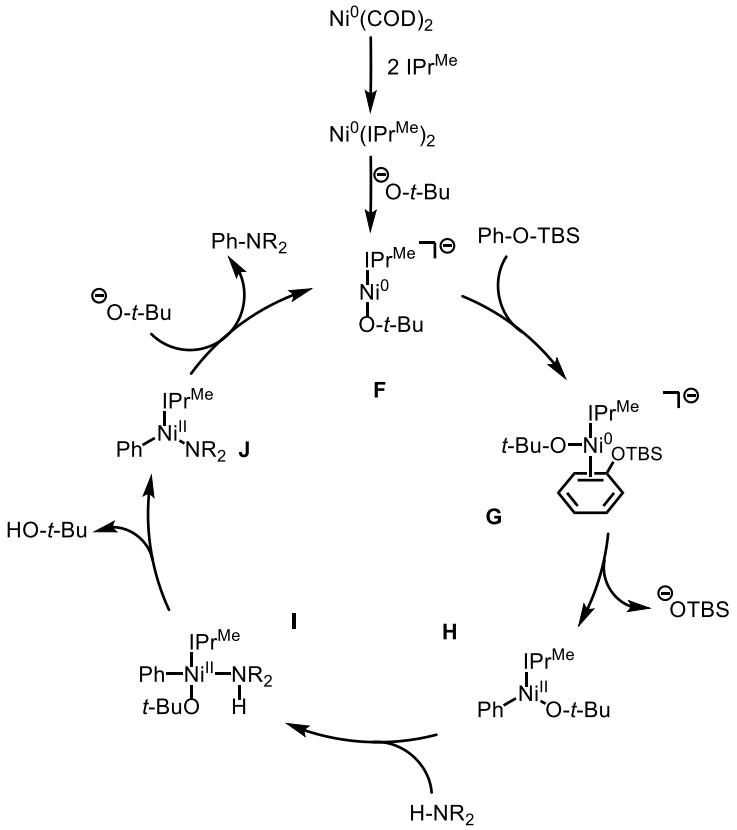

Scheme 3-3. Proposed Mechanism for Nickel-Catalyzed C-O Bond Amination of Silyloxyarenes.

This mechanism is proposed based on empirical findings through discoveries in our developed silyloxyarene C-O bond couplings and computational reports on related methods, see section 2.3.3 for a more detailed discussion. Our mechanism does not fully explain the difference between our reported method and aryl methyl ether C-O bond amination. A similar ligand is used and presumably goes through a related mechanism. The difference in poor reactivity with aryl methyl ethers can be explained by the stronger C-O bond as compared to silyloxyarene C-O bonds. However, the improved amine scope in our methodology is not explained and could be due to a variety of reasons, including a full amine scope was not explored, a different mechanism is operating, or the protecting group is resulting in improved scope for the reaction. Additionally, the methoxy group could be resulting in off cycle intermediates, such as nickel carbonyl complexes through β-hydride elimination and resulting in undesired outcomes.

3.3 C-O Bond Borylation and Suzuki Couplings of Silyloxyarenes

In addition to developing Buchwald-Hartwig type aminations through C-O bond activation of silyloxyarenes, C-C bond forming reactions were desired. Due to the widespread use of Suzuki couplings in organic synthesis, development of a Suzuki coupling with silyloxyarene C-O bonds would be attractive for C-C bond formation and has not been previously explored. Therefore, we investigated C-O bond activation with nickel catalysts for development of a Suzuki coupling, which we believed could lead to improvements for current inert C-O bond coupling methods and prove complementary to these existing procedures.

3.3.1 Background in Suzuki-Miyaura Couplings of C-O Bonds

Several methods exist for Suzuki coupling or borylation of C-O bonds using carbonyl or aryl methyl ether derivatives. An example of using carbamates as aryl C-O electrophiles for borylation was reported with yields ranging from 42-84% (Scheme 3-4).[46] However, use of a

strong base, sodium *tert*-butoxide, resulted in poor results when moving from naphthyl substrates to biphenyl and isolated aromatics. They could obtain improved yields by using increased temperatures and a weaker base, potassium phosphate. Notably, they also showed several heterocyclic substrates and alkenyl substrates for generation of heterocyclic aryl or vinyl boranes. Other groups have also explored borylation of more activated aryl C-O bonds, such as 2-pyridyl protecting groups, with nickel[117] or rhodium[113] catalysts. However, inert C-O bond borylations have been limited to aryl methyl ethers.

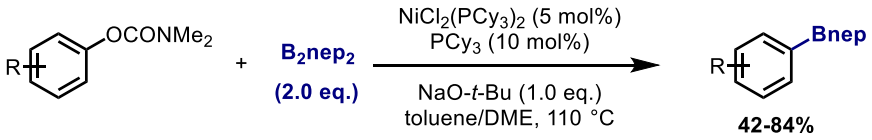

Scheme 3-4. Nickel-Catalyzed C-O Borylation of Aryl Carbamates with Bis(neopentyl glycolato)diboron.

An example for borylation of aryl methyl ethers was displayed where many naphthyl and extended aryl systems (**3-38**) gave good yields.[107] However, due to low C-O bond reactivity of aryl methyl ethers, use of isolated aromatics were not general as electron-deficient groups were required to act as directing groups for the nickel catalyst to obtain moderate yields (Table 3-6). Substrates with ortho-ester groups (**3-39, 3-40**) or an ortho-trifluoromethyl group (**3-41**) were the only isolated aromatic derivatives that were shown to result in product.

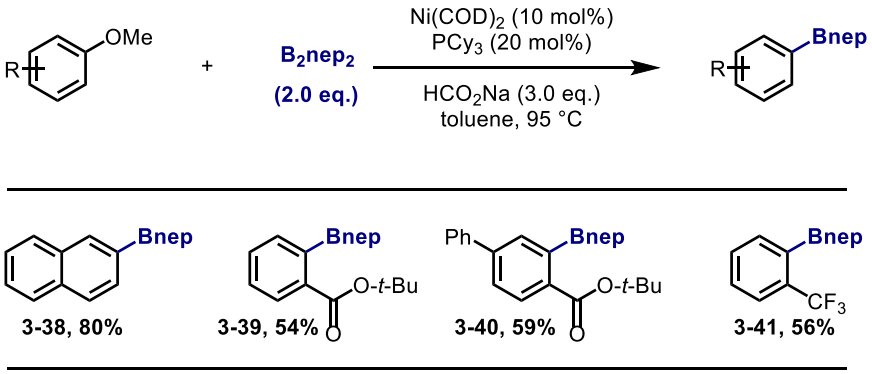

Table 3-6. Nickel-Catalyzed C-O Borylation of Aryl Methyl Ethers with Bis(neopentyl glycolato)diboron.

An earlier report described that some aryl methyl ether substrates could be used in homocouplings with bis(neopentyl glycolato)diboron as reductant, where the aryl boron is generated in-situ (Scheme 3-5).[103] Although yields were good for extended aryl systems, use of isolated aromatics gave poor yields, with anisole resulting in a 33% yield. In addition to this example of in-situ generation of an aryl boron reagent for Suzuki couplings, many direct Suzuki couplings with aryl borons have been reported.

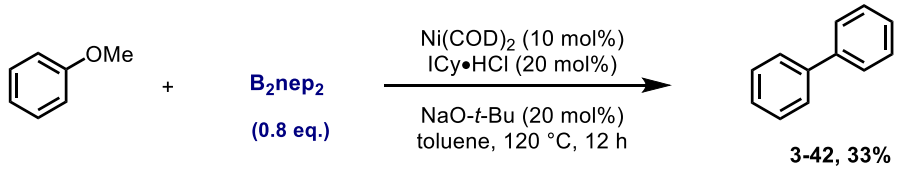

Scheme 3-5. Nickel-Catalyzed C-O Homocoupling of Aryl Methyl Ethers with Bis(neopentyl glycolato)diboron.

Early developments by Garg,[58] Shi,[57] and Snieckus[39] showed Suzuki couplings of carbonyl derivatives, such as pivalates, acetates, and carbamates, with boronic acids or boroxines. These methods used nickel catalysts with tricyclohexylphosphine as a ligand, four equivalents of aryl borane, and more than five equivalents of potassium phosphate. In general, high yields were obtained for the substrates explored. Early findings by Snieckus showed that excess water impeded the reaction and that boroxines did not couple under strictly anhydrous conditions; therefore, a 10:1 ratio of boroxine to boronic acid was used.[39] Due to some discrepancies between the work of Garg and Snieckus, they followed up by exploring Suzuki couplings of aryl carbamates experimentally and computationally with Houk.[41] They found water stabilized the resting state and a five-membered transition state was operable for oxidative addition, leading to improved results.

Other coupling partners have also been used for Suzuki couplings of C-O bonds, including more activated aryl C-O electrophilic coupling partners.[112,115] Furthermore, aryl boronic esters can also be utilized, as was later displayed in Suzuki couplings of aryl carbamates using aliphatic NHC

ligands and nickel catalysts.[42] There has also been a couple of examples using more inert aryl electrophiles, which would be advantageous for late-stage coupling.

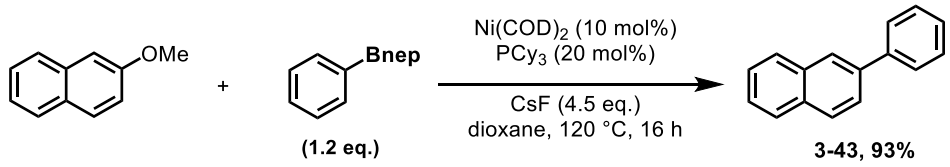

Scheme 3-6. Nickel-Catalyzed Suzuki Coupling of Aryl Methyl Ether with Nickel(0) Cyclooctadiene and Tricyclohexylphosphine.

An early example of coupling aryl methyl ethers was limited to naphthyl substrates, and other extended ring systems, using tricyclohexylphosphine, nickel(0) pre-catalyst, and cesium fluoride (Scheme 3-6).[89] The scope for this reaction was quite limited as few functional groups were tolerated in the reaction. As few base sensitive functional groups were displayed, this Suzuki coupling presented few advantages over coupling reactions using strongly nucleophilic coupling partners, where high yields are obtained for even isolated aromatics.[128] However, it was a important initial discovery early in the development of aryl methyl ether couplings with milder nucleophilic coupling partners.

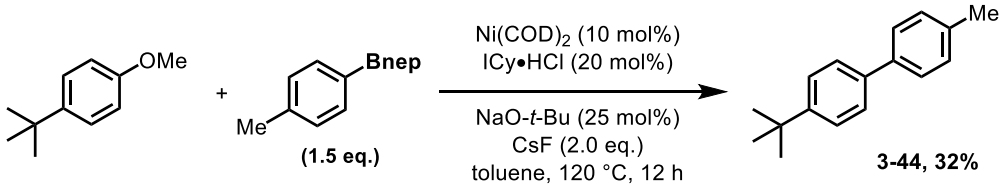

Scheme 3-7. Nickel-Catalyzed Suzuki Coupling of Aryl Methyl Ethers using Aliphatic NHC Ligands and Cesium Fluoride.

The method was later explored, with improved conditions obtained for Suzuki couplings of aryl methyl ethers and aryl boronate esters, using aliphatic NHC ligands, nickel(0) pre-catalyst, and cesium fluoride (Scheme 3-7).[90] Although significantly higher yields were obtained with biphenyl substrates, isolated aromatics still suffered from low yield with 1-(*tert*-butyl)-4-methoxybenzene resulting in a 32% yield (**3-44**). Use of benzylic methyl ethers were also shown to be competent in the developed Suzuki coupling for Csp_2-Csp_3 coupling, with even higher yields

obtained over aryl methyl ether C-O bond coupling. One interesting discovery was the necessity of cesium fluoride in the original method for Suzuki coupling with tricyclohexylphosphine. Cesium fluoride was found to not be needed with aliphatic NHCs in the Suzuki coupling of aryl methyl ethers. This difference was explored computationally, and was determined to derive from a lowering of the transition state energy by forming a quaternary complex with tricyclohexylphosphine. This stabilization was not necessary for the aliphatic NHC method due to increased stabilization of the nickel catalyst by the NHC ligand.[180] Of the inert C-O bonds, only aryl methyl ethers have been utilized in Suzuki-Miyaura couplings and we sought to develop Suzuki-Miyaura couplings of silyloxyarene C-O bonds to further show the utility of these aryl electrophiles and potentially increased the substrate scope for inert C-O bond couplings.

3.3.2 C-O Bond Borylation of Silyloxyarenes

Nickel-catalyzed C-O bond borylation of silyloxyarenes was explored as another method of transforming the C-O bond of silyloxyarenes into an aryl nucleophile. Previous work (chapter 2) displays generation of aryl silanes from silyloxyarene C-O bonds. However, current use of such products has only limited use as nucleophilic coupling partners in Hiyama-Denmark reactions and development of a more useful aryl nucleophile would be advantageous. Therefore, due to the prevalence of Suzuki couplings, borylation, or Miyaura couplings, was explored.

3.3.2.1 Optimization for C-O Bond Borylation of Silyloxyarenes

Initial experiments began by exploring H-Bpin for the coupling partner, as a method to expand on our silylation methodology by switching Bpin for $SiEt_3$. However, due to initial experiments showing instability of H-Bpin to our reaction conditions, use of H-Bpin was not further explored. Instead, diboron reagents were explored with our catalyst systems for silyloxyarene C-O bond activation, a nickel(0) pre-catalysts and IPr^{Me}. However, no product was

observed while screening many bases and solvents. Therefore, co-catalysts were explored that are known to rapidly transmetallate with diboron species and generate metal-boronates. Copper appeared to be an ideal candidate due to prevalence in borylation reactions[181,182] and previously shown compatibility with nickel catalysis.[73] Indeed, when a range of copper sources were explored, product was observed (Table 3-7). There did not seem to be a significant difference or any observable trend between copper(II) or copper (I) sources, as both copper(II) and copper(I) acetates resulted in observed product. However, there did appear to be an importance on the anionic ligand, as copper(II) triflate did not work (Table 3-7, entries 1-3). In general, copper(I) generally gave the best results across halide derivatives and discrete copper complexes (Table 3-7, entries 4-11).

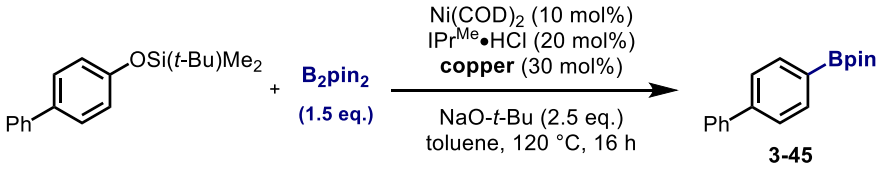

Entry	copper	product observed
1	$Cu(OAc)_2$	✓
2	Cu(OAc)	✓
3	$Cu(OTf)_2$	✗
4	CuF_2	✗
5	CuCl	✓
6	$CuBr_2$	✗
7	CuI	✓
8	IPrCuCl	✓
9	IMesCuCl	✓
10	ICyCuCl	✓
11	$(PPh_3)_3CuBr$	✗

✓ = product observed. ✗ = no product observed.
✓ = trace product observed

Table 3-7. Copper Screen for Nickel-Catalyzed Borylation of Silyloxyarene C-O Bonds.

Based on conversion to the silyloxyarene to product, copper(II) acetate and IMesCuCl were further optimized. Initial optimization of IMesCuCl resulted in yields around 50%. However, further optimization proved challenging as yields plateaued and altering other reaction conditions

did not result in improved yields. Therefore, copper(II) acetate was then explored as an alternative copper co-catalyst, which was advantages due the low cost.

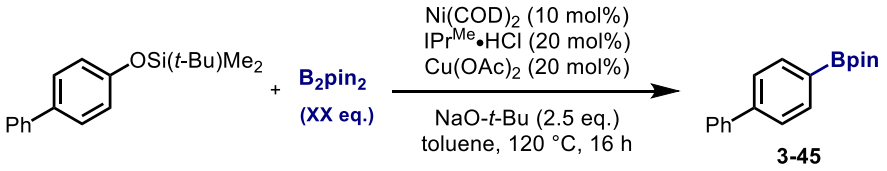

Entry	B_2pin_2 equivalents	yield[a]
1	1.0	**trace**
2	1.5	**9%**
3	2.0	**55%**
4	2.5	**72%**
5	3.0	**83%**
6	4.0	**79%**
7	5.0	**5%**

(a) Yields were determined by GCFID with tridecane as internal standard.

Table 3-8. Diboron Equivalents in C-O Bond Borylation of Silyloxyarenes.

Equivalents of the diboron reagent was explored, where low yield were observed with fewer than 1.5 equivalents (Table 3-8, entries 1-2). Two equivalents gave a moderate yield of 55% (Table 3-8, entry 3), but increasing to 2.5 and 3.0 equivalents gave good yields of 72 and 83%, respectively (Table 3-8, entries 4-5). Increasing further resulted in decreased yields, with only a small amount of product using five equivalents of B_2pin_2 (Table 3-8, entries 6-7). The amount of diboron used going forward was 2.5 equivalents, to balance yield and the amount of B_2pin_2.

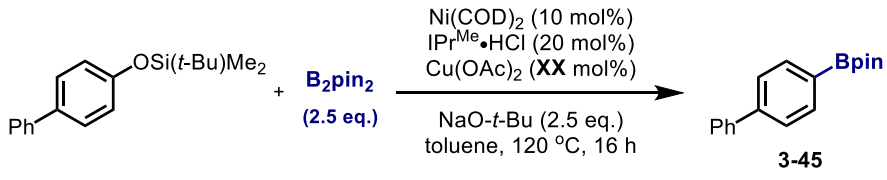

Entry	$Cu(OAc)_2$ (mol %)	yield[a]
1	10	**60%**
2	20	**72%**
3	30	**61%**
4	40	**60%**
5	50	**trace**

(a) Yields were determined by GCFID with tridecane as internal standard.

Table 3-9. Copper Loading in C-O Bond Borylation of Silyloxyarenes.

Next, amounts of copper co-catalyst was then explored. Based on the amount of nickel catalyst, a 1:1 ratio of copper to nickel resulted in inferior results than the 2:1 ratio previously used (Table 3-9, entries 1-2). A 2:1 ratio proved to be optimal between copper and nickel, with increased amounts of copper resulting in inferior results (Table 3-9, entries 3-4). Interestingly, increasing further to a 5:1 ratio of copper to nickel resulted in only trace product being observed (Table 3-9, entry 5). Several solvents were explored, which all proved inferior to toluene, although cyclopentyl methyl ether resulted in only a small decrease in yield. Therefore, a 2:1 ratio of copper to nickel and toluene were kept as the optimal conditions going forward.

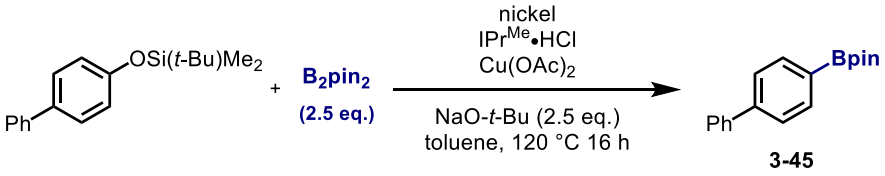

Entry	Nickel (mol %)	IPr^{Me}•HCl (mol %)	$Cu(OAc)_2$ (mol %)	yield[a]
1	$Ni(COD)_2$ 10 mol%	20	20	**72%**
2	$Ni(COD)_2$ 5 mol%	10	10	**50%**
3	$Ni(acac)_2$ 10 mol%	20	20	**>98%**
4	$Ni(acac)_2$ 5 mol%	10	10	**92%**
5	$Ni(acac)_2$ 2.5 mol%	5	5	**34%**

(a) Yields were determined by GCFID with tridecane as internal standard.

Table 3-10. Catalyst Optimization in C-O Bond Borylation of Silyloxyarenes.

The nickel catalyst was then explored, looking at catalysts loadings and other pre-catalysts. Using bis(1,5-cyclooctadiene) nickel(0), cutting the catalyst loading in half to 5 mol% resulted in a 50% yield, from 72% yield (Table 3-10, entries 1-2). However, using 10 mol% nickel(II) acetylacetonate resulted in near quantitative yield (Table 3-10, entry 3). The catalyst loading could be cut in half without any significant decrease in yield (Table 3-10, entry 4), although decreasing catalyst loadings by half again resulted in only 34% yield (Table 3-10, entry 5). Switching to a nickel(II) pre-catalyst also allowed the reaction to be set up without a glovebox. Due to only a

small decrease in yield by cutting the catalyst loading to 5 mol% with nickel(II) acetylacetonate, this pre-catalyst and loading was used for further optimization.

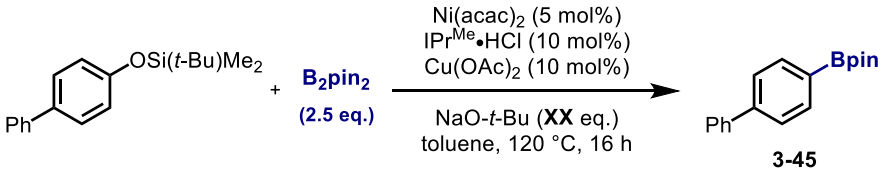

Entry	NaO-*t*-Bu equivalents	yield[a]
1	0.2	**trace**
2	1.0	**15%**
3	1.5	**70%**
4	2.0	**79%**
5	2.5	**92%**
6	3.0	**42%**
7	5.0	**24%**

(a) Yields were determined by GCFID with tridecane as internal standard.

Table 3-11. Sodium *tert*-butoxide Equivalents in C-O Bond Borylation of Silyloxyarenes.

The stoichiometry of sodium *tert*-butoxide was next investigated, and using catalytic amounts only gave trace product (Table 3-11, entry 1). Increasing to one equivalent also resulted in poor yield, with 15% product observed (Table 3-11, entry 2). Although use of 1.5 or 2.0 equivalents gave good yields (Table 3-11, entries 3-4), they were both inferior to the 2.5 equivalents used in previous studies (Table 3-11, entry 5). Additional equivalents of base above 2.5 resulted in poor yields (Table 3-11, entries 6-7).

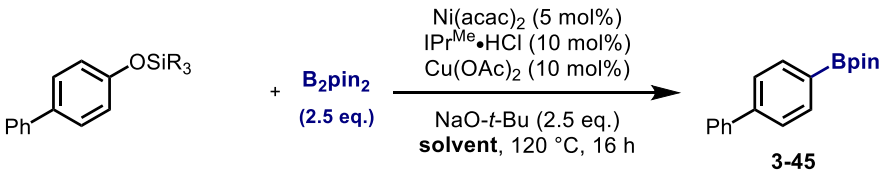

Entry	Silane Protecting Group	yield[a]
1	TES	**77%**
2	TBS	**92%**
3	TIPS	**46%**

(a) Yields were determined by GCFID with tridecane as internal standard.

Table 3-12. Silane Protecting Groups in C-O Bond Borylation of Silyloxyarenes.

Finally, several different silane protecting groups were explored to ensure *tert*-butyldimethysilyl was again optimal. A smaller silane protecting group, triethylsilyl, resulted in only a small decrease in yield with 77% product observed (Table 3-12, entry 1). A larger silane protecting group, triisopropysilyl, resulted in a moderate yield of 46% (Table 3-12, entry 3). Therefore, *tert*-butyldimethylsilyl was maintained as the optimal protecting group. Control reactions were also run to ensure all catalytic components were required for product formation, and no product was observed without nickel pre-catalyst, ligand, or base. However, a moderate yield of 34% can be obtained without copper co-catalyst.

3.3.2.2 Substrate Scope for C-O Bond Borylation of Silyloxyarenes

After good yields were obtained for C-O bond borylation of silyloxyarenes, an initial substrate scope was explored (Table 3-13). In addition to our model substrate (**3-45**), other simple biphenyl and naphthyl silyloxyarenes were borylated under our reaction conditions in good yields. Both meta (**3-48**) and ortho substitution resulted in good yields, with only a 10% decrease in the case of 1-naphthyl (**3-48**) substrate, compared to the 2-naphthyl (**3-47**) compound. Finally, isolated aromatic substrates (**3-49, 3-50**) also gave good yields of the borylated product, considering the difficulty in activating the C-O bond of these isolated aromatic systems. For example, the method reported for C-O borylation of aryl methyl ethers was unable to borylate isolated aromatic systems without directing groups. Heterocycles were also explored and currently result in modest yield (**3-51**). The decreased yield for these substrates results from mixtures of products derived from C-H borylation, where an increased acidity of C-H bonds on heterocyclic substrates result in increased borylation. Such C-H borylations have been reported recently.[183,184] However, this currently complicates use of heterocyclic substrates in this C-O bond borylation of silyloxyarenes.

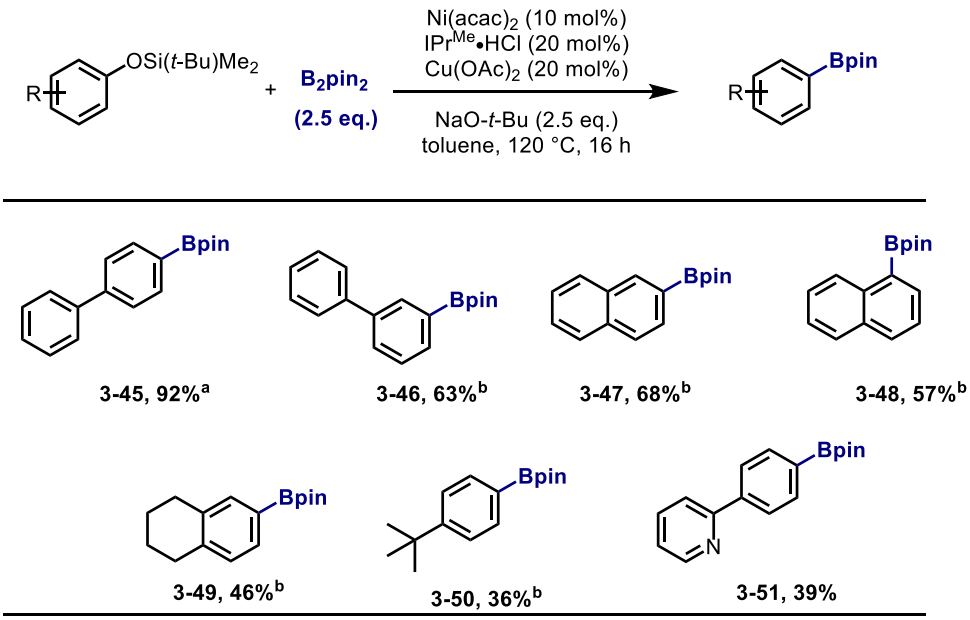

(a) Reactin used 5 mol% $Ni(acac)_2$, 10 mol% IPr^{Me}•HCl, 10 mol% $Cu(OAc)_2$ and yields were determined by GCFID with tridecane as internal standard. (b) Cyclopentylmethyl ether used as solvent.

Table 3-13. Initial Substrate Scope for C-O Bond Borylation of Silyloxyarenes.

3.3.2.3 Mechanism for C-O Bond Borylation of Silyloxyarenes

Although no detailed mechanistic investigations have been conducted, our proposed mechanism is based on reaction trends observed in our silyloxyarene C-O bond couplings and literature precedent. Our proposed mechanism for borylation is analogous to our proposed mechanism for C-O bond reduction of silyloxyarenes, with a more complete mechanistic description on aspects of the proposed mechanism available in section 2.3.3. Generation of $Ni(IPr^{Me})_2$ is proposed, which then produces the catalytically active catalyst through substitution of one NHC ligand with *tert*-butoxide, generating complex **K**. Next, coordination of nickel catalyst of substrate, through η^2 coordination, makes complex **L**. Oxidative addition of the silyloxyarene C-O bond to the nickel catalyst and dissociation of one alkoxide generates a neutral nickel complex (**M**). With a copper co-catalyst, copper(II) acetate produces a copper alkoxide through ligand substitution, which transmetallates with bispinacolatodiboron, to form a copper-boryl complex for transmetallation with nickel complex **M**. This regenerates copper alkoxide and produces a nickel-

boryl complex (**N**). Alternatively, nickel complex **M** can directly transmetallate with bispinacolatodiboron to generate complex **N**, which then undergoes reductive elimination to produce the aryl boron and close the catalytic cycle upon association of *tert*-butoxide. As copper is not required to obtain moderate yields of product, direct transmetallation of B_2pin_2 with complex **M** is operable but competitive with the copper co-catalyzed pathway in the presence of copper(II) acetate.

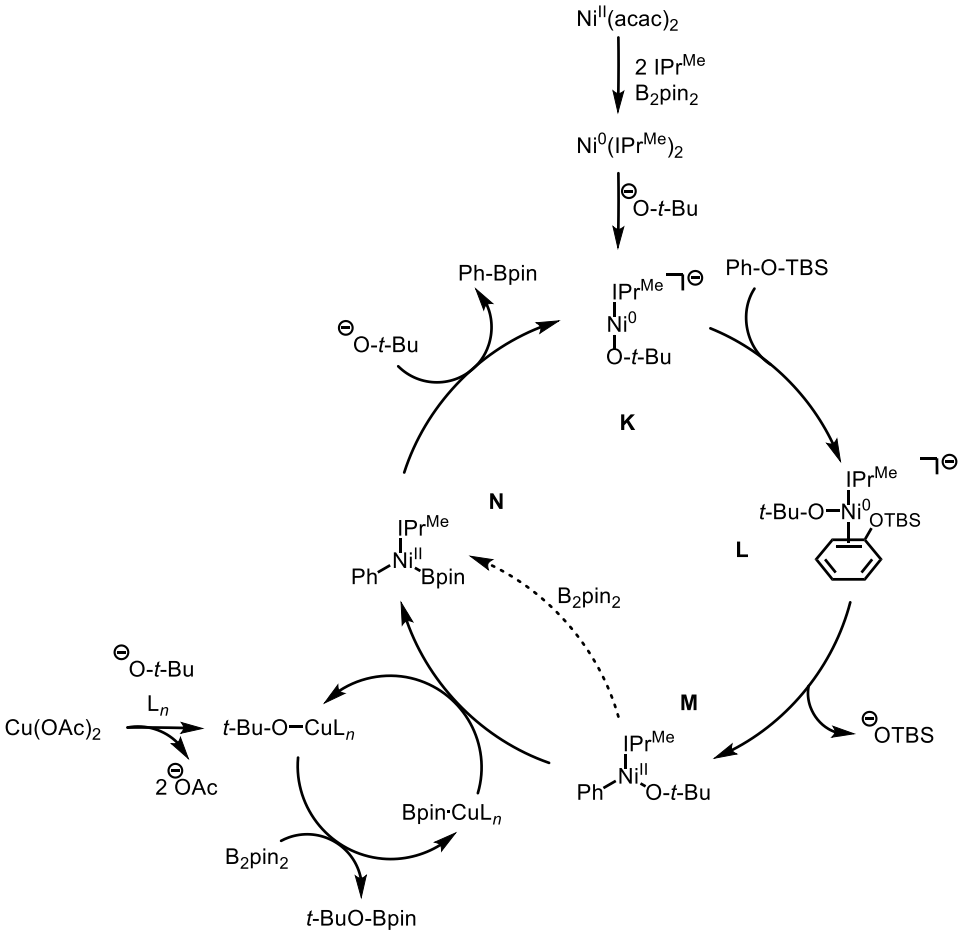

Scheme 3-8. Proposed Mechanism for C-O Bond Borylation of Silyloxyarenes.

3.3.3 C-O Bond Suzuki Coupling of Silyloxyarenes

Direct aryl-aryl coupling of silyloxyarene C-O bonds and aryl borons was also explored to access biaryl compounds. Furthermore, the unexpected C-H borylation currently presents

limitations in the in C-O bond borylation with heterocyclic substrates, and direct coupling was explored as a complementary and alternative method by focusing on using heterocyclic silyloxyarene substrates.

3.3.3.1 Optimization for C-O Bond Suzuki Coupling of Silyloxyarenes

Suzuki coupling of silyloxyarene C-O bonds was first explored with inspiration from Garg.[57] Similar conditions were explored using combinations of sodium *tert*-butoxide and potassium phosphate. However, no product was observed using combinations of these bases across a variety of ligands commonly employed for inert C-O bond activation, such as electron-rich phosphines and aliphatic or aryl NHC ligands. Some dual-catalytic methods were also briefly explored using palladium or copper co-catalysts; however, this approach did not result in the desired product. Drawing inspiration from aryl methyl ether C-O bond Suzuki coupling, addition of cesium fluoride resulted in product formation, although yields were low (Scheme 3-9). Aryl boronate esters derived from Bpin could also be used and generally resulted in slightly better yields.

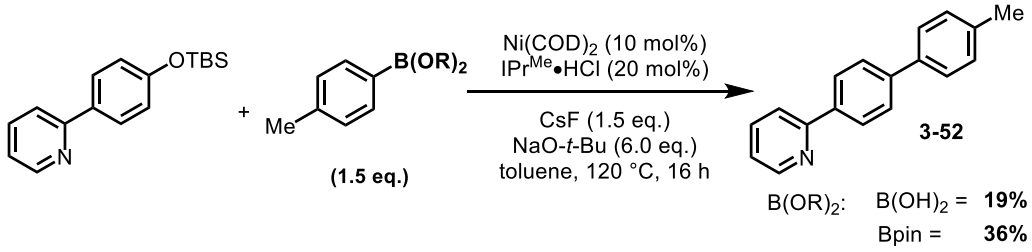

Scheme 3-9. Initial Suzuki Coupling of Boronic Acids and C-O Bonds of Silyloxyarene with Cesium Fluoride.

In addition to the low yields, high loadings of base and cesium fluoride were used and further optimization was necessary to move away from these limitations. A range of different solvents were explored but did not improve yields. Water as a co-solvent was employed but did not result any significant product. Other ligands used in inert C-O bond activation were explored but did not result in improved yields. Higher yields could be obtained by decreasing the amounts

of both bases and moving to a conjugated silyloxyarene substrate (Scheme 3-10). These conditions also gave similar yields using ([1,1'-biphenyl]-4-yloxy)(*tert*-butyl)dimethylsilane as a substrate.

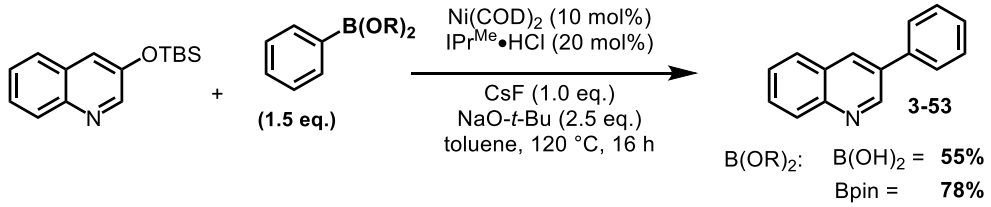

Scheme 3-10. Suzuki Coupling of Aryl Borons and C-O Bonds of Silyloxyarenes with Cesium Fluoride.

Several heterocyclic silyloxyarene substrates were explored, including 6-((*tert*-butyldimethylsilyl)oxy)-2-methylquinoline, 3-((*tert*-butyldimethylsilyl)oxy)pyridine, 2-((*tert*-butyldimethylsilyl)oxy)pyridine, and 2-(4-((*tert*-butyldimethylsilyl)oxy)phenyl)pyridine, all resulting in yields ranging from 30-60%. These substrates showed a variety of heterocyclic silyloxyarene substrates would be compatible with the methodology. However, improved yields were desired, and the ratio of aryl boron to silyloxyarene was then explored for optimization. Yields decreased when using a lower ratio than 1.5:1, and increased slightly when 1.75 equivalents of aryl boron to silyloxyarene were used. However, a 1.5:1 ratio of aryl boron to silyloxyarene was maintained as the optimal conditions, where increased amounts of aryl boron could be used for challenging substrate.

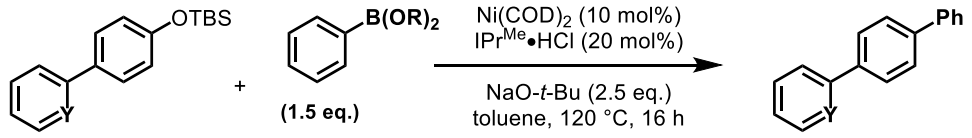

entry	$B(OR)_2$	Y	yield[a]
1	$B(OH)_2$	CH	**NP**
2	Bpin	CH	**34%**
3	$B(OH)_2$	N	**38%**
4	Bpin	N	**67%**

Table 3-14. Suzuki Coupling of Aryl Boronic Acid or Boronate Esters and C-O Bonds of Silyloxyarenes with or without Lewis Basic Sites.

Interesting, looking at lower loadings of either cesium fluoride or sodium *tert*-butoxide, ranging from catalytic amounts to four equivalents, did not result in a change to the yield outside of the 60-70% range, with 3-((*tert*-butyldimethylsilyl)oxy)quinoline and phenyl boronic acid pinacol ester as substrates. This questioned the role of cesium fluoride in these reactions. Through some control experiments across several different substrates, cesium fluoride was found to be required for reactivity when using aryl boronic acids and simple silyloxyarenes without Lewis basic sites. However, cesium fluoride was not required for heterocyclic aryl boronic acids or for both classes of substrates with aryl boronate ester coupling partners (Table 3-14).

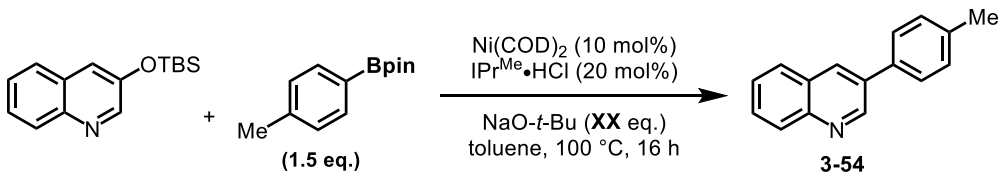

entry	NaO-*t*-Bu Equivalents	yield[a]
1	0.5 eq. NaO-*t*-Bu	**89%**
2	2.5 eq. NaO-*t*-Bu	**92%**

(a) Yield determined by NMR with dibromomethane as internal standard. Isolated yields are in parentheses.

Table 3-15. Current Optimized Conditions for Suzuki Coupling of 3-((*tert*-butyldimethylsilyl)oxy)quinoline.

Fewer equivalents of sodium *tert*-butoxide could also be used with activated substrates containing Lewis basic sites on the silyloxyarene or aryl boron coupling partner. Additionally, for activated naphthyl substrates, slightly higher yields were obtained using lower reaction temperatures to 110 or 100 degrees Celsius. More optimization needs to be conducted to obtain higher yields, and currently there are two different conditions based on the substrate employed. One for the highly reactive 3-quinoline substrate, where yields in the 90s are obtained (Table 3-15), and another for other silyloxyarene substrates which are not as activated, and do not have the C-O bond on the heterocyclic ring (Table 3-16). Slightly higher yield in these reactions can be obtained by increasing the amount of aryl boron.

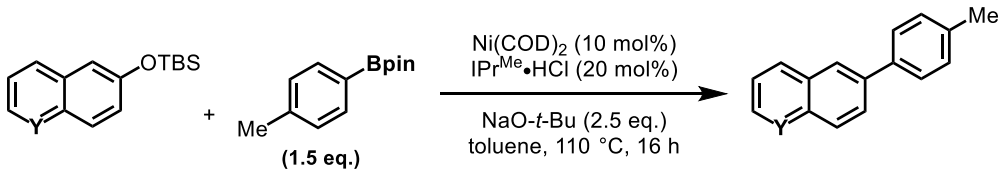

entry	Y	yield[a]
1	N	**52%**
2	CH	**54%**

(a) Yield determined by NMR with dibromomethane as internal standard. Isolated yields are in parentheses.

Table 3-16. Current Optimized Conditions for Suzuki Coupling of Silyloxyarene.

3.3.3.2 Substrate Scope for C-O Bond Suzuki Coupling of Silyloxyarenes

An exploration of substrate scope has not been conducted yet as further optimization needs to be preformed to obtain higher yields. However, after further optimization, the method should be general to a range of substrates, as several different heterocyclic silyloxyarene substrates have already been shown to be competent in the Suzuki reaction. One area that needs further attention is the use of isolated aromatic substrates. These substrates were briefly explored in our optimization but due to low yields in the 20s-30s, biphenyl and naphthyl substrates when then explored for ease of isolation.

3.4 Conclusions and Future Directions for C-O Bond Amination, Borylation, and Suzuki Coupling of Silyloxyarenes

A variety of transformations have been developed to display the toolbox of methods that could be used in late-stage silyloxyarene C-O bond coupling, including, amination, borylation, and Suzuki coupling. Development of C-O bond amination of silyloxyarenes has improved the reaction scope for inert C-O bonds, allowing for isolated aromatic substrates and primary aliphatic amines. Miyaura couplings have also led to improvements in scope for inert C-O bonds, as isolated aromatics systems without a directing group can now be utilized as substrates. Further work needs to be conducted to fully explore the capabilities of both the borylation and Suzuki reactions.

However, early findings suggest both reactions should have good substrate scope and be broadly applicable.

Future directions include completing the substrate scope for Miyaura coupling. Additionally, direct coupling of the in-situ generated aryl boronate ester should be, allowing for homocoupling of silyloxyarene C-O bonds. This was briefly explored but may be easier to develop after we have a greater understanding of the Suzuki coupling reaction. This would allow silyloxyarene C-O bonds to be used as both electrophilic and nucleophilic coupling partners in homo or heterocoupling reactions. Other future directions related to these projects are described in chapter 5.

Chapter 4

Nickel-Catalyzed Sequential and Orthogonal Couplings of Silyloxyarenes

4.1 Introduction to Sequential and Orthogonal Couplings

The ability to conduct a late-stage, selective coupling is important to medicinal chemists for rapid diversification of a common intermediate, allowing for molecules to be efficiently stitched together and to rapidly build up complexity. Two methods are commonly employed, iterative and sequential derivatization (Scheme 4-1).[185] Whereas iterative routes have intermediate deprotection or deprotection-activation strategies, sequential routes allow for direct coupling of functional groups in a molecule in succession, without intermediate steps. Iterative routes are commonly employed in synthesis; however, the increased step count from deprotection or deprotecting-activation make them less advantageous than direct sequential routes (Scheme 4-1).

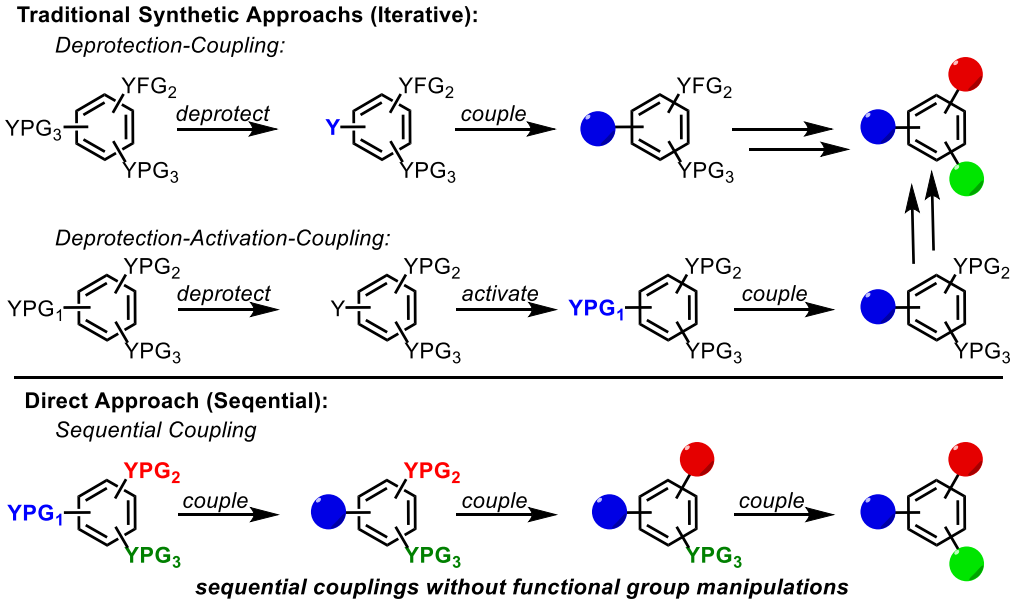

Scheme 4-1. Iterative Diversification and Sequential Diversification.

Sequential diversification allows for a rapid growth in complexity of a core scaffold and efficiently accesses related molecules for creating chemical libraries. Most importantly, utilizing routes that do not require intermediate protecting group manipulations provides the most direct and attractive routes due to minimization of step count, time, reagents, and waste generated in such steps. However, development of sequential diversification routes is challenging, often due to the similarity in reactivity of coupling groups. Therefore, sequential coupling strategies are typically limited to two or three steps. Commonly utilized strategies to obtain high selectivity is through attenuating reactivity of the electrophile and selectivity derived from the nucleophile or catalyst system. The most commonly explored area for developing sequential coupling routes are with aryl electrophiles due to the diverse number of electrophilic derivatives and coupling methods.

Aryl electrophiles are attractive because of the large range of reactivity in common aryl electrophilic coupling partners, from aryl iodides to aryl methyl ethers, where the large range of reactivity allows for sequential couplings. Sequential couplings with aryl electrophiles demonstrates a proof-of-principle on how other substrate classes could be developed. Utilizing methods with coupling groups that are typically considered inert is necessary for sequential couplings as later steps require these handles to be stable through previous steps. In this way, the same properties that make inert electrophiles useful for late-stage diversification, also make them relevant in sequential couplings. However, sequential coupling routes of aryl electrophiles are still challenging to design due to the lability of some aryl electrophiles and low functional group tolerance or low activity in a coupling reaction. Despite many challenges, there have been several examples of sequential coupling routes using aryl electrophiles.

The vast majority of sequential couplings only display two sequential couplings in a row, where few examples show three sequential couplings. Therefore, this background section will

focus on sequential couplings of aryl electrophiles with greater than two steps, concentrating on how longer sequential couplings could be developed. An early example displayed use of a trisubstituted benzene ring (**4-1**) with chloride, nitrile, and methoxy groups for sequential coupling.[186] This allowed them to access a benzene product (**4-4**) with three different aryl substituents by coupling from most reactive chloride to least reactive methoxy (Scheme 4-2). Two Suzuki couplings were used to install the first two aryl groups and a Kumada coupling installed the final phenyl group.

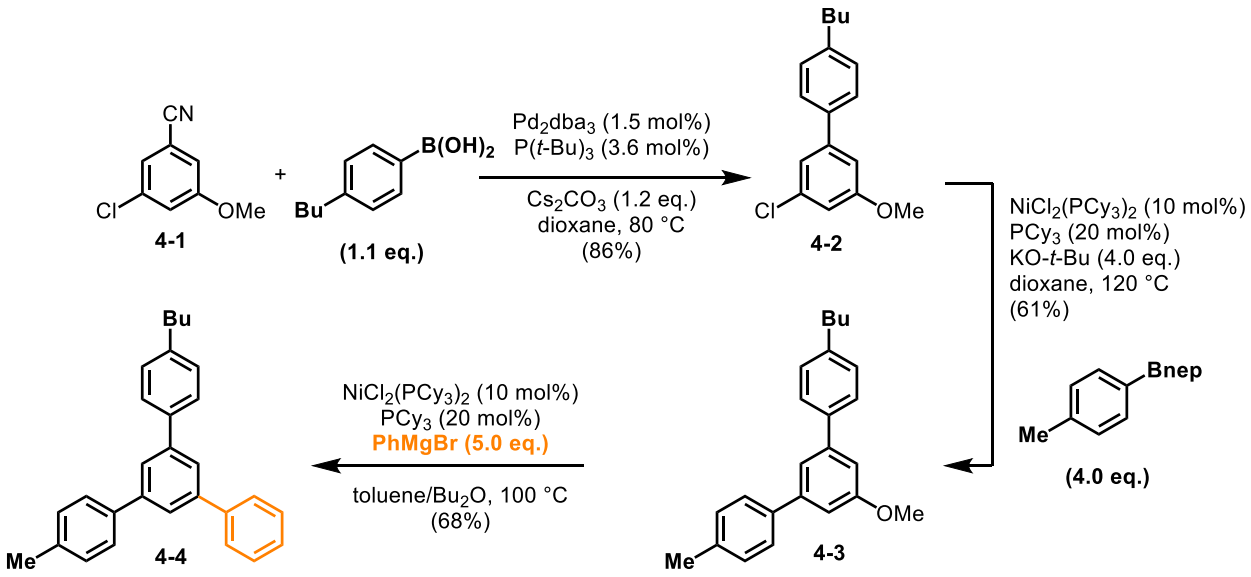

Scheme 4-2. Sequential Coupling towards Trisubstituted Benzene using Chloride, Nitrile, and Methoxy Groups.

This approach for generation of tri-substituted benzene compounds was further expanded with a full publication dedicated to the programmed selective couplings of C-O bonds (Scheme 4-3).[187] Substrate scopes for each of the three coupling reactions was displayed, where three different C-O electrophilic coupling partners were utilized (**4-5**). Use of three different protected C-O bonds, triflate, carbamate, and methoxy, allowed for a range of reactivity of the C-O bonds and for selective coupling of the most activated C-O bond, triflate, to the most inert C-O bond, methoxy.

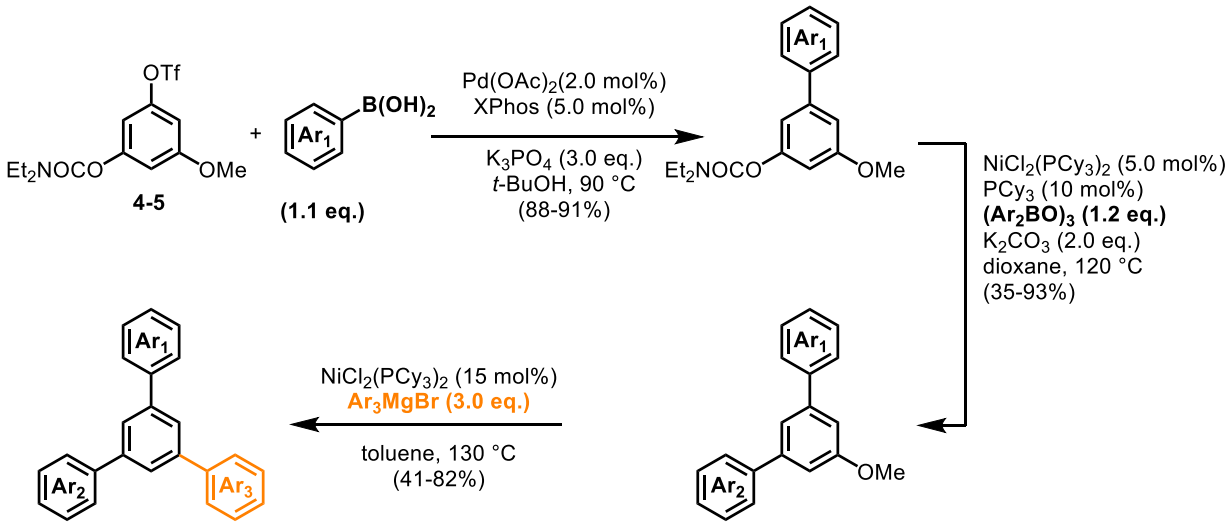

Scheme 4-3. Programmed Selective Sequential Coupling using Triflate, Carbamates, and Methoxy Groups.

Since these two initial reports, other analogous strategies have been used with the same tri-substituted starting material. A similar sequential coupling using three C-O bonds was reported, except a pivalate (**4-6**) was used instead of the carbamate (Scheme 4-4).[38] Although they utilized the same first step, a Suzuki coupling mediated by palladium catalysis for C-O bond coupling of the triflate, the strategies diverged by using two aryl-alkyl couplings for subsequent steps. First the pivalate (**4-7**) was coupled with an alkyl boron and then the methyl ether (**4-8**) was coupled with an organolithium reagent to generate the final product (**4-9**).

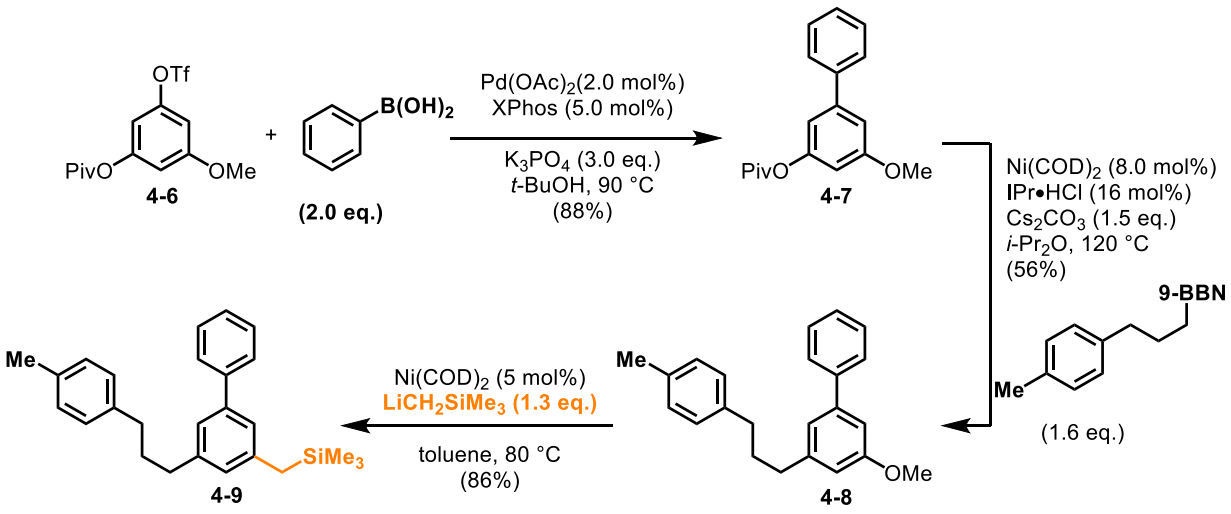

Scheme 4-4. Programmed Selective Sequential Coupling Using Triflate, Pivalate, and Methoxy Groups.

One final example explored a similar strategy with the tri-functionalized benzene ring, containing bromo, chloro, and pivalate electrophiles (Scheme 4-5).[74] This displayed tolerance of pivalates in two transition metal-catalyzed couplings of a bromide and a chloride. Additionally, use of three different transition metals for the three different couplings added significance to this example. A copper-catalyzed amination of the aryl bromide (**4-10**), palladium-catalyzed Suzuki coupling of the aryl chloride (**4-11**), and nickel-catalyzed stannylation of the pivalate (**4-12**) displayed the reactivity order of these aryl electrophiles.

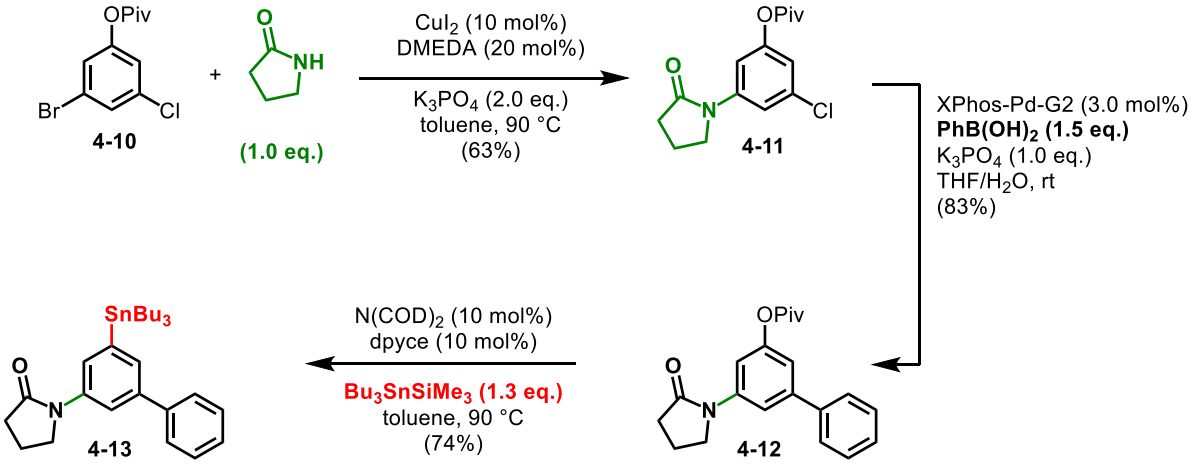

Scheme 4-5. Programmed Selective Sequential Coupling Using Bromo, Chloro, and Pivalate Groups.

The above examples are excellent illustrations of how these commonly utilized C-O bond electrophiles can be utilized in selective, sequential couplings. However, as they all utilize the same starting material scaffold, other configurations of electrophiles would further show the significance of this strategy. Furthermore, adding additional couplings would substantially increase the diversity and modularity of the final compound. In addition to developing longer and more diverse sequential coupling routes, ideally being able to reverse the inherent reactivity that determines coupling order of aryl electrophiles would be even more advantageous and add additional modularity to these approaches.

This ability to orthogonally couple aryl electrophiles would represent a large advance and be useful for applications in sequential couplings and for organic synthesis. Orthogonal couplings are attractive because divergent, selective coupling of two different aryl electrophiles allows for increased modularity in synthetic routes (Scheme 4-6). However, this is even more challenging than developing sequential couplings, and has only been displayed on unbiased substrates between aryl triflates and aryl chlorides or bromides. This is due to the difficultly in overcoming the inherent reactivity of one of the coupling partners while maintaining high selectivity.

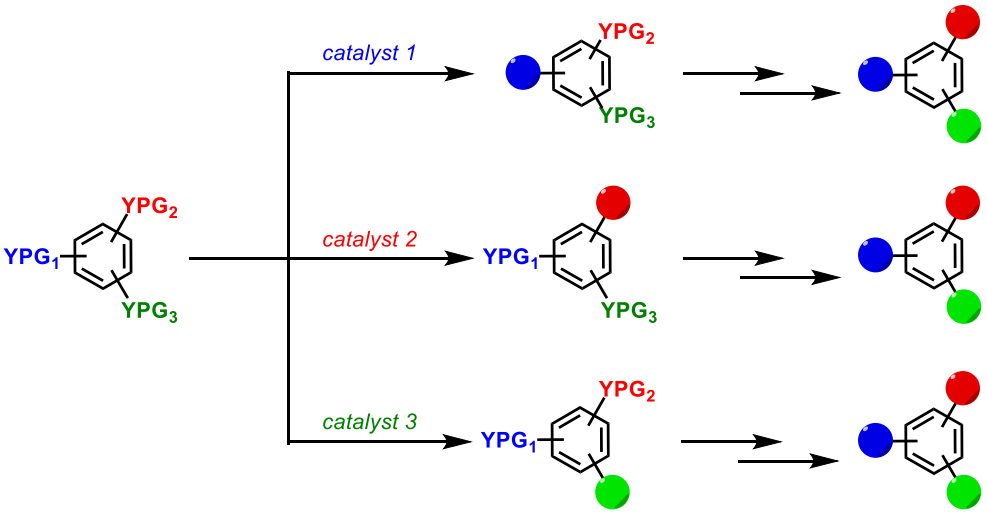

Scheme 4-6. Orthogonal Coupling Strategies.

One of the early examples in exploring orthogonality between two aryl electrophiles (**4-13**) was conducted in Stille couplings with vinyl stannanes (Scheme 4-7).[188] Decent selectivity was observed between bromide and triflate, based on the starting catalyst and solvent choice. Non-polar solvents with tetrakis(triphenylphosphine)palladium(0) resulted in moderate selectivity for coupling the bromide (**4-14**) and polar solvents with bis(triphenylphosphine)palladium(II) dichloride resulted in moderate selectivity for coupling the triflate (**4-15**). Higher selectivity was observed when temperatures were decreased for these reactions. The observed selectivity between

triflate and bromide electrophiles was proposed to derive from coordination number on the palladium catalyst and ability of the triflate to direct the palladium catalyst.

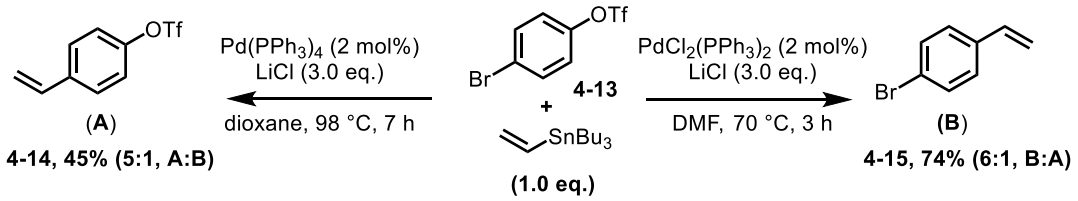

Scheme 4-7. Orthogonal Coupling of Aryl Bromide and Aryl Triflate in Palladium-catalyzed Stille Couplings.

Hayashi explored the orthogonal coupling of 4-bromophenyl trifluoromethanesulfonate (**4-13**) in Kumada couplings with phenyl magnesium bromide.[189] It was found that a bidentate ligand, 1,3-bis(diphenylphosphino)propane, resulted in selective coupling of the triflate (**4-17**), and a monodentate ligand, 2-(diphenylphosphino)-2'-methoxy-1,l'-binaphthyl, resulted in selective coupling of the bromide (**4-16**, Scheme 4-8). No traces of coupling the opposite aryl electrophile first was observed, although small amounts of the di-coupled products were detected. This was the first successful example of orthogonal coupling with a palladium catalyst, determined solely by choice of ligand.

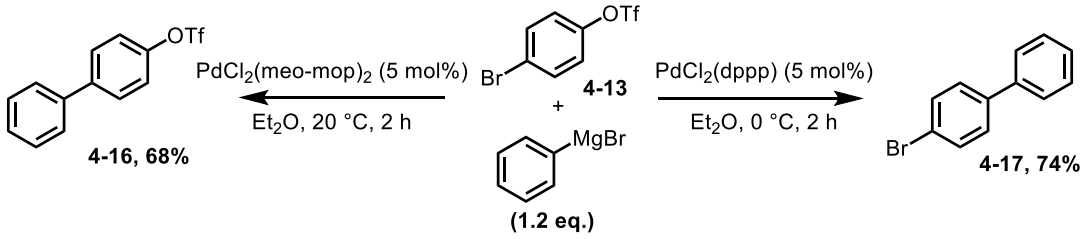

Scheme 4-8. Orthogonal Coupling of Aryl Bromide and Aryl Triflate in Palladium-catalyzed Kumada Couplings.

Another example of orthogonal coupling of aryl electrophiles was described by the Fu group (Scheme 4-9).[190] The unbiased substrate utilized in the orthogonal couplings was 4-chlorophenyl trifluoromethanesulfonate (**4-18**), where a phenyl ring contained para-substituted chloride and triflate electrophiles. The Fu group found that judicious choice of catalyst enabled orthogonal coupling of these aryl electrophile in a Suzuki coupling. Using

tris(dibenzylideneacetone)dipalladium(0) with tri-*tert*-butylphosphine the aryl chloride was coupled (**4-19**), and using palladium(II) acetate with tricyclohexylphosphine the aryl triflate was reacted (**4-20**).

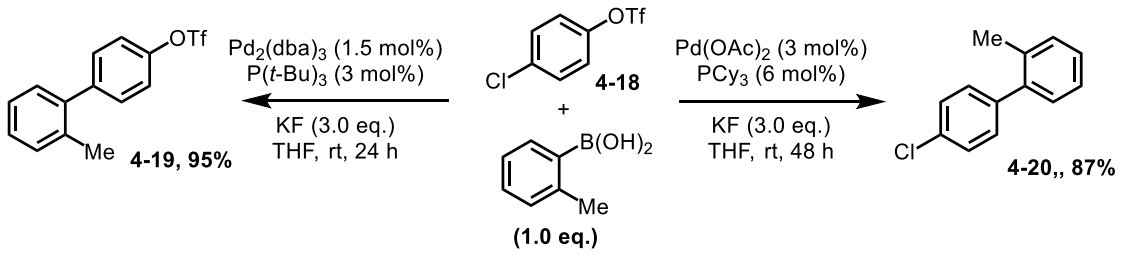

Scheme 4-9. Orthogonal Coupling of Aryl Chloride and Aryl Triflate in Palladium-catalyzed Suzuki Couplings.

Houk and Schoenebeck explored the origin of selectivity for the above example (Scheme 4-9) and found that reversal in the inherent reactivity of the aryl chloride is due to having a monoligated palladium complex. This complex reacts with the weaker aryl electrophile C-X bond, the aryl chloride C-Cl bond. Selectivity for the triflate C-O bond is due to having a di-ligated palladium complex that is directed by the triflate protecting group.[191] Subsequent studies further explored this catalyst selectivity by investigating a larger range of phosphines.[192] Schoenbeck further explored solvent effects in this system and also found that selective coupling of the triflate was possible using conditions to couple the aryl chloride (**4-21**), except using a polar solvent, acetonitrile. (Scheme 4-10).[193]

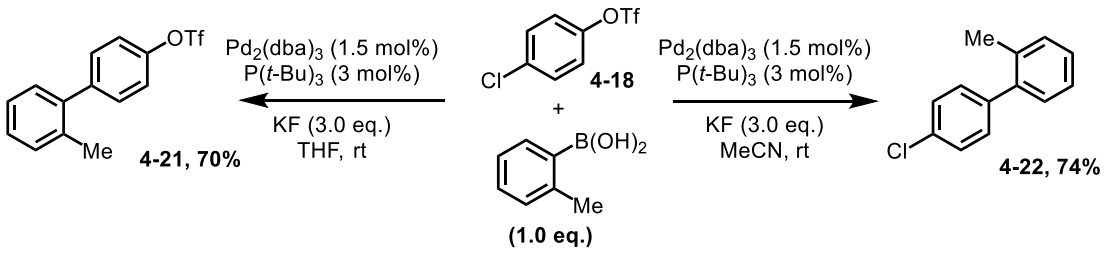

Scheme 4-10. Orthogonal Coupling of Aryl Chloride and Aryl Triflate in Palladium-catalyzed Suzuki Couplings Based on Solvent.

Schoenbeck went on to show selectivity between the two aryl electrophiles in nonpolar or polar solvents was derived from generation of an anionic palladium complex. Initially,

computations were conducted to explore solvent coordination or electrostatic stabilization, but neither was shown to support the observed selectivity. Another proposal involved coordination of a fluoride ion to generate an anionic palladium complex and activate the triflate. This was supported by using the Stille coupling as a model reaction, as the stannane coupling partners are not coordinating and can be conducted without additives. These experiments validated this proposal where Stille couplings with a coordinating ion, fluoride, results in coupling of the triflate (**4-23**) and use of a non-coordinating ion, PF_6, resulted in coupling of the aryl chloride (**4-24**, Scheme 4-11).[193,194]

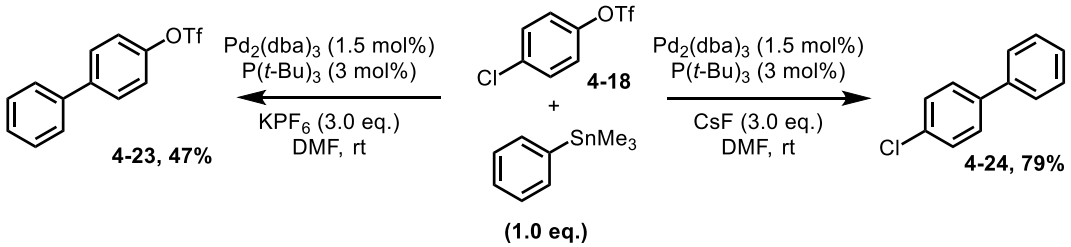

Scheme 4-11. Orthogonal Coupling of Aryl Chloride and Aryl Triflate in Palladium-catalyzed Stille Couplings Based on Additive.

An example showing orthogonal selectivity based on the nucleophilic coupling partner has also been described between triflate and bromide.[195] Based off of the above works by Hayashi[189] and Fu,[190] a variety of different coupling reactions were explored and discovered that using the same reactions conditions for Suzuki couplings with boronic acids resulted in coupling the aryl bromide. However, other common nucleophilic coupling partners reacted with the triflate, including Kumada, Negishi, Stille, amination, and Heck reactions (Scheme 4-12).[195] They proposed the observed selectivity was determined by the nucleophilic coupling partner. The difference between the boronic acid and the other coupling partners was proposed to derive from activation of the boronic acid by the bromide. However, they also propose that other activation processes for the boron species could be operable and no support for any of these hypotheses was included.

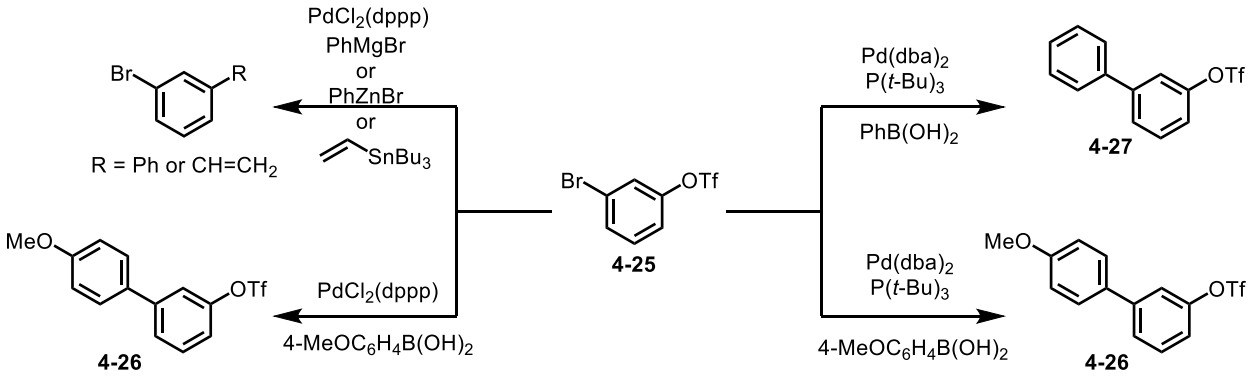

Scheme 4-12. Orthogonal Couplings of Triflate and Bromide Based on Nucleophilic Coupling Partner.

A recent example explored use of a palladium-catalyzed amino carbonylation reaction for orthogonal couplings of bromide and triflate electrophiles (Scheme 4-13).[196] Chemoselective coupling was observed based on the ligand and solvent utilized. A combination of xantphos and toluene resulted in coupling of the aryl bromide (**4-28**), where dppf ligand and dimethylsulfoxide resulted in coupling of the triflate (**4-29**). A large solvent effect was observed for these two ligands. Interestingly, when instead exploring bulky, monodentate phosphine ligands, solvent choice did not influence the chemoselectivity. They supported the empirical findings through computations and found that differences in polarities of the bromide and triflate C-X bonds resulted in the selectivity, as triflate activation required polar solvents to stabilize the transition state and the bromide did not.

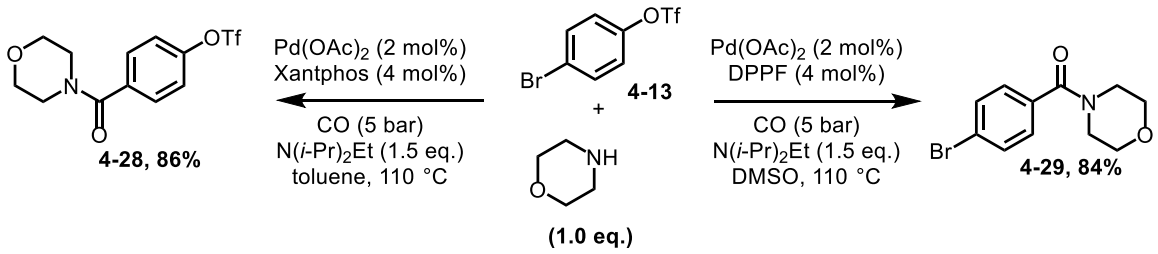

Scheme 4-13. Orthogonal Coupling of Aryl Bromide and Aryl Triflate in Palladium-catalyzed Carbonylation Based on Solvent and Ligand.

In addition to the above examples for unbiased orthogonal couplings, where chemoselectivity is derived from the catalyst or nucleophilic coupling partner, there are also many

examples using biased substrates where selectivity is determined on the electrophilic coupling partner. A recent example of utilizing biased substrates to obtain orthogonal coupling is from the Sigman group.[197] Although these cases are useful, they are limited to the specific substrate explored and are not general as if unbiased substrates were not used the same selectivity would not be obtained. Thus, the development of methods that have catalyst selectivity are the most useful for general application. All the above examples have utilized activated electrophilic coupling partners and palladium catalysts. Therefore, developing orthogonal couplings using inert protecting groups and nickel catalysts would both explore new areas in the field of orthogonal couplings.

4.2 Orthogonal Couplings with Silyloxyarenes and Aryl Methyl Ethers

Inspired by palladium-catalyzed orthogonal couplings of triflates with bromides or chlorides, the use of aryl methyl ethers and silyloxyarenes as orthogonal coupling partners was envisioned under nickel catalysis. This approach was hypothesized, as aryl methyl ethers are well tolerated under reaction conditions we developed for silyloxyarene C-O bond coupling. However, as the aryl methyl ether C-O bond is stronger than a silyloxyarene C-O bond, this result follows the reactivity order of the two inert C-O bonds. The more challenging part of developing orthogonal couplings of aryl methyl ethers and silyloxyarenes would be reversing this inherent selectivity to couple the aryl methyl ether C-O bond first.

Reversing coupling order is extremely challenging and has only been demonstrated using triflates in the field of cross-coupling. The ability of the triflate to act as a directing group allows a palladium catalyst to activate the stronger aryl C-O bond over the aryl C-Br or C-Cl bonds. The difference between aryl C-OMe and aryl C-$OSiR_3$ bonds is less significant than the difference between aryl C-OSO_2CF_3 and aryl C-Br or C-Cl. Neither aryl methyl ethers nor silyloxyarenes

possess significant directing capabilities for a transition metal catalyst, and the only major difference between the groups is their size. Silane protecting groups utilized in C-O couplings are typically large compared to a methyl group. Therefore, finding a method that could utilize the steric differences between the two electrophiles, with the higher reactivity of silyloxyarene C-O bonds, could lead to orthogonal couplings of the two groups (Scheme 4-14).

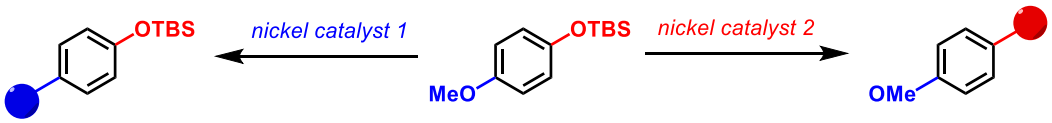

Scheme 4-14. Sequential Coupling Strategy of Aryl Methyl Ethers and Silyloxyarenes.

One key finding towards orthogonal coupling of aryl methyl ethers and silyloxyarenes was discovered through optimization of silyloxyarene C-O bond coupling reactions (Chapters 2 and 3). Use of phosphine ligands and aliphatic NHC ligands, common ligands for aryl methyl ether C-O activation, did not activate the silyloxyarene C-O bond. This suggested that catalyst selectivity could be feasible and lead to selective activation of the more inert aryl C-OMe bond with these ligands. Furthermore, support for this approach was found by use of very large TIPS protecting groups being tolerated in aryl methyl ether C-O bond couplings.[88,107]

Studies exploring orthogonal couplings began with an unbiased, difunctionalized naphthyl substrate with methoxy and silyloxy substituents (**4-30**). A naphthyl substrate was explored due to the low reactivity of aryl methyl ethers with biphenyl or isolated aromatic systems under nickel catalysis. Additionally, milder nucleophilic coupling partners were explored as strongly nucleophilic reagents have been shown to couple silyloxyarene C-O bonds under nickel catalysis with phosphine ligands.[161]

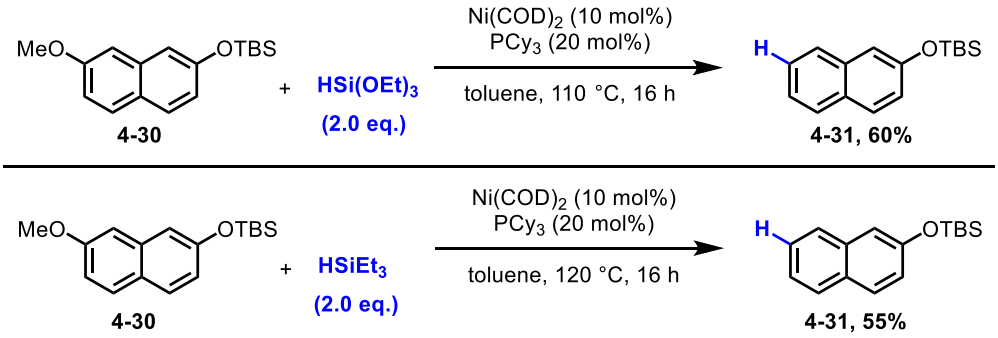

Scheme 4-15. Aryl Methyl Ether C-O Bond Reductive Deoxygenations of *tert*-butyl((7-methoxynaphthalen-2-yl)oxy)dimethylsilane.

Initial experiments suggested that selective coupling of the aryl methyl ether C-O bond could prove general with phosphine ligands, as good yields were obtained in reductive deoxygenation reactions using silane reductants. Both trialkoxysilanes[100] and trialkylsilanes[65] resulted in good yields of the desired product with only trace amounts of products derived from silyloxyarene C-O bond coupling (Scheme 4-15).

We also found that silylation of the aryl methyl ether C-O bond can be favored by use of previously reported methods using silylborons with nickel catalysts, which presumably makes a silyl anion.[104] Although this reaction does not use a mild coupling partner or a ligand, and could thus couple the silyloxyarene C-O bond, it was explored to determine the origin of selectivity. Conversion for this reaction was low, but the major product was silylation of the aryl methyl ether C-O bond, with significant amounts of disilylation (Scheme 2-13). However, no appreciable amounts of the product corresponding to initial silylation of the silyloxyarene C-O bond were observed, where the silyloxyarene C-O bond was coupled and the aryl methyl ether remained untouched. Interestingly. the opposite selectivity was observed with our silylation method (Scheme 2-14). Other reactions were also explored following previously published methods, including amination,[105] borylation,[107] and Suzuki reactions.[180] However, compatibility issues with ligand or bases used in these reactions need to be resolved as poor results are currently obtained.

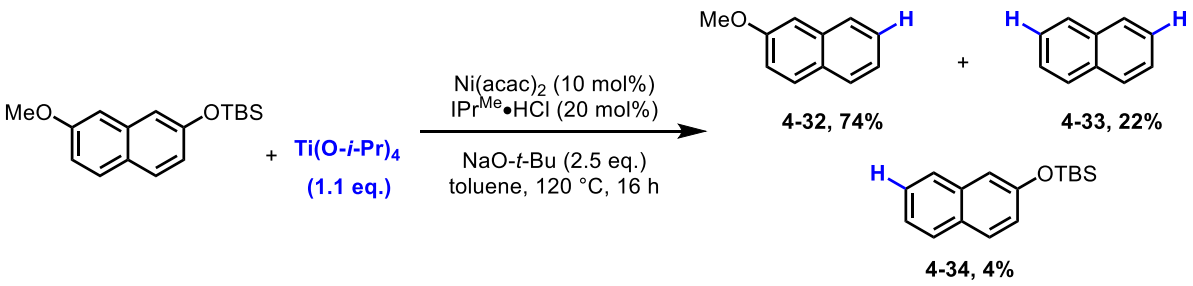

Scheme 4-16. Silyloxyarene C-O Bond Reductive Deoxygenation of *tert*-butyl((7-methoxynaphthalen-2-yl)oxy)dimethylsilane.

Looking at selective coupling of the silyloxyarene C-O bond, the same reductive deoxygenative coupling can be conducted, resulting in a high yield of the desired product using our developed method (Scheme 4-16). Even though C-O bond selectivity was high, there were small amounts of products derived from activation of the aryl methyl ether C-O bond, primarily naphthalene due to over reduction of the substrate after silyloxyarene C-O bond reduction.

Next, coupling reactions to increase functionality through C-O bond coupling of silyloxyarenes and aryl methyl ethers were explored to illustrate orthogonal coupling routes. Starting from the same difunctionalized naphthyl substrate (**4-30**), use of our amination methodology with octylamine results in coupling of the silyloxyarene C-O bond (**4-35**, Scheme 4-17). Subsequent coupling of the remaining aryl methyl ether C-O bond, using a reported method for Csp^2-Csp^3 coupling with an aliphatic NHC ligand,[96] resulted in alkylation of the aryl methyl ether (**4-36**). The low yield for this coupling was likely due to the use of an unprotected primary aliphatic amine.

Orthogonality was then shown by starting from the same difunctionalized naphthyl starting material (**4-30**), where the product (**4-36**) can be accessed by reversing the order of the steps. Trimethylaluminum can again be used for selective coupling of the aryl methyl ether C-O bond (**4-37**). Next, the silyloxyarene C-O bond can be coupled with octylamine to generate the same final product in good yield (**4-36)**. This divergent, convergent sequence displays the orthogonality

of aryl methyl ether with silyloxyarenes. However, due to moderate yields being obtained, alternative coupling partners were explored to obtain higher yields.

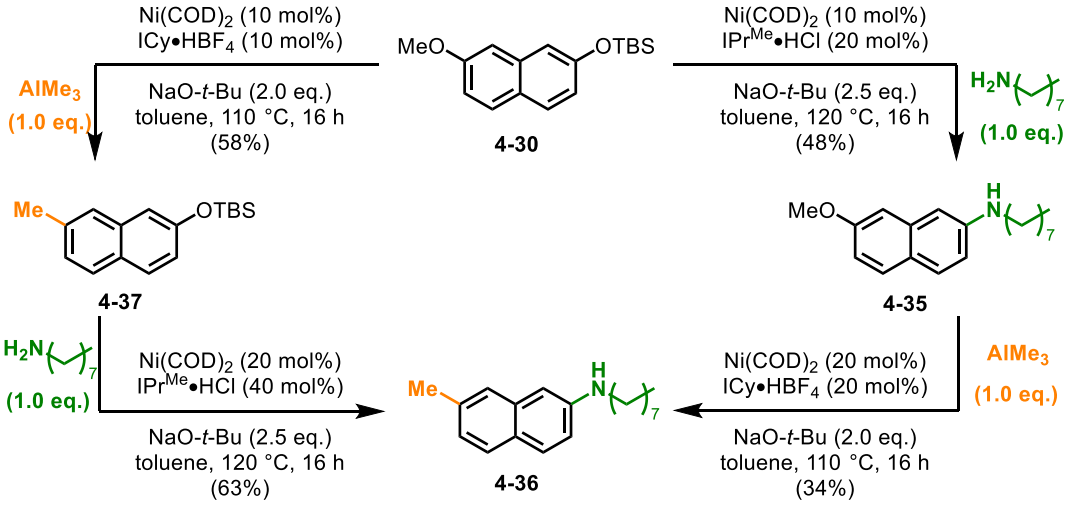

Scheme 4-17. Orthogonal Coupling Routes with Octylamine and Trimethylaluminum.

As secondary aliphatic amines typically result in higher yields in our developed nickel-catalyzed amination reactions of silyloxyarene C-O bonds than primary aliphatic amines, they were explored to improve the yield (Scheme 4-18). Simply switching amines did resulted in an improved yield for product, where selective coupling of the silyloxyarene C-O bond with 1-methypiperazine was observed (**4-38**). Next, coupling of the aryl methyl ether C-O bond with triethylaluminium gave a good yield of the product (**4-39**), where a bidentate phosphine ligand could be used.[97] The order of reactions can again be reversed by first coupling the aryl methyl ether C-O bond with triethylaluminium (**4-40**). Coupling of the aryl methyl ether C-O bond first showed excellent selectivity, where no product derived from silyloxyarene C-O bond coupling was observed. Finally, the same product (**4-39**) can be obtained by coupling the silyloxyarene C-O bond with 1-methypiperazine in high yield. Use of different coupling partners resulted in higher yields, but both of these orthogonal coupling routes explicitly show the first display of switching the selectivity between aryl methyl ethers and silyloxyarenes.

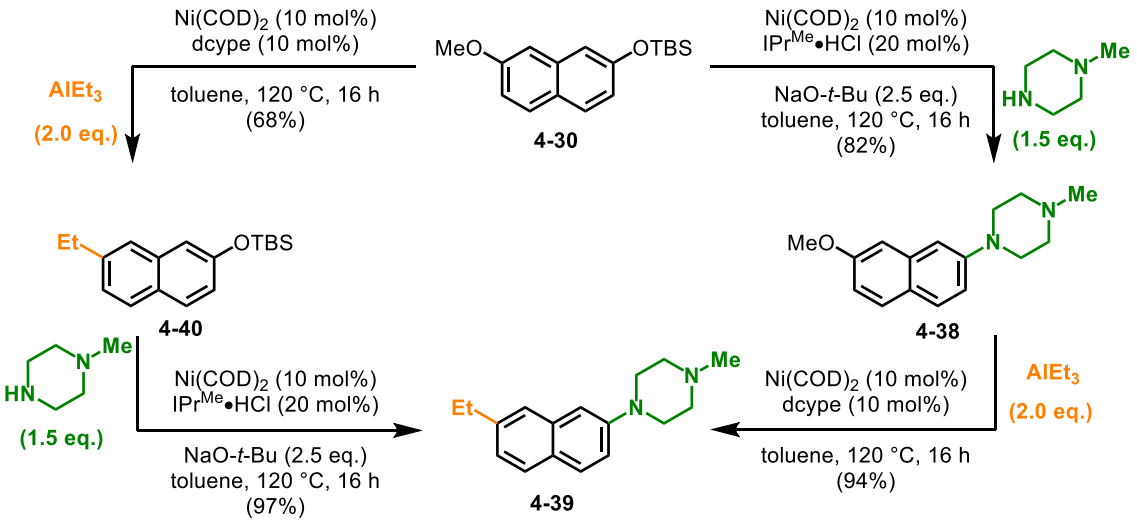

Scheme 4-18. Orthogonal Coupling Routes with 1-methylpiperazine and Triethylaluminum.

The origin of the selectivity between aryl methyl ether C-O bonds and silyloxyarene C-O bonds could be due to several different reasons, including selectivity derived from the catalyst, electrophilic partner, or nucleophilic partner. As an unbiased substrate (**4-30**) was utilized in these orthogonal coupling experiments, the electrophilic coupling partner is not resulting in the observed selectivity. Additionally, the nucleophilic coupling partner is unlikely resulting in the observed selectivity as several nucleophilic coupling partners have been shown to generate the same selectivity, including, silanes, trialkylaluminum reagents, silylboranes, and amines. Finally, the most likely factor that determines orthogonal coupling of the two electrophiles is catalyst selectivity, which derives from the ligands utilized in the two couplings.

A range of ligands has been shown to selectively activate aryl methyl ether C-O bonds while not activating silyloxyarene C-O bonds, such as, PCy_3, ICy, and dcype. This suggests that chemoselectivity is derived from the catalyst system. Furthermore, selectivity is poor when ligands are removed from the reaction (Scheme 2-13). Additionally, use of a ligand that has been shown to activate aryl methyl ether C-O bonds and silyloxyarene C-O bonds, such as amination methods for aryl methyl ethers,[105,106] shows a mixture of products. Strong evidence for catalyst selectivity

is observed when looking at silane coupling partners, as the nucleophilic coupling partner does not change but orthogonal reactivity is still observed due to differences in the ligands for the two reactions (Scheme 4-19). Despite the lower yields observed for these reactions, reaction trends suggest ligands are influencing the selectivity.

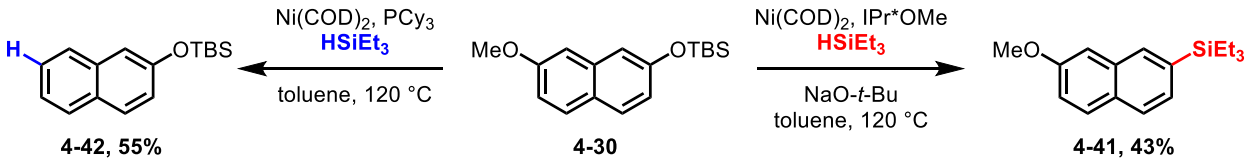

4-42, 55% **4-30** **4-41, 43%**

Scheme 4-19. Orthogonal Coupling of Aryl Methyl Ethers and Silyloxyarene C-O Bonds with Silanes.

One possibility of how the ligands are influencing selectivity can be observed by evaluating the catalyst employed. Aryl methyl ether C-O bond activation with PCy_3 and ICy use a 2:1 ratio of ligand to nickel catalyst. It is proposed that having two of these ligands on nickel is too large to allow for activation of the silyloxyarene C-O bond due to the large silane protecting group. The presence of a di-ligated nickel complex using these mono-dentate ligands is supported by use of a bidentate phosphine ligand, dcype, which also selectively activates the aryl methyl ether C-O bond. In our catalyst system, the active catalyst is proposed to only have one NHC ligand bound. Having one large NHC ligand is not too sterically encumbered to approach the large silyl protecting group, allowing for activation of the more reactive C-O bond. Additionally, another reason for our catalyst system favoring the silyloxyarene C-O bond could be generation of inactive catalysts if an aryl methyl ether C-O bond is activated by generation of a nickel carbonyl complex[148,151]

However, further studies need to be conducted to confirm catalyst selectivity and rule out the influence of the nucleophilic coupling partner on selectivity. Although preliminary studies have been conducted, current methods that use the same nucleophilic coupling partner for both C-O bonds need to be further developed. Currently, poor yields are obtained for aryl methyl ether coupling due to inefficient catalysts for electron-rich aryl systems or having a ligand that activates

both C-O bonds with conjugated aryl systems. For example, aminations of aryl methyl ethers use IPr as a ligand, which is a moderate ligand for silyloxyarene C-O activation, and mixtures of products are observed. Suzuki or borylation couplings of aryl methyl ethers use bases that result in some deprotection of the silyloxy group or have low reactivity for the aryl methyl ether C-O bond. Even with some uncertainty in the mode of selectivity, implications of the general orthogonal coupling strategy are very exciting and should be a powerful method alongside other coupling reactions.

4.3 Sequential Couplings with Silyloxyarenes

Having developed orthogonal couplings of aryl methyl ethers and silyloxyarenes, applications of this orthogonality was explored in sequential couplings. Furthermore, demonstration of silyloxyarene C-O bonds for late-stage coupling was envisioned, where the inert silyloxyarene C-O bond could be carried through multiple steps and coupled late in the sequence. Therefore, two distinct sequential coupling routes were envisioned where the orthogonality of silyloxyarenes and aryl methyl ethers could be displayed by switching the order of their couplings.

Planning for the first sequential coupling began by exploring benzene rings with three unique aryl electrophiles, where a fourth would be introduced through the first aryl coupling reaction and generate a biphenyl scaffold. Selective generation of the biphenyl scaffold would demonstrate a coupling of one aryl electrophile in the presence of four possible aryl electrophilic coupling partners. Sequential coupling of the three remaining aryl electrophiles on the biphenyl scaffold would then demonstrate four sequential couplings without any protecting group manipulations.

Studies began by exploring 2-bromo-5-chlorophenol (**4-43**) and (4-((tert-butyldimethylsilyl)oxy)phenyl)boronic acid (**4-45**) as the two substrates contained four different

aryl electrophiles, where coupling would generate the biphenyl scaffold (Scheme 4-20). Initial protection of the phenol with a methyl group set all the aryl electrophiles, thereby removing intermediate protecting group manipulations between coupling reactions. Initial coupling of the aryl bromide (**4-44**) and boronic acid (**4-45**) under palladium catalysis gave a good yield of the biphenyl scaffold containing chloro, methoxy, and silyloxy electrophiles (**4-46**).

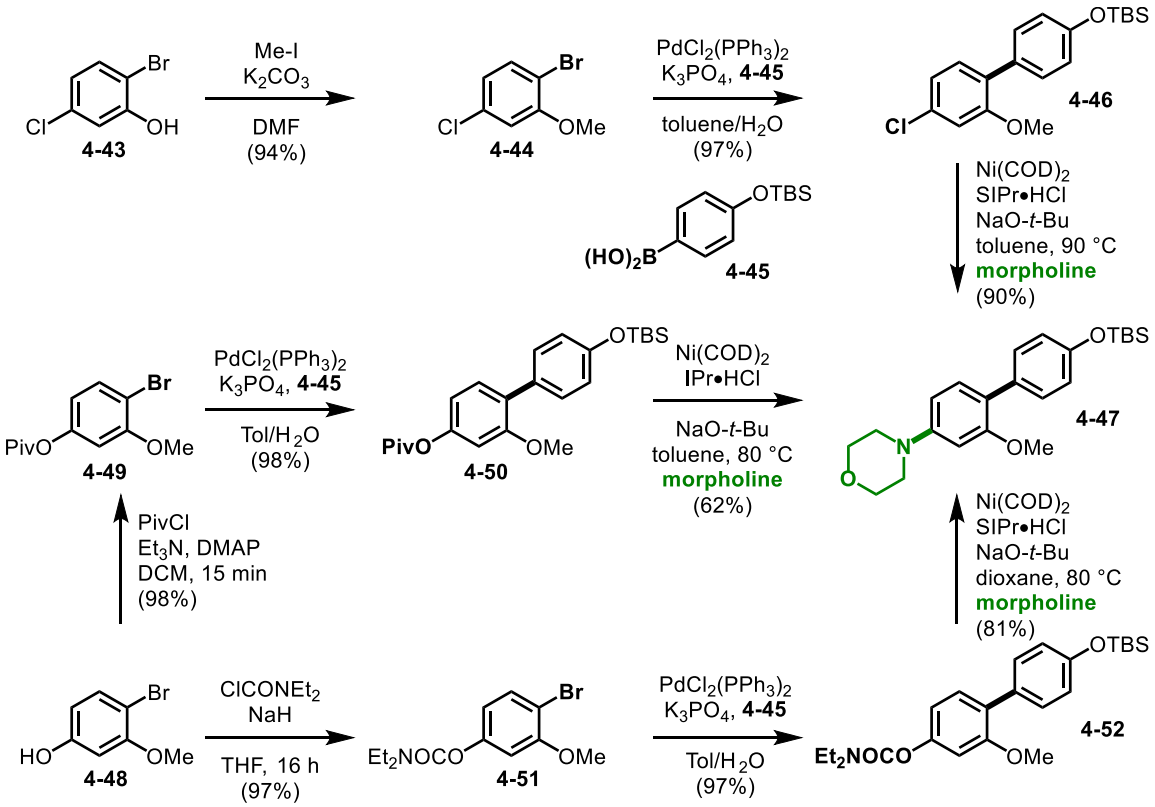

Scheme 4-20. Sequential Coupling with Biphenyl Scaffold with Bromo, Chloro, Pivalate, and Carbamate.

A range of commonly utilized aryl electrophiles was desired to describe how a variety of substrates could be utilized alongside silyloxyarenes in future coupling reactions or sequential coupling routes. Therefore, 4-bromo-3-methoxyphenol (**4-49**) was also explored and was considered analogous to 2-bromo-5-chlorophenol (**4-43**), upon protection with a carboxylate or carbamate protecting group. This would maintain the bromide as the most activated partner and generate the same scaffold derived from 2-bromo-5-chlorophenol (**4-46**), where an activated C-O

bond replaced the chloro substituent. Protection of 4-bromo-3-methoxy with pivaloyl chloride or diethylcarbamoyl chloride gave the desired intermediates (**4-59, 4-51**), which were carried on to the same palladium-catalyzed Suzuki coupling with (4-((tert-butyldimethylsilyl)oxy)phenyl)boronic acid (**4-45**) to give the analogous biphenyl scaffold (**4-50, 4-52**) previously obtained (**4-46**).

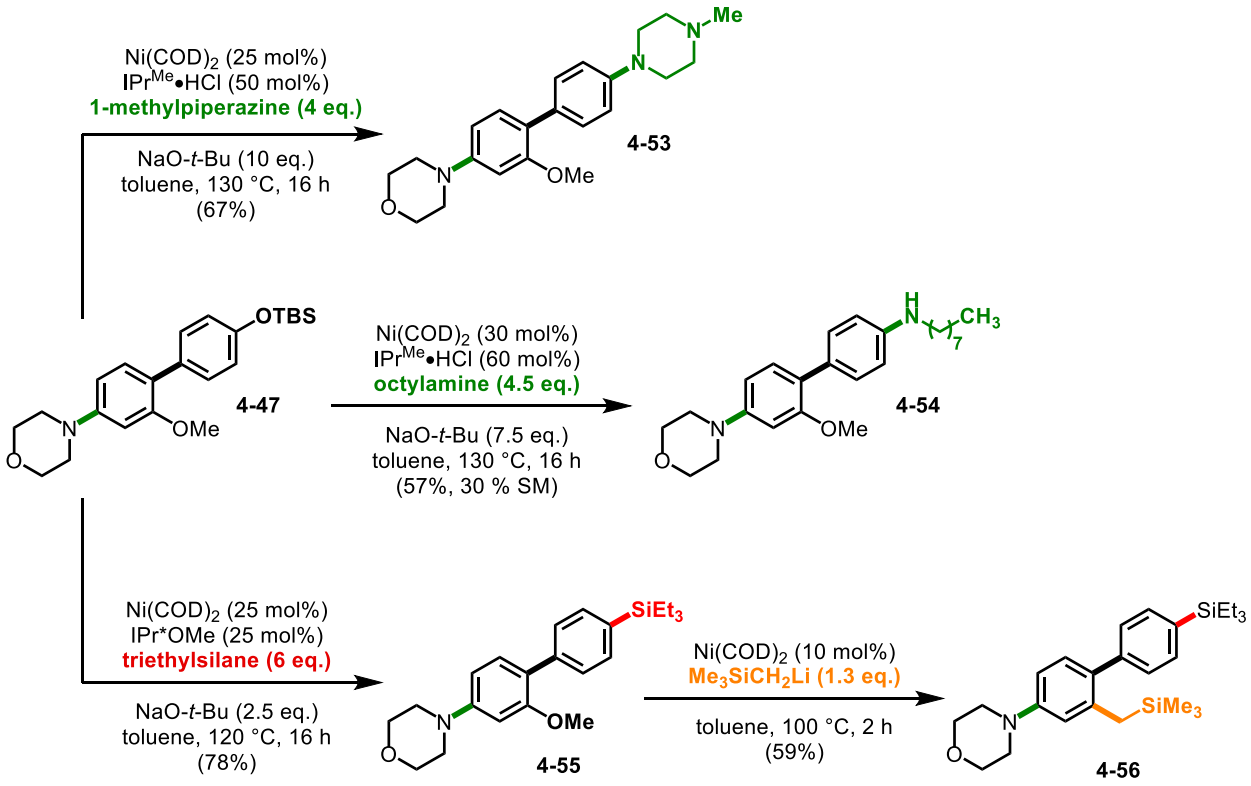

Scheme 4-21. Sequential Coupling with Biphenyl Scaffold with Silyloxyarene and Aryl Methyl Ether.

For the next step, several coupling reactions were envisioned with the chloro, pivalate, or carbamate. Initially, another Suzuki coupling was explored with a heterocyclic aryl boronic acid to add polarity and show tolerance of heterocyclic substrates in subsequent reactions. However, this coupling proved unsuccessful as a large quantity of deprotection was observed. Additionally, a convergent approach was desired where all three substrates would generate a single product through coupling each of the three aryl electrophiles, pivalate, carbamate, and chloro. Therefore, to provide diversity in the type of coupling reactions used in this sequential coupling route, and to

allow for high functional group tolerance to be displayed in subsequent couplings, a Buchwald-Hartwig amination was explored.

Based on previously reported methods, a nickel catalysts with a NHC ligand was utilized in each of the three couplings with chloro,[198] pivalate,[63] and carbamate[47] electrophiles. The pivalate proved to be the most problematic electrophilic coupling partner as the standard conditions for amination of aryl pivalates only resulted in a 14% yield, with the remaining mass balance being primarily deprotection. However, adding higher loadings of catalyst, ligand, amine, and base gave a good yield of 62%. This decrease in yield from the standard conditions is likely due to the large amount of electron-density in the aryl ring, slowing the oxidative addition and leading to competing deprotection. Higher yields were obtained for both carbamate and chloro electrophiles when using the same catalyst loading, allowing for direct comparison. Although, lower yields were also observed using 5 or 10 mol% catalyst for these two electrophiles, significantly higher yields were observed compared to coupling of the pivalate.

Having all three starting aryl scaffolds converge to a single product (**4-47**), a divergent approach was then envisioned going forward to display the toolbox of couplings that we have currently developed for silyloxyarenes (Scheme 4-21). Amination and silylation reactions were conducted on the biphenyl scaffold (**4-47**), which contained both silyloxy and methoxy functionalities. Both secondary (**4-53**) and primary (**4-54**) aliphatic amines can be coupled in good yield, with slightly lower yields observed with primary aliphatic amines on the electron rich biphenyl substrate (**4-47**). No coupling of the aryl methyl ether is observed and most of the remaining mass-balance of the reactions can be recovered as starting material. Use of our silylation methodology also resulted in a good yield of the aryl silane product (**4-55**), with great selectivity between the two inert aryl electrophiles.

For the final step, a variety of reactions were explored for aryl methyl ether C-O bond coupling. Initial use of a Suzuki coupling reaction[90] resulted in low conversion of the C-O bond and only gave reduction of the C-O bond. Use of stronger nucleophilic coupling partners was then explored. However, in-situ generation of heterocyclic, aryl organolithium reagents resulted in low conversion, where starting material was recovered. Therefore, use of preformed trimethylsilylmethyl lithium can be utilized following a reported methodology[95] to give the final product (**4-56**). Although the yield is moderate for this last step, the reported method notes that presence of an ortho-phenyl substituent hinders conversion for their reaction, as they saw a 68% yield for 2-methoxy-1,1'-biphenyl. Coupling the aryl methyl ether in this final step displays a sequential coupling sequence of four steps that circumvents intermediate protecting group manipulations or activations. To the best of our knowledge, this is the first example of such a route (Scheme 4-22).

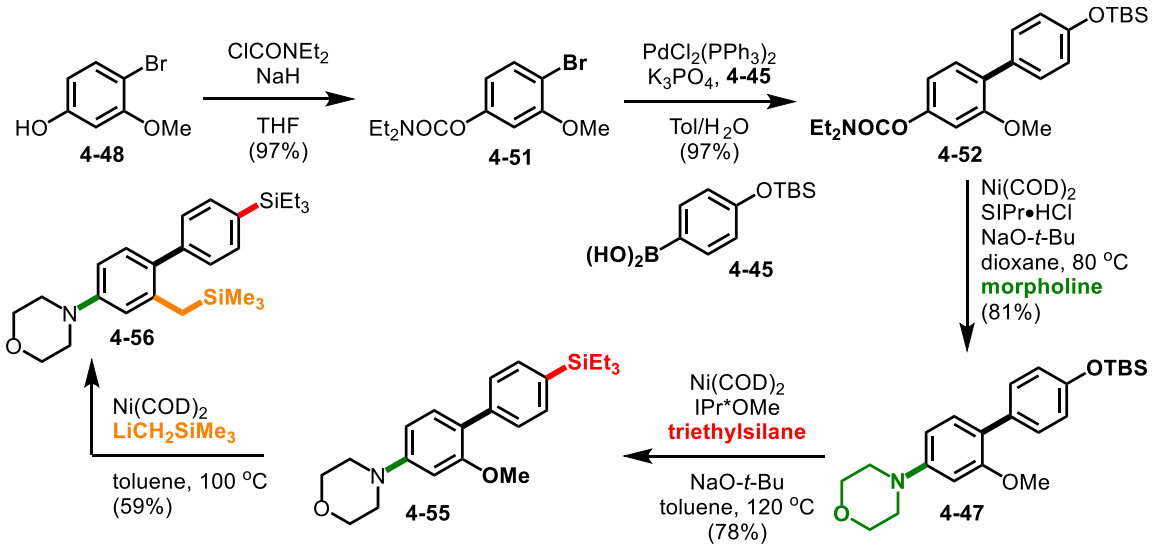

Scheme 4-22. Four-step Sequential Coupling Sequence without Protecting Group Manipulations of Biphenyl Scaffold.

Next, having developed orthogonal couplings between aryl methyl ethers and silyloxyarenes, the reversal in inherent reactivity of the C-O bonds was demonstrated in another sequential coupling. Studies began with generation of an aryl methyl ether (**4-58**) through

protection of 6-bromonaphthalen-2-ol (**4-57**). Suzuki coupling of the aryl bromide with a difunctionalized boronic acid (**4-59**) gave a naphthyl scaffold with three different aryl electrophiles (**4-60,** Scheme 4-23).

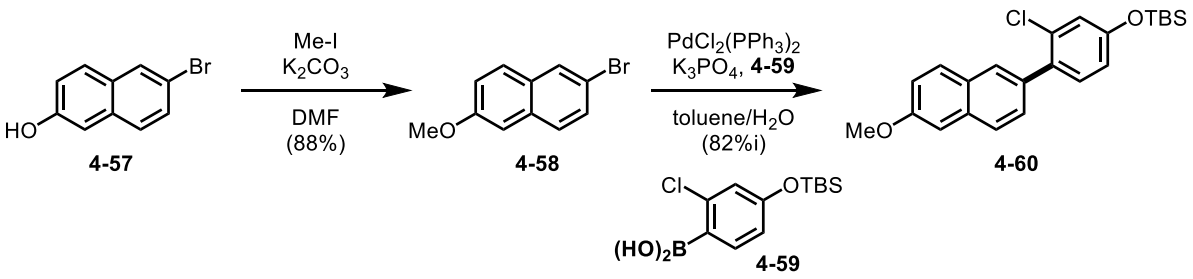

Scheme 4-23. Synthesis of Naphthyl Scaffold for Sequential Coupling Route.

Subsequent coupling began with the aryl chloride (**4-60**), the next most reactive aryl electrophile. Upon exploring potential coupling reactions, it was found that very few coupling reactions of aryl chlorides tolerate an ortho-phenyl or ortho-naphthyl group. An amination reaction with morpholine was first explored using a nickel-NHC catalyst.[199] However, as this method did not report any large ortho substituents in the substrate scope, the yield for coupling this sterically hindered aryl chloride was a modest 36% yield. However, switching to a palladium catalyst,[200] an improved yield of 65% was obtained with morpholine (**4-61**, Scheme 4-24). Next, coupling of the aryl methyl ether C-O bond, and reversing the inherent order of reactivity with silyloxyarenes was explored. However, using a method reported for alkylation[96] of aryl methyl ethers gave poor yields of the coupled product (**4-62**). Therefore, alternate routes were explored due to the low yields for these two steps.

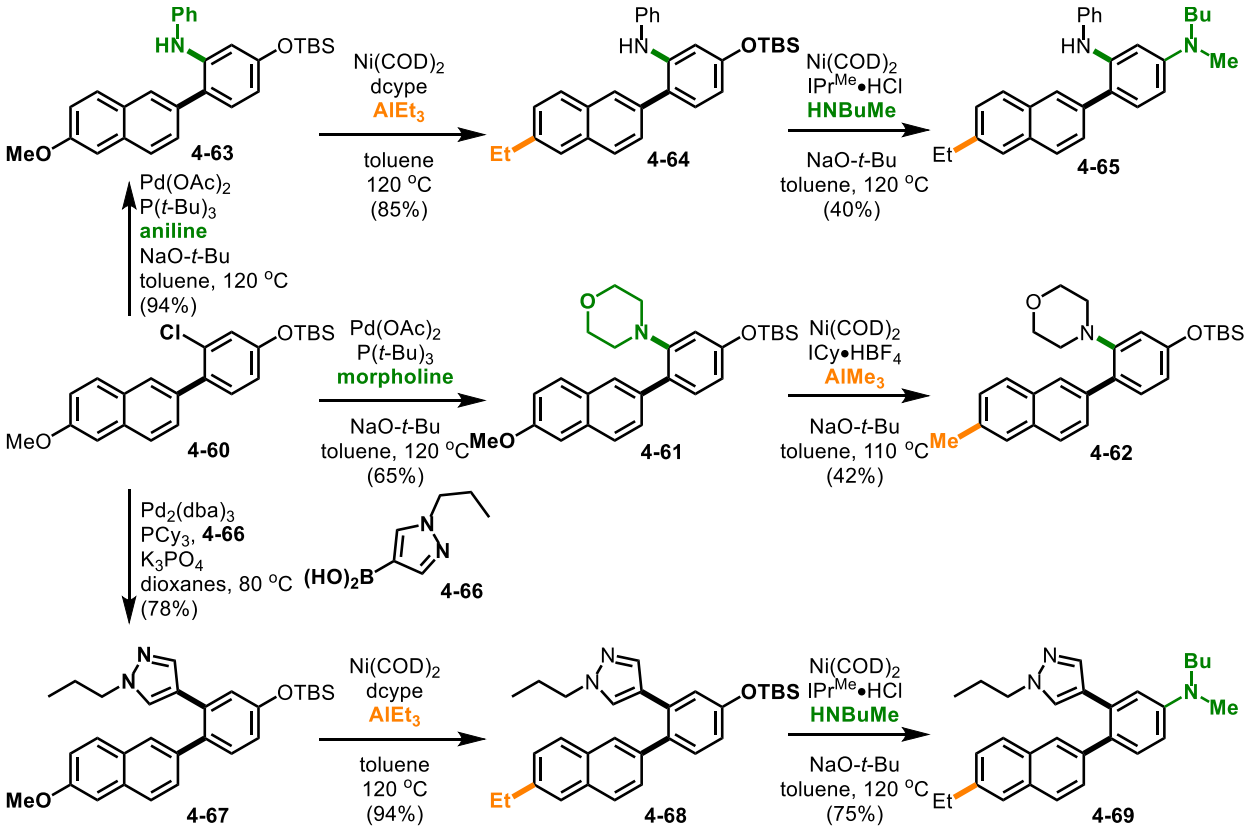

Scheme 4-24. Sequential Coupling of Naphthyl Scaffold.

Starting from the aryl chloride (**4-60**), a less hindered amine was utilized to give a higher yield. Use of aniline resulted in a higher yield of the coupled product (**4-63**), using the same palladium-catalyzed method used with morpholine. Next, coupling of the aryl methyl ether C-O bond with triethylaluminium gave a high yield of the desired product (**4-64**). Finally, coupling of the silyloxyarene C-O bond, which was carried through all previous coupling steps intact, was conducted using our developed amination methodology. However, the presence of the unprotected aniline proved problematic as a low yield was obtained due to competing coupling, as a mixture of products was observed. Additionally, low conversion was observed due to the electron-rich nature of the silyloxyarene substrate. Therefore, to improve yields, another route was constructed that would increase yields for the final step by removing competing reactions and decrease the electron density on the silyloxyarene.

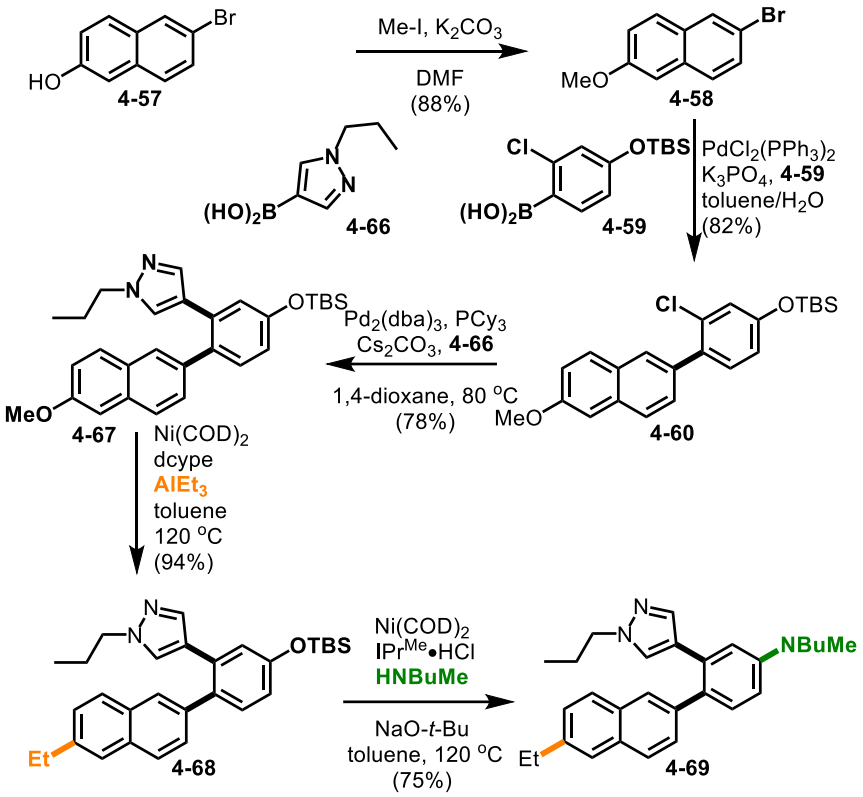

Scheme 4-25. Four-step Sequential Coupling of Naphthyl Scaffold.

Installation of a heterocycle at the aryl chloride was explored to withdraw electron density from the silyloxyarene ring. Initially, a C-H coupling was investigated using substrates with acidic C-H bonds, such as 4,5-dimethylthiazole. However, deprotection was observed as the major product. Thus, a Suzuki coupling[201] was explored using (1-propyl-1*H*-pyrazol-4-yl)boronic acid (**4-66**), which resulted in a good yield of the desired product (**4-67**). Coupling of the aryl methyl ether C-O bond with triethylaluminium gave a very good yield of the product (**4-68**). Finally, coupling of the silyloxyarene C-O bond with our amination methodology gave the fully functionalized product (**4-69**) in high yield with N-methylbutylamine as the coupling partner. Cyclohexylamine could also be utilized in this step, but a lower yield of 54% was obtained due to the more challenging primary aliphatic amine coupling partner. This sequential coupling sequence is another example of four sequential coupling reactions without any protecting group manipulations. Furthermore, it displays a practical example of the reversal in the inherent coupling

order between aryl methyl ethers and silyloxyarene C-O bonds (Scheme 4-25), and a late-stage coupling of a silyloxyarene C-O bond in the last step.

4.4 Conclusions and Future Directions of Sequential and Orthogonal Couplings if Silyloxyarenes

Exploring nickel-catalyzed C-O bond coupling of silyloxyarenes has led to the development of orthogonal and sequential couplings. Orthogonal coupling of aryl methyl ethers and silyloxyarenes was discovered though the optimization of silyloxyarene couplings. Selectivity derives from the ligand used in the nickel-catalyzed coupling reaction. This is the first example of utilizing inert C-O bonds in orthogonal couplings. Four step sequential coupling routes have also been developed, where no intermediate activation or protecting group manipulations were required. Previous methods have been limited to three steps and these two examples are the first instances of sequential couplings with aryl electrophiles that are greater than three steps. Although palladium has been the transition metal of choice for orthogonal couplings, nickel has been proven to be a competent transition metal for developing orthogonal and sequential routes. Our newly developed strategies have been paired with known routes that utilized pallidum for coupling aryl halides. These developments will hopefully lead to further advancements and result in improvements for the synthesis of complex molecules.

Future directions on these projects include further validating catalyst selectivity in orthogonal couplings of silyloxyarenes and aryl methyl ethers by utilizing the same coupling partner with only a change in ligand. Additionally, moving to a phenyl system instead of the highly explored naphthyl system would be important, as phenyl scaffold are significantly more prevalent than naphthyl scaffolds. However, due the lower reactivity of aryl methyl ether C-O bonds, further developments would first be required in aryl methyl ether C-O bond activation to obtain reactivity

that is robust enough to realize this goal. Further applications of our developed orthogonal and sequential couplings would also be important to show, such as applications in the synthesis of a biologically relevant compound to highlight the power of these strategies. An interesting orthogonal coupling example that was briefly explored, and needs to be further developed, was using orthogonality between triflates and aryl chlorides or bromides under palladium catalysis along with our developed orthogonality to show the modularity these approaches allow.

For future directions in development of sequential couplings, additional routes containing a larger variety of electrophiles and transformations would be useful. However, applying these sequential and late-stage couplings of silyloxyarenes in syntheses is the next area that needs to be developed, demonstrating these methods on biologically relevant scaffolds. I hope that these initial discoveries in orthogonal, sequential, and late-stage couplings of silyloxyarenes prove useful in organic synthesis.

Chapter 5

Beyond Silyloxyarene: Future Directions of Nickel-catalyzed C-O Couplings of Silyl Ethers

5.1 General Introduction on Silyl-Protected C-O Bonds as Electrophilic Coupling Partners

Phenol derivatives were initially explored as a direct method to explore their reactivity compared to other inert aryl electrophilic coupling partners. However, other silyl ether derivatives beyond silyloxyarenes could also be used as C-O electrophilic coupling partners. Expansion of current nickel-catalyzed methods for aryl C-OSiR_3 activation to other silyl-protected electrophilic coupling partners would allow for derivatization of many common organic scaffolds, including alkyl, allylic, and vinyl alcohols. This chapter provides future directions regarding C-O bond coupling of a more diverse range of silyl ethers.

5.2 Silyl-Protected Allylic Alcohols as C-O Bond Electrophilic Coupling Partners

Allylic alcohols are attractive handles for functionalization due to their prevalence in biologically relevant compounds. Due to the abundance of allylic alcohols, there are numerous methods for their synthesis, and many more for modulation of the allylic alcohol scaffold. In addition to traditional syntheses adding vinyl nucleophiles to aldehydes or reducing α-β unsaturated ketones, new variations on these methods have also been developed. For example, the Nozaki-Hiyama-Kishi (NHK) reaction is an in-situ, transition metal mediated method of generating a nucleophilic vinyl species and adding them to aldehydes with a nickel catalyst and stoichiometric chromium. The NHK reaction has become a powerful method due to high functional group compatibility; however, use of vinyl halides and stoichiometric chromium present

limitations.[202] An alternative method is the nickel-catalyzed reductive coupling of an aldehyde and alkyne with a mild reducing agent, which has been developed by our group (Scheme 5-1).[203,204]

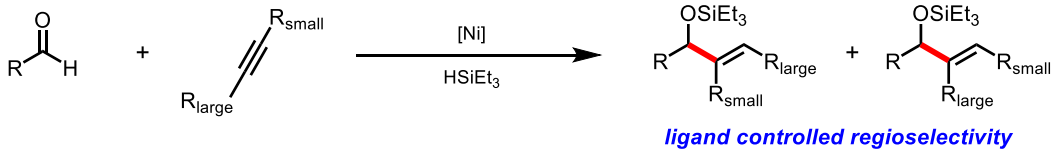

Scheme 5-1. Regiocontrol in Nickel-Catalyzed Reductive Coupling of Aldehydes and Alkynes with Silane Reductants.

With powerful methods of generating silyl-protected allylic alcohols in our group, expansion of silyloxyarene couplings to these derivatives was explored to allow for further functionalization. Transition metal-catalyzed methods for the diversification of allylic alcohols have been widely developed and have been shown to be extremely useful synthetic tools.[205] However, most of these methods have used allylic alcohols with activated protecting groups and a palladium catalyst. Only few reactions have been developed with inert ether protecting groups.

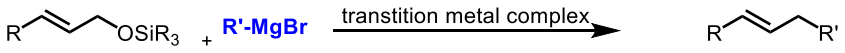

Scheme 5-2. Diversification of Silyl-Protected Allylic Alcohols.

There have been many methods using other inert protecting groups,[206] or those that directly use the unprotected alcohol.[207] However, only few reports exist using silyl-protected allylic alcohols as electrophilic coupling partners. Furthermore, as with silyloxyarene substrates for C-O bond activation, most reactions use strong nucleophilic coupling partners, such as Grignard reactions (Scheme 5-2).[208,209,210]

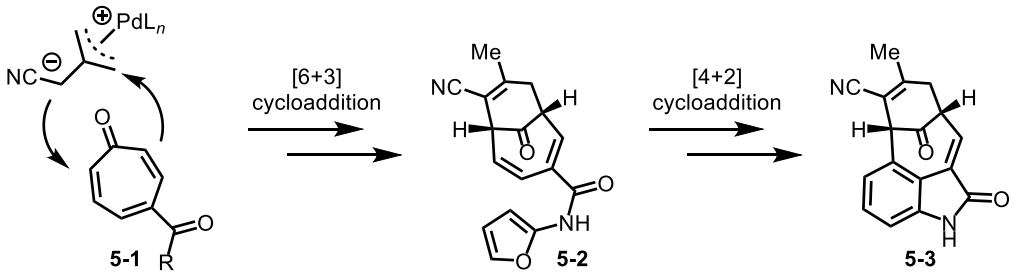

Scheme 5-3. Synthesis of Welwitindolinone Core Through Cycloaddition with Trimethylenemethane Precursor.

One application we became interested in that would utilize both our current reductive coupling methodology to synthesize allylic alcohol derivatives and allow for diversification of silyl-protected allylic alcohols through C-O bond coupling was synthesis of trimethylenemethane (TMM) precursors. The Trost group has developed allylic alcohol derivatives with strongly activating protecting groups that generate trimethylenemethane complexes with palladium. They have shown many applications of these complexes in cycloaddition reactions, where a range of five or seven membered products are generated.[211–213] Additionally, they have shown many applications of the developed methods in several syntheses, such as the welwitindolinone core (**5-3**, Scheme 5-3).[214–217] However, trimethylenemethane precursors are not readily available and require three steps for an unsubstituted derivative, or four to six steps for more substituted derivatives.[211] Therefore, we proposed rapid access to a library of substituted trimethylenemethane precursors through the nickel-catalyzed reductive coupling of propargyl silanes and aldehydes.

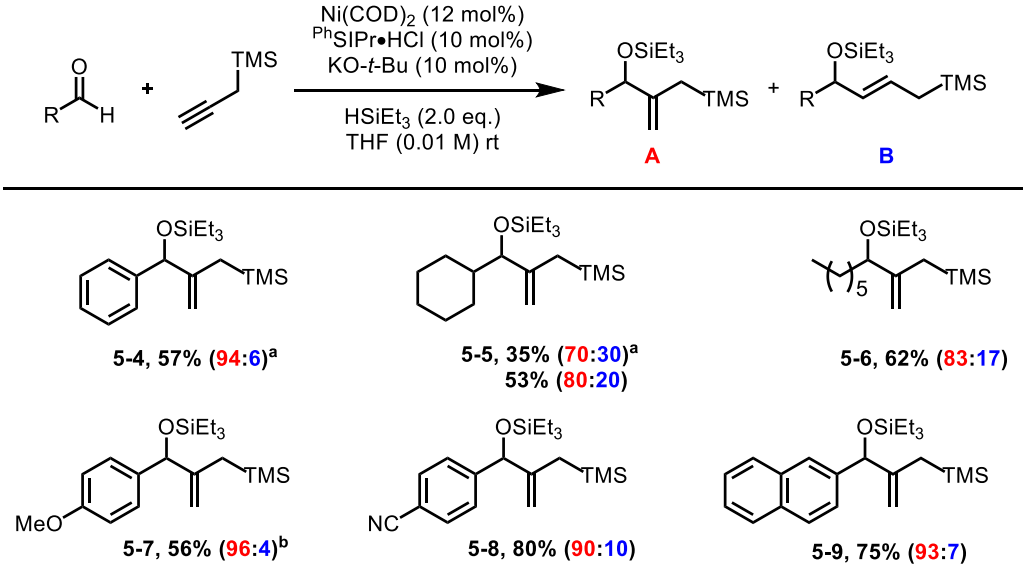

(a) Reaction run under concentrated conditions, 0.1M.

Table 5-1. Scope of Nickel-Catalyzed Reductive Coupling toward Trimethylmethaneprecursors.

The same TMM precursors would be accessible, except with a silane protecting group on the alcohol instead of a more activated protecting group, such as an acetate or phosphate. After

some optimization, good yields of the desired products were possible using conditions derived from our nickel-catalyzed reductive couplings of terminal alkynes. A brief exploration of substrate scope tested generality for a variety of functionalities (Table 5-1). Benzaldehyde and trimethylpropargyl silane resulted in a good yield and high ratio of branched to linear products. Although aliphatic aldehydes resulted in lower yields and a decreased ratio of products, both yield and product ratio could be improved by decreasing the concentration of the reaction. Electron-rich and electron-deficient aryl substituents both resulted in good yields and good ratios of products.

Having developed access to silyl-protected trimethylenemethane precursors, development of a nickel-catalyzed method for the [3+2] cycloaddition was explored. Nickel-catalyzed [3+2] cycloadditions of TMM precursors with activating protecting groups has been described once before.[218] However, after exploring several nickel and palladium catalyst systems, cycloaddition product was not observed. As an alternative route, a protecting group swap was conducted to replace the silane protecting group with a more activating protecting group, accessing the same TMM precursors previously utilized in [3+2] cycloadditions with palladium catalysts. However, as a direct route from silyl-protected TMM precursors was still desired, other reactions were explored to validate activation of the silyl-protected allylic alcohol C-O bond.

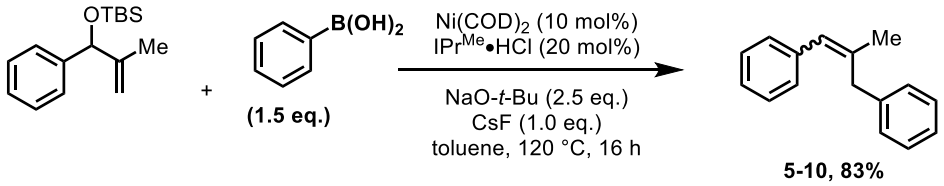

Scheme 5-4. Nickel-Catalyzed Suzuki Coupling of Silyl-Protected Allylic Alcohols.

Initially, a model substrate similar to the silyl-protected TMM precursors was explored, resulting in good yields for Suzuki coupled products, where a 2:1 ratio of E:Z isomers was obtained (Scheme 5-4). The ability to readily activate and couple these silyl-protected allylic alcohol derivatives suggested that activation of the silyl-protected TMM precursors was not limiting

reactivity. Therefore, the [3+2] cycloaddition was likely problematic. This was supported by finding that ligands used to activate the C-O bond had not been shown for the [3+2] cycloaddition. Based on these findings, other coupling reactions of silyl-protected allylic alcohols were explored.

To show generality in coupling of silyl-protected allylic alcohol substrates, other substitution patterns were explored using our reductive deoxygenation or Suzuki coupling reaction conditions. With terminal allylic alcohol compunds derived from cinnamaldehyde, a good yield of the Suzuki coupling product was obtained at 40 degrees Celsius, with both higher and lower temperatures resulting in lower yields (Scheme 5-5). Use of our conditions for our reduction reaction on a fully conjugated and symmetrical allylic alcohol derivative resulted in a good yield of the alkene at 80 degrees Celsius, again with lower yields being obtained at both higher and lower temperatures (Scheme 5-6).

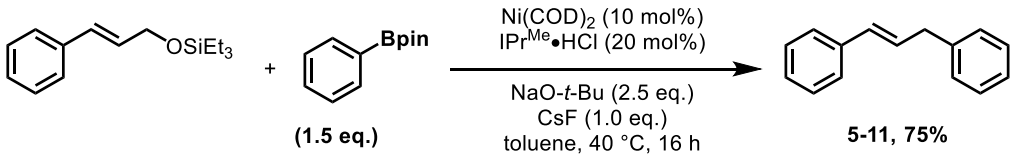

Scheme 5-5. Suzuki Coupling of Silyl-Protected Allylic Alcohol Derivatives.

Future work should build on these initial results for C-O bond coupling of silyl-protected allylic alcohol derivatives. One area that needs to be further explored is the regioselectivity for these reactions by examining different substrates classes and ligands to control the product distribution. Expansion to other reactions previously developed for silyloxyarenes would also be beneficial, such as generation of allylic boron or silicon reagents. Finally, expanding beyond allylic derivatives to benzylic or aliphatic silyl ether C-O bonds would allow nearly any alcohol to be functionalized. Although this is extremely challenging, and a unique reaction pathway would have to be developed, reports do exist for aliphatic C-O diversification with methyl protecting groups.[219]

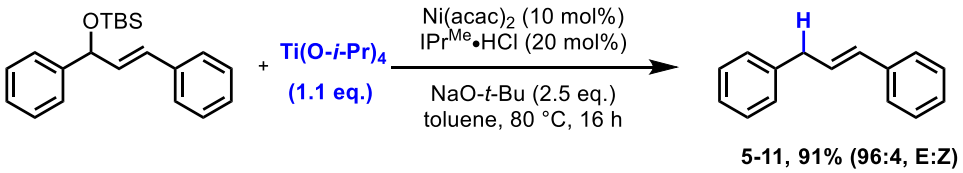

Scheme 5-6. Reduction of Silyl-Protected Allylic Alcohol Derivative.

5.3 Enol Silanes as C-O Bond Electrophilic Coupling Partners

In addition to silyloxyarenes and silyl-protected allylic alcohols, silyl enol ethers, or enol silanes, are the other major C-O electrophilic coupling partner that would be attractive. Additionally, considering other traditionally used vinyl electrophiles, enol silanes are arguably even more attractive compared to the advantages of using silyloxyarenes over other aryl electrophiles. These advantages for enol silanes derive from the utility of enol silanes in synthesis, where their regioselective synthesis allows for excellent control of regiochemical outcomes in synthesis (Scheme 1-4),[220] a common limitation of vinyl halides. Additionally, enols are easily prepared from readily available ketones or aldehydes. Enol triflates are commonly used as the enol derivative for vinyl C-O bond coupling. Development of enol silane C-O bond coupling could result in complementary and new reactivity. Despite the advantages of enol silanes, they have not been widely used beyond α-functionalization and their use as electrophilic, vinyl coupling partners would be valuable.

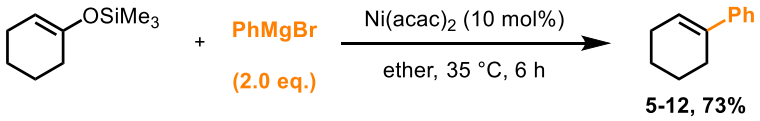

Scheme 5-7. Kumada Coupling of Enol Silanes under Nickel Catalysis.

Enol silanes, along with other ether protecting groups, have been explored previously as electrophilic C-O coupling partners, with some representative examples described using methyl enol ethers,[81,83,99,221–223] cyclic alkyl enol systems,[224–226] pivalates.[227] One of the early examples of using enol silanes as electrophilic coupling partners was by Kumada in 1980 (Scheme 5-7).[228]

However, deprotection of the TMS group needs to be considered, as strongly nucleophilic coupling partners can deprotect these labile silane protecting groups. Furthermore, the desired product derived from the deprotected ketone, where addition of Grignard to the carbonyl carbon and subsequent elimination would access the same product as the coupled compound.

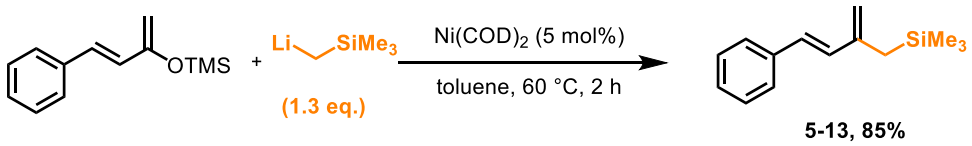

Scheme 5-8. Enol Silane Coupling with Organolithium Reagents under Nickel Catalysis.

Regardless, other reports of enol silane C-O bond coupling has been reported, although the focus has been on use of strongly nucleophilic coupling partners. Another, more recent example uses Grignard reagents with TMS-protected enol silanes with a nickel catalyst.[161] Use of organolithium reagents has also been described in coupling of enol silane C-O bonds, where 1.3 equivalents of organolithium was used with a nickel(0) pre-catalyst (Scheme 5-8).[223] Many other reports of using enol silanes as vinyl electrophilic coupling partners have been described, often as an isolated example in a substrate table.[93,98,99,102] However, all of these methods are generally limited by two constraints, use of strongly nucleophilic coupling partners and/or necessitating conjugation of the enol silane to an aryl system. Therefore, a general coupling method with mild coupling partners, across conjugated and non-conjugated enol silanes would be beneficial.

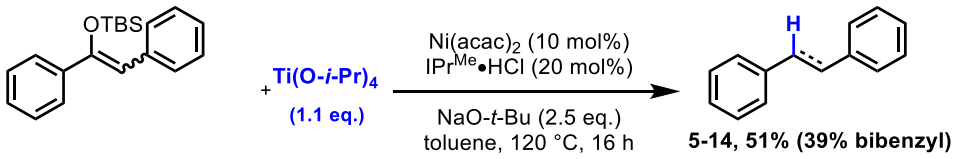

Scheme 5-9. Nickel-Catalyzed Reduction of Conjugated Enol Silane C-O Bonds.

Use of mild coupling partners with enol silanes was initially explored in conjugated systems to explore reactivity of the C-O bond. Use of our reductive deoxygenation reaction conditions resulted in high conversion of the starting enol silane and good yield of product (**5-14**),

although over reduction of stilbene to the alkane was a major byproduct (Scheme 5-9). To confirm the order of reduction steps to the alkane, stilbene was subjected to the same reaction conditions and reduction to alkane was again observed. This suggested that the enol silane C-O bond was initially reduced, followed by reduction of the alkene. Decreasing the amount of alkane byproduct should be possible by exploring milder conditions and shorter reaction times, but this was not explored.

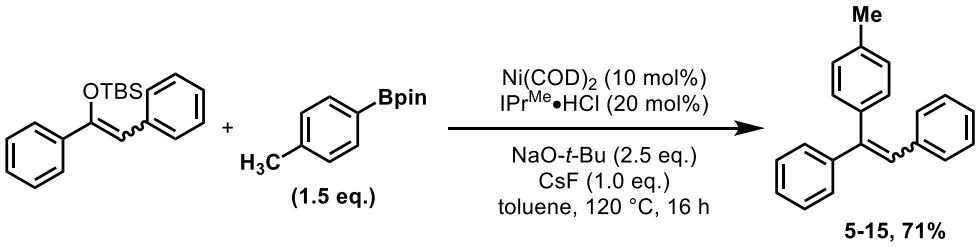

Scheme 5-10. Nickel-Catalyzed Suzuki Coupling of Conjugated Enol Silane C-O Bonds.

Instead, a Suzuki coupling of enol silanes was next explored to increase complexity, instead of removing functionality. High reactivity was again observed with conjugated enol silanes under our Suzuki coupling conditions, generating a trisubstituted olefin in good yield (**5-15**, Scheme 5-10). Interestingly, replacing the α-phenyl with an α-methyl resulted in only trace product. This suggests that sterics are influencing reactivity of this substrate or the α-phenyl group is resulting in increased yields through additional conjugation or by acting as a directing group. Other reactions developed for silyloxyarenes were also explored, including silylation and borylation, but only trace product was observed with this substrate.

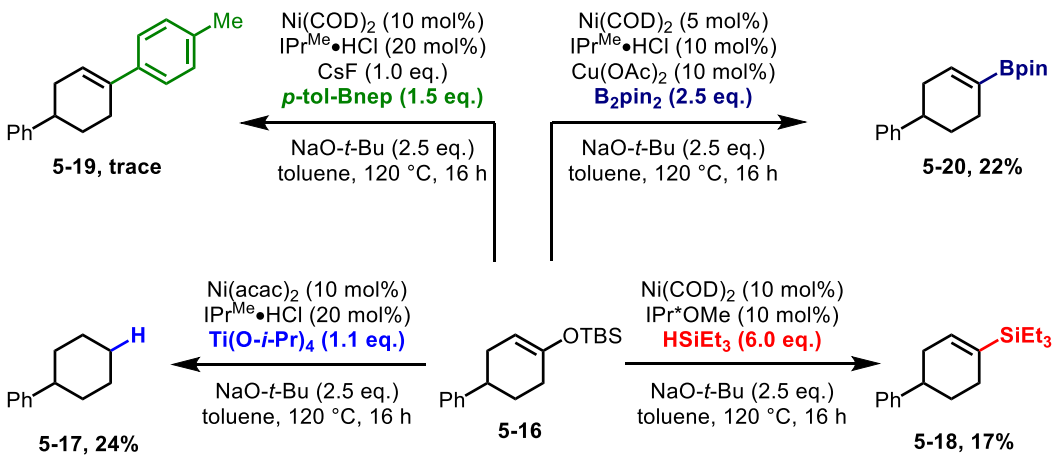

Scheme 5-11. Nickel-Catalyzed Coupling of Isolated Enol Silane C-O Bonds.

Another substrate was then explored to move away from the more reactive, conjugated enol silanes. Using our reduction methodology for silyloxyarenes on an enol silane derived from 4-phenylcyclohexanone, low conversion to phenyl cyclohexane was observed, where over reduction of the alkene was the major product. This reaction demonstrated the drastic difference in reactivity between conjugated and non-conjugated enol silanes (Scheme 5-11). Use of our silylation and borylation methodology generates vinyl nucleophiles, although low yields were again observed. Suzuki coupling with these challenging enol silane substrates only resulted in trace product. However, comparable yields to silylation and borylation should be obtainable once Suzuki coupling of silyloxyarene C-O bonds is optimized. Importantly, low yields of the products were not due to degradation of starting material, but low reactivity of the C-O bond as starting material was the only other major species observed from these reactions. Therefore, this low conversion can be overcome with further optimization.

Of all the silyl-protected alcohol derivatives, enol silanes are the most attractive and should be a major area of focus for future development. Exciting preliminary results show that current methods could be generally applied across even challenging isolated enol silanes. One explanation for the reactivity difference between conjugated and isolated enol silanes could be the poor

coordinating ability of isolated systems over conjugated systems. This is analogues to differences between naphthyl and isolated aromatics in aryl C-O bond couplings. One solution that was briefly explored to overcome this lack of reactivity was installing a directing group in the silane protecting group, such as aryl or pyridyl. Other methods of increasing conversion for C-O bond coupling of these inert enol silanes should be explored, such as exploring new catalysts systems or ligands to improve reactivity.

Another area that was briefly explored for catalyst improvement was exploring different ligands. Optimization of an improved catalysts system could lead to a broader substrate scope, lower reaction temperatures, and lower catalyst loadings for currently developed coupling reactions. In addition, this could allow for higher conversion of challenging substrates, such as isolated aryl and vinyl silyl ethers. As oxidative addition is presumed the rate determining step, ligands were explored that could lower the activation barrier by stabilizing the nickel complex. Such ligands explored were similar in structre but were more donating thatn IPr^{Me}, such as those with anionic donating groups[229] or CAAC ligands.[230] These ligands were explored for in-situ generation of the catalyst. However, no product was observed, which could be due to their higher pKas. Therefore, future work with these ligands should be to synthesize discrete complexes and explore their reactivity.

5.4 Conclusions on Silyl-Protected C-O Bonds as Electrophilic Coupling Partners

Future directions in silyloxyarene C-O bond couplings include further mechanistic investigations, development of new coupling reactions, improvements on currently developed methods, and new sequential or orthogonal coupling routes. Other transition metals such as iron[231] or cobalt[232] may allow for these improvements and should be explored. Outside of continuing to improve current methods, future directions should focus on other silyl-protected alcohol

derivatives, namely silyl-protected allylic alcohols and enol silanes. Preliminary studies have shown these substrates to be competent coupling partners with our developed reaction, but additional work is necessary to improve selectivity, conversion, and generality across substrate classes. Gaining mechanistic insights for current methods, and further development of reactions for these electrophiles, would solidify silyl ethers as a ubiquitous class of electrophiles in transition metal-catalyzed cross-coupling reactions. Furthermore, they could be used in a complementary, or even standalone fashion, for orthogonal and sequential coupling strategies, which will have a profound impact on the late-stage diversification of complex molecules.

Chapter 6

Supporting Information

6.1 General Supporting Information

Unless otherwise noted, all reactions were conducted in flame-dried or oven-dried (120 °C) sealed tubes with magnetic stirring sealed in a nitrogen glovebox. Solvents were purified under nitrogen using a solvent purification system (Innovative Technology, Inc. Model # SPS-400-3 and PS-400-3). Et_3SiH (Sigma-Aldrich), *i*-$PrMe_2SiH$ (Gelest Chemicals) and $BnMe_2SiH$ (Gelest Chemicals) were passed through basic alumina before use and stored under nitrogen. All liquid amines were distilled over calcium hydride before use and stored under nitrogen and solid amines were used without further purification, morpholine (Sigma-Aldrich), N-methylbutylamine (Sigma-Aldrich), dibutylamine (Sigma-Aldrich), 2-methylpiperdine (Sigma-Aldrich), 2,6-dimethylpiperdine, predominantly cis (Alfa Aesar), 1-methylpiperazine (Sigma-Aldrich), N-methylbenzylamine (Sigma-Aldrich), N-methylaniline (Sigma-Aldrich), 2,4,6-trimethylaniline (Oakwood Chemicals), 2,6-diisopropylaniline (Oakwood Chemicals), aniline (Sigma-Aldrich), octylamine (Sigma-Aldrich), sec-butylamine (Sigma-Aldrich), iso-butylamine (Sigma-Aldrich), cyclohexylamine (Sigma-Aldrich), 1-adamantylamine (Oakwood Chemicals), butylamine (Sigma-Aldrich), benzylamine (Sigma-Aldrich), pyrrolidine (Sigma-Aldrich), piperazine (Sigma-Aldrich), 2-(piperazin-1-yl)pyrimidine (Oakwood Chemicals). Bis(pinacolato) diboron and all other diboron reagents (Combi Blocks) were recrystallized in pentane before use. All aryl boron species (Combi Blocks) were used as received without any further purification. Anhydrous $Ni(acac)_2$ (Strem Chemicals), $Ni(COD)_2$ (Strem Chemicals), IPr^{Me}·HCl (made from known procedure[233]), $IMes^{Me}$·HCl (made from known procedure[233]), ICy·HCl (Sigma-Aldrich), IAd·HCl (Sigma-Aldrich), IPr^{Cl}·HCl (made from known procedure[234]), IPr·HCl (made from known procedure[235]), IMes·HCl (made from known procedure[235]), IPr*OMe·HCl (made from known procedure[236]), IPr*OMe (Strem Chemicals), and NaO-*t*-Bu (Strem Chemicals) were stored and weighed in an inert atmosphere glovebox.

Analytical thin layer chromatography (TLC) was performed on Kieselgel 60 F254 (250 μm silica gel) glass plates and compounds were visualized with UV light and *p*-anisaldehyde, potassium permanganate or ceric ammonium molybdate stains. Flash column chromatography was performed using Kieselgel 60 (230-400 mesh) silica gel. Eluent mixtures are reported as v:v percentages of the minor constituent in the major constituent. All compounds purified by column chromatography were sufficiently pure for use in further experiments unless otherwise indicated.

^{1}H NMR spectra were collected at 400 MHz on a Varian MR400, at 500 MHz on a Varian Inova 500 or Varian vnmrs 500, or at 700 MHz on a Varian vnmrs 700 instrument. The proton signal of the residual, nondeuterated solvent (δ 7.26 for $CHCl_3$ or 7.15 for C_6D_6) was used as the internal reference for ^{1}H NMR spectra. ^{13}C NMR spectra were completely heterodecoupled and measured at 125 MHz or 175 MHz. Chloroform-d (δ 77.00), dimethylsulfoxide-d_6 (δ 39.95), or benzene-d_6 (δ 128.0) was used as an internal reference. High resolution mass spectra were recorded on a VG 70-250-s spectrometer manufactured by Micromass Corp. (Manchester UK) at the University of Michigan Mass Spectrometry Laboratory. GCMS analysis was carried out on a HP 6980 Series GC system with HP-5MS column (30 m x 0.250 mm x 0.25 μm). GCFID analysis was carried out on a HP 6980N Series GC system with a HP-5 column (30 m x 0.32 mm x 0.25 μm).

6.2 Experimental Details for Chapter 2

6.2.1 General Procedures for Chapter 2

General Procedure the for Ni(COD)$_2$/IPr*OMe promoted silylation or reduction of silyloxyarenes using titanium isopropoxide and triethylsilane or triisopropylsilane (A):

A reaction tube containing a stir bar was charged with aryl silyl ether (1 equiv), NaO-*t*-Bu (2.5 equiv), Ni(acac)$_2$ (10 mol%) and IPr*OMe (10 mol%) in a nitrogen atmosphere glovebox. The sealed reaction tube was brought outside the glovebox where toluene (0.5 M), silane (6 equiv), and titanium isopropoxide (2.0 equiv) were sequentially added via syringe. The reaction tube was then placed in a heated block set to 120 °C and stirred for 16 h. The mixture was allowed to reach rt, internal standard was added (tridecane, 40 µL, 0.164 mmol), diluted with EtOAc (5 mL) and deionized water (3 mL), then extracted with EtOAc (3 x 5 mL), dried over $MgSO_4$, filtered, concentrated under reduced pressure and purified by flash column chromatography on silica gel to afford the desired product.

General Procedure for the Ni(acac)$_2$/IPr^{Me}·HCl promoted reductive deoxygenation of silyloxyarenes using titanium(IV) isopropoxide (B):

A reaction tube containing a stir bar was charged with aryl silyl ether (1 equiv), NaO-*t*-Bu (2.5 equiv), Ni(acac)$_2$ (5 mol%) and IPr^{Me}·HCl (10 mol%). The reaction tube was sealed and pump/purged with nitrogen three times. Toluene (0.5 M) and titanium (IV) isopropoxide (1.1 equiv) were sequentially added via syringe, and the reaction tube was then placed in a heated block set to 120 °C and stirred for 6 h. The mixture was allowed to reach rt, internal standard was added (tridecane, 40 µL, 0.164 mmol), diluted with EtOAc (5 mL) and 1 M HCl (3 mL), then extracted with EtOAc (3 x 5 mL), dried over $MgSO_4$, filtered, concentrated under reduced pressure and purified by flash column chromatography on silica gel to afford the desired product. Note: slightly higher yields (5-10%) were obtained by utilizing a nitrogen atmosphere glovebox and yields in the text utilized the glovebox procedure.

General Procedure the for Ni(COD)$_2$/IPr*OMe promoted silylation of silyloxyarenes using triethylsilane (C):

A reaction tube containing a stir bar was charged with aryl silyl ether (1 equiv), NaO-*t*-Bu (2.5 equiv), Ni(COD)$_2$ (10 mol%) and IPr*OMe (10 mol%) in a nitrogen atmosphere glovebox. The

sealed reaction tube was brought outside the glovebox where toluene (0.5 M) and silane (6 equiv) were sequentially added via syringe. The reaction tube was then placed in a heated block set to 120 °C and stirred for 16 h. The mixture was allowed to reach rt, internal standard was added (tridecane, 40 µL, 0.164 mmol), diluted with EtOAc (5 mL) and deionized water (3 mL), then extracted with EtOAc (3 x 5 mL), dried over $MgSO_4$, filtered, concentrated under reduced pressure and purified by flash column chromatography on silica gel to afford the desired product.

6.2.2 Procedure for Generating Calibration Curves Utilizing a GC-FID

Solutions containing a constant concentration of an internal standard (tridecane (0.164 M) and varying concentrations of the desired product (0.05, 0.10, 0.15 and 0.20 M) were prepared in ethyl acetate. Each was analyzed by GC-FID and the response factor (F) calculated by solving equation S1 for the area of product to give equation S2, where the response factor (F) is the slope. Yields of crude reactions mixtures, containing a known amount of internal standard, were then determined by solving Equation S1 for the concentration of the product to give Equation S3 and filling in the known data from a crude reaction.

$$\frac{\boldsymbol{Area\ of\ Product}}{\boldsymbol{Concentration\ of\ Product}} = \boldsymbol{F}\left(\frac{\boldsymbol{Area\ of\ Standard}}{\boldsymbol{Concentration\ of\ Standard}}\right)$$

Equation 1. Response Factor.

$$\boldsymbol{Area\ of\ Product} = \boldsymbol{F}\left(\frac{(\boldsymbol{Area\ of\ Standard})(\boldsymbol{Concentration\ of\ Product})}{\boldsymbol{Concentration\ of\ Standard}}\right)$$

Equation 2. Area of Product.

$$\boldsymbol{Concentration\ of\ Product} = \frac{(\boldsymbol{Concentration\ of\ Standard})(\boldsymbol{Area\ of\ Product})}{\boldsymbol{F}(\boldsymbol{Area\ of\ Standard})}$$

Equation 3. Concentration of Product.

Calibration Curve for biphenyl:

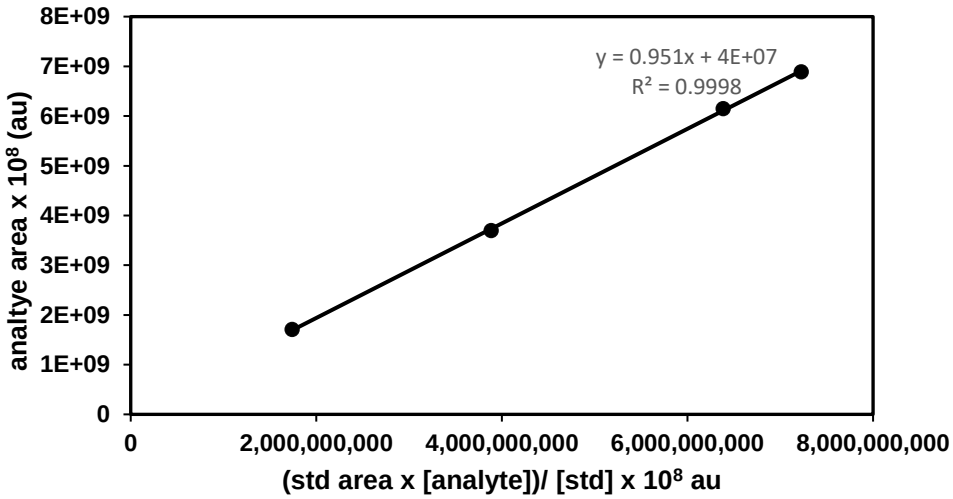

Plot of analyte area versus (std area x [analyte]) / [std] fitted to y = *m*x + *b* where *m* = 0.951 and *b* = 4 x 10^7 with a R^2 of 0.9998.

concentration of analyte	area of analyte	area tridecane (std)	(std area x [analyte]) / [std]
0.0509	17.07 x 10^8	56.48 x 10^8	17.42 x 10^8
0.0966	37.00 x 10^8	65.97 x 10^8	38.86 x 10^8
0.1582	61.49 x 10^8	66.22 x 10^8	63.88 x 10^8
0.1920	68.92 x 10^8	61.77 x 10^8	72.28 x 10^8

Table 6-1. Calibration Curve for biphenyl.

Calibration Curve for [1,1'-biphenyl]-4-yltriethylsilane.

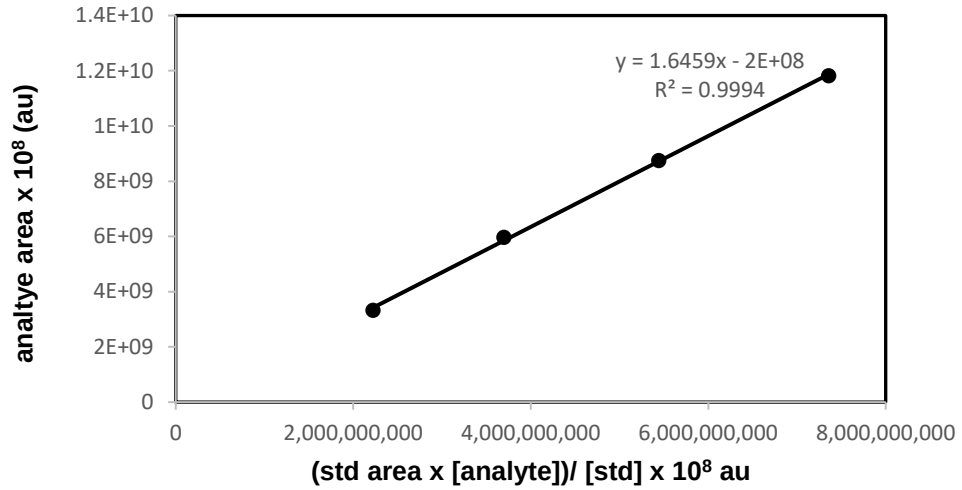

Plot of analyte area versus (std area x [analyte]) / [std] fitted to y = *m*x + *b* where *m* = 1.6459 and *b* = -2 x 10^8 with a R^2 of 0.9994.

Concentration of analyte	Area of analyte	area tridecane (std)	(std area x [analyte]) / [std]
0.0484	33.29 x 10^8	75.35 x 10^9	22.25 x 10^8
0.0872	59.61 x 10^8	69.62 x 10^9	36.99 x 10^8
0.1430	87.51 x 10^8	62.43 x 10^9	54.43 x 10^8
0.1929	11.81 x 10^9	62.54 x 10^9	73.57 x 10^8

Table 6-2. Calibration Curve for [1,1'-biphenyl]-4-yltriethylsilane.

Calibration Curve for naphthalene.

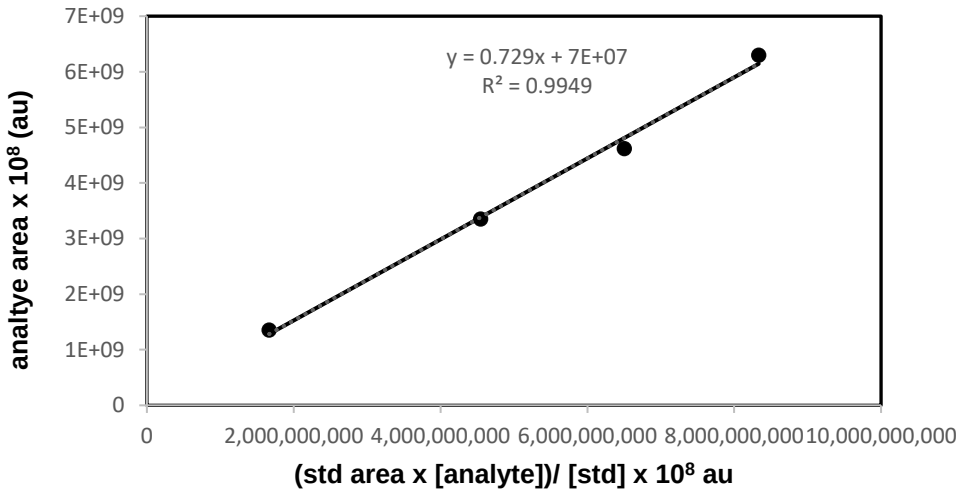

Plot of analyte area versus (std area x [analyte]) / [std] fitted to y = *m*x + *b* where *m* = 0.729 and *b* = 7 x 10^7 with a R^2 of 0.9949.

Concentration of analyte	Area of analyte	area tridecane (std)	(std area x [analyte]) / [std]
0.0492	13.53 x 10^8	55.61 x 10^9	16.66 x 10^8
0.1038	33.53 x 10^8	71.85 x 10^9	45.45 x 10^8
0.1545	46.15 x 10^8	69.04 x 10^9	65.02 x 10^8
0.2013	62.96 x 10^8	67.90 x 10^9	83.33 x 10^8

Table 6-3. Calibration Curve for naphthalene.

Calibration Curve for 4-phenylmorpholine.

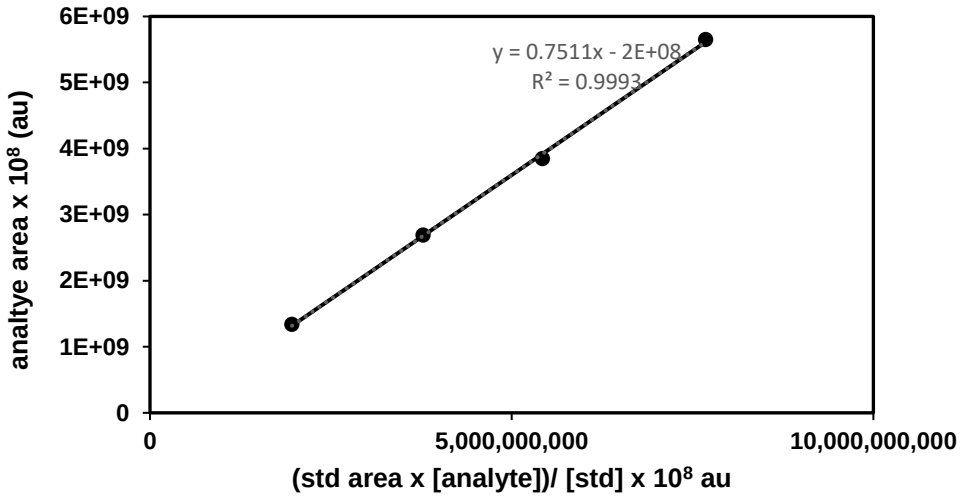

Plot of analyte area versus (std area x [analyte]) / [std] fitted to y = *m*x + *b* where *m* = 0.7511 and *b* = -2 x 10^8 with a R^2 of 0.9993.

Concentration of analayte	area of analyte	area tridecane (std)	(std area x [analyte]) / [std]
0.0545	13.38 x 10^8	59.08 x 10^8	19.63 x 10^9
0.1017	26.91 x 10^8	60.88 x 10^8	37.75 x 10^9
0.1482	38.17 x 10^8	60.03 x 10^8	54.24 x 10^9
0.2169	56.51 x 10^8	58.08 x 10^8	76.80 x 10^9

Table 6-4. Calibration Curve for 4-phenylmorpholine.

Calibration Curve for *N*-phenylacetamide.

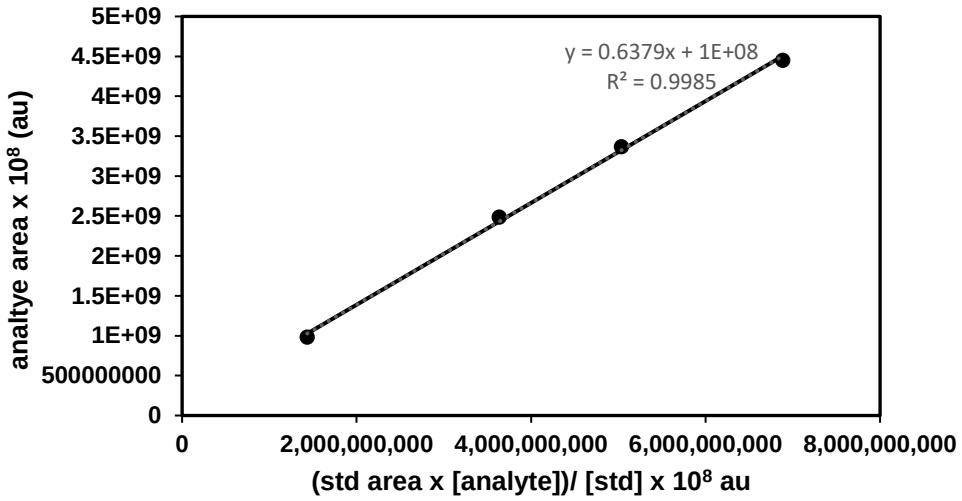

Plot of analyte area versus (std area x [analyte]) / [std] fitted to y = *m*x + *b* where *m* = 0.6379 and *b* = 1 x 10^8 with a R^2 of 0.9985.

Concentration of analyte	area of analyte	area tridecane (std)	(std area x [analyte]) / [std]
0.0444	9.806 x 10^8	53.02 x 10^8	14.35 x 10^9
0.0888	24.84 x 10^8	67.18 x 10^8	36.36 x 10^9
0.1480	33.68 x 10^8	55.81 x 10^8	50.34 x 10^9
0.1850	44.52 x 10^8	61.05 x 10^8	68.83 x 10^9

Table 6-5. Calibration Curve for *N*-phenylacetamide.

Calibration Curve for *tert*-butylbenzene.

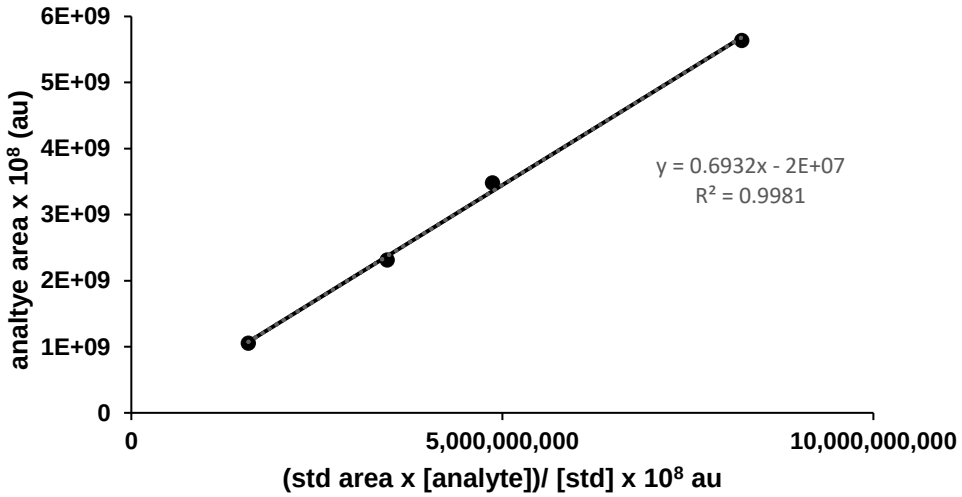

Plot of analyte area versus (std area x [analyte]) / [std] fitted to y = *m*x + *b* where *m* = 0.6932 and *b* = -2 x 10^7 with a R^2 of 0.9981.

Concentration of analyte	area of analyte	area tridecane (std)	(std area x [analyte]) / [std]
0.0425	10.52 x 10^8	60.91 x 10^8	15.77 x 10^8
0.0969	23.16 x 10^8	58.41 x 10^8	34.49 x 10^8
0.1378	34.82 x 10^8	57.91 x 10^8	48.66 x 10^8
0.2161	56.38 x 10^8	62.45 x 10^8	82.26 x 10^8

Table 6-6. Calibration Curve for *tert*-butylbenzene.

Calibration Curve for 2,3-dihydro-1H-indene.

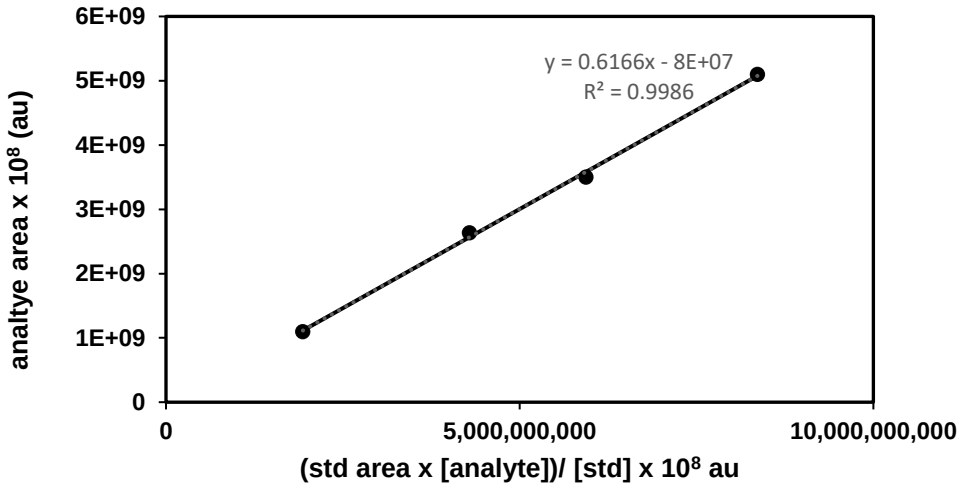

Plot of analyte area versus (std area x [analyte]) / [std] fitted to y = *m*x + *b* where *m* = 0.6166 and *b* = -8 x 10^7 with a R^2 of 0.9986.

Concentration of analyte	area of analyte	area tridecane (std)	(std area x [analyte]) / [std]
0.0550	10.99 x 10^8	57.69 x 10^8	19.34 x 10^8
0.1090	26.37 x 10^8	64.57 x 10^8	42.91 x 10^8
0.1506	35.03 x 10^8	64.65 x 10^8	59.36 x 10^8
0.2488	50.99 x 10^8	55.12 x 10^8	83.61 x 10^8

Table 6-7. Calibration Curve for 2,3-dihydro-1H-indene.

Calibration Curve for 1,2,3,4-tetrahydronaphthalene.

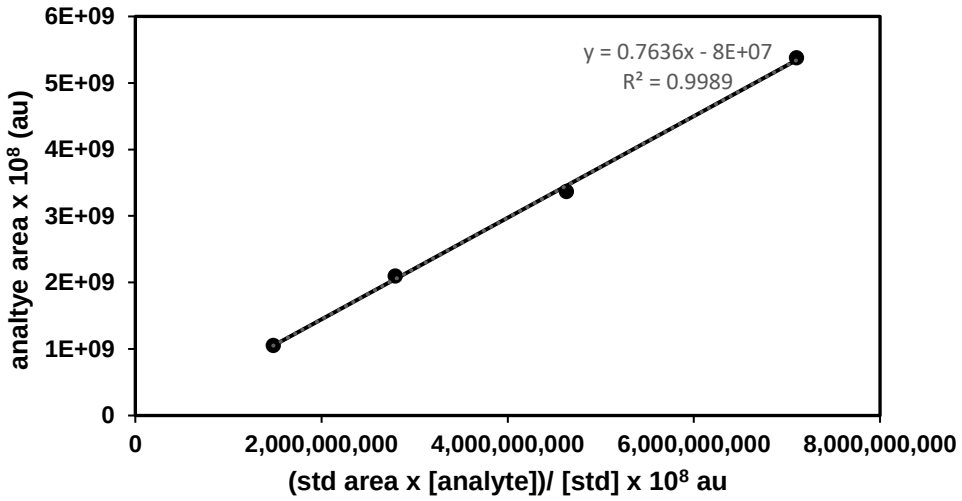

Plot of analyte area versus (std area x [analyte]) / [std] fitted to y = *m*x + *b* where *m* = 0.7636 and *b* = -8 x 10^7 with a R^2 of 0.9989.

Concentration of analyte	area of analyte	area tridecane (std)	(std area x [analyte]) / [std]
0.0431	10.52 x 10^8	56.40 x 10^8	14.82 x 10^8
0.0938	20.99 x 10^8	48.83 x 10^8	27.93 x 10^8
0.1354	33.67 x 10^8	56.08 x 10^8	46.29 x 10^8
0.2080	53.80 x 10^8	56.01 x 10^8	71.03 x 10^8

Table 6-8. Calibration Curve for 1,2,3,4-tetrahydronaphthalene.

Calibration Curve for 2-([1,1'-biphenyl]-4-yl)-4,4,5,5-tetramethyl-1,3,2-dioxaborolane:

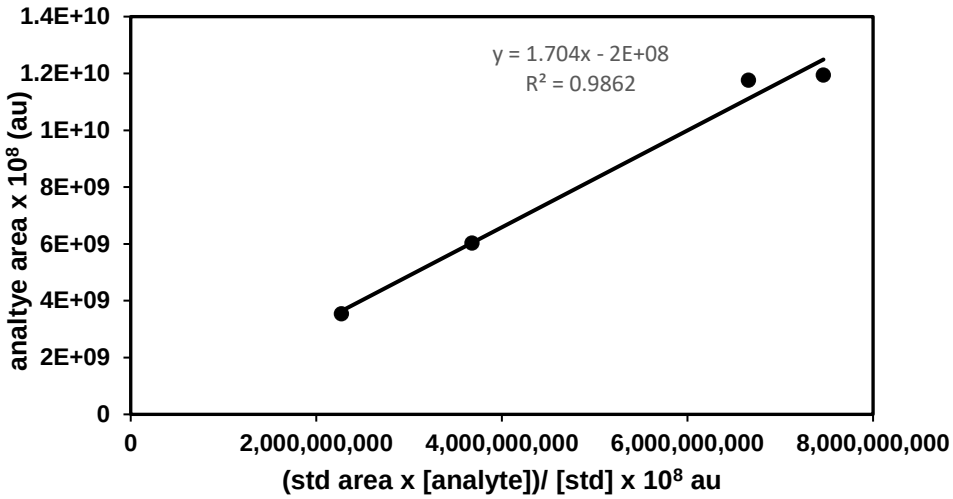

Plot of analyte area versus (std area x [analyte]) / [std] fitted to y = *m*x + *b* where *m* = 1.704 and *b* = -2 x 10^8 with a R^2 of 0.9862.

concentration of analyte	area of analyte	area tridecane (std)	(std area x [analyte]) / [std]
0.0532	35.45 x 10^8	70.06 x 10^8	22.71 x 10^8
0.0974	60.30 x 10^8	61.94 x 10^8	36.79 x 10^8
0.1545	11.77 x 10^9	70.68 x 10^8	66.60 x 10^8
0.1981	11.94 x 10^9	61.82 x 10^8	74.65 x 10^8

Table 6-9. Calibration Curve for 2-([1,1'-biphenyl]-4-yl)-4,4,5,5-tetramethyl-1,3,2-dioxaborolane.

Calibration Curve for 2-methoxynaphthalene:

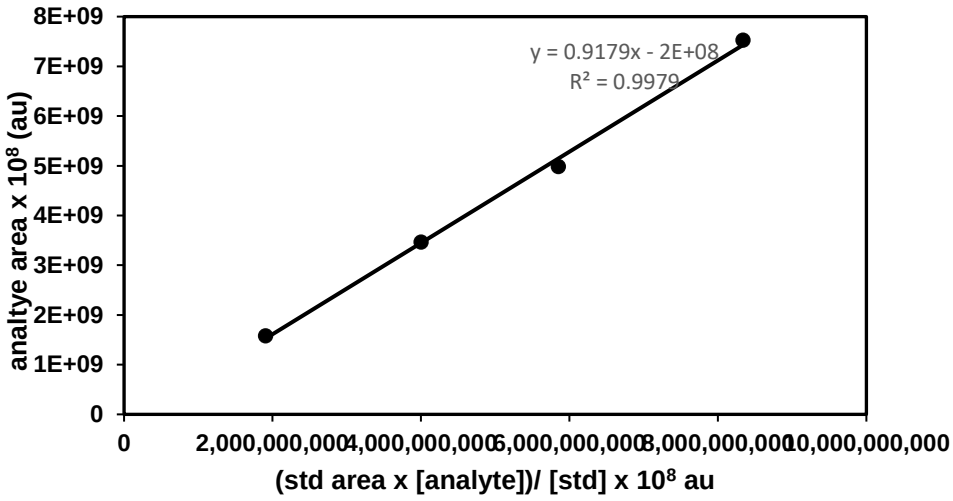

Plot of analyte area versus (std area x [analyte]) / [std] fitted to y = *m*x + *b* where *m* = 0.9179 and *b* = -2 x 10^8 with a R^2 of 0.9979.

concentration of analyte	area of analyte	area tridecane (std)	(std area x [analyte]) / [std]
0.0487	15.82 x 10^8	64.28 x 10^8	19.07 x 10^8
0.0967	34.62 x 10^8	67.89 x 10^8	40.03 x 10^8
0.1479	49.84 x 10^8	64.91 x 10^8	58.53 x 10^8
0.2035	75.29 x 10^8	67.22 x 10^8	83.41 x 10^8

Table 6-10. Calibration Curve for 2-methoxynaphthalene.

Calibration Curve for *tert*-butyldimethyl(naphthalen-2-yloxy)silane:

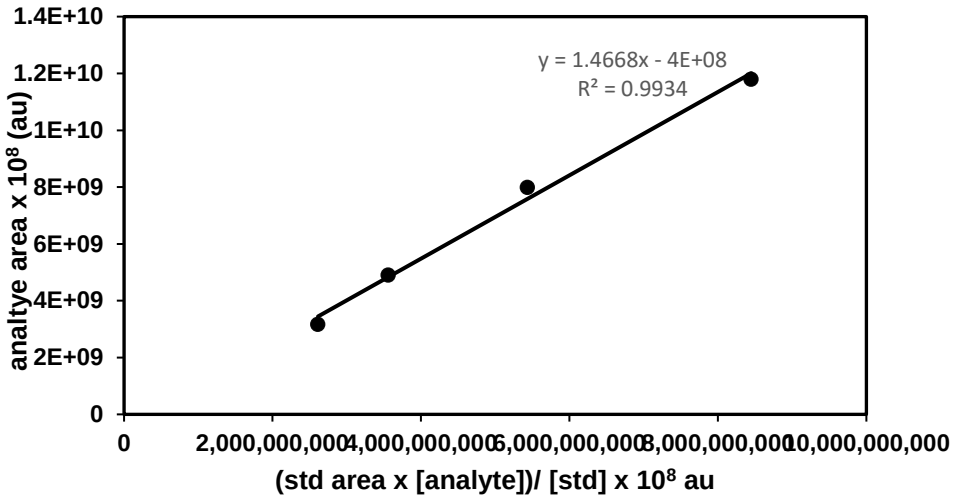

Plot of analyte area versus (std area x [analyte]) / [std] fitted to y = *m*x + *b* where *m* = 1.4668 and *b* = -4 x 10^8 with a R^2 of 0.9934.

concentration of analyte	area of analyte	area tridecane (std)	(std area x [analyte]) / [std]
0.0518	31.73 x 10^8	82.65 x 10^8	26.13 x 10^8
0.0987	49.09 x 10^8	59.15 x 10^8	35.58 x 10^8
0.1517	79.87 x 10^8	58.76 x 10^8	54.34 x 10^8
0.1981	11.80 x 10^9	69.96 x 10^8	84.49 x 10^8

Table 6-11. Calibration Curve for *tert*-butyldimethyl(naphthalen-2-yloxy)silane.

Calibration Curve for 4,4,5,5-tetramethyl-2-(1,2,3,6-tetrahydro-[1,1'-biphenyl]-4-yl)-1,3,2-dioxaborolane:

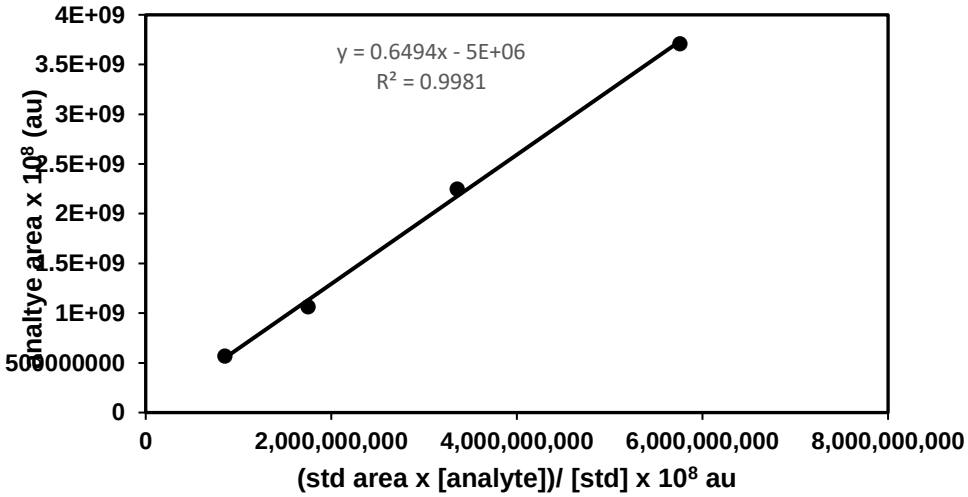

Plot of analyte area versus (std area x [analyte]) / [std] fitted to y = *m*x + *b* where *m* = 0.6494 and *b* = -5 x 10^6 with a R^2 of 0.9981.

concentration of analyte	area of analyte	area tridecane (std)	(std area x [analyte]) / [std]
0.0242	5.68 x 10^8	57.63 x 10^8	8.53 x 10^8
0.0510	10.66 x 10^8	56.34 x 10^8	17.52 x 10^8
0.0989	22.50 x 10^8	55.70 x 10^8	33.57 x 10^8
0.1548	37.09 x 10^8	61.00 x 10^8	57.58 x 10^8

Table 6-12. Calibration Curve for 4,4,5,5-tetramethyl-2-(1,2,3,6-tetrahydro-[1,1'-biphenyl]-4-yl)-1,3,2-dioxaborolane.

6.2.3 Table 2-9 Substrate Scope

1,1'-biphenyl [CAS: 92-52-4].

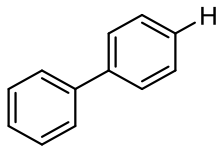

Table 2-9, 2-21B: Following general procedure B, $Ni(acac)_2$ (1.9 mg, 0.0075 mmol), IPr^{Me}·HCl (6.8 mg, 0.015 mmol), NaO-*t*-Bu (36.0 mg, 0.375 mmol), ([1,1'-biphenyl]-4-yloxy)(*tert*-butyl)dimethylsilane (42.0 mg, 0.148 mmol) and titanium(IV) isopropoxide (49 μL, 0.165 mmol) gave a crude residue. The yield was determined by GC-FID analysis using tridecane as an internal standard due to volatility of the product (tridecane integration: 329116406, biphenyl integration: 265260257, 0.139 mmol, 94%). The spectral data matches that previously reported in the literature.

^{1}H-NMR (500 MHz, $CDCl_3$): δ 7.61 (d, *J* = 7.5 Hz, 4H), 7.45 (t, *J* = 7.5 Hz, 4H), 7.36 (t, *J* = 7.5 Hz, 2H).

naphthalene [CAS: 91-20-3].

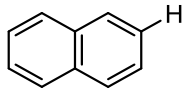

Table 2-9, 2-20B: Following a modified general procedure B, $Ni(acac)_2$ (1.9 mg, 0.0075 mmol), IPr^{Me}·HCl (6.8 mg, 0.015 mmol), NaO-*t*-Bu (36.0 mg, 0.375 mmol), *tert*-butyldimethyl(naphthalen-2-yloxy)silane (39.0 mg, 0.151 mmol), and titanium(IV) isopropoxide (49 μL, 0.165 mmol) at 120 °C for 3 h gave a crude residue. The yield was determined by GC-FID analysis using tridecane as an internal standard due to volatility of the product (tridecane integration: 332901580, naphthalene integration: 191812112, 0.130 mmol, 86%). The spectral data matches that previously reported in the literature.

^{1}H-NMR (500 MHz, $CDCl_3$): δ 7.85 (m, 4H), 7.49 (m, 4H).

naphthalene [CAS: 91-20-3].

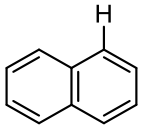

Table 2-9, 2-37B: Following a modified general procedure B, $Ni(acac)_2$ (1.9 mg, 0.0075 mmol), IPr^{Me}·HCl (6.8 mg, 0.015 mmol), NaO-*t*-Bu (36.0 mg, 0.375 mmol), *tert*-butyldimethyl(naphthalen-1-yloxy)silane (39.4 mg, 0.152 mmol), and titanium(IV) isopropoxide (49 μL, 0.165 mmol) at 120 °C for 3 h gave a crude residue. The yield was determined by GC-FID analysis using tridecane as an internal standard due to volatility of the product (tridecane integration: 229475874, naphthalene integration: 127832132, 0.125 mmol, 82%). The spectral data matches that previously reported in the literature.

^{1}H-NMR (500 MHz, $CDCl_3$): δ 7.85 (m, 4H), 7.49 (m, 4H).

trimethyl(naphthalen-2-yl)silane.

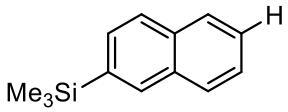

Table 2-9, 2-23B: Following a modified general procedure B, $Ni(acac)_2$ (1.9 mg, 0.0075 mmol), IPr^{Me}·HCl (6.8 mg, 0.015 mmol), NaO-*t*-Bu (36.0 mg, 0.375 mmol), *tert*-butyldimethyl((6-(trimethylsilyl)naphthalen-2-yl)oxy)silane (50.0 mg, 0.151 mmol), and titanium(IV) isopropoxide (49 μL, 0.165 mmol) at 120 °C for 3 h gave a crude residue which was purified by flash chromatography (100% hexanes) to afford the desired product (25.4 mg, 0.127 mmol, 84% yield). The spectral data matches that previously reported in the literature.

^{1}H-NMR (500 MHz, $CDCl_3$): δ 8.01 (s, 1H), 7.84 (m, 3H), 7.61 (d, *J* = 8.0 Hz, 1H), 7.48 (m, 2H), 0.34 (s, 3H).

[1,1'-biphenyl]-4-ol [CAS: 92-69-3].

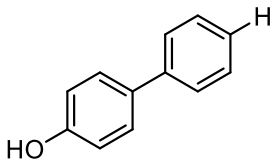

Table 2-9, 2-25B: Following a modified general procedure B, $Ni(acac)_2$ (3.9 mg, 0.015 mmol), IPr^{Me}·HCl (13.6 mg, 0.030 mmol), NaO-*t*-Bu (57.7 mg, 0.6 mmol), 4'-((*tert*-butyldimethylsilyl)oxy)-[1,1'-biphenyl]-4-ol (45.1 mg, 0.15 mmol), and titanium(IV) isopropoxide (49 μL, 0.165 mmol) at 120 °C for 16 h gave a crude residue which was purified by flash chromatography (hexanes: ethyl acetate 95:5) to afford the desired product (17.7 mg, 0.104 mmol, 69% yield). The spectral data matches that previously reported in the literature.

^{1}H-NMR (500 MHz, $CDCl_3$): δ 7.54 (m, 2H), 7.48 (m, 2H), 7.41 (t, *J* = 7.5 Hz, 2H), 7.32 (m, 1H), 6.91 (m, 2H), 4.70 (br, 1H).

([1,1'-biphenyl]-4-ylmethoxy)(*tert*-butyl)dimethylsilane.

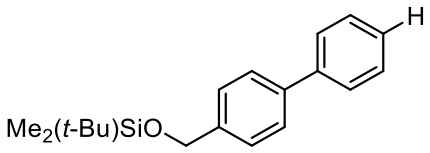

Table 2-9, 2-26B: Following a modified general procedure B, $Ni(acac)_2$ (1.9 mg, 0.0075 mmol), IPr^{Me}·HCl (6.8 mg, 0.015 mmol), NaO-*t*-Bu (36.0 mg, 0.375 mmol), *tert*-butyl((4'-((*tert*-butyldimethylsilyl)oxy)-[1,1'-biphenyl]-4-yl)methoxy)dimethylsilane (68.5 mg, 0.15 mmol), and

titanium(IV) isopropoxide (49 μL, 0.165 mmol) at 120 °C for 16 h gave a crude residue which was purified by flash chromatography (100% hexanes) to afford the desired product (41.3 mg, 0.138 mmol, 91% yield). The spectral data matches that previously reported in the literature.

^{1}H-NMR (500 MHz, $CDCl_3$): δ 7.58 (m, 4H), 7.42 (m, 4H), 7.33 (t, *J* = 7.5 Hz, 1H), 4.79 (s, 2H), 0.96 (s, 9H), 0.13 (s, 6H).

4-methoxy-1,1'-biphenyl [CAS: 613-37-6].

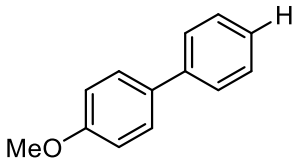

Table 2-9, 2-27B: Following a modified general procedure B, $Ni(acac)_2$ (1.9 mg, 0.0075 mmol), IPr^{Me}•HCl (6.8 mg, 0.015 mmol), NaO-*t*-Bu (36.0 mg, 0.375 mmol), *tert*-butyl((4'-methoxy-[1,1'-biphenyl]-4-yl)oxy)dimethylsilane (48.1 mg, 0.153 mmol), and titanium(IV) isopropoxide (49 μL, 0.165 mmol) at 120 °C for 16 h gave a crude residue which was purified by flash chromatography (hexanes: ethyl acetate 99:1) to afford the desired product (18.6 mg, 0.101 mmol, 66% yield). The spectral data matches that previously reported in the literature. [A 6:1 (4-methoxy-1,1'-biphenyl and 1,1'-biphenyl) ratio of products was observed.]

^{1}H-NMR (500 MHz, $CDCl_3$): δ 7.55 (m, 4H), 7.42 (t, *J* = 7.5 Hz, 2H), 7.31 (t, *J* = 7.5 Hz, 1H), 6.99 (m, *2*H), 3.86 (s, 3H).

1,1'-biphenyl [CAS: 92-52-4].

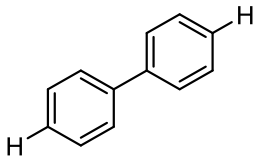

Table 2-9, 2-38B: Following a modified general procedure B, $Ni(acac)_2$ (3.9 mg, 0.015 mmol), IPr^{Me}·HCl (13.6 mg, 0.030 mmol), NaO-*t*-Bu (57.7 mg, 0.6 mmol), 4,4'-bis((*tert*-butyldimethylsilyl)oxy)-1,1'-biphenyl (61.8 mg, 0.149 mmol) and titanium(IV) isopropoxide (98 μL, 0.330 mmol) at 130 °C for 16 h gave a crude residue. The yield was determined by GC-FID analysis using tridecane as an internal standard due to volatility of the product (tridecane integration: 254280859, biphenyl integration: 144283275, 0.098 mmol, 66%). The spectral data matches that previously reported in the literature.

^{1}H-NMR (500 MHz, $CDCl_3$): δ 7.61 (d, *J* = 7.5 Hz, 4H), 7.45 (t, *J* = 7.5 Hz, 4H), 7.36 (t, *J* = 7.5 Hz, 2H).

2-methylquinoline.

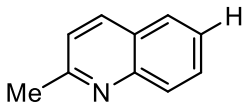

Table 2-9, 2-39B: Following a modified general procedure B, $Ni(acac)_2$ (1.9 mg, 0.0075 mmol), IPr^{Me}·HCl (6.8 mg, 0.015 mmol), NaO-*t*-Bu (36.0 mg, 0.375 mmol), 6-((*tert*-butyldimethylsilyl)oxy)-2-methylquinoline (40.9 mg, 0.150 mmol), and titanium(IV) isopropoxide (49 μL, 0.165 mmol) at 120 °C for 3 h gave a crude residue which was purified by flash chromatography (hexanes: ethyl acetate 90:10) to afford the desired product (15.8 mg, 0.110 mmol, 74% yield). The spectral data matches that previously reported in the literature.

^{1}H-NMR (500 MHz, $CDCl_3$): δ 8.04 (m, 2H), 7.77 (d, *J* = 7.0 Hz, 1H), 7.68 (t, *J* = 7.0 Hz, 1H), 7.48 (t, *J* = 7.5 Hz, 1H), 7.29 (d, *J* = 8.5 Hz, 1H), 2.75 (s, 3H).

9-methyl-9H-carbazole [CAS: 1484-12-4].

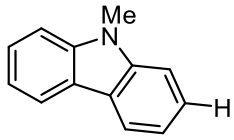

Table 2-9, 2-28B: Following general procedure B, $Ni(acac)_2$ (1.9 mg, 0.0075 mmol), IPr^{Me}·HCl (6.8 mg, 0.015 mmol), NaO-*t*-Bu (36.0 mg, 0.375 mmol), 2-((*tert*-butyldimethylsilyl)oxy)-9-methyl-9H-carbazole (47.2 mg, 0.152 mmol), and titanium(IV) isopropoxide (49 μL, 0.165 mmol) gave a crude residue which was purified by flash chromatography (hexanes: ethyl acetate 98:2) to afford the desired product (22.7 mg, 0.125 mmol, 83% yield). The spectral data matches that previously reported in the literature.

^{1}H-NMR (500 MHz, $CDCl_3$): δ 8.11 (d, *J* = 7.5 Hz, 2H), 7.49 (t, *J* = 7.5 Hz, 2H), 7.41 (d, *J* = 8.0 Hz, 2H), 7.24 (t, *J* = 7.0 Hz, 2H), 3.87 (s, 3H).

2-phenylpyridine [CAS: 1008-89-5].

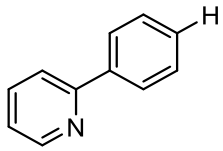

Table 2-9, 2-29B: Following a modified general procedure B, $Ni(acac)_2$ (1.9 mg, 0.0075 mmol), IPr^{Me}·HCl (6.8 mg, 0.015 mmol), NaO-*t*-Bu (36.0 mg, 0.375 mmol), 2-(4-((*tert*-butyldimethylsilyl)oxy)phenyl)pyridine (42.9 mg, 0.150 mmol), and titanium(IV) isopropoxide (49 μL, 0.165 mmol) at 120 °C for 3 h gave a crude residue which was purified by flash chromatography (hexanes: ethyl acetate 95:5) to afford the desired product (19.8 mg, 128 mmol, 85% yield). The spectral data matches that previously reported in the literature.

^{1}H-NMR (500 MHz, $CDCl_3$): δ 8.73 (d, *J* = 5.0 Hz, 1H), 8.02 (d, *J* = 8.0 Hz, 2H), 7.79 (m, *2*H), 7.51 (t, *J* = 7.5 Hz, 2H), 7.44 (t, *J* = 7.5 Hz, 1H), 7.27 (m, 1H).

4-phenylmorpholine [CAS: 92-53-5].

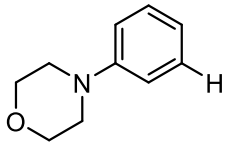

Table 2-9, 2-40B: Following a modified general procedure B, $Ni(acac)_2$ (3.9 mg, 0.015 mmol), IPr^{Me}·HCl (13.6 mg, 0.030 mmol), NaO-*t*-Bu (57.7 mg, 0.60 mmol), 4-(3-((*tert*-butyldimethylsilyl)oxy)phenyl)morpholine (44.5 mg, 0.152 mmol), and titanium(IV) isopropoxide (49 μL, 0.165 mmol) at 130 °C for 16 h gave a crude residue. The yield was determined by GC-FID analysis using tridecane as an internal standard due to volatility of the product (tridecane integration: 289820445, 4-phenylmorpholine integration: 61169732, 0.046 mmol, 30%). The spectral data matches that previously reported in the literature.

^{1}H-NMR (500 MHz, $CDCl_3$): δ 7.29 (m, 2H), 6.93 (d, *J* = 8.5 Hz, 2H), 6.89 (t, *J* = 7.5 Hz, 1H), 3.87 (t, *J* = 5.0 Hz, 4H), 3.16 (t, *J* = 5.0 Hz, 4H).

N-phenylacetamide [CAS: 103-84-4].

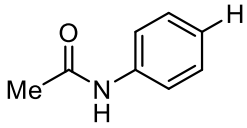

Table 2-9, 2-41B: Following a modified general procedure B, $Ni(acac)_2$ (3.9 mg, 0.015 mmol), IPr^{Me}·HCl (13.6 mg, 0.030 mmol), NaO-*t*-Bu (57.7 mg, 0.60 mmol), *N*-(4-((*tert*-butyldimethylsilyl)oxy)phenyl)acetamide (39.0 mg, 0.147 mmol), and titanium(IV) isopropoxide

(49 μL, 0.165 mmol) at 130 °C for 16 h gave a crude residue. The yield was determined by GC-FID analysis using tridecane as an internal standard due to volatility of the product (tridecane integration: 258912979, N-phenylacetamide integration: 22126637, 0.022 mmol, 15%). The spectral data matches that previously reported in the literature.

^{1}H-NMR (500 MHz, $CDCl_3$): δ 7.50 (d, *J* = 8.0 Hz, 2H), 7.32 (t, *J* = 8.0 Hz, 2H), 7.4-7.2 (br, 1H), 7.11 (t, *J* = 7.5 Hz, 1H), 2.18 (s, 3H).

***tert*-butylbenzene [CAS: 98-06-6].**

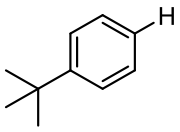

Table 2-9, 2-42B: Following a modified general procedure B, $Ni(COD)_2$ (4.1 mg, 0.015 mmol), IPr^{Me}·HCl (13.6 mg, 0.030 mmol), NaO-*t*-Bu (57.7 mg, 0.60 mmol), *tert*-butyl(4-(*tert*-butyl)phenoxy)dimethylsilane (39.8 mg, 0.150 mmol), and titanium(IV) isopropoxide (49 μL, 0.165 mmol) at 130 °C for 16 h gave a crude residue. The yield was determined by GC-FID analysis using tridecane as an internal standard due to volatility of the product (tridecane integration: 581498251, *tert*-butylbenzene integration: 170920319, 0.070 mmol, 46%). The spectral data matches that previously reported in the literature.

^{1}H-NMR (500 MHz, $CDCl_3$): δ 7.41 (d, *J* = 7.5 Hz, 2H), 7.32 (t, *J* = 7.5 Hz, 2H), 7.19 (t, *J* = 7.5 Hz, 1H), 1.34 (s, 9H).

2,3-dihydro-1H-indene [CAS: 496-11-7].

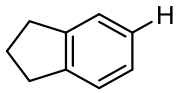

Table 2-9, 2-33B: Following a modified general procedure B, $Ni(acac)_2$ (3.9 mg, 0.015 mmol), IPr^{Me}·HCl (13.6 mg, 0.030 mmol), NaO-*t*-Bu (57.7 mg, 0.60 mmol), *tert*-butyl((2,3-dihydro-1H-inden-5-yl)oxy)dimethylsilane (37.0 mg, 0.149 mmol), and titanium(IV) isopropoxide (49 μL, 0.165 mmol) at 130 °C for 16 h gave a crude residue. The yield was determined by GC-FID analysis using tridecane as an internal standard due to volatility of the product (tridecane integration: 355781667, 2,3-dihydro-1H-indene integration: 153470439, 0.117 mmol, 77%). The spectral data matches that previously reported in the literature.

^{1}H-NMR (500 MHz, $CDCl_3$): δ 7.26 (m, 2H), 7.16 (m, 2H), 2.94 (t, *J* = 7.5 Hz, 4H, 2.10 (pentet, *J* = 7.5 Hz, 2H).

1,2,3,4-tetrahydronaphthalene [CAS: 119-64-2].

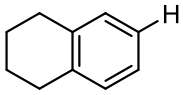

Table 2-9, 2-34B: Following a modified general procedure B, $Ni(acac)_2$ (3.9 mg, 0.015 mmol), IPr^{Me}·HCl (13.6 mg, 0.030 mmol), NaO^{t}Bu (57.7 mg, 0.60 mmol), *tert*-butyldimethyl((5,6,7,8-tetrahydronaphthalen-2-yl)oxy)silane (39.5 mg, 0.150 mmol), triisopropylsilane (184 μL, 0.9 mmol), and titanium(IV) isopropoxide (89 μL, 0.3 mmol) at 130 °C for 16 hours gave a crude residue. The yield was determined by GC-FID analysis using tridecane as an internal standard due to volatility of the product (tridecane integration: 377773699, 1,2,3,4-tetrahydronaphthalene integration: 153470439, 0.109 mmol, 73%). The spectral data matches that previously reported in the literature.

^{1}H-NMR (500 MHz, $CDCl_3$): δ 7.02 (m, 4H), 2.73 (m, 4H), 1.76 (m, 4H).

***tert*-butyldimethyl(((8R,9S,13S,14S,17S)-13-methyl-7,8,9,11,12,13,14,15,16,17-decahydro-6H-cyclopenta[a]phenanthren-17-yl)oxy)silane.**

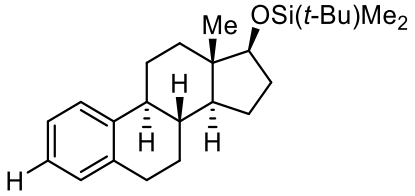

Table 2-9, 2.35B: Following a modified general procedure B, $Ni(acac)_2$ (3.9 mg, 0.015 mmol), IPr^{Me}·HCl (13.6 mg, 0.030 mmol), NaO-*t*-Bu (57.7 mg, 0.60 mmol), (((8R,9S,13S,14S,17S)-13-methyl-7,8,9,11,12,13,14,15,16,17-decahydro-6H-cyclopenta[a]phenanthrene-3,17-diyl)bis(oxy))bis(*tert*-butyldimethylsilane) (75.0 mg, 0.15 mmol), and titanium(IV) isopropoxide (49 μL, 0.165 mmol) at 130 °C for 16 h gave a crude residue which was purified by flash chromatography (100% hexanes) to afford the desired product as a white solid (42.5 mg, 0.115 mmol, 76% yield).

^{1}H-NMR (700 MHz, $CDCl_3$): δ 7.30 (d, *J* = 7.0 Hz, 1H), 7.14 (t, *J* = 7.0 Hz, 1H), 7.11 (t, *J* = 7.0 Hz, 1H), 7.08 (d, *J* = 7.0 Hz, 1H), 3.65 (t, *J* = 8.4 Hz, 1H), 2.86 (m, 2H), 2.32 (m, 1H), 2.23 (m, 1H), 1.89 (m, 3H), 1.66 (m, 1H), 1.50 (m, 4H), 1.33 (m, 2H), 1.18 (m, 3H), 0.90 (s, 9H), 0.75 (s, 3H), 0.03 (d, *J* = 9.1 Hz, 6H).
^{13}C-NMR (175 MHz, $CDCl_3$): δ 140.5, 136.8, 129.0, 125.5, 125.5, 125.3, 81.8, 49.8, 44.6, 43.6, 38.6, 37.2, 31.0, 29.6, 27.3, 26.3, 25.9, 23.3, 18.1, 11.4, 4.5, 4.8.
IR (film, cm^{-1}): 2923, 2852, 1469, 1247, 1097.
HRMS (EI) *m/z*: $[M]^+$ predicted for $C_{24}H_{38}OSi$, 370.2692; found, 370.2689.

6.2.4 Scheme 2-12 Deuterium Labeling Studies

tetrakis((propan-2-yl-d_7)oxy)titanium.

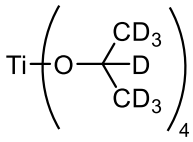

Titanium(IV) isopropoxide (1.0 ml, 3.4 mmol) was added to a flame dried round bottom under a nitrogen atmosphere. To this was added 2-propanol-d_8 (99.5%) (2.0 ml, 26.1 mmol) and the mixture was allowed to stir for 2 h. The reaction mixture was then concentrated, and the addition of 2-propanol-d_8 (99.5%) (2.0 ml, 26.1 mmol) and subsequent concentration after stirring for two h was repeated two more times to afford the desired product with 92% deuterium incorporation.

Standard Titanium(IV) isopropoxide, MS (EI) m/z: $[M\text{-}CH_3]+$ calc. for $C_{12}H_{28}O_4Ti$, 269.12, found, 269.1.

Titanium(IV) isopropoxide-d_{28} MS (EI) m/z: $[M\text{-}CD_3]+$ calc. for $C_{12}D_{28}O_4Ti$, 294.28, found, 294.3. Small amounts of d_{21}, d_{14}, or d_7 products detected. Characteristic peaks at m/z 290.3, 287.2, 283.2, 280.2, 276.2, and 273.1 indicate incomplete deuterium incorporation. Relative intensities:

M/Z	Intensity	Percent Deuterium	Deuterium Intensity
294.2 (d_{28})(-CD_3)	10330	100	10330
290.3 (d_{21})(-CH_3)	960	75	720
287.2 (d_{21})(-CD_3)	1562	75	1171.5
283.2 (d_{14})(-CH_3)	109.5	50	54.75
280.2 (d_{14})(-CD_3)	274.4	50	137.2
276.2 (d_7)(-CH_3)	128.3	25	32.075
273.1 (d_7)(-CD_3)	191.3	25	47.825
Total:	13555.5		12493.35

$$\frac{12493.35}{13555.5} = 0.92 = 92\% \text{ deuterium incorporation}$$

4-(trifluoromethyl)-1,1'-biphenyl.

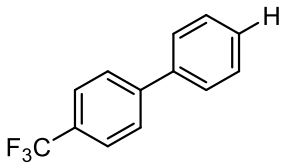

Following general procedure B, $Ni(acac)_2$ (1.9 mg, 0.0075 mmol), IPr^{Me}·HCl (6.8 mg, 0.015 mmol), NaO-*t*-Bu (36.0 mg, 0.375 mmol), *tert*-butyldimethyl((4'-(trifluoromethyl)-[1,1'-biphenyl]-4-yl)oxy)silane (56.6 mg, 0.161 mmol) and titanium(IV) isopropoxide (49 μL, 0.165 mmol) gave a crude residue which was purified by flash chromatography (100% hexanes) to afford the desired product as a white solid (19.2 mg, 0.086 mmol, 54% yield). The spectral data matches that previously reported in the literature.

^{1}H-NMR (500 MHz, $CDCl_3$): δ 7.70 (m, 4H), 7.60 (d, *J* = 7.0 Hz, 2H), 7.48 (t, *J* = 7.0 Hz, 2H), 7.41 (t, *J* = 7.0 Hz, 1H).

4-(trifluoromethyl)-1,1'-biphenyl-4'-*d*.

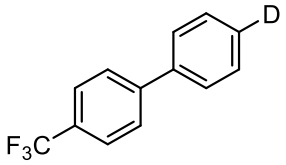

Scheme 2-12, 2-36D: Following a modified general procedure B, $Ni(COD)_2$ (4.1 mg, 0.015 mmol), IPr^{Me}·HCl (13.6 mg, 0.030 mmol), NaO-*t*-Bu (36.0 mg, 0.375 mmol), *tert*-butyldimethyl((4'-(trifluoromethyl)-[1,1'-biphenyl]-4-yl)oxy)silane (52.7 mg, 0.150 mmol) and tetrakis((propan-2-yl-d_7)oxy)titanium (51.5 mg, 0.165 mmol) gave a crude residue which was purified by flash chromatography (100% hexanes) to afford the desired product as a white solid (13.3 mg, 0.060 mmol, 40% yield) with 89% deuterium incorporation at the proton shown above, as determined by ^{1}H-NMR.

^{1}H-NMR (500 MHz, $CDCl_3$): δ 7.70 (m, 4H), 7.64 (d, *J* = 8.0 Hz, 2H), 7.48 (d, *J* = 7.5 Hz, 2H), 7.43 (t, *J* = 7.5 Hz, 0.11H).

^{13}C-NMR (175 MHz, $CDCl_3$): δ 144.7, 139. 7, 129.3 (q, *J* = 32.6 Hz), 128.9, 127.9 (t, *J* = 24.4 Hz), 127.4, 127.3, 126.2 (q, *J* = 3.7 Hz), 124.3 (q, *J* = 270.3 Hz). (minor proteo peak at 128.2)

IR (film, cm^{-1}): 2924, 2854, 2360, 1614, 1396, 1327.

HRMS (EI) *m/z*: $[M]^+$ predicted for $C_{13}H_8DF_3$, 223.0714; found, 223.0711.

6.2.5 Table 2-14 Substrate Scope

[1,1'-biphenyl]-4-yl(ethyl)dimethylsilane.

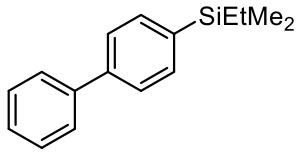

Table 2-14, entry 1: Following general procedure C, $Ni(COD)_2$ (4.1 mg, 0.015 mmol), IPr*OMe (14.2 mg, 0.015 mmol), NaO^{t}Bu (36.0 mg, 0.375 mmol), ([1,1'-biphenyl]-4-yloxy)(*tert*-butyl)dimethylsilane (43.4 mg, 0.153 mmol), and dimethylethylsilane (119 μL, 0.9 mmol) gave a crude residue which was purified by flash chromatography (100% hexanes) to afford the desired product (26.6 mg, 0.111 mmol, 73% yield). The yield for biphenyl was determined by GC-FID analysis using tridecane as an internal standard due to sublimability of the product (tridecane integration: 318617645, biphenyl integration: 12130473, 0.007 mmol, 4%).

^{1}H-NMR (500 MHz, $CDCl_3$): δ 7.61 (m, 6H), 7.45 (t, *J* = 7.5 Hz, 2H), 7.36 (t, *J* = 7.5 Hz, 1H), 1.00 (t, *J* = 7.5 Hz, 3H), 0.78 (q, *J* = 7.5 Hz, 2H), 0.30 (s, 6H).

^{13}C-NMR (125 MHz, $CDCl_3$): δ 141.5, 141.2, 138.2, 134.1, 128.7, 127.3, 127.1, 126.4, 7.4, 3.5.

IR (film, cm^{-1}): 3023, 2953, 2873, 1597, 1484, 1247.

HRMS (EI) *m/z*: $[M]^+$ predicted for $C_{16}H_{20}Si$, 240.1334; found, 240.1326.

[1,1'-biphenyl]-4-yldiethyl(methyl)silane.

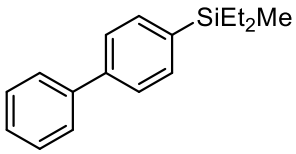

Table 2-14, entry 2: Following general procedure C, $Ni(COD)_2$ (4.1 mg, 0.015 mmol), IPr*OMe (14.2 mg, 0.015 mmol), NaO^tBu (36.0 mg, 0.375 mmol), ([1,1'-biphenyl]-4-yloxy)(*tert*-butyl)dimethylsilane (42.4 mg, 0.149 mmol), and diethylmethylsilane (131 µL, 0.9 mmol) gave a crude residue which was purified by flash chromatography (100% hexanes) to afford the desired product (28.3 mg, 0.111 mmol, 75% yield). The yield for biphenyl was determined by GC-FID analysis using tridecane as an internal standard due to sublimability of the product (tridecane integration: 231029643, biphenyl integration: 6144535, 0.005 mmol, 3%).

^{1}H-NMR (500 MHz, $CDCl_3$): δ 7.62 (m, 6H), 7.45 (t, *J* = 7.5 Hz, 2H), 7.36 (t, *J* = 7.5 Hz, 1H), 1.00 (t, *J* = 7.5 Hz, 6H), 0.81 (q, *J* = 7.5 Hz, 4H), 0.29 (s, 6H).
^{13}C-NMR (125 MHz, $CDCl_3$): δ 141.5, 141.2, 137.2, 134.4, 128.7, 127.3, 127.1, 126.4, 7.4, 5.5, -6.0
IR (film, cm^{-1}): 3022, 2952, 2873, 1597, 1484, 1251.
HRMS (EI) *m/z*: $[M]^+$ predicted for $C_{17}H_{22}Si$, 254.1491; found, 254.1491.

[1,1'-biphenyl]-4-yl(isopropyl)dimethylsilane.

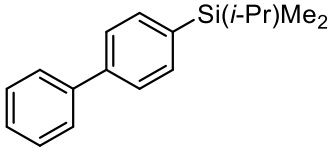

Table 2-14, entry 4: Following general procedure C, $Ni(COD)_2$ (4.1 mg, 0.015 mmol), IPr*OMe (14.2 mg, 0.015 mmol), NaO^tBu (36.0 mg, 0.375 mmol), ([1,1'-biphenyl]-4-yloxy)(*tert*-butyl)dimethylsilane (44.1 mg, 0.155 mmol), and dimethylisopropylsilane (127 µL, 0.9 mmol)

gave a crude residue which was purified by flash chromatography (100% hexanes) to afford the desired product (31.3 mg, 0.123 mmol, 79% yield). The yield for biphenyl was determined by GC-FID analysis using tridecane as an internal standard due to sublimability of the product (tridecane integration: 217553870, biphenyl integration: 11731319, 0.009 mmol, 6%).

^{1}H-NMR (500 MHz, $CDCl_3$): δ 7.61 (m, 6H), 7.45 (t, *J* = 7.5 Hz, 2H), 7.35 (t, *J* = 7.5 Hz, 1H), 1.00 (m, 7H), 0.28 (s, 6H).
^{13}C-NMR (125 MHz, $CDCl_3$): δ 141.5, 141.1, 137.4, 134.4, 128.7, 127.3, 127.1, 126.3, 17.6, 13.8, -5.3.
IR (film, cm^{-1}): 2953, 2862, 1597, 1484, 1383, 1249, 1114.
HRMS (EI) *m/z*: $[M]^+$ predicted for $C_{17}H_{22}Si$, 254.1491; found, 254.1495.

[1,1'-biphenyl]-4-yltripropylsilane.

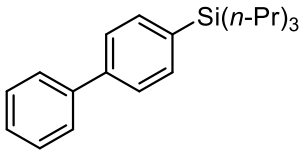

Table 2-14, entry 5: Following general procedure C, $Ni(COD)_2$ (4.1 mg, 0.015 mmol), IPr*OMe (14.2 mg, 0.015 mmol), NaO^tBu (36.0 mg, 0.375 mmol), ([1,1'-biphenyl]-4-yloxy)(*tert*-butyl)dimethylsilane (43.5 mg, 0.153 mmol), and tripropylsilane (188 µL, 0.9 mmol) gave a crude residue which was purified by flash chromatography (100% hexanes) to afford the desired product (40.7 mg, 0.131 mmol, 85% yield). The yield for biphenyl was determined by GC-FID analysis using tridecane as an internal standard due to sublimability of the product (tridecane integration: 296020364, biphenyl integration: 26809476, 0.016 mmol, 10%).

^{1}H-NMR (500 MHz, $CDCl_3$): δ 7.60 (m, 6H), 7.45 (t, *J* = 7.5 Hz, 2H), 7.35 (t, *J* = 7.5 Hz, 1H), 1.40 (m, 6H), 0.99 (t, *J* = 7.5 Hz, 9H), 0.83 (m, 6H).
^{13}C-NMR (125 MHz, $CDCl_3$): δ 141.3, 141.2, 137.0, 134.6, 128.7, 127.2, 127.1, 126.3, 18.6, 17.5, 15.3.

IR (film, cm^{-1}): 2952, 2922, 2866, 1597, 1484, 1196.

HRMS (EI) *m/z*: $[M]^+$ predicted for $C_{21}H_{30}Si$, 310.2117; found, 310.2117.

[1,1'-biphenyl]-4-yl(*tert*-butyl)dimethylsilane

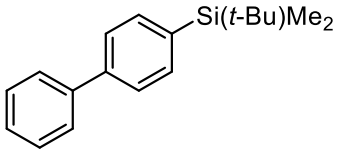

Table 2-14, entry 6: Following general procedure C, $Ni(COD)_2$ (4.1 mg, 0.015 mmol), IPr*OMe (14.2 mg, 0.015 mmol), NaO^{t}Bu (36.0 mg, 0.375 mmol), ([1,1'-biphenyl]-4-yloxy)(*tert*-butyl)dimethylsilane (40.2 mg, 0.141 mmol), and *tert*-butyldimethylsilane (150 µL, 0.9 mmol) gave a crude residue which was purified by flash chromatography (100% hexanes) to afford the desired product (05.3 mg, 0.020 mmol, 14% yield). The yield for biphenyl was determined by GC-FID analysis using tridecane as an internal standard due to sublimability of the product (tridecane integration: 323972611, biphenyl integration: 93135824, 0.050 mmol, 34%).

^{1}H-NMR (500 MHz, $CDCl_3$): δ 7.59 (m, 6H), 7.44 (t, *J* = 7.5 Hz, 2H), 7.35 (t, *J* = 7.5 Hz, 1H), 0.91 (s, 9H), 0.30 (s, 6H).

^{13}C-NMR (125 MHz, $CDCl_3$): δ 141.4, 141.1, 136.6, 134.9, 128.7, 127.3, 127.1, 126.1, 26.5, 16.9, 6.1.

IR (film, cm^{-1}): 2924, 2852, 1595, 1468, 1252.

HRMS (EI) *m/z*: $[M]^+$ predicted for $C_{18}H_{24}Si$, 268.1647; found, 268.1648.

[1,1'-biphenyl]-4-yl(benzyl)dimethylsilane

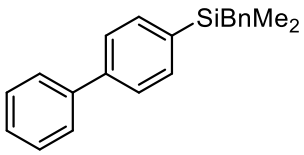

Table 2-14, entry 8: Following general procedure C, $Ni(COD)_2$ (4.1 mg, 0.015 mmol), IPr*OMe (14.2 mg, 0.015 mmol), NaO^{t}Bu (36.0 mg, 0.375 mmol), ([1,1'-biphenyl]-4-yloxy)(*tert*-butyl)dimethylsilane (43.3 mg, 0.152 mmol), and benzyldimethylsilane (140 µL, 0.9 mmol) gave a crude residue which was purified by flash chromatography (100% hexanes) to afford the desired product (20.0 mg, 0.066 mmol, 43% yield). The yield for biphenyl was determined by GC-FID analysis using tridecane as an internal standard due to sublimability of the product (tridecane integration: 244625734, biphenyl integration: 27662478, 0.020 mmol, 12%).

^{1}H-NMR (500 MHz, $CDCl_3$): δ 7.56 (m, 6H), 7.47 (t, *J* = 7.5 Hz, 2H), 7.37 (t, *J* = 7.5 Hz, 1H), 7.21 (t, *J* = 7.5 Hz, 2H), 7.09 (t, *J* = 7.5 Hz, 1H), 6.98 (d, *J* = 7.5 Hz, 2H), 2.36 (s, 2H), 0.30 (s, 6H).
^{13}C-NMR (125 MHz, $CDCl_3$): δ 141.8, 141.0, 139.6, 137.2, 134.2, 128.8, 128.3, 128.1, 127.4, 127.1, 126.4, 124.1, 26.2, 3.4.
IR (film, cm^{-1}): 3026, 2961, 2889, 1596, 1492, 1483, 1246.
HRMS (EI) *m/z*: $[M]^+$ predicted for $C_{21}H_{22}Si$, 302.1491; found, 302.1491.

6.2.6 Table 2-15 Substrate Scope

[1,1'-biphenyl]-4-yltriethylsilane.

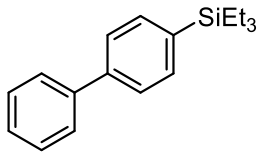

Table 2-15, 2-21A: Following general procedure C, $Ni(COD)_2$ (4.1 mg, 0.015 mmol), IPr*OMe (14.2 mg, 0.015 mmol), NaO-*t*-Bu (36.0 mg, 0.375 mmol), ([1,1'-biphenyl]-4-yloxy)(*tert*-butyl)dimethylsilane (42.6 mg, 0.15 mmol), and triethylsilane (144 µL, 0.9 mmol) gave a crude residue which was purified by flash chromatography (100% hexanes) to afford the desired product (36.6 mg, 0.137 mmol, 91% yield). The yield for biphenyl was determined by GC-FID analysis

using tridecane as an internal standard due to volatility of the product (tridecane integration: 163648334, biphenyl integration: 776212, 0.0008 mmol, 1%; [1,1'-biphenyl]-4-yltriethylsilane integration: 238889415, 0.145 mmol, 97%). The spectral data matches that previously reported in the literature.

^{1}H-NMR (500 MHz, $CDCl_3$): δ 7.64 - 7.58 (m, 6H), 7.46 (dt, *J* = 7.3, 0.7 Hz, 2H), 7.36 (m, 1H), 1.02 (t, *J* = 8.0 Hz, 9H), 0.85 (q, *J* = 8.0, 6H).

triethyl(naphthalen-2-yl)silane.

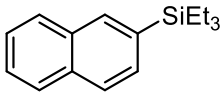

Table 2-15, 2-20A: Following general procedure C, $Ni(COD)_2$ (4.1 mg, 0.015 mmol), IPr*OMe (14.2 mg, 0.015 mmol), NaO-*t*-Bu (36.0 mg, 0.375 mmol), *tert*-butyldimethyl(naphthalen-2-yloxy)silane (39.1 mg, 0.151 mmol), and triethylsilane (144 μL, 0.9 mmol) gave a crude residue which was purified by flash chromatography (100% hexanes) to afford the desired product (27.2 mg, 0.112 mmol, 74% yield). The spectral data matches that previously reported in the literature.

^{1}H-NMR (500 MHz, $CDCl_3$): δ 8.0 (s, 1H), 7.83 (m, 3H), 7.58 (d, J = 8.0, 1H), 7.49 (dd, J = 6.3, 3.2 Hz, 2H), 1.02 (t, J = 7.5 Hz, 9H), 0.89 (q, J = 7.6 Hz, 6H).

triethyl(naphthalen-1-yl)silane.

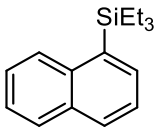

Table 2-15, 2-37A: Following a modified general procedure C, $Ni(COD)_2$ (10.3 mg, 0.038 mmol), IPr*OMe (35.5 mg, 0.038 mmol), NaO-*t*-Bu (36.0 mg, 0.375 mmol), *tert*-butyldimethyl(naphthalen-1-yloxy)silane (39.3 mg, 0.152 mmol), and triethylsilane (144 μL, 0.9 mmol) at 130 °C for 24 h gave a crude residue which was purified by flash chromatography (100% hexanes) to afford the desired product (22.9 mg, 0.094 mmol, 62% yield). The spectral data matches that previously reported in the literature.

^{1}H-NMR (500 MHz, $CDCl_3$): δ 8.10 (d, *J* = 7.5 Hz, 1H), 7.86 (m, 2H), 7.8 (m, 1H), 7.47 (m, 3H), 0.99 (m, 15H).

triethyl(6-(trimethylsilyl)naphthalen-2-yl)silane.

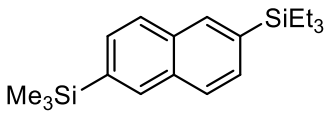

Table 2-15, 2-33A: Following general procedure C, $Ni(COD)_2$ (4.1 mg, 0.015 mmol), IPr*OMe (14.2 mg, 0.015 mmol), NaO-*t*-Bu (36.0 mg, 0.375 mmol), *tert*-butyldimethyl((6-(trimethylsilyl)naphthalen-2-yl)oxy)silane (49.3 mg, 0.149 mmol), and triethylsilane (144 μL, 0.9 mmol) gave a crude residue which was purified by flash chromatography (100% hexanes) to afford the desired product (37.1 mg, 0.118 mmol, 79% yield).

^{1}H-NMR (500 MHz, $CDCl_3$): δ 7.989 (s, 1H), 7.97 (s, 1H), 7.82 (dd, *J* = 8.0, 4.5 Hz, 2H), 7.61 (d, *J* = 8.0 Hz, 1H), 7.58 (d, *J* = 8.5 Hz, 1H), 1.00 (t, *J* = 8.5 Hz, 9H), 0.88 (q, *J* = 8.0 Hz, 6H), 0.35 (s, 9H).
^{13}C-NMR (125 MHz, $CDCl_3$): δ 138.3, 135.4, 134.6, 133.5, 133.1, 133.0, 130.7, 129.7, 127.0, 126.8, 7.4, 3.4, 1.1.
IR (film, cm^{-1}): 3039, 2952, 2874, 1577, 1456, 1312, 1246.
HRMS (EI) *m/z*: $[M]^+$ predicted for $C_{19}H_{30}Si_2$, 314.1886; found, 314.1889.

4'-(triethylsilyl)-[1,1'-biphenyl]-4-ol.

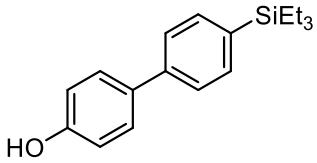

Table 2-15, 2-25A: Following a modified general procedure C, $Ni(COD)_2$ (10.3 mg, 0.038 mmol), IPr*OMe (35.5 mg, 0.038 mmol), NaO-*t*-Bu (36.0 mg, 0.375 mmol), 4'-((*tert*-butyldimethylsilyl)oxy)-[1,1'-biphenyl]-4-ol (44.3 mg, 0.147 mmol), and triethylsilane (144 μL, 0.9 mmol) at 120 °C for 16 h gave a crude residue which was purified by flash chromatography (hexanes: ethyl acetate 95:5) to afford the desired product (30.4 mg, 0.107 mmol, 72% yield).

^{1}H-NMR (500 MHz, $CDCl_3$): δ 7.55 - 7.49 (m, 6H), 6.90 (dt, *J* = 8.8, 2.2 Hz, 2H), 4.78 (s, 1H), 1.00 (t, *J* = 8.3 Hz, 9H), 0.83 (q, *J* = 7.8 Hz, 6H).
^{13}C-NMR (125 MHz, $CDCl_3$): δ 155.1, 140.9, 135.5, 134.7, 134.0, 128.4, 125.9, 115.6, 7.4, 3.4.
IR (film, cm^{-1}): 3290, 2951, 2873, 1596, 1521, 1458, 1244.
HRMS (EI) *m/z*: $[M]^+$ predicted for $C_{18}H_{24}OSi$, 284.1596; found, 284.1606.

***tert*-butyldimethyl((4'-(triethylsilyl)-[1,1'-biphenyl]-4-yl)methoxy)silane.**

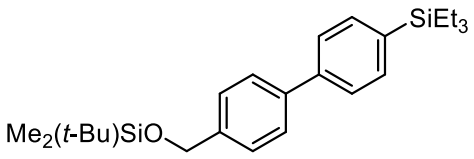

Table 2-15, 2-26A: Following a modified general procedure C, $Ni(COD)_2$ (10.3 mg, 0.038 mmol), IPr*OMe (35.5 mg, 0.038 mmol), NaO-*t*-Bu (36.0 mg, 0.375 mmol), *tert*-butyl((4'-((*tert*-butyldimethylsilyl)oxy)-[1,1'-biphenyl]-4-yl)methoxy)dimethylsilane (67.3 mg, 0.157 mmol), and triethylsilane (144 μL, 0.9 mmol) at 100 °C for 8 h gave a crude residue which was purified by flash chromatography (100% hexanes) to afford the desired product (50.2 mg, 0.122 mmol, 78% yield).

^{1}H-NMR (500 MHz, $CDCl_3$): δ 7.58 (m, 6H), 7.40 (d, *J* = 8.0 Hz, 2H), 1.00 (t, *J* = 8.0 Hz, 9H), 0.97 (s, 9H), 0.83 (q, *J* = 8.0 Hz, 6H), 0.13 (s, 6H).

^{13}C-NMR (125 MHz, $CDCl_3$): δ 141.3, 140.5, 139.8, 136.0, 134.7, 126.9, 126.5, 126.3, 64.8, 26.0, 18.5, 7.4, 3.4, -5.2.

IR (film, cm^{-1}): 2951, 2874, 1599, 1462, 1375, 1252.

HRMS (EI) *m/z*: $[M]^+$ predicted for $C_{25}H_{40}OSi_2$, 412.2618; found, 412.2628.

triethyl(4'-methoxy-[1,1'-biphenyl]-4-yl)silane.

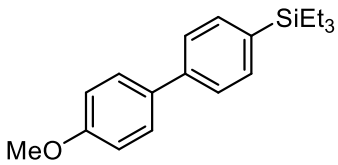

Table 2-15, 2-27A: Following a modified general procedure C, $Ni(COD)_2$ (10.3 mg, 0.038 mmol), IPr*OMe (35.5 mg, 0.038 mmol), NaO-*t*-Bu (36.0 mg, 0.375 mmol), *tert*-butyl((4'-methoxy-[1,1'-biphenyl]-4-yl)oxy)dimethylsilane (45.9 mg, 0.146 mmol), and triethylsilane (144 μL, 0.9 mmol) at 100 °C for 8 h gave a crude residue which was purified by flash chromatography (hexanes: ethyl acetate 99:1) to afford the desired product (31.1 mg, 0.104 mmol, 71% yield). [A 37:7:1 (triethyl(4'-methoxy-[1,1'-biphenyl]-4-silane:4-methoxy-1,1'-biphenyl:[1,1'-biphenyl]-4-yloxy)(*tert*-butyl)dimethylsilane) ratio of products was observed.]

^{1}H-NMR (500 MHz, $CDCl_3$): δ 7.55 (m, 6H), 6.98 (dt, *J* = 8.8 Hz, 2H), 3.86 (s, 3H), 1.00 (t, *J* = 8.1 Hz, 9H), 0.81 (q, *J* = 7.8 Hz, 6H).

^{13}C-NMR (125 MHz, $CDCl_3$): δ 159.2, 141.0, 135.4, 134.7, 133.7, 128.1, 125.9, 114.2, 55.3, 7.4, 3.4.

IR (film, cm^{-1}): 2952, 1602, 1492, 1462, 1248.

HRMS (EI) *m/z*: $[M]^+$ predicted for $C_{19}H_{26}OSi$, 298.1753; found, 298.1763.

4,4'-bis(triethylsilyl)-1,1'-biphenyl.

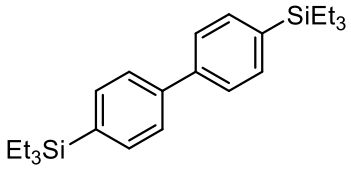

Table 2-15, 2-38A: Following a modified general procedure C, $Ni(COD)_2$ (10.3 mg, 0.038 mmol), IPr*OMe (35.5 mg, 0.038 mmol), NaO-*t*-Bu (36.0 mg, 0.375 mmol), 4,4'-bis((*tert*-butyldimethylsilyl)oxy)-1,1'-biphenyl (63.9 mg, 0.154 mmol), and triethylsilane (144 μL, 0.9 mmol) at 120 °C for 16 h gave a crude residue which was purified by flash chromatography (100% hexanes) to afford the desired product (43.1 mg, 0.113 mmol, 73% yield).

^{1}H-NMR (500 MHz, $CDCl_3$): δ 7.58 (m, 8 H), 1.0 (t, *J* = 8.0 Hz, 18H), 0.83 (q, *J* = 8.0 Hz, 12H).
^{13}C-NMR (125 MHz, $CDCl_3$): δ 141.4, 136.2, 134.7, 126.3, 7.4, 3.4.
IR (film, cm^{-1}): 3068, 2950, 2872, 1594, 1455, 1380, 1236.
HRMS (EI) *m/z*: $[M]^+$ predicted for $C_{19}H_{26}OSi$, 382.2512; found, 382.2510.

2-methyl-6-(triethylsilyl)quinolone.

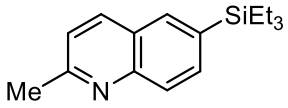

Table 2-15, 2-39A: Following general procedure C, $Ni(COD)_2$ (4.1 mg, 0.015 mmol), IPr*OMe (14.2 mg, 0.015 mmol), NaO-*t*-Bu (36.0 mg, 0.375 mmol), 6-((*tert*-butyldimethylsilyl)oxy)-2-methylquinoline (44.7 mg, 0.163 mmol), and triethylsilane (144 μL, 0.9 mmol) gave a crude residue which was purified by flash chromatography (hexanes: ethyl acetate 95:5) to afford the desired product (22.5 mg, 0.087 mmol, 53% yield).

^{1}H-NMR (500 MHz, $CDCl_3$): δ 8.04 (d, *J* = 8.5Hz, 1H), 7.98 (d, *J* = 8.5 Hz, 1H), 7.89 (s, 1H), 7.77 (d, *J* = 8.0 Hz, 1H), 7.28 (d, *J* = 8.0 Hz, 1H), 2.75 (s, 3H), 0.94 (t, *J* = 8.0 Hz, 9H), 0.88 (q, *J* = 8.0 Hz, 6H).

^{13}C-NMR (125 MHz, $CDCl_3$): δ 159.2, 136.2, 135.1, 134.3, 134.3, 129.6, 127.5, 126.0, 121.9, 25.4, 7.4, 3.4.

IR (film, cm^{-1}): 2950, 2873, 1612, 1560, 1465, 1223.

HRMS (ESI+) *m/z*: $[M+H]^+$ predicted for $C_{16}H_{23}NSi$, 258.1673; found, 258.1671.

9-methyl-2-(triethylsilyl)-9H-carbazole.

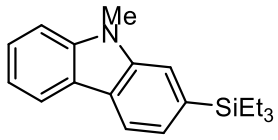

Table 2-15, 2-28A: Following general procedure C, $Ni(COD)_2$ (4.1 mg, 0.015 mmol), IPr*OMe (14.2 mg, 0.015 mmol), NaO-*t*-Bu (36.0 mg, 0.375 mmol), 2-((*tert*-butyldimethylsilyl)oxy)-9-methyl-9H-carbazole (46.1 mg, 0.148 mmol), and triethylsilane (144 μL, 0.9 mmol)gave a crude residue which was purified by flash chromatography (hexanes: ethyl acetate 99:1) to afford the desired product (38.1 mg, 0.130 mmol, 87% yield). The spectral data matches that previously reported in the literature.

^{1}H-NMR (500 MHz, $CDCl_3$): δ 8.10 (m, 2H), 7.53 (d, *J* = 2.5 Hz, 1H), 7.47 (t, *J* = 7.0 Hz, 1H), 7.41 (d, *J* = 8.0 Hz, 1H), 7.37 (dd, *J* = 7.5, 3.0 Hz, 1H), (7.23, dt, *J* = 8.0, 2.5 Hz, 1H), 3.89 (s, 3H), 1.03 (dt, *J* = 8.0 Hz, 3.5 Hz, 9H), 0.91 (dq, *J* = 8.0, 3.5 Hz, 6H).

2-(4-(triethylsilyl)phenyl)pyridine.

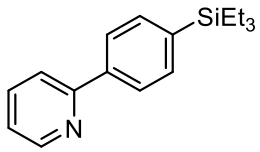

Table 2-15, 2-29A: Following general procedure C, $Ni(COD)_2$ (4.1 mg, 0.015 mmol), IPr*OMe (14.2 mg, 0.015 mmol), NaO-*t*-Bu (36.0 mg, 0.375 mmol), 2-(4-((*tert*-butyldimethylsilyl)oxy)phenyl)pyridine (40.0 mg, 0.139 mmol), and triethylsilane (144 μL, 0.9 mmol) gave a crude residue which was purified by flash chromatography (hexanes: ethyl acetate 90:10) to afford the desired product (26.4 mg, 0.098 mmol, 70% yield).

^{1}H-NMR (500 MHz, $CDCl_3$): δ 8.70 (d, *J* = 5.0 Hz, 1H), 7.97 (d, *J* = 8.0 Hz, 2H), 7.76 (m, 2H), 7.61 (d, *J* = 8.0 Hz, 2H), 7.24 (m, 1H), 0.98 (t, *J* = 8.0 Hz, 9H), 0.83 (q, *J* = 8.0 Hz, 6H).
^{13}C-NMR (125 MHz, $CDCl_3$): δ 157.6, 149.7, 139.6, 138.4, 136.7, 134.7, 126.0, 122.1, 120.6, 7.4, 3.3.
IR (film, cm^{-1}): 2951, 2873, 1586, 1464, 1430, 1382, 1236.
HRMS (ESI+) *m/z*: $[M+H]^+$ predicted for $C_{17}H_{23}NSi$, 286.1622; found, 286.1623.

4-(3-(triethylsilyl)phenyl)morpholine.

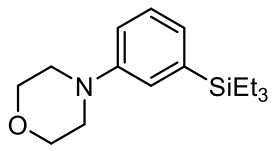

Table 2-15, 2-40A: Following a modified general procedure C, $Ni(COD)_2$ (10.3 mg, 0.038 mmol), IPr*OMe (35.5 mg, 0.038 mmol), NaO-*t*-Bu (36.0 mg, 0.375 mmol), 4-(3-((*tert*-butyldimethylsilyl)oxy)phenyl)morpholine (44.0 mg, 0.15 mmol), and triethylsilane (144 μL, 0.9 mmol) at 130 °C for 24 h gave a crude residue which was purified by flash chromatography (100% hexanes) to afford the desired product (32.0 mg, 0.116 mmol, 77% yield).

^{1}H-NMR (500 MHz, $CDCl_3$): δ 7.28 (d, *J* = 7.6 Hz, 1H), 7.05 (d, *J* = 2.5 Hz, 1H), 7.02 (d, *J* = 7.1 Hz, 1H), 6.91 (dd, *J* = 8.1, 2.5 Hz, 1H), 3.88 (t, *J* = 4.9 Hz, 4H), 3.17 (t, *J* = 4.9 Hz, 4H), 0.97 (t, *J* = 7.8 Hz, 9H), 0.78 (q, *J* = 7.8 Hz, 6H).

^{13}C-NMR (125 MHz, $CDCl_3$): δ 150.6, 138.4, 128.5, 126.1, 121.6, 116.2, 67.0, 49.6, 7.5, 3.4.

IR (film, cm^{-1}): 2953, 2873, 1586, 1449, 1229.

HRMS (EI) *m/z*: $[M]^+$ predicted for $C_{16}H_{27}NOSi$, 277.1862; found, 277.1863.

N-(4-(triethylsilyl)phenyl)acetamide.

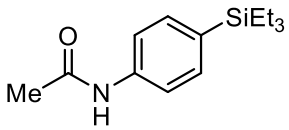

Table 2-15, 2-41A: Following a modified general procedure C, $Ni(COD)_2$ (10.3 mg, 0.038 mmol), IPr*OMe (35.5 mg, 0.038 mmol), NaO-*t*-Bu (36.0 mg, 0.375 mmol), N-(4-((*tert*-butyldimethylsilyl)oxy)phenyl)acetamide (39.8 mg, 0.15 mmol), and triethylsilane (144 μL, 0.9 mmol) at 130 °C for 24 h gave a crude residue which was purified by flash chromatography (100% hexanes) to afford the desired product (27.7 mg, 0.111 mmol, 74% yield).

^{1}H-NMR (500 MHz, $CDCl_3$): δ 7.46 (m, 4H), 7.30 (b, 1H), 2.17 (s, 3H), 0.95 (t, *J* = 8.0 Hz, 9H), 0.77 (q, *J* = 8.0 Hz, 6H).

^{13}C-NMR (125 MHz, $CDCl_3$): δ 168.3, 138.3, 135.0, 133.0, 119.0, 24.6, 7.3, 3.6.

IR (film, cm^{-1}): 3307, 2952, 2874, 1669, 1590, 1526, 1388.

HRMS (EI) *m/z*: $[M]^+$ predicted for $C_{14}H_{23}NOSi$, 249.1549; found, 249.1548.

(4-(*tert*-butyl)phenyl)triethylsilane.

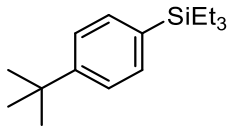

Table 2-15, 2-42A: Following a modified general procedure C, $Ni(COD)_2$ (10.3 mg, 0.038 mmol), IPr*OMe (35.5 mg, 0.038 mmol), NaO-*t*-Bu (36.0 mg, 0.375 mmol), *tert*-butyl(4-(*tert*-butyl)phenoxy)dimethylsilane (39.6 mg, 0.15 mmol), and triethylsilane (144 μL, 0.9 mmol) at 130 °C for 24 h gave a crude residue which was purified by flash chromatography (100% hexanes) to afford the desired product (34.0 mg, 0.137 mmol, 91% yield). The spectral data matches that previously reported in the literature.

^{1}H-NMR (500 MHz, $CDCl_3$): δ 7.43 (m, 2H), 7.37 (m, 2H), 1.32 (s, 9H), 0.97 (t, *J* = 7.5 Hz, 9H), 0.78 (q, *J* = 7.5 Hz, 6H).

(2,3-dihydro-1H-inden-5-yl)triethylsilane.

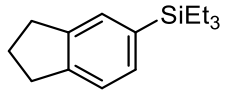

Table 2-15, 2-33A: Following a modified general procedure C, $Ni(COD)_2$ (10.3 mg, 0.038 mmol), IPr*OMe (35.5 mg, 0.038 mmol), NaO-*t*-Bu (36.0 mg, 0.375 mmol), *tert*-butyl((2,3-dihydro-1H-inden-5-yl)oxy)dimethylsilane (37.2 mg, 0.15 mmol) and triethylsilane (144 μL, 0.9 mmol) at 130 °C for 24 h gave a crude residue which was purified by flash chromatography (100% hexanes) to afford the desired product (29.7 mg, 0.128 mmol, 85% yield).

^{1}H-NMR (500 MHz, $CDCl_3$): δ 7.37 (s, 1H), 7.25 (m, 2H), 2.92 (dt, *J* = 7.5, 3.0 Hz, 4H), 2.06 (pentet, *J* = 7.5 Hz, 2H), 0.97 (t, *J* = 7.5 Hz, 9H), 0.78 (q, *J* = 7.5 Hz, 6H).

^{13}C-NMR (125 MHz, $CDCl_3$): δ 145.0, 143.5, 134.5, 132.0, 130.1, 123.9, 32.9, 32.8, 25.1, 7.5, 3.5.

IR (film, cm^{-1}): 2950, 2873, 1458, 1415, 1236.

HRMS (EI) *m/z*: $[M]^+$ predicted for $C_{15}H_{24}Si$, 232.1647; found, 232.1646.

triethyl(5,6,7,8-tetrahydronaphthalen-2-yl)silane.

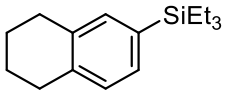

Table 2-15, 2-34A: Following a modified general procedure C, $Ni(COD)_2$ (10.3 mg, 0.038 mmol), IPr*OMe (35.5 mg, 0.038 mmol), NaO^tBu (36.0 mg, 0.375 mmol), *tert*-butyldimethyl((5,6,7,8-tetrahydronaphthalen-2-yl)oxy)silane (39.1 mg, 0.149 mmol), and triethylsilane (144 μL, 0.9 mmol) at 130 °C for 24 hours gave a crude residue which was purified by flash chromatography (100% hexanes) to afford the desired product (29.3 mg, 0.119 mmol, 82% yield).

^{1}H-NMR (500 MHz, $CDCl_3$): δ 7.21 (d, *J* = 7.5 Hz, 1H), 7.18 (s, 1H), 7.05 (d, *J* = 7.5 Hz, 1H), 2.78 (m, 4H), 1.81 (m, 4H), 0.98 (t, *J* = 8.0 Hz, 9H), 0.78 (q, *J* = 8.0 Hz, 6H).

^{13}C-NMR (125 MHz, $CDCl_3$): δ 137.8, 136.3, 135.2, 133.9, 131.2, 128.5, 29.42, 29.39, 23.3, 23.2, 7.5, 3.4.

IR (film, cm^{-1}): 2929, 2873, 1458, 1415, 1236.

HRMS (EI) *m/z*: $[M]^+$ predicted for $C_{16}H_{26}Si$, 246.1804; found, 246.1807.

***tert*-butyldimethyl(((8R,9S,13S,14S,17S)-13-methyl-3-(triethylsilyl)-7,8,9,11,12,13,14,15,16,17-decahydro-6H-cyclopenta[a]phenanthren-17-yl)oxy)silane.**

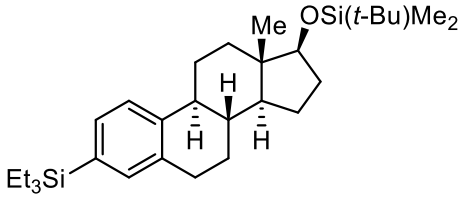

Table 2-15, 2-35A: Following a modified general procedure C, $Ni(COD)_2$ (10.3 mg, 0.038 mmol), IPr*OMe (35.5 mg, 0.038 mmol), NaO-*t*-Bu (36.0 mg, 0.375 mmol), (((8R,9S,13S,14S,17S)-13-methyl-7,8,9,11,12,13,14,15,16,17-decahydro-6H-cyclopenta[a]phenanthrene-3,17-diyl)bis(oxy))bis(*tert*-butyldimethylsilane) (77.4 mg, 0.155 mmol), and triethylsilane (144 μL, 0.9 mmol) at 130 °C for 24 h gave a crude residue which was purified by flash chromatography (100% hexanes) to afford the desired product (70.2 mg, 0.148 mmol, 94% yield).

^{1}H-NMR (500 MHz, $CDCl_3$): δ 7.28 (m, 2H), 7.19 (s, 1H), 3.65 (t, J = 8.0 Hz, 1H), 2.86 (m, 2H), 2.31 (m, 1H), 2.24 (dt, *J* = 11.5, 4.0 Hz, 1H), 1.89 (m, 3H), 1.66 (m, 1H), 1.49 (m, 3H), 1.32 (m, 2H), 1.18 (m, 2H), 0.97 (t, *J* = 7.5 Hz, 9H), 0.90 (s, 9H), 0.77 (q, *J* = 8.0 Hz, 6H), 0.74 (s, 3H), 0.03 (d, *J* = 6.5 Hz, 6H).
^{13}C-NMR (125 MHz, $CDCl_3$): δ 141.1, 135.9, 135.0, 134.0, 131.5, 124.6. 81.7, 49.9, 44.7, 43.6, 38.6, 37.2, 31.0, 29.7, 27.3, 26.0, 25.9, 23.3, 18.2, 11.4, 7.5, 3.4, -4.5, -4.8.
IR (film, cm^{-1}): 2949, 2866, 1594, 1462, 1371, 1253.
HRMS (EI) *m/z*: $[M]^+$ predicted for $C_{30}H_{52}OSi_2$, 484.3557; found, 484.3558.

6.3 General Experimental Details for Chapter 3

6.3.1 General Procedures for Chapter 3

General Procedure for the $Ni(COD)_2/IPr^{Me}\cdot HCl$ promoted amination of silyloxyarenes using amines (D):

A reaction tube containing a stir bar was charged with aryl silyl ether (1 equiv.), $Ni(COD)_2$ (5 mol%), $IPr^{Me}\cdot HCl$ (10 mol%), NaO-*t*-Bu (2.5 equiv.), toluene (0.5 M) and amine. The sealed reaction tube was brought outside the glovebox and placed in a heated block set to 120 ^oC and stirred for 16 hours, unless noted otherwise. The mixture was cooled to room temperature, quenched with dichloromethane (1 mL), and diluted with EtOAc (3 mL). The mixture was then run through a silica plug, concentrated under reduced pressure and purified by flash column chromatography on silica gel to afford the desired product.

General Procedure for the $Ni(acac)_2/IPr^{Me}\cdot HCl$ and $Cu(OAc)_2$ promoted borylation of silyloxyarenes using bis(pinacolato)diboron (E):

A reaction tube containing a stir bar was charged with aryl silyl ether (1 equiv), NaO-*t*-Bu (2.5 equiv), $Ni(acac)_2$ (10 mol%), $IPr^{Me}\cdot HCl$ (20 mol%), $Cu(OAc)_2$ (20 mol%), and B_2pin_2 (2.5 equiv). Toluene (0.3 M) was then added added, and the reaction tube was then placed in a heated block set to 120 °C and stirred for 16 h. The mixture was allowed to reach rt, taken up in ethyl acetate and filtered through silica (boric acid impregnated silica) plug via a glass fritted filter and concentrated under reduced pressure. The crude material was placed under reduced pressure via high vacuum until purification via column chromatography (boric acid impregnated silica gel) to afford the desired product.

General Procedure for the $Ni(COD)_2/IPr^{Me}\cdot HCl$ promoted Suzuki coupling of silyloxyarenes using aryl boronate esters (F):

A reaction tube containing a stir bar was charged with aryl silyl ether (1 equiv.), $Ni(COD)_2$ (10 mol%), $IPr^{Me}\cdot HCl$ (20 mol%), NaO-*t*-Bu (2.5 equiv.), aryl boronate ester (1.5 equiv), and toluene (0.3 M). The sealed reaction tube was brought outside the glovebox and placed in a heated block set to 120 ^oC and stirred for 16 hours, unless noted otherwise. The mixture was cooled to room temperature, quenched with dichloromethane (1 mL), and diluted with EtOAc (3 mL). The mixture

was then run through a silica plug, concentrated under reduced pressure and purified by flash column chromatography on silica gel to afford the desired product.

6.3.2 Table 3-3 Substrate Scope

***N*-octyl-4-(pyridin-2-yl)aniline.**

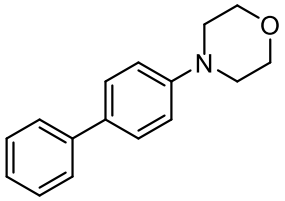

Table 3-3, 3-4: Following a modified general procedure D, $Ni(COD)_2$ (4.1 mg, 0.015 mmol), IPr^{Me}·HCl (13.6 mg, 0.03 mmol), NaO-*t*-Bu (72.0 mg, 0.750 mmol), ([1,1'-biphenyl]-4-yloxy)(*tert*-butyl)dimethylsilane (79.3 mg, 0.279 mmol), and morpholine (39 µL, 0.45 mmol) at 120 °C for 16 h gave a crude residue which was purified by flash chromatography (hexanes: ethyl acetate 92.5:7.5) to afford the desired product (62.3 mg, 0.260 mmol, 93% yield). The spectral data matches that previously reported in the literature.

^{1}H-NMR (500 MHz, $CDCl_3$): δ 7.55 (m, 4H), 7.41 (t, *J* = 7.5 Hz, 2H), 7.29 (t, *J* = 7.5 Hz, 1H), 6.98 (d, *J* = 8.5 Hz, 2H), 3.89 (t, *J* = 5.0 Hz, 4H), 3.22 (t, *J* = 5.0 Hz, 4H).

1-([1,1'-biphenyl]-4-yl)-4-methylpiperazine.

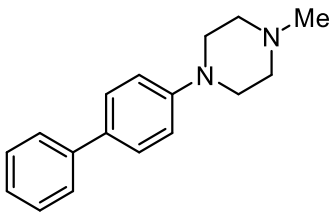

Table 3-3, 3-5: Following a modified general procedure D, $Ni(COD)_2$ (8.2 mg, 0.03 mmol), IPr^{Me}·HCl (27.2 mg, 0.06 mmol), NaO-*t*-Bu (72.0 mg, 0.750 mmol), ([1,1'-biphenyl]-4-yloxy)(*tert*-butyl)dimethylsilane (84.0 mg, 0.295 mmol), and 1-methylpiperazine (50 µL, 0.45 mmol) at 120 °C for 16 h gave a crude residue which was purified by flash chromatography (hexanes: ethyl acetate:triethylamine 72.5:25:2.5) to afford the desired product (64.6 mg, 0.256 mmol, 87% yield). The spectral data matches that previously reported in the literature.

^{1}H-NMR (500 MHz, $CDCl_3$): δ 7.58 (d, *J* = 7.0 Hz, 2H), 7.54 (dd, *J* = 8.0 Hz, 3.0 Hz, 2H), 7.42 (t, *J* = 7.5 Hz, 2H), 7.30 (t, *J* = 7.5 Hz, 1H), 7.01 (d, *J* = 7.5 Hz, 2H), 3.29 (t, *J* = 5.0 Hz, 4H), 2.61 (t, *J* = 5.0 Hz, 4H), 2.38 (s, 3H).

1-([1,1'-biphenyl]-4-yl)-2-methylpiperidine.

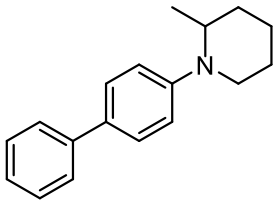

Table 3-3, 3-6: Following a modified general procedure D, $Ni(COD)_2$ (8.2 mg, 0.03 mmol), IPr^{Me}·HCl (27.2 mg, 0.06 mmol), NaO-*t*-Bu (72.0 mg, 0.750 mmol), ([1,1'-biphenyl]-4-yloxy)(*tert*-butyl)dimethylsilane (85.3 mg, 0.300 mmol), and 2-methylpiperidine (53 µL, 0.45 mmol) at 120 °C for 16 h gave a crude residue which was purified by flash chromatography (hexanes: ethyl acetate 95:5) to afford the desired product (57.9 mg, 0.230 mmol, 77% yield). The spectral data matches that previously reported in the literature.

^{1}H-NMR (500 MHz, $CDCl_3$): δ 7.56 (d, *J* = 8.0 Hz, 2H), 7.50 (d, *J* = 7.5 Hz, 2H), 7.40 (t, *J* = 8.0 Hz, 2H), 7.27 (m, 1H), 6.98 (d, *J* = 7.5 Hz, 2H), 4.02 (s, 1H), 3.32 (dt, *J* = 12.2, 4.0 Hz, 1H), 3.0 (t, *J* = 10.0 Hz, 1H), 1.88 (m, 1H), 1.77 (m, 1H), 1.62 (m, 4H), 1.05 (d, *J* = 6.5 Hz, 3H).

1-([1,1'-biphenyl]-4-yl)-2,6-dimethylpiperidine.

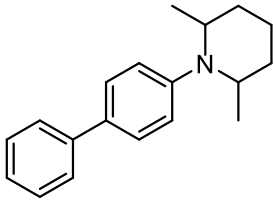

Table 3-3, 3-7: Following a modified general procedure D, $Ni(COD)_2$ (8.3 mg, 0.03 mmol), IPr^{Me}·HCl (27.2 mg, 0.06 mmol), NaO-*t*-Bu (72.0 mg, 0.750 mmol), ([1,1'-biphenyl]-4-yloxy)(*tert*-butyl)dimethylsilane (84.0 mg, 0.295 mmol), and 2,6-dimethylpiperdine (49 µL, 0.45 mmol) at 120 °C for 16 h gave a crude residue which was purified by flash chromatography (hexanes: ethyl acetate 95:5) to afford the desired product (18.3 mg, 0.069 mmol, 23% yield).

^{1}H-NMR (500 MHz, $CDCl_3$): δ 7.59 (d, *J* = 8.5 Hz, 2H), 7.53 (d, *J* = 8.5 Hz, 2H), 7.42 (t, *J* = 8.0 Hz, 2H), 7.30 (t, *J* = 7.0 Hz, 1H), 7.16 (d, *J* = 8.5 Hz, 2H), 3.10 (m, 2H), 1.77 (m, 3H), 1.53 (m, 3H), 0.87 (d, *J* = 6.5 Hz, 6H).
^{13}C-NMR (125 MHz, $CDCl_3$): δ 150.0, 140.9, 136.3, 128.7, 128.3, 126.8, 126.7, 124.9, 55.9, 34.5, 22.6, 21.4.
IR (film, cm^{-1}): 2956, 2924, 2855, 2791, 1602, 1485.
HRMS (ESI+) *m/z*: $[M+H]^+$ predicted for $C_{19}H_{23}N$, 266.1903; found, 266.1903.

***N*,*N*-diisobutyl-[1,1'-biphenyl]-4-amine.**

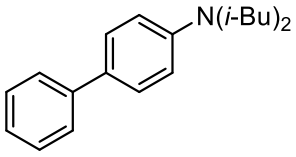

Table 3-3, 3-8: Following a modified general procedure D, $Ni(COD)_2$ (12.4 mg, 0.045 mmol), IPr^{Me}·HCl (40.8 mg, 0.09 mmol), NaO-*t*-Bu (72.0 mg, 0.750 mmol), ([1,1'-biphenyl]-4-yloxy)(*tert*-butyl)dimethylsilane (87.4 mg, 0.307 mmol), and diisobutylamine (131 µL, 0.75

mmol) at 120 °C for 16 h gave a crude residue which was purified by flash chromatography (hexanes) to afford the desired product (16.4 mg, 0.058 mmol, 19% yield).

^{1}H-NMR (500 MHz, $CDCl_3$): δ 7.54 (d, *J* = 8.0 Hz, 2H), 7.46 (d, *J* = 7.5 Hz, 2H), 7.38 (t, *J* = 7.5 Hz, 2H), 7.23 (t, *J* = 7.5 Hz, 1H), 6.71 (d, *J* = 8.5 Hz, 2H), 3.19 (d, *J* = 7.0 Hz, 4H), 2.13 (septet, *J* = 7.0 Hz, 2H), 0.92 (d, *J* = 7.0 Hz, 12H).
^{13}C-NMR (125 MHz, $CDCl_3$): δ 147.6, 141.3, 128.8, 128.7, 128.6, 126.1, 125.7, 115.5, 60.4, 26.4, 20.4.
IR (film, cm^{-1}): 2948, 2929, 2863, 1609, 1518, 1486.
HRMS (ESI+) *m/z*: $[M+H]^+$ predicted for $C_{20}H_{27}N$, 282.2216; found, 282.2219.

***N*,*N*-dibutyl-[1,1'-biphenyl]-4-amine.**

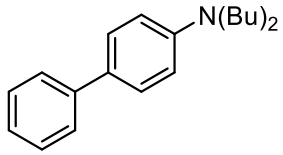

Table 3-3, 3-9: Following a modified general procedure D, $Ni(COD)_2$ (12.4 mg, 0.045 mmol), IPr^{Me}·HCl (40.8 mg, 0.09 mmol), NaO-*t*-Bu (72.0 mg, 0.750 mmol), ([1,1'-biphenyl]-4-yloxy)(*tert*-butyl)dimethylsilane (85.9 mg, 0.302 mmol), and dibutylamine (126 µL, 0.75 mmol) at 120 °C for 16 h gave a crude residue which was purified by flash chromatography (hexanes: ethyl acetate 99:1) to afford the desired product (69.8 mg, 0.248 mmol, 82% yield). The spectral data matches that previously reported in the literature.

^{1}H-NMR (500 MHz, $CDCl_3$): δ 7.55 (d, *J* = 8.0 Hz, 2H), 7.47 (d, *J* = 8.0 Hz, 2H), 7.24 (m, 1H), 6.71 (d, *J* = 8.0 Hz, 2H), 3.31 (t, *J* = 8.0 Hz, 4H), 1.61 (m, 4H), 1.38 (m, 4H), 0.98 (t, *J* = 7.5 Hz, 6H).

***N*-butyl-*N*-methyl-[1,1'-biphenyl]-4-amine.**

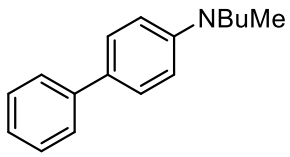

Table 3-3, 3-10: Following a modified general procedure D, $Ni(COD)_2$ (8.2 mg, 0.03 mmol), IPr^{Me}·HCl (27.2 mg, 0.06 mmol), NaO-*t*-Bu (72.0 mg, 0.750 mmol), ([1,1'-biphenyl]-4-yloxy)(*tert*-butyl)dimethylsilane (84.8 mg, 0.298 mmol), and *N*-methylbutylamine (53 µL, 0.45 mmol) at 120 °C for 16 h gave a crude residue which was purified by flash chromatography (hexanes: ethyl acetate 95:5) to afford the desired product (63.8 mg, 0.267 mmol, 89% yield).

^{1}H-NMR (500 MHz, $CDCl_3$): δ 7.56 (d, *J* = 7.5 Hz, 2H), 7.51 (d, *J* = 8.0 Hz, 2H), 7.39 (t, *J* = 7.0 Hz, 2H), 7.25 (m, 1H), 6.77 (d, *J* = 8.0 Hz, 2H), 3.36 (t, *J* = 7.5 Hz, 2H), 2.98 (s, 3H), 1.60 (m, 2H), 1.38 (m, 2H), 0.97 (t, *J* = 7.5 Hz, 3H).
^{13}C-NMR (125 MHz, $CDCl_3$): δ 148.7, 141.3, 128.6, 128.4, 127.7, 126.2, 125.8, 112.2, 52.5, 38.4, 28.9, 20.4, 14.0.
IR (film, cm^{-1}): 3033, 2952, 2870, 1608, 1527, 1491.
HRMS (ESI+) *m/z*: $[M+H]^+$ predicted for $C_{17}H_{21}N$, 240.1747; found, 240.1748.

***N*-methyl-*N*-phenyl-[1,1'-biphenyl]-4-amine.**

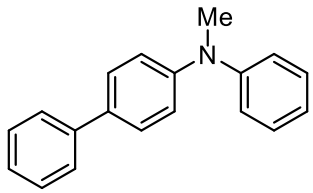

Table 3-3, 3-11: Following a modified general procedure D, $Ni(COD)_2$ (8.2 mg, 0.03 mmol), IPr^{Me}·HCl (27.2 mg, 0.06 mmol), NaO-*t*-Bu (72.0 mg, 0.750 mmol), ([1,1'-biphenyl]-4-yloxy)(*tert*-butyl)dimethylsilane (84.8 mg, 0.298 mmol), and *N*-methylaniline (81 µL, 0.75 mmol)

at 120 °C for 16 h gave a crude residue which was purified by flash chromatography (hexanes: toluene 90:10) to afford the desired product (33.2 mg, 0.128 mmol, 43% yield). The spectral data matches that previously reported in the literature.

^{1}H-NMR (500 MHz, $CDCl_3$): δ 7.56 (d, *J* = 7.0 Hz, 2H), 7.50 (d, *J* = 7.5 Hz, 2H), 7.41 (t, *J* = 7.5 Hz, 2H), 7.31 (m, 2H), 7.11 (d, *J* = 8.0 Hz, 2H), 7.06 (d, *J* = 8.5 Hz, 2H), 7.01 (t, *J* = 7.0 Hz, 1H), 3.36 (s, 3H).

***N*-mesityl-[1,1'-biphenyl]-4-amine.**

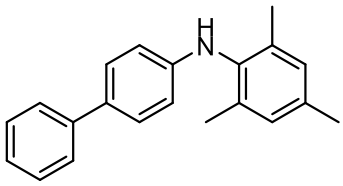

Table 3-3, 3-12: Following a modified general procedure D, $Ni(COD)_2$ (8.2 mg, 0.03 mmol), IPr^{Me}·HCl (27.6 mg, 0.06 mmol), NaO-*t*-Bu (72.0 mg, 0.750 mmol), ([1,1'-biphenyl]-4-yloxy)(*tert*-butyl)dimethylsilane (84.1 mg, 0.296 mmol), and 2,4,6-trimethylaniline (63 µL, 0.45 mmol) at 120 °C for 16 h gave a crude residue which was purified by flash chromatography (hexanes: ethyl acetate 95:5) to afford the desired product (68.0 mg, 0.237 mmol, 80% yield).

^{1}H-NMR (500 MHz, $CDCl_3$): δ 7.54 (d, *J* = 8.0 Hz, 2H), 7.41 (m, 4H), 7.26 (t, *J* = 7.5 Hz, 1H), 6.98 (s, 2H), 6.57 (d, *J* = 8.5 Hz, 2H), 2.34 (s, 3H), 2.22 (s, 6H).
^{13}C-NMR (125 MHz, $CDCl_3$): δ 146.1, 141.2, 136.0, 135.5, 135.3, 130.8, 129.2, 128.6, 127.9, 126.3, 126.1, 113.5, 20.9, 18.3.
IR (film, cm^{-1}): 3390, 3022, 2916, 1613, 1519, 1484.
HRMS (ESI+) *m/z*: $[M+H]^+$ predicted for $C_{21}H_{21}N$, 288.1747; found, 288.1753.

***N*-(2,6-diisopropylphenyl)-[1,1'-biphenyl]-4-amine.**

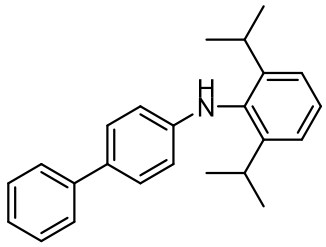

Table 3-3, 3-13: Following a modified general procedure D, $Ni(COD)_2$ (12.4 mg, 0.045 mmol), IPr^{Me}·HCl (40.8 mg, 0.09 mmol), NaO-*t*-Bu (72.0 mg, 0.750 mmol), ([1,1'-biphenyl]-4-yloxy)(*tert*-butyl)dimethylsilane (84.7 mg, 0.298 mmol), and 2,6-diisopropylaniline (131 µL, 0.75 mmol) at 120 °C for 16 h gave a crude residue which was purified by flash chromatography (hexanes: ethyl acetate 95:5) to afford the desired product (54.0 mg, 0.164 mmol, 55% yield).

^{1}H-NMR (500 MHz, $CDCl_3$): δ 7.56 (d, *J* = 7.5 Hz, 2H), 7.40 (m, 4H), 7.33 (t, *J* = 7.5 Hz, 1H), 7.26 (m, 2H), 6.57 (d, *J* = 8.0 Hz, 2H), 5.21 (s, 1H), 3.25 (septet, *J* = 7.0 Hz, 2H), 1.18 (d, *J* = 7.0 Hz, 12H).
^{13}C-NMR (125 MHz, $CDCl_3$): δ 147.6, 141.1, 135.0, 130.5, 128.6, 127.8, 127.3, 126.2, 126.0, 123.9, 115.6, 113.2, 28.2, 23.9.
IR (film, cm^{-1}): 3398, 3031, 2961, 2867, 1612, 1521, 1486.
HRMS (ESI+) *m/z*: $[M+H]^+$ predicted for $C_{24}H_{27}N$, 330.2216; found, 330.2217.

***N*-phenyl-[1,1'-biphenyl]-4-amine.**

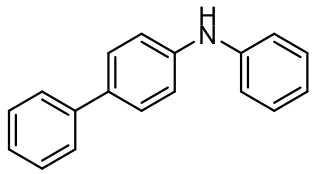

Table 3-3, 3-14: Following a modified general procedure D, $Ni(COD)_2$ (12.4 mg, 0.045 mmol), IPr^{Me}·HCl (40.8 mg, 0.09 mmol), NaO-*t*-Bu (72.0 mg, 0.750 mmol), ([1,1'-biphenyl]-4-

yloxy)(*tert*-butyl)dimethylsilane (84.7 mg, 0.298 mmol), and aniline (68 µL, 0.75 mmol) at 120 °C for 16 h gave a crude residue which was analyzed by ^{1}H-NMR and GC-MS where the product was observed. The spectral data matches that previously reported in the literature.

***N*-cyclohexyl-[1,1'-biphenyl]-4-amine.**

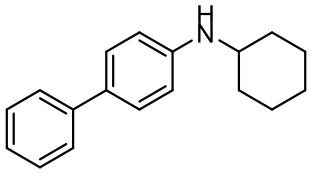

Table 3-3, 3-15: Following a modified general procedure D, $Ni(COD)_2$ (4.1 mg, 0.015 mmol), IPr^{Me}·HCl (13.6 mg, 0.03 mmol), NaO-*t*-Bu (36.0 mg, 0.375 mmol), ([1,1'-biphenyl]-4-yloxy)(*tert*-butyl)dimethylsilane (41.2 mg, 0.145 mmol), and cyclohexylamine (26 µL, 0.225 mmol) at 120 °C for 16 h gave a crude residue which was purified by flash chromatography (hexanes: ethyl acetate 95:5) to afford the desired product (31.8 mg, 0.127 mmol, 87% yield). The spectral data matches that previously reported in the literature.

^{1}H-NMR (500 MHz, $CDCl_3$): δ 7.52 (d, *J* = 7.5 Hz, 2H), 7.42 (d, *J* = 8.0 Hz, 2H), 7.38 (t, *J* = 8.0 Hz, 2H), 7.24 (m, 1H), 6.69 (m, 2H), 3.67 (bs, 1H), 3.30 (m, 1H), 2.09 (dd, *J* = 12.5 Hz, 3.0 Hz, 2H), 13.5 Hz, 4.0 Hz, 2H), 1.66 (m, 1H), 1.38 (m, 2H), 1.28-1.19 (m, 3H).

***N*-(cyclopropylmethyl)-[1,1'-biphenyl]-4-amine.**

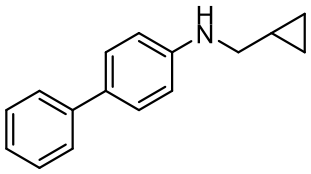

Table 3-3, 3-16: Following a modified general procedure D, $Ni(COD)_2$ (8.2 mg, 0.03 mmol), IPr^{Me}·HCl (27.6 mg, 0.06 mmol), NaO-*t*-Bu (72.0 mg, 0.750 mmol), ([1,1'-biphenyl]-4-yloxy)(*tert*-butyl)dimethylsilane (85.4 mg, 0.300 mmol), and cyclopropylmethylamine (65 µL, 0.75 mmol) at 120 °C for 16 h gave a crude residue which was purified by flash chromatography (hexanes: ethyl acetate 95:5) to afford the desired product (47.4 mg, 0.212 mmol, 71% yield).

^{1}H-NMR (500 MHz, $CDCl_3$): δ 7.54 (d, *J* = 7.5 Hz, 2H), 7.45 (d, *J* = 8.5 Hz, 2H), 7.39 (t, *J* = 7.5 Hz, 2H), 7.26 (m, 1H), 6.69 (d, *J* = 8.5 Hz, 2H), 3.88 (br, 1H), 3.01 (d, *J* = 7.0 Hz, 2H), 1.13 (m, 1H), 0.57 (d, *J* = 7.5 Hz, 2H), 0.27 (d, *J* = 5.0 Hz, 2H).
^{13}C-NMR (125 MHz, $CDCl_3$): δ 147.9, 141.3, 130.1, 128.6, 127.9, 126.3, 126.0, 113.0, 49.1, 10.9, 3.5.
IR (film, cm^{-1}): 2926, 2853, 1609, 1503, 1471.
HRMS (ESI+) *m/z*: $[M+H]^+$ predicted for $C_{16}H_{17}N$, 224.1434; found, 224.1433.

***N*-butyl-[1,1'-biphenyl]-4-amine.**

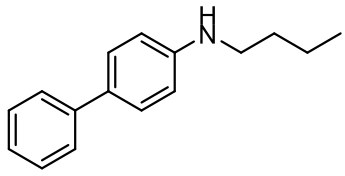

Table 3-3, 3-17: Following a modified general procedure D, $Ni(COD)_2$ (8.2 mg, 0.03 mmol), IPr^{Me}·HCl (27.2 mg, 0.06 mmol), NaO-*t*-Bu (72.0 mg, 0.750 mmol), ([1,1'-biphenyl]-4-yloxy)(*tert*-butyl)dimethylsilane (87.3 mg, 0.307 mmol), and butylamine (74 µL, 0.75 mmol) at 120 °C for 16 h gave a crude residue which was purified by flash chromatography (hexanes: ethyl acetate 95:5) to afford the desired product (48.0 mg, 0.213 mmol, 69% yield). The spectral data matches that previously reported in the literature.

^{1}H-NMR (500 MHz, $CDCl_3$): δ 7.53 (d, *J* = 7.0 Hz, 2H), 7.44 (d, *J* = 8.5 Hz, 2H), 7.39 (t, *J* = 8.0 Hz, 2H), 7.25 (m, 1H), 6.70 (d, *J* = 8.5 Hz, 2H), 3.91 (bs, 1H), 3.16 (t, *J* = 7.0 Hz, 2H), 1.64 (pentet, *J* = 7.5 Hz, 2H), 1.45 (sextet, *J* = 7.5 Hz, 2H), 0.97 (t, *J* = 7.5 Hz, 3H).

***N*-isobutyl-[1,1'-biphenyl]-4-amine.**

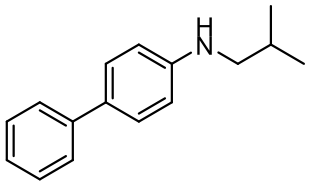

Table 3-3, 3-18: Following a modified general procedure D, $Ni(COD)_2$ (8.2 mg, 0.03 mmol), IPr^{Me}·HCl (27.2 mg, 0.06 mmol), NaO-*t*-Bu (72.0 mg, 0.750 mmol), ([1,1'-biphenyl]-4-yloxy)(*tert*-butyl)dimethylsilane (83.9 mg, 0.295 mmol), and isobutylamine (75 µL, 0.75 mmol) at 120 °C for 16 h gave a crude residue which was purified by flash chromatography (hexanes: ethyl acetate 95:5) to afford the desired product (50.0 mg, 0.222 mmol, 75% yield).

^{1}H-NMR (500 MHz, $CDCl_3$): δ 7.57 (d, *J* = 6.5 Hz, 2H), 7.47 (d, *J* = 8.5 Hz, 2H), 7.42 (t, *J* = 7.5 Hz, 2H), 7.28 (t, *J* = 7.0 Hz, 1H), 6.70 (d, *J* = 8.5 Hz, 2H), 3.83 (bs, 1H), 3.00 (d, *J* = 7.0 Hz, 2H), 1.95 (septet, *J* = 7.0 Hz, 1H), 1.03 (d, *J* = 6.5 Hz, 6H).
^{13}C-NMR (125 MHz, $CDCl_3$): δ 148.0, 141.3, 129.8, 128.6, 127.9, 126.2, 125.9, 112.8, 51.8, 28.0, 20.5.
IR (film, cm^{-1}): 3393, 2951, 2927, 2854, 1610, 1492.
HRMS (EI) *m/z*: $[M]^+$ predicted for $C_{16}H_{19}N$, 225.1517; found, 225.1513.

***N*-(*sec*-butyl)-[1,1'-biphenyl]-4-amine.**

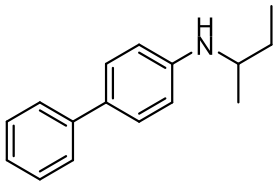

Table 3-3, 3-19: Following a modified general procedure D, $Ni(COD)_2$ (8.2 mg, 0.03 mmol), IPr^{Me}·HCl (27.2 mg, 0.06 mmol), NaO-*t*-Bu (72.0 mg, 0.750 mmol), ([1,1'-biphenyl]-4-yloxy)(*tert*-butyl)dimethylsilane (86.0 mg, 0.302 mmol), and sec-butylamine (76 µL, 0.75 mmol)

at 120 °C for 16 h gave a crude residue which was purified by flash chromatography (hexanes: ethyl acetate 95:5) to afford the desired product (45.4 mg, 0.201 mmol, 67% yield). The spectral data matches that previously reported in the literature.

^{1}H-NMR (500 MHz, $CDCl_3$): δ 7.53 (d, *J* = 8.0 Hz, 2H), 7.44-7.37 (m, 4H), 7.25 (m, 11H), 6.65 (d, *J* = 7.0 Hz, 2H), 3.55 (bs, 1H), 3.44 (m, 1H), 1.61 (m, 1H), 1.50 (m, 1H), 1.21 (d, *J* = 5.5 Hz, 3H), 0.98 (t, *J* = 7.0 Hz, 3H).

***N*-cyclobutyl-[1,1'-biphenyl]-4-amine.**

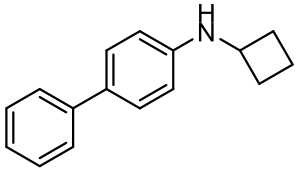

Table 3-3, 3-20: Following a modified general procedure D, $Ni(COD)_2$ (8.2 mg, 0.03 mmol), IPr^{Me}·HCl (27.2 mg, 0.06 mmol), NaO-*t*-Bu (72.0 mg, 0.750 mmol), ([1,1'-biphenyl]-4-yloxy)(*tert*-butyl)dimethylsilane (87.5 mg, 0.308 mmol), and cyclobutylamine (64 µL, 0.75 mmol) at 120 °C for 16 h gave a crude residue which was purified by flash chromatography (hexanes: ethyl acetate 95:5) to afford the desired product (37.7 mg, 0.169 mmol, 55% yield).

^{1}H-NMR (500 MHz, $CDCl_3$): δ 7.56 (d, *J* = 7.0 Hz, 2H), 7.45 (d, *J* = 8.5 Hz, 2H), 7.41 (t, *J* = 7.5 Hz, 2H), 7.27 (t, *J* = 7.5 Hz, 1H), 6.64 (d, *J* = 8.5 Hz, 2H), 3.98 (m, 1H), 3.92 (bs, 1H), 2.47 (m, 2H), 1.88 (m, 4H).
^{13}C-NMR (125 MHz, $CDCl_3$): δ 146.6, 141.3, 130.2, 128.6, 127.9, 126.3, 126.0, 113.2, 48.9, 31.2, 15.3.
IR (film, cm^{-1}): 3380, 2954, 2928, 2853, 1607, 1518, 1472.
HRMS (ESI+) *m/z*: $[M+H]^+$ predicted for $C_{16}H_{17}N$, 224.1434; found, 224.1438.

***N*-(*tert*-butyl)-[1,1'-biphenyl]-4-amine.**

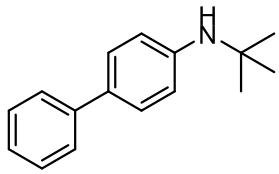

Table 3-3, 3-21: Following a modified general procedure D, $Ni(COD)_2$ (8.2 mg, 0.03 mmol), IPr^{Me}·HCl (27.2 mg, 0.06 mmol), NaO-*t*-Bu (72.0 mg, 0.750 mmol), ([1,1'-biphenyl]-4-yloxy)(*tert*-butyl)dimethylsilane (83.2 mg, 0.292 mmol), and *tert*-butylamine (79 µL, 0.75 mmol) at 120 °C for 16 h gave a crude residue which was purified by flash chromatography (hexanes: ethyl acetate 95:5) to afford the desired product (10.2 mg, 0.045 mmol, 15% yield). The spectral data matches that previously reported in the literature.

^{1}H-NMR (500 MHz, $CDCl_3$): δ 7.54 (d, *J* = 7.5 Hz, 2H), 7.43-7.37 (m, 4H), 7.26 (m, 1H), 6.82 (m, 2H), 3.62 (bs, 1H), 1.38 (s, 9H).

(3s,5s,7s)-*N*-([1,1'-biphenyl]-4-yl)adamantan-1-amine.

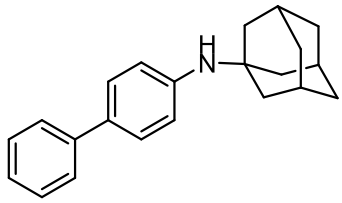

Table 3-3, 3-22: Following a modified general procedure D, $Ni(COD)_2$ (12.4 mg, 0.045 mmol), IPr^{Me}·HCl (40.8 mg, 0.09 mmol), NaO-*t*-Bu (72.0 mg, 0.750 mmol), ([1,1'-biphenyl]-4-yloxy)(*tert*-butyl)dimethylsilane (87.5 mg, 0.308 mmol), and 1-adamantylamine (113.4 mg, 0.75 mmol) at 120 °C for 16 h gave a crude residue which was purified by flash chromatography (hexanes: ethyl acetate 95:5) to afford the desired product (51.9 mg, 0.171 mmol, 56% yield). The spectral data matches that previously reported in the literature.

^{1}H-NMR (500 MHz, $CDCl_3$): δ 7.53 (d, *J* = 7.5 Hz, 2H), 7.41-7.37 (m, 4H), 7.26 (m, 1H), 6.65 (d, *J* = 8.0 Hz, 2H), 3.45 (bs, 1H), 2.13 (m, 3H), 1.92 (m, 6H), 1.69 (m, 6H).

6.3.3 Table 3-5 Substrate Scope

***N*-benzylnaphthalen-1-amine.**

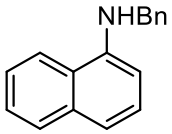

Table 3-5, 3-23: Following a modified general procedure D, $Ni(COD)_2$ (8.2 mg, 0.03 mmol), IPr^{Me}·HCl (27.2 mg, 0.06 mmol), NaO-*t*-Bu (115.6 mg, 1.20 mmol), *tert*-butyldimethyl(naphthalen-1-yloxy)silane (77.5 mg, 0.300 mmol), and benzylamine (50 µL, 0.45 mmol) at 120 °C for 16 h gave a crude residue which was purified by flash chromatography (hexanes: ethyl acetate 99:1) to afford the desired product (53.0 mg, 0.227 mmol, 76% yield). The spectral data matches that previously reported in the literature.

^{1}H-NMR (500 MHz, $CDCl_3$): δ 7.83 (t, *J* = 7.5 Hz, 2H), 7.46 (m, 4H), 7.39 (t, *J* = 7.5 Hz, 2H), 7.34 (m, 2H), 7.27 (m, 1H), 6.65 (d, *J* = 7.5 Hz, 1H), 4.71 (b, 1H), 4.51 (s, 2H).

***N*-isobutylnaphthalen-2-amine.**

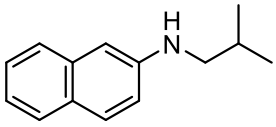

Table 3-5, 3-24: Following a modified general procedure D, $Ni(COD)_2$ (8.2 mg, 0.03 mmol), IPr^{Me}·HCl (27.2 mg, 0.06 mmol), NaO-*t*-Bu (72.0 mg, 0.75 mmol), *tert*-butyldimethyl(naphthalen-2-yloxy)silane (79.4 mg, 0.307 mmol), and isobutylamine (45 µL, 0.45 mmol) at 120 °C for 16 h

gave a crude residue which was purified by flash chromatography (hexanes: ethyl acetate 95:5) to afford the desired product (42.5 mg, 0.213 mmol, 69% yield). The spectral data matches that previously reported in the literature.

^{1}H-NMR (500 MHz, $CDCl_3$): δ 7.66 (8.0 Hz, 1H), 7.61 (m, 2H), 7.35 (t, *J* = 7.5 Hz, 1H), 7.18 (t, *J* = 7.5 Hz, 2H), 6.88 (dd, *J* = 8.5 Hz, 2.0 Hz, 1H), 6.80 (d, *J* = 2.0 Hz, 1H), 3.90 (bs, 1H), 3.05 (d, *J* = 7.0 Hz, 2H), 1.98 (septet, *J* = 6.5 Hz, 1H), 1.04 (d, *J* = 7.0 Hz, 6H).
^{13}C-NMR (125 MHz, $CDCl_3$): δ 146.2, 135.3, 128.8, 127.6, 127.3, 126.2, 125.8, 121.7, 117.9, 104.1, 51.8, 28.0, 20.6.
IR (film, cm^{-1}): 3421, 3050, 2955, 2868, 1629, 1522.
HRMS (ESI+) *m/z*: $[M+H]^+$ predicted for $C_{14}H_{17}N$, 200.1434; found, 200.1439.

***N*-methyl-*N*-phenyl-6-(trimethylsilyl)naphthalen-2-amine.**

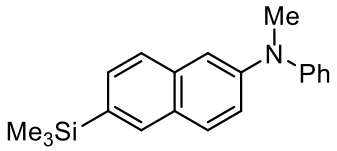

Table 3-5, 3-25: Following general procedure D, $Ni(COD)_2$ (8.2 mg, 0.03 mmol), IPr^{Me}·HCl (27.2 mg, 0.06 mmol), NaO-*t*-Bu (72.0 mg, 0.750 mmol), *tert*-butyldimethyl((6-(trimethylsilyl)naphthalen-2-yl)oxy)silane (99.8 mg, 0.302 mmol), and *N*-methylaniline (49 µL, 0.45 mmol) gave a crude residue which was purified by flash chromatography (hexanes: ethyl acetate 99:1) to afford the desired product (56.4 mg, 0.184 mmol, 61% yield).

^{1}H-NMR (500 MHz, $CDCl_3$): δ 7.91 (s, 1H), 7.69 (d, *J* = 8.5 Hz, 2H), 7.55 (d, *J* = 8.0 Hz, 1H), 7.32 (m, 3H), 7.21 (m, 1H), 7.12 (d, *J* = 8.5 Hz, 2H), 7.04 (t, *J* = 7.5 Hz, 1H), 3.44 (s, 3H), 0.36 (s, 9H).
^{13}C-NMR (125 MHz, $CDCl_3$): δ 149.0, 146.9, 135.1, 134.9, 133.4, 130.3, 129.3, 128.7, 128.6, 125.8, 122.1, 121.64, 121.61, 114.0, 40.6, -1.0.
IR (film, cm^{-1}): 3038, 2952, 1625, 1589, 1488.

HRMS (ESI+) *m/z*: $[M+H]^+$ predicted for $C_{20}H_{23}NSi$, 306.1673; found, 306.1669.

***N*-benzyl-*N*,3-dimethyl-[1,1'-biphenyl]-4-amine.**

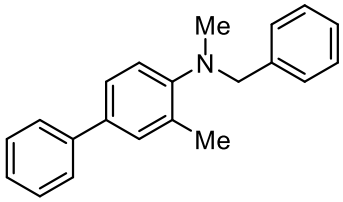

Table 3-5, 3-26: Following a modified general procedure D, $Ni(COD)_2$ (4.1 mg, 0.015 mmol), IPr^{Me}·HCl (13.6 mg, 0.03 mmol), NaO-*t*-Bu (36.0 mg, 0.375 mmol), *tert*-butyldimethyl((3-methyl-[1,1'-biphenyl]-4-yl)oxy)silane (46.2 mg, 0.155 mmol), and *N*-benzylmethylamine (29 µL, 0.225 mmol) at 120 °C for 16 h gave a crude residue which was purified by flash chromatography (hexanes: ethyl acetate 95:5) to afford the desired product (28.9 mg, 0.101 mmol, 65% yield).

^{1}H-NMR (500 MHz, $CDCl_3$): δ 7.59 (d, *J* = 7.5 Hz, 2H), 7.46-7.16 (m, 10H), 7.15 (d, *J* = 8.0 Hz, 1H), 4.10 (s, 2H), 2.64 (s, 3H), 2.48 (s, 3H).
^{13}C-NMR (125 MHz, $CDCl_3$): δ 151.8, 141.0, 139.0, 135.7, 132.9, 129.9, 128.6, 128.32, 128.30, 127.0, 126.8, 126.7, 125.1, 120.2, 60.7, 40.8, 18.7.
IR (film, cm^{-1}): 3060, 3028, 2948, 2791, 1603, 1485.
HRMS (ESI+) *m/z*: $[M+H]^+$ predicted for $C_{21}H_{22}N$, 288.1747; found, 288.1748.

4-(6-((*tert*-butyldimethylsilyl)oxy)-[1,1'-biphenyl]-3-yl)morpholine.

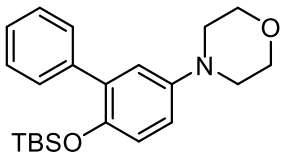

Table 3-5, 3-27: Following a modified general procedure D, $Ni(COD)_2$ (6.2 mg, 0.0225 mmol), IPr^{Me}·HCl (20.4 mg, 0.045 mmol), NaO-*t*-Bu (57.7 mg, 0.6 mmol), ([1,1'-biphenyl]-2,5-diylbis(oxy))bis(*tert*-butyldimethylsilane) (63.2 mg, 0.152 mmol), and morpholine (33 µL, 0.375 mmol) at 120 °C for 16 h gave a crude residue which was purified by flash chromatography (hexanes: ethyl acetate 95:5) to afford the desired product (27.0 mg, 0.073 mmol, 48% yield). The product was isolated as a mixture of the desired product and 4-([1,1'-biphenyl]-3-yl)morpholine. The spectral data for 4-([1,1'-biphenyl]-3-yl)morpholine matches that previously reported in the literature.

^{1}H-NMR (500 MHz, $CDCl_3$): δ 7.48 (d, *J* = 7.5 Hz, 2H), 7.37 (t, *J* = 7.5 Hz, 2H), 7.29 (t, *J* = 7.5 Hz, 1H), 6.88 (d, *J* = 3.0 Hz, 1H), 6.84 (d, *J* = 9.0 Hz, 1H), 6.80 (dd, *J* = 8.5, 2.5 Hz, 1H), 3.86 (t, *J* = 5.0 Hz, 4H), 3.11 (t, *J* = 5.0 Hz, 4H), 0.80 (s, 9H), -0.11 (s, 6H).

Minor product peaks of 4-([1,1'-biphenyl]-3-yl)morpholine: 7.57 (d, *J* = 7.5 Hz, 0.43H), 7.43 (t, *J* = 7.5 Hz, 0.48H), 7.35 (m, 0.26), 7.11 (m, 0.50H), 6.93 (m, 0.26H), 3.89 (t, *J* = 5.0 Hz, 0.90H), 3.23 (t, *J* = 5.0 Hz, 0.71H),

^{13}C-NMR (175 MHz, $CDCl_3$): δ 146.5, 145.9, 139.4, 133.8, 129.7, 127.8, 126.7, 120.9, 119.2, 118.9, 116.2, 67.1, 50.5, 25.6, 18.0, -4.7.

Minor product peaks of 4-([1,1'-biphenyl]-3-yl)morpholine: 129.5, 128.7, 127.2, 114.76, 114.66, 66.9, 49.4.

IR (film, cm^{-1}): 3032, 2957, 2928, 2855, 1599, 1486.

HRMS (ESI+) *m/z*: $[M+H]^+$ predicted for $C_{22}H_{31}NO_2S$, 370.2197; found, 370.2206.

2-methyl-6-(4-(pyrimidin-2-yl)piperazin-1-yl)quinolone.

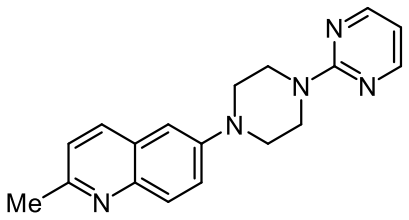

Table 3-5, 3-28: Following a modified general procedure D, $Ni(COD)_2$ (8.2 mg, 0.03 mmol), IPr^{Me}·HCl (27.2 mg, 0.06 mmol), NaO-*t*-Bu (72.0 mg, 0.750 mmol), 6-((*tert*-butyldimethylsilyl)oxy)-2-methylquinoline (82.6 mg, 0.302 mmol), and 1-(2-pyrimidyl)piperazine (106 µL, 0.75 mmol) at 120 °C for 16 h gave a crude residue which was purified by flash chromatography (hexanes: ethyl acetate: triethylamine 85:12.5:2.5) to afford the desired product (65.8 mg, 0.215 mmol, 71% yield).

^{1}H-NMR (500 MHz, $CDCl_3$): δ 8.35 (d, *J* = 5 Hz, 2H), 7.92 (t, *J* = 9.0 Hz, 2H), 7.51 (dd, *J* = 7.0, 1.5 Hz, 1H), 7.21 (d, *J* = 7.5 Hz, 1H), 7.05 (d, *J* = 1.5 Hz, 1H), 6.53 (t, *J* = 4.5 Hz, 2H), 4.04 (t, *J* = 5.0 Hz, 4H), 3.36 (t, *J* = 5.0Hz, 4H), 2.70 (s, 3H).
^{13}C-NMR (125 MHz, $CDCl_3$): δ 161.7, 157.7, 156.2, 148.8, 143.6, 135.0, 129.4, 127.4, 122.7, 122.2, 110.2, 110.0, 109.8, 49.5, 43.6, 25.0.
IR (film, cm^{-1}): 2362, 2322, 1584, 1546, 1498, 1448.
HRMS (ESI+) *m/z*: $[M+H]^+$ predicted for $C_{18}H_{19}N_5$, 306.1713; found, 306.1708.

***N*-octyl-4-(pyridin-2-yl)aniline.**

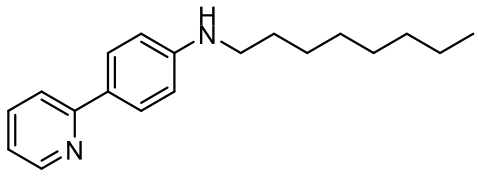

Table 3-5, 3-29: Following general procedure D, $Ni(COD)_2$ (8.2 mg, 0.03 mmol), IPr^{Me}·HCl (27.2 mg, 0.06 mmol), NaO-*t*-Bu (72.0 mg, 0.750 mmol), 2-(4-((*tert*-butyldimethylsilyl)oxy)phenyl)pyridine (85.0 mg, 0.298 mmol), and *N*-octylamine (73 µL, 0.45 mmol) gave a crude residue which was purified by flash chromatography (hexanes: ethyl acetate 90:10) to afford the desired product (62.0 mg, 0.220 mmol, 74% yield).

^{1}H-NMR (500 MHz, $CDCl_3$): δ 8.61 (d, *J* = 5.0 Hz, 1H), 7.86 (d, *J* = 9.0 Hz, 2H), 7.64 (m, 2H), 7.09 (t, *J* = 5.5 Hz, 1H), 6.67 (d, *J* = 8.5 Hz, 2H), 3.83 (b, 1H), 3.16 (t, *J* = 7.0 Hz, 2H), 1.63 (pentet, *J* = 7.5 Hz, 2H), 1.40 (m, 2H), 1.31 (m, 8H), 0.90 (t, *J* = 8.0 Hz, 3H).

^{13}C-NMR (125 MHz, $CDCl_3$): δ 157.6, 149.3, 149.3, 136.4, 128.0, 127.9, 120.5, 119.0, 112.5, 43.8, 29.5, 29.4, 29.2, 27.1, 22.6, 14.

IR (film, cm^{-1}): 3392, 2922, 2851, 2361, 1612, 1582, 1460.

HRMS (EI) *m/z*: $[M]^+$ predicted for $C_{19}H_{26}N_2$, 282.2096; found, 282.2093.

***N*-cyclohexyl-9-methyl-*9H*-carbazol-2-amine.**

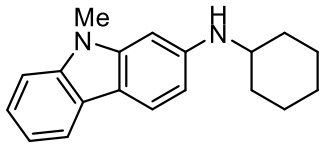

Table 3-5, 3-30: Following a modified general procedure D, $Ni(COD)_2$ (4.1 mg, 0.015 mmol), IPr^{Me}·HCl (13.6 mg, 0.03 mmol), NaO-*t*-Bu (36.0 mg, 0.375 mmol), 2-((*tert*-butyldimethylsilyl)oxy)-9-methyl-9H-carbazole (46.9 mg, 0.151 mmol), and cyclohexylamine (26 µL, 0.225 mmol) at 120 °C for 16 h gave a crude residue which was purified by flash chromatography (hexanes: ethyl acetate 95:5) to afford the desired product (30.4 mg, 0.109 mmol, 73% yield).

^{1}H-NMR (500 MHz, $CDCl_3$): δ 7.90 (d, *J* = 7.5 Hz, 1H), 7.81 (d, *J* = 8.5 Hz, 1H), 7.34-7.28 (m, 2H), 7.15 (t, *J* = 7.5 Hz, 1H), 6.53 (dd, *J* = 8.0, 2.0 Hz, 1H), 6.51 (d, *J* = 2.0 Hz, 1H), 3.75 (s, 3H), 3.42 (m, 1H), 2.15 (dd, *J* = 13.5, 4.0 Hz, 2H), 1.81 (m, 2H), 1.70 (m, 1H), 1.45 (m, 2H), 1.25 (m, 3H).

^{13}C-NMR (125 MHz, $CDCl_3$): δ 146.8, 143.1, 140.7, 123.64, 123.61, 123.3, 121.1, 118.6, 114.1, 107.8, 107.6, 91.2, 52.2, 33.6, 28.9, 26.0, 25.1.

IR (film, cm^{-1}): 3033, 2952, 2870, 1608, 1527, 1491.

HRMS (ESI+) *m/z*: $[M+H]^+$ predicted for $C_{19}H_{22}N_2$, 279.1856; found, 279.1862.

***N*,*N*-dibutylquinolin-3-amine.**

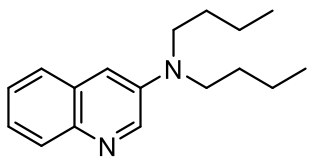

Table 3-5, 3-31: Following a modified general procedure D, $Ni(COD)_2$ (4.1 mg, 0.015 mmol), IPr^{Me}·HCl (13.6 mg, 0.03 mmol), NaO-*t*-Bu (36.0 mg, 0.375 mmol), 3-((*tert*-butyldimethylsilyl)oxy)quinoline (40.7 mg, 0.157 mmol), and dibutylamine (63 µL, 0.375 mmol) at 120 °C for 16 h gave a crude residue which was purified by flash chromatography (hexanes: ethyl acetate 95:5) to afford the desired product (25.5 mg, 0.099 mmol, 63% yield).

^{1}H-NMR (500 MHz, $CDCl_3$): δ 8.63 (d, *J* = 3.0 Hz, 1H), 7.91 (d, *J* = 7.5 Hz, 1H), 7.59 (d, *J* = 7.0 Hz, 1H), 7.38 (m, 2H), 7.04 (d, *J* = 3.0 Hz, 1H), 3.39 (t, *J* = 8.0 Hz, 4H), 1.63 (pentet, *J* = 8.0 Hz, 4H), 1.40 (sextet, *J* = 7.5 Hz, 4H), 0.98 (t, *J* = 7.5 Hz, 6H).
^{13}C-NMR (125 MHz, $CDCl_3$): δ 141.7, 141.1, 140.8, 129.5, 128.8, 126.7, 125.8, 124.4, 111.4, 50.8, 29.3, 20.3, 14.0.
IR (film, cm^{-1}): 3062, 2956, 2929, 2871, 2208, 1697, 1594.
HRMS (ESI+) *m/z*: $[M+H]^+$ predicted for $C_{17}H_{24}N_2$, 257.2012; found, 257.2014.

1-(4'-methoxy-[1,1'-biphenyl]-4-yl)-4-methylpiperazine.

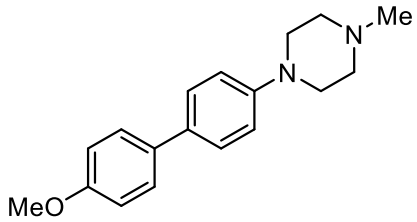

Table 3-5, 3-32: Following a modified general procedure D, $Ni(COD)_2$ (12.4 mg, 0.045 mmol), IPr^{Me}·HCl (40.8 mg, 0.09 mmol), NaO-*t*-Bu (115.3 mg, 1.20 mmol), *tert*-butyl((4'-methoxy-[1,1'-biphenyl]-4-yl)oxy)dimethylsilane (95.4 mg, 0.303 mmol), and 1-methylpiperazine (50 µL, 0.45

mmol) at 120 °C for 16 h gave a crude residue which was purified by flash chromatography (hexanes: ethyl acetate: triethylamine 85:12.5:2.5) to afford the desired product (54.0 mg, 0.191 mmol, 63% yield).

^{1}H-NMR (500 MHz, $CDCl_3$): δ 7.48 (t, *J* = 8.0 Hz, 4H), 6.98 (m, 4H), 3.84 (m, 3H), 3.26 (t, *J* = 5.0 Hz, 4H), 2.60 (t, *J* = 5.0 Hz, 4H), 2.37 (s, 3H).
^{13}C-NMR (125 MHz, $CDCl_3$): δ 158.5, 150.1, 133.5, 132.0, 127.5, 127.3, 116.1, 114.1, 55.3, 55.1, 49.0, 46.1.
IR (film, cm^{-1}): 2932, 2840, 2790, 1606, 1500, 1443.
HRMS (ESI+) *m/z*: $[M+H]^+$ predicted for $C_{18}H_{22}N_2O$, 283.1805; found, 283.1802.

***tert*-butyl 4-([1,1'-biphenyl]-3-ylamino)piperidine-1-carboxylate.**

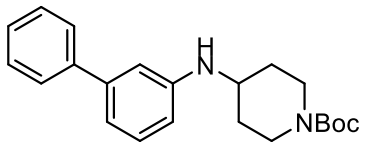

Table 3-5, 3-33: Following a modified general procedure D, $Ni(COD)_2$ (4.1 mg, 0.015 mmol), IPr^{Me}·HCl (13.6 mg, 0.03 mmol), NaO-*t*-Bu (36.0 mg, 0.375 mmol), ([1,1'-biphenyl]-3-yloxy)(*tert*-butyl)dimethylsilane (41.8 mg, 0.147 mmol), and *tert*-butyl 4-aminopiperidine-1-carboxylate (45.1 mg, 0.225 mmol) at 120 °C for 16 h gave a crude residue which was purified by flash chromatography (hexanes: ethyl acetate 95:5) to afford the desired product (30.0 mg, 0.085 mmol, 60% yield).

^{1}H-NMR (700 MHz, $CDCl_3$): δ 7.56 (d, *J* = 7.7 Hz, 2H), 7.42 (t, *J* = 7.7 Hz, 2H), 7.34 (t, *J* = 7.0 Hz, 1H), 7.24 (t, *J* = 7.7 Hz, 1H), 6.93 (d, *J* = 7.7 Hz, 1H), 6.80 (s, 1H), 6.60 (d, *J* = 7.7 Hz, 1H), 4.11 (m, 2H), 3.62 (s, 1H), 3.50 (pentet, *J* = 8.4 Hz, 1H), 2.94 (s, 2H), 2.07 (d, *J* = 13.3 Hz, 2H), 1.47 (s, 9H), 1.37 (m, 2H).
^{13}C-NMR (175 MHz, $CDCl_3$): δ 154.8, 147.1, 142.6, 141.7, 129.7, 128.6, 127.18, 127.16, 116.7, 112.2, 112.1, 79.6, 50.1, 32.4, 28.4.

IR (film, cm^{-1}): 3366, 2974, 2931, 2854, 1679, 1598, 1448.

HRMS (ESI+) *m/z*: $[M+H]^+$ predicted for $C_{22}H_{28}N_2O_2$, 353.2224; found, 353.2230.

4-(3-(2-methylpiperidin-1-yl)phenyl)morpholine.

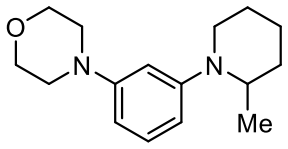

Table 3-5, 3-34: Following a modified general procedure D, $Ni(COD)_2$ (6.2 mg, 0.0225 mmol), IPr^{Me}·HCl (20.4 mg, 0.045 mmol), NaO-*t*-Bu (57.7 mg, 0.6 mmol), 4-(3-((*tert*-butyldimethylsilyl)oxy)phenyl)morpholine (45.6 mg, 0.155 mmol), and 2-methylpiperidine (44 µL, 0.375 mmol) at 120 °C for 16 h gave a crude residue which was purified by flash chromatography (hexanes: ethyl acetate 90:10) to afford the desired product (25.0 mg, 0.096 mmol, 62% yield).

^{1}H-NMR (700 MHz, $CDCl_3$): δ 7.15 (t, *J* = 7.7 Hz, 1H), 6.52 (m, 2H), 6.43 (d, *J* = 8.4 Hz, 1H), 3.86 (m, 5H), 3.15 (m, 5H), 2.98 (dd, *J* = 10.5, 3.5 Hz, 1H), 1.86 (m, 1H), 1.74 (m, 1H), 1.64 (m, 2H), 1.57 (m, 2H), 0.99 (d, *J* = 7.0 Hz, 3H).

^{13}C-NMR (175 MHz, $CDCl_3$): δ 152.6, 152.3, 129.4, 110.3, 107.5, 106.2, 67.0, 51.8, 49.7, 45.6, 31.9, 26.2, 19.9, 14.1.

IR (film, cm^{-1}): 2928, 2850, 2816, 1595, 1576, 1498, 1448.

HRMS (ESI+) *m/z*: $[M+H]^+$ predicted for $C_{16}H_{24}N_2O$, 261.1961; found, 261.1964.

***N*-(4-(butyl(methyl)amino)phenyl)acetamide.**

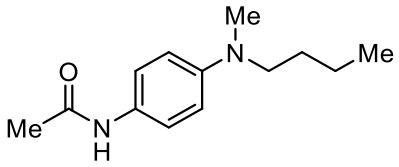

Table 3-5, 3-35: Following a modified general procedure D, $Ni(COD)_2$ (6.2 mg, 0.0225 mmol), IPr^{Me}·HCl (20.4 mg, 0.045 mmol), NaO-*t*-Bu (57.7 mg, 0.60 mmol), *N*-(4-((*tert*-butyldimethylsilyl)oxy)phenyl)acetamide (42.4 mg, 0.160 mmol), and *N*-methylbutylamine (44 µL, 0.375 mmol) at 120 °C for 16 h gave a crude residue which was purified by flash chromatography (hexanes: ethyl acetate 90:10) to afford the desired product (15.2 mg, 0.069 mmol, 43% yield).

^{1}H-NMR (500 MHz, $CDCl_3$): δ 7.28 (d, *J* = 9.0 Hz, 2H), 7.00 (br, 1H), 6.64 (d, *J* = 9.0 Hz, 2H), 3.27 (t, *J* = 7.5 Hz, 2H), 2.89 (s, 3H), 2.13 (s, 3H), 1.53 (pentet, *J* = 7.5 Hz, 2H), 1.32 (sextet, *J* = 7.5 Hz, 2H), 0.93 (t, *J* = 7.5 Hz, 3H).
^{13}C-NMR (125 MHz, $CDCl_3$): δ 168.1, 146.8, 127.9, 126.9, 122.3, 112.4, 112.0, 52.8, 38.4, 28.7, 24.2, 20.3, 14.0
IR (film, cm^{-1}): 3284, 2955, 2870, 1653, 1598.
HRMS (ESI+) *m/z*: $[M+H]^+$ predicted for $C_{13}H_{20}N_2O$, 220.1576; found, 220.1572.

1-(5,6,7,8-tetrahydronaphthalen-2-yl)pyrrolidine.

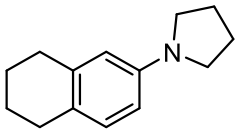

Table 3-5, 3-36: Following a modified general procedure D, $Ni(COD)_2$ (12.4 mg, 0.045 mmol), IPr^{Me}·HCl (40.8 mg, 0.09 mmol), NaO-*t*-Bu (115.6 mg, 1.20 mmol), *tert*-butyldimethyl((5,6,7,8-tetrahydronaphthalen-2-yl)oxy)silane (79.7 mg, 0.300 mmol), and pyrrolidine (38 µL, 0.45 mmol) at 120 °C for 16 h gave a crude residue which was purified by flash chromatography (hexanes: ethyl acetate 99.5:0.5) to afford the desired product (44.3 mg, 0.220 mmol, 72% yield). The spectral data matches that previously reported in the literature.

^{1}H-NMR (500 MHz, $CDCl_3$): δ 6.93 (d, *J* = 8.0 Hz, 1H), 6.40 (dd, *J* = 8.5, 2.5 Hz, 1H), 6.28 (s, 1H), 3.25 (m, 4H), 2.71 (m, 4H), 1.98 (m, 4H), 1.77 (m, 4H).

1-((8*R*,9*S*,13*S*,14*S*,17*S*)-17-((*tert*-butyldimethylsilyl)oxy)-13-methyl-7,8,9,11,12,13,14,15,16,17-decahydro-6*H*-cyclopenta[a]phenanthren-3-yl)piperidine.

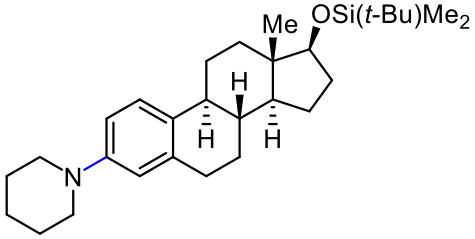

Table 3-5, 3-37: Following a modified general procedure A, $Ni(COD)_2$ (6.2 mg, 0.0225 mmol), IPr^{Me}·HCl (20.4 mg, 0.045 mmol), NaO-*t*-Bu (57.7 mg, 0.60 mmol), (((8R,9S,13S,14S,17S)-13-methyl-7,8,9,11,12,13,14,15,16,17-decahydro-6H-cyclopenta[a]phenanthrene-3,17-diyl)bis(oxy))bis(*tert*-butyldimethylsilane) (75.7 mg, 0.151 mmol), and piperidine (37 µL, 0.375 mmol) at 120 °C for 16 h gave a crude residue which was purified by flash chromatography (hexanes: ethyl acetate 95:5) to afford the desired product (65.0 mg, 0.143 mmol, 95% yield).

^{1}H-NMR (500 MHz, $CDCl_3$): δ 7.18 (d, *J* = 8.5 Hz, 1H), 6.77 (dd, *J* = 8.5, 2.5 Hz, 1H), 6.67 (d, *J* = 3.0 Hz, 1H), 3.65 (t, *J* = 8.5 Hz, 1H), 3.10 (t, *J* = 5.5 Hz, 4H), 2.82 (m, 2H), 2.28 (dd, *J* = 13.5, 4.0 Hz, 1H), 2.16 (m, 1H), 1.94-1.85 (m, 3H), 1.73-1.62 (m, 5H), 1.58-1.12 (m, 10H), 0.91 (s, 9H), 0.75 (s, 3H), 0.04 (d, *J* = 6.0 Hz, 6H).
^{13}C-NMR (125 MHz, $CDCl_3$): δ 150.2, 137.2, 131.7, 125.9, 117.0, 114.5, 81.8, 51.0, 49.7, 44.1, 43.6, 39.0, 37.2, 31.0, 30.0, 27.5, 26.3, 26.0, 25.9, 24.3, 23.3, 18.1, 11.4, -4.5, -4.8.
IR (film, cm^{-1}): 2926, 2854, 1608, 1503, 1450, 1127.
HRMS (ESI+) *m/z*: $[M+H]^+$ predicted for $C_{29}H_{47}NOSi$, 454.3500; found, 454.3504.

6.3.4 Table 3-13 Substrate Scope

2-([1,1'-biphenyl]-4-yl)-4,4,5,5-tetramethyl-1,3,2-dioxaborolane.

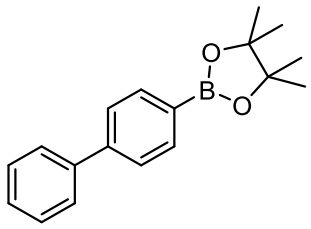

Table 3-13, 3-45: Following a modified general procedure E, $Ni(acac)_2$ (1.9 mg, 0.0075 mmol), IPr^{Me}·HCl (6.8 mg, 0.015 mmol), NaO-*t*-Bu (36.0 mg, 0.375 mmol), $Cu(OAc)_2$ (2.8 mg, 0.150 mmol), ([1,1'-biphenyl]-4-yloxy)(*tert*-butyl)dimethylsilane (39.4 mg, 0.139 mmol), B_2pin_2 (95.2 mg, 0.375 mmol), and toluene (0.3 M) at 120 °C for 16 h gave a crude residue. The yield was determined by GC-FID analysis using tridecane (40 µL, 0.164 mmol) as an internal standard (tridecane integration: 273004807, product integration: 361762783, 0.128 mmol, 92%). The spectral data matches that previously reported in the literature.

^{1}H-NMR (500 MHz, $CDCl_3$): δ 7.88 (d, *J* = 8.0 Hz, 2H), 7.62 (m, 4H), 7.44 (m, 2H), 7.36 (m, 1H), 1.35 (s,12H).

4,4,5,5-tetramethyl-2-(naphthalen-2-yl)-1,3,2-dioxaborolane.

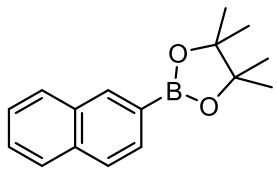

Table 3-13, 3-46: Following a modified general procedure E, $Ni(acac)_2$ (3.9 mg, 0.015 mmol), IPr^{Me}·HCl (13.6 mg, 0.03 mmol), NaO-*t*-Bu (72.0 mg, 0.750 mmol), $Cu(OAc)_2$ (5.5 mg, 0.300 mmol), *tert*-butyldimethyl(naphthalen-2-yloxy)silane (39.0 mg, 0.147 mmol), B_2pin_2 (95.2 mg, 0.375 mmol), and cyclopenylmethylether (0.3 M) at 120 °C for 16 h gave a crude residue which was purified by flash chromatography (boric acid impregnated silica gel, hexanes: ethyl acetate

95:5) to afford the desired product (25.4 mg, 0.100 mmol, 68% yield). The spectral data matches that previously reported in the literature. Experiment was conducted by Wesley Pein.

^{1}H-NMR (500 MHz, $CDCl_3$): δ 8.36 (s, 1H), 7.85 (m, 4H), 7.50 (m, 2H), 1.38 (s, 12H).

2-([1,1'-biphenyl]-3-yl)-4,4,5,5-tetramethyl-1,3,2-dioxaborolane.

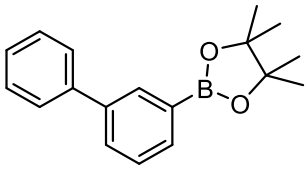

Table 3-13, 3-47: Following a modified general procedure E, $Ni(acac)_2$ (3.9 mg, 0.015 mmol), IPr^{Me}·HCl (13.6 mg, 0.03 mmol), NaO-*t*-Bu (72.0 mg, 0.750 mmol), $Cu(OAc)_2$ (5.5 mg, 0.300 mmol), ([1,1'-biphenyl]-3-yloxy)(*tert*-butyl)dimethylsilane (42.7 mg, 0.150 mmol), B_2pin_2 (95.2 mg, 0.375 mmol), and cyclopenylmethylether (0.3 M) at 120 °C for 16 h gave a crude residue which was purified by flash chromatography (boric acid impregnated silica gel, hexanes: ethyl acetate 95:5) to afford the desired product (26.5 mg, 0.094 mmol, 63% yield). The spectral data matches that previously reported in the literature. Experiment was conducted by Wesley Pein.

^{1}H-NMR (500 MHz, $CDCl_3$): δ 8.04 9s, 1H), 7.79 (d, *J* = 7.5 Hz, 1H), 7.68 (d, *J* = 7.5 Hz, 1H), 7.63 (d, *J* = 7.5 Hz, 2H), 7.44 (m, 3H), 7.33 (m, 1H), 1.35 (s, 12H).

4,4,5,5-tetramethyl-2-(naphthalen-1-yl)-1,3,2-dioxaborolane.

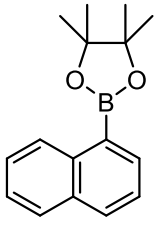

Table 3-13, 3-48: Following a modified general procedure E, $Ni(acac)_2$ (3.9 mg, 0.015 mmol), IPr^{Me}·HCl (13.6 mg, 0.03 mmol), NaO-*t*-Bu (72.0 mg, 0.750 mmol), $Cu(OAc)_2$ (5.5 mg, 0.300 mmol), *tert*-butyldimethyl(naphthalen-1-yloxy)silane (46.0 mg, 0.180 mmol), B_2pin_2 (95.2 mg, 0.375 mmol), and cyclopenylmethylether (0.3 M) at 120 °C for 16 h gave a crude residue which was purified by flash chromatography (boric acid impregnated silica gel, hexanes: ethyl acetate 95:5) to afford the desired product (25.8 mg, 0.101 mmol, 57% yield). The spectral data matches that previously reported in the literature. Experiment was conducted by Wesley Pein.

^{1}H-NMR (500 MHz, $CDCl_3$): δ 8.65 (d, *J* = 8.0 Hz, 1H), 8.08 (s, *J* = 7.0 Hz, 1H), 7.93 (d, *J* = 8.0 Hz, 1H), 7.82 (d, *J* = 8.0 Hz, 1H), 7.53 (m, 1H), 7.47 (m, 2H), 1.43 (s, 12H).

4,4,5,5-tetramethyl-2-(5,6,7,8-tetrahydronaphthalen-2-yl)-1,3,2-dioxaborolane.

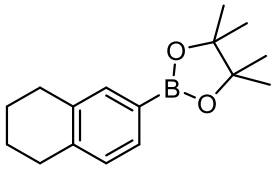

Table 3-13, 3-49: Following a modified general procedure E, $Ni(acac)_2$ (3.9 mg, 0.015 mmol), IPr^{Me}·HCl (13.6 mg, 0.03 mmol), NaO-*t*-Bu (72.0 mg, 0.750 mmol), $Cu(OAc)_2$ (5.5 mg, 0.300 mmol), *tert*-butyldimethyl((5,6,7,8-tetrahydronaphthalen-2-yl)oxy)silane (39.3 mg, 0.150 mmol), B_2pin_2 (95.2 mg, 0.375 mmol), and cyclopenylmethylether (0.3 M) at 120 °C for 16 h gave a crude residue which was purified by flash chromatography (boric acid impregnated silica gel, hexanes: ethyl acetate 95:5) to afford the desired product (17.8 mg, 0.069 mmol, 46% yield). The spectral data matches that previously reported in the literature. Experiment was conducted by Wesley Pein.

^{1}H-NMR (500 MHz, $CDCl_3$): δ 7.52 (m, 2H), 7.09 (d, *J* = 7.5 Hz, 1H), 2.80 (m, 4H), 1.8 (m, 4H), 1.38 (s, 12H).

2-(4-(tert-butyl)phenyl)-4,4,5,5-tetramethyl-1,3,2-dioxaborolane.

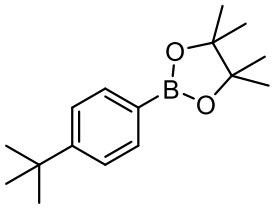

Table 3-13, 3-50: Following a modified general procedure E, $Ni(acac)_2$ (3.9 mg, 0.015 mmol), IPr^{Me}·HCl (13.6 mg, 0.03 mmol), NaO-*t*-Bu (72.0 mg, 0.750 mmol), $Cu(OAc)_2$ (5.5 mg, 0.300 mmol), *tert*-butyl(4-(*tert*-butyl)phenoxy)dimethylsilane (39.8 mg, 0.151), B_2pin_2 (95.2 mg, 0.375 mmol), and cyclopenylmethylether (0.3 M) at 120 °C for 16 h gave a crude residue which was purified by flash chromatography (boric acid impregnated silica gel, hexanes: ethyl acetate 95:5) to afford the desired product (14.1, 0.054 mmol, 36% yield). The spectral data matches that previously reported in the literature. Experiment was conducted by Wesley Pein.

^{1}H-NMR (500 MHz, $CDCl_3$): δ 7.78 (d, *J* = 8.0 Hz, 2H), 7.42 (d, *J* = 8.0 Hz, 2H), 1.34 (s, 9H), 1.35 (s, 12H).

2-(4-(4,4,5,5-tetramethyl-1,3,2-dioxaborolan-2-yl)phenyl)pyridine.

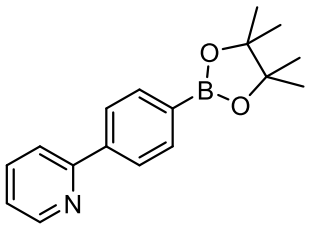

Table 3-13, 3-51: Following a modified general procedure E, $Ni(acac)_2$ (3.9 mg, 0.015 mmol), IPr^{Me}·HCl (13.6 mg, 0.03 mmol), NaO-*t*-Bu (72.0 mg, 0.750 mmol), $Cu(OAc)_2$ (5.5 mg, 0.300 mmol), 2-(4-((*tert*-butyldimethylsilyl)oxy)phenyl)pyridine (41.5 mg, 0.145 mmol), B_2pin_2 (95.2 mg, 0.375 mmol), and toluene (0.3 M) at 120 °C for 16 h gave a crude residue which was purified

by flash chromatography (hexanes: ethyl acetate 95:5) to afford the desired product (16.0 mg, 0.57 mmol, 39% yield). The spectral data matches that previously reported in the literature.

^{1}H-NMR (500 MHz, $CDCl_3$): δ 8.72 (m, 1H), 8.02 (d, *J* = 8.0 Hz, 2H), 7.92 (d, *J* = 8.2 Hz, 2H), 7.75 (m, 2H), 7.25 (m, 1H), 1.35 (s, 12H).

6.4 General Experimental Details for Chapter 4

6.4.1 Scheme 4-17 Substrates

7-methoxy-*N*-octylnaphthalen-2-amine.

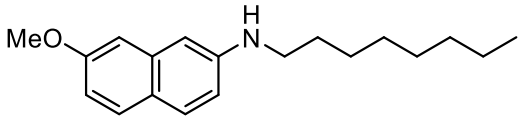

Scheme 4-17, 4-35: Following a modified general procedure D, $Ni(COD)_2$ (4.1 mg, 0.015 mmol), IPr^{Me}·HCl (13.6 mg, 0.03 mmol), NaO-*t*-Bu (36.0 mg, 0.375 mmol), *tert*-butyl((7-methoxynaphthalen-2-yl)oxy)dimethylsilane (44.0 mg, 0.153 mmol), and octylamine (30 µL, 0.18 mmol) at 120 °C for 16 h gave a crude residue which was purified by flash chromatography (hexanes: ethyl acetate 85:15) to afford the desired product (20.8 mg, 0.0729 mmol, 48% yield). The spectral data matches that previously reported in the literature.

^{1}H-NMR (500 MHz, $CDCl_3$): δ 7-55 (m, 2H), 6.96 (d, *J* = 2.0 Hz, 1H), 6.86 (m, 1H), 6.72 (m, 2H), 3.90 (s, 3H), (3.20 (t, *J* = 7.0 Hz, 2H), 1.68 (m, 2H), 1.38 (m, 10H), 0.91 (t, *J* = 7.0 Hz, 3H).

7-methyl-*N*-octylnaphthalen-2-amine.

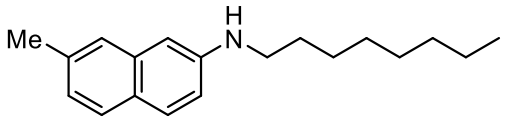

Scheme 4-17, 4-36: Following a modified previously published procedure,[96] $Ni(COD)_2$ (3.5 mg, 0.0126 mmol), ICy·HBF_4 (4.0 mg, 0.0126 mmol), NaO-*t*-Bu (12.1 mg, 0.126 mmol), 7-methoxy-*N*-octylnaphthalen-2-amine (18.0 mg, 0.063 mmol), and trimethylaluminum (2 M in hexanes, 63 µL) at 120 °C for 16 h gave a crude residue which was purified by flash chromatography (hexanes: ethyl acetate 95:5) to afford the desired product (5.8 mg, 0.022 mmol, 34% yield).

^{1}H-NMR (500 MHz, $CDCl_3$): δ 7.56 (dd, *J* = 9.0, 2.0 Hz, 2H), 7.40 (s, 1H), 7.02 (dd, *J* = 8.5, 2.0 Hz, 1H), 6.80 (dd, *J* = 9.0, 2.5 Hz, 1H), 6.73 (d, *J* = 2.0 Hz, 1H), 3.74 (br, 1H), 3.20 (t, *J* = 7.5 Hz, 2H), 2.46 (s, 3H), 1.68 (pentet, *J* = 7.5 Hz, 2H), 1.44 (m, 2H), 1.34 (m, 10H), 0.90 (t, *J* = 7.0 Hz, 3H).

^{13}C-NMR (125 MHz, $CDCl_3$): δ 146.2, 135.8, 135.5, 128.5, 127.4, 125.6, 125.0, 124.0, 117.0, 103.8, 44.1, 31.8, 29.5, 29.4, 29.3, 27.2, 22.6, 21.8, 14.1.

***tert*-butyldimethyl((7-methylnaphthalen-2-yl)oxy)silane.**

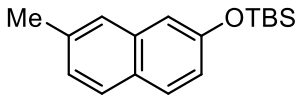

Scheme 4-17, 4-37: Following a modified previously published procedure,[96] $Ni(COD)_2$ (4.1 mg, 0.015 mmol), ICy·HBF_4 (4.8 mg, 0.015 mmol), NaO-*t*-Bu (28.8 mg, 0.30 mmol), *tert*-butyl((7-methoxynaphthalen-2-yl)oxy)dimethylsilane (43.3 mg, 0.150 mmol), and trimethylaluminum (2 M in hexanes, 75 µL) at 120 °C for 16 h gave a crude residue which was purified by flash chromatography (hexanes) to afford the desired product (23.7 mg, 0.087 mmol, 58% yield).

^{1}H-NMR (500 MHz, $CDCl_3$): δ 7.65 (m,2H), 7.12 (d, *J* = 2.5 Hz, 1H), 7.01 (m, 2H), 6.93 (dd, *J* = 9.0, 2.5 Hz, 1H), 3.91 (s, 3H), 1.04 (s, 9H), 0.26 (s, 6H).

^{13}C-NMR (125 MHz, $CDCl_3$): δ 153.5, 135.8, 134.8, 129.0, 127.5, 127.4, 126.0, 125.7, 121.1, 114.4, 25.7, 21.7, 18.3, -4.3.

7-methyl-*N*-octylnaphthalen-2-amine.

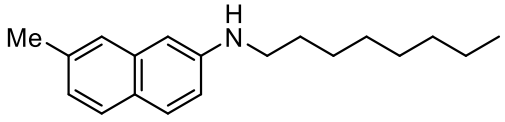

Scheme 4-17, 4-36: Following a modified general procedure D, $Ni(COD)_2$ (4.8 mg, 0.0175 mmol), IPr^{Me}·HCl (15.9 mg, 0.035 mmol), NaO-*t*-Bu (21.1 mg, 0.220 mmol), *tert*-butyldimethyl((7-methylnaphthalen-2-yl)oxy)silane (24.0 mg, 0.088 mmol), and octylamine (18 µL, 0.106 mmol) at 120 °C for 16 h gave a crude residue which was purified by flash chromatography (hexanes: ethyl acetate 95:5) to afford the desired product (14.9 mg, 0.055 mmol, 63% yield).

^{1}H-NMR (500 MHz, $CDCl_3$): δ 7.56 (dd, *J* = 9.0, 2.0 Hz, 2H), 7.40 (s, 1H), 7.02 (dd, *J* = 8.5, 2.0 Hz, 1H), 6.80 (dd, *J* = 9.0, 2.5 Hz, 1H), 6.73 (d, *J* = 2.0 Hz, 1H), 3.74 (br, 1H), 3.20 (t, *J* = 7.5 Hz, 2H), 2.46 (s, 3H), 1.68 (pentet, *J* = 7.5 Hz, 2H), 1.44 (m, 2H), 1.34 (m, 10H), 0.90 (t, *J* = 7.0 Hz, 3H).
^{13}C-NMR (125 MHz, $CDCl_3$): δ 146.2, 135.8, 135.5, 128.5, 127.4, 125.6, 125.0, 124.0, 117.0, 103.8, 44.1, 31.8, 29.5, 29.4, 29.3, 27.2, 22.6, 21.8, 14.1.

6.4.2 Scheme 4-18 Substrates

***tert*-butyl((7-methoxynaphthalen-2-yl)oxy)dimethylsilane.**

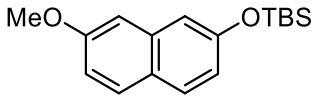

Scheme 4-18, 4-30: Following a previously published procedure,[179] 7-methoxynaphthalen-2-ol (890 mg, 5.1 mmol), imidazole (681 mg, 10 mmol), *tert*-butyldimethylsilyl chloride (1.13 g, 7.5 mmol) gave a crude residue which was purified by flash chromatography (hexanes: ethyl acetate = 99:1) to afford the desired product as a clear oil (1.43 g, 4.96 mmol, 97% yield).

^{1}H-NMR (500 MHz, $CDCl_3$): δ 7.65 (t, *J* = 8.5 Hz, 2H), 7.11 (m, 1H), 6.99 (m, 2H), 6.93 (dt, *J* = 9.0 Hz, 2.5 Hz, 1H), 3.91 (s, 3H), 1.03 (s, 9H), 0.25 (s, 6H).
^{13}C-NMR (125 MHz, $CDCl_3$): δ 158.0, 154.1, 135.9, 129.1, 129.0, 124.7, 119.5, 116.5, 114.2, 104.8, 55.2, 25.7, 18.3, -4.3.
IR (film, cm^{-1}): 2954, 2928, 2857, 1631, 1511.

HRMS (ESI+) *m/z*: $[M+H]^+$ predicted for $C_{17}H_{24}O_2Si$, 289.1618; found, 289.1620.

1-(7-methoxynaphthalen-2-yl)-4-methylpiperazine.

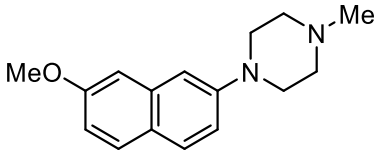

Scheme 4-18, 4-38: Following a modified general procedure D, $Ni(COD)_2$ (4.1 mg, 0.015 mmol), IPr^{Me}·HCl (13.6 mg, 0.03 mmol), NaO-*t*-Bu (36.0 mg, 0.375 mmol), *tert*-butyl((7-methoxynaphthalen-2-yl)oxy)dimethylsilane (44.2 mg, 0.153 mmol), and 1-methylpiperazine (25 µL, 0.225 mmol) at 120 °C for 16 h gave a crude residue which was purified by flash chromatography (hexanes: ethyl acetate: triethylamine 75:24:1) to afford the desired product (32.2 mg, 0.125 mmol, 82% yield).

^{1}H-NMR (700 MHz, $CDCl_3$): δ 7.64 (d, *J* = 8.4Hz, 1H), 7.62 (d, *J* = 8.4 Hz, 1H), 7.12 (d, *J* = 9.1 Hz, 1H), 7.05 (s, 1H), 7.02 (s, 1H), 6.95 (d, *J* = 9.1 Hz, 1H), 3.99 (s, 3H), 3.32 (t, *J* = 4.9 Hz, 4H), 2.63 (t, *J* = 4.9 Hz, 4H), 2.38 (s, 3H).
^{13}C-NMR (175 MHz, $CDCl_3$): δ 158.1, 149.6, 135.8, 128.9, 128.4, 123.8, 116.8, 115.8, 109.4, 105.1, 55.2, 55.1, 49.4, 46.2.
IR (film, cm^{-1}): 2932, 2839, 2798, 1629, 1515, 1462.
HRMS (ESI+) *m/z*: $[M+H]^+$ predicted for $C_{16}H_{20}N_2O$, 257.1648; found, 257.1653.

1-(7-ethylnaphthalen-2-yl)-4-methylpiperazine.

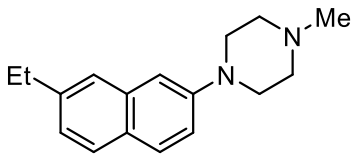

Scheme 4-18, 4-39: Following a modified published procedure,[97] $Ni(COD)_2$ (1.7 mg, 0.0062 mmol), 1,2-bis(dicylohexylphosphino)ethane (dcype) (2.6 mg, 0.0062 mmol), 1-(7-methoxynaphthalen-2-yl)-4-methylpiperazine (16.0 mg, 0.062 mmol), triethylaluminum (25 wt% in toluene, 34 µL), toluene (0.3 mL), and diisopropylether (0.3 mL) at 120 °C for 16 h gave a crude residue which was purified by flash chromatography (hexanes: ethyl acetate: triethylamine 72.5:25:2.5) to afford the desired product (15.0 mg, 0.059 mmol, 94% yield).

^{1}H-NMR (500 MHz, $CDCl_3$): δ 7.68 (d, *J* = 9.1 Hz, 1H), 7.64 (d, *J* = 8.4 Hz, 1H), 7.49 (s, 1H), 7.21 (d, *J* = 8.4 Hz, 1H), 7.17 (d, *J* = 7.7 Hz, 1H), 7.09 (s, 1H), 3.32 (t, *J* = 4.9 Hz, 4H), 2.77 (q, *J* = 7.7 Hz, 2H), 2.64 (t, *J* = 4.9 Hz, 4H), 2.39 (s, 3H), 1.31 (t, *J* = 7.7 Hz, 3H).
^{13}C-NMR (125 MHz, $CDCl_3$): δ 149.2, 142.2, 134.8, 128.4, 127.3, 127.0, 124.6, 124.5, 118.6, 110.0, 55.1, 49.5, 46.2, 29.1, 15.5.
IR (film, cm^{-1}): 2963, 2928, 2839, 2787, 1629, 1514.
HRMS (ESI+) *m/z*: $[M+H]^+$ predicted for $C_{17}H_{22}N_2$, 255.1856; found, 255.1856.

***tert*-butyl((7-ethylnaphthalen-2-yl)oxy)dimethylsilane.**

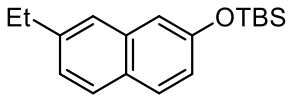

Scheme 4-18, 4-40: Following a modified published procedure,[97] $Ni(COD)_2$ (4.1 mg, 0.015 mmol), 1,2-bis(dicylohexylphosphino)ethane (dcype) (6.3 mg, 0.015 mmol), *tert*-butyl((7-methoxynaphthalen-2-yl)oxy)dimethylsilane (43.2 mg, 0.150 mmol), triethylaluminum (25 wt% in toluene, 161 µL), toluene (0.3 mL), and diisopropylether (0.3 mL) at 120 °C for 16 h gave a crude residue which was purified by flash chromatography (hexanes) to afford the desired product (29.2 mg, 0.102 mmol, 68% yield).

^{1}H-NMR (500 MHz, $CDCl_3$): δ 7.69 (m, 2H), 7.49 (s, 1H), 7.21 (dd, *J* = 8.5, 2.0 Hz, 1H), 7.15 (d, *J* = 2.0 Hz, 7.02 (dd, *J* = 9.0, 2.5 Hz, 1H), 2.79 (q, *J* = 8.0 Hz, 2H), 1.33 (t, *J* = 8.0 Hz, 3H), 1.03 (s, 9H), 0.25 (s, 6H).

^{13}C-NMR (125 MHz, $CDCl_3$): δ 153.5, 142.1, 134.9, 129.0, 127.7, 127.5, 125.0, 124.4, 121.2, 114.6, 29.0, 25.7, 18.3, 15.5, -4.3.

IR (film, cm^{-1}): 2958, 2929, 2857, 1632, 1606, 1511, 1461.

HRMS (ESI+) *m/z*: $[M+H]^+$ predicted for $C_{18}H_{26}OSi$, 287.1826; found, 287.1829.

1-(7-ethylnaphthalen-2-yl)-4-methylpiperazine.

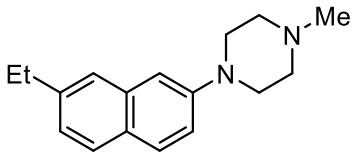

Scheme 4-18, 4-39: Following a modified general procedure D, $Ni(COD)_2$ (3.0 mg, 0.011 mmol), IPr^{Me}·HCl (9.80 mg, 0.022 mmol), NaO-*t*-Bu (25.9 mg, 0.270 mmol), *tert*-butyl((7-ethylnaphthalen-2-yl)oxy)dimethylsilane (31.0 mg, 0.108 mmol), and 1-methylpiperazine (18 µL, 0.162 mmol) at 120 °C for 16 h gave a crude residue which was purified by flash chromatography (hexanes: ethyl acetate:triethylamine 72.5:25:2.5) to afford the desired product (26.8 mg, 0.105 mmol, 97% yield).

^{1}H-NMR (500 MHz, $CDCl_3$): δ 7.68 (d, *J* = 9.1 Hz, 1H), 7.64 (d, *J* = 8.4 Hz, 1H), 7.49 (s, 1H), 7.21 (d, *J* = 8.4 Hz, 1H), 7.17 (d, *J* = 7.7 Hz, 1H), 7.09 (s, 1H), 3.32 (t, *J* = 4.9 Hz, 4H), 2.77 (q, *J* = 7.7 Hz, 2H), 2.64 (t, *J* = 4.9 Hz, 4H), 2.39 (s, 3H), 1.31 (t, *J* = 7.7 Hz, 3H).

^{13}C-NMR (125 MHz, $CDCl_3$): δ 149.2, 142.2, 134.8, 128.4, 127.3, 127.0, 124.6, 124.5, 118.6, 110.0, 55.1, 49.5, 46.2, 29.1, 15.5.

IR (film, cm^{-1}): 2963, 2928, 2839, 2787, 1629, 1514.

HRMS (ESI+) *m/z*: $[M+H]^+$ predicted for $C_{17}H_{22}N_2$, 255.1856; found, 255.1856.

6.4.3 Scheme 4-19 Substrates

triethyl(7-methoxynaphthalen-2-yl)silane.

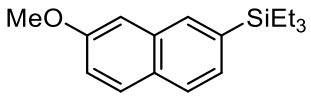

Scheme 4-19, 4-41: Following a modified general procedure A, $Ni(acac)_2$ (3.9 mg, 0.015 mmol), IPr*OMe (14.2 mg, 0.015 mmol), NaO-*t*-Bu (36.0 mg, 0.375 mmol), *tert*-butyl((7-methoxynaphthalen-2-yl)oxy)dimethylsilane (45.1 mg, 0.156 mmol), titanium(IV) isopropoxide (89 μL, 0.90 mmol), and triethylsilane (144 μL, 0.90 mmol) at 120 °C for 5 h gave a crude residue which was purified by flash chromatography (hexanes: ethyl acetate 98:2) to afford the desired product (16.0 mg, 0.059 mmol, 43% yield). The spectral data matches that previously reported in the literature.

^{1}H-NMR (500 MHz, $CDCl_3$): δ 7.88 (s, 1H), 7.73 (m, 2H), 7.43 (dd, *J* = 8.0, 2.0 Hz, 1H), 7.15 (m, 2H), 3.93 (s, 3H), 1.00 (m, 9H), 0.88 (m, 6H).

***tert*-butyldimethyl(naphthalen-2-yloxy)silane.**

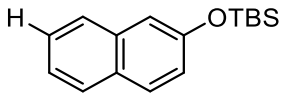

Scheme 4-19, 4-42: Following a modified published procedure,[151] $Ni(COD)_2$ (4.1 mg, 0.015 mmol), PCy_3 (8.4 mg, 0.030 mmol), *tert*-butyl((7-methoxynaphthalen-2-yl)oxy)dimethylsilane (42.6 mg, 0.148 mmol), and triethylsilane (48 μL, 0.30 mmol) at 120 °C for 16 h gave a crude residue which was purified by flash chromatography (hexanes: ethyl acetate 98:2) to afford the desired product (20.7 mg, 0.080 mmol, 55% yield). The spectral data matches that previously reported in the literature.

^{1}H-NMR (500 MHz, $CDCl_3$): δ 7.77 (d, *J* = 8.0 Hz, 1H), 7.72 (d, *J* = 8.8, 1H), 7.69 (d, *J* = 8.3 Hz, 1H), 7.42 (dt, *J* = 7.8, 1.2 Hz, 1H), 7.33 (dt, *J* = 6.8, 1.2, 1H), 7.19 (d, *J* = 2.2, 1H), 7.08 (dd, *J* = 8.8, 2.2 Hz, 1H), 1.04 (s, 9H), 0.26 (s, 6H).

6.4.4 Scheme 4-20 Substrates

1-bromo-4-chloro-2-methoxybenzene.

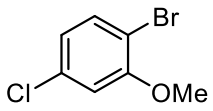

Scheme 4-20, 4-44: Following a previously reported procedure,[179] 2-bromo-5-chlorophenol (2.09 g, 10.1 mmol), K_2CO_3 (2.76 g, 10 mmol), methyl iodide (1.25 mL, 20 mmol), and DMF (10 mL) gave a crude residue which was purified by flash chromatography (hexanes) to afford the desired product as a white solid (2.1 g, 9.48 mmol, 94% yield). The spectral data matches that previously reported in the literature.

^{1}H-NMR (500 MHz, $CDCl_3$): δ 7.43 (d, *J* = 8.0 Hz, 1H), 6.87 (s, 1H), 6.83 (d, *J* = 7.5 Hz, 1H), 3.88 (s, 3H).

***tert*-butyl((4'-chloro-2'-methoxy-[1,1'-biphenyl]-4-yl)oxy)dimethylsilane.**

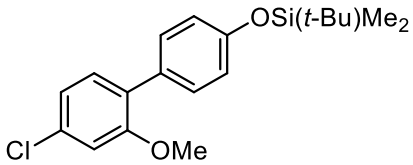

Scheme 4-20, 4-46: Following a previously reported procedure,[179] 1-bromo-4-chloro-2-methoxybenzene (32.7 mg, 0.148 mmol), (4-((tert-butyldimethylsilyl)oxy)phenyl)boronic acid

(56.7 mg, 0.225 mmol), K_3PO_4 (191 mg, 0.9 mmol), $PdCl_2(PPh_3)_2$ (5.3 mg, 0.0075 mmol), toluene (0.45 mL), and degassed H_2O (0.45 mL) at 90 ºC for 16 hours gave a crude residue which was purified by flash chromatography (hexanes: ethyl acetate = 98:2) to afford the desired product (50.1 mg, 0.144 mmol, 97% yield).

^{1}H-NMR (500 MHz, $CDCl_3$): δ 7.35 (d, *J* = 8.0 Hz, 2H), 7.21 (d, *J* = 8.0 Hz, 1H), 6.99 (dd, *J* = 8.0, 1.5 Hz, 1H), 6.94 (d, *J* = 1.5 Hz, 1H), 6.86 (d, *J* = 8.5 Hz, 2H), 3.81 (s, 3H), 1.00 (s, 9H), 0.23 (s, 6H).
^{13}C-NMR (125 MHz, $CDCl_3$): δ 156.9, 155.0, 133.3, 131.3, 130.4, 130.3, 129.0, 120.8, 119.6, 111.8, 55.8, 25.7, 18.2, -4.4.
IR (film, cm^{-1}): 2955, 2929, 2857, 1606, 1514, 1483.
HRMS (ESI+) *m/z*: $[M+H]^+$ predicted for $C_{19}H_{25}ClO_2Si$, 349.1385; found, 349.1386.

4-(4'-((*tert*-butyldimethylsilyl)oxy)-2-methoxy-[1,1'-biphenyl]-4-yl)morpholine.

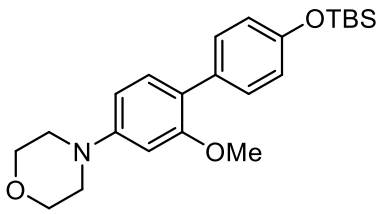

Scheme 4-20, 4-47: Following a previously reported procedure,[237] *tert*-butyl((4'-chloro-2'-methoxy-[1,1'-biphenyl]-4-yl)oxy)dimethylsilane (53.5 mg, 0.153 mmol), NaO-*t*-Bu (25.9 mg, 0.27 mmol), $Ni(COD)_2$ (6.2 mg, 0.0225 mmol), SIPr·HCl (9.6 mg, 0.0225 mmol), morpholine (20 µL, 0.225 mmol) gave a crude residue which was purified by flash chromatography (hexanes: ethyl acetate = 95:5) to afford the desired product (55.4 mg, 0.139 mmol, 90% yield).

^{1}H-NMR (500 MHz, $CDCl_3$): δ 7.37 (d, *J* = 8.5 Hz, 2H), 7.21 (d, *J* = 8.5 Hz, 1H), 6.84 (d, *J* = 8.5 Hz, 2H), 6.55 (m, 2H), 3.89 (t, *J* = 5.0 Hz, 4H), 3.80 (s, 3H), 3.21 (t, *J* = 5.0 Hz, 4H), 1.00 (s, 9H), 0.23 (s, 6H).

^{13}C-NMR (125 MHz, $CDCl_3$): δ 157.2, 154.3, 151.6, 131.3, 131.0, 130.3, 122.6, 119.4, 107.9, 99.9, 66.9, 55.5, 49.5, 25.7, 18.2, -4.4.

IR (film, cm^{-1}): 2955, 2856, 1606, 1496, 1448.

HRMS (ESI+) *m/z*: $[M+H]^+$ predicted for $C_{23}H_{33}NO_3Si$, 400.2302; found, 400.2299.

4-bromo-3-methoxyphenyl pivalate.

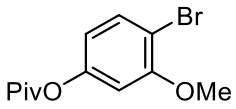

Scheme 4-20, 4-49: Following a modified reported procedure,[57] 4-bromo-3-methoxyphenol (1.22 g, 6.01 mmol), triethylamine (0.84 mL, 6 mmol), *N*,*N*-dimethylpyridin-4-amine (73.3 mg, 0.6 mmol), pivaloyl chloride (0.74 mL, 6 mmol) gave a crude residue which was purified by flash chromatography (hexanes: ethyl acetate = 95:5) to afford the desired product as a white solid (1.69 g, 5.91 mmol, 98% yield).

^{1}H-NMR (500 MHz, $CDCl_3$): δ 7.50 (d, *J* = 8.5 Hz, 1H), 6.63 (d, *J* = 1.0 Hz, 1H), 6.57 (dd, *J* = 8.5, 1.0 Hz, 1H), 3.88 (s, 3H), 1.35 (s, 9H).

^{13}C-NMR (125 MHz, $CDCl_3$): δ 176.7, 156.4, 151.3, 133.2, 114.7, 108.0, 106.2, 56.3, 39.1, 27.1.

IR (film, cm^{-1}): 2979, 747, 1595, 1479, 1395, 1272.

HRMS (EI) *m/z*: $[M]^+$ predicted for $C_{12}H_{15}BrO_3$, 286.0205; found, 286.0205.

4'-((*tert*-butyldimethylsilyl)oxy)-2-methoxy-[1,1'-biphenyl]-4-yl pivalate.

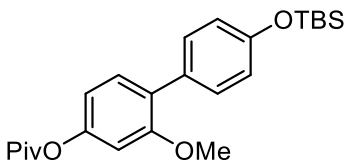

Scheme 4-20, 4-50: Following a modified reported procedure,[179] 4-bromo-3-methoxyphenyl pivalate (141.2 mg, 0.494 mmol), 4-(*tert*-Butyldimethylsilyloxy)phenylboronic acid (189 mg, 0.75 mmol), Bis(triphenylphosphine)palladium(II) dichloride (35.0 mg, 0.05 mmol), potassium phosphate (635 mg, 3 mmol) gave a crude residue which was purified by flash chromatography (hexanes: ethyl acetate = 99:1) to afford the desired product as a white solid (200 mg, 0.482 mmol, 98% yield).

^{1}H-NMR (500 MHz, $CDCl_3$): δ 7.37 (d, *J* = 8.5 Hz, 2H), 7.27 (m, 1H), 6.86 (d, *J* = 8.5 Hz, 2H), 6.71 (dd, *J* = 8.0, 2.0 Hz, 1H), 6.67 (d, *J* = 2.0, 1H), 3.80 (s, 3H), 1.38 (s, 9H), 1.00 (s, 9H), 0.23 (s, 6H).
^{13}C-NMR (125 MHz, $CDCl_3$): δ 157.0, 154.8, 151.0, 130.9, 130.7, 130.5, 127.9, 119.5, 113.4, 105.1, 55.7, 39.1, 27.2, 25.7, 18.2, -4.4.
IR (film, cm^{-1}): 2932, 2858, 1746, 1600, 1490, 1253.
HRMS (ESI+) *m/z*: $[M+H]^+$ predicted for $C_{24}H_{34}O_4Si$, 415.2299; found, 415.2298.

4-(4'-((*tert*-butyldimethylsilyl)oxy)-2-methoxy-[1,1'-biphenyl]-4-yl)morpholine.

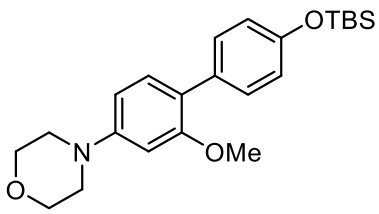

Scheme 4-20, 4-47: Following a previously reported procedure,[63] 4'-((*tert*-butyldimethylsilyl)oxy)-2-methoxy-[1,1'-biphenyl]-4-yl pivalate (61.7 mg, 0.149 mmol), NaO-*t*-Bu (31.7 mg, 0.33 mmol), $Ni(COD)_2$ (6.3 mg, 0.0225 mmol), IPr·HCl (19.2 mg, 0.045 mmol), morpholine (24 µL, 0.27 mmol) gave a crude residue which was purified by flash chromatography (hexanes: ethyl acetate = 95:5) to afford the desired product as a white solid (36.6 mg, 0.092 mmol, 62% yield).

^{1}H-NMR (500 MHz, $CDCl_3$): δ 7.37 (d, *J* = 8.5 Hz, 2H), 7.21 (d, *J* = 8.5 Hz, 1H), 6.84 (d, *J* = 8.5 Hz, 2H), 6.55 (m, 2H), 3.89 (t, *J* = 5.0 Hz, 4H), 3.80 (s, 3H), 3.21 (t, *J* = 5.0 Hz, 4H), 1.00 (s, 9H), 0.23 (s, 6H).

^{13}C-NMR (125 MHz, $CDCl_3$): δ 157.2, 154.3, 151.6, 131.3, 131.0, 130.3, 122.6, 119.4, 107.9, 99.9, 66.9, 55.5, 49.5, 25.7, 18.2, -4.4.

IR (film, cm^{-1}): 2955, 2856, 1606, 1496, 1448.

HRMS (ESI+) *m/z*: $[M+H]^+$ predicted for $C_{23}H_{33}NO_3Si$, 400.2302; found, 400.2299.

4-bromo-3-methoxyphenyl diethylcarbamate.

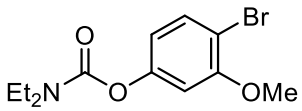

Scheme 4-20, 4-51: Following a previously reported procedure,[47] 4-bromo-3-methoxyphenol (1.014 g, 4.99 mmol), sodium hydride (300.0 mg, 12.5 mmol), Diethylcarbamoyl chloride (0.79 mL, 6.25 mmol) gave a crude residue which was purified by flash chromatography (hexanes: ethyl acetate = 90:10) to afford the desired product (1.468 g, 4.86 mmol, 97% yield).

^{1}H-NMR (500 MHz, $CDCl_3$): δ 7.48 (d, *J* = 8.5 Hz, 1H), 6.73 (d, *J* = 2.5 Hz, 1H), 6.64 (m, 1H), 3.88 (s, 3H), 3.41 (m, 4H), 1.22 (m, 6H).

^{13}C-NMR (125 MHz, $CDCl_3$): δ 156.2, 153.7, 151.7, 132.9, 114.9, 107.4, 106.5, 56.3, 42.3, 41.9, 14.2, 13.3.

IR (film, cm^{-1}): 2973, 1712, 1594, 1472, 1416.

HRMS (ESI+) *m/z*: $[M+H]^+$ predicted for $C_{12}H_{16}BrNO_3$, 302.0386; found, 302.0382.

4'-((*tert*-butyldimethylsilyl)oxy)-2-methoxy-[1,1'-biphenyl]-4-yl diethylcarbamate.

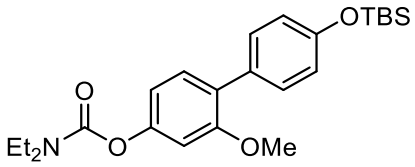

Scheme 4-20, 4-52: Following a previously reported procedure,[179] 4-bromo-3-methoxyphenyl diethylcarbamate (1.35 g, 0.447 mmol), 4-(*tert*-Butyldimethylsilyloxy)phenylboronic acid (1.70 g, 6.75 mmol), Bis(triphenylphosphine)palladium(II) dichloride (158 mg, 0.225 mmol), potassium phosphate (5.73 g, 27 mmol) gave a crude residue which was purified by flash chromatography (hexanes: ethyl acetate = 90:10) to afford the desired product (1.87 g, 4.35 mmol, 97% yield).

^{1}H-NMR (500 MHz, $CDCl_3$): δ 7.37 (m, 2H), 7.26 (m, 1H), 6.86 (m, 2H), 6.78 (m, 2H), 3.80 (s, 3H), 3.43 (m, 4H), 1.25 (m, 6H), 1.02 (s, 9H) -0.24 (s, 6H).
^{13}C-NMR (125 MHz, $CDCl_3$): δ 156.8, 154.6, 154.2, 151.4, 130.9, 130.7, 130.4, 127.4, 119.4, 113.7, 105.5, 55.6, 42.2, 41.9, 25.7, 18.2, 14.2, 13.4, -4.4.
IR (film, cm^{-1}): 2931, 2857, 1718, 1604, 1492, 1417.
HRMS (ESI+) *m/z*: $[M+H]^+$ predicted for $C_{24}H_{35}NO_4Si$, 430.2408; found, 430.2403.

4-(4'-((*tert*-butyldimethylsilyl)oxy)-2-methoxy-[1,1'-biphenyl]-4-yl)morpholine.

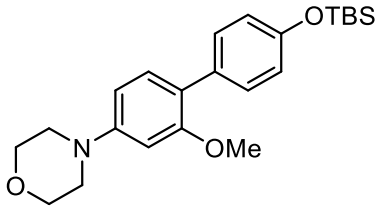

Scheme 4-20, 4-47: Following a previously reported procedure,[47] 4'-((*tert*-butyldimethylsilyl)oxy)-2-methoxy-[1,1'-biphenyl]-4-yl diethylcarbamate (428.3 mg, 0.997 mmol), NaO-*t*-Bu (211.8 mg, 2.2 mmol), $Ni(COD)_2$ (41.3 mg, 0.15 mmol), SIPr·HCl (178.1 mg,

0.3 mmol), morpholine (157 µL, 1.8 mmol) gave a crude residue which was purified by flash chromatography (hexanes: ethyl acetate = 95:5) to afford the desired product as a white solid (324.0 mg, 0.811 mmol, 81% yield).

^{1}H-NMR (500 MHz, $CDCl_3$): δ 7.37 (d, *J* = 8.5 Hz, 2H), 7.21 (d, *J* = 8.5 Hz, 1H), 6.84 (d, *J* = 8.5 Hz, 2H), 6.55 (m, 2H), 3.89 (t, *J* = 5.0 Hz, 4H), 3.80 (s, 3H), 3.21 (t, *J* = 5.0 Hz, 4H), 1.00 (s, 9H), 0.23 (s, 6H).
^{13}C-NMR (125 MHz, $CDCl_3$): δ 157.2, 154.3, 151.6, 131.3, 131.0, 130.3, 122.6, 119.4, 107.9, 99.9, 66.9, 55.5, 49.5, 25.7, 18.2, -4.4.
IR (film, cm^{-1}): 2955, 2856, 1606, 1496, 1448.
HRMS (ESI+) *m/z*: $[M+H]^+$ predicted for $C_{23}H_{33}NO_3Si$, 400.2302; found, 400.2299.

6.4.5 Scheme 4-21 Substrates

4-(2-methoxy-4'-(4-methylpiperazin-1-yl)-[1,1'-biphenyl]-4-yl)morpholine.

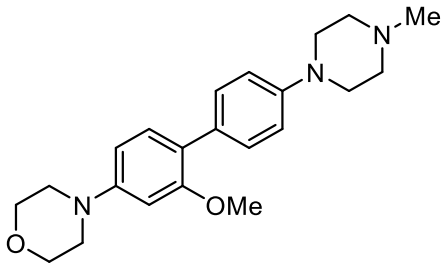

Scheme 4-21, 4-53: Following a modified general procedure D, $Ni(COD)_2$ (10.3 mg, 0.038 mmol), IPr^{Me}·HCl (34.0 mg, 0.075 mmol), NaO-*t*-Bu (144.2 mg, 1.50 mmol), 4-(4'-((*tert*-butyldimethylsilyl)oxy)-2-methoxy-[1,1'-biphenyl]-4-yl)morpholine (60.8 mg, 0.152 mmol) and 1-methylpiperazine (67 µL, 0.60 mmol) at 130 °C for 16 h gave a crude residue which was purified by flash chromatography (hexanes: ethyl acetate: triethylamine = 50:47.5:2.5) to afford the desired product as a tan solid (37.5 mg, 0.102 mmol, 67% yield).

^{1}H-NMR (500 MHz, $CDCl_3$): δ 7.42 (d, *J* = 8.5 Hz, 2H), 7.22 (d, *J* = 8.5 Hz, 1H), 6.95 (d, *J* = 8.5 Hz, 2H), 6.56 (dd, *J* = 8.5, 2.0 Hz, 1H), 6.53 (d, *J* = 2.0 Hz, 1H), 3.88 (t, *J* = *J* = 5 Hz, 4H), 3.79 (s, 3H), 3.25 (t, *J* = 5 Hz, 4H), 3.20 (t, *J* = 5 Hz, 4H), 2.59 (t, *J* = 5 Hz, 4H), 2.36 (s, 3H).
^{13}C-NMR (125 MHz, $CDCl_3$): δ 157.2, 151.5, 149.7, 130.8, 129.9, 127.1, 122.6, 115.5, 107.8, 99.8, 66.9, 55.5, 55.1, 49.5, 49.0, 46.1.
IR (film, cm^{-1}): 2933, 2824, 1607, 1499, 1446, 1234.
HRMS (ESI+) *m/z*: $[M+H]^+$ predicted for $C_{22}H_{29}N_3O_2$, 368.2333; found, 368.2337.

2'-methoxy-4'-morpholino-*N*-octyl-[1,1'-biphenyl]-4-amine.

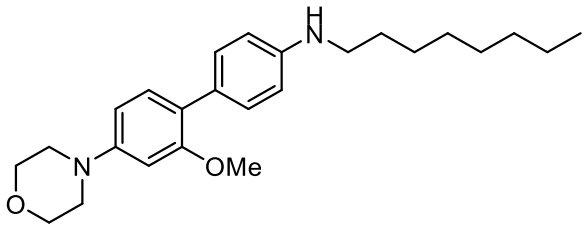

Scheme 4-21, 4-54: Following a modified general procedure D, $Ni(COD)_2$ (8.2 mg, 0.03 mmol), IPr^{Me}·HCl (27.2 mg, 0.06 mmol), NaO-*t*-Bu (72.0 mg, 0.75 mmol), 4-(4'-((*tert*-butyldimethylsilyl)oxy)-2-methoxy-[1,1'-biphenyl]-4-yl)morpholine (43.3 mg, 0.108 mmol) and octylamine (73 μL, 0.45 mmol) at 130 °C for 16 h gave a crude residue which was purified by flash chromatography (hexanes: ethyl acetate = 90:10) to afford the desired product (24.5 mg, 0.062 mmol, 57% yield).

^{1}H-NMR (500 MHz, $CDCl_3$): δ 7.34 (d, *J* = 8.0 Hz, 1H), 7.21 (d, *J* = 8.0 Hz, 1H), 6.63 (d, *J* = 8.0 Hz, 1H), 6.55 (m, 2H), 3.89 (t, *J* = 4.5 Hz, 4H), 3.80 (s, 3H), 3.65 (b, 1H), 3.20 (t, *J* = 4.5 Hz, 4H), 3.13 (t, *J* = 7.5 Hz, 2H), 1.63 (p, *J* = 7.0 Hz, 2H), 1.40 (m, 2H), 1.31 (m, 8H), 0.90 (t, *J* = 7.5 Hz, 3H).
^{13}C-NMR (125 MHz, $CDCl_3$): δ 157.2, 151.2, 147.2, 130.7, 130.1, 127.0, 123.2, 112.3, 107.9, 100.0, 66.9, 55.5, 49.6, 44.0, 33.8, 29.6, 29.4, 29.3, 27.2, 22.6, 14.1.
IR (film, cm^{-1}): 2924, 2853, 1610, 1501, 1447.
HRMS (ESI+) *m/z*: $[M+H]^+$ predicted for $C_{25}H_{36}N_2O_2$, 397.2850; found, 397.2847.

4-(2-methoxy-4'-(triethylsilyl)-[1,1'-biphenyl]-4-yl)morpholine.

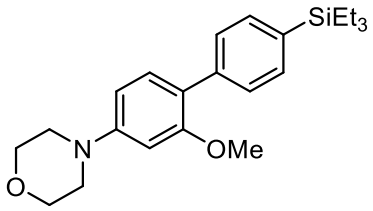

Scheme 4-21, 4-55: Following a modified general procedure C, $Ni(COD)_2$ (10.3 mg, 0.0375 mmol), IPr*OMe (35.4 mg, 0.0375 mmol), NaO-*t*-Bu (36.0 mmol, 0.375 mmol), 4-(4'-((*tert*-butyldimethylsilyl)oxy)-2-methoxy-[1,1'-biphenyl]-4-yl)morpholine (60.4 mg, 0.151 mmol) and triethylsilane (144 μL, 0.90 mmol) at 120 °C for 16 h gave a crude residue which was purified by flash chromatography (hexanes: ethyl acetate = 90:10) to afford the desired product (18.9 mg, 0.05 mmol, 64% yield).

^{1}H-NMR (500 MHz, $CDCl_3$): δ 7.51 (s, 4H), 7.26 (m, 1H), 6.57 (dd, *J* = 8.0 Hz, 2.0 Hz, 1H), 6.54 (d, *J* = 2.0 Hz, 1H), 3.89 (t, *J* = 5.0 Hz, 4H), 3.82 (s, 3H), 3.23 (t, *J* = 5.0 Hz, 4H), 1.00 (t, *J* = 7.5 Hz, 9H), 0.81 (q, *J* = 8.0 Hz, 6H).
^{13}C-NMR (125 MHz, $CDCl_3$): δ 157.3, 152.0, 138.7, 135.0, 133.9, 131.3, 128.5, 122.6, 107.8, 99.5, 66.9, 55.5, 49.4, 7.5, 3.5.
IR (film, cm^{-1}): 2955, 2874, 1608, 1567, 1518, 1447.
HRMS (ESI+) *m/z*: $[M+H]^+$ predicted for $C_{23}H_{33}NO_2Si$, 384.2353; found, 384.2349.

4-(4'-(triethylsilyl)-2-((trimethylsilyl)methyl)-[1,1'-biphenyl]-4-yl)morpholine.

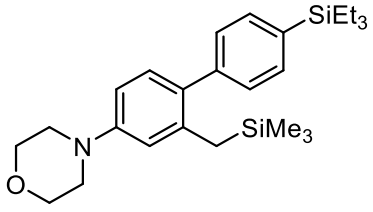

Scheme 4-21, 4-56: Following a modified previously published procedure,[95] $Ni(COD)_2$ (1.1 mg, 0.004 mmol), 4-(2-methoxy-4'-(triethylsilyl)-[1,1'-biphenyl]-4-yl)morpholine (15.0 mg, 0.039 mmol) and (trimethylsilyl)methyllithium (51 μL, 0.051 mmol) at 100 °C for 2 h gave a crude residue which was purified by flash chromatography (hexanes: ethyl acetate = 95:5) to afford the desired product as a clear oil (10.1 mg, 0.023 mmol, 59% yield).

^{1}H-NMR (500 MHz, $CDCl_3$): δ 7.48 (d, *J* = 8.0 Hz, 2H), 7.27 (d, *J* = 8.0 Hz, 2H), 7.11 (d, *J* = 8.5 Hz, 1H), 6.72 (dd, *J* = 8.0, 2.5 Hz, 1H), 6.63 (d, *J* = 2.5 Hz, 1H), 3.88 (t, *J* = 5.0 Hz, 4H), 3.18 (t, *J* = 5.0 Hz, 4H), 2.22 (s, 2H), 0.99 (t, *J* = 7.5 Hz, 9H), 0.82 (q, *J* = 8.0 Hz, 6H), -0.20 (s, 9H).
^{13}C-NMR (125 MHz, $CDCl_3$): δ 150.1, 142.5, 139.1, 134.7, 133.8, 132.9, 131.0, 129.1, 116.2, 111.9, 67.0, 49.4, 24.0, 7.4, 3.4, -1.2.
IR (film, cm^{-1}): 2954, 2821**,** 1608, 1500, 1448, 1236.
HRMS (ESI+) *m/z*: $[M+H]^+$ predicted for $C_{26}H_{41}NOSi_2$, 440.2799; found, 440.2806.

6.4.6 Scheme 4-23 Substrates

2-bromo-6-methoxynaphthalene.

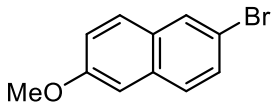

Scheme 4-23, 4-58: Following a previously reported procedure,[179] 6-bromonaphthalen-2-ol (2.2 g, 9.86 mmol), K_2CO_3 (2.76 g, 10 mmol), methyl iodide (1.25 mL, 20 mmol), and DMF (10 mL) gave a crude residue which was purified by flash chromatography (hexanes) to afford the desired product as a white solid (2.065 g, 8.71 mmol, 88% yield).

^{1}H-NMR (700 MHz, $CDCl_3$): δ 7.92 (s, 1H), 7.65 (d, *J* = 9.0 Hz, 1H), 7.61 (d, *J* = 8.6 Hz, 1H), 7.50 (d, *J* = 8.8 Hz, 1H), 7.17 (d, *J* = 9.0 Hz, 1H), 7.10 (s, 1H), 3.92 (s, 3H).

^{13}C-NMR (175 MHz, $CDCl_3$): δ 157.9, 133.0, 130.0, 129.64, 129.60, 128.5, 128.4, 119.8, 117.0, 105.7, 55.3.

IR (film, cm^{-1}): 3061, 2966, 2840, 1625, 1584, 1498.

HRMS (EI) *m/z*: $[M]^+$ predicted for $C_{11}H_9BrO$, 235.9837; found, 235.9836.

***tert*-butyl(3-chloro-4-(6-methoxynaphthalen-2-yl)phenoxy)dimethylsilane.**

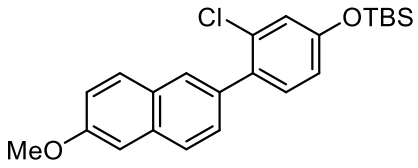

Scheme 4-23, 4-60: Following a previously reported procedure,[179] 2-bromo-6-methoxynaphthalene (36.2 mg, 0.153 mmol), (4-((*tert*-butyldimethylsilyl)oxy)-2-chlorophenyl)boronic acid (64.5 mg, 0.225 mmol), K_3PO_4 (191 mg, 0.9 mmol), $PdCl_2(PPh_3)_2$ (5.3 mg, 0.0075 mmol), toluene (0.45 mL), and degassed H_2O (0.45 mL) at 90 ^oC for 16 hours gave a crude residue which was purified by flash chromatography (hexanes: ethyl acetate = 98:2) to afford the desired product (49.7 mg, 0.125 mmol, 82% yield).

^{1}H-NMR (700 MHz, $CDCl_3$): δ 7.79 (s, 1H), 7.77 (m, 2H), 7.54 (d, *J* = 8.2 Hz, 1H), 7.29 (d, *J* = 8.7 Hz, 1H), 7.18 (s, 2H), 7.00 (s, 1H), 6.83 (s, *J* = 8.3 Hz, 1H), 3.95 (s, 3H), 1.02 (s, 9H), 0.26 (s, 6H).

^{13}C-NMR (175 MHz, $CDCl_3$): δ 157.8, 155.4, 134.6, 133.64, 133.60, 132.8, 132.0, 129.6, 128.4, 128.1, 126.2, 121.4, 119.0, 118.8, 105.6, 55.3, 25.6, 18.2, -4.4.

IR (film, cm^{-1}): 2951, 2929, 2856, 1603, 1496, 1471.

HRMS (ESI+) *m/z*: $[M+H]^+$ predicted for $C_{23}H_{27}ClO_2Si$, 399.1542; found, 399.1540.

6.4.7 Scheme 4-24 Substrates

4-(5-((tert-butyldimethylsilyl)oxy)-2-(6-methoxynaphthalen-2-yl)phenyl)morpholine.

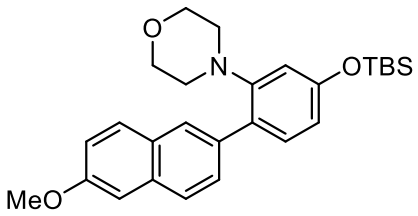

Scheme 4-24, 4-61: Following a previously reported procedure,[238] *tert*-butyl(3-chloro-4-(6-methoxynaphthalen-2-yl)phenoxy)dimethylsilane (61.0 g, 0.153 mmol), NaO-*t*-Bu (21.6 mg, 0.225 mmol), $Pd(OAc)_2$ (3.4 mg, 0.015 mmol), P(*t*-Bu)$_3$ (6.1 mg, 0.03 mmol), morpholine (16 µL, 0.18 mmol), and toluene (0.2 M) at 120 ºC for 16 hours gave a crude residue which was purified by flash chromatography (hexanes: ethyl acetate 90:10) to afford the desired product (44.8 mg, 0.100 mmol, 65% yield).

^{1}H-NMR (500 MHz, $CDCl_3$): δ 7.90 (s, 1H), 7.84 (d, *J* = 8.5 Hz, 1H), 7.73 (t, *J* = 9.0 Hz, 2H), 7.20 (d, *J* = 8.0 Hz, 1H), 7.15 (m, 2H), 6.60 (dd, *J* = 8.5, 2.5 Hz, 1H), 6.54 (d, *J* = 2.0 hz, 1H), 3.94 (s, 3H), 3.58 (t, *J* = 4.5 Hz, 4H), 2.82 (t, *J* = 4.5 Hz, 4H), 1.02 (s, 9H), 0.26 (s, 6H).

4-(5-((*tert*-butyldimethylsilyl)oxy)-2-(6-methylnaphthalen-2-yl)phenyl)morpholine.

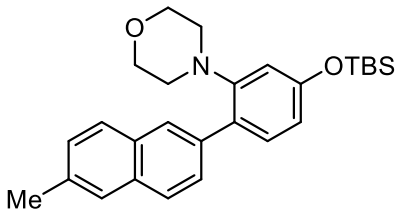

Scheme 4-24, 4-62: Following a previously reported procedure,[96] 4-(5-((*tert*-butyldimethylsilyl)oxy)-2-(6-methoxynaphthalen-2-yl)phenyl)morpholine (18.0 mg, 0.040 mmol), NaO-*t*-Bu (7.7 mg, 0.080 mmol), $Ni(COD)_2$ (2.2 mg, 0.008 mmol), ICy·HBF_4 (3.6 mg, 0.011 mmol), trimethylaluminum (2 M in hexanes, 24 µL), and toluene (0.5 M) at 120 ºC for 16

hours gave a crude residue which was purified by flash chromatography (hexanes: ethyl acetate 90:10) to afford the desired product (7.3 mg, 0.017 mmol, 42% yield).

^{1}H-NMR (500 MHz, $CDCl_3$): δ 7.92 (s, 1H), 7.84 (d, *J* = 8.5 Hz, 1H), 7.74 (dd, *J* = 7.5, 2.0 Hz, 2H), 7.62 (s, 1H), 7.32 (d, *J* = 8.0 Hz, 1H), 7.21 (d, *J* = 8.5 Hz, 1H), 6.60 (dd, *J* = 8.0, 2.0 Hz, 1H), 6.54 (d, *J* = 2.0 Hz, 1H), 3.57 (t, *J* = 4.0 Hz, 4H), 2.81 (t, *J* = 4.5 Hz, 4H), 2.53 (s, 3H), 1.02 (s, 9H), 0.28 (s, 6H).

5-((*tert*-butyldimethylsilyl)oxy)-2-(6-methoxynaphthalen-2-yl)-*N*-phenylanilinedimethylsilane.

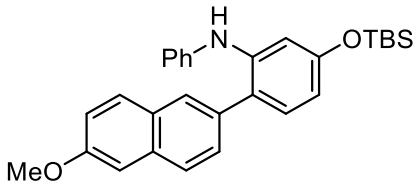

Scheme 4-24, 4-63: Following a previously reported procedure,[238] *tert*-butyl(3-chloro-4-(6-methoxynaphthalen-2-yl)phenoxy)dimethylsilane (392.4 mg, 0.983 mmol), NaO-*t*-Bu (144.2 mg, 1.50 mmol), $Pd(OAc)_2$ (11.2 mg, 0.05 mmol), P(*t*-Bu)$_3$ (20.2 mg, 0.10 mmol), aniline (109 µL, 1.20 mmol) at 120 ^oC for 16 hours gave a crude residue which was purified by flash chromatography (hexanes: ethyl acetate 90:10) to afford the desired product (419.1 mg, 0.920 mmol, 94% yield).

^{1}H-NMR (500 MHz, $CDCl_3$): δ 7.81 (s, 1H), 7.45 (m, 2H), 7.50 (dd, *J* = 8.5, 3.0 Hz, 1H), 7.27 (m, 2H), 7.19 (m, 3H), 7.06 (d, *J* = 7.5 Hz, 2H), 6.94 (m, 2H), 6.53 (dd, *J* = 8.0, 2.5 Hz, 1H), 3.95 (s, 3H), 1.01 (s, 9H), 0.24 (s, 6H).
^{13}C-NMR (125 MHz, $CDCl_3$): δ 157.8, 155.8, 143.2, 141.2, 134.1, 133.5, 131.7, 129.5, 129.3, 129.2, 128.3, 128.0, 127.1, 124.7, 121.1, 119.1, 118.3, 113.0, 108.7, 105.6, 55.4, 25.7, 18.2, -4.3.
IR (film, cm^{-1}): 3348, 2956, 2928, 2855, 1630, 1488.
HRMS (ESI+) *m/z*: $[M+H]^+$ predicted for $C_{29}H_{33}NO_2Si$, 456.2353; found, 456.2358.

5-((*tert*-butyldimethylsilyl)oxy)-2-(6-ethylnaphthalen-2-yl)-*N*-phenylaniline.

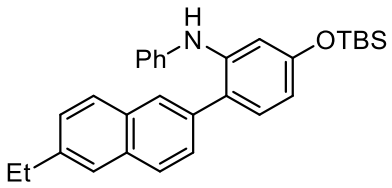

Scheme 4-24, 4-64: Following a previously reported procedure,[97] 5-((*tert*-butyldimethylsilyl)oxy)-2-(6-methoxynaphthalen-2-yl)-*N*-phenylanilinedimethylsilane (66.0 mg, 0.145 mmol), $Ni(COD)_2$ (4.0 mg, 0.0145 mmol), 1,2-bis(dicylohexylphosphino)ethane (dcype) (6.1 mg, 0.0144 mmol), triethylaluminum (25 wt% in toluene, 156 µL), toluene (0.29 mL), and diisopropylether (0.29 mL) at 120 °C for 16 h gave a crude residue which was purified by flash chromatography (hexanes: ethyl acetate 90:10) to afford the desired product (55.6 mg, 0.123 mmol, 85% yield).

^{1}H-NMR (500 MHz, $CDCl_3$): δ 7.80 (m, 3H), 7.65 (s, 1H), 7.51 (d, *J* = 8.5 Hz, 1H), 7.37 (d, *J* = 8.5 Hz, 1H), 7.26 (m, 2H), 7.19 (d, *J* = 8.0 Hz, 1H), 7.04 (d, *J* = 8.0 Hz, 2H), 6.96 (t, *J* = 7.5 Hz, 1H), 6.90 (d, *J* = 2.5 Hz, 1H), 6.53 (dd, *J* = 8.0, 2.5 Hz, 1H), 5.64 (br, 1H), 2.83 (quartet, *J* = 7.5 Hz, 2H), 1.34 (t, *J* = 7.5 Hz, 3H), 1.00 (s, 9H), 0.234 (s, 6H).
^{13}C-NMR (125 MHz, $CDCl_3$): δ 155.9, 143.1, 142.1, 141.2, 135.6, 132.7, 132.2, 131.7, 129.3, 127.90, 127.89, 127.86, 127.64, 127.5, 1125.3, 124.7, 121.1, 118.3, 113.0, 108.6, 29.1, 25.7, 18.2, 15.6, -4.3.

4-(5-((*tert*-butyldimethylsilyl)oxy)-2-(6-methoxynaphthalen-2-yl)phenyl)-1-propyl-1H-pyrazole.

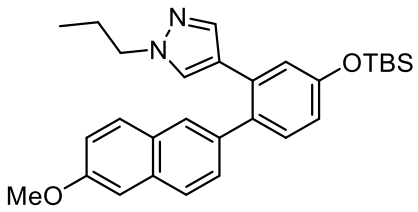

Scheme 4-24, 4-67: Following a modified previously reported procedure,[239] *tert*-butyl(3-chloro-4-(6-methoxynaphthalen-2-yl)phenoxy)dimethylsilane (52.3 mg, 0.131 mmol), (1-propyl-1*H*-pyrazol-4-yl)boronic acid (23.1 mg, 0.15 mmol), K_3PO_4 (45.1 mg, 0.213 mmol), Pd_2dba_3 (11.4 mg, 0.0125 mmol), PCy_3 (3.5 mg, 0.0125 mmol), and dioxane (0.25 mL) at 80 °C for 16 hours gave a crude residue which was purified by flash chromatography (hexanes: ethyl acetate 90:10) to afford the desired product (48.4 mg, 0.102 mmol, 78% yield).

^{1}H-NMR (700 MHz, $CDCl_3$): δ 7.69 (m, 2H), 7.61 (d, *J* = 8.4 Hz, 1H), 7.38 (s, 1H), 7.25 (m, 2H), 7.13 (m, 2H), 6.90 (s, 1H), 6.81 (d, *J* = 8.3 Hz, 1H), 6.74 (s, 1H), 3.93 (s, 3H), 3.84 (t, *J* = 6.9 Hz, 2H), 1.67 (m, 2H), 1.04 (s, 9H), 0.72 (t, *J* = 7.4 Hz, 3H), 0.28 (s, 6H).
^{13}C-NMR (175 MHz, $CDCl_3$): δ 157.6, 155.1, 138.5, 133.30, 133.28, 132.5, 131.9, 129.4, 128.9, 128.5, 127.9, 126.1, 121.4, 120.3, 118.7, 118.1, 105.6, 55.3, 53.6, 25.7, 23.6, 18.2, 10.9, -4.3.
IR (film, cm^{-1}): 2956, 2929, 2857, 1605, 1496.
HRMS (ESI+) *m/z*: $[M+H]^+$ predicted for $C_{29}H_{36}N_2O_2Si$, 473.2619; found, 473.2619.

4-(5-((*tert*-butyldimethylsilyl)oxy)-2-(6-ethylnaphthalen-2-yl)phenyl)-1-propyl-1*H*-pyrazole.

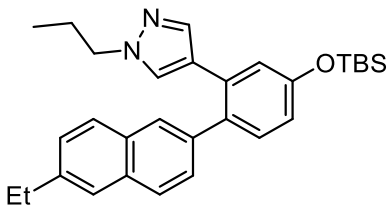

Scheme 4-24, 4-68: Following a previously reported procedure,[97] 4-(5-((*tert*-butyldimethylsilyl)oxy)-2-(6-methoxynaphthalen-2-yl)phenyl)-1-propyl-1*H*-pyrazole (33.0 mg, 0.070 mmol), $Ni(COD)_2$ (1.9 mg, 0.007 mmol), 1,2-bis(dicylohexylphosphino)ethane (dcype) (3.0 mg, 0.007 mmol), triethylaluminum (25 wt% in toluene, 75 µL), toluene (0.14 mL), and diisopropylether (0.14 mL) at 120 °C for 16 h gave a crude residue which was purified by flash chromatography (hexanes: ethyl acetate 90:10) to afford the desired product (31.0 mg, 0.066 mmol, 94% yield).

^{1}H-NMR (700 MHz, $CDCl_3$): δ 7.72 (t, *J* = 4.0 Hz, 2H), 7.64 (d, *J* = 8.4 Hz, 1H), 7.60 (s, 1H), 7.38 (s, 1H), 7.35 (d, *J* = 8.3 Hz, 1H), 7.25 (m, 2H), 6.99 (s, 1H), 6.81 (d, *J* = 8.3 Hz, 1H), 6.74 (s, 1H), 3.84 (t, *J* = 7.0 Hz, 2H), 2.82 (q, *J* = 7.6 Hz, 2H), 1.66 (sextet, *J* = 7.2 Hz, 2H), 1.34 (t, *J* = 7.6 Hz, 3H), 1.04 (s, 9H), 0.72 (t, *J* = 7.7 Hz), 3H), 0.28 (s, 6H).

^{13}C-NMR (175 MHz, $CDCl_3$): δ 155.1, 141.7, 138.8, 138.5, 133.3, 132.5, 132.4, 132.0, 131.9, 128.5, 127.83, 127.77, 127.2, 126.7, 125.3, 121.4, 120.3, 118.1, 53.6, 29.0, 25.7, 23.6, 18.2, 15.5, 10.9, -4.3.

IR (film, cm^{-1}): 2959, 2929, 2857, 1602, 1495, 1472.

HRMS (ESI+) *m/z*: $[M+H]^+$ predicted for $C_{30}H_{38}N_2OSi$, 471.2826; found, 471.2833.

***N*-butyl-4-(6-ethylnaphthalen-2-yl)-*N*-methyl-3-(1-propyl-1*H*-pyrazol-4-yl)aniline.**

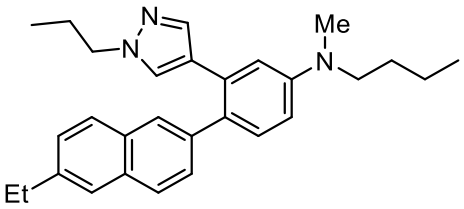

Scheme 4-24, 4-69: Following a modified general procedure D, 4-(5-((*tert*-butyldimethylsilyl)oxy)-2-(6-ethylnaphthalen-2-yl)phenyl)-1-propyl-1*H*-pyrazole (42.8 mg, 0.091 mmol), $Ni(COD)_2$ (2.5 mg, 0.0091 mmol), IPr^{Me}·HCl (8.2 mg, 0.0182 mmol), NaO-*t*-Bu (21.9 mg, 0.228 mmol), and *N*-methylbutylamine (16.2 µL, 0.136 mmol) at 120 °C for 16 h gave a crude residue which was purified by flash chromatography (hexanes: ethyl acetate 90:10) to afford the desired product (29.0 mg, 0.068 mmol, 75% yield).

^{1}H-NMR (700 MHz, $CDCl_3$): δ 7.72 (m, 2H), 7.60 (m, 2H), 7.47 (s, 1H), 7.33 (d, *J* = 8.4 Hz, 1H), 7.30 (d, *J* = 8.4 Hz, 1H), 7.25 (m, 1H), 6.80 (s, 1H), 6.78 (s, 1H), 6.72 (d, *J* = 8.4 Hz, 1H), 3.85 (t, *J* = 7.0 Hz, 2H), 3.39 (t, *J* = 7.7 Hz, 2H), 3.02 (s, 3H), 2.82 (q, *J* = 7.0 Hz, 2H), 1.66 (m, 4H), 1.41 (sextet, *J* = 7.0 Hz, 2H), 1.34 (t, *J* = 7.7 Hz, 3H), 0.99 (t, *J* = 7.0 Hz, 3H), 0.73 (t, *J* = 7.0 Hz, 3H).

^{13}C-NMR (175 MHz, $CDCl_3$): δ 148.8, 141.3, 139.2, 138.5, 132.2, 132.03, 131.97, 128.9, 128.7, 128.0, 127.7, 127.6, 127.0, 126.5, 125.2, 122.3, 115.5, 110.7, 55.6, 52.5, 38.4, 29.02, 29.01, 23.6, 20.4, 15.6, 14.0, 10.9.

IR (film, cm^{-1}): 2961, 2930, 2871, 1604, 1514, 1455.

HRMS (ESI+) *m/z*: $[M+H]^+$ predicted for $C_{29}H_{35}N_3$, 426.2904; found, 426.2912.

6.5 General Experimental Details for Chapter 5

6.5.1 General Procedures for Chapter 5

General Procedure for the Ni(acac)$_2$/IPr^{Me}·HCl promoted reductive deoxygenation of silyloxyarenes using titanium(IV) isopropoxide (B):

A reaction tube containing a stir bar was charged with aryl silyl ether (1 equiv), NaO-*t*-Bu (2.5 equiv), Ni(acac)$_2$ (5 mol%) and IPr^{Me}·HCl (10 mol%). The reaction tube was sealed and pump/purged with nitrogen three times. Toluene (0.5 M) and titanium (IV) isopropoxide (1.1 equiv) were sequentially added via syringe, and the reaction tube was then placed in a heated block set to 120 °C and stirred for 6 h. The mixture was allowed to reach rt, internal standard was added (tridecane, 40 µL, 0.164 mmol), diluted with EtOAc (5 mL) and 1 M HCl (3 mL), then extracted with EtOAc (3 x 5 mL), dried over $MgSO_4$, filtered, concentrated under reduced pressure and purified by flash column chromatography on silica gel to afford the desired product. Note: slightly higher yields (5-10%) were obtained by utilizing a nitrogen atmosphere glovebox and yields in the text utilized the glovebox procedure.

General Procedure the for Ni(COD)$_2$/IPr*OMe promoted silylation of silyloxyarenes using triethylsilane (C):

A reaction tube containing a stir bar was charged with aryl silyl ether (1 equiv), NaO-*t*-Bu (2.5 equiv), Ni(COD)$_2$ (10 mol%) and IPr*OMe (10 mol%) in a nitrogen atmosphere glovebox. The sealed reaction tube was brought outside the glovebox where toluene (0.5 M) and silane (6 equiv) were sequentially added via syringe. The reaction tube was then placed in a heated block set to 120 °C and stirred for 16 h. The mixture was allowed to reach rt, internal standard was added (tridecane, 40 µL, 0.164 mmol), diluted with EtOAc (5 mL) and deionized water (3 mL), then extracted with EtOAc (3 x 5 mL), dried over $MgSO_4$, filtered, concentrated under reduced pressure and purified by flash column chromatography on silica gel to afford the desired product.

General Procedure for the Ni(COD)$_2$/IPr^{Me}·HCl promoted amination of silyloxyarenes using amines (D):

A reaction tube containing a stir bar was charged with aryl silyl ether (1 equiv.), Ni(COD)$_2$ (5 mol%), IPr^{Me}·HCl (10 mol%), NaO-*t*-Bu (2.5 equiv.), toluene (0.5 M) and amine. The sealed reaction tube was brought outside the glovebox and placed in a heated block set to 120 ^{o}C and

stirred for 16 hours, unless noted otherwise. The mixture was cooled to room temperature, quenched with dichloromethane (1 mL), and diluted with EtOAc (3 mL). The mixture was then run through a silica plug, concentrated under reduced pressure and purified by flash column chromatography on silica gel to afford the desired product.

General Procedure for the $Ni(acac)_2$/IPr^{Me}·HCl and $Cu(OAc)_2$ promoted borylation of silyloxyarenes using bis(pinacolato)diboron (E):

A reaction tube containing a stir bar was charged with aryl silyl ether (1 equiv), NaO-*t*-Bu (2.5 equiv), $Ni(acac)_2$ (10 mol%), IPr^{Me}·HCl (20 mol%), $Cu(OAc)_2$ (20 mol%), and B_2pin_2 (2.5 equiv). Toluene (0.3 M) was then added added, and the reaction tube was then placed in a heated block set to 120 °C and stirred for 16 h. The mixture was allowed to reach rt, taken up in ethyl acetate and filtered through silica (boric acid impregnated silica) plug via a glass fritted filter and concentrated under reduced pressure. The crude material was placed under reduced pressure via high vacuum until purification via column chromatography (boric acid impregnated silica gel) to afford the desired product.

General Procedure for the $Ni(COD)_2$/IPr^{Me}·HCl promoted Suzuki coupling of silyloxyarenes using aryl boronate esters (F):

A reaction tube containing a stir bar was charged with aryl silyl ether (1 equiv.), $Ni(COD)_2$ (10 mol%), IPr^{Me}·HCl (20 mol%), NaO-*t*-Bu (2.5 equiv.), aryl boronate ester (1.5 equiv), and toluene (0.3 M). The sealed reaction tube was brought outside the glovebox and placed in a heated block set to 120 ^{o}C and stirred for 16 hours, unless noted otherwise. The mixture was cooled to room temperature, quenched with dichloromethane (1 mL), and diluted with EtOAc (3 mL). The mixture was then run through a silica plug, concentrated under reduced pressure and purified by flash column chromatography on silica gel to afford the desired product.

General Procedure for the $Ni(COD)_2$/^{Ph}SIPr·HCl promoted reductive coupling of propargyl silanes, aldehydes and triethyl silane (G):

A round bottom flask containing a stir bar was charged with $Ni(COD)_2$ (12 mol%), ^{Ph}SIPr·HCl (10 mol%), KO-*t*-Bu (10 mol%). The flask was sealed, brought out of the glovebox, and THF (0.1 M) was added. The solution was stirred for 10 minutes at rt until the solution turned light yellow

brown. Alkyne (1.2 equiv), aldehyde (1.0 equiv), and silane (2.0 equiv) were combined in 2 mL of THF and added to the flask over 60 minutes using a syringe pump and stirred overnight. The reaction was run through a silica plug, concentrated under reduced pressure and purified by flash column chromatography on silica gel to afford the desired product.

6.5.2 Scheme 5-4 Substrates

(Z)-(2-methylprop-1-ene-1,3-diyl)dibenzene.

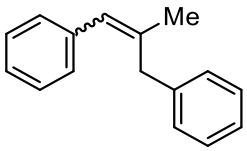

Scheme 5-4, 5-10: Following general procedure F, *tert*-butyldimethyl((2-methyl-1-phenylallyl)oxy)silane (38.5 mg, 0.147 mmol), $Ni(COD)_2$ (4.1 mg, 0.015 mmol), IPr^{Me}·HCl (13.6 mg, 0.030 mmol), NaO-*t*-Bu (36.0 mg, 0.375 mmol), CsF (22.8 mg, 0.15 mmol), phenyl boronic acid (27.4 mg, 0.225 mmol), and toluene (0.3 M) at 120 ^{o}C for 16 hours, gave a crude residue which was purified by flash chromatography (hexanes: ethyl acetate 99:1) to afford the desired product (25.3 mg, 0.121 mmol, 83% yield) as a 2:1 mixture of E:Z isomers. The spectral data matches that previously reported in the literature.

^{1}H-NMR (500 MHz, $CDCl_3$): δ major E isomer: 7.29 (m, 10H), 6.40 (s, 1H), 3.50 (s, 2H), 1.82 (m, 3H). minor E isomer: 2.75 (m, 4.5H), 6.54 (s, 0.45), 3.63 (s, 1H), 1.83 (m, 1.5H).

6.5.3 Scheme 5-5 Substrates

(E)-prop-1-ene-1,3-diyldibenzene.

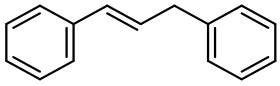

Scheme 5-5, 5-11: Following general procedure F, *tert*-butyl(cinnamyloxy)dimethylsilane (38.0 mg, 0.153 mmol), $Ni(COD)_2$ (4.1 mg, 0.015 mmol), IPr^{Me}·HCl (13.6 mg, 0.030 mmol), NaO-*t*-Bu (36.0 mg, 0.375 mmol), CsF (22.8 mg, 0.15 mmol), phenyl boronic acid pinacol ester (45.9 mg, 0.225 mmol), and toluene (0.3 M) at 40 ^{o}C for 16 hours, gave a crude residue. The 75% yield was determined by ^{1}H-NMR yield with dibromomethane as internal standard (21µL, 0.30 mmol). The spectral data matches that previously reported in the literature.

^{1}H-NMR (500 MHz, $CDCl_3$): δ 7.31 (m, 10H), 6.48 (d, *J* = 15.5 Hz, 1H), 6.39 (m, 1H), 3.58 (d, *J* = 6.5 Hz, 2H).

6.5.4 Scheme 5-6 Substrates

(E)-prop-1-ene-1,3-diyldibenzene.

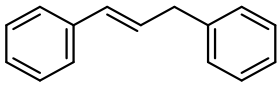

Scheme 5-6, 5-11: Following general procedure B, (E)-*tert*-butyl((1,3-diphenylallyl)oxy)dimethylsilane (48.0 mg, 0.148 mmol), $Ni(acac)_2$ (3.9 mg, 0.015 mmol), IPr^{Me}·HCl (13.6 mg, 0.030 mmol), NaO-*t*-Bu (36.0 mg, 0.375 mmol), titanium(IV) isopropoxide (49 µL, 0.165 mmol), and toluene (0.5 M) at 80 ^{o}C for 16 hours, gave a crude residue which was purified by flash chromatography (hexanes: ethyl acetate 99:1) to afford the desired product (26.1 mg, 0.134 mmol, 91% yield) as a 94:4 ratio of E:Z isomers. The spectral data matches that previously reported in the literature.

^{1}H-NMR (500 MHz, $CDCl_3$): δ 7.31 (m, 10H), 6.48 (d, *J* = 15.5 Hz, 1H), 6.39 (m, 1H), 3.58 (d, *J* = 6.5 Hz, 2H).

6.5.5 Scheme 5-9 Substrates

(E)-1,2-diphenylethene.

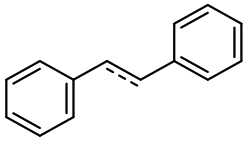

Scheme 5-9, 5-14: Following general procedure B, *tert*-butyl((1,2-diphenylvinyl)oxy)dimethylsilane (47.6 mg, 0.153 mmol), $Ni(acac)_2$ (3.9 mg, 0.015 mmol), IPr^{Me}·HCl (13.6 mg, 0.030 mmol), NaO-*t*-Bu (36.0 mg, 0.375 mmol), titanium(IV) isopropoxide (49 µL, 0.165 mmol), and toluene (0.5 M) at 120 °C for 16 hours, gave a crude residue. The 51% yield for (E)-1,2-diphneylethene and 39% yield for 1,2-diphenylethane was determined by ^{1}H-NMR yield with dibromomethane as internal standard (21µL, 0.30 mmol). The spectral data matches that previously reported in the literature.

6.5.6 Scheme 5-10 Substrates

(Z)-(1-(*p*-tolyl)ethene-1,2-diyl)dibenzene.

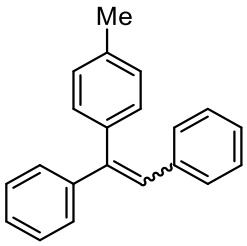

Scheme 5-10, 5-15: Following general procedure F, *tert*-butyl((1,2-diphenylvinyl)oxy)dimethylsilane (47.0 mg, 0.151 mmol), $Ni(COD)_2$ (4.1 mg, 0.015 mmol), IPr^{Me}·HCl (13.6 mg, 0.030 mmol), NaO-*t*-Bu (36.0 mg, 0.375 mmol), CsF (22.8 mg, 0.15 mmol), 4,4,5,5-tetramethyl-2-(p-tolyl)-1,3,2-dioxaborolane (49.2 mg, 0.225 mmol), and toluene (0.3 M) at 120 °C for 16 hours, gave a crude residue which was purified by flash chromatography (hexanes:

ethyl acetate 99:1) to afford the desired product (29.0 mg, 0.107 mmol, 71% yield) as a 9.4:1 mixture of Z:E isomers. The spectral data matches that previously reported in the literature.

6.5.7 Scheme 5-11 Substrates

Cyclohexylbenzene.

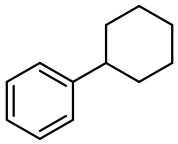

Table 5-11, 5-17: Following general procedure B, *tert*-butyldimethyl((1,2,3,6-tetrahydro-[1,1'-biphenyl]-4-yl)oxy)silane (43.6 mg, 0.151 mmol), $Ni(acac)_2$ (3.9 mg, 0.015 mmol), IPr^{Me}·HCl (13.6 mg, 0.030 mmol), NaO-*t*-Bu (36.0 mg, 0.375 mmol), titanium(IV) isopropoxide (49 µL, 0.165 mmol), and toluene (0.5 M) at 120 °C for 16 hours, gave a crude residue. The yield was determined by GC-FID analysis using tridecane (40 µL, 0.164 mmol) as an internal standard (tridecane integration: 15632686, product integration: 3154344, 0.036 mmol, 24%). The spectral data matches that previously reported in the literature.

^{1}H-NMR (500 MHz, $CDCl_3$): δ 7.30 (m, 2H), 7.19 (m, 3H), 2.50 (m, 1H), 1.90 (m, 4H), 1.76 (m, 1H), 1.30 (m, 5H).

triethyl(1,2,3,6-tetrahydro-[1,1'-biphenyl]-4-yl)silane.

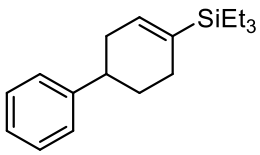

Table 5-11, 5-18: Following general procedure C, *tert*-butyldimethyl((1,2,3,6-tetrahydro-[1,1'-biphenyl]-4-yl)oxy)silane (44.3 mg, 0.154 mmol), $Ni(COD)_2$ (4.1 mg, 0.015 mmol), IPr*OMe (14.2 mg, 0.015 mmol), NaO-*t*-Bu (36.0 mg, 0.375 mmol), triethylsilane (144 µL, 0.90 mmol), and toluene (0.5 M) at 120 ºC for 16 hours, gave a crude residue which was purified by flash chromatography (hexanes: ethyl acetate 99:1) to afford the desired product (7.0 mg, 0.026 mmol, 17% yield). The spectral data matches that previously reported in the literature.

^{1}H-NMR (500 MHz, $CDCl_3$): δ 7.39 (m, 1H), 7.32 (t, *J* = 7.5 Hz, 2H), 7.24 (m, 2H), 6.14 (m, 1H), 2.79 (m, 1H), 2.37 (m, 2H), 2.21 (m, 2H), 1.97 (m, 1H), 1.74 (m, 1H), 0.98 (m, 9H), 0.62 (m, 6H).

4,4,5,5-tetramethyl-2-(1,2,3,6-tetrahydro-[1,1'-biphenyl]-4-yl)-1,3,2-dioxaborolane.

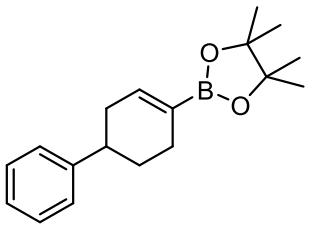

Table 5-11, 3-45: Following a modified general procedure E, $Ni(acac)_2$ (1.9 mg, 0.0075 mmol), IPr^{Me}·HCl (6.8 mg, 0.015 mmol), NaO-*t*-Bu (36.0 mg, 0.750 mmol), $Cu(OAc)_2$ (2.8 mg, 0.150 mmol), *tert*-butyldimethyl((1,2,3,6-tetrahydro-[1,1'-biphenyl]-4-yl)oxy)silane (42.6 mg, 0.148 mmol), B_2pin_2 (95.2 mg, 0.375 mmol), and toluene (0.3 M) at 120 °C for 16 h gave a crude residue. The yield was determined by GC-FID analysis using tridecane (40 µL, 0.164 mmol) as an internal standard (tridecane integration: 427319552, product integration: 82868177, 0.032 mmol, 22%). The spectral data matches that previously reported in the literature.

^{1}H-NMR (500 MHz, $CDCl_3$): δ 7.30 (t, *J* = 7.0 Hz, 2H), 7.21 (m, 3H), 6.66 (dd, *J* = 5.5, 2.5 Hz, 1H), 2.77 (m, 1H), 2.33 (m, 4H), 1.96 (m, 1H), 1.71 (m, 1H), 1.28 (s, 12H).

6.6 Spectra of New Compounds

Table 2-9, *tert*-butyldimethyl(((8R,9S,13S,14S,17S)-13-methyl-7,8,9,11,12,13,14,15,16,17-decahydro-6H-cyclopenta[a]phenanthren-17-yl)oxy)silane (2-35B).

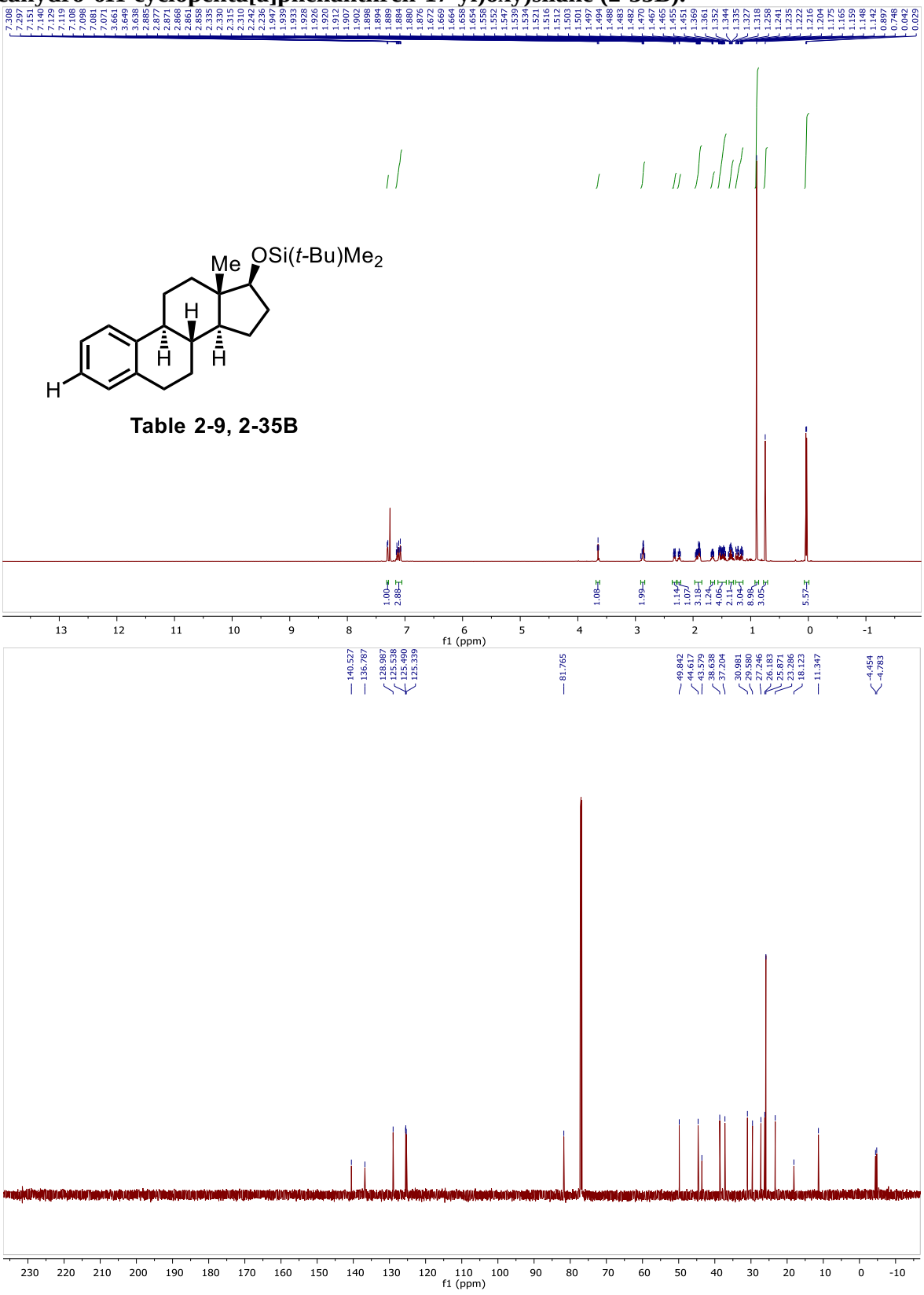

Scheme 2-12, 4-(trifluoromethyl)-1,1'-biphenyl (2-36B).

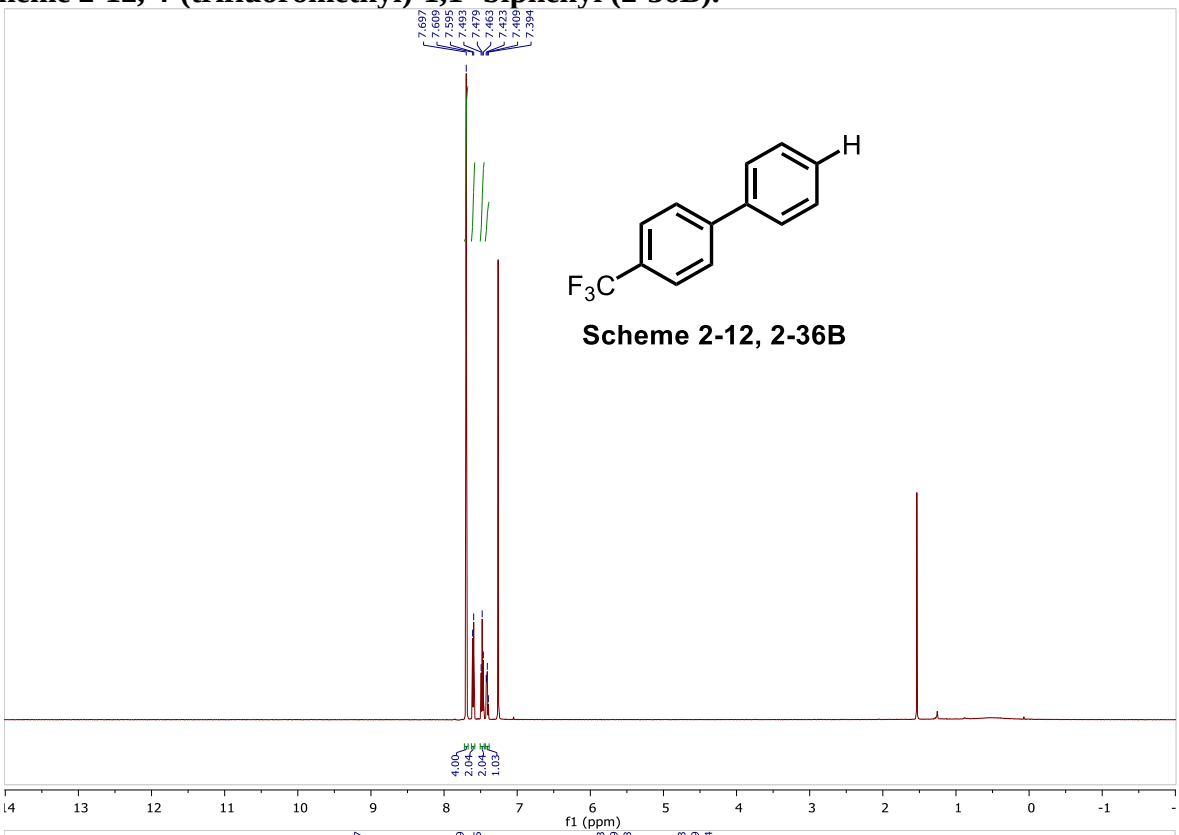

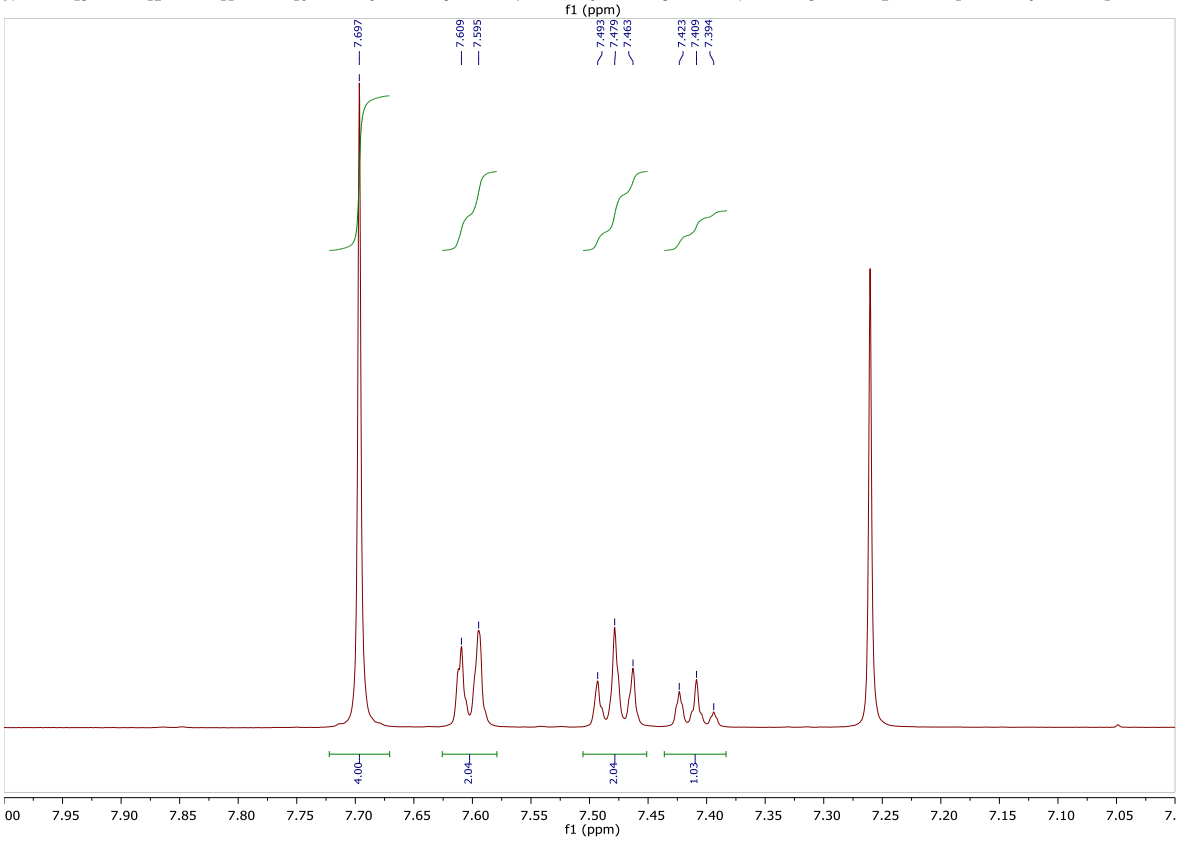

Scheme 2-12, 4-(trifluoromethyl)-1,1'-biphenyl-4'-*d* (2-36D).

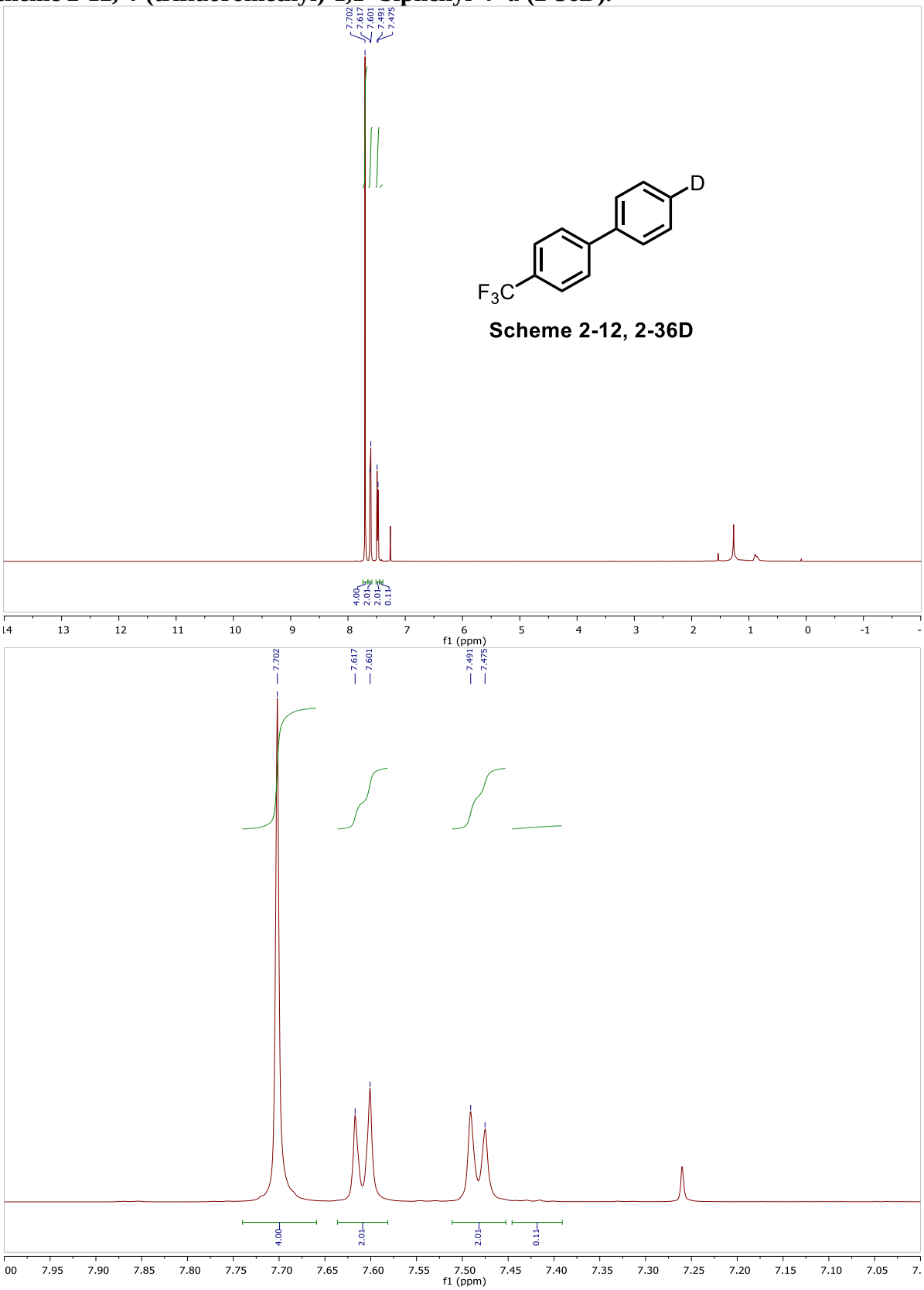

Scheme 2-12, 4-(trifluoromethyl)-1,1'-biphenyl-4'-*d* (2-36D).

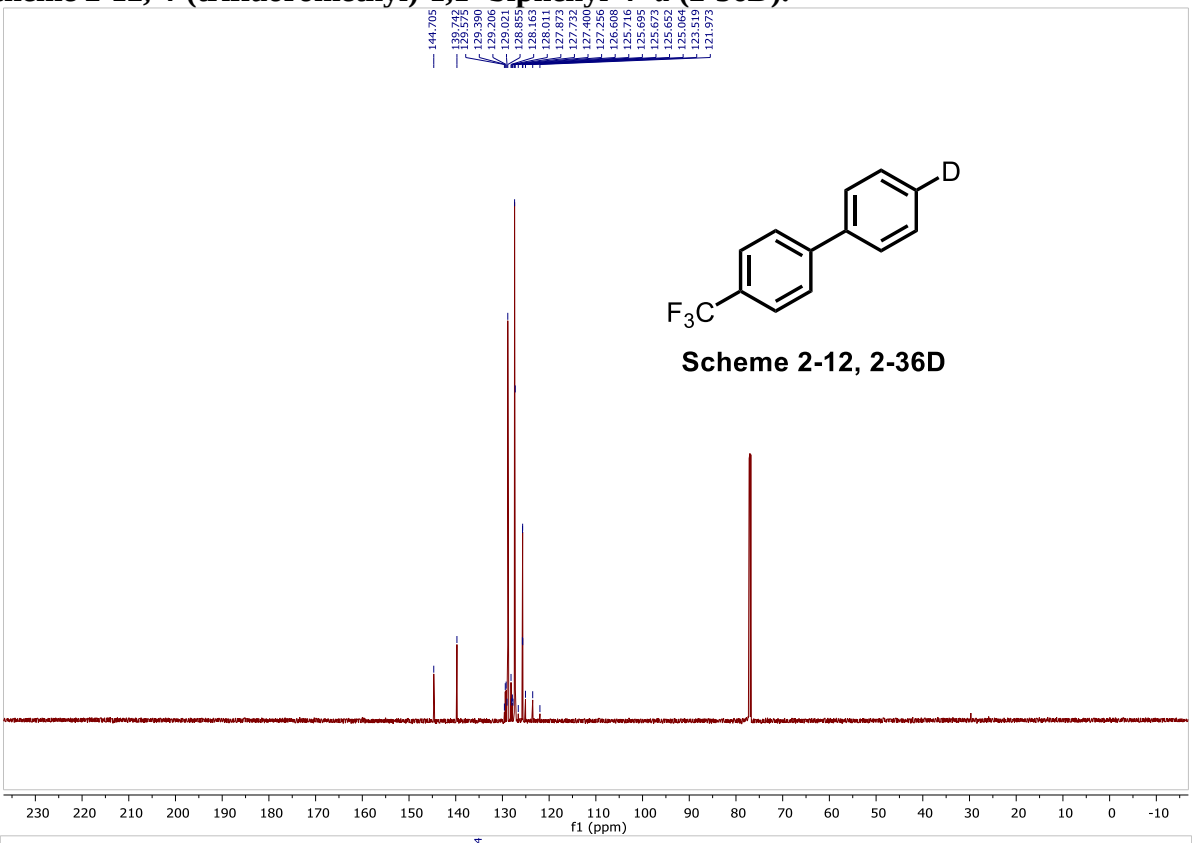

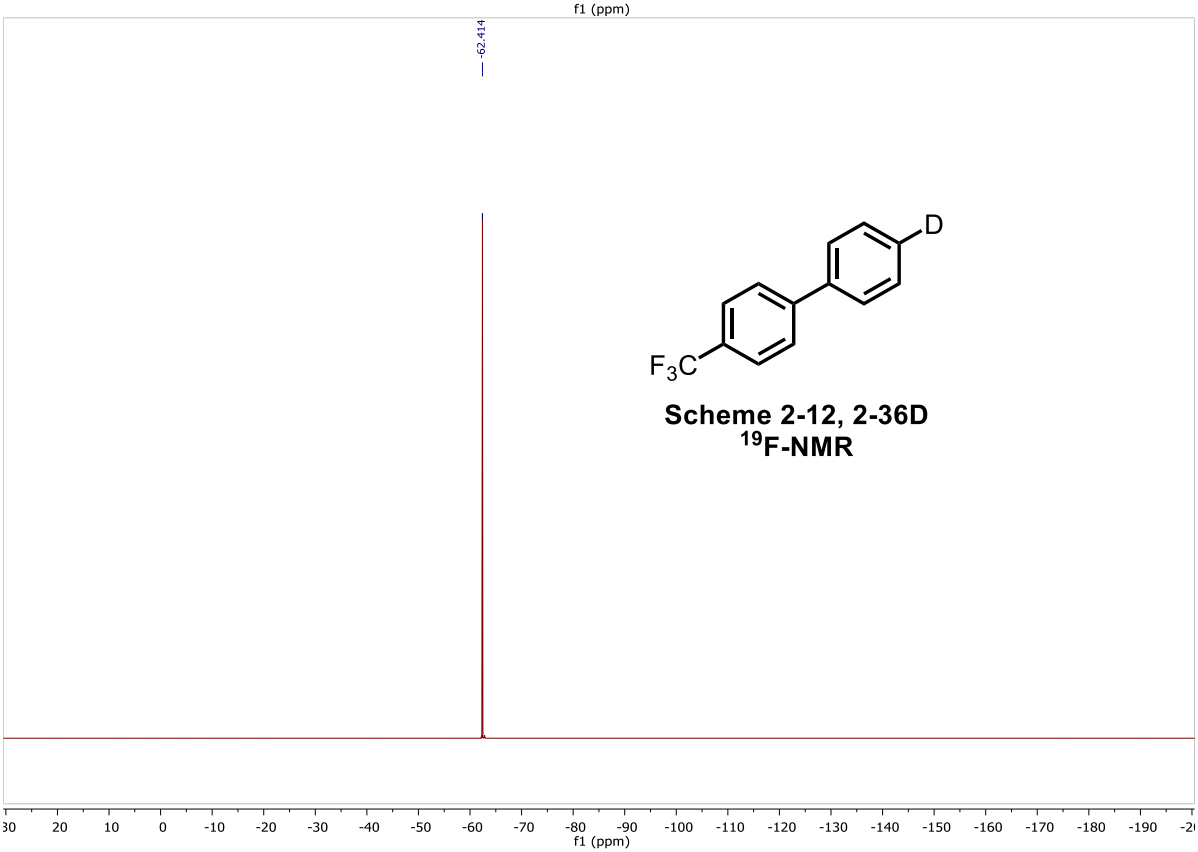

Table 2-14, [1,1'-biphenyl]-4-yl(ethyl)dimethylsilane (entry 1).

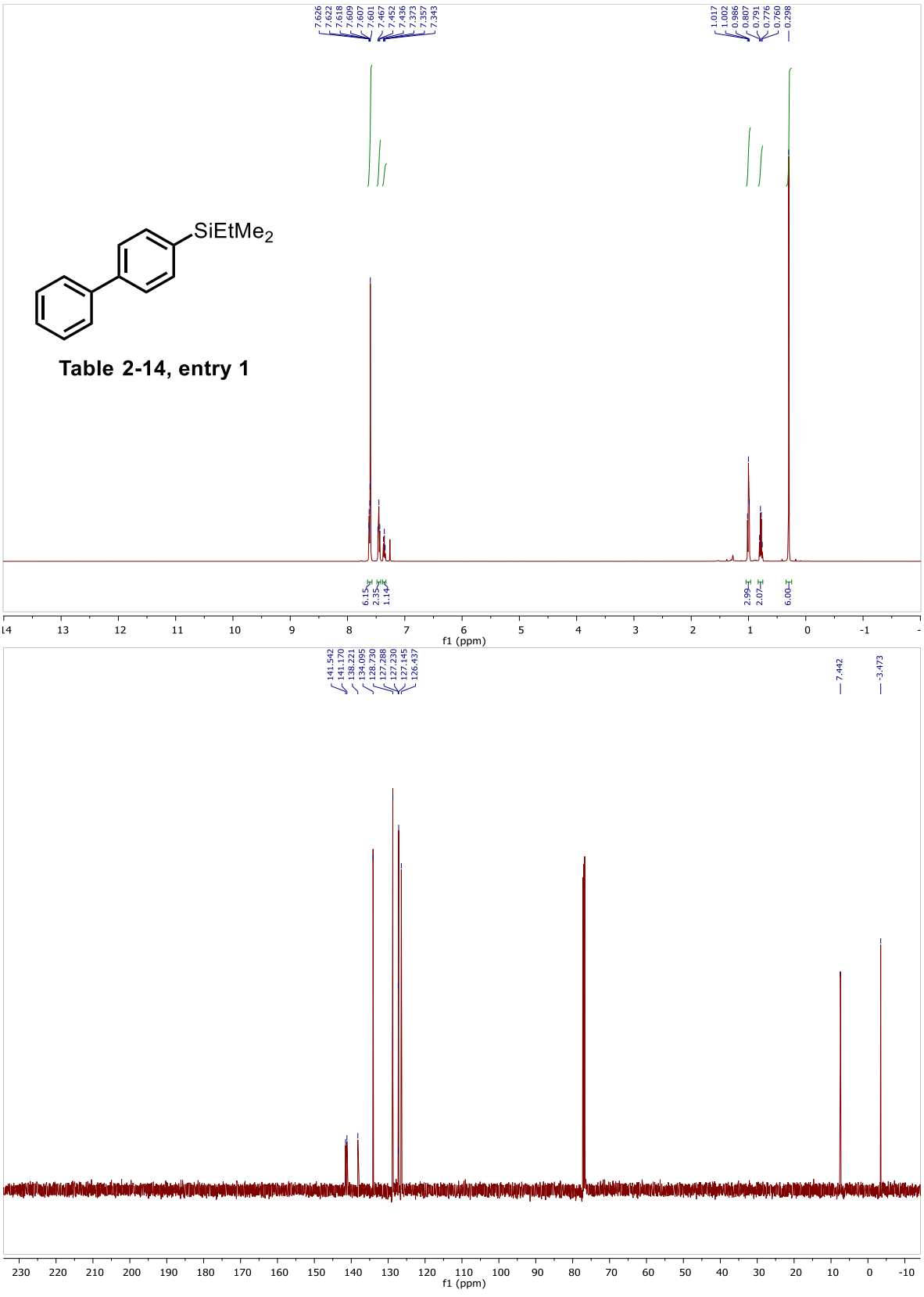

Table 2-14, [1,1'-biphenyl]-4-yldiethyl(methyl)silane (entry 2).

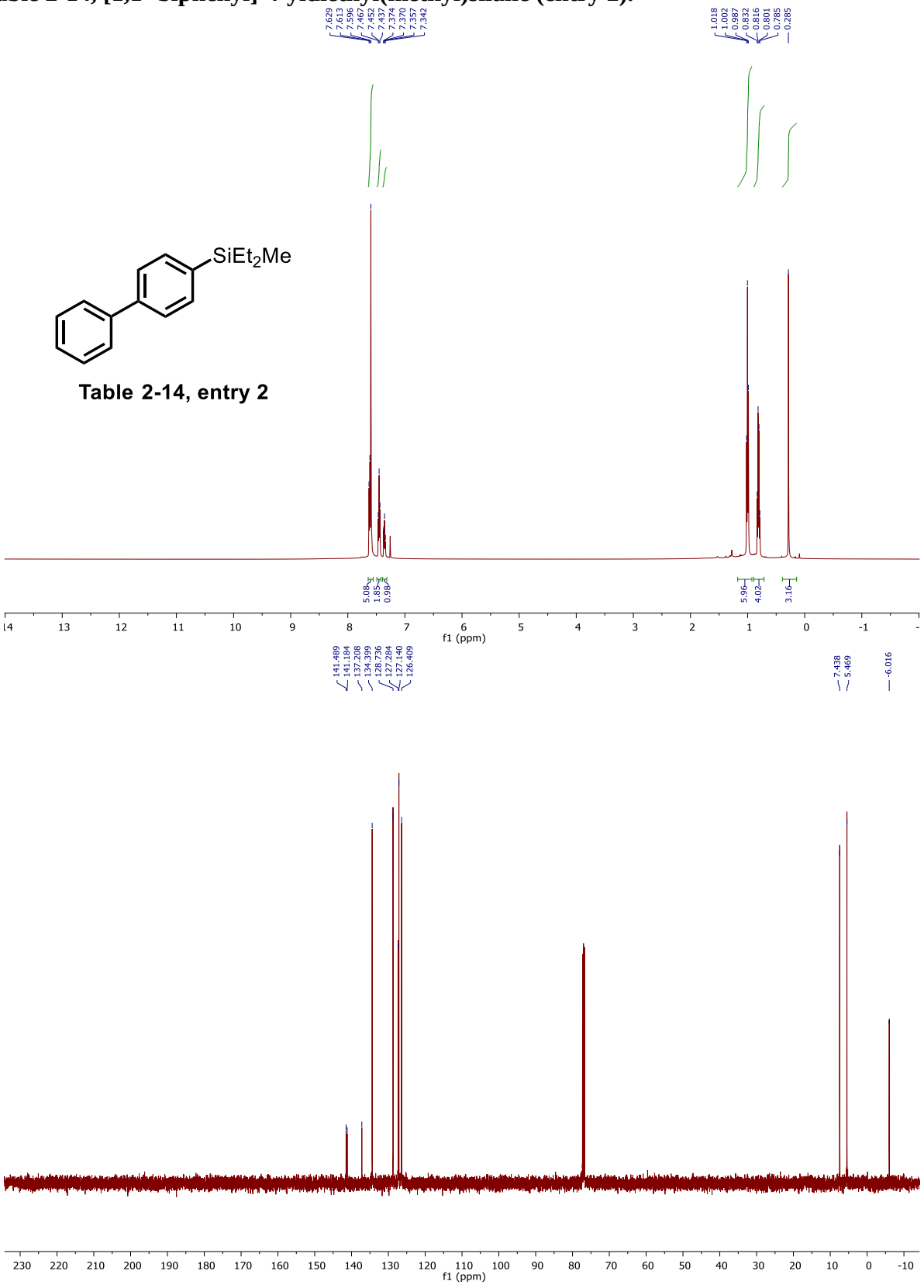

Table, 2-14, [1,1'-biphenyl]-4-yl(isopropyl)dimethylsilane (entry 4).

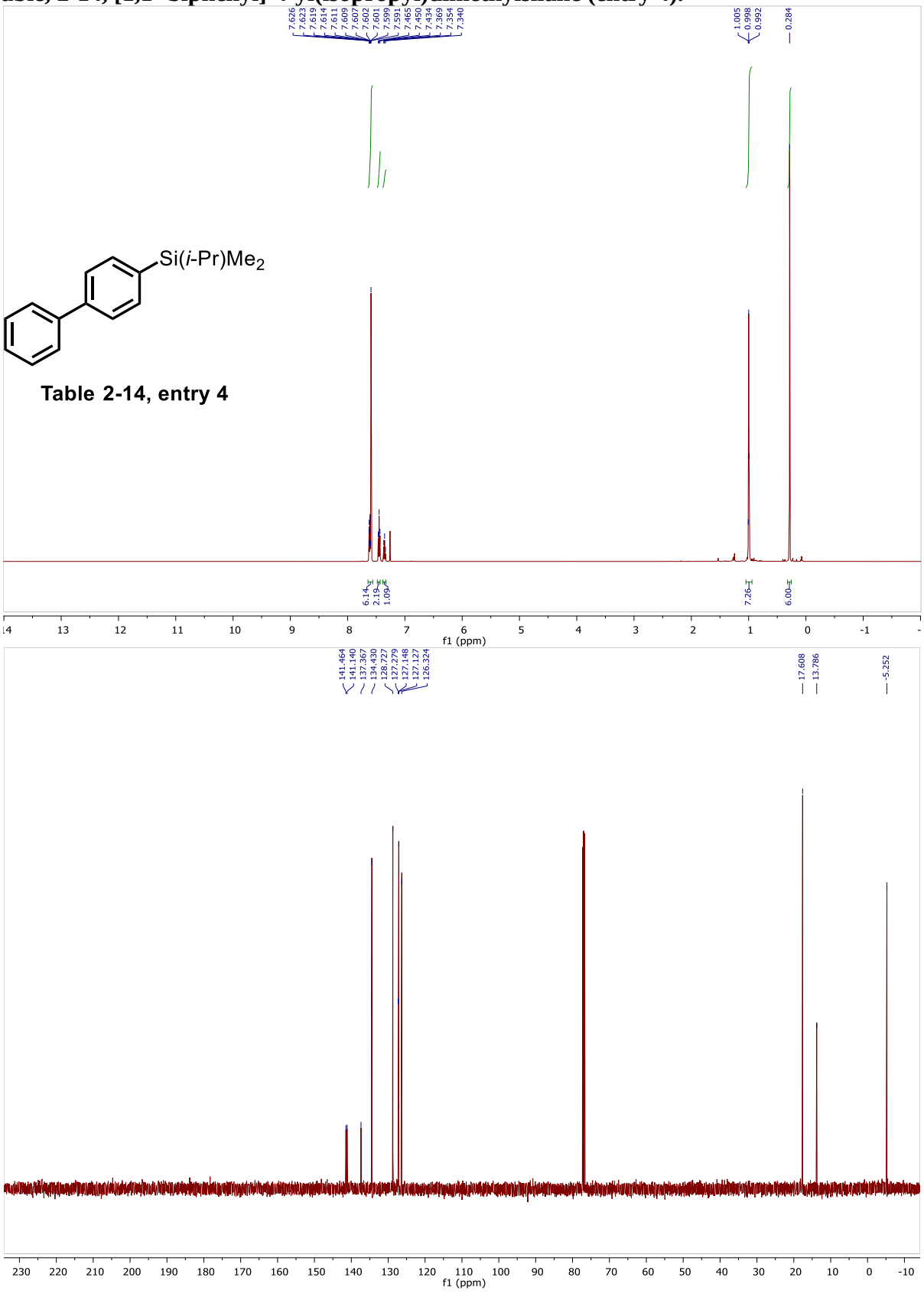

Table 2-14, [1,1'-biphenyl]-4-yltripropylsilane (entry 5).

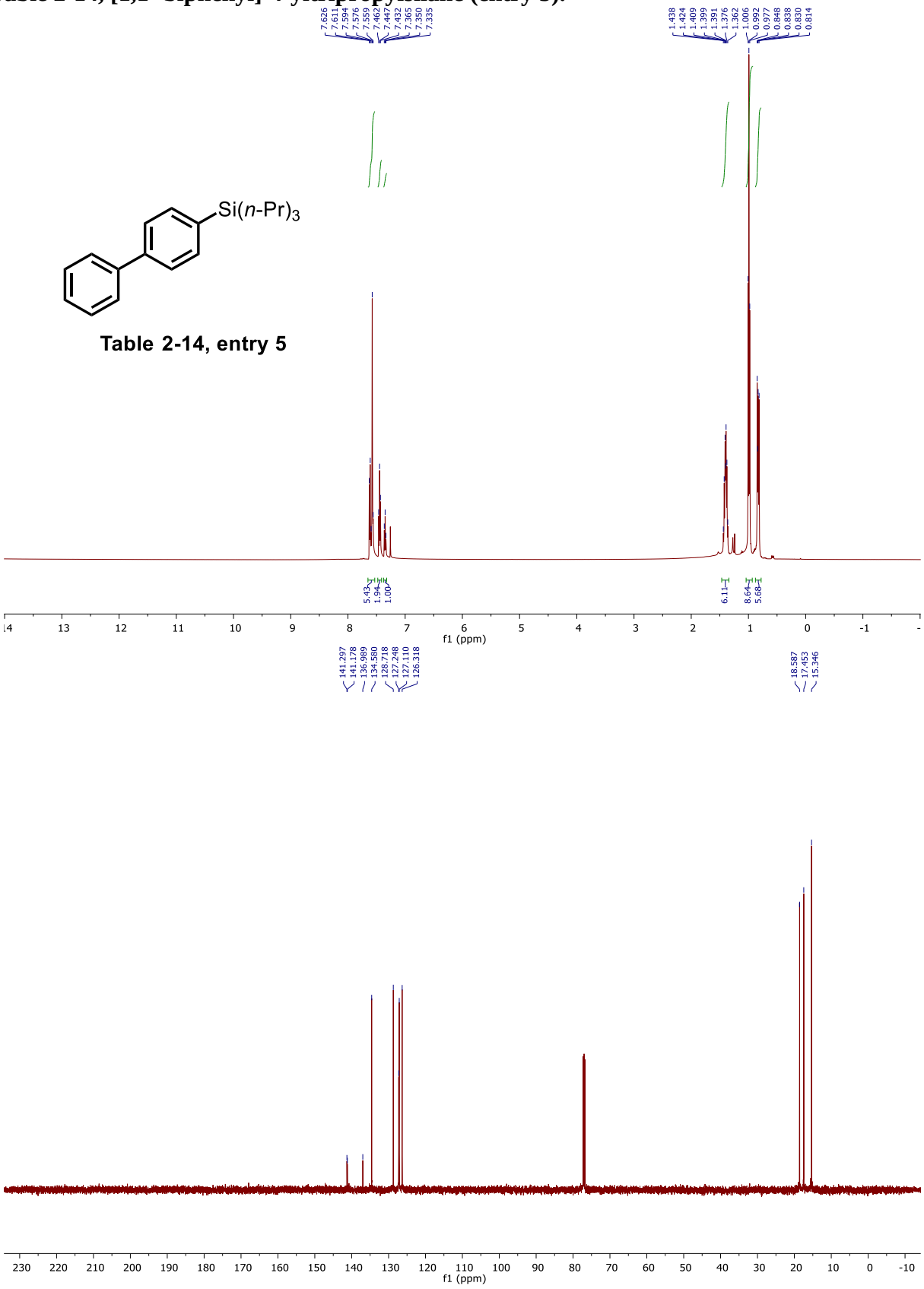

Table 2-14, [1,1'-biphenyl]-4-yl(*tert*-butyl)dimethylsilane (entry 6).

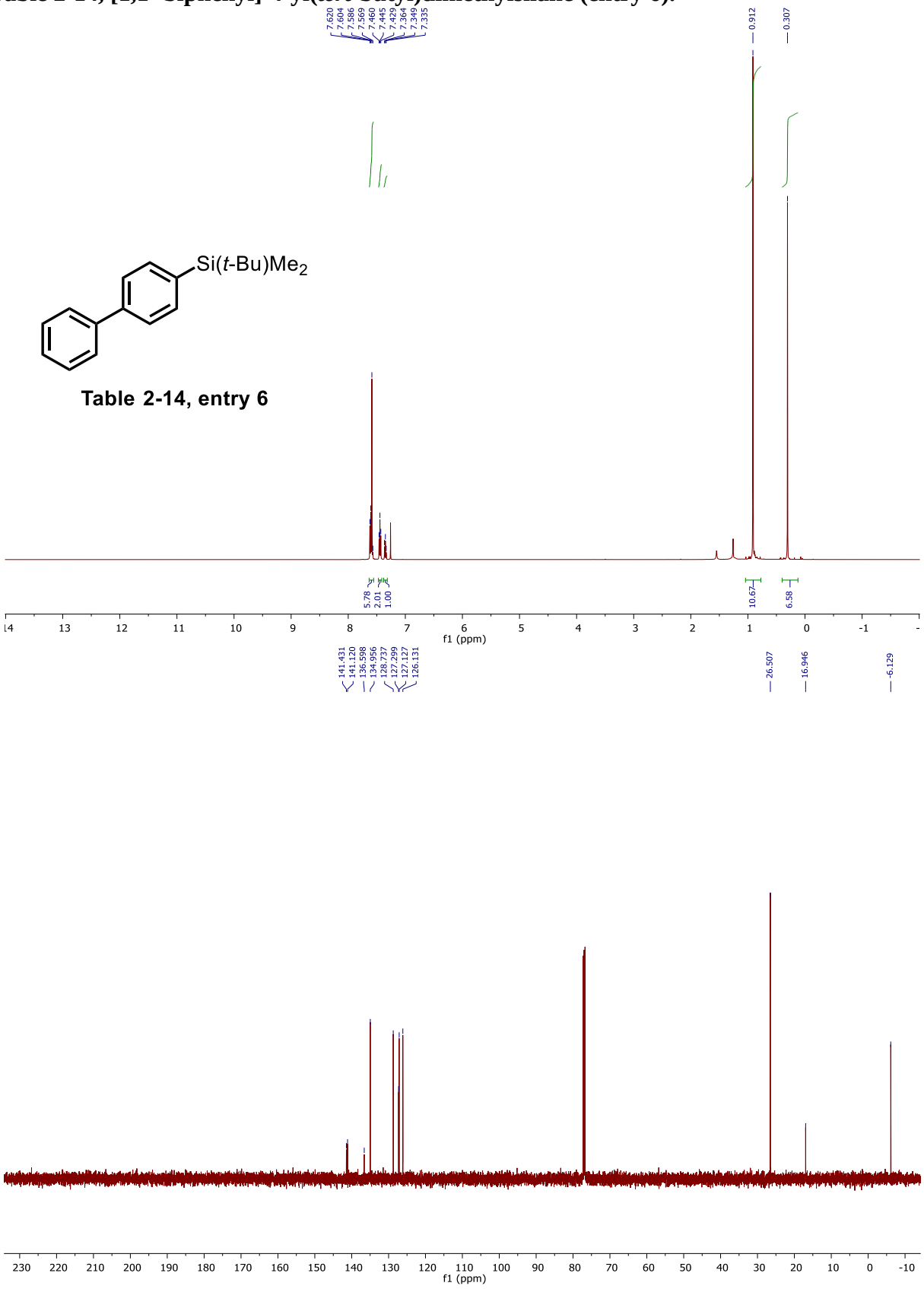

Table 2-14, [1,1'-biphenyl]-4-yl(benzyl)dimethylsilane (entry 8).

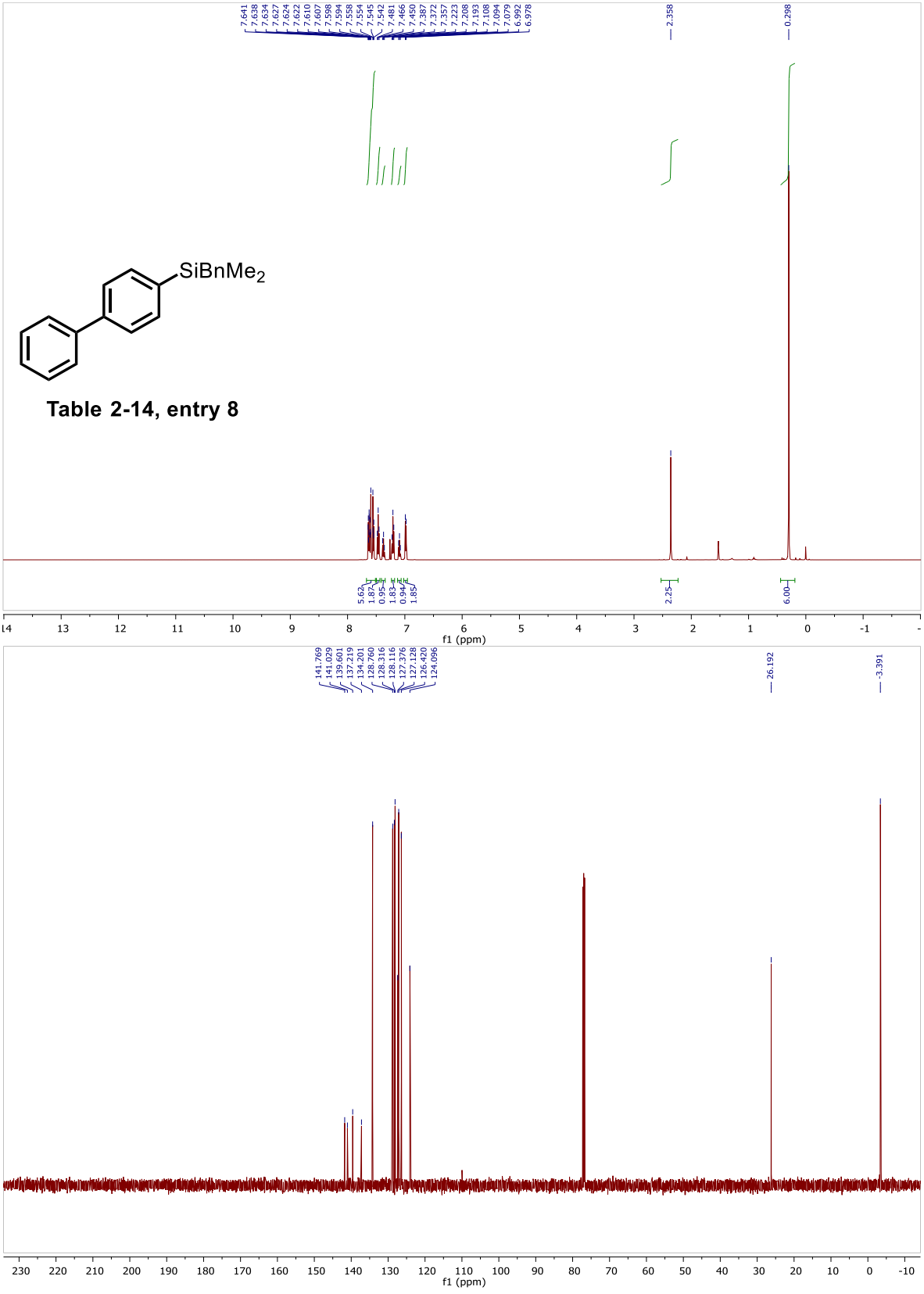

Table 2-15, triethyl(6-(trimethylsilyl)naphthalen-2-yl)silane (2-33A).

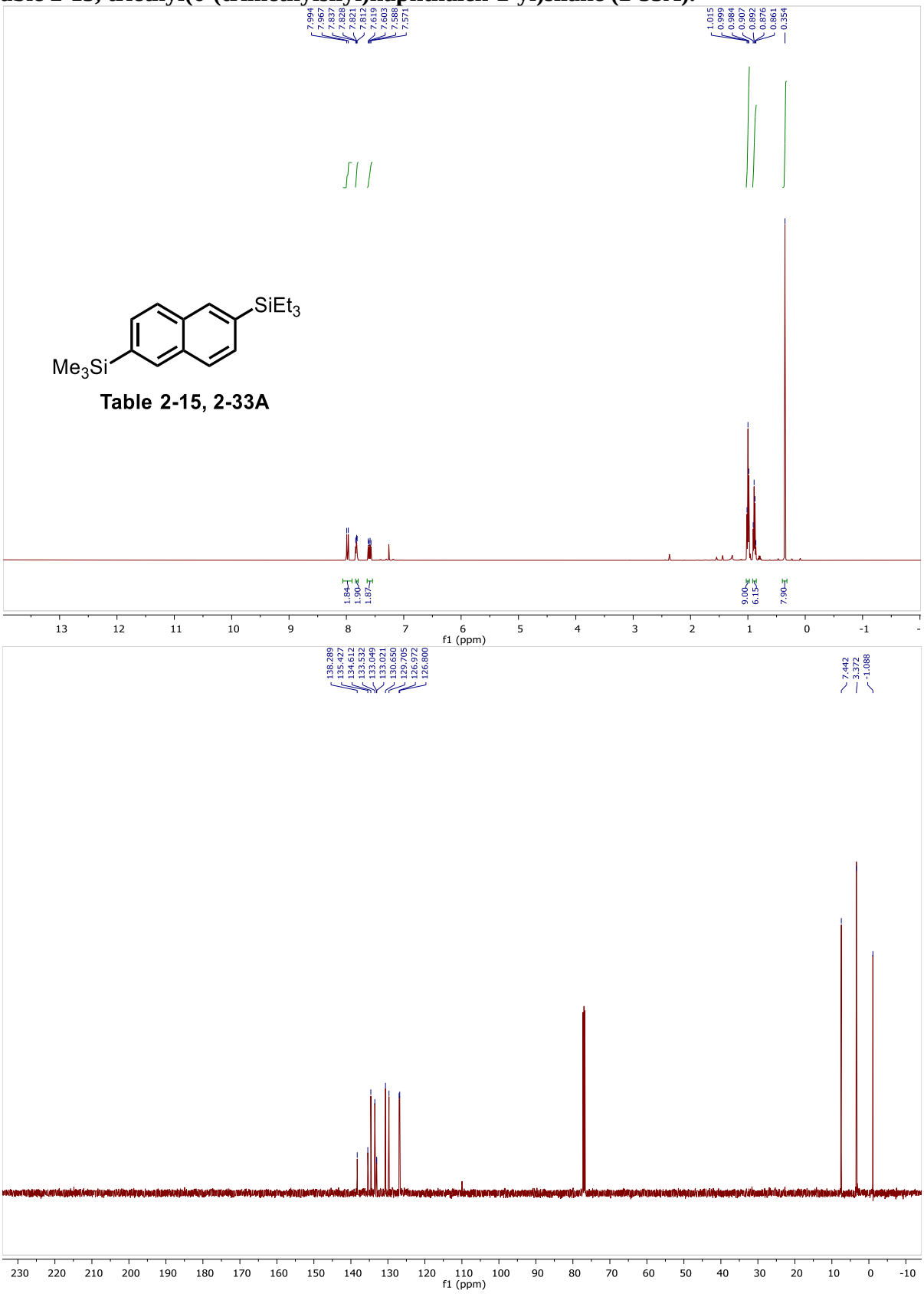

Table 2-15, 4'-(triethylsilyl)-[1,1'-biphenyl]-4-ol (2-25A).

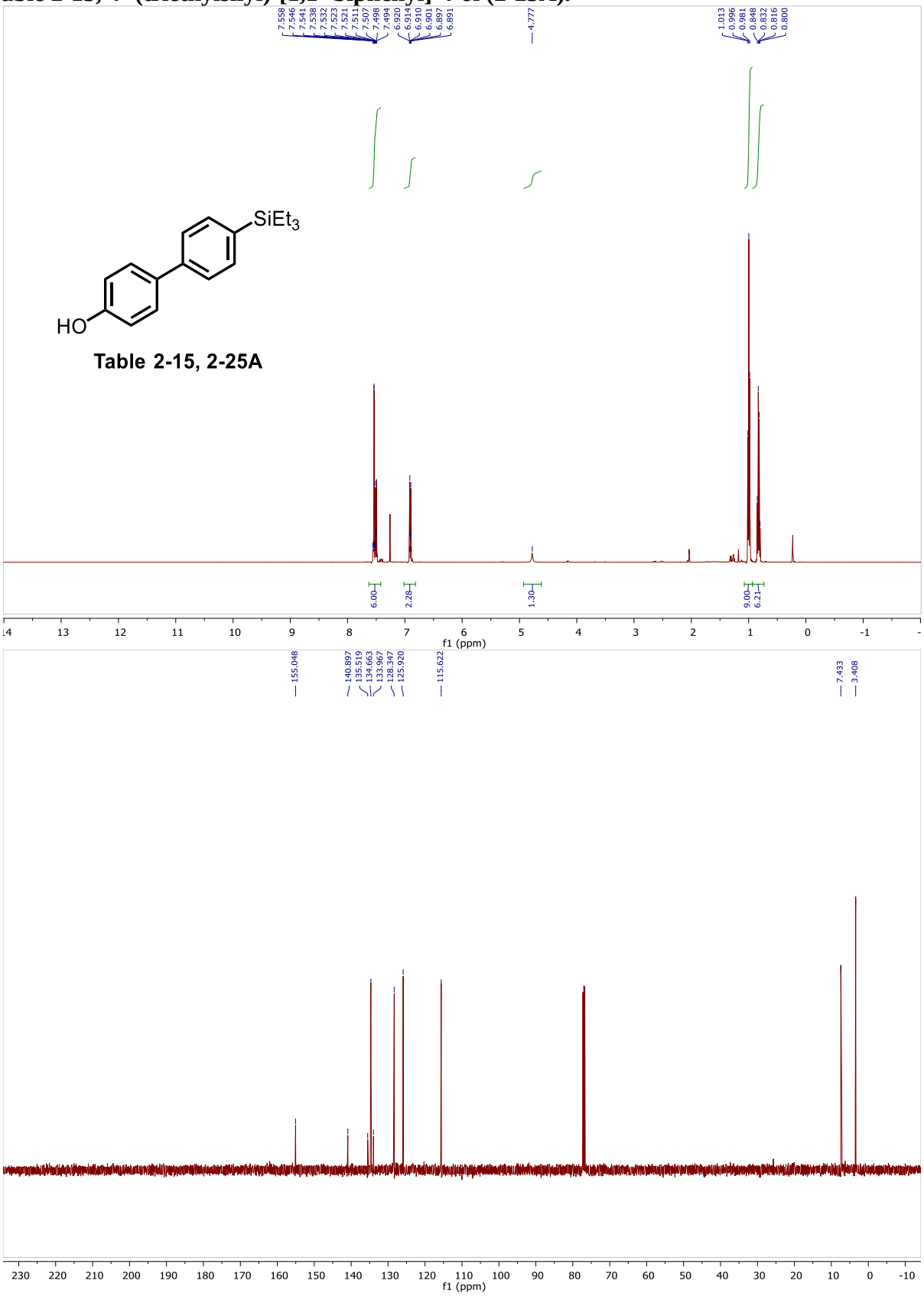

Table 2-15, *tert*-butyldimethyl((4'-(triethylsilyl)-[1,1'-biphenyl]-4-yl)methoxy)silane (2-26A).

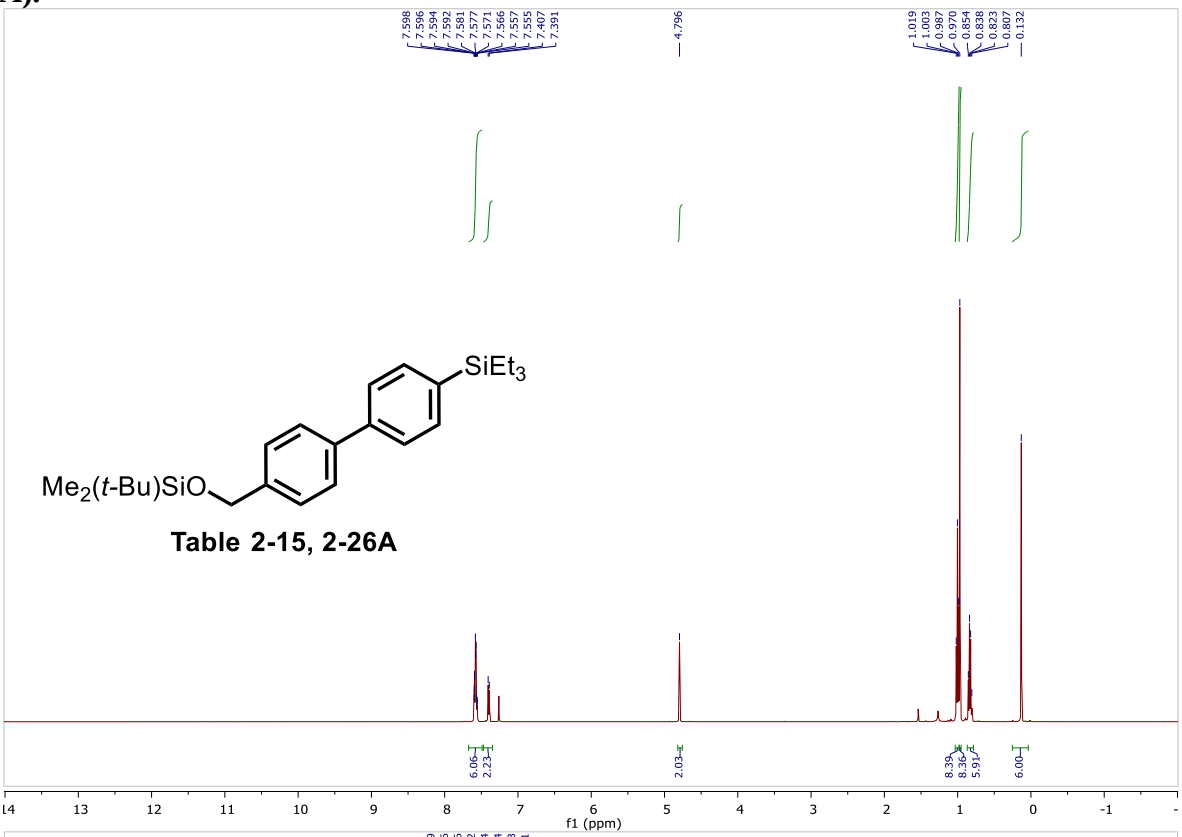

Table 2-15, 2-26A

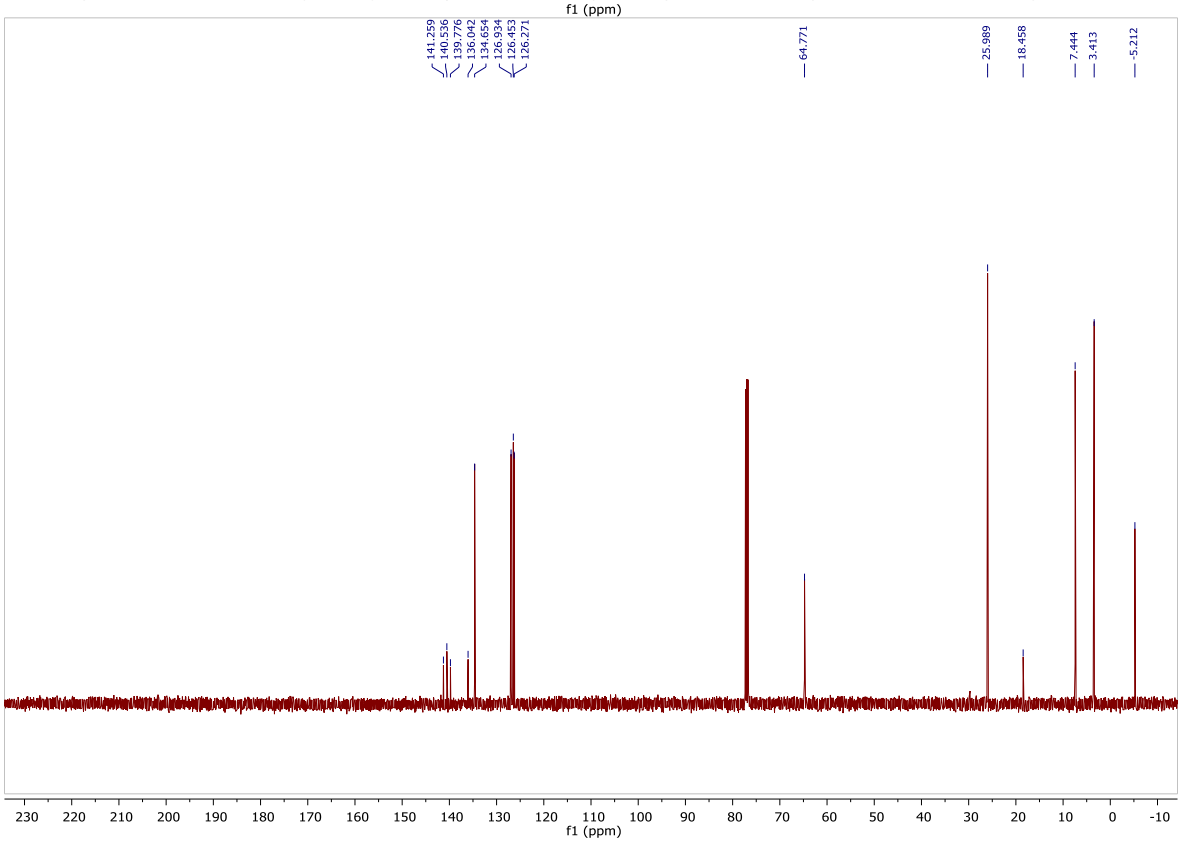

Table 2-15, triethyl(4'-methoxy-[1,1'-biphenyl]-4-yl)silane (2-27A).

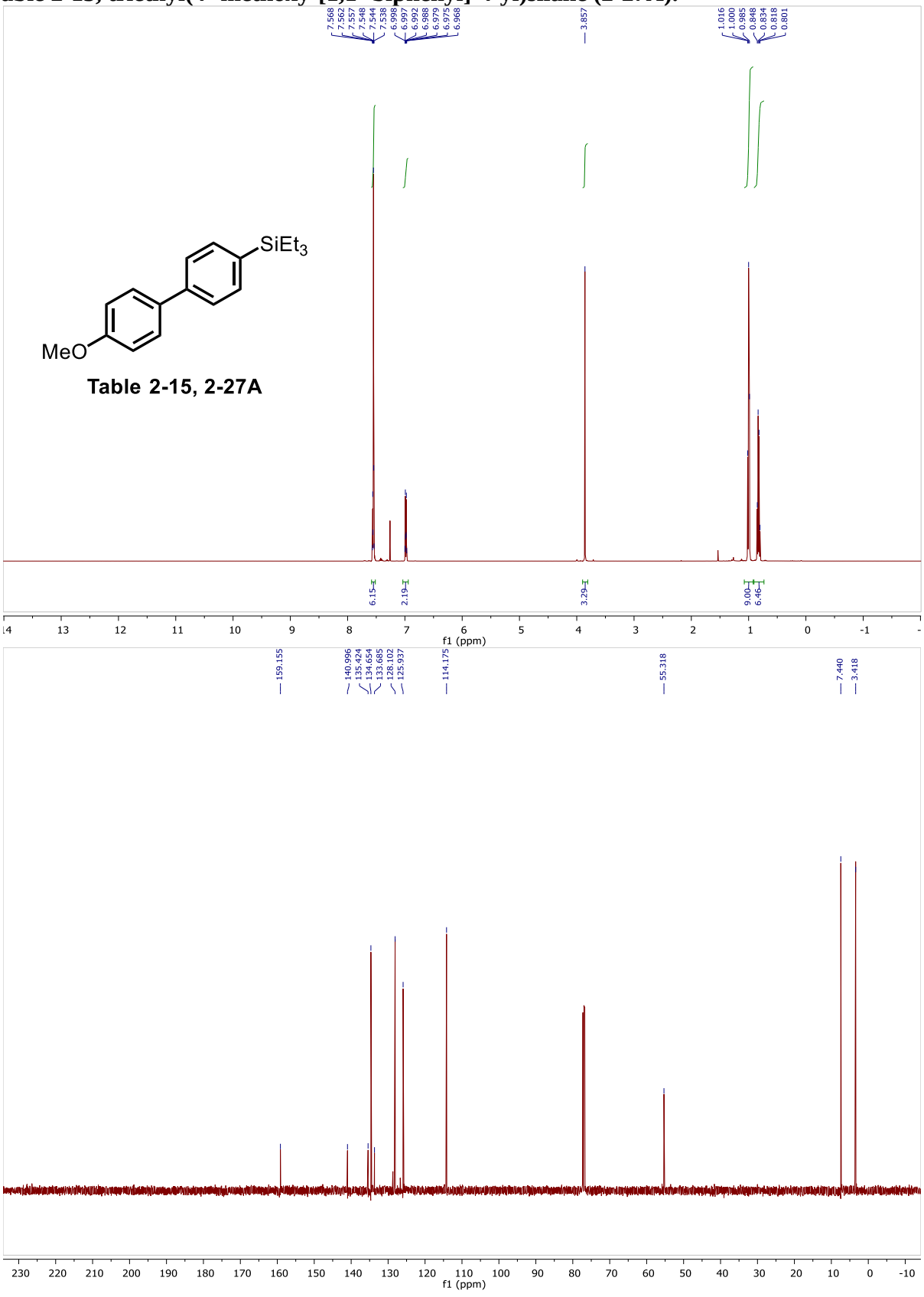

Table 2-15, 4,4'-bis(triethylsilyl)-1,1'-biphenyl (2-38A).

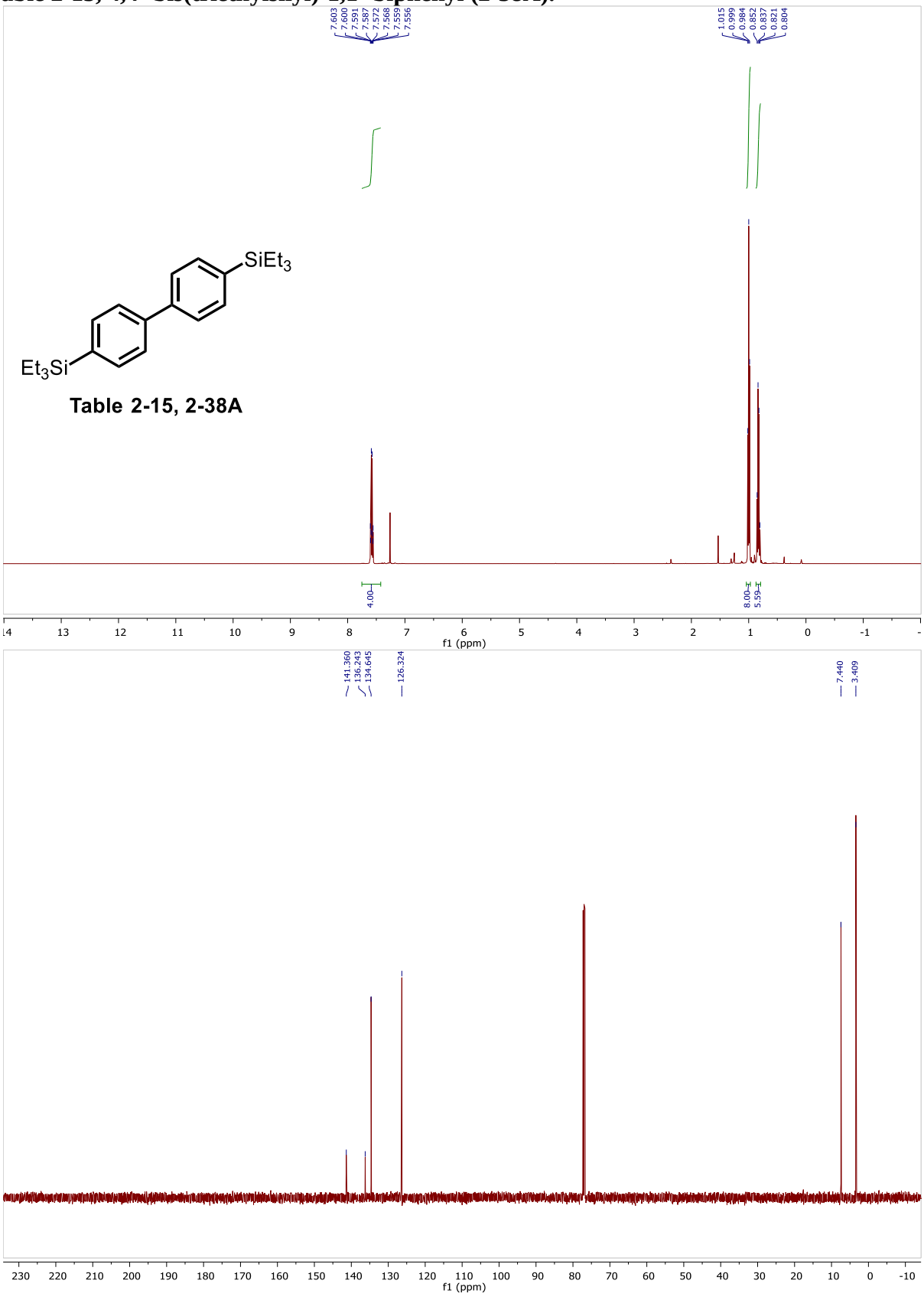

Table 2-15, 2-methyl-6-(triethylsilyl)quinolone (2-39A).

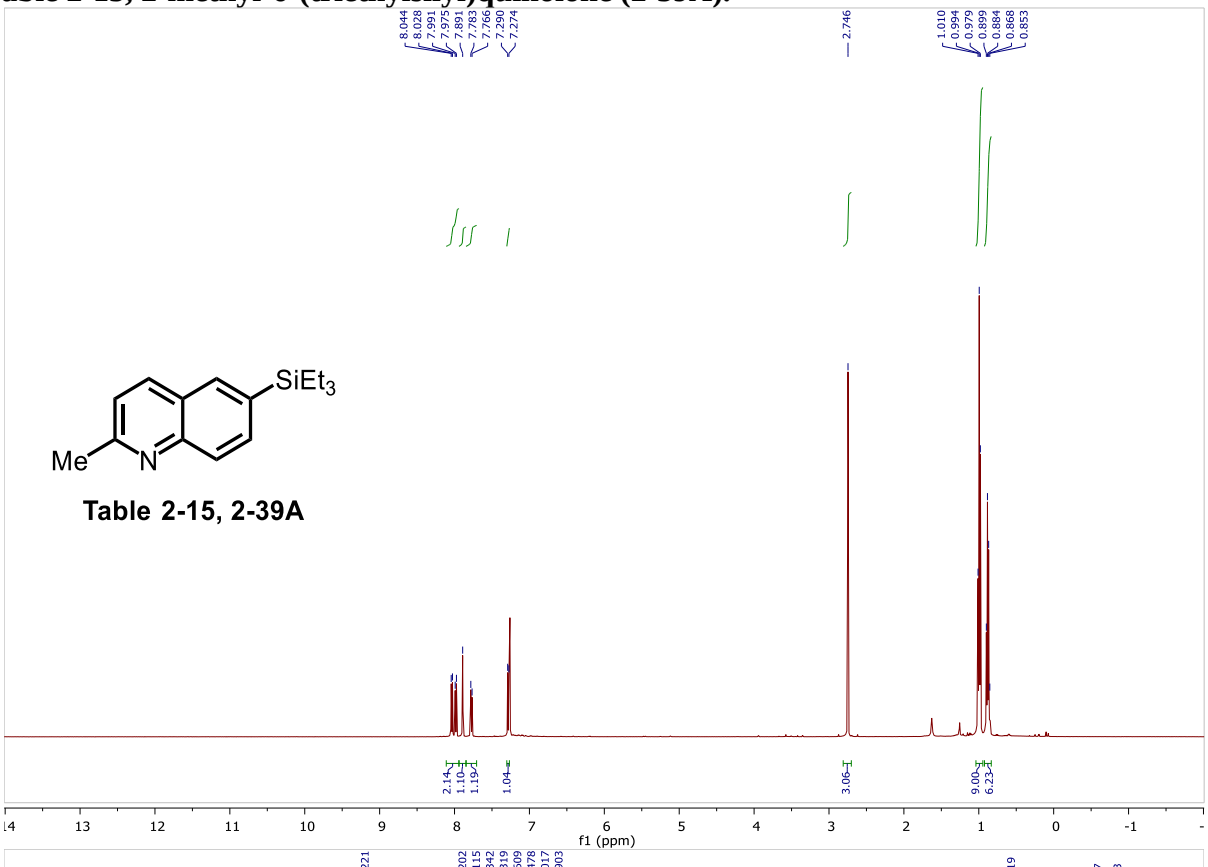

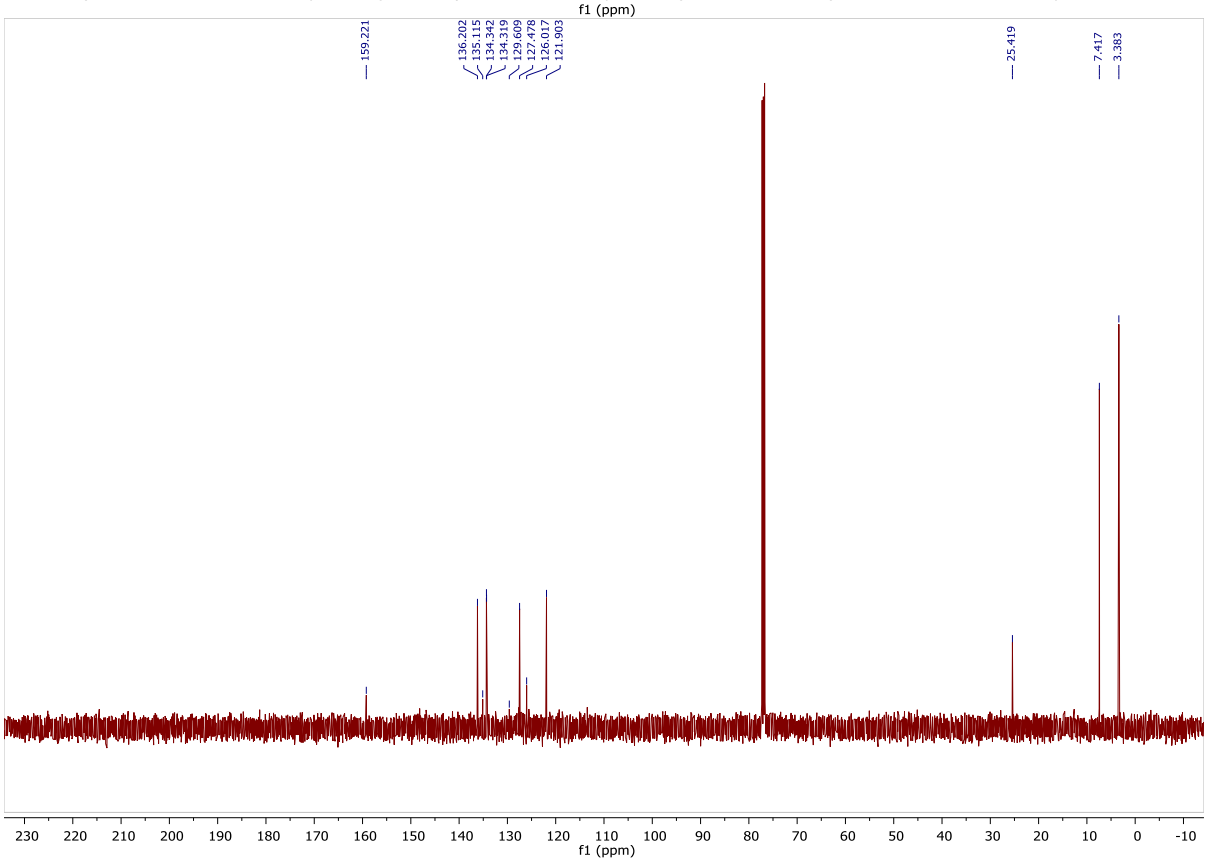

Table 2-15, 2-(4-(triethylsilyl)phenyl)pyridine (2-28A).

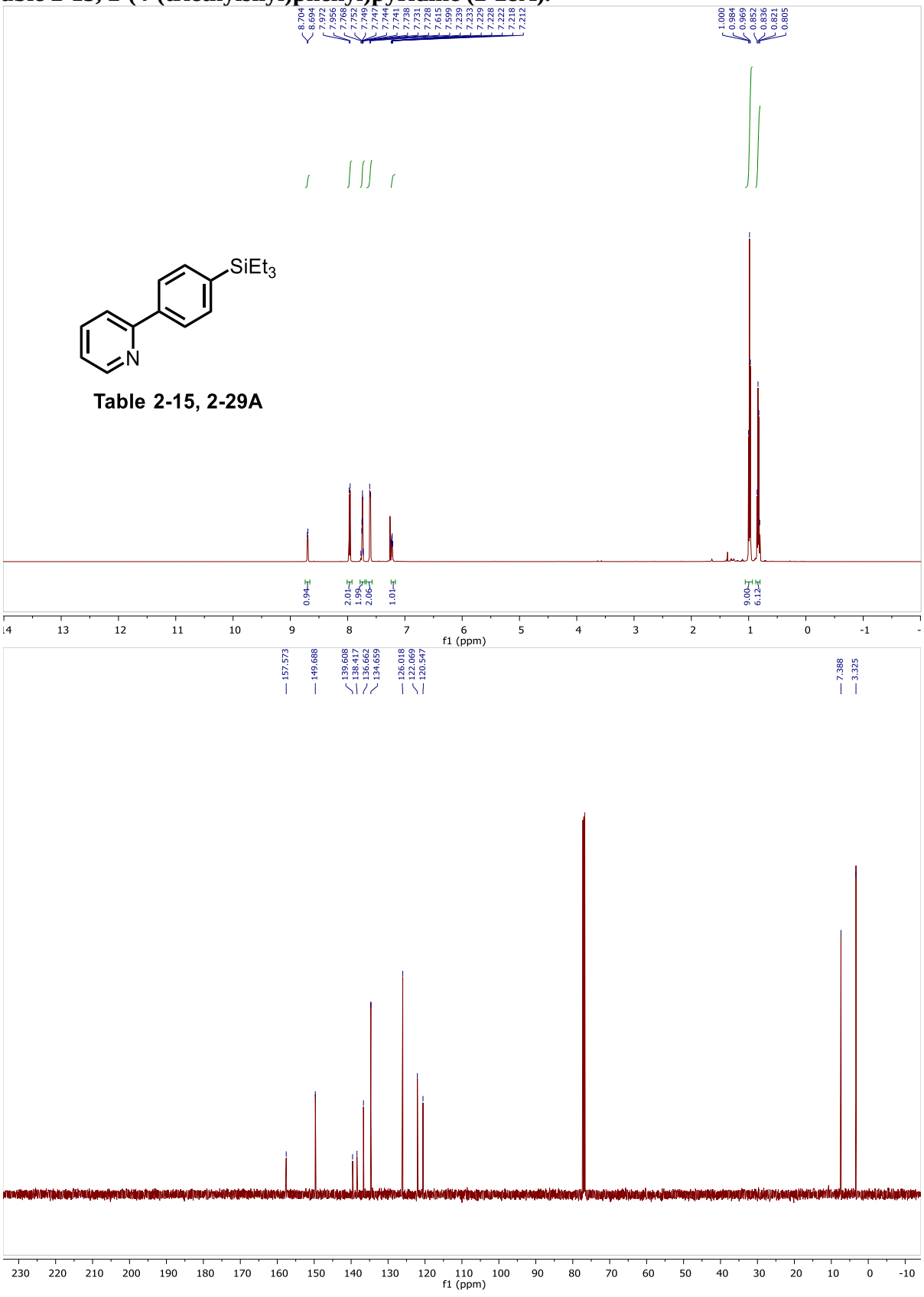

Table 2-15, 4-(3-(triethylsilyl)phenyl)morpholine (2-40A).

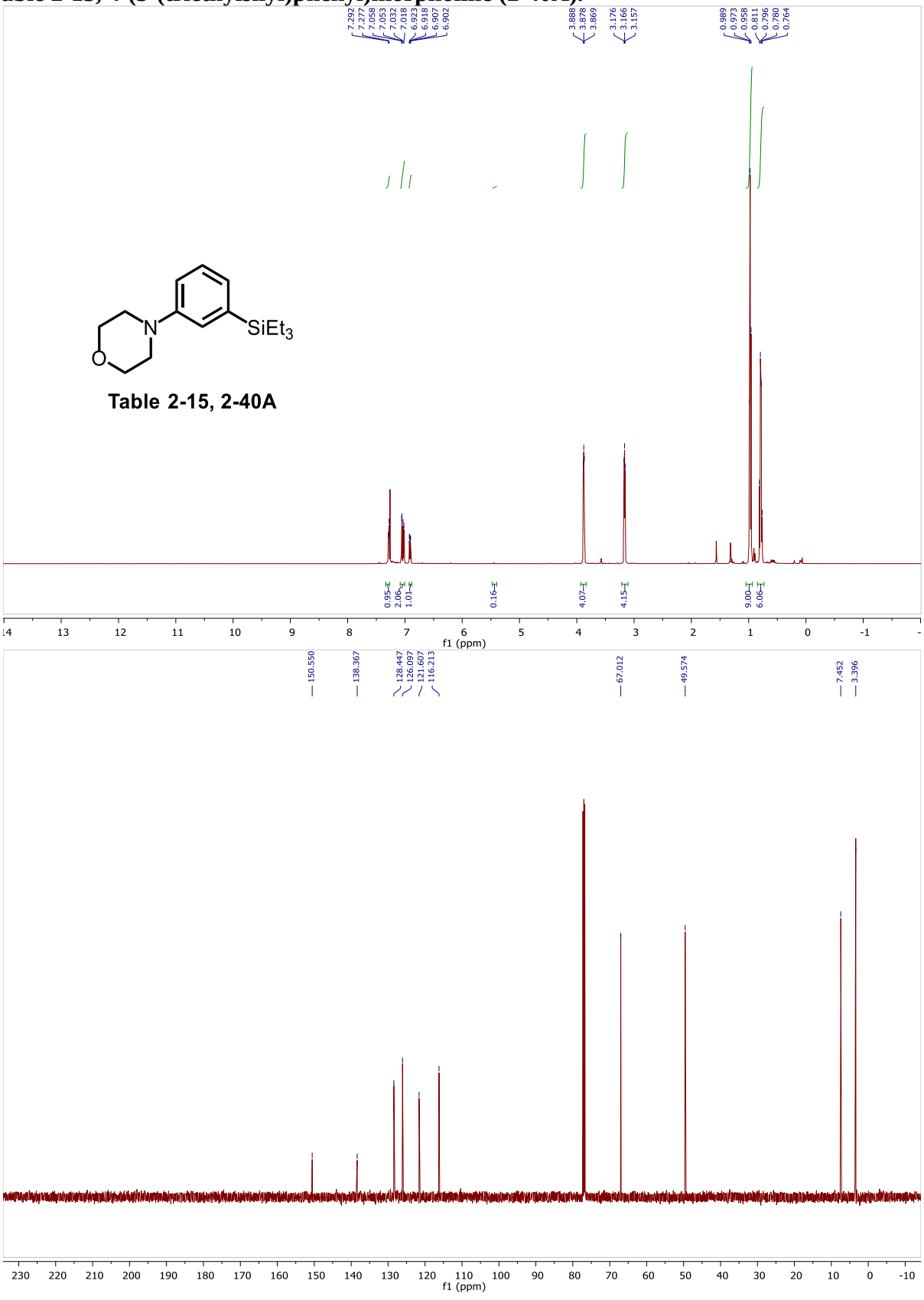

Table 2-15, 2-40A

Table 2-15, N-(4-(triethylsilyl)phenyl)acetamide (2-41A).

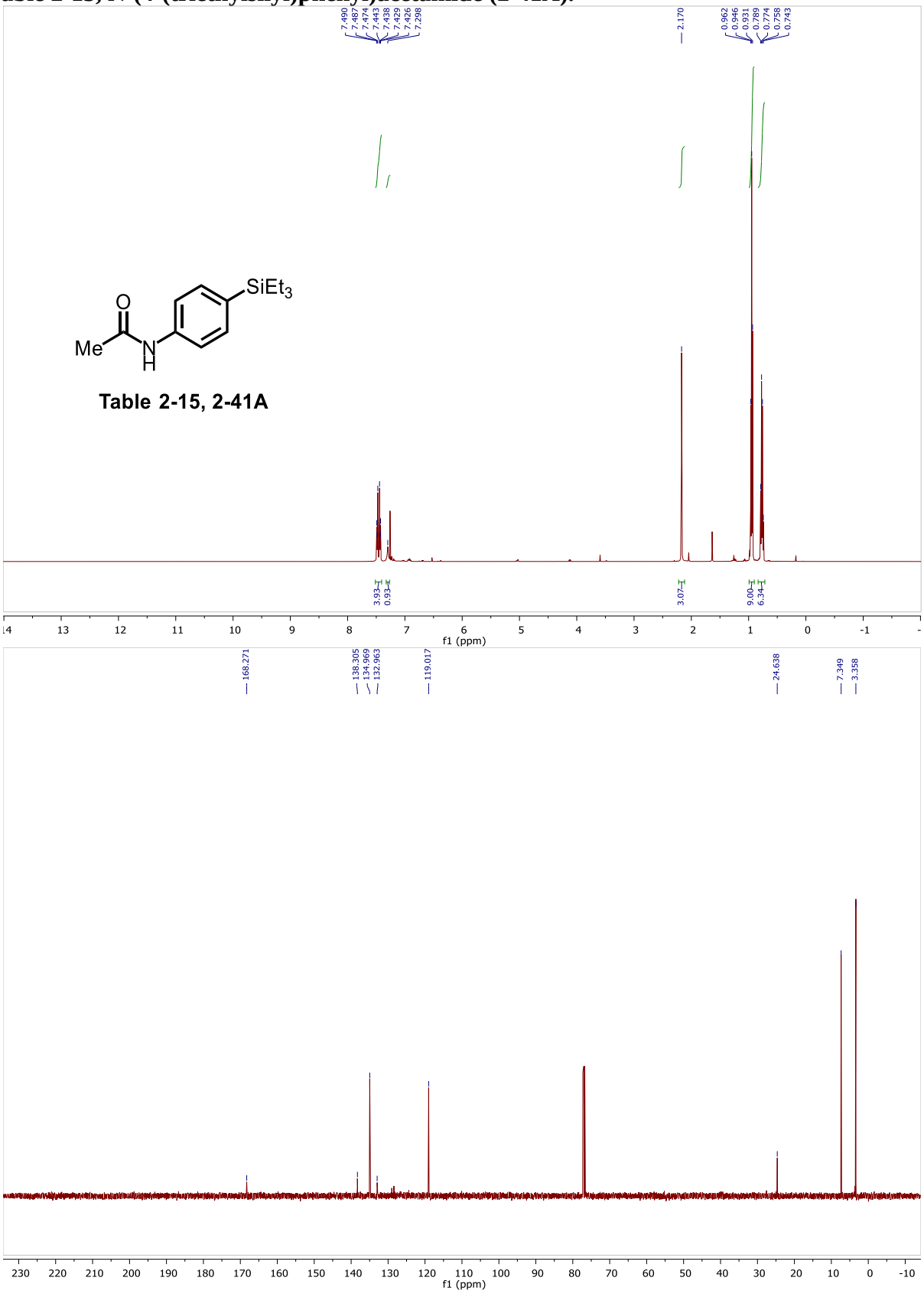

Table 2-15, (2,3-dihydro-1H-inden-5-yl)triethylsilane (2-33A).

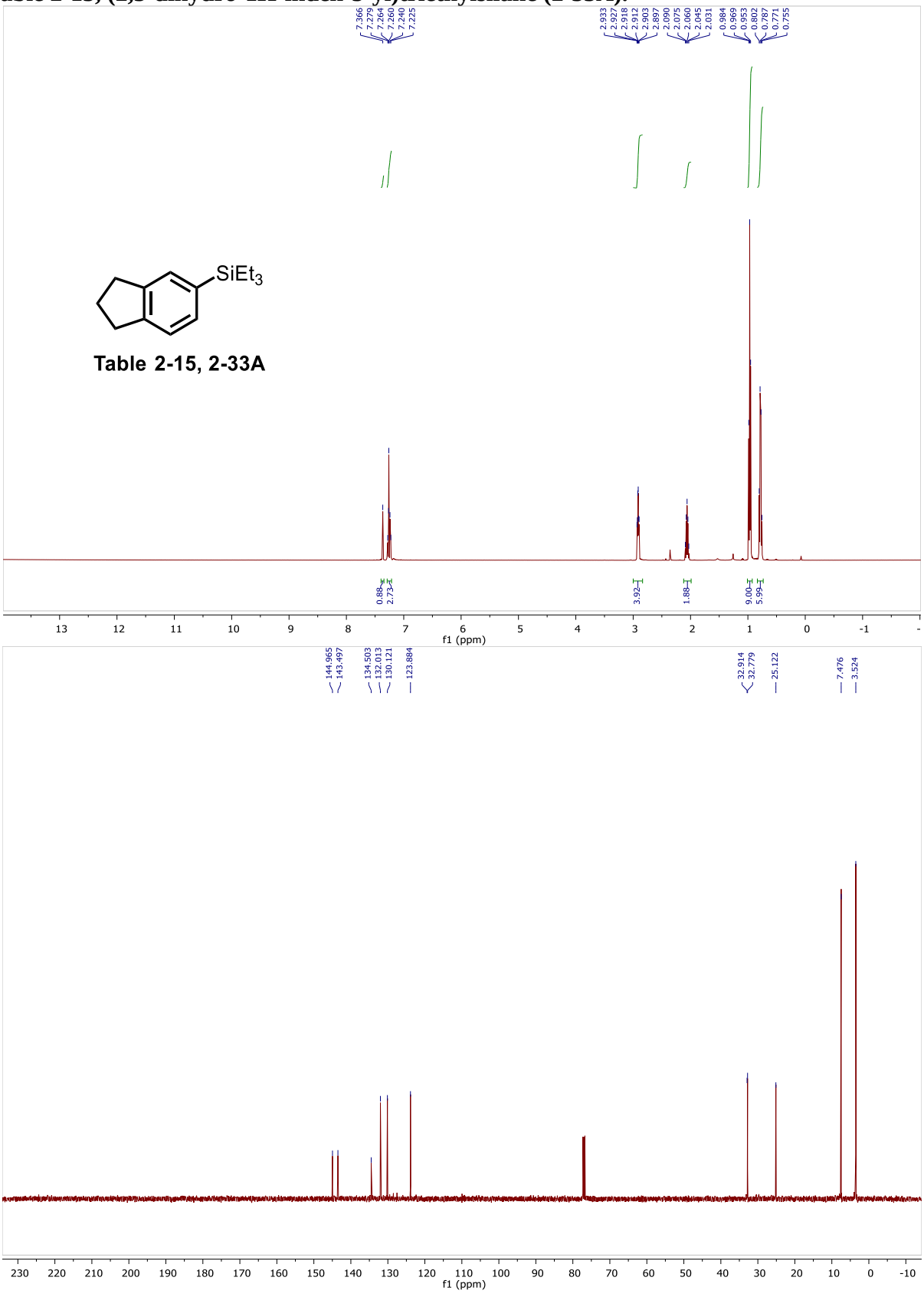

Table 2-15, triethyl(5,6,7,8-tetrahydronaphthalen-2-yl)silane (2-34A).

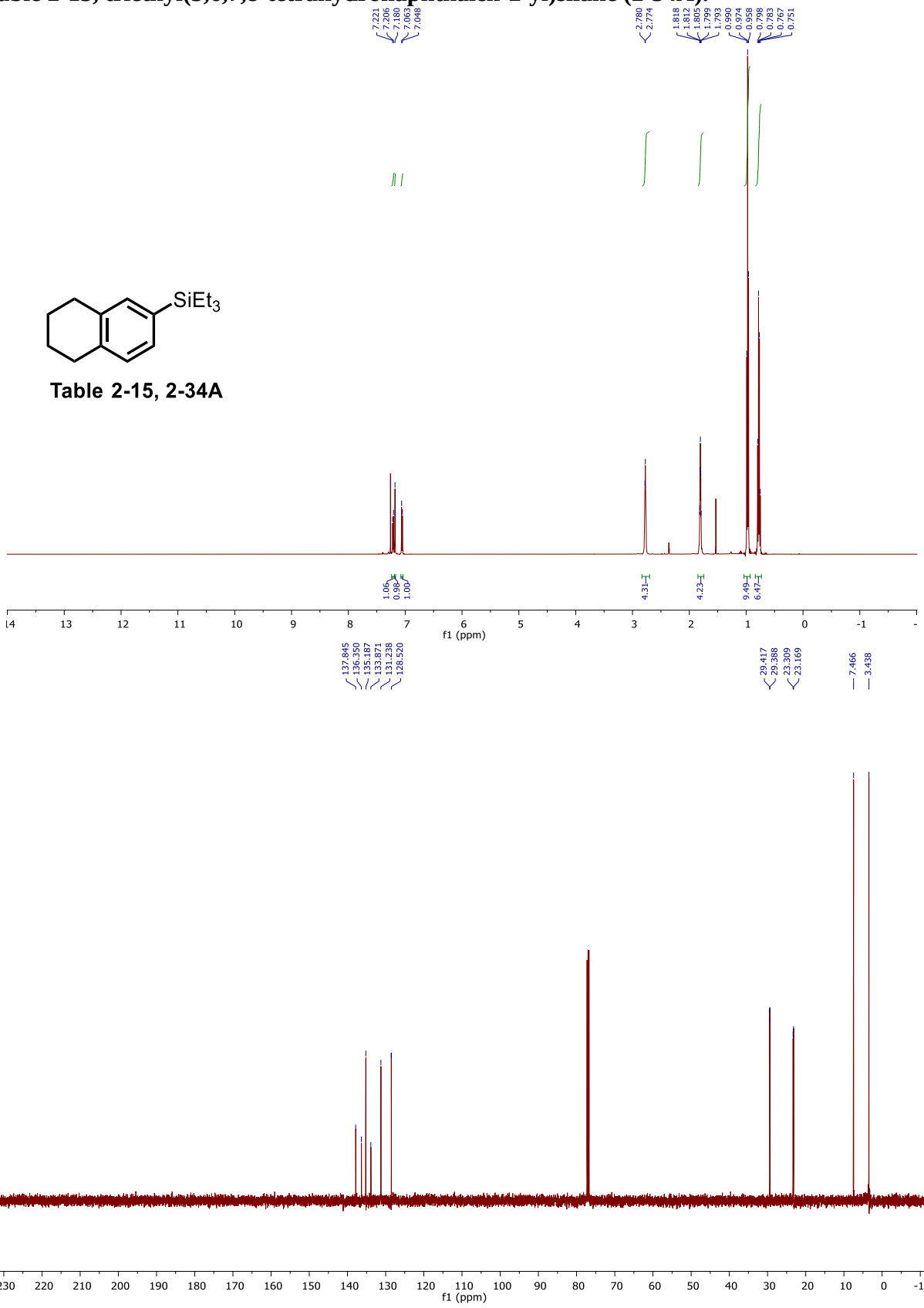

Table 2-15, *tert*-butyldimethyl(((8R,9S,13S,14S,17S)-13-methyl-3-(triethylsilyl)-7,8,9,11,12,13,14,15,16,17-decahydro-6H-cyclopenta[a]phenanthren-17-yl)oxy)silane (2-35A).

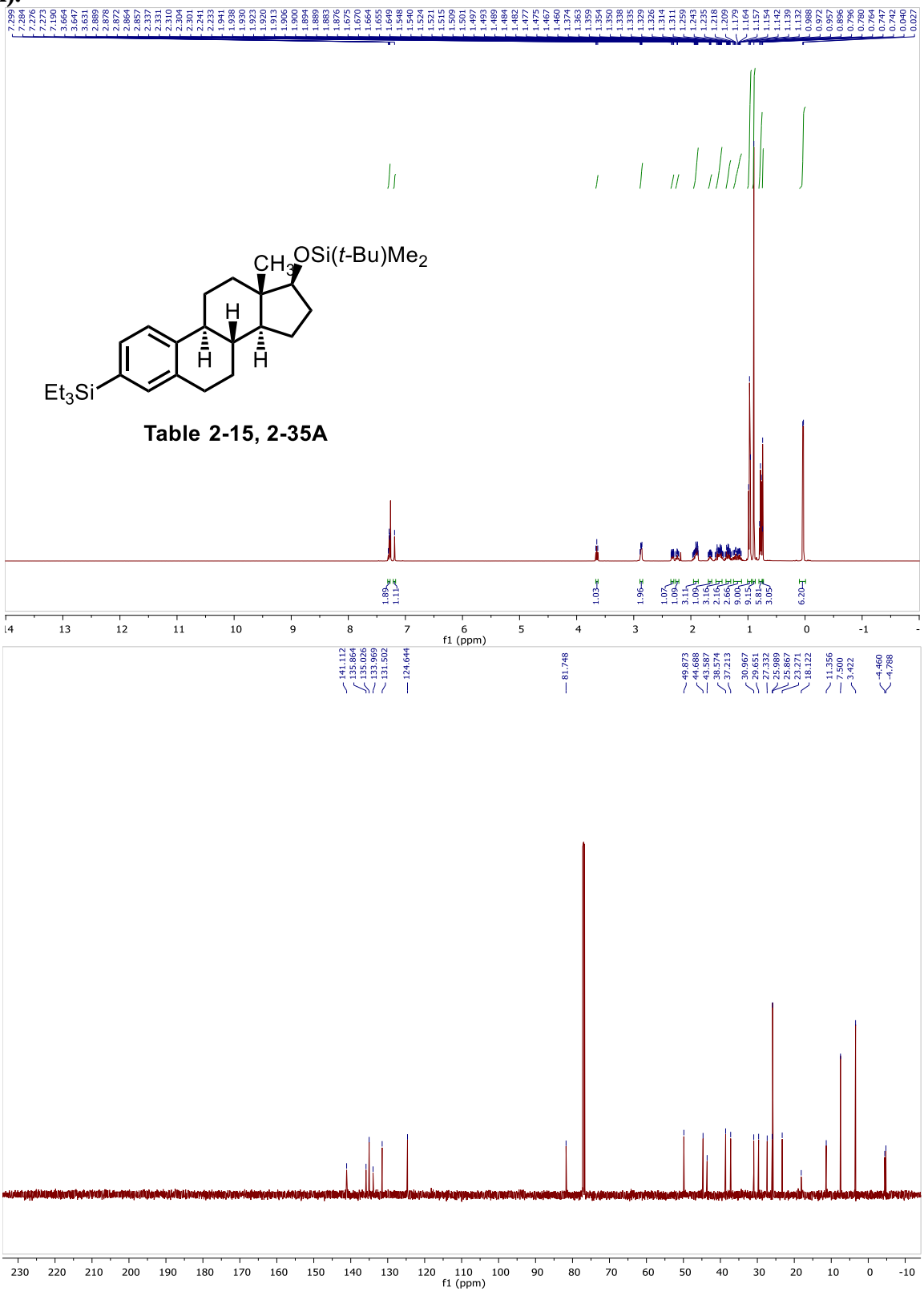

Table 3-3, 1-([1,1'-biphenyl]-4-yl)-2,6-dimethylpiperidine (3-7).

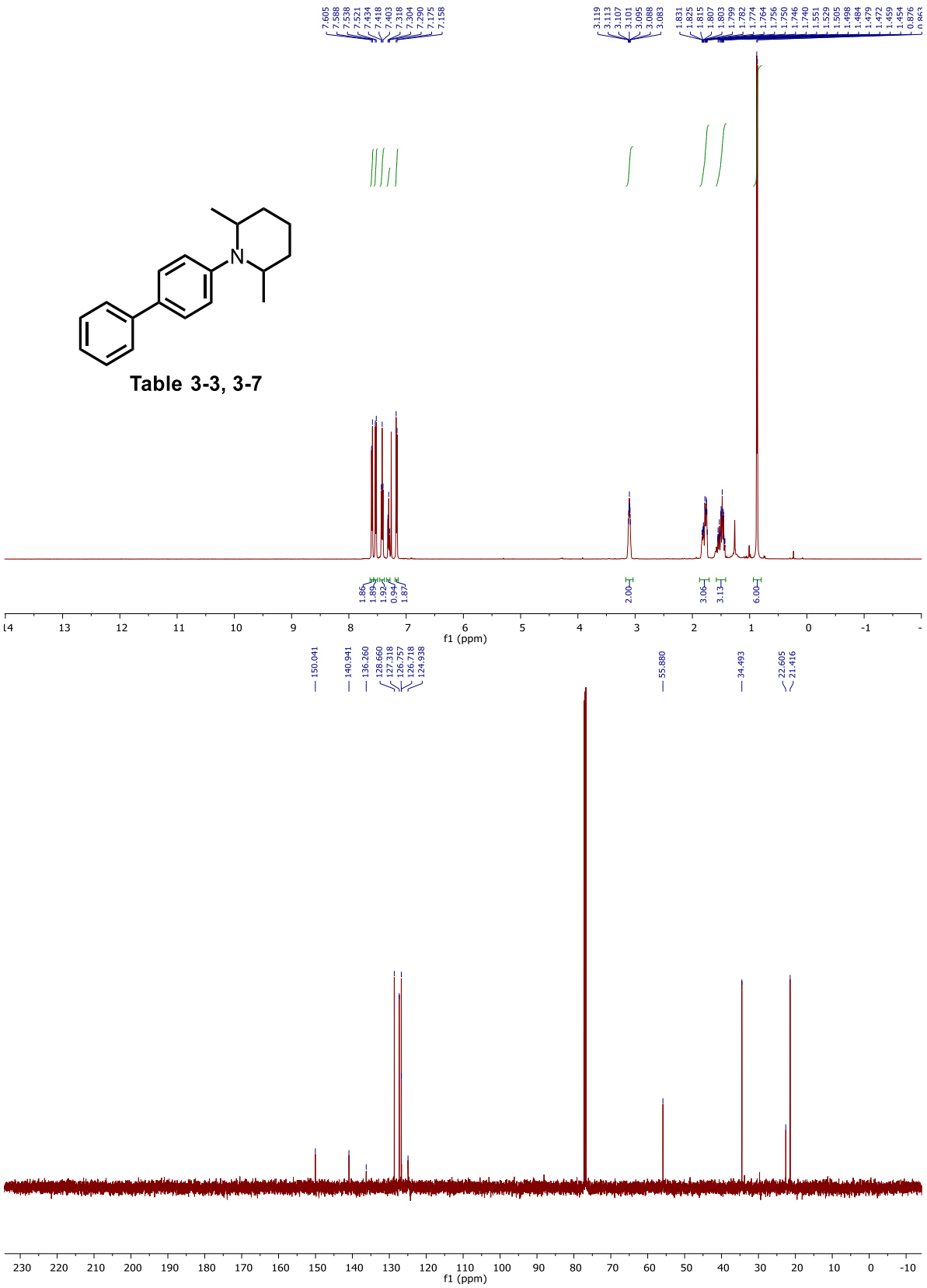

Table 3-3, *N*,*N*-diisobutyl-[1,1'-biphenyl]-4-amine (3-8).

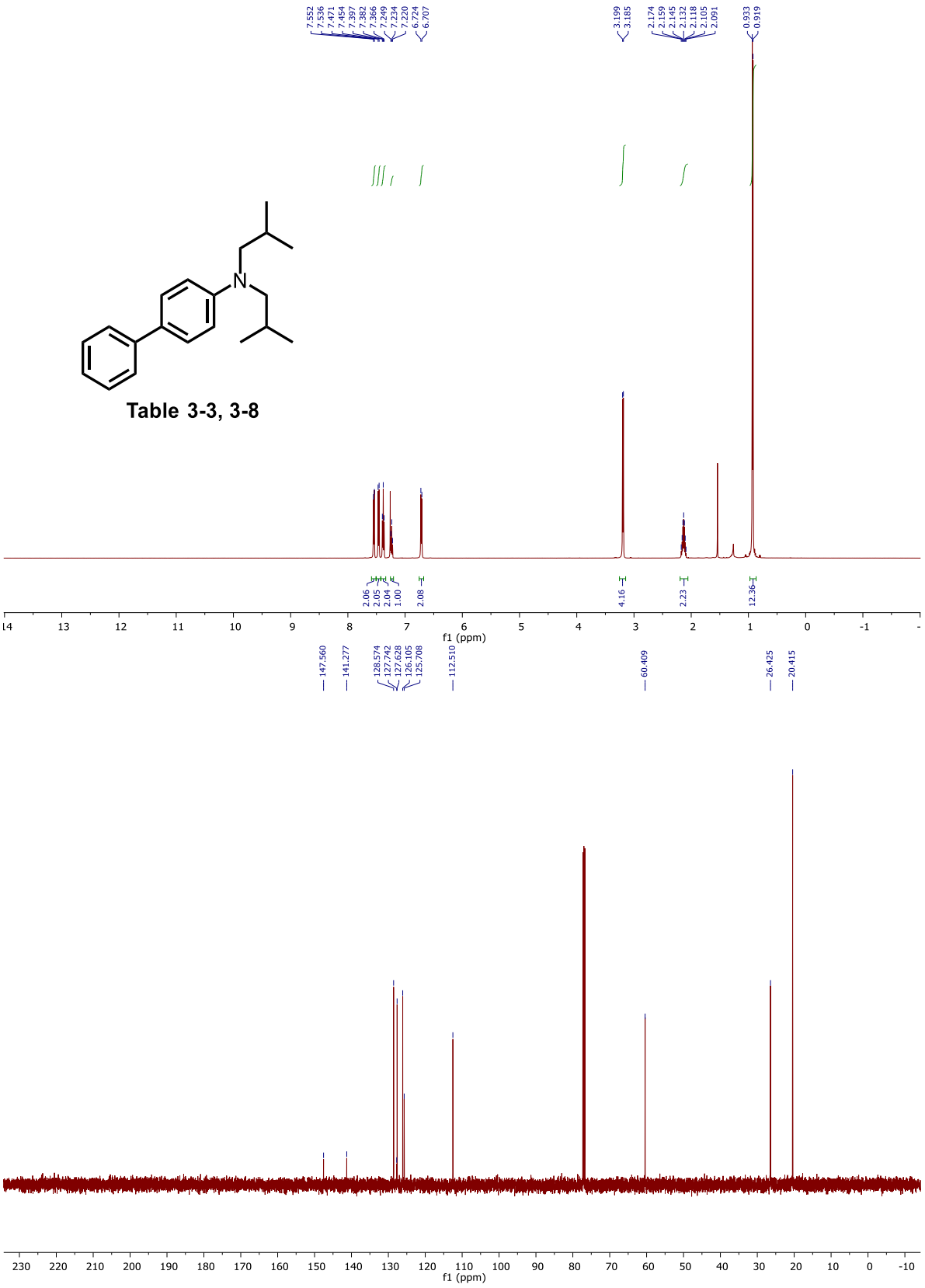

Table 3-3, *N*-butyl-*N*-methyl-[1,1'-biphenyl]-4-amine (3-10).

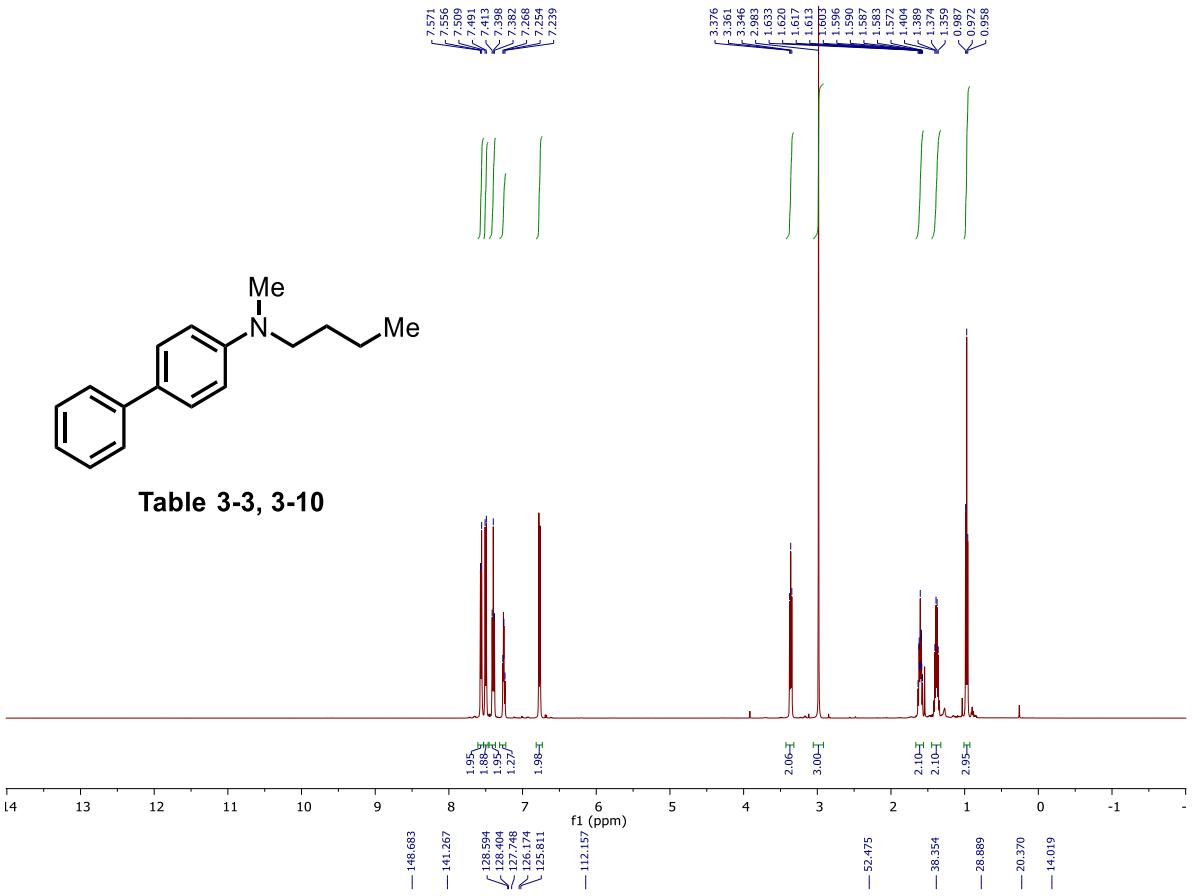

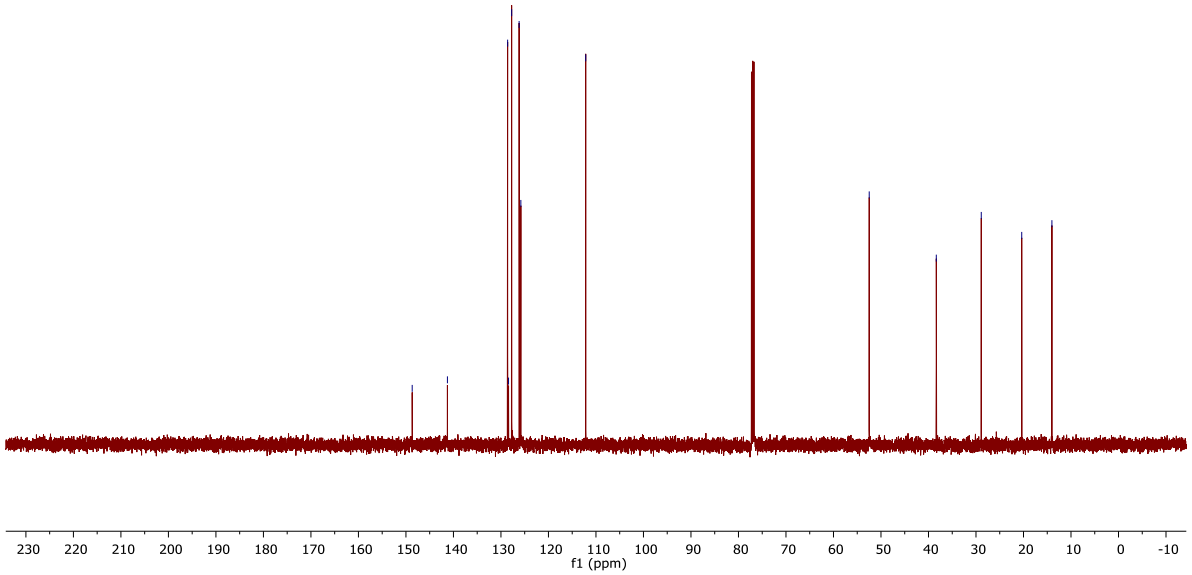

Table 3-3, *N*-mesityl-[1,1'-biphenyl]-4-amine (3-12).

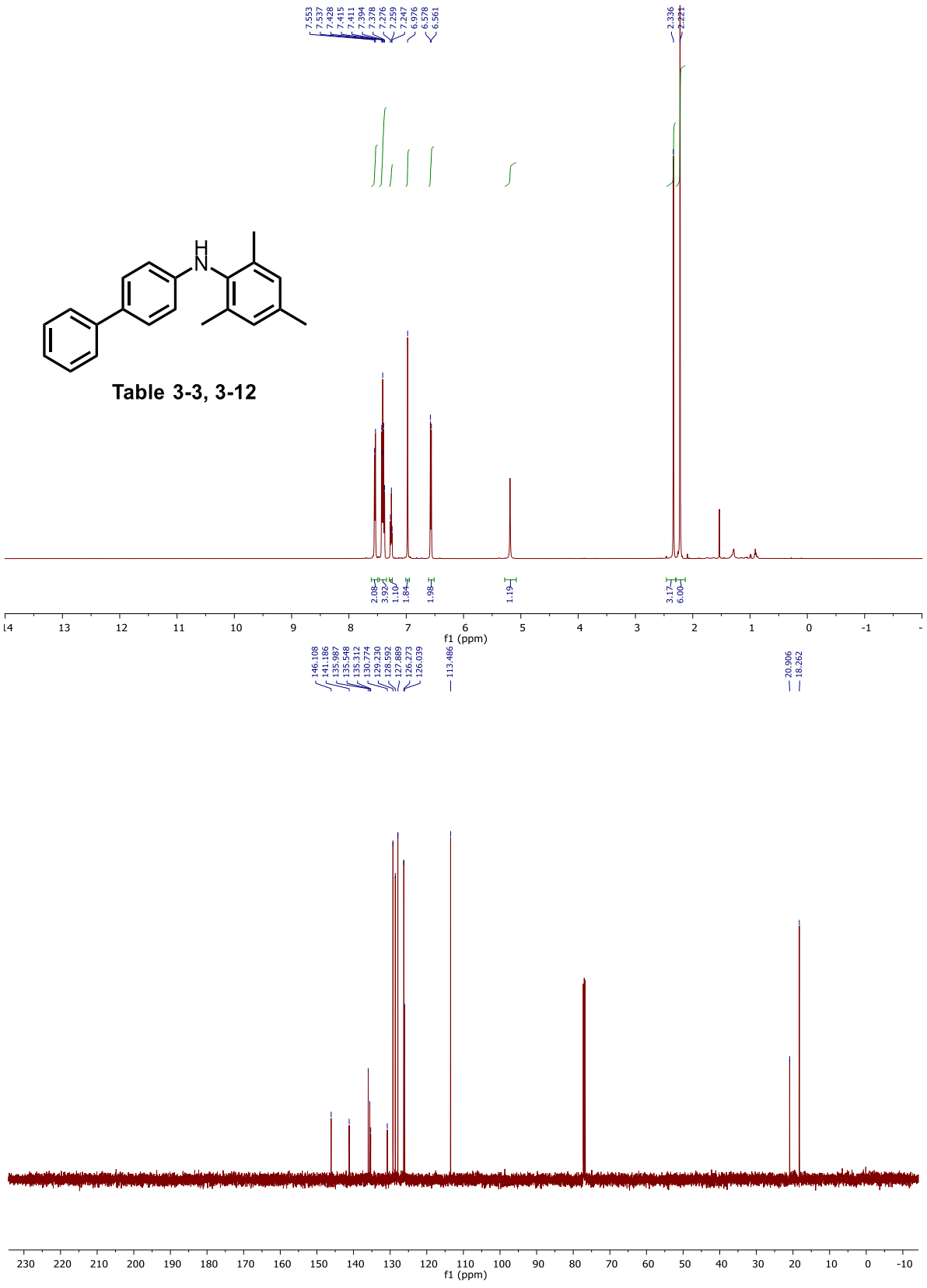

Table 3-3, *N*-(2,6-diisopropylphenyl)-[1,1'-biphenyl]-4-amine (3-13).

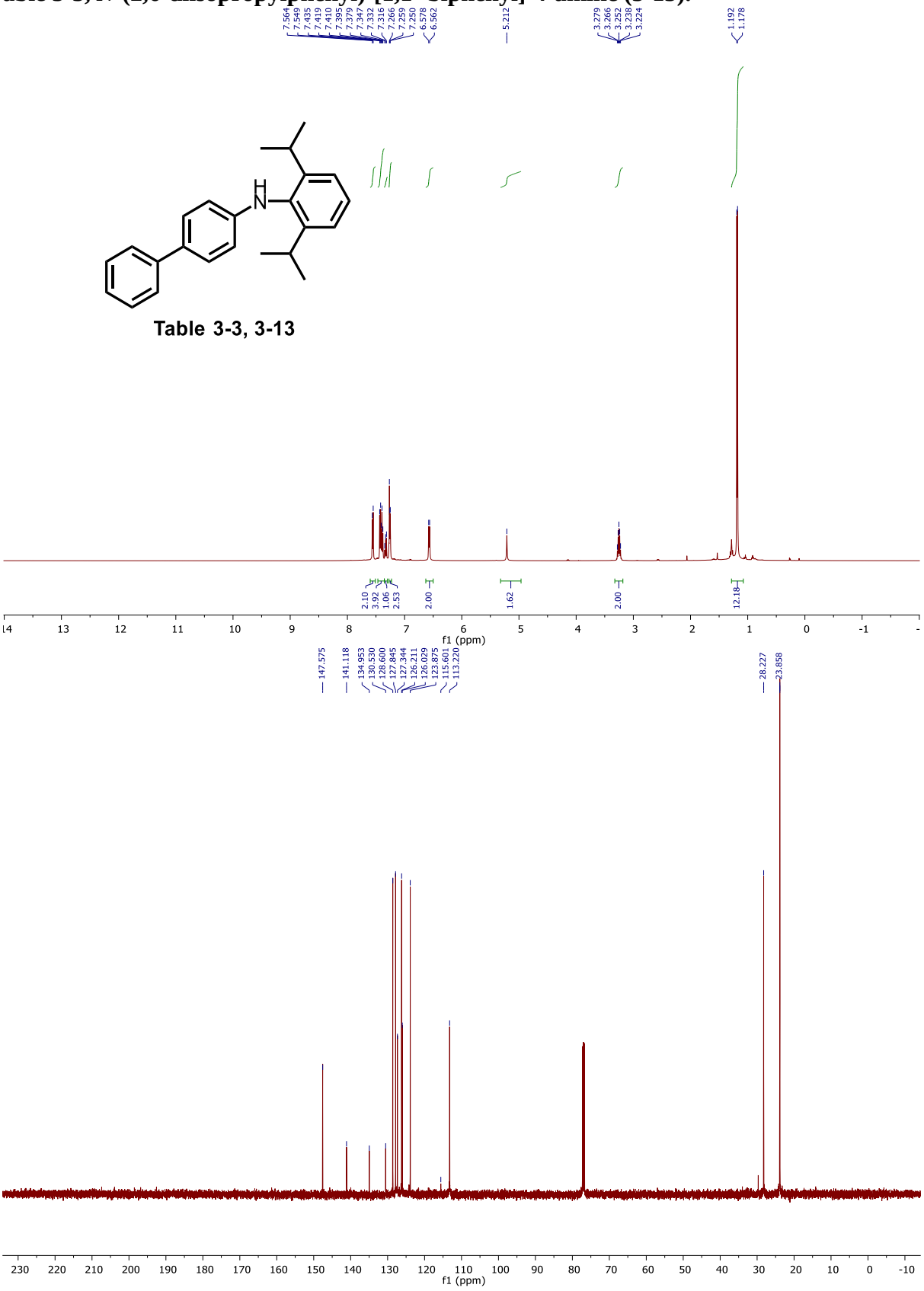

Table 3-3, *N*-(cyclopropylmethyl)-[1,1'-biphenyl]-4-amine (3-16).

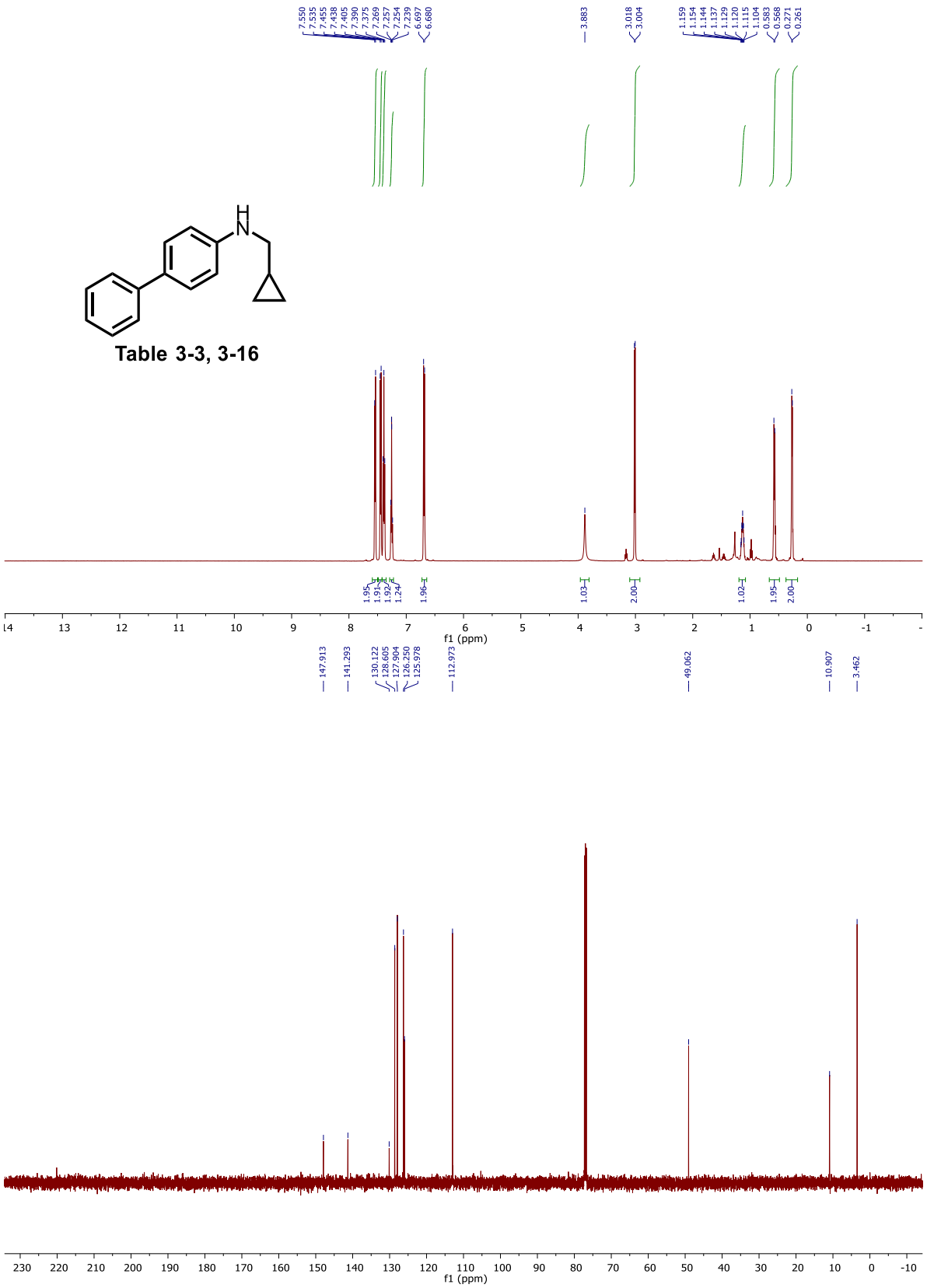

Table 3-3, *N*-isobutyl-[1,1'-biphenyl]-4-amine (3-18).

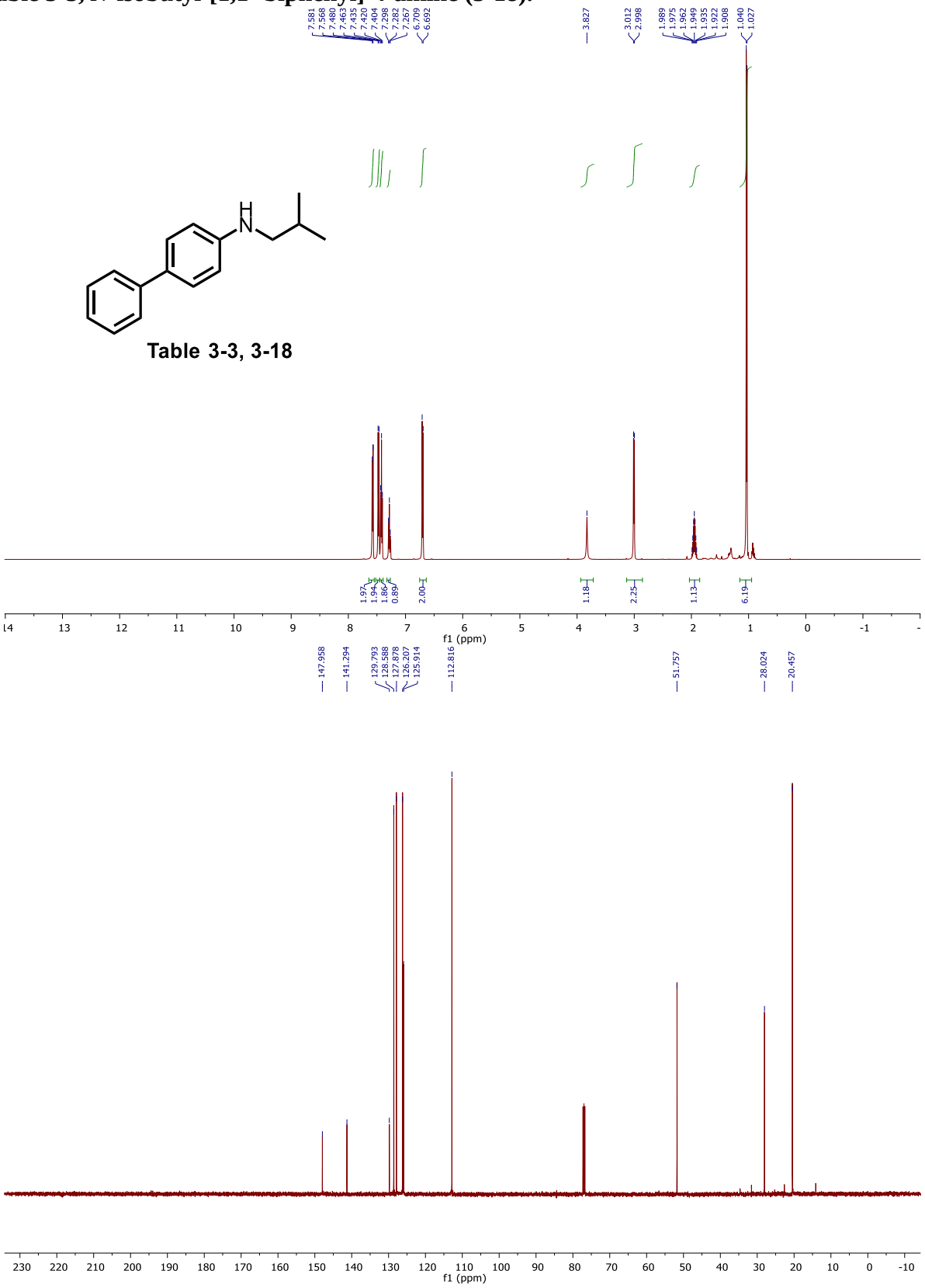

Table 3-3, *N*-cyclobutyl-[1,1'-biphenyl]-4-amine 3-20).

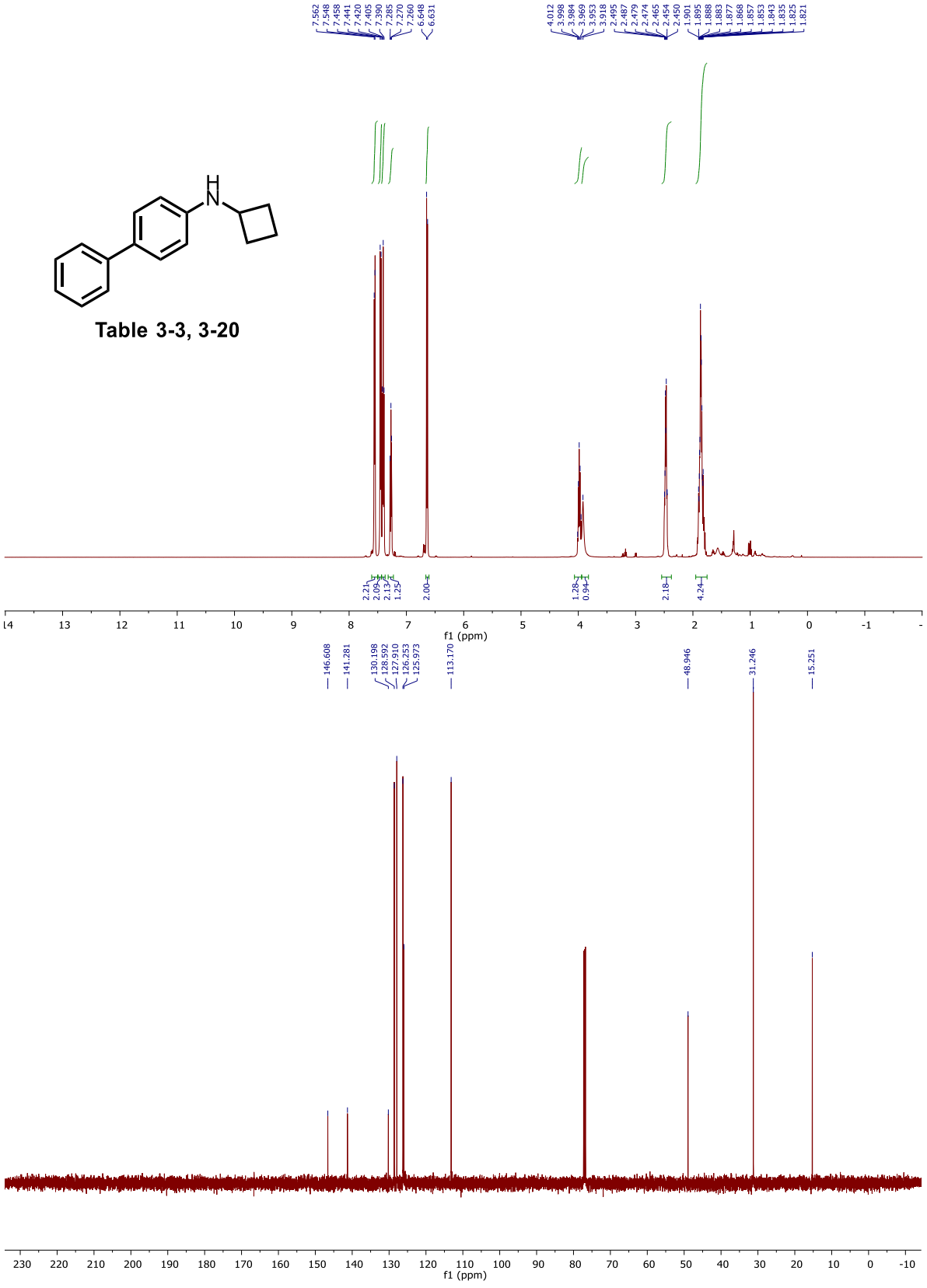

Table 3-5, *N*-isobutylnaphthalen-2-amine (3-24).

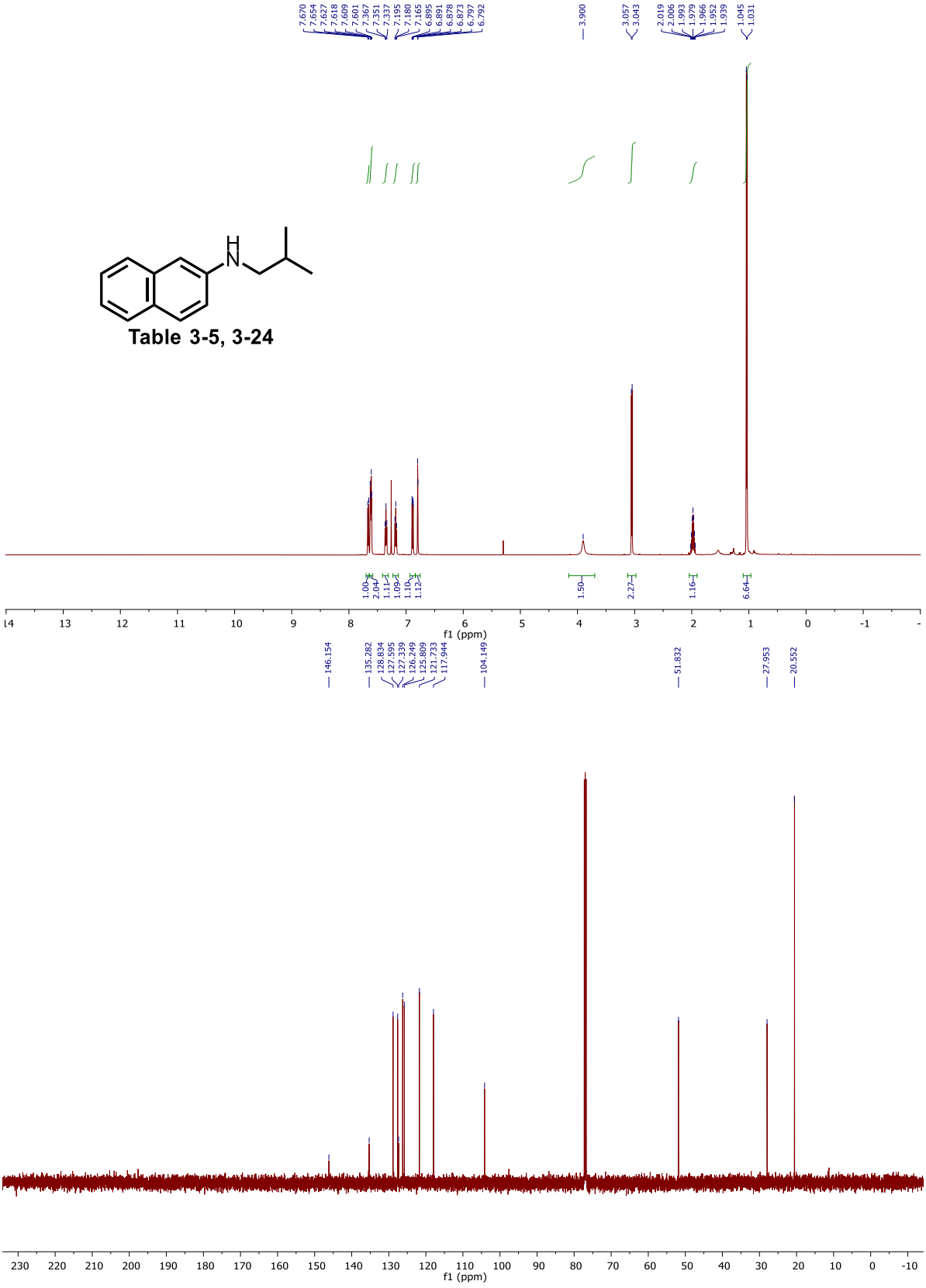

Table 3-5, *N*-methyl-*N*-phenyl-6-(trimethylsilyl)naphthalen-2-amine (3-25).

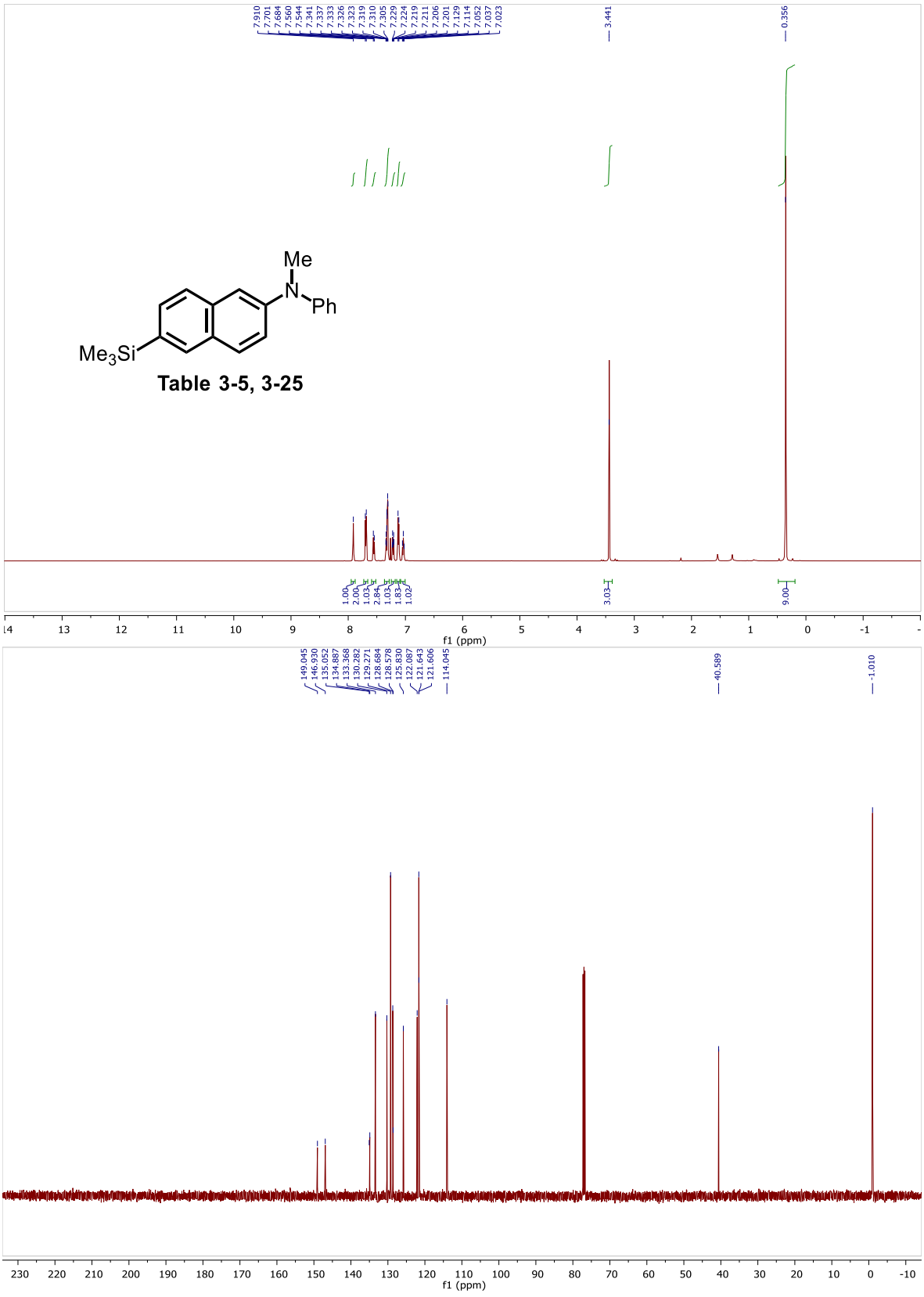

Table 3-5, *N*-benzyl-*N*,3-dimethyl-[1,1'-biphenyl]-4-amine (3-26).

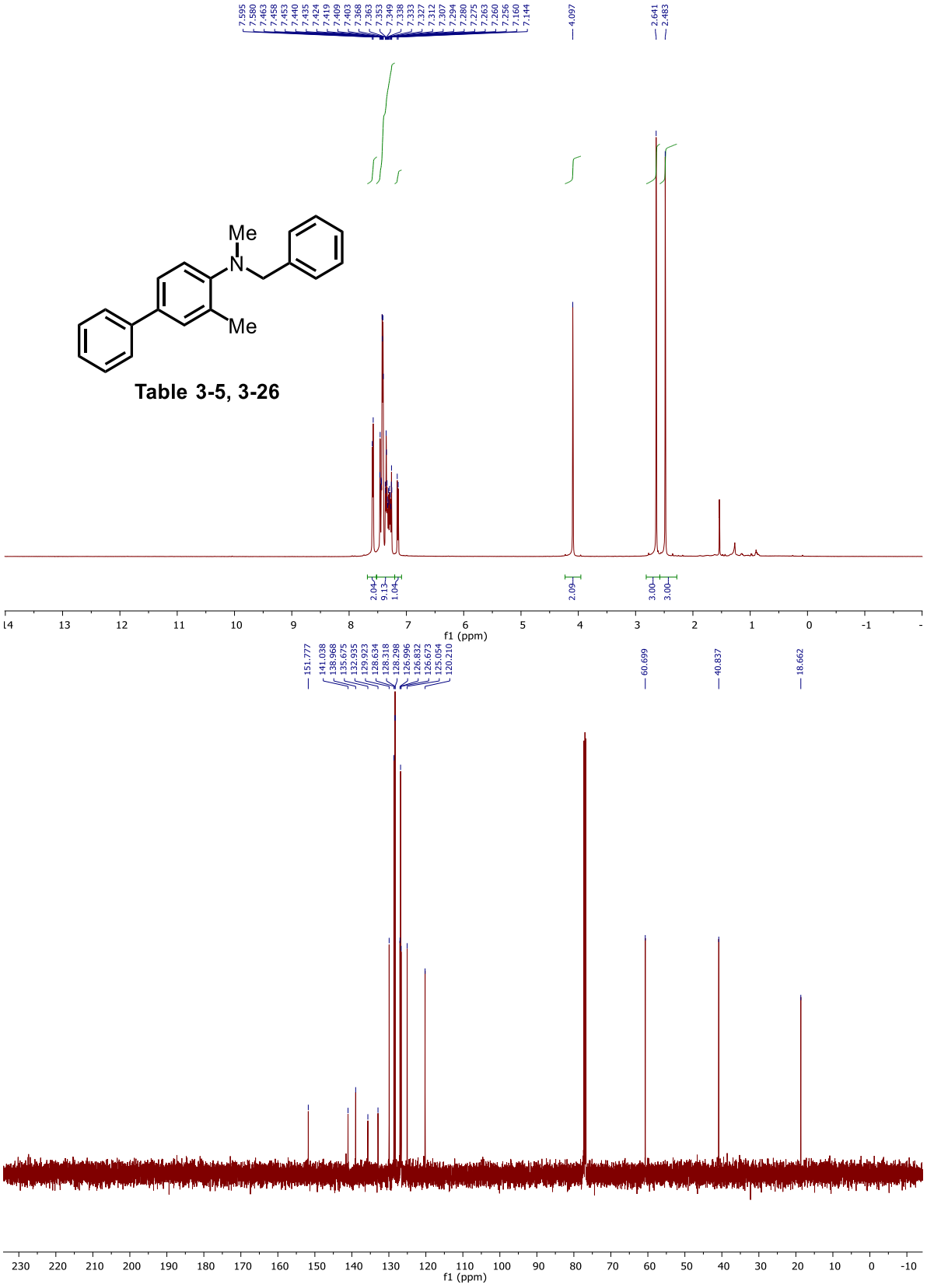

Table 3-5, 4-(6-((*tert*-butyldimethylsilyl)oxy)-[1,1'-biphenyl]-3-yl)morpholine (3-27) and 4-([1,1'-biphenyl]-3-yl)morpholine.

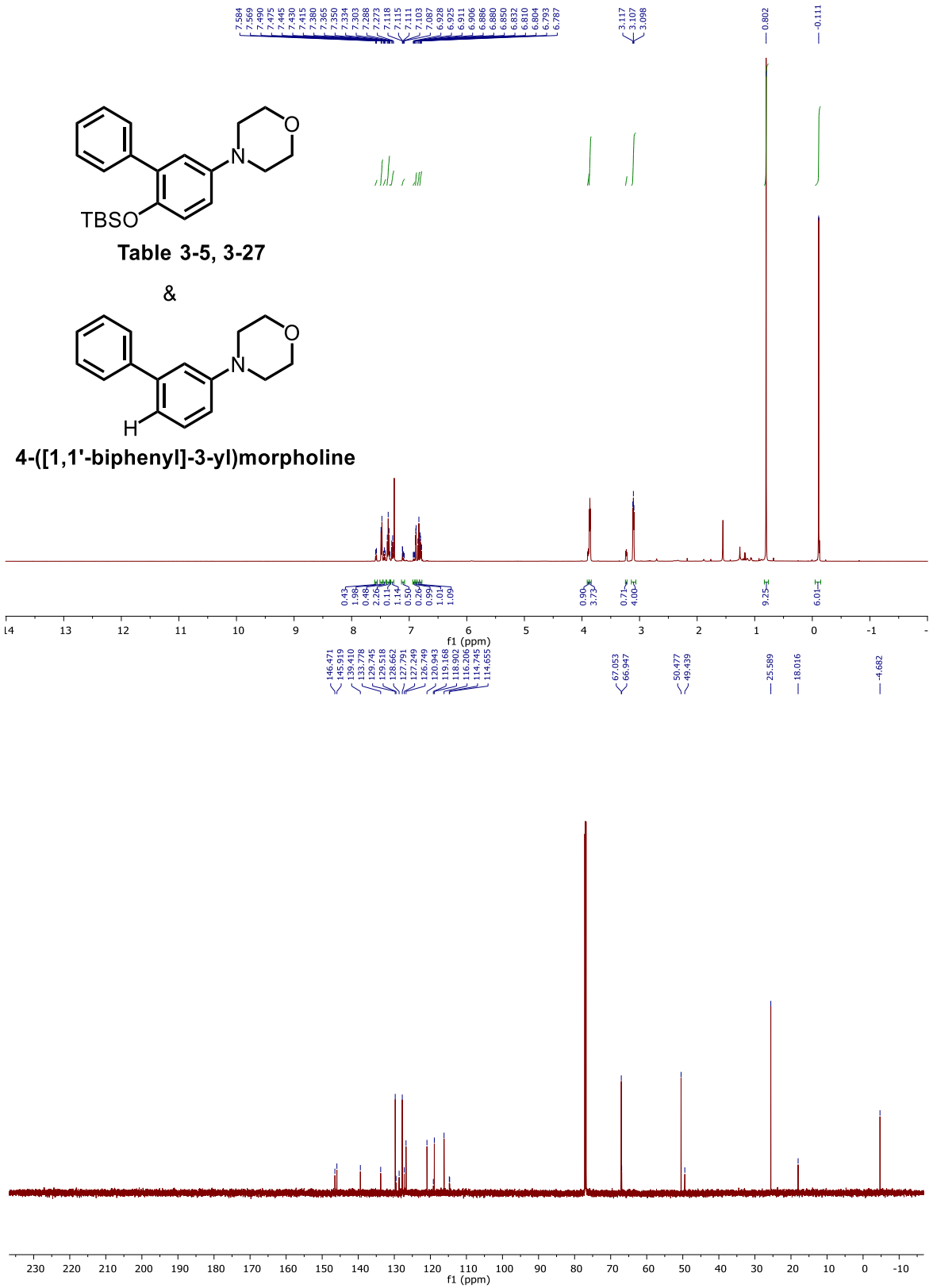

Table 3-5, 2-methyl-6-(4-(pyrimidin-2-yl)piperazin-1-yl)quinolone (3-28).

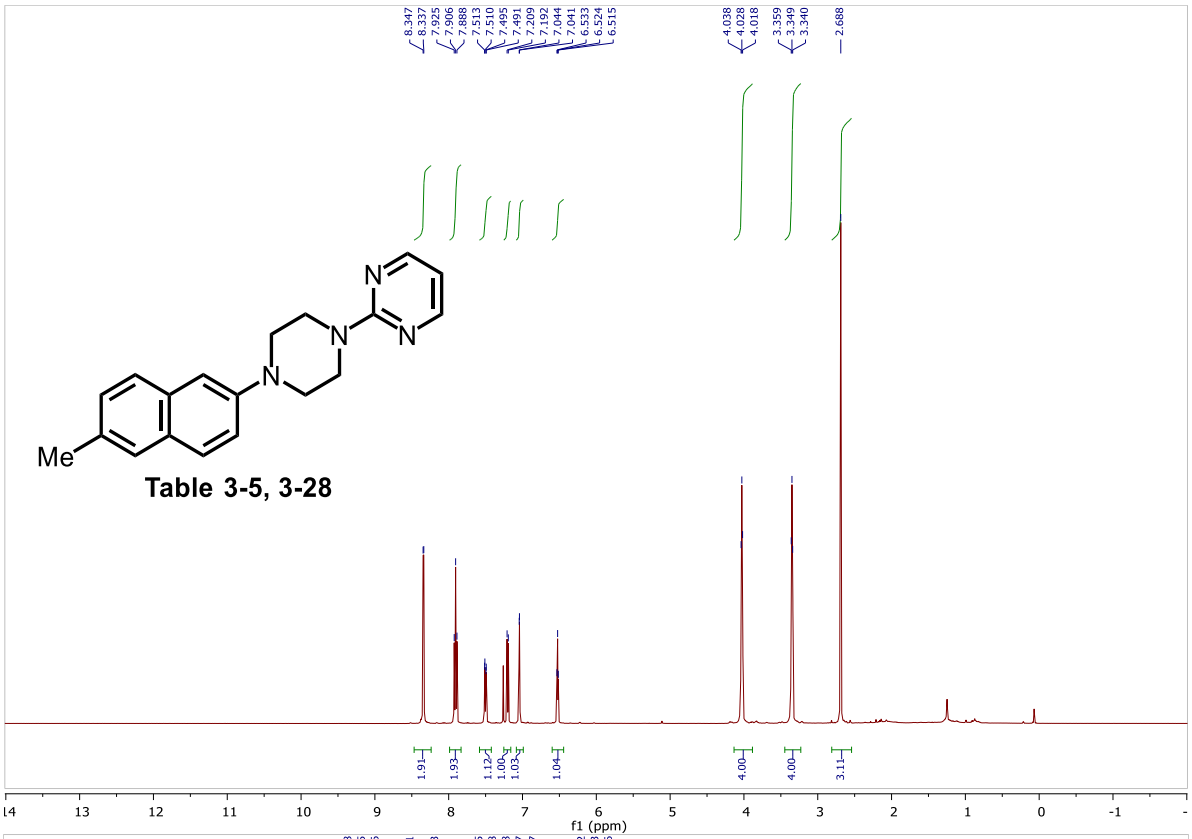

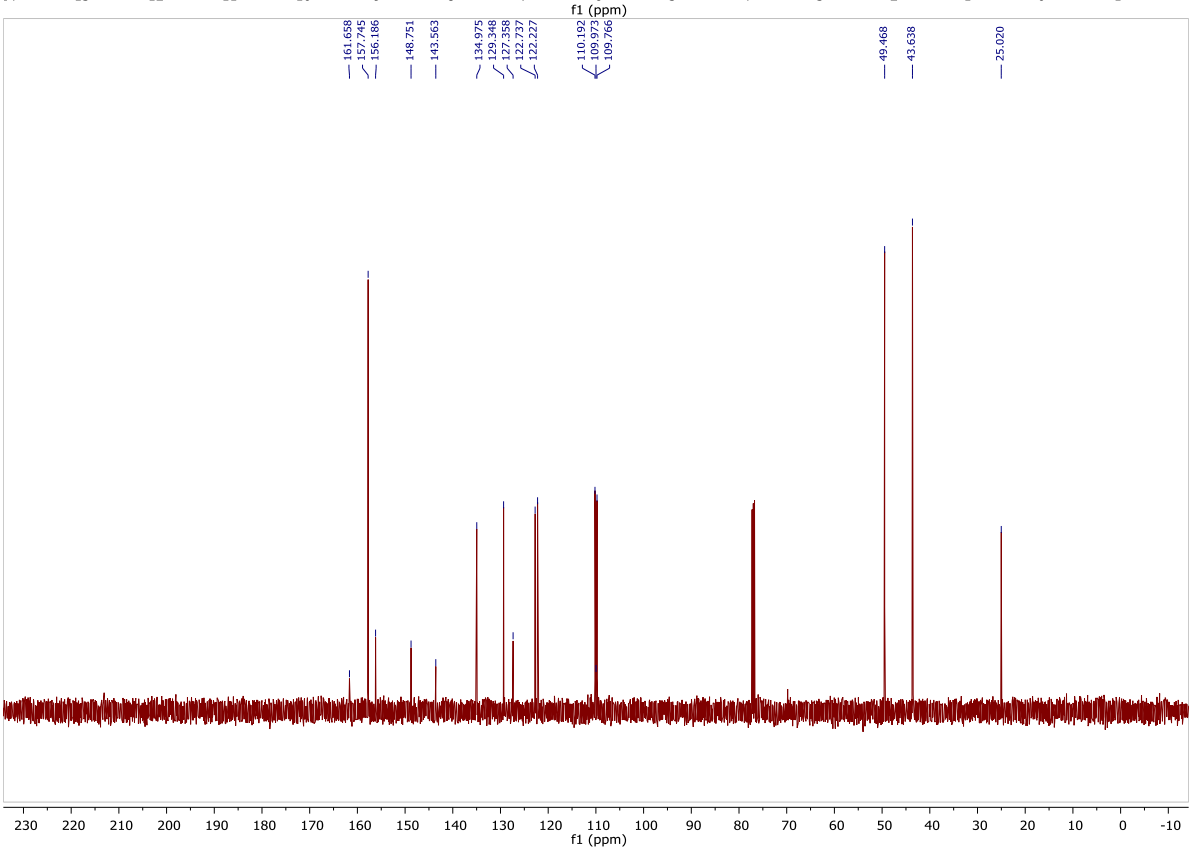

Table 3-5, *N*-octyl-4-(pyridin-2-yl)aniline (3-29).

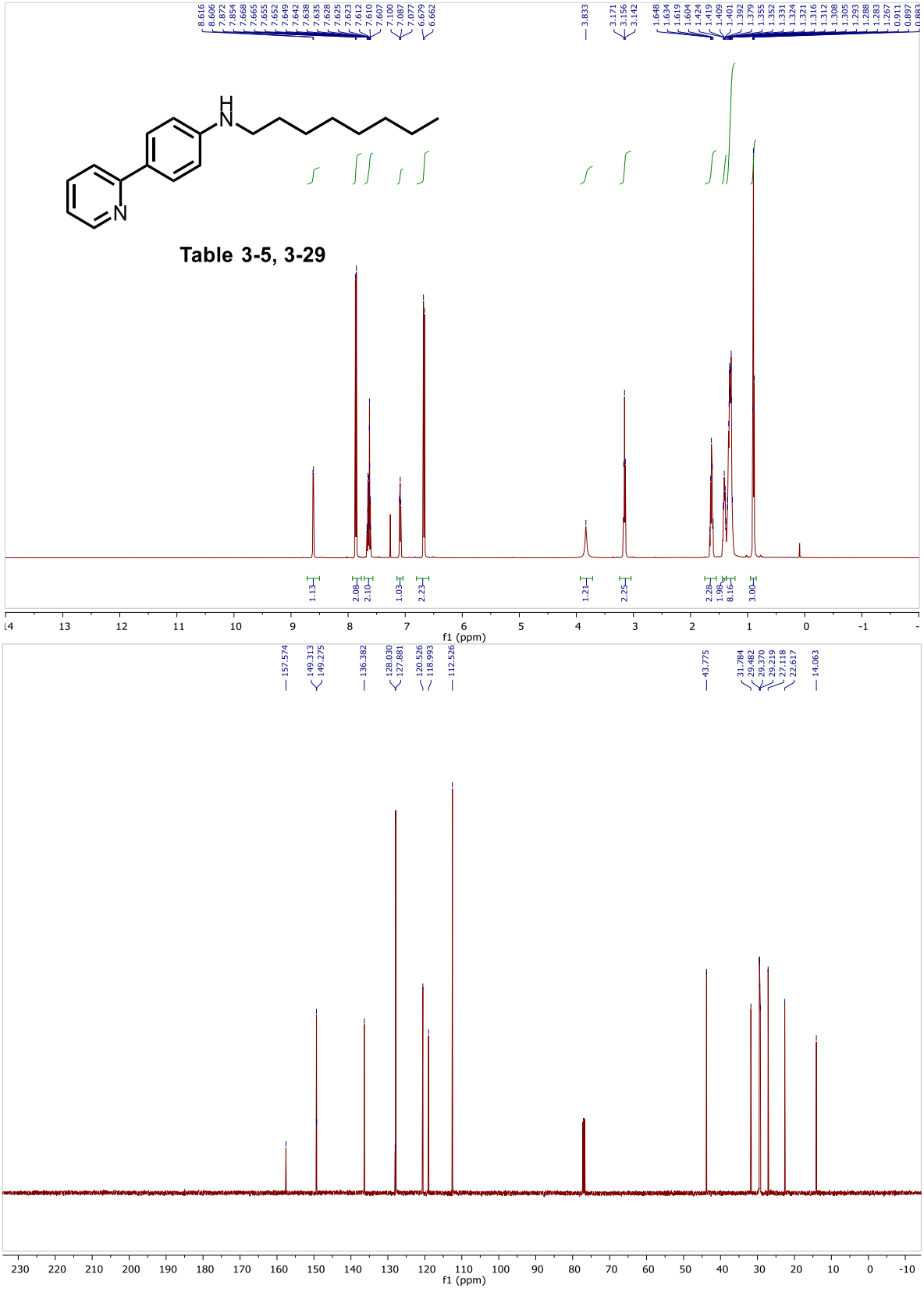

Table 3-5, *N*-cyclohexyl-9-methyl-*9H*-carbazol-2-amine (3-30).

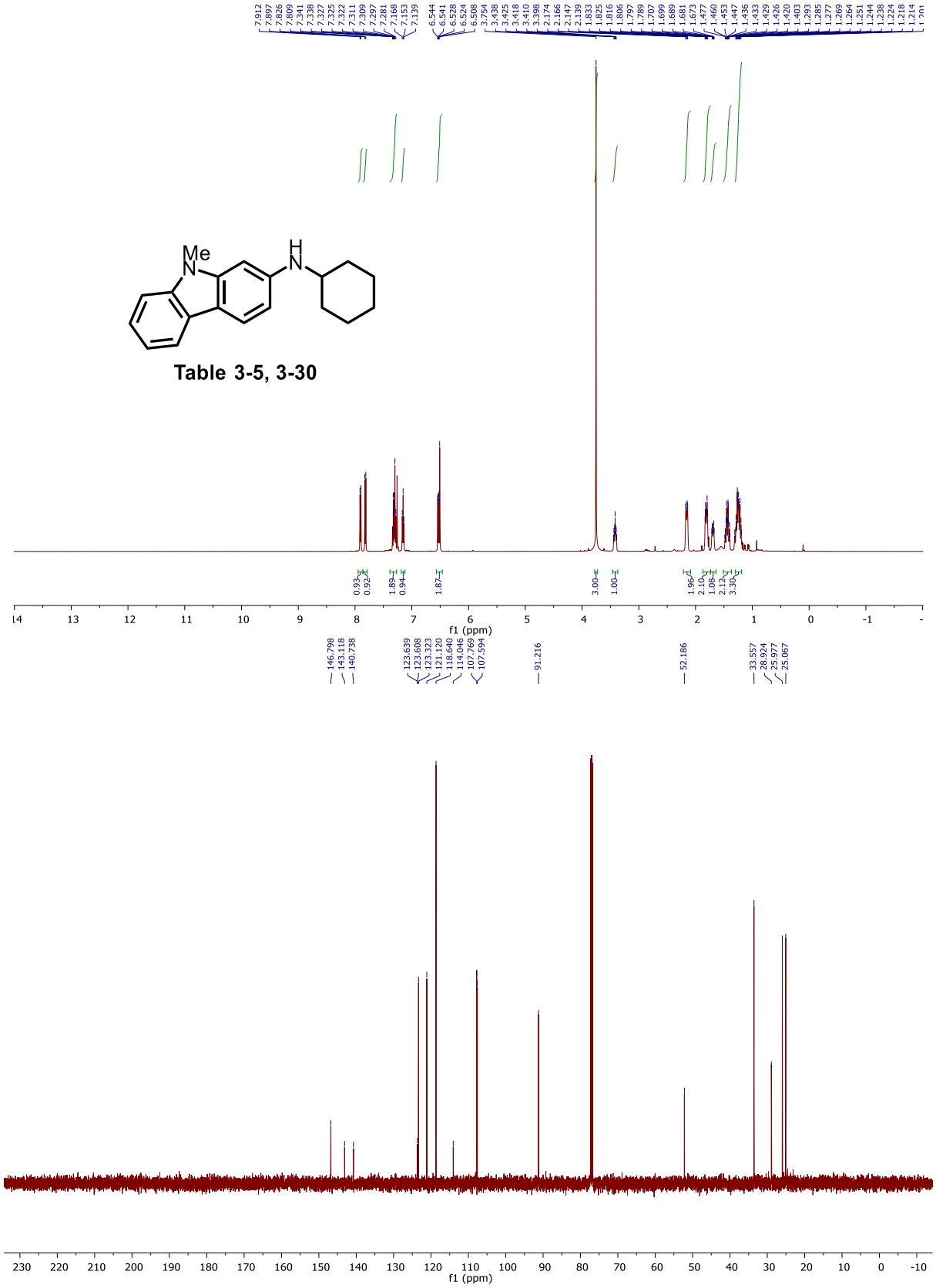

Table 3-5, *N*,*N*-dibutylquinolin-3-amine (3-31).

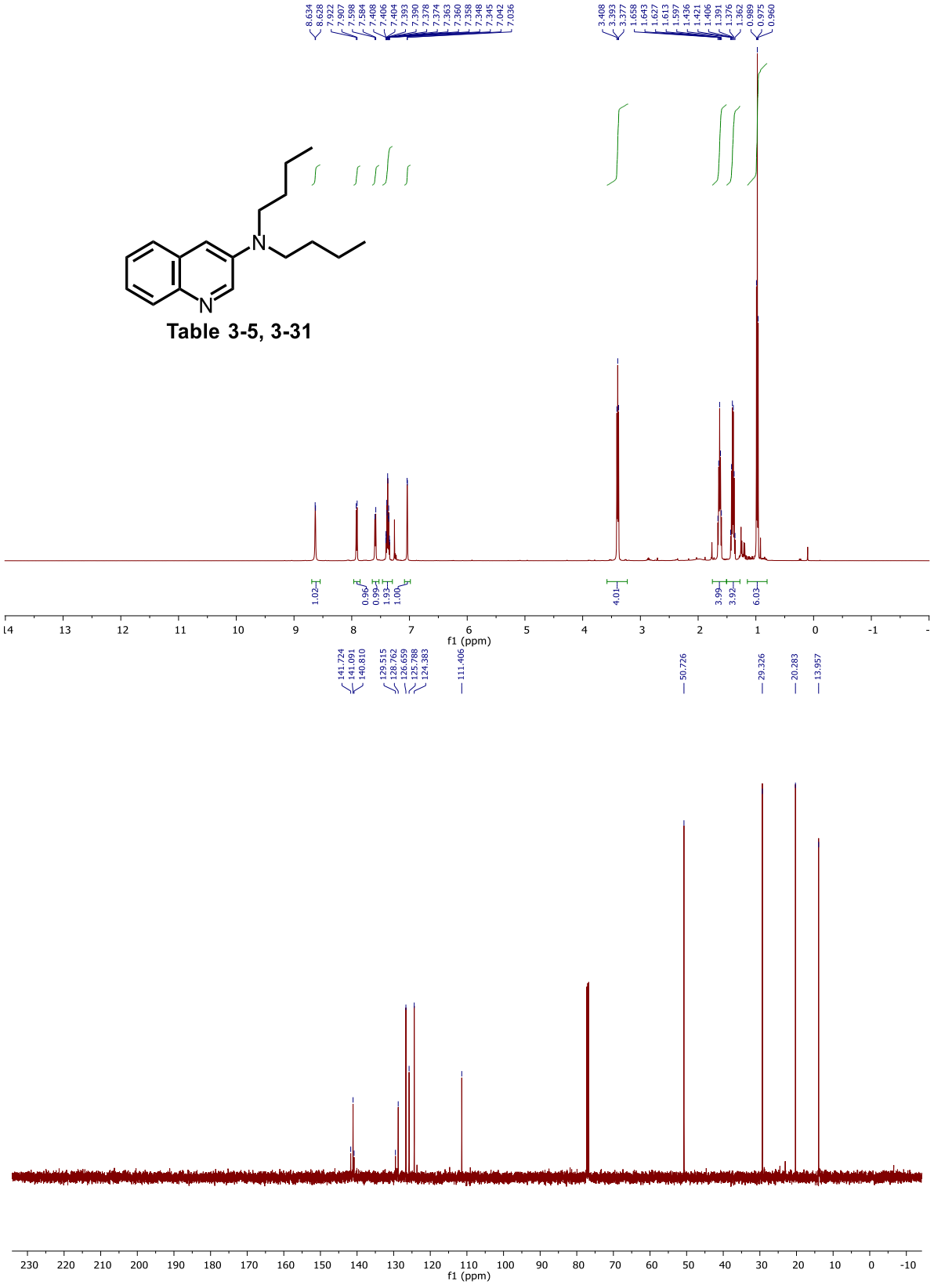

Table 3-5, 1-(4'-methoxy-[1,1'-biphenyl]-4-yl)-4-methylpiperazine (3-32).

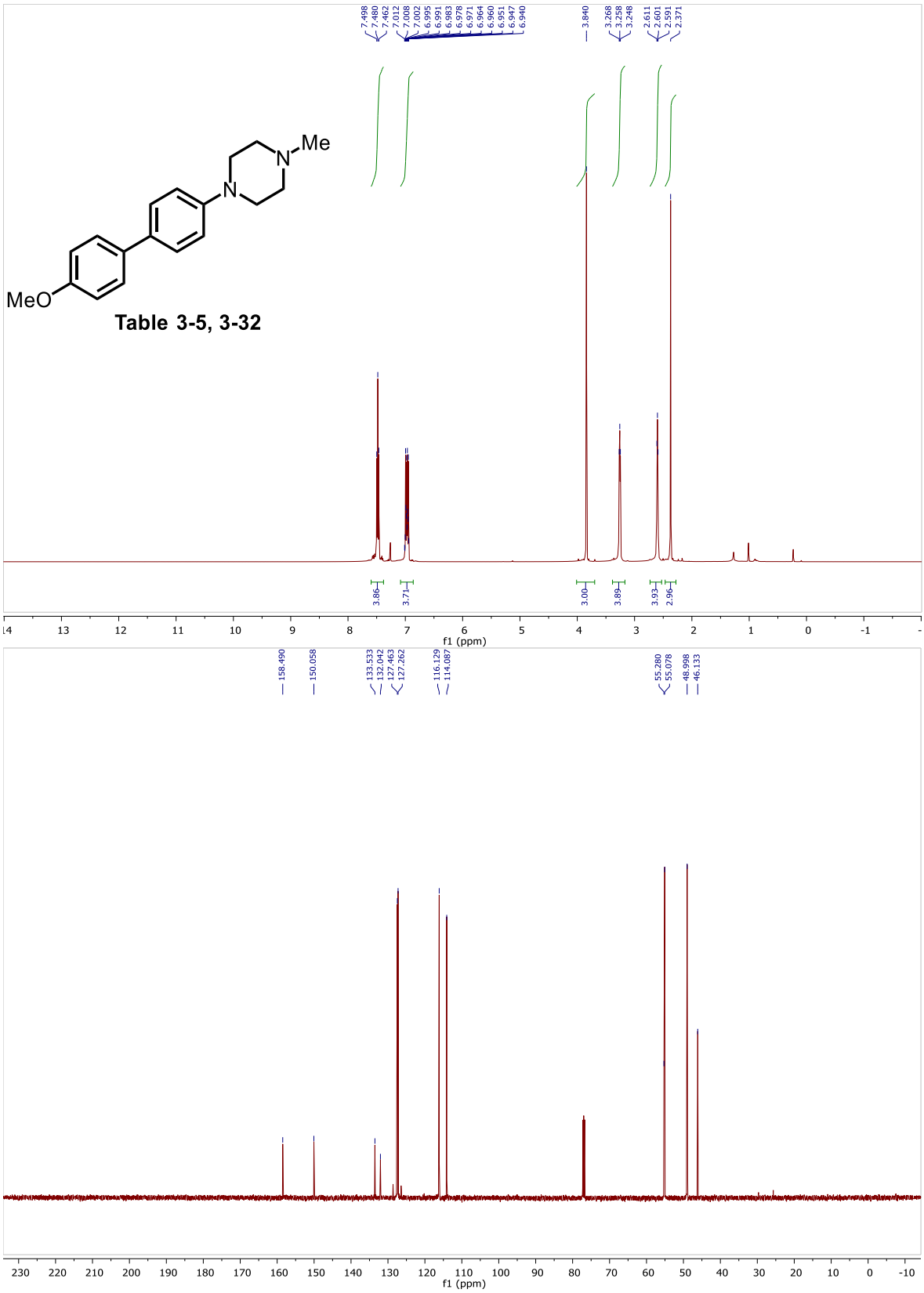

Table, 3-5, *tert*-butyl 4-([1,1'-biphenyl]-3-ylamino)piperidine-1-carboxylate (3-33).

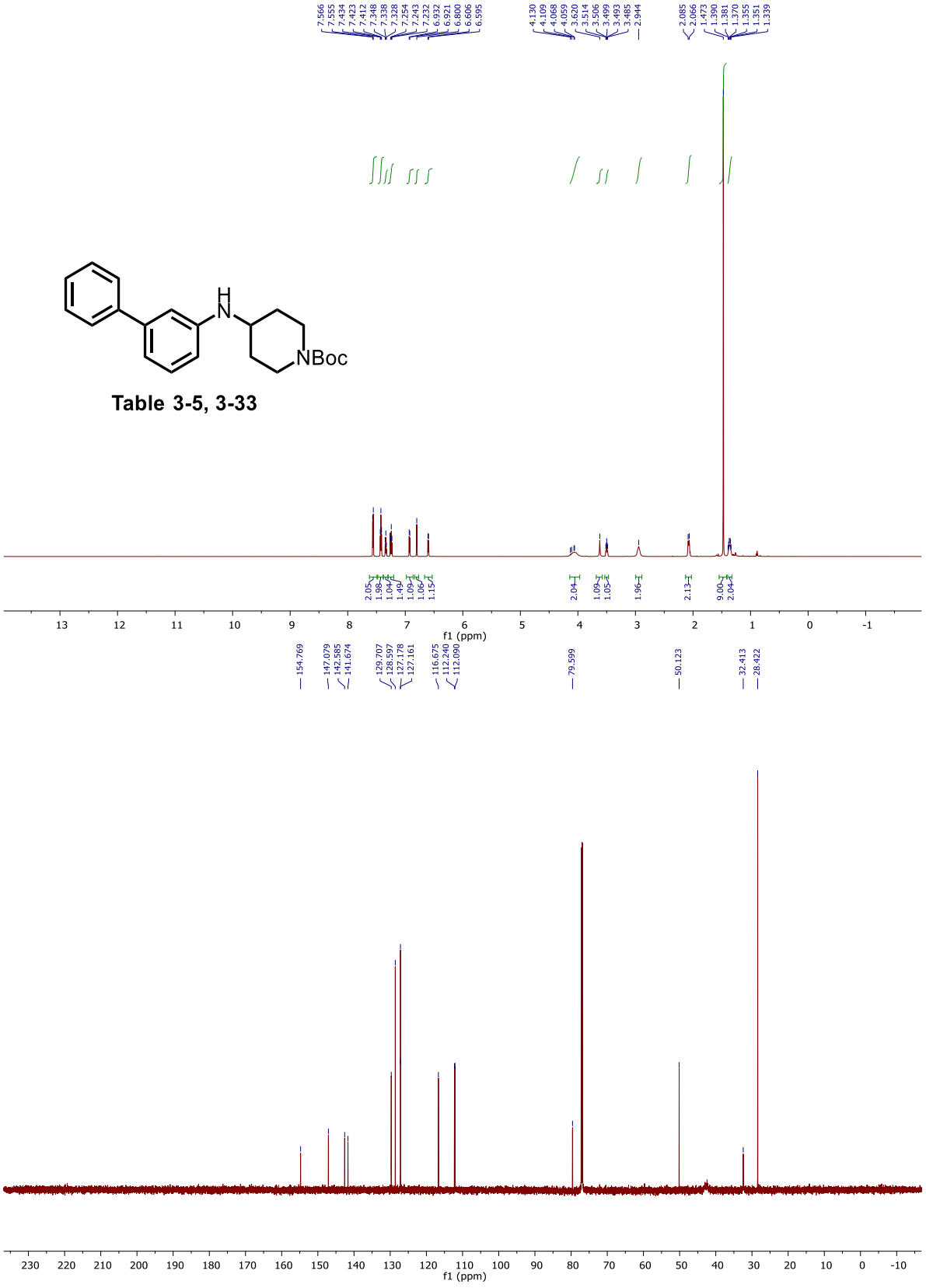

Table 3-5, 4-(3-(2-methylpiperidin-1-yl)phenyl)morpholine (3-34).

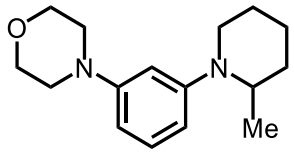

Table 3-5, 3-34

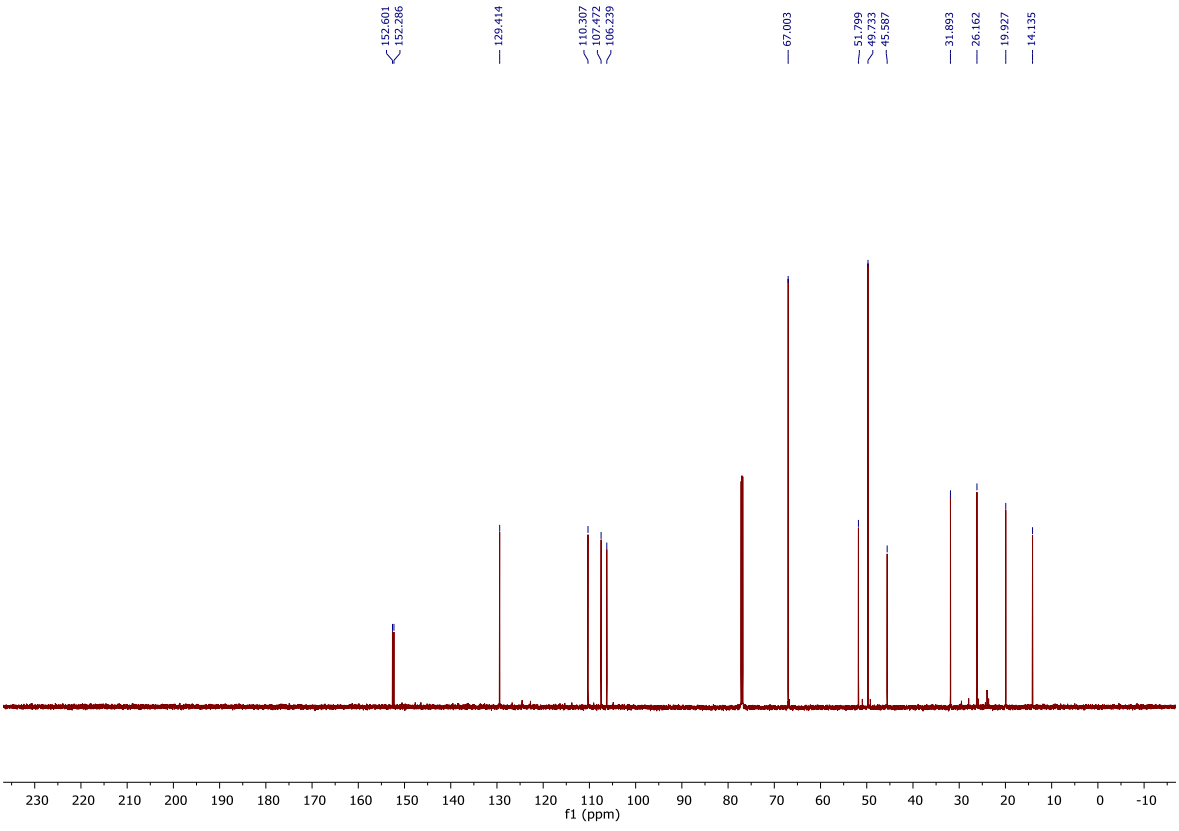

Table 3-5, *N*-(4-(butyl(methyl)amino)phenyl)acetamide (3-35).

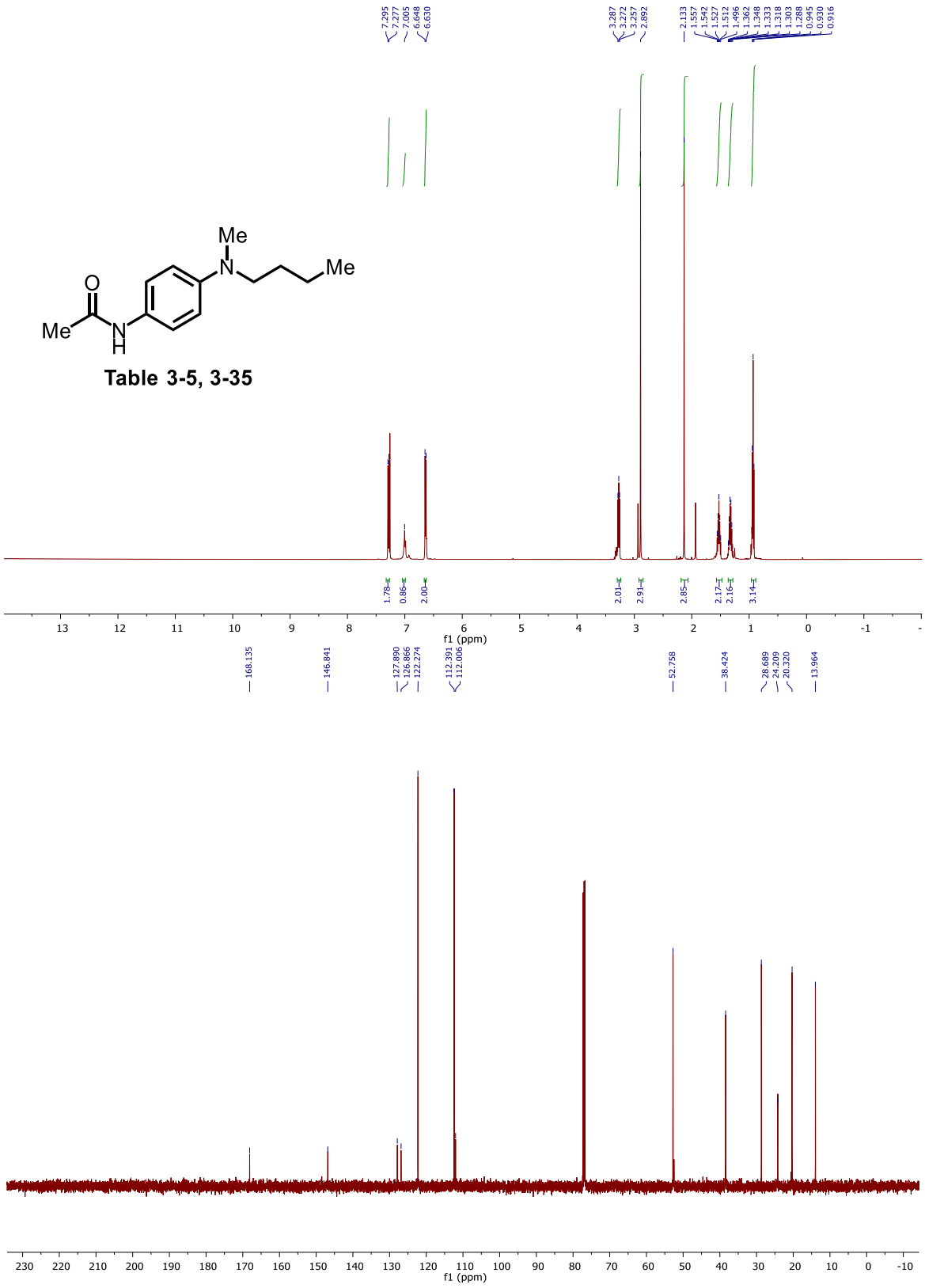

Table 3-5, 1-((8*R*,9*S*,13*S*,14*S*,17*S*)-17-((*tert*-butyldimethylsilyl)oxy)-13-methyl-7,8,9,11,12,13,14,15,16,17-decahydro-6*H*-cyclopenta[a]phenanthren-3-yl)piperidine (3-45).

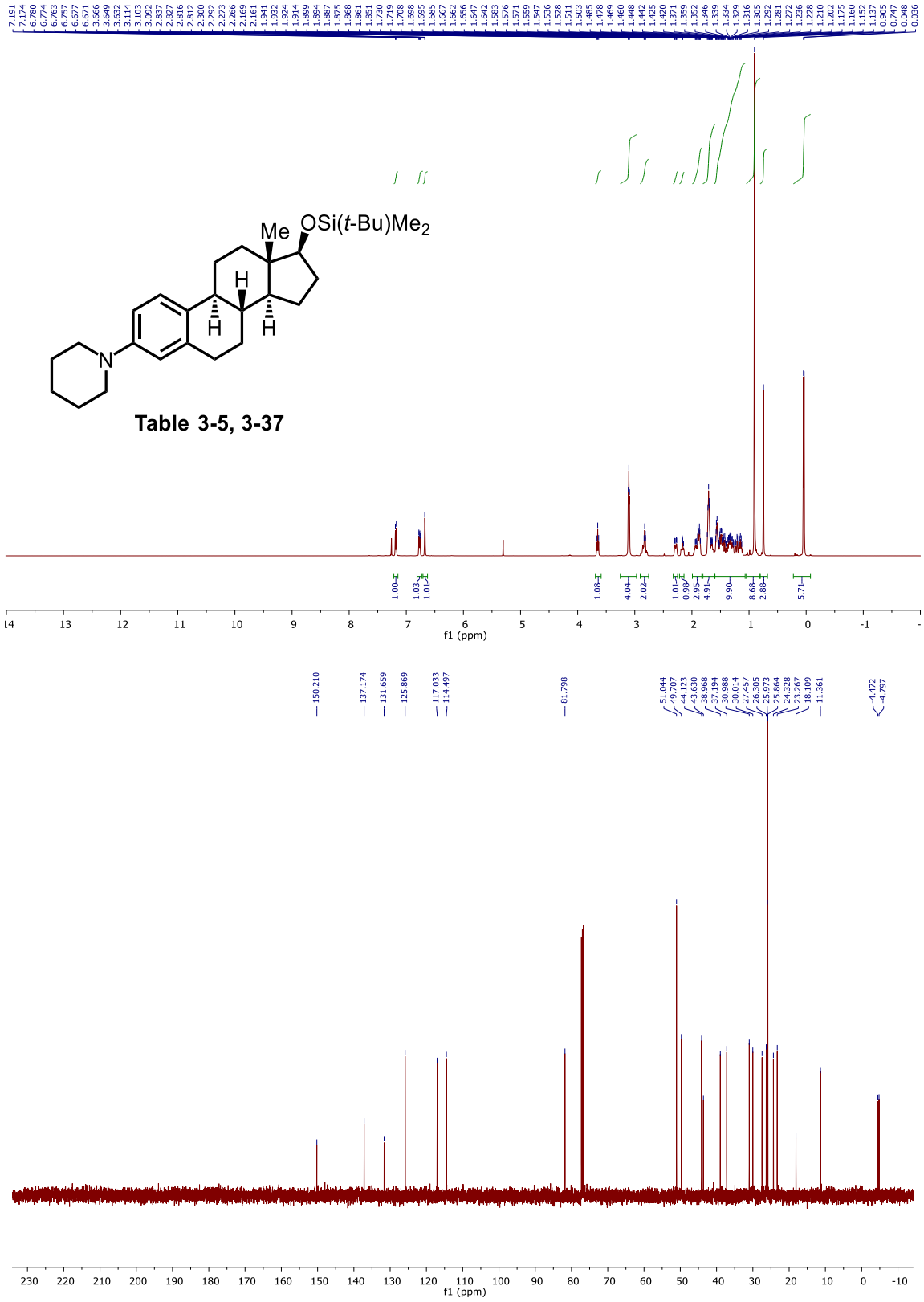

Scheme 4-17, 7-methyl-*N*-octylnaphthalen-2-amine (4-36).

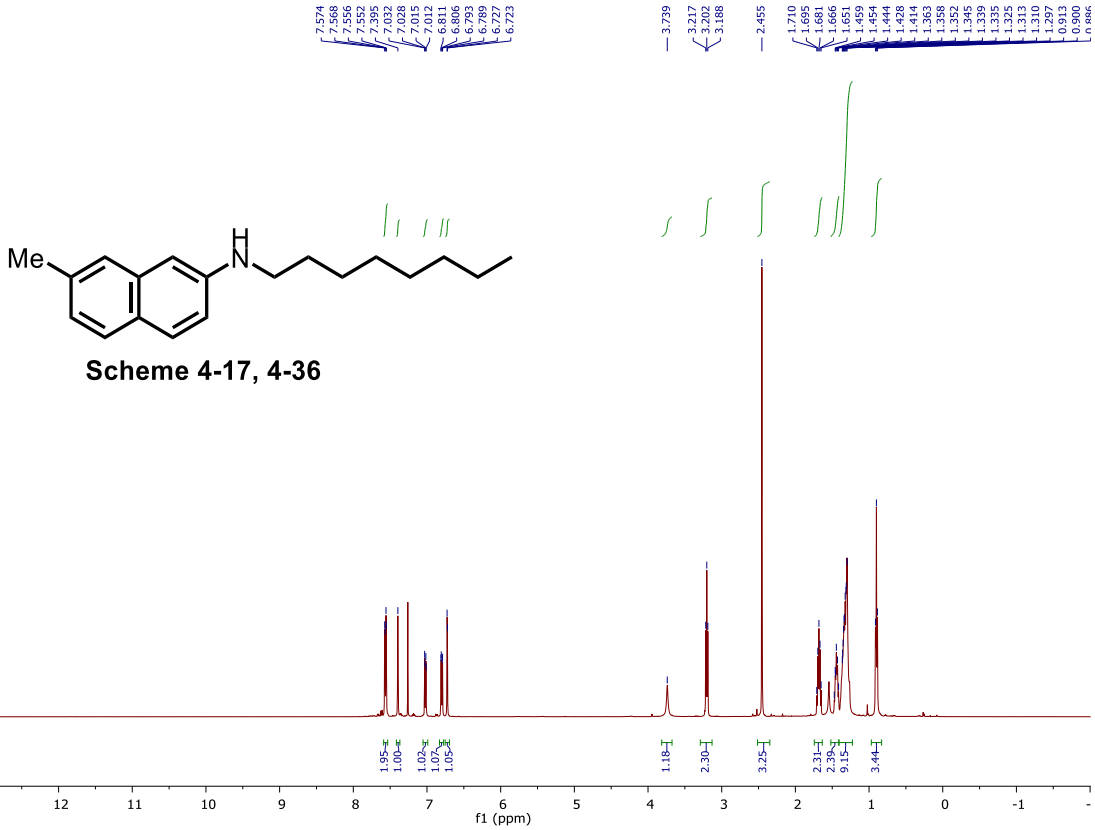

Scheme 4-17, 4-36

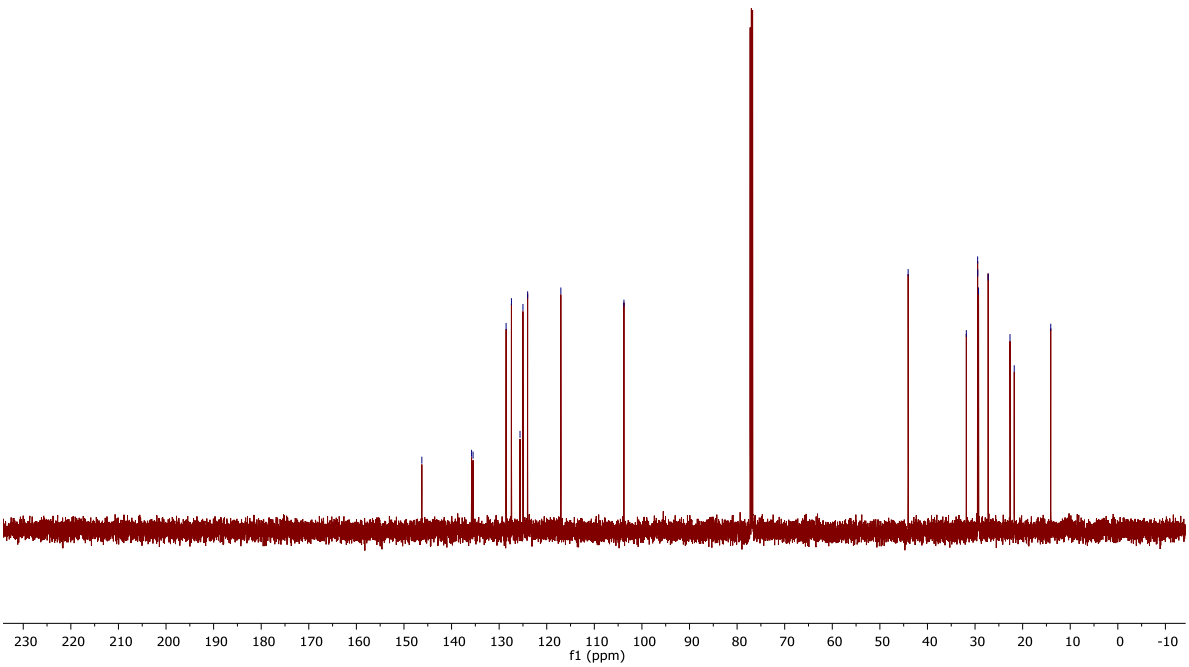

Scheme 4-17, *tert*-butyldimethyl((7-methylnaphthalen-2-yl)oxy)silane (4-37).

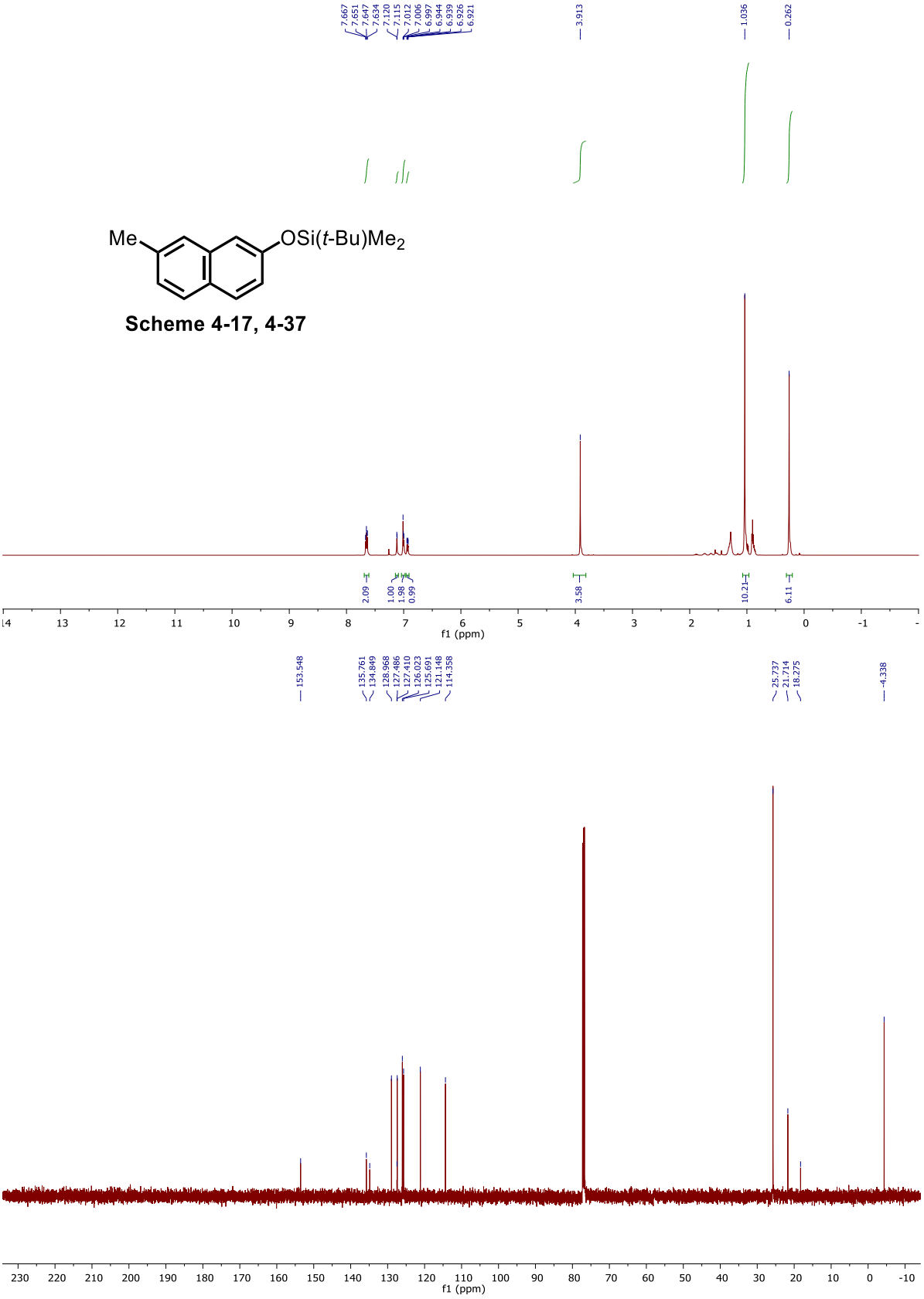

Scheme 4-18, *tert*-butyl((7-methoxynaphthalen-2-yl)oxy)dimethylsilane (4-30).

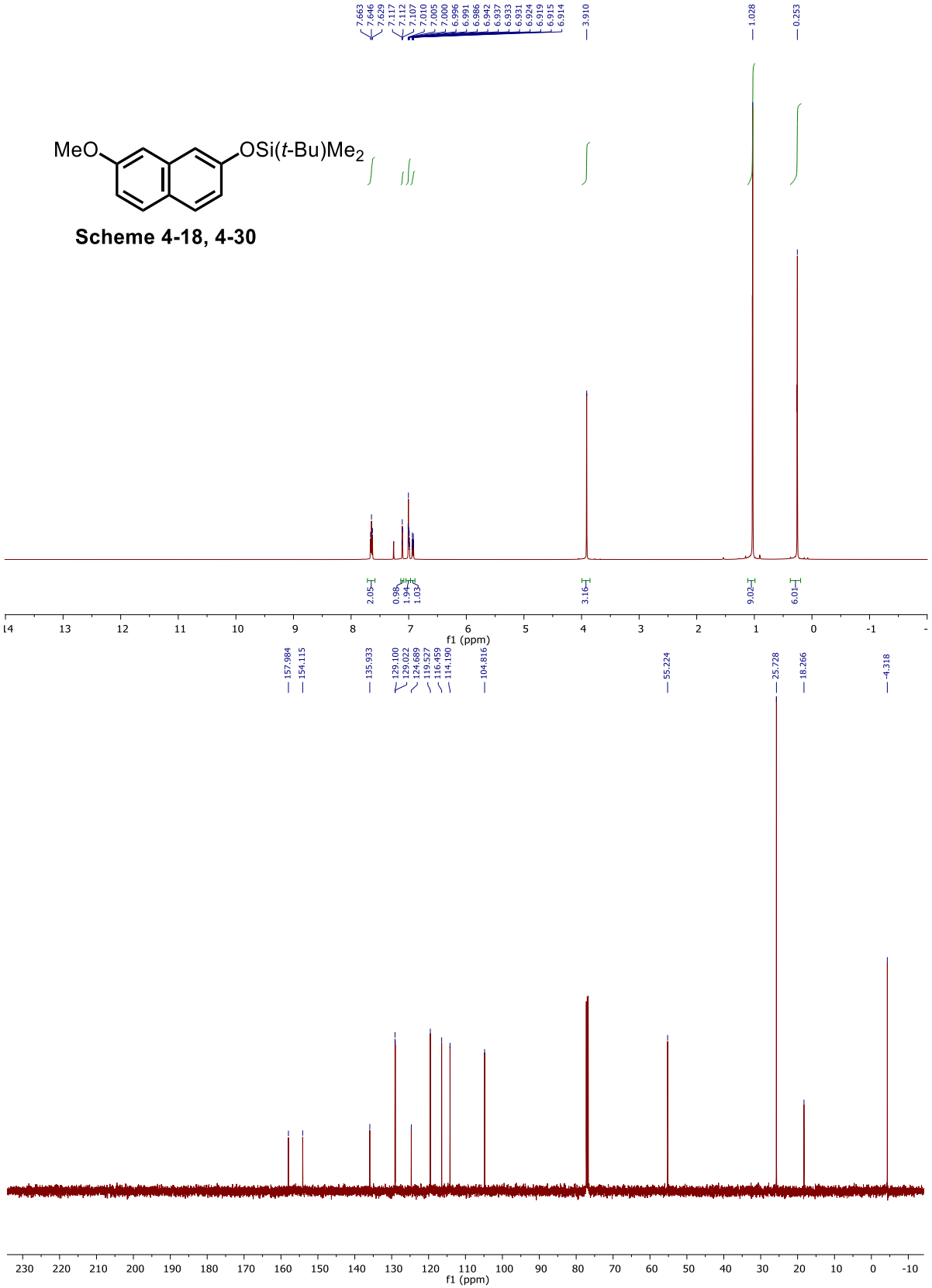

Scheme 4-18, 1-(7-methoxynaphthalen-2-yl)-4-methylpiperazine (4-38).

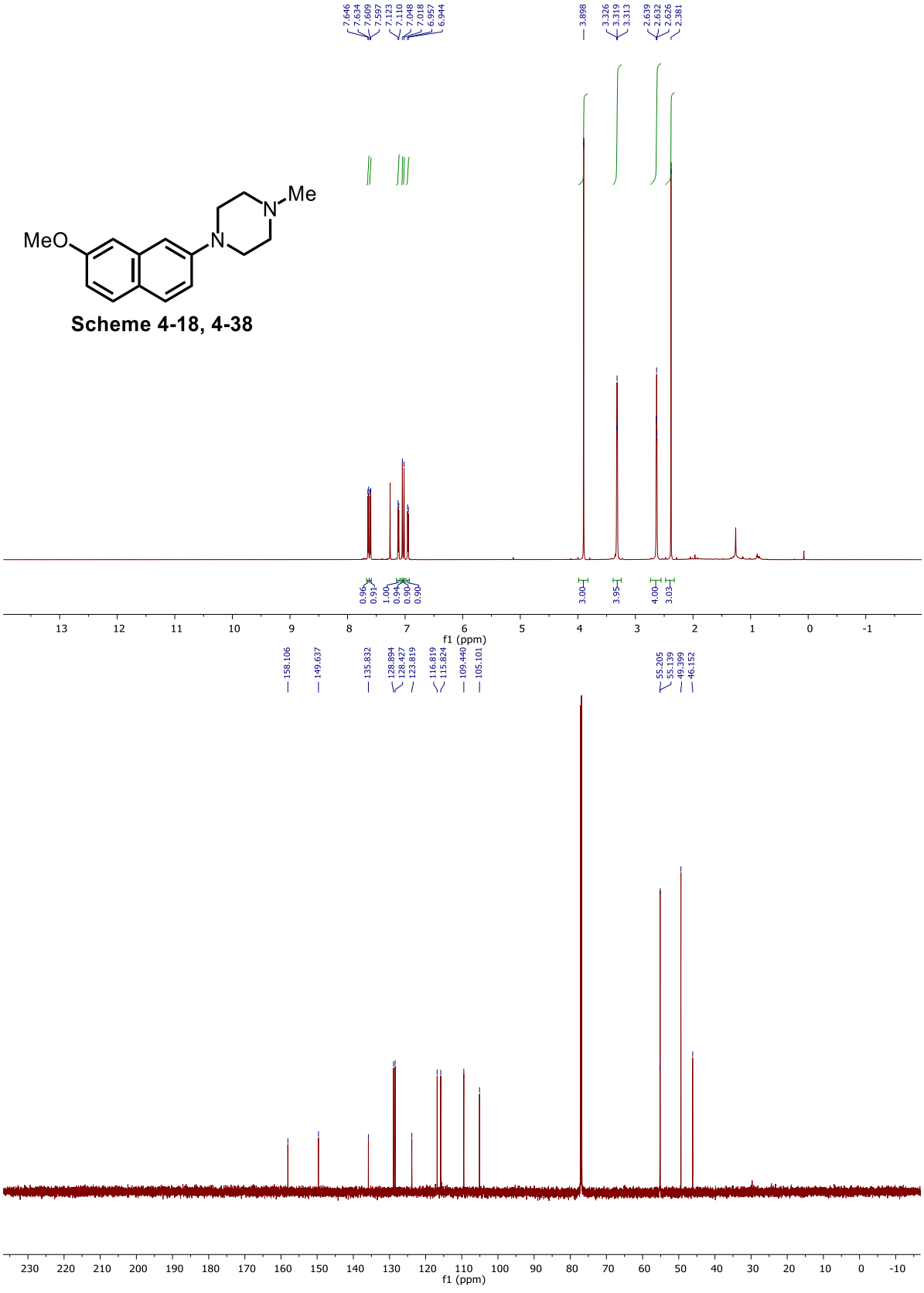

Scheme 4-18, 1-(7-ethylnaphthalen-2-yl)-4-methylpiperazine (4-39).

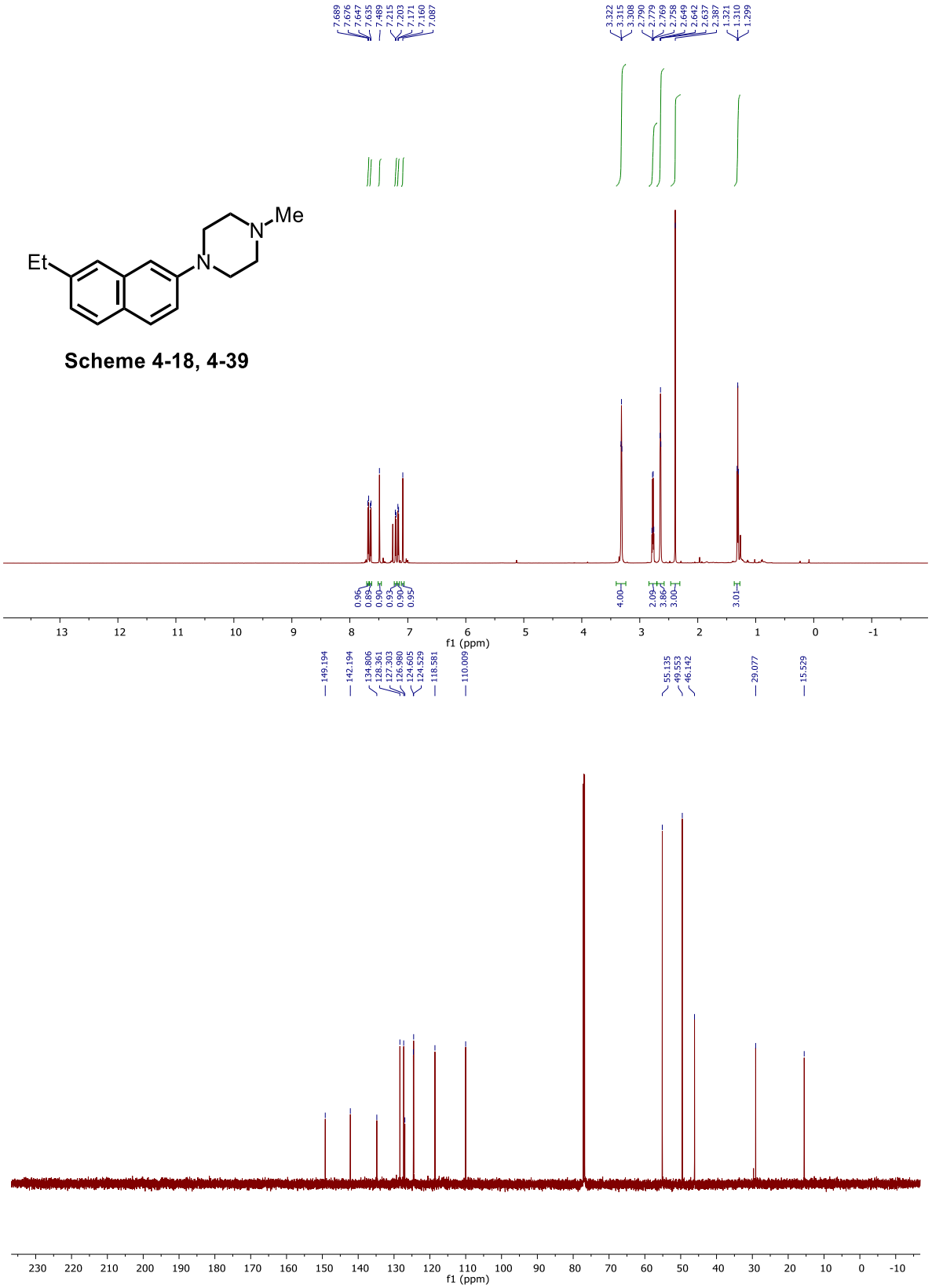

Scheme 4-18, *tert*-butyl((7-ethylnaphthalen-2-yl)oxy)dimethylsilane (4-40).

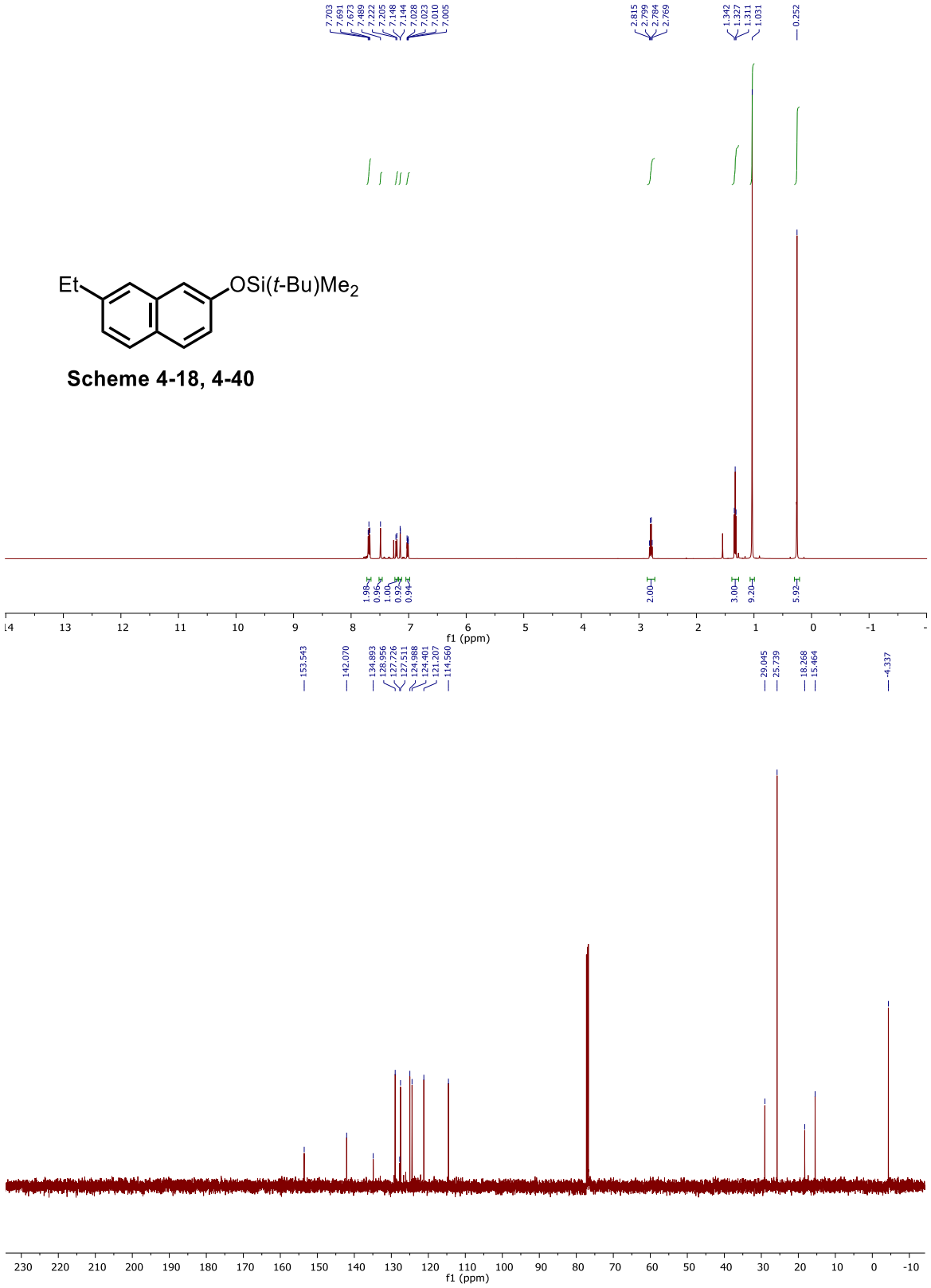

Scheme 4-20, *tert*-butyl((4'-chloro-2'-methoxy-[1,1'-biphenyl]-4-yl)oxy)dimethylsilane (4-46).

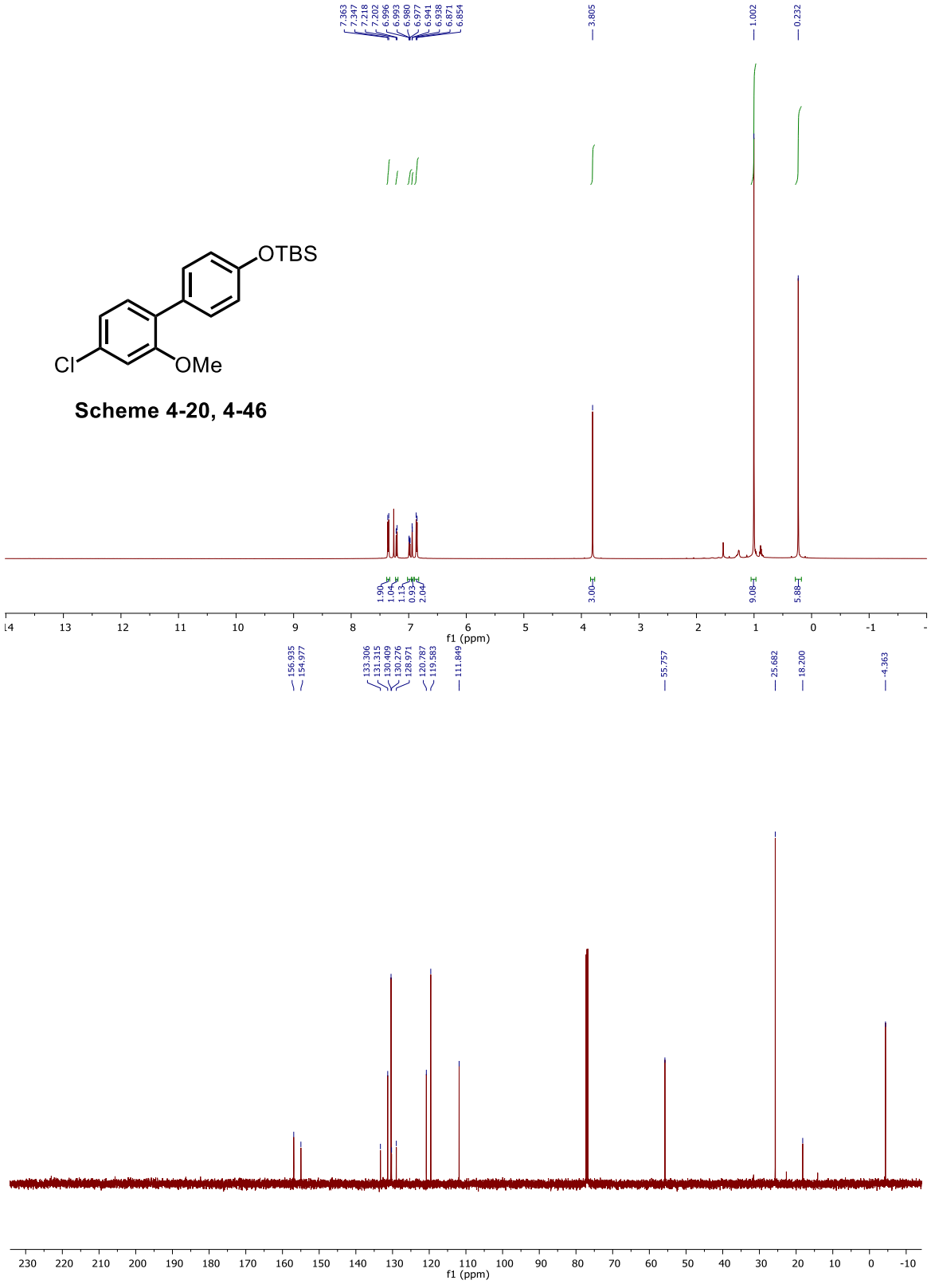

Scheme 4-20, 4-(4'-((*tert*-butyldimethylsilyl)oxy)-2-methoxy-[1,1'-biphenyl]-4-yl)morpholine (4-47).

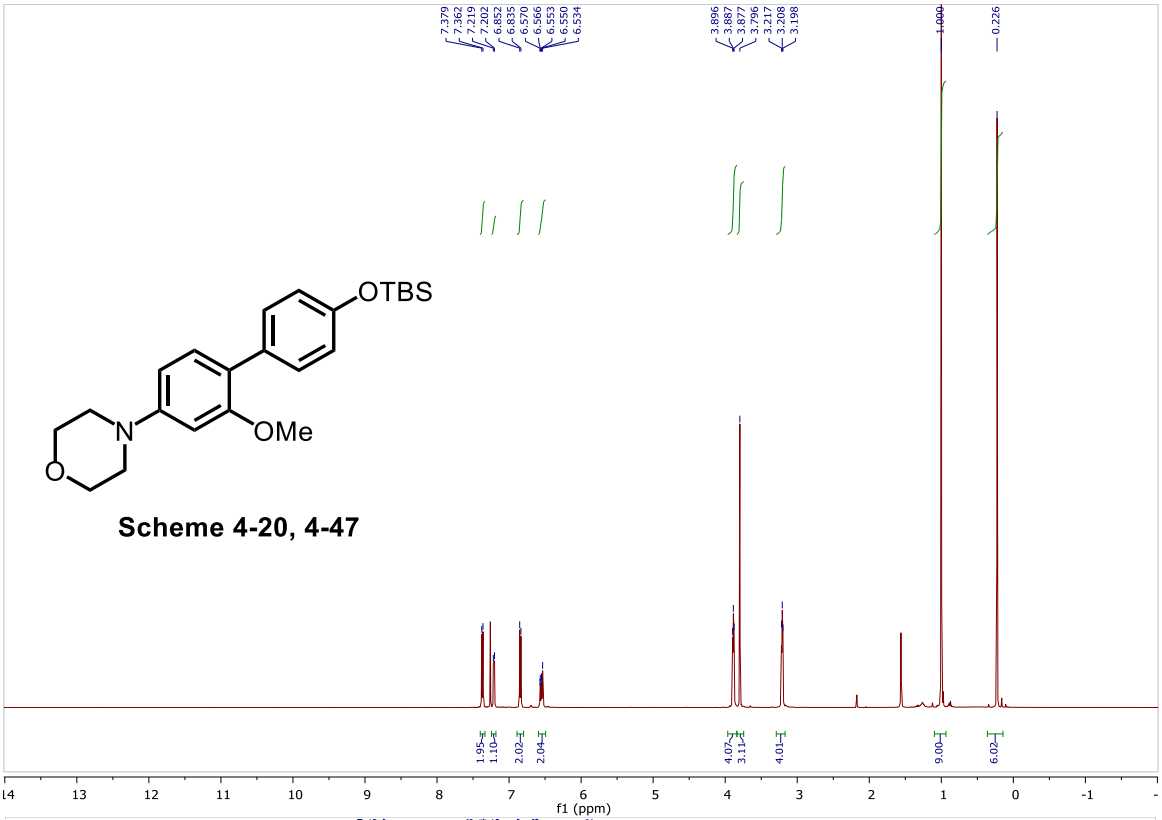

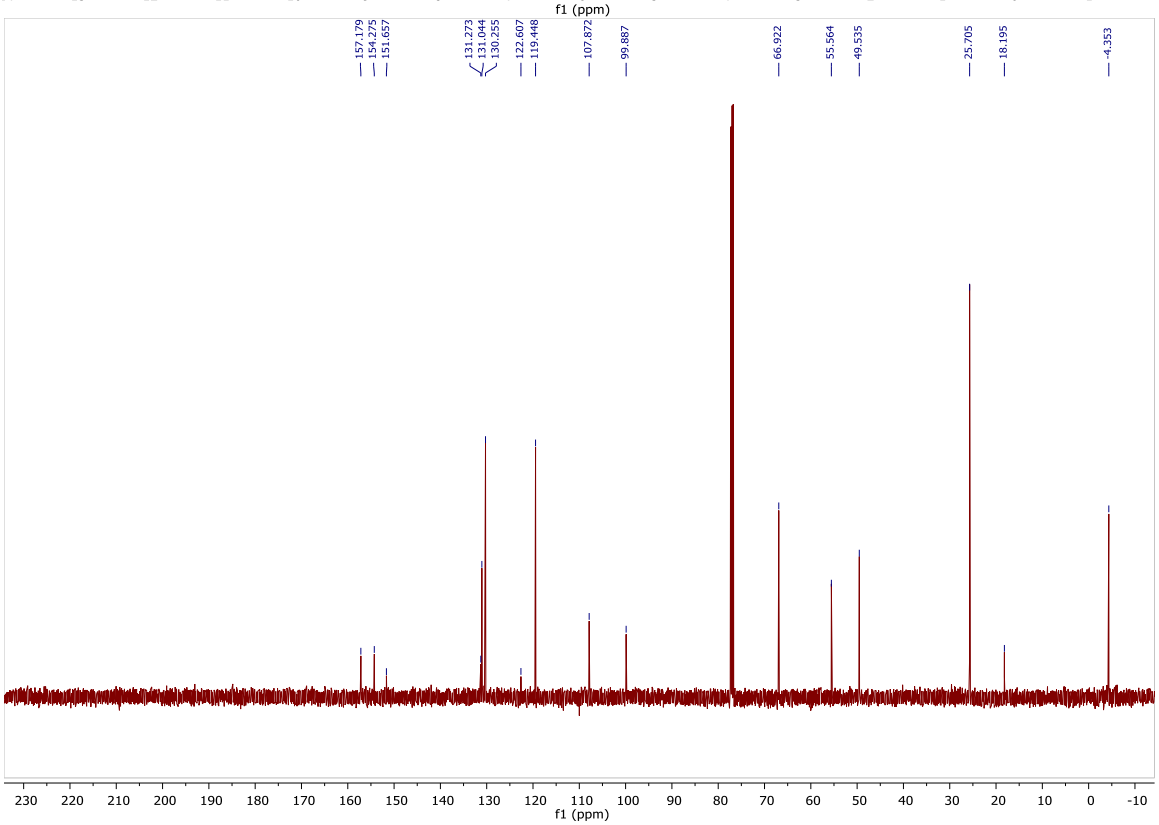

Scheme 4-20, 4-bromo-3-methoxyphenyl pivalate (4-49).

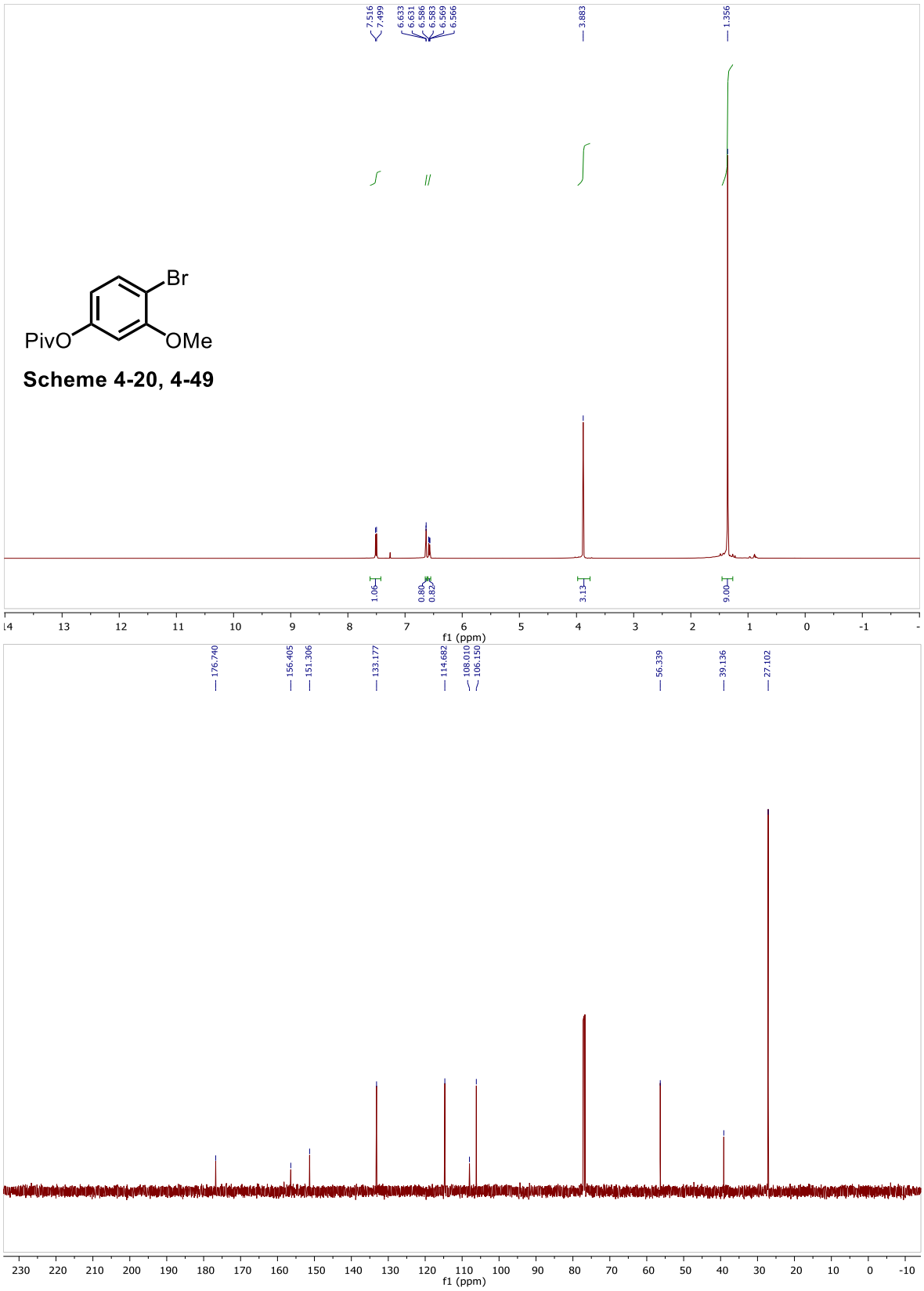

Scheme 4-20, 4'-((*tert*-butyldimethylsilyl)oxy)-2-methoxy-[1,1'-biphenyl]-4-yl pivalate (4-50).

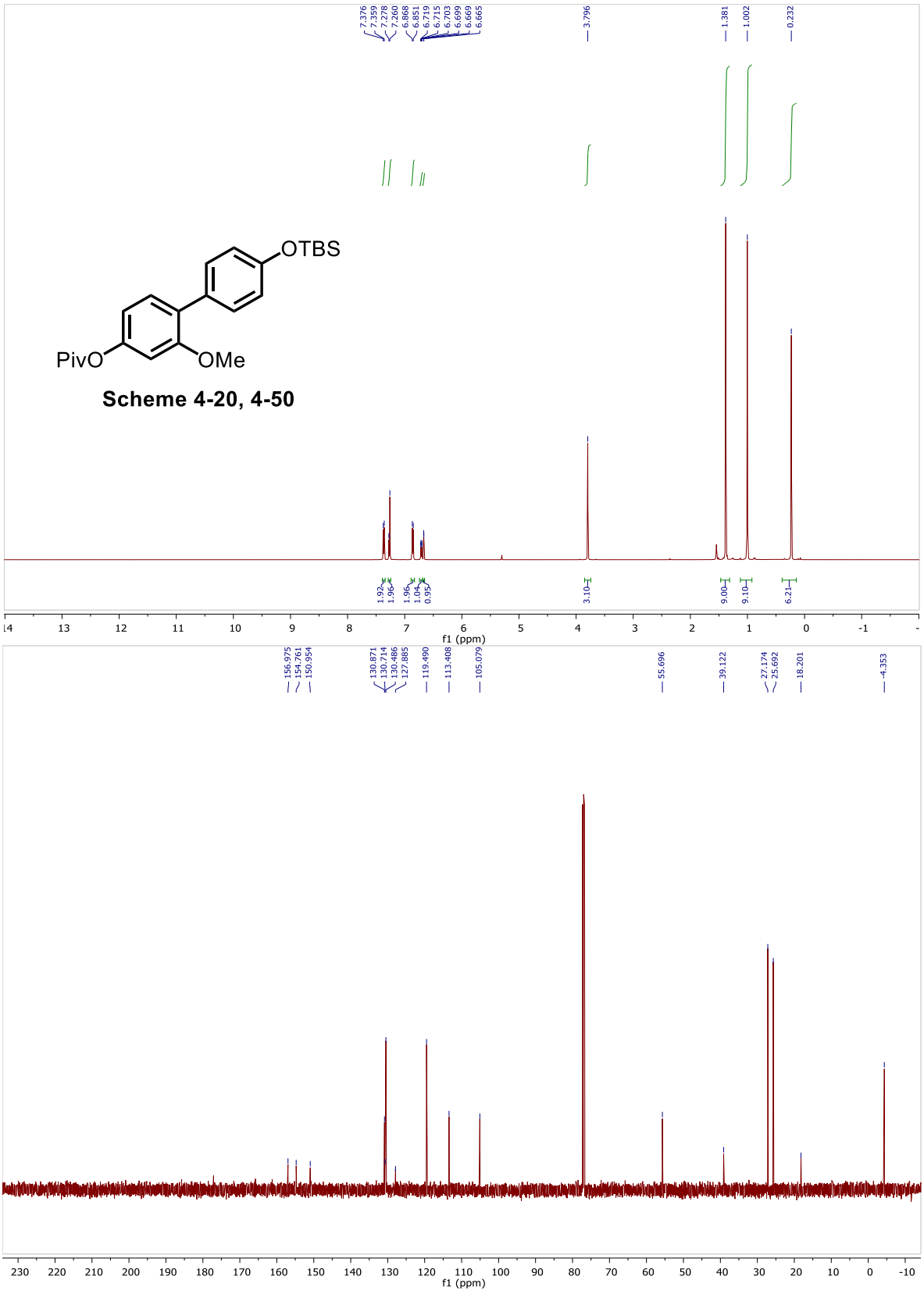

Scheme 4-20, 4-bromo-3-methoxyphenyl diethylcarbamate (4-51).

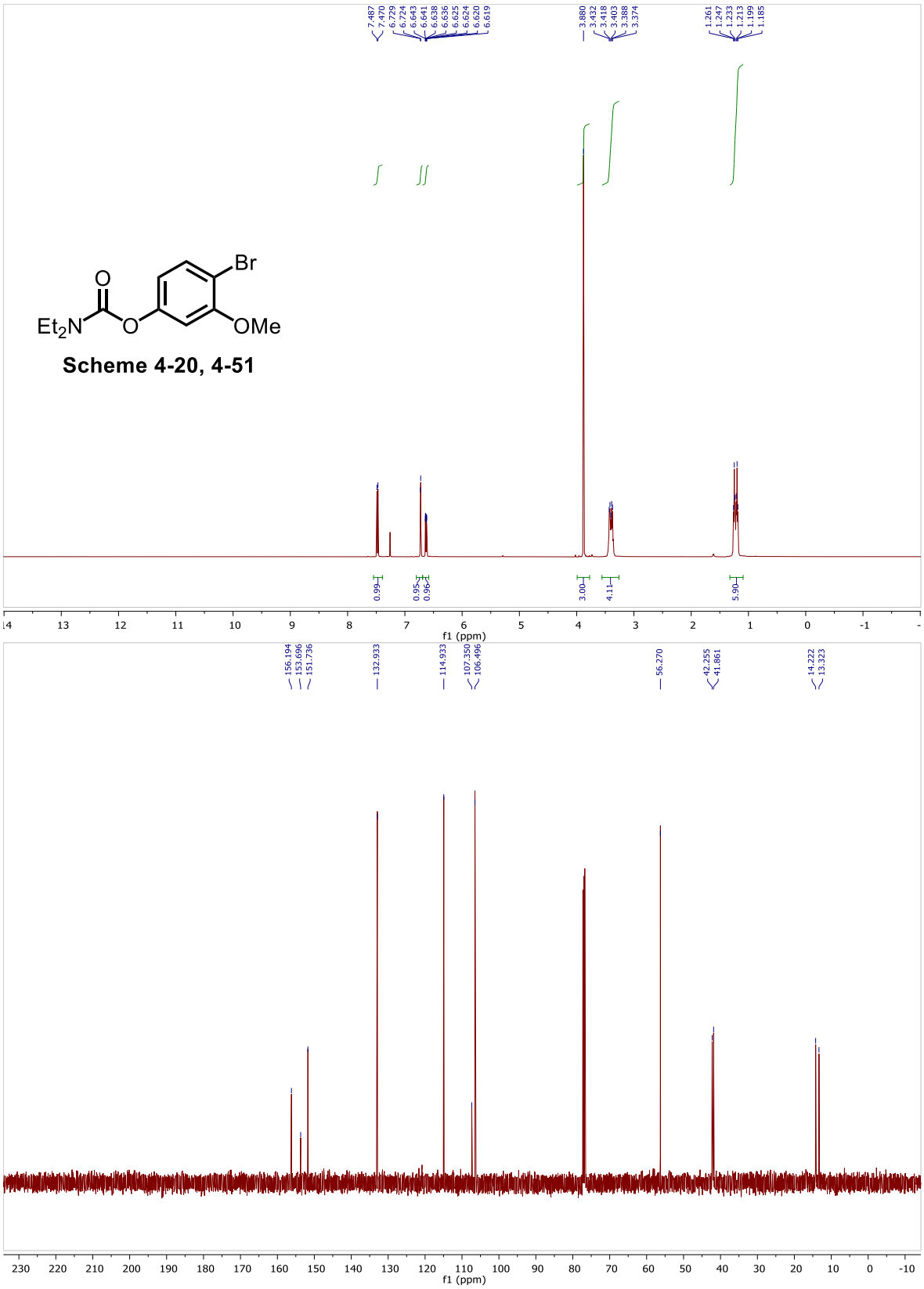

Scheme 4-20, 4'-((*tert*-butyldimethylsilyl)oxy)-2-methoxy-[1,1'-biphenyl]-4-yl diethylcarbamate (4-52).

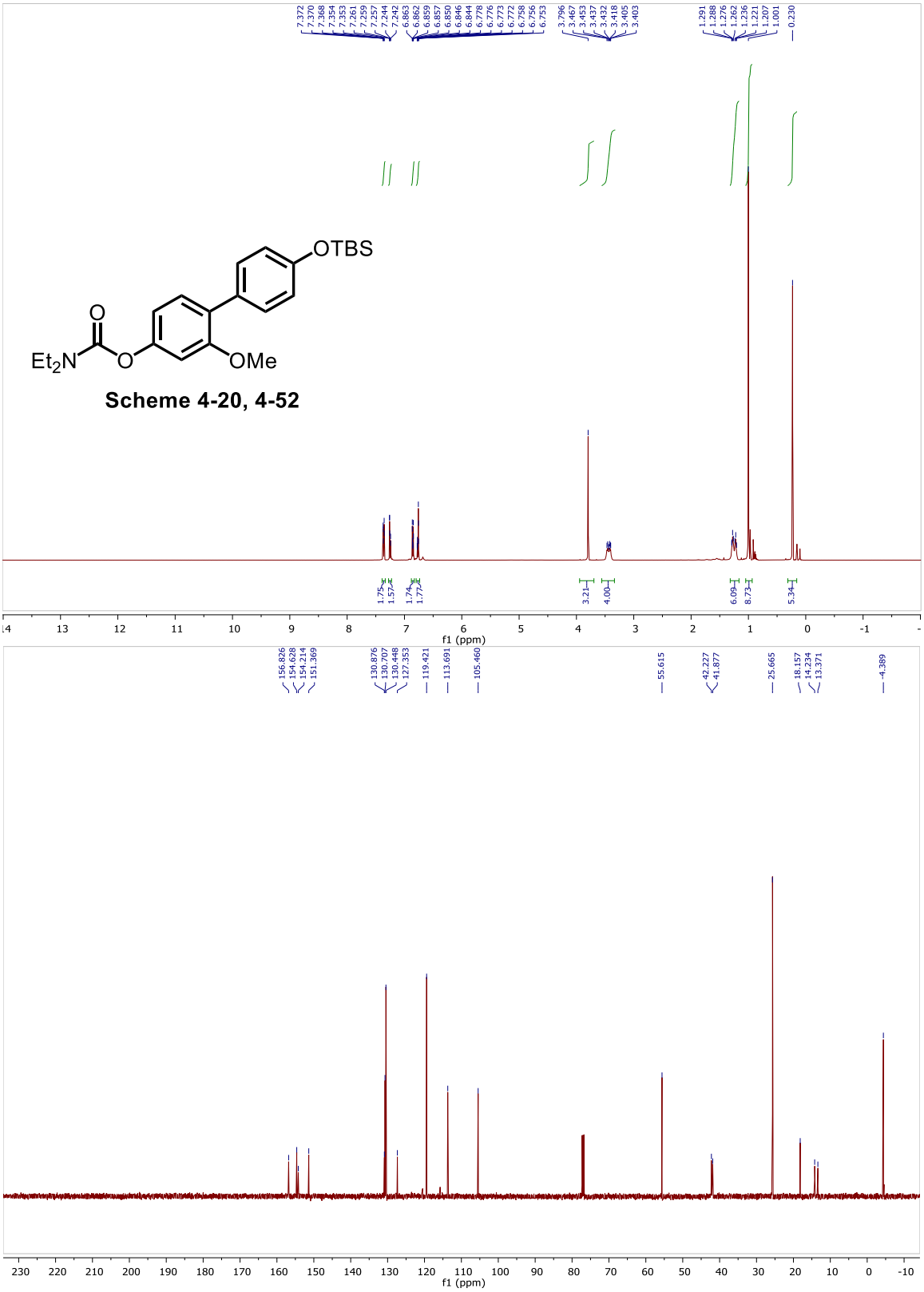

Scheme 4-21, 4-(2-methoxy-4'-(4-methylpiperazin-1-yl)-[1,1'-biphenyl]-4-yl)morpholine (4-53).

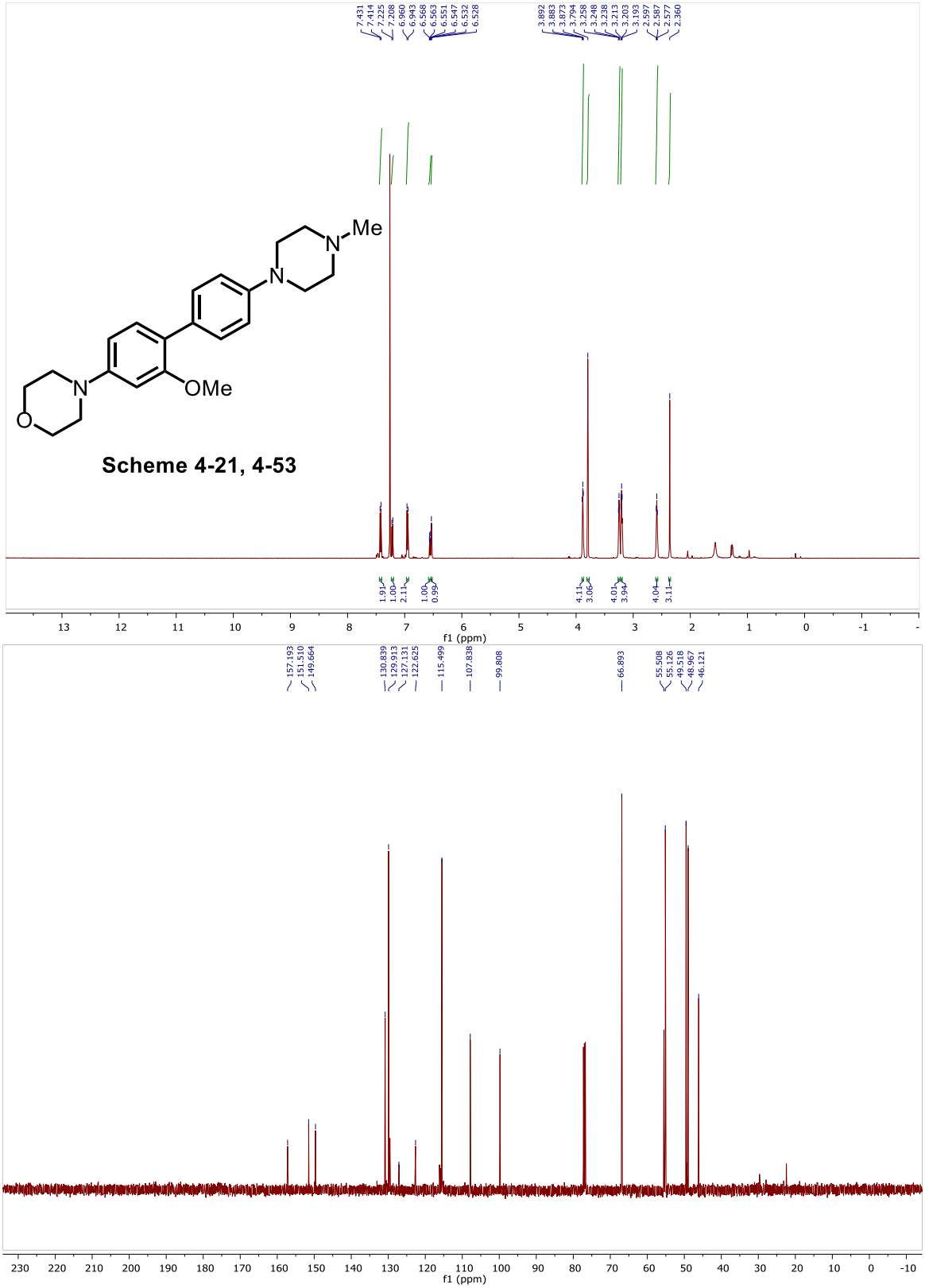

Scheme 4-21, 2'-methoxy-4'-morpholino-*N*-octyl-[1,1'-biphenyl]-4-amine (4-54).

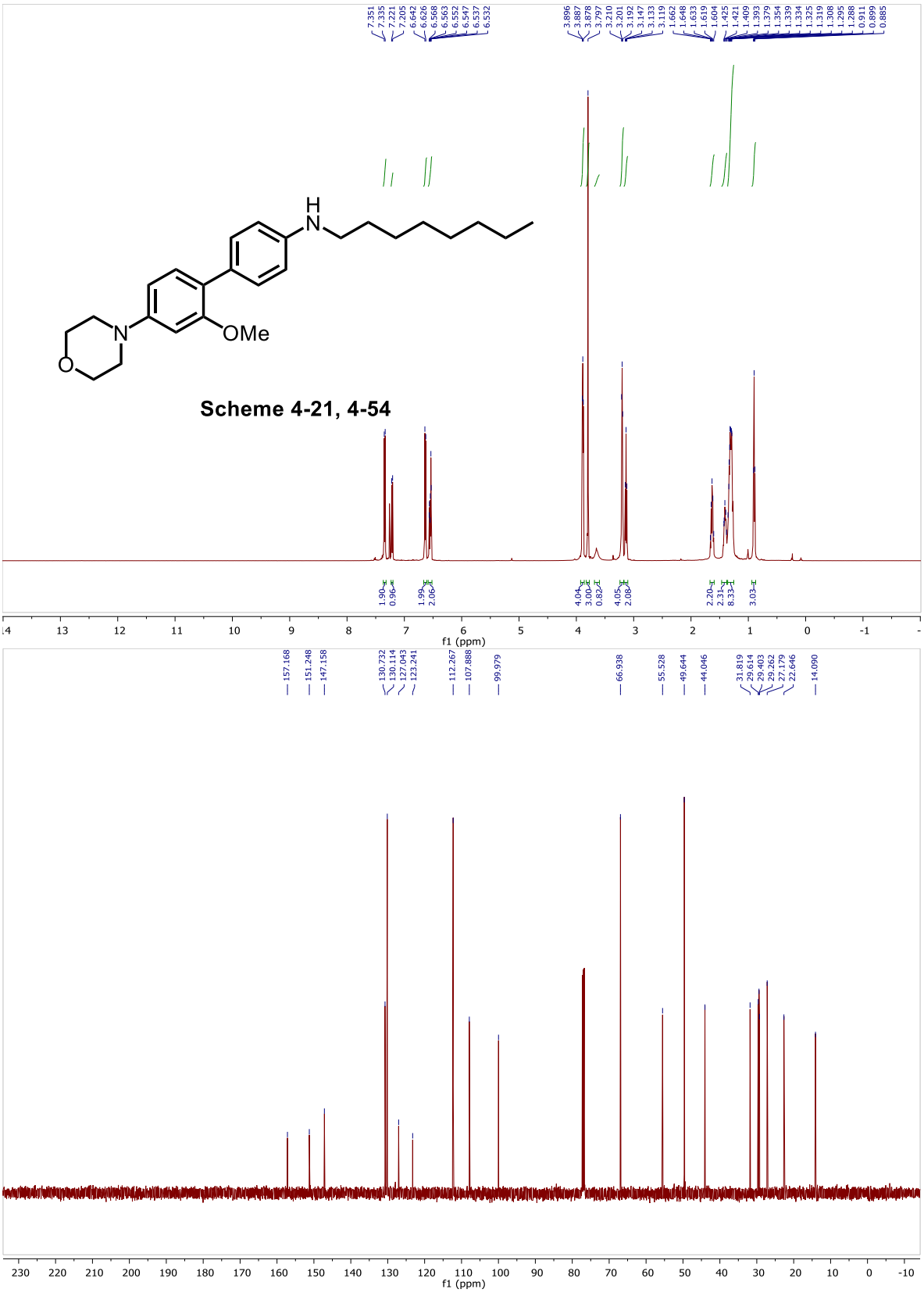

Scheme 4-21, 4-(2-methoxy-4'-(triethylsilyl)-[1,1'-biphenyl]-4-yl)morpholine (4-55).

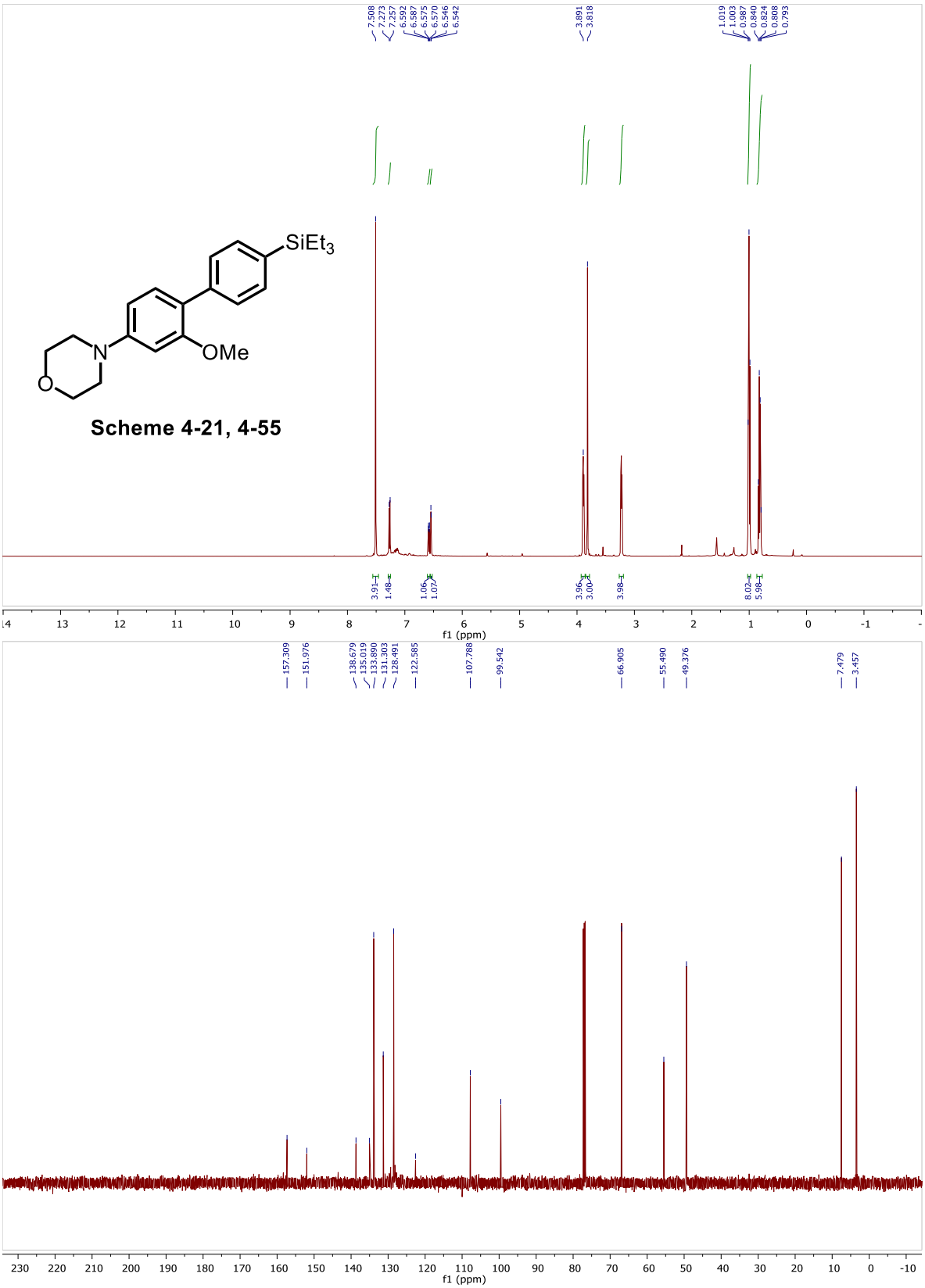

Scheme 4-21, 4-(4'-(triethylsilyl)-2-((trimethylsilyl)methyl)-[1,1'-biphenyl]-4-yl)morpholine(4-56).

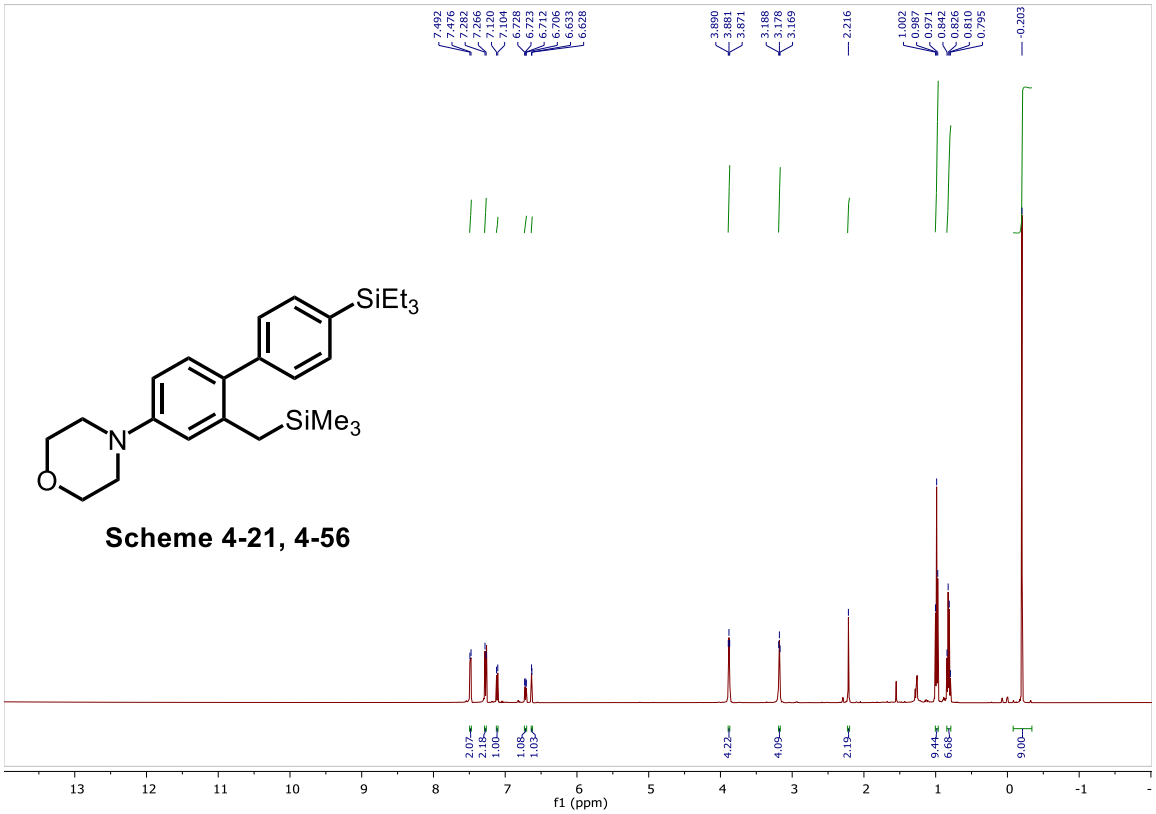

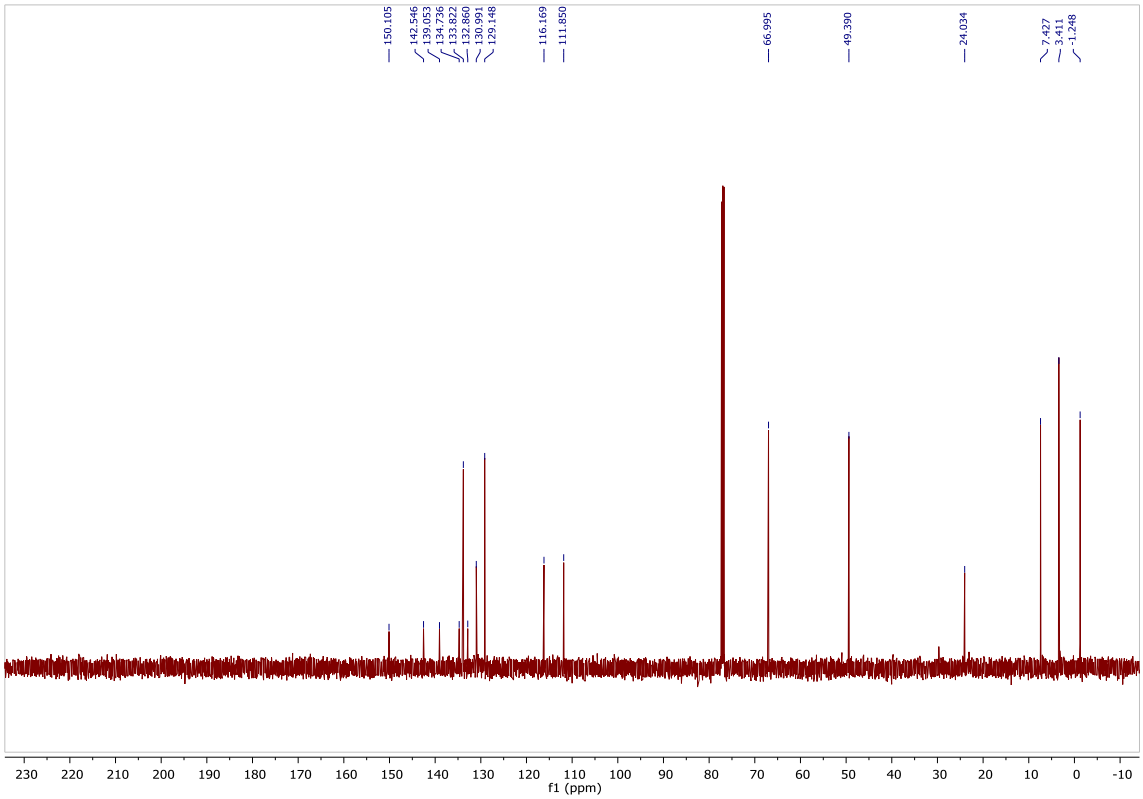

Scheme 4-23, 2-bromo-6-methoxynaphthalene (4-58).

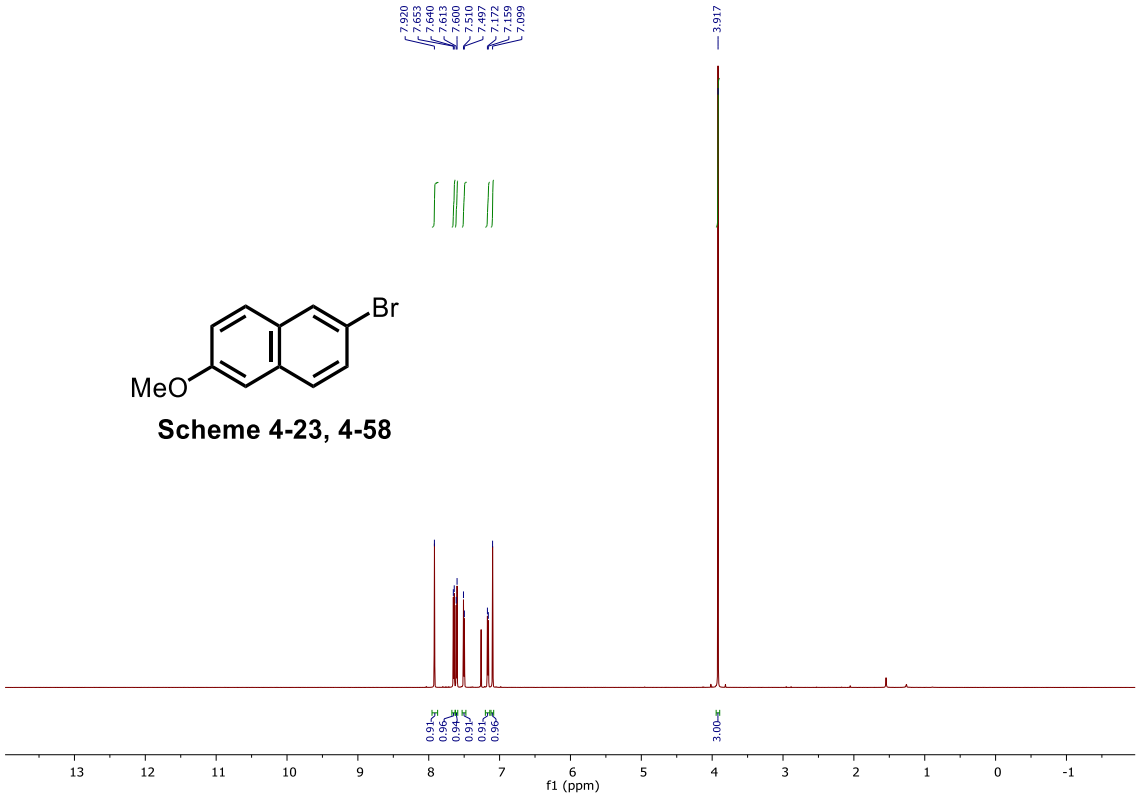

Scheme 4-23, 4-58

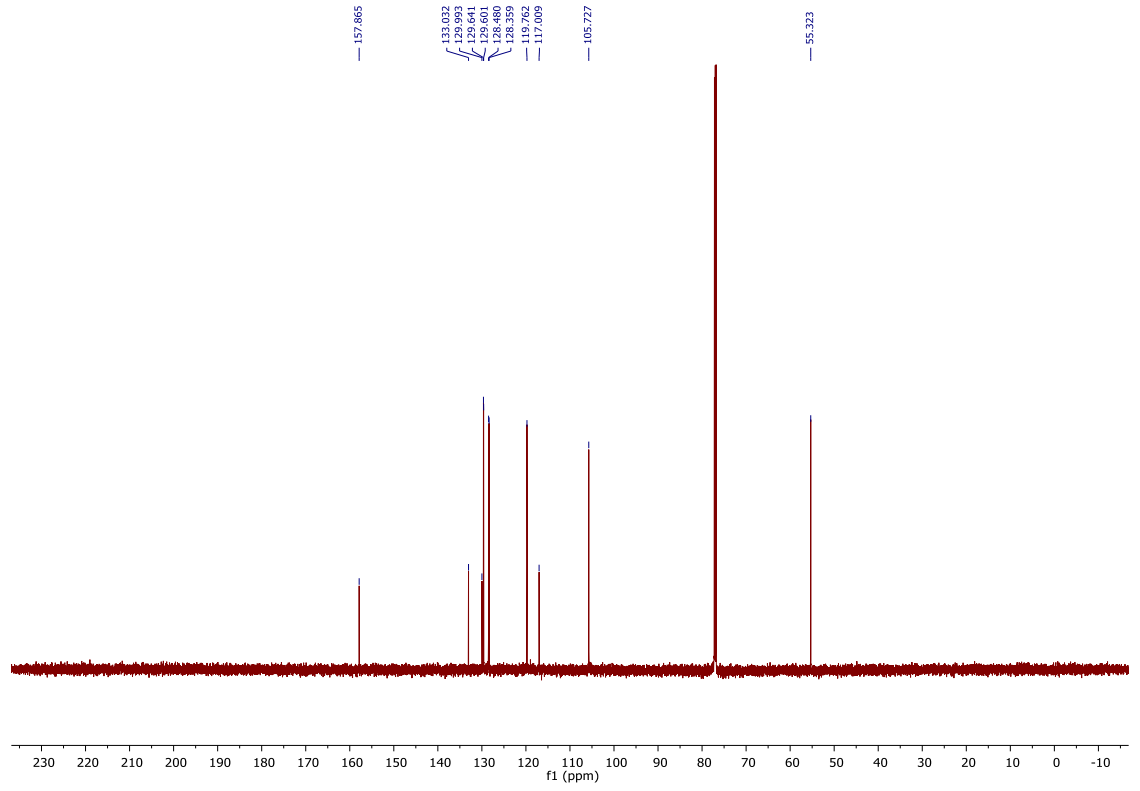

Scheme 4-23, *tert*-butyl(3-chloro-4-(6-methoxynaphthalen-2-yl)phenoxy)dimethylsilane (4-60).

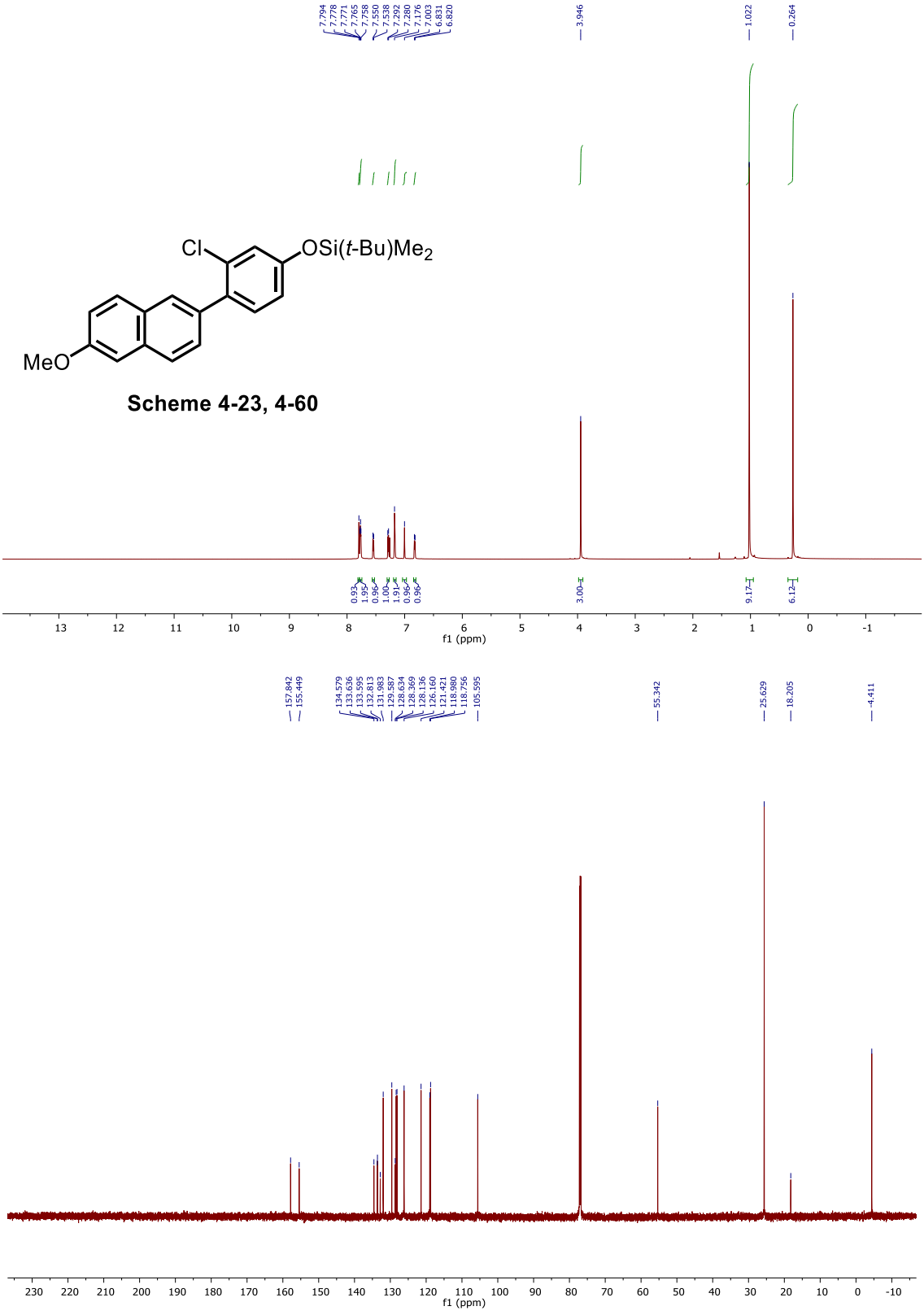

Scheme 4-23, 5-((*tert*-butyldimethylsilyl)oxy)-2-(6-methoxynaphthalen-2-yl)-*N*-phenylanilinedimethylsilane (4-63).

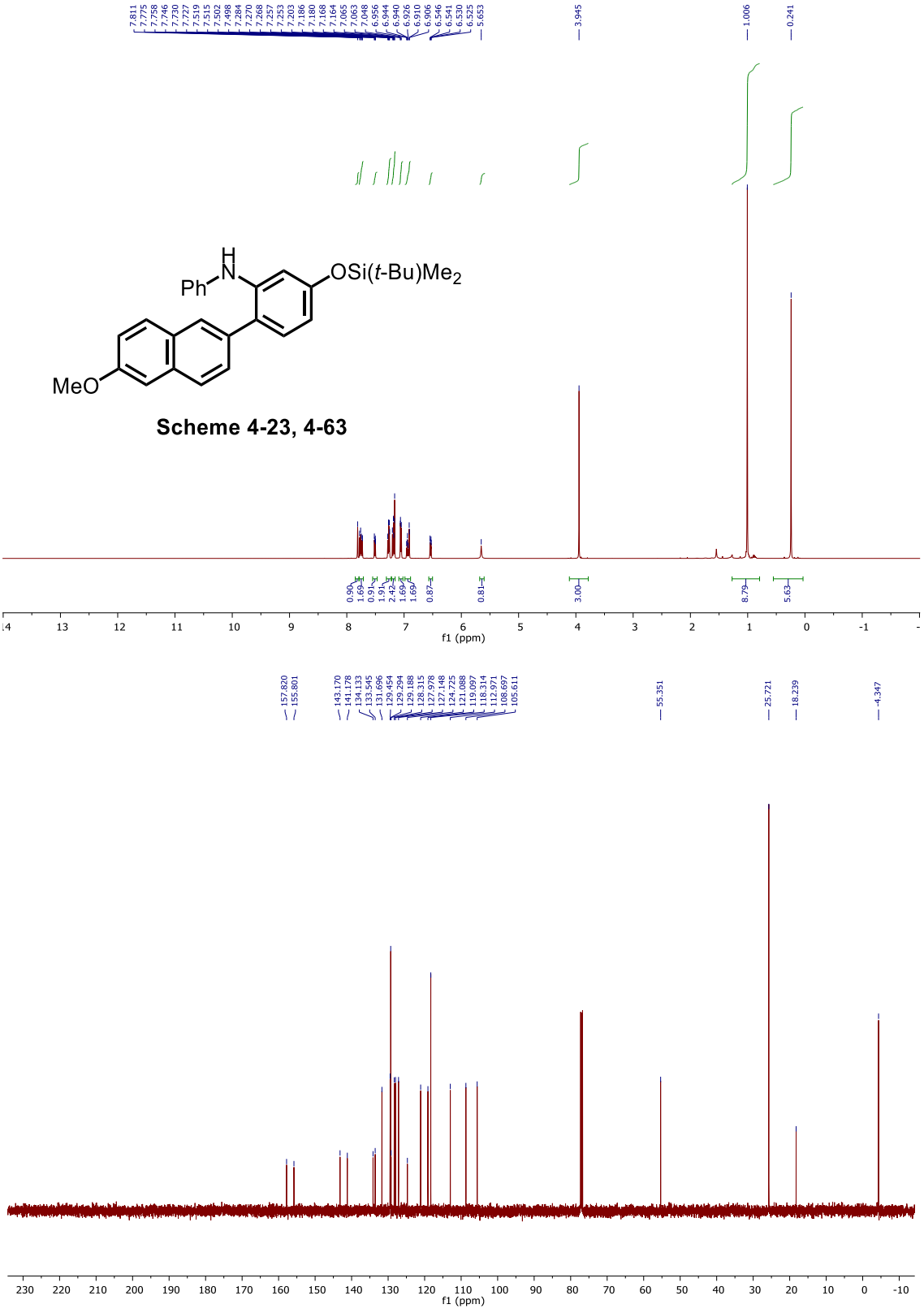

Scheme 4-23, 4-63

Scheme 4-23, 5-((*tert*-butyldimethylsilyl)oxy)-2-(6-ethylnaphthalen-2-yl)-*N*-phenylaniline (4-64).

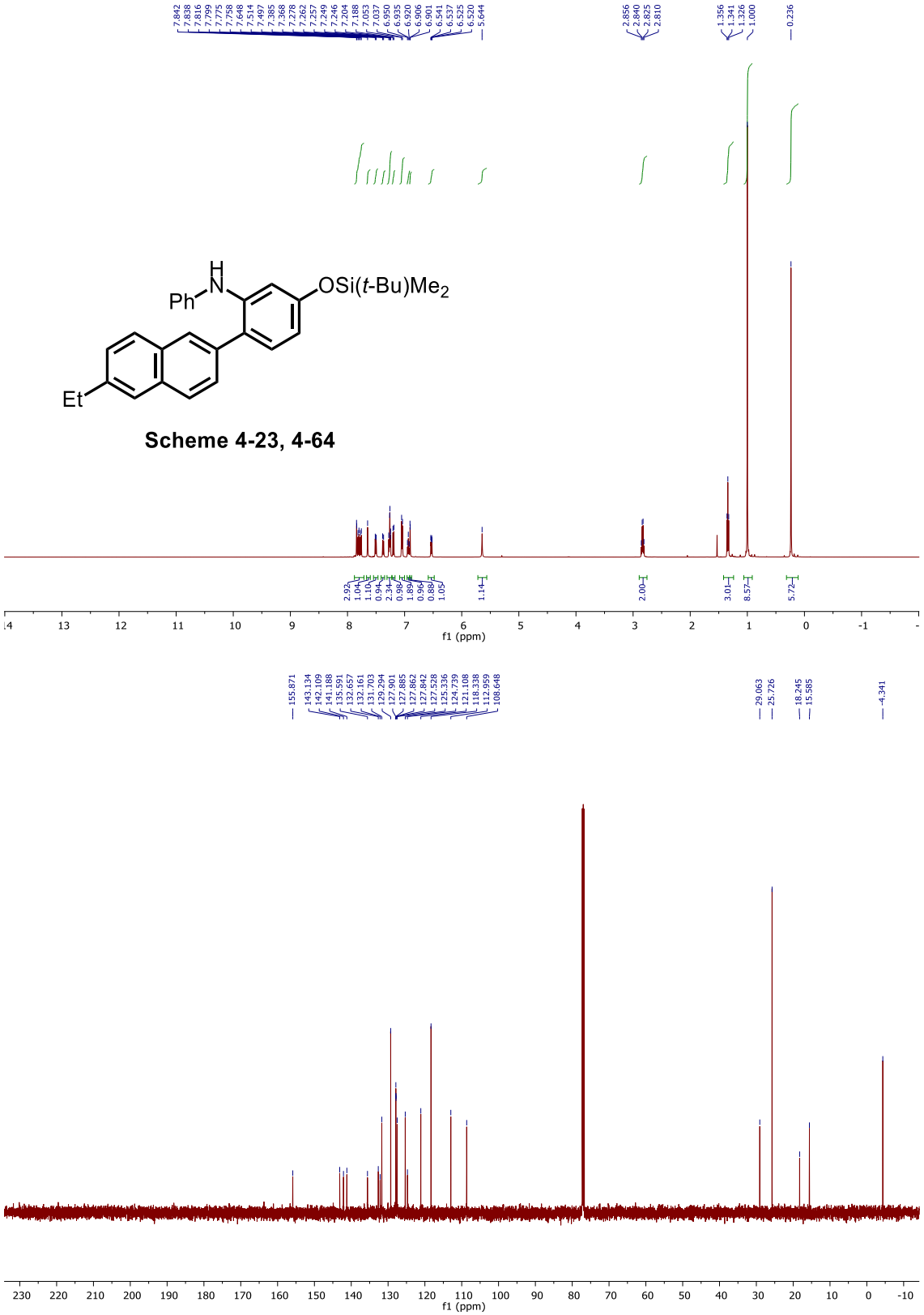

Scheme 4-23, 4-64

Scheme 4-23, 4-(5-((*tert*-butyldimethylsilyl)oxy)-2-(6-methoxynaphthalen-2-yl)phenyl)-1-propyl-1H-pyrazole (4-67).

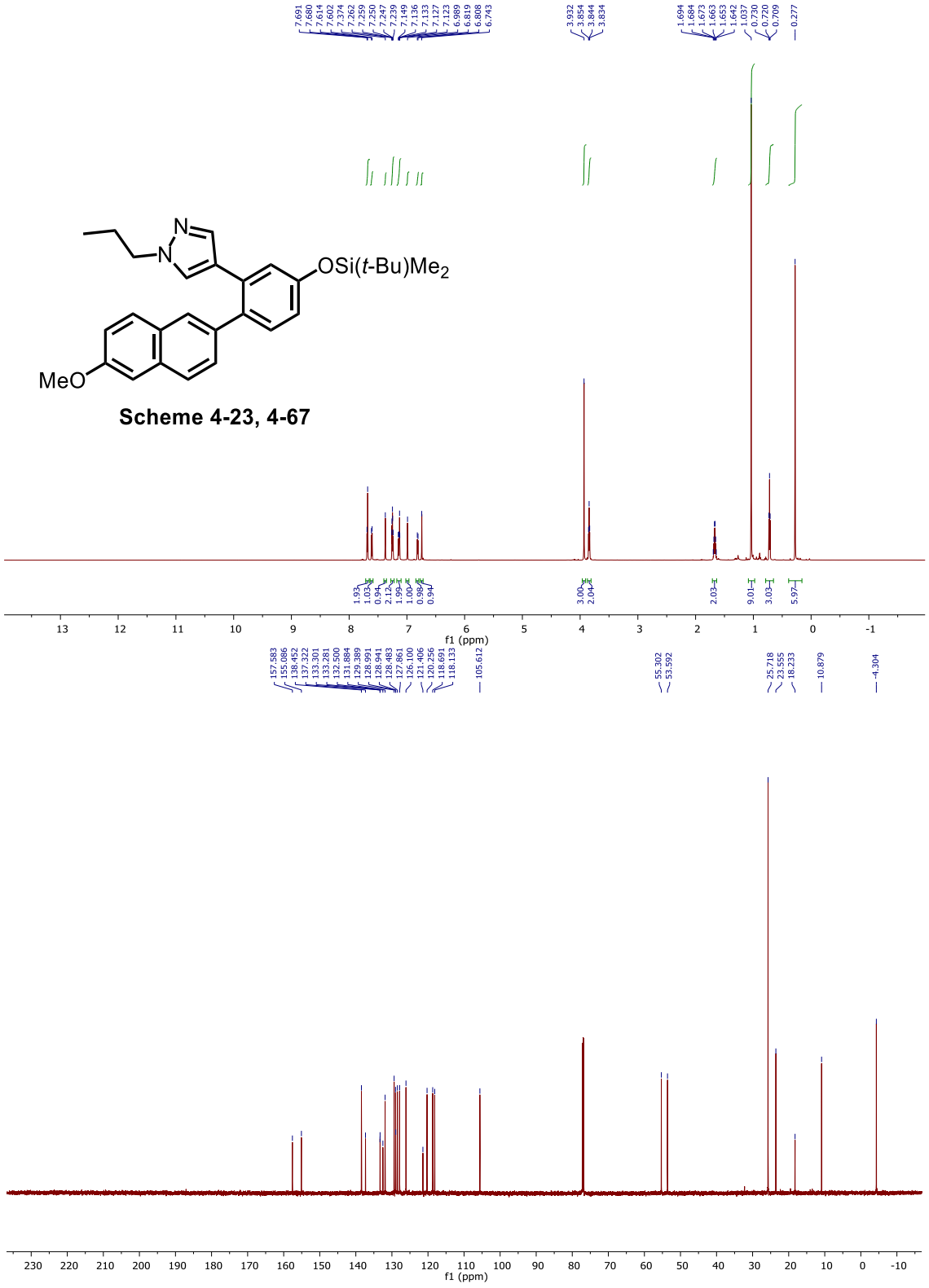

Scheme 4-23, 4-67

Scheme 4-23, 4-(5-((*tert*-butyldimethylsilyl)oxy)-2-(6-ethylnaphthalen-2-yl)phenyl)-1-propyl-1*H*-pyrazole (4-69).

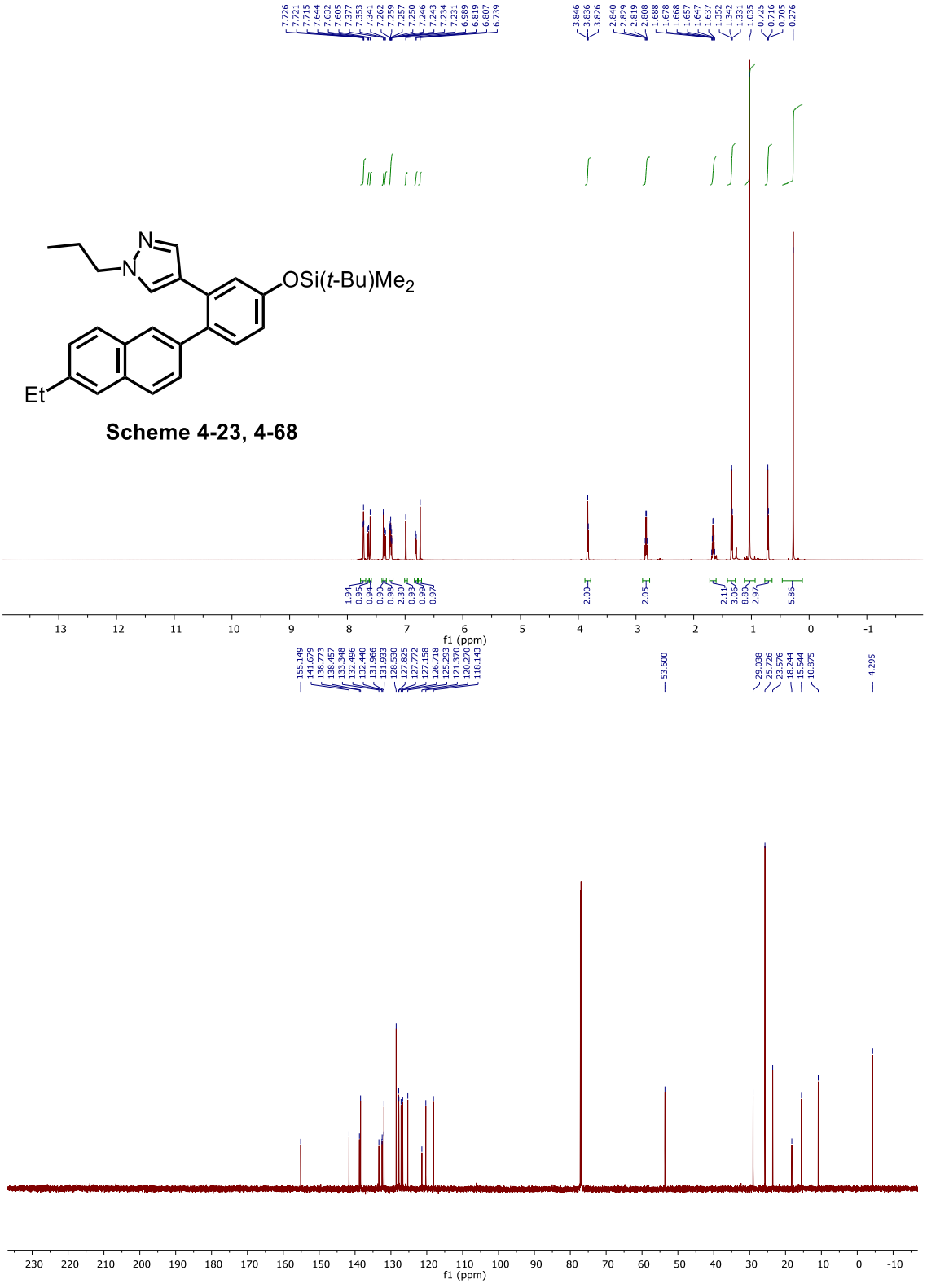

Scheme 4-23, *N*-butyl-4-(6-ethylnaphthalen-2-yl)-*N*-methyl-3-(1-propyl-1*H*-pyrazol-4-yl)aniline (4-69).

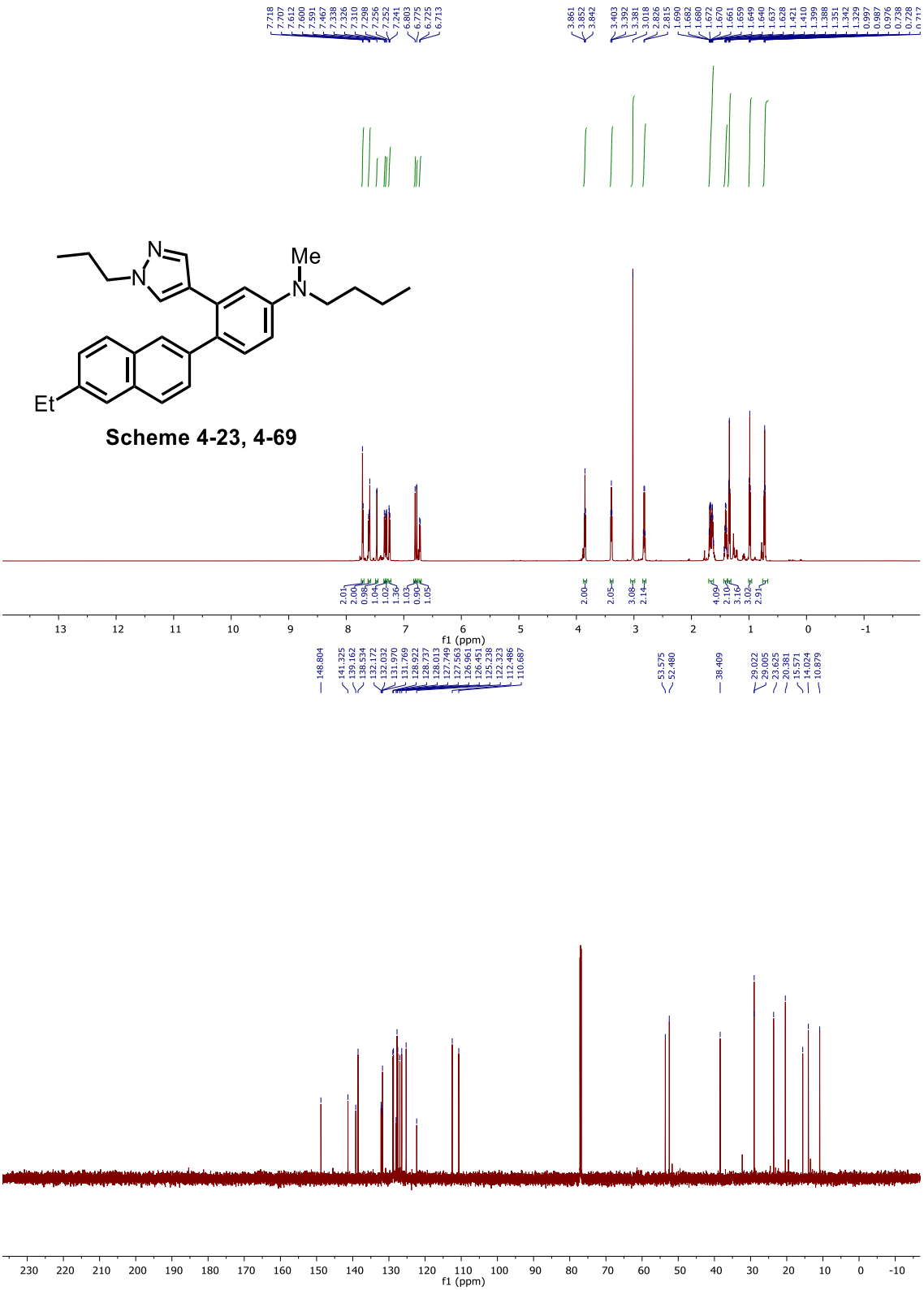

References

(1) Mkhalid, I. A. I.; Barnard, J. H.; Marder, T. B.; Murphy, J. M.; Hartwig, J. F. *Chem. Rev.* **2010**, *110*, 890.

(2) Johansson Seechurn, C. C. C.; Kitching, M. O.; Colacot, T. J.; Snieckus, V. *Angew. Chem. Int. Ed.* **2012**, *51*, 5062.

(3) Gildner, P. G.; Colacot, T. J. *Organometallics* **2015**, *34*, 5497.

(4) Nicolaou, K. C.; Bulger, P. G.; Sarlah, D. *Angew. Chem. Int. Ed.* **2005**, *44*, 4442.

(5) Torborg, C.; Beller, M. *Adv. Synth. Catal.* **2009**, *351*, 3027.

(6) Busacca, C. A.; Fandrick, D. R.; Song, J. J.; Senanayake, C. H. *Adv. Synth. Catal.* **2011**, *353*, 1825.

(7) Rosen, B. M.; Quasdorf, K. W.; Wilson, D. a; Zhang, N.; Resmerita, A.-M.; Garg, N. K.; Percec, V. *Chem. Rev.* **2011**, *111*, 1346.

(8) Amii, H.; Uneyama, K. *Chem. Rev.* **2009**, *109*, 2119.

(9) Ahrens, T.; Kohlmann, J.; Ahrens, M.; Braun, T. *Chem. Rev.* **2015**, *115*, 931.

(10) Neumann, C. N. Late-Stage Fluorination With 19F and 18F via Concerted Nucleophilic Aromatic Substitution, Harvard, 2016.

(11) Terrier, F. In *Modern Nucleophilic Aromatic Substitution*; Wiley-VCH Verlag GmbH & Co. KGaA: Weinheim, Germany, 2013; pp 1–94.

(12) Fier, P. S.; Hartwig, J. F. *J. Am. Chem. Soc.* **2014**, *136*, 10139.

(13) Poliakoff, M. *Science* **2002**, *297*, 807.

(14) Wenkert, E.; Han, A.-L.; Jenny, C.-J. *J. Chem. Soc., Chem. Commun.* **1988**, No. 14, 975.

(15) Yu, D.-G.; Li, B.-J.; Shi, Z.-J. *Acc. Chem. Res.* **2010**, *43*, 1486.

(16) Li, B.-J.; Yu, D.-G.; Sun, C.-L.; Shi, Z.-J. *Chem. Eur. J.* **2011**, *17*, 1728.

(17) Mesganaw, T.; Garg, N. K. *Org. Process Res. Dev.* **2013**, *17*, 29.

(18) Han, F.-S. *Chem. Soc. Rev. Chem. Soc. Rev* **2013**, *42*, 5270.

(19) Fujimoto, T.; Ritter, T. *Org. Lett.* **2015**, *17*, 544.

(20) Tobisu, M.; Chatani, N. *Acc. Chem. Res.* **2015**, *48*, 1717.

(21) Zeng, H.; Qiu, Z.; Domínguez-Huerta, A.; Hearne, Z.; Chen, Z.; Li, C.-J. *ACS Catal.* **2017**, *7*, 510.

(22) Zarate, C.; van Gemmeren, M.; Somerville, R. J.; Martin, R. *Phenol Derivatives: Modern Electrophiles in Cross-Coupling Reactions*, 1st ed.; Elsevier Inc., 2016; Vol. 66.

(23) Chen, Q.-Y.; Yang, Z.-Y. *Tetrahedron Lett.* **1986**, *27*, 1171.

(24) Scott, W. J.; Crisp, G. T.; Stille, J. K. *J. Am. Chem. Soc.* **1984**, *106*, 4630.

(25) Matsushita, H.; Negishi, E. *J. Org. Chem.* **1982**, *47*, 4161.

(26) Yamashita, J.; Inoue, Y.; Kondo, T.; Hashimoto, H. *Chem. Lett.* **1986**, *15*, 407.

(27) Percec, V.; Bae, J.-Y.; Zhao, M.; Hill, D. H. *J. Org. Chem.* **1995**, *60*, 176.

(28) Leowanawat, P.; Zhang, N.; Percec, V. *J. Org. Chem.* **2012**, *77*, 1018.

(29) Wender, P. A.; Verma, V. A.; Paxton, T. J.; Pillow, T. H. *Acc. Chem. Res.* **2008**, *41*, 40.

(30) Hilf, J. A.; Witthoft, L. W.; Woerpel, K. A. *J. Org. Chem.* **2015**, *80*, 8262.

(31) Brown, D. G.; Boström, J. *J. Med. Chem.* **2016**, *59*, 4443.

(32) Roughley, S. D.; Vernalis, A. M. J. *J. Med. Chem* **2011**, *54*, 3451.

(33) Young, I. S.; Baran, P. S. *Nat. Chem.* **2009**.

(34) Roulland, E. *Angew. Chem. Int. Ed.* **2011**, *50*, 1226.

(35) Sengupta, S.; Leite, M.; Raslan, D. S.; Quesnelle, C.; Snieckus, V. *J. Org. Chem.* **1992**, *57*, 4066.

(36) Snieckus, V. *Chem. Rev. Chem. Rev.* **1990**, *90*, 879.

(37) Mesganaw, T.; Fine Nathel, N. F.; Garg, N. K. *Org. Lett.* **2012**, *14*, 2918.

(38) Guo, L.; Hsiao, C.-C.; Yue, H.; Liu, X.; Rueping, M. *ACS Catal.* **2016**, *6*, 4438.

(39) Antoft-Finch, A.; Blackburn, T.; Snieckus, V. *J. Am. Chem. Soc.* **2009**, *131*, 17750.

(40) Quasdorf, K. W.; Riener, M.; Petrova, K. V; Garg, N. K. *J. Am. Chem. Soc.* **2009**, *131*, 17748.

(41) Quasdorf, K. W.; Antoft-Finch, A.; Liu, P.; Silberstein, A. L.; Komaromi, A.; Blackburn,

T.; Ramgren, S. D.; Houk, K. N.; Snieckus, V.; Garg, N. K. *J. Am. Chem. Soc* **2011**, *133*, 6352.

(42) Ohtsuki, A.; Yanagisawa, K.; Furukawa, T.; Tobisu, M.; Chatani, N. *J. Org. Chem.* **2016**, *81*, 9409.

(43) Shi, W. J.; Zhao, H. W.; Wang, Y.; Cao, Z. C.; Zhang, L. S.; Yu, D. G.; Shi, Z. J. *Adv. Synth. Catal.* **2016**, *358*, 2410.

(44) Ogawa, H.; Yang, Z.-K.; Minami, H.; Kojima, K.; Saito, T.; Wang, C.; Uchiyama, M. *ACS Catal.* **2017**, *7*, 3988.

(45) Yang, Z.-K.; Wang, C.; Uchiyama, M. *Synlett* **2017**, *28*, 2565.

(46) Huang, K.; Yu, D.-G.; Zheng, S.-F.; Wu, Z.-H.; Shi, Z.-J. *Chem. Eur. J.* **2011**, *17*, 786.

(47) Mesganaw, T.; Silberstein, A. L.; Ramgren, S. D.; Nathel, N. F. F.; Hong, X.; Liu, P.; Garg, N. K. *Chem. Sci.* **2011**, *2*, 1766.

(48) Hie, L.; Ramgren, S. D.; Mesganaw, T.; Garg, N. K. *Org. Lett.* **2012**, *14*, 4182.

(49) Koch, E.; Takise, R.; Studer, A.; Yamaguchi, J.; Itami, K. *Chem. Commun. Chem. Commun* **2015**, *51*, 855.

(50) Muto, K.; Hatakeyama, T.; Yamaguchi, J.; Itami, K. *Chem. Sci.* **2015**, *6*, 6792.

(51) Takise, R.; Itami, K.; Yamaguchi, J. *Org. Lett.* **2016**, *18*, 4428.

(52) Wang, Y.; Wu, S.-B.; Shi, W.-J.; Shi, Z.-J. *Org. Lett.* **2016**, *18*, 2548.

(53) Song, W.; Ackermann, L. *Angew. Chem. Int. Ed.* **2012**, *51*, 8251.

(54) Silberstein, A. L.; Ramgren, S. D.; Garg, N. K. *Org. Lett.* **2012**, *14*, 3796.

(55) Nakamura, K.; Yasui, K.; Tobisu, M.; Chatani, N. *Tetrahedron* **2015**, *71*, 4484.

(56) Yasui, K.; Higashino, M.; Chatani, N.; Tobisu, M. *Synlett* **2017**, *28*, 2569.

(57) Quasdorf, K. W.; Tian, X.; Garg, N. K. *J. Am. Chem. Soc.* **2008**, *130*, 14422.

(58) Guan, B.-T.; Wang, Y.; Li, B.-J.; Yu, D.-G.; Shi, Z.-J. *J. Am. Chem. Soc.* **2008**, *130*, 14468.

(59) Li, B. J.; Li, Y. Z.; Lu, X. Y.; Liu, J.; Guan, B. T.; Shi, Z. J. *Angew. Chem. Int. Ed.* **2008**, *47*, 10124.

(60) Yang, J.; Chen, T.; Han, L.-B. *J. Am. Chem. Soc.* **2015**, *137*, 1782.

(61) Yang, J.; Xiao, J.; Chen, T.; Han, L.-B. *J. Org. Chem.* **2016**, *81*, 3911.

(62) Ehle, A. R.; Zhou, Q.; Watson, M. P. *Org. Lett.* **2012**, *14*, 1202.

(63) Shimasaki, T.; Tobisu, M.; Chatani, N. *Angew. Chem. Int. Ed.* **2010**, *49*, 2929.

(64) Yue, H.; Guo, L.; Liu, X.; Rueping, M. *Org. Lett.* **2017**, *19*, 1788.

(65) Tobisu, M.; Yamakawa, K.; Shimasaki, T.; Chatani, N. *Chem. Commun.* **2011**, *47*, 2946.

(66) Xi, X.; Chen, T.; Zhang, J.-S.; Han, L.-B. *Chem. Commun.* **2018**, *54*, 1521.

(67) Muto, K.; Yamaguchi, J.; Itami, K. *J. Am. Chem. Soc.* **2012**, *134*, 169.

(68) Wang, J.; Ferguson, D. M.; Kalyani, D. *Tetrahedron* **2013**, *69*, 5780.

(69) Takise, R.; Muto, K.; Yamaguchi, J.; Itami, K. *Angew. Chem. Int. Ed.* **2014**, *53*, 6791.

(70) Cornella, J.; Jackson, E. P.; Martin, R. *Angew. Chem. Int. Ed.* **2015**, *54*, 4075.

(71) Correa, A.; León, T.; Martin, R. *J. Am. Chem. Soc.* **2014**, *136*, 1062.

(72) Correa, A.; Martin, R. *J. Am. Chem. Soc.* **2014**, *136*, 7253.

(73) Zarate, C.; Martin, R. *J. Am. Chem. Soc.* **2014**, *136*, 2236.

(74) Gu, Y.; Martín, R. *Angew. Chem. Int. Ed.* **2017**, *56*, 3187.

(75) Li, B.-J.; Xu, L.; Wu, Z.-H.; Guan, B.-T.; Sun, C.-L.; Wang, B.-Q.; Shi, Z.-J. *J. Am. Chem. Soc.* **2009**, *131*, 14656.

(76) Kinuta, H.; Hasegawa, J.; Tobisu, M.; Chatani, N. *Chem. Lett.* **2015**, *44*, 366.

(77) Yamamoto, T.; Ishizu, J.; Kohara, T.; Komiya, S.; Yamamoto, A. *J. Am. Chem. Soc.* **1980**, *102*, 3758.

(78) Li, Z.; Zhang, S.-L.; Fu, Y.; Guo, Q.-X.; Liu, L. *J. Am. Chem. Soc.* **2009**, *131*, 8815.

(79) Meng, G.; Shi, S.; Szostak, M. *Synlett* **2016**, *27*, 2530.

(80) Dander, J. E.; Garg, N. K. *ACS Catal.* **2017**, *7*, 1413.

(81) Wenkert, E.; Michelotti, E. L.; Swindell, C. S. *J. Am. Chem. Soc.* **1979**, *101*, 2246.

(82) Dankwardt, J. W. *Angew. Chem. Int. Ed.* **2004**, *43*, 2428.

(83) Xie, L. G.; Wang, Z. X. *Chem. Eur. J.* **2011**, *17*, 4972.

(84) Iglesias, M. J.; Prieto, A.; Nicasio, M. C. *Org. Lett.* **2012**, *14*, 4318.

(85) Zhang, J.; Xu, J.; Xu, Y.; Sun, H.; Shen, Q.; Zhang, Y. *Organometallics* **2015**, *34*, 5792.

(86) Harkness, G. J.; Clarke, M. L. *Catal. Sci. Technol.* **2018**, *8*, 328.

(87) Wang, C.; Ozaki, T.; Takita, R.; Uchiyama, M. *Chem. Eur. J.* **2012**, *18*, 3482.

(88) Yang, Z.-K.; Wang, D.-Y.; Minami, H.; Ogawa, H.; Ozaki, T.; Saito, T.; Miyamoto, K.; Wang, C.; Uchiyama, M. *Chem. Eur. J.* **2016**, *22*, 15693.

(89) Tobisu, M.; Shimasaki, T.; Chatani, N. *Angew. Chem. Int. Ed.* **2008**, *47*, 4866.

(90) Tobisu, M.; Yasutome, A.; Kinuta, H.; Nakamura, K.; Chatani, N. *Org. Lett.* **2014**, *16*, 5572.

(91) Cao, Z.-C.; Luo, Q.-Y.; Shi, Z.-J. *Org. Lett.* **2016**, *18*, 5978.

(92) Guan, B.-T.; Xiang, S.-K.; Wu, T.; Sun, Z.-P.; Wang, B.-Q.; Zhao, K.-Q.; Shi, Z.-J. *Chem. Commun.* **2008**, *2*, 1437.

(93) Tobisu, M.; Takahira, T.; Chatani, N. *Org. Lett.* **2015**, *17*, 4352.

(94) Rasheed, S.; Rao, D. N.; Das, P. *Asian J. Org. Chem.* **2016**, *5*, 1499.

(95) Leiendecker, M.; Hsiao, C. C.; Guo, L.; Alandini, N.; Rueping, M. *Angew. Chem. Int. Ed.* **2014**, *53*, 12912.

(96) Morioka, T.; Nishizawa, A.; Nakamura, K.; Tobisu, M.; Chatani, N. *Chem. Lett.* **2015**, *3*, 1729.

(97) Liu, X.; Hsiao, C.; Kalvet, I.; Leiendecker, M.; Guo, L.; Schoenebeck, F.; Rueping, M. *Angew. Chem. Int. Ed.* **2016**, *55*, 6093.

(98) Tobisu, M.; Takahira, T.; Morioka, T.; Chatani, N. *J. Am. Chem. Soc.* **2016**, *138*, 6711.

(99) Guo, L.; Liu, X.; Baumann, C.; Rueping, M. *Angew. Chem. Int. Ed.* **2016**, *55*, 15415.

(100) Álvarez-Bercedo, P.; Martin, R. *J. Am. Chem. Soc.* **2010**, *132*, 17352.

(101) Tobisu, M.; Morioka, T.; Ohtsuki, A.; Chatani, N. *Chem. Sci.* **2015**, *6*, 3410.

(102) Tobisu, M.; Takahira, T.; Ohtsuki, A.; Chatani, N. *Org. Lett.* **2015**, *17*, 680.

(103) Nakamura, K.; Tobisu, M.; Chatani, N. *Org. Lett.* **2015**, *17*, 6142.

(104) Zarate, C.; Nakajima, M.; Martin, R. *J. Am. Chem. Soc.* **2017**, *139*, 1191.

(105) Tobisu, M.; Shimasaki, T.; Chatani, N. *Chem. Lett.* **2009**, *38*, 710.

(106) Tobisu, M.; Yasutome, A.; Yamakawa, K.; Shimasaki, T.; Chatani, N. *Tetrahedron* **2012**, *68*, 5157.

(107) Zarate, C.; Manzano, R.; Martin, R. *J. Am. Chem. Soc.* **2015**, *137*, 6754.

(108) Sergeev, A. G.; Hartwig, J. F. *Science* **2011**, *332*, 439.

(109) Sergeev, A. G.; Webb, J. D.; Hartwig, J. F. *J. Am. Chem. Soc.* **2012**, *134*, 20226.

(110) Gao, F.; Webb, J. D.; Hartwig, J. F. *Angew. Chem. Int. Ed.* **2016**, *55*, 1474.

(111) Saper, N. I.; Hartwig, J. F. *J. Am. Chem. Soc.* **2017**, *139*, 17667.

(112) Li, X.-J.; Zhang, J.-L.; Geng, Y.; Jin, Z. *J. Org. Chem.* **2013**, *78*, 5078.

(113) Kinuta, H.; Tobisu, M.; Chatani, N. *J. Am. Chem. Soc.* **2015**, *137*, 1593.

(114) Ueno, S.; Mizushima, E.; Chatani, N.; Kakiuchi, F. *J. Am. Chem. Soc.* **2006**, *128*, 16516.

(115) Iranpoor, N.; Panahi, F.; Jamedi, F. *J. Organomet. Chem.* **2015**, *781*, 6.

(116) Kurata, Y.; Otsuka, S.; Fukui, N.; Nogi, K.; Yorimitsu, H.; Osuka, A. *Org. Lett.* **2017**, *19*, 1274.

(117) Tobisu, M.; Zhao, J.; Kinuta, H.; Furukawa, T.; Igarashi, T.; Chatani, N. *Adv. Synth. Catal.* **2016**, *358*, 2417.

(118) Iranpoor, N.; Panahi, F. *Adv. Synth. Catal.* **2014**, *356*, 3067.

(119) Li, J.; Wang, Z.-X. *Org. Lett.* **2017**, *19*, 3723.

(120) Iranpoor, N.; Panahi, F. *Org. Lett.* **2015**, *17*, 214.

(121) Etemadi-Davan, E.; Iranpoor, N. *Chem. Commun.* **2017**, *53*, 12794.

(122) Li, J.; Wang, Z.-X. *Chem. Commun.* **2018**, *54*, 2138.

(123) Peng, Z.; Yu, Z.; Li, T.; Li, N.; Wang, Y.; Song, L.; Jiang, C. *Organometallics* **2017**, *36*, 2826.

(124) van der Boom, M. E.; Liou, S.-Y.; Ben-David, Y.; Vigalok, A.; Milstein, D. *Angew. Chem. Int. Ed.* **1997**, *36*, 625.

(125) van der Boom, M. E.; Liou, S.-Y.; Ben-David, Y.; Shimon, L. J. W.; Milstein, D. *J. Am. Chem. Soc.* **1998**, *120*, 6531.

(126) Edouard, G. A.; Kelley, P.; Herbert, D. E.; Agapie, T. *Organometallics* **2015**, *34*, 5254.

(127) Kelley, P.; Lin, S.; Edouard, G.; Day, M. W.; Agapie, T. *J. Am. Chem. Soc.* **2012**, *134*, 5480.

(128) Kelley, P.; Edouard, G. A.; Lin, S.; Agapie, T. *Chem. Eur. J.* **2016**, *22*, 17173.

(129) Kakiuchi, F.; Usui, M.; Ueno, S.; Chatani, N.; Murai, S. *J. Am. Chem. Soc.* **2004**, *126*, 2706.

(130) Zhao, Y.; Snieckus, V. *J. Am. Chem. Soc.* **2014**, *136*, 11224.

(131) da Frota, L.; Schneider, C.; de Amorim, M.; da Silva, A.; Snieckus, V. *Synlett* **2017**, *28*, 2587.

(132) Cong, X.; Tang, H.; Zeng, X. *J. Am. Chem. Soc.* **2015**, *137*, 14367.

(133) Tang, J.; Luo, M.; Zeng, X. *Synlett* **2017**, *28*, 2577.

(134) Hibe, Y.; Ebe, Y.; Nishimura, T.; Yorimitsu, H. *Chem. Lett.* **2017**, *46*, 953.

(135) Chen, Z.; Liu, J.; Pei, H.; Liu, W.; Chen, Y.; Wu, J.; Li, W.; Li, Y. *Org. Lett.* **2015**, *17*, 3406.

(136) Ren, Y.; Yan, M.; Wang, J.; Zhang, Z. C.; Yao, K. *Angew. Chem. Int. Ed.* **2013**, *52*, 12674.

(137) Ren, Y.-L.; Tian, M.; Tian, X.-Z.; Wang, Q.; Shang, H.; Wang, J.; Zhang, Z. C. *Catal. Commun.* **2014**, *52*, 36.

(138) Miller, A. J. M.; Kaminsky, W.; Goldberg, K. I. *Organometallics* **2014**, *33*, 1245.

(139) Cong, X.; Tang, H.; Zeng, X. *J. Am. Chem. Soc.* **2015**, *137*, 14367.

(140) Kusumoto, S.; Nozaki, K. *Nat. Commun.* **2015**, *6*, 6296.

(141) Wu, W.-B.; Huang, J.-M. *J. Org. Chem.* **2014**, *79*, 10189.

(142) Xu, H.; Yu, B.; Zhang, H.; Zhao, Y.; Yang, Z.; Xu, J.; Han, B.; Liu, Z. *Chem. Commun. Chem. Commun* **2015**, *51*, 12212.

(143) Xu, H.; Liu, X.; Zhao, Y.; Wu, C.; Chen, Y.; Gao, X.; Liu, Z. *Chin. J. Chem* **2017**, *35*, 938.

(144) Samant, B. S.; Kabalka, G. W. *Chem. Commun. Chem. Commun* **2012**, *48*, 8658.

(145) Ogawa, H.; Minami, H.; Ozaki, T.; Komagawa, S.; Wang, C.; Uchiyama, M. *Chem. Eur. J.* **2015**, *21*, 13904.

(146) Xu, L.; Chung, L. W.; Wu, Y. D. *ACS Catal.* **2016**, *6*, 483.

(147) Sawatlon, B.; Wititsuwannakul, T.; Tantirungrotechai, Y.; Surawatanawong, P. *Dalt. Trans.* **2014**, *43*, 18123.

(148) Wititsuwannakul, T.; Tantirungrotechai, Y.; Surawatanawong, P. *ACS Catal.* **2016**, *6*, 1477.

(149) Kojima, K.; Yang, Z.-K.; Wang, C.; Uchiyama, M. *Chem. Pharm. Bull* **2017**, *862*, 862.

(150) Wang, B.; Zhang, Q.; Jiang, J.; Yu, H.; Fu, Y. *Chem. Eur. J.* **2017**, *23*, 17249.

(151) Cornella, J.; Gómez-Bengoa, E.; Martin, R. *J. Am. Chem. Soc.* **2013**, *135*, 1997.

(152) Greene, T. W.; Wuts, P. G. M. In *Greene's Protective Groups in Organic Synthesis*; John Wiley & Sons, Inc.: Hoboken, NJ, USA, 1999; Vol. 9, pp 16–366.

(153) Corey, E. J.; Venkateswarlu, A. *J. Am. Chem. Soc.* **1972**, *94*, 6190.

(154) Lalonde, M.; Chan, T. H. *Synthesis* **1985**, *1985*, 817.

(155) Crouch, R. D. *Synth. Commun.* **2013**, *43*, 2265.

(156) Nelson, T. D.; Crouch, R. D. *Synthesis* **1996**, *1996*, 1031.

(157) David Crouch, R. *Tetrahedron* **2004**, *60*, 5833.

(158) Carreira, E. M.; Du Bois, J. *J. Am. Chem. Soc.* **1994**, *116*, 10825.

(159) Askin, D.; Angst, C.; Danishefsky, S. *J. Org. Chem.* **1987**, *52*, 622.

(160) Holton, R. A.; Kim, H. B.; Somoza, C.; Liang, F.; Biediger, R. J.; Boatman, P. D.; Shindo, M.; Smith, C. C.; Kim, S. *J. Am. Chem. Soc.* **1994**, *116*, 1599.

(161) Zhao, F.; Yu, D.-G.; Zhu, R.-Y.; Xi, Z.; Shi, Z.-J. *Chem. Lett.* **2011**, *40*, 1001.

(162) Yu, D.-G.; Li, B.-J.; Zheng, S.-F.; Guan, B.-T.; Wang, B.-Q.; Shi, Z.-J. *Angew. Chem. Int. Ed.* **2010**, *49*, 4566.

(163) Ohgi, A.; Nakao, Y. *Chem. Lett.* **2016**, *45*, 45.

(164) Murata, M.; Suzuki, K.; Watanabe, S.; Masuda, Y. *J. Org. Chem.* **1997**, *62*, 8569.

(165) Xu, Z.; Huang, W. S.; Zhang, J.; Xu, L. W. *Synth.* **2015**, *47*, 3645.

(166) Denmark, S. E.; Kallemeyn, J. M. *Org. Lett.* **2003**, *5*, 3483.

(167) Iizuka, M.; Kondo, Y. *European J. Org. Chem.* **2008**, *2008*, 1161.

(168) Yamanoi, Y. *J. Org. Chem.* **2005**, *70*, 9607.

(169) Matsumoto, H.; Nagashima, S.; Yoshihiro, K.; Nagai, Y. *J. Organomet. Chem.* **1975**, *85*, C1.

(170) Shirakawa, E.; Kurahashi, T.; Yoshida, H.; Hiyama, T. *Chem. Commun.* **2000**, *0*, 1895.

(171) Jain, P.; Pal, S.; Avasare, V. *Organometallics* **2018**, *37*, 1141.

(172) Malik, H. a; Sormunen, G. J.; Montgomery, J. *J. Am. Chem. Soc.* **2010**, *132*, 6304.

(173) Komiyama, T.; Minami, Y.; Hiyama, T. *Angew. Chem. Int. Ed.* **2016**, *2*, 2.

(174) Komiyama, T.; Minami, Y.; Furuya, Y.; Hiyama, T. *Angew. Chem. Int. Ed.* **2018**, *57*, 1987.

(175) Komiyama, T.; Minami, Y.; Hiyama, T. *Angew. Chem. Int. Ed.* **2016**, *55*, 15787.

(176) Ruiz-Castillo, P.; Buchwald, S. L. *Chem. Rev.* **2016**, *116*, 12564.

(177) Tassone, J. P.; MacQueen, P. M.; Lavoie, C. M.; Ferguson, M. J.; McDonald, R.; Stradiotto, M. *ACS Catal.* **2017**, 6048.

(178) MacQueen, P.; Stradiotto, M. *Synlett* **2017**, *28*, 1652.

(179) Wiensch, E. M.; Todd, D. P.; Montgomery, J. *ACS Catal.* **2017**, *7*, 5568.

(180) Schwarzer, M. C.; Konno, R.; Hojo, T.; Ohtsuki, A.; Nakamura, K.; Yasutome, A.; Takahashi, H.; Shimasaki, T.; Tobisu, M.; Chatani, N.; Mori, S. *J. Am. Chem. Soc.* **2017**, *139*, 10347.

(181) Kleeberg, C.; Dang, L.; Lin, Z.; Marder, T. B. *Angew. Chem. Int. Ed.* **2009**, *48*, 5350.

(182) Niwa, T.; Ochiai, H.; Hosoya, T. *ACS Catal.* **2017**, *7*, 4535.

(183) Furukawa, T.; Tobisu, M.; Chatani, N. *Chem. Commun.* **2015**, *51*, 6508.

(184) Zhang, H.; Hagihara, S.; Itami, K. *Chem. Lett.* **2015**, *44*, 779.

(185) Dobrounig, P.; Trobe, M.; Breinbauer, R. *Monatshefte für Chemie - Chem. Mon.* **2017**, *148*, 3.

(186) Yu, D.-G.; Yu, M.; Guan, B.-T.; Li, B.-J.; Zheng, Y.; Wu, Z.-H.; Shi, Z.-J. *Org. Lett.* **2009**, *11*, 3374.

(187) Zhao, F.; Zhang, Y. F.; Wen, J.; Yu, D. G.; Wei, J. B.; Xi, Z.; Shi, Z. J. *Org. Lett.* **2013**, *15*, 3230.

(188) Echavarren, A. M.; Stille, J. K. *J. Am. Chem. Soc.* **1987**, *109*, 5478.

(189) Kamikawa, T.; Hayashi, T. *Tetrahedron Lett.* **1997**, *38*, 7087.

(190) Littke, A. F.; Dai, C.; Fu, G. C. *J. Am. Chem. Soc.* **2000**, *122*, 4020.

(191) Schoenebeck, F.; Houk, K. N. *J. Am. Chem. Soc.* **2010**, *132*, 2496.

(192) Niemeyer, Z. L.; Milo, A.; Hickey, D. P.; Sigman, M. S. *Nat. Chem.* **2016**, *8*, 610.

(193) Proutiere, F.; Schoenebeck, F. *Angew. Chem. Int. Ed.* **2011**, *50*, 8192.

(194) Proutiere, F.; Schoenebeck, F. *Synlett* **2012**, *23*, 645.

(195) Espino, G.; Kurbangalieva, A.; Brown, J. M. *Chem. Commun.* **2007**, *0*, 1742.

(196) Shen, C.; Wei, Z.; Jiao, H.; Wu, X.-F. *Chem. Eur. J.* **2017**, *23*, 13369.

(197) Keylor, M. H.; Niemeyer, Z. L.; Sigman, M. S.; Tan, K. L. *J. Am. Chem. Soc.* **2017**, *139*, 10613.

(198) Desmarets, C.; Schneider, R.; Fort, Y. *J. Org. Chem.* **2002**, *67*, 3029.

(199) Fine Nathel, N. F.; Kim, J.; Hie, L.; Jiang, X.; Garg, N. K. *ACS Catal.* **2014**, *4*, 3289.

(200) Hatakeyama, T.; Hashimoto, S.; Seki, S.; Nakamura, M. *J. Am. Chem. Soc* **2011**, *133*, 18614.

(201) Littke, A. F.; Fu, G. C. *Angew. Chem. Int. Ed* **1998**, *37*, 3387.

(202) Hargaden, G. C.; Guiry, P. J. *Adv. Synth. Catal.* **2007**, *349*, 2407.

(203) Oblinger, E.; Montgomery, J.; Comprehensi, P. I.; Organic, V. *J. Am. Chem. Soc.* **1997**, *7863*, 9065.

(204) Jackson, E. P.; Malik, H. a.; Sormunen, G. J.; Baxter, R. D.; Liu, P.; Wang, H.; Shareef, A.-R.; Montgomery, J. *Acc. Chem. Res.* **2015**, *48*, 1736.

(205) Trost, B. M.; Van Vranken, D. L. *Chem. Rev.* **1996**, *96*, 395.

(206) Didiuk, M. T.; Morken, J. P.; Hoveyda, A. H. *J. Am. Chem. Soc* **1995**, *117*, 7273.

(207) Hayashi, T.; Konishi, M.; Kumada, M. *J. Organomet. Chem.* **1980**, *186*, C1.

(208) Seto, C.; Otsuka, T.; Takeuchi, Y.; Tabuchi, D.; Nagano, T. *Synlett* **2018**, *29*, A.

(209) Naitoh, Y.; Bando, F.; Terao, J.; Otsuki, K.; Kuniyasu, H.; Kambe, N. *Chem. Lett.* **2007**, *36*, 236.

(210) Hayashi, T.; Konishi, M.; Yokota, K.; Kumada, M. *J. Chem. Soc. Chem. Commun.* **1981**, No. 7, 313.

(211) Trost, B. M.; Nanninga, T. N.; Satoh, T. *J. Am. Chem. Soc.* **1985**, *107*, 721.

(212) Trost, B. M.; Silverman, S. M.; Stambuli, J. P. *J. Am. Chem. Soc.* **2011**, *133*, 19483.

(213) Trost, B. M. *Angew. Chem. Int. Ed.* **1986**, *25*, 1.

(214) Trost, B. M.; McDougall, P. J. *Org. Lett.* **2009**, *11*, 3782.

(215) Trost, B. M.; Cramer, N.; Bernsmann, H. *J. Am. Chem. Soc.* **2007**, *129*, 3086.

(216) Trost, B. M.; McDougall, P. J.; Hartmann, O.; Wathen, P. T. *J. Am. Chem. Soc.* **2008**, *130*, 14960.

(217) Trost, B. M.; Cramer, N.; Silverman, S. M. *J. Am. Chem. Soc.* **2007**, *129*, 12396.

(218) Jones, M. D.; Kemmitt, R. D. W. *J. Chem. Soc., Chem. Commun.* **1986**, *0*, 1201.

(219) Luo, S.; Yu, D.-G.; Zhu, R.-Y.; Wang, X.; Wang, L.; Shi, Z.-J. *Chem. Commun.* **2013**, *49*, 7794.

(220) Poirier, J.-M. *Org. Prep. Proced. Int.* **1988**, *20*, 317.

(221) Hostier, T.; Neouchy, Z.; Ferey, V.; Gomez Pardo, D.; Cossy, J. *Org. Lett.* **2018**, *20*, 1815.

(222) Iwasaki, T.; Akimoto, R.; Kuniyasu, H.; Kambe, N. *Chem. - An Asian J.* **2016**, *11*, 2834.

(223) Guo, L.; Leiendecker, M.; Hsiao, C.-C.; Baumann, C.; Rueping, M. *Chem. Commun.* **2014**, *51*, 2.

(224) Kocieński, P. J.; Pritchard, M.; Wadman, S. N.; Whitby, R. J.; Yeates, C. L. *J. Chem. Soc., Perkin Trans. 1* **1992**, *1*, 3419.

(225) Wenkert, E.; Michelotti, E. L.; Swindell, C. S.; Tingoli, M. *J. Org. Chem* **1984**, *49*, 4894.

(226) Ohtsuki, A.; Sakurai, S.; Tobisu, M.; Chatani, N. *Chem. Lett.* **2016**, *45*, 1277.

(227) Li, B.-J.; Xu, L.; Wu, Z.-H.; Guan, B.-T.; Sun, C.-L.; Wang, B.-Q.; Shi, Z.-J. *J. Am. Chem. Soc.* **2009**, *131*, 14656.

(228) Hayashi, T.; Katsuro, Y.; Kumada, M. *Tetrahedron Lett.* **1980**, *21*, 3915.

(229) Biju, A. T.; Hirano, K.; Fröhlich, R.; Glorius, F. *Chem. - An Asian J.* **2008**, *4*, 1786.

(230) Melaimi, M.; Jazzar, R.; Soleilhavoup, M.; Bertrand, G. *Angew. Chem. Int. Ed.* **2017**, *56*, 10046.

(231) Bisz, E.; Szostak, M. *ChemSusChem* **2017**, *10*, 3964.

(232) Asghar, S.; Tailor, S. B.; Elorriaga, D.; Bedford, R. B. *Angew. Chem. Int. Ed.* **2017**, *56*, 16367.

(233) Van Ausdall, B. R.; Glass, J. L.; Wiggins, K. M.; Aarif, A. M.; Louie, J. *J. Org. Chem.* **2009**, *74*, 7935.

(234) Pompeo, M.; Froese, R. D. J.; Hadei, N.; Organ, M. G. *Angew. Chem. Int. Ed.* **2012**, *51*, 11354.

(235) Bantreil, X.; Nolan, S. P. *Nat. Protoc.* **2011**, *6*, 69.

(236) Meiries, S.; Speck, K.; Cordes, D. B.; Slawin, A. M. Z.; Nolan, S. P. *Organometallics* **2013**, *32*, 330.

(237) Desmarets, C.; Schneider, R.; Fort, Y. *J. Org. Chem.* **2002**, *67*, 3029.

(238) Hatakeyama, T.; Hashimoto, S.; Seki, S.; Nakamura, M. *J. Am. Chem. Soc.* **2011**, *133*, 18614.

(239) Littke, A. F.; Fu, G. C. *Angew. Chem. Int. Ed.* **1999**, *37*, 3387.